

June 2008

Yucca Mountain Repository License Application

SAFETY ANALYSIS REPORT

**Chapter 1:
Repository Safety
Before Permanent Closure**

This publication was produced by the U.S. Department of Energy
Office of Civilian Radioactive Waste Management.

For further information contact:
U.S. Department of Energy
Office of Civilian Radioactive Waste Management
1551 Hillshire Drive
Las Vegas, Nevada 89134

or call:
Yucca Mountain Information Center
1-800-225-6972

or visit:
Office of Civilian Radioactive Waste Management website
<http://www.ocrwm.doe.gov>

Section 508 Accessibility Elements Included in this Document

The PDF version of this report includes features that address applicable accessibility standards in the 1998 amendment to Section 508 of the Rehabilitation Act. These features include tagged text, which is available to assistive technologies such as screen readers; alternative text (alt text), which complements graphic materials; and bookmarks and hyperlinks, which allow efficient navigation of the report.

If you require an alternative format of this report, or interpretive services, please contact our toll-free information line, at 1-800-225-6972.

LIST OF EFFECTIVE SECTIONS

Section	Title	Revision
1	Repository Safety before Permanent Closure	Rev. 0
1.1	Site Description as It Pertains to Preclosure Safety Analysis	Rev. 0
1.2	Surface Facility Structures, Systems, and Components and Operational Process Activities	Rev. 0
1.2.1	Surface Operations Overview	Rev. 0
1.2.2	Surface Facilities Structural, Mechanical Handling Equipment, and Heating, Ventilation, and Air-Conditioning System Design	Rev. 0
1.2.3	Initial Handling Facility	Rev. 0
1.2.4	Canister Receipt and Closure Facility	Rev. 0
1.2.5	Wet Handling Facility	Rev. 0
1.2.6	Receipt Facility	Rev. 0
1.2.7	Aging Facility	Rev. 0
1.2.8	Balance of Plant Facilities	Rev. 0
1.3	Subsurface Structures, Systems, and Components and Operational Process Activities	Rev. 0
1.3.1	Subsurface Operations Overview	Rev. 0
1.3.2	General Subsurface Design Considerations	Rev. 0
1.3.3	Nonemplacement Areas of the Subsurface Facility	Rev. 0
1.3.4	Emplacement Areas of the Subsurface Facility	Rev. 0
1.3.5	Subsurface Facility Ventilation	Rev. 0
1.3.6	Subsurface Facility Closure	Rev. 0
1.4	Infrastructure Structures, Systems, Components, Equipment, and Operational Process Activities	Rev. 0
1.4.1	Electric Power	Rev. 0
1.4.2	Controls and Monitoring	Rev. 0
1.4.3	Fire Protection	Rev. 0

LIST OF EFFECTIVE SECTIONS (Continued)

Section	Title	Revision
1.4.4	Plant Services	Rev. 0
1.4.5	Waste Management	Rev. 0
1.5	Waste Form and Waste Package	Rev. 0
1.5.1	Characteristics of Spent Nuclear Fuel and High-Level Radioactive Waste	Rev. 0
1.5.2	Waste Packages and Their Components	Rev. 0
1.6	Identification of Hazards and Initiating Events	Rev. 0
1.7	Event Sequence Analysis	Rev. 0
1.8	Consequence Analysis	Rev. 0
1.9	Structures, Systems, and Components Important to Safety; Natural and Engineered Barriers Important to Waste Isolation; Safety Controls; and Measures to Ensure Availability of the Safety Systems	Rev. 0
1.10	Meeting the As Low As Is Reasonably Achievable Requirements for Normal Operations and Category 1 Event Sequences	Rev. 0
1.11	Plans for Retrieval and Alternate Storage of Radioactive Wastes	Rev. 0
1.12	Plans for Permanent Closure, Decontamination, and Dismantlement of Surface Facilities	Rev. 0
1.13	Equipment Qualification Program	Rev. 0
1.14	Nuclear Criticality Safety	Rev. 0
2	Repository Safety after Permanent Closure	Rev. 0
2.1	System Description and Demonstration of Multiple Barriers	Rev. 0
2.2	Scenario Analysis and Event Probability	Rev. 0
2.3	Model Abstraction	Rev. 0
2.3.1	Climate and Infiltration	Rev. 0
2.3.2	Unsaturated Zone Flow	Rev. 0

LIST OF EFFECTIVE SECTIONS (Continued)

Section	Title	Revision
2.3.3	Water Seeping into Drifts	Rev. 0
2.3.4	Mechanical Degradation of the Engineered Barrier System	Rev. 0
2.3.5	In-Drift Physical and Chemical Environment	Rev. 0
2.3.6	Waste Package and Drip Shield Corrosion	Rev. 0
2.3.7	Waste Form Degradation and Mobilization and Engineered Barrier System Flow and Transport	Rev. 0
2.3.8	Radionuclide Transport in Unsaturated Zone	Rev. 0
2.3.9	Saturated Zone Flow and Transport	Rev. 0
2.3.10	Biosphere Transport and Exposure	Rev. 0
2.3.11	Igneous Activity	Rev. 0
2.4	Demonstration of Compliance with the Postclosure Public Health and Environmental Standards	Rev. 0
3	Research and Development Program to Resolve Safety Questions	Rev. 0
4	Performance Confirmation Program	Rev. 0
5	Management Systems	Rev. 0
5.1	Quality Assurance	Rev. 0
5.2	Records, Reports, Tests, and Inspections	Rev. 0
5.3	Training and Certification of Personnel	Rev. 0
5.4	Expert Elicitation	Rev. 0
5.5	Plans for Initial Startup Activities and Testing	Rev. 0
5.6	Plans and Procedures for Conduct of Normal Activities, Including Operations, Maintenance, Surveillance, and Periodic Testing	Rev. 0
5.7	Emergency Planning	Rev. 0
5.8	Controls to Restrict Access and Regulate Land Uses	Rev. 0

LIST OF EFFECTIVE SECTIONS (Continued)

Section	Title	Revision
5.9	Uses of the Geologic Repository Operations Area for Purposes Other Than Disposal of Radioactive Wastes	Rev. 0
5.10	License Specifications	Rev. 0
5.11	Operational Radiation Protection Program	Rev. 0

CONTENTS

	Page
1. REPOSITORY SAFETY BEFORE PERMANENT CLOSURE	1-1
1.1 SITE DESCRIPTION AS IT PERTAINS TO PRECLOSURE SAFETY ANALYSIS	1.1-1
1.1.1 Site Geography	1.1-1
1.1.1.1 Repository Boundaries	1.1-2
1.1.1.2 Natural Features	1.1-3
1.1.1.3 Man-Made Features	1.1-4
1.1.2 Regional Demography	1.1-23
1.1.2.1 Demographic Study Area	1.1-23
1.1.2.2 Population Centers	1.1-24
1.1.2.3 Population Projections	1.1-25
1.1.3 Local Meteorology and Regional Climatology	1.1-25
1.1.3.1 Meteorological Monitoring	1.1-26
1.1.3.2 Data Summary	1.1-36
1.1.3.3 Atmospheric Dispersion Characteristics	1.1-41
1.1.3.4 Atmospheric Stability	1.1-42
1.1.3.5 Meteorological Summary	1.1-44
1.1.3.6 Severe Weather Characteristics	1.1-45
1.1.4 Regional and Local Surface and Groundwater Hydrology	1.1-48
1.1.4.1 Surface Water Hydrology	1.1-49
1.1.4.2 Groundwater Hydrology	1.1-50
1.1.4.3 Hydrologic Engineering Studies for Surface Facilities	1.1-53
1.1.5 Site Geology and Seismology	1.1-55
1.1.5.1 Site Geology	1.1-55
1.1.5.2 Site Seismology	1.1-65
1.1.5.3 Geotechnical Properties and Conditions	1.1-101
1.1.6 Igneous Activity	1.1-134
1.1.6.1 Location of Volcanism in the Yucca Mountain Region	1.1-135
1.1.6.2 Probabilistic Volcanic Hazard Analysis	1.1-137
1.1.6.3 Potential Hazard from Ash Fall	1.1-138
1.1.7 Site Geomorphology	1.1-139
1.1.7.1 Geomorphic Information and Tectonic Activity	1.1-139
1.1.7.2 Variability in Quaternary Processes	1.1-140
1.1.8 Geochemistry	1.1-142
1.1.8.1 Introduction	1.1-142
1.1.8.2 Geochemical Composition of Subsurface Waters	1.1-143
1.1.8.3 Geochemical Conditions in the Preclosure Emplacement Drift Environment	1.1-144

CONTENTS (Continued)

	Page	
1.1.8.4	Geochemical Alteration to Host-Rock Properties Environment	1.1-145
1.1.9	Land Use, Structures and Facilities, and Residual Radioactivity.	1.1-148
1.1.9.1	Previous Land Uses within the Land Withdrawal Area	1.1-149
1.1.9.2	Previous Land Uses in the Vicinity of the Proposed Land Withdrawal Area	1.1-152
1.1.9.3	Location and Description of Existing Man-Made Structures or Facilities.	1.1-156
1.1.9.4	Identification of Residual Radiation	1.1-161
1.1.10	General References.	1.1-164
1.2	SURFACE FACILITY STRUCTURES, SYSTEMS, AND COMPONENTS AND OPERATIONAL PROCESS ACTIVITIES.	1.2-1
1.2.1	Surface Operations Overview.	1.2.1-1
1.2.1.1	Overview of Transportation Casks, Waste Packages, and Canisters	1.2.1-2
1.2.1.2	Major Surface Facility Structures and Systems.	1.2.1-5
1.2.1.3	Overview of Operations.	1.2.1-8
1.2.1.4	Loading Plans	1.2.1-13
1.2.1.5	Phased Operation and Construction Activities	1.2.1-20
1.2.1.6	General References	1.2.1-21
1.2.2	Surface Facilities Structural, Mechanical Handling Equipment, and Heating, Ventilation, and Air-Conditioning System Design.	1.2.2-1
1.2.2.1	Structural Design	1.2.2-1
1.2.2.2	Mechanical Handling Equipment Design	1.2.2-21
1.2.2.3	HVAC Systems Design	1.2.2-29
1.2.2.4	Regulatory Guidance and Other Design Codes and Standards	1.2.2-37
1.2.2.5	General References	1.2.2-38
1.2.3	Initial Handling Facility	1.2.3-1
1.2.3.1	Initial Handling Facility Description.	1.2.3-1
1.2.3.2	Mechanical Handling Systems	1.2.3-9
1.2.3.3	Process Systems.	1.2.3-23
1.2.3.4	Initial Handling Facility Heating, Ventilation, and Air-Conditioning Systems.	1.2.3-24
1.2.3.5	General References	1.2.3-27
1.2.4	Canister Receipt and Closure Facility	1.2.4-1
1.2.4.1	Canister Receipt and Closure Facility Description	1.2.4-1
1.2.4.2	Mechanical Handling System	1.2.4-9
1.2.4.3	Process Systems.	1.2.4-49

CONTENTS (Continued)

	Page
1.2.4.4 Canister Receipt and Closure Facility Heating, Ventilation, and Air-Conditioning Systems	1.2.4-53
1.2.4.5 General References	1.2.4-65
1.2.5 Wet Handling Facility	1.2.5-1
1.2.5.1 Wet Handling Facility Description	1.2.5-1
1.2.5.2 Mechanical Handling System	1.2.5-11
1.2.5.3 Process Systems	1.2.5-35
1.2.5.4 Shielded Transfer Cask	1.2.5-50
1.2.5.5 Wet Handling Facility Heating, Ventilation, and Air-Conditioning System	1.2.5-56
1.2.5.6 General References	1.2.5-62
1.2.6 Receipt Facility	1.2.6-1
1.2.6.1 Receipt Facility Description	1.2.6-1
1.2.6.2 Mechanical Handling System	1.2.6-8
1.2.6.3 Process Systems	1.2.6-16
1.2.6.4 Receipt Facility HVAC System	1.2.6-16
1.2.6.5 General References	1.2.6-21
1.2.7 Aging Facility	1.2.7-1
1.2.7.1 Aging Facility Description	1.2.7-2
1.2.7.2 Operational Processes	1.2.7-8
1.2.7.3 Safety Category Classification	1.2.7-10
1.2.7.4 Procedural Safety Controls to Prevent Event Sequences or Mitigate Their Effects	1.2.7-10
1.2.7.5 Design Bases and Design Criteria	1.2.7-11
1.2.7.6 Design Methodologies	1.2.7-11
1.2.7.7 Consistency of Materials with Design Methodologies	1.2.7-14
1.2.7.8 Design Codes and Standards	1.2.7-14
1.2.7.9 Design Load Combinations	1.2.7-14
1.2.7.10 General References	1.2.7-15
1.2.8 Balance of Plant Facilities	1.2.8-1
1.2.8.1 Balance of Plant Facility Descriptions	1.2.8-1
1.2.8.2 ITS Diesel Generator Mechanical Support Systems	1.2.8-8
1.2.8.3 Balance of Plant Facilities Heating, Ventilation, and Air-Conditioning	1.2.8-21
1.2.8.4 Surface Transportation	1.2.8-31
1.2.8.5 General References	1.2.8-43
1.3 SUBSURFACE STRUCTURES, SYSTEMS, AND COMPONENTS AND OPERATIONAL PROCESS ACTIVITIES	1.3-1
1.3.1 Subsurface Operations Overview	1.3.1-1
1.3.1.1 Major Subsurface Facility Structures and Equipment	1.3.1-1

CONTENTS (Continued)

	Page
1.3.1.2	Subsurface Facility Operations 1.3.1-7
1.3.1.3	Subsurface Facility Interfaces with Facilities and Systems 1.3.1-35
1.3.1.4	Conformance of Design to Criteria and Bases 1.3.1-37
1.3.1.5	General References 1.3.1-37
1.3.2	General Subsurface Design Considerations 1.3.2-1
1.3.2.1	General Design Approach 1.3.2-2
1.3.2.2	Design Considerations 1.3.2-4
1.3.2.3	Design of Subsurface Mechanical Handling Equipment 1.3.2-7
1.3.2.4	Design of Subsurface Facility Structures, Systems, and Components 1.3.2-11
1.3.2.5	Design Methodologies for Subsurface Structures, Systems, and Components 1.3.2-25
1.3.2.6	Performance and Documentation of Design Analyses 1.3.2-27
1.3.2.7	Design Codes and Standards 1.3.2-28
1.3.2.8	Design Loads and Load Combinations 1.3.2-29
1.3.2.9	Conformance of Design to Criteria and Bases 1.3.2-33
1.3.2.10	General References 1.3.2-33
1.3.3	Nonemplacement Areas of the Subsurface Facility 1.3.3-1
1.3.3.1	Nonemplacement Areas Design Description 1.3.3-3
1.3.3.2	Excavation 1.3.3-13
1.3.3.3	Ground Support System 1.3.3-14
1.3.3.4	Invert System 1.3.3-25
1.3.3.5	Waste Package Transportation System 1.3.3-27
1.3.3.6	Conformance of Design to Criteria and Bases 1.3.3-47
1.3.3.7	General References 1.3.3-47
1.3.4	Emplacement Areas of the Subsurface Facility 1.3.4-1
1.3.4.1	Description of Subsurface Facility Emplacement Areas 1.3.4-1
1.3.4.2	Emplacement Areas Design Description 1.3.4-3
1.3.4.3	Excavation 1.3.4-7
1.3.4.4	Ground Support System 1.3.4-8
1.3.4.5	Invert System 1.3.4-16
1.3.4.6	Waste Package Emplacement Pallet System 1.3.4-21
1.3.4.7	Drip Shield System 1.3.4-26
1.3.4.8	Waste Package Emplacement System 1.3.4-33
1.3.4.9	Conformance of Design to Criteria and Bases 1.3.4-39
1.3.4.10	General References 1.3.4-39
1.3.5	Subsurface Facility Ventilation 1.3.5-1

CONTENTS (Continued)

	Page
1.3.5.1 System Description	1.3.5-4
1.3.5.2 Operational Processes and Procedures	1.3.5-15
1.3.5.3 Safety Category Classification	1.3.5-19
1.3.5.4 Design Codes and Standards	1.3.5-25
1.3.5.5 Conformance of Design to Criteria and Bases	1.3.5-26
1.3.5.6 General References	1.3.5-27
1.3.6 Subsurface Facility Closure	1.3.6-1
1.3.6.1 Closure Processes	1.3.6-1
1.3.6.2 Operational Processes	1.3.6-8
1.3.6.3 Safety Category Classification	1.3.6-8
1.3.6.4 Procedural Safety Controls to Prevent Event Sequences or Mitigate Their Effects	1.3.6-8
1.3.6.5 Design Criteria and Design Bases	1.3.6-8
1.3.6.6 Design Methodologies	1.3.6-9
1.3.6.7 Consistency of Materials with Design Methodologies	1.3.6-9
1.3.6.8 Design Codes and Standards	1.3.6-9
1.3.6.9 Design Load Combinations	1.3.6-9
1.3.6.10 Conformance of Design to Criteria and Bases	1.3.6-9
1.3.6.11 General References	1.3.6-9
1.4 INFRASTRUCTURE STRUCTURES, SYSTEMS, COMPONENTS, EQUIPMENT, AND OPERATIONAL PROCESS ACTIVITIES	1.4-1
1.4.1 Electric Power	1.4.1-1
1.4.1.1 Normal Electrical Power	1.4.1-1
1.4.1.2 ITS Power	1.4.1-7
1.4.1.3 ITS DC Electrical Power and Uninterruptible Power Supply	1.4.1-14
1.4.1.4 Electrical Support Subsystems	1.4.1-17
1.4.1.5 General References	1.4.1-21
1.4.2 Controls and Monitoring	1.4.2-1
1.4.2.1 Digital Control and Management Information	1.4.2-2
1.4.2.2 Radiation/Radiological Monitoring	1.4.2-7
1.4.2.3 Environmental/Meteorological Monitoring System	1.4.2-9
1.4.2.4 Communications	1.4.2-13
1.4.2.5 Postevent Monitoring	1.4.2-19
1.4.2.6 General References	1.4.2-20
1.4.3 Fire Protection	1.4.3-1
1.4.3.1 Fire Hazard Analyses	1.4.3-1
1.4.3.2 Fire Protection System Description	1.4.3-3
1.4.3.3 Operational Processes	1.4.3-15

CONTENTS (Continued)

	Page
1.4.3.4	Design Codes and Standards 1.4.3-17
1.4.3.5	Fire Protection Program. 1.4.3-18
1.4.3.6	General References 1.4.3-21
1.4.4	Plant Services 1.4.4-1
1.4.4.1	General Purpose and Instrument Air Subsystems 1.4.4-2
1.4.4.2	Service Gases Subsystems. 1.4.4-3
1.4.4.3	Fuel Oil Subsystem 1.4.4-4
1.4.4.4	Raw, Potable, and Deionized Water Subsystems 1.4.4-5
1.4.4.5	Hot Water Heating and Chilled Water Cooling Subsystems 1.4.4-7
1.4.4.6	General References 1.4.4-8
1.4.5	Waste Management 1.4.5-1
1.4.5.1	Low-Level Radioactive Waste Management 1.4.5-1
1.4.5.2	Nonradiological Waste Management 1.4.5-7
1.4.5.3	General References 1.4.5-9
1.5	WASTE FORM AND WASTE PACKAGE 1.5-1
1.5.1	Characteristics of Spent Nuclear Fuel and High-Level Radioactive Waste 1.5.1-1
1.5.1.1	Commercial SNF 1.5.1-8
1.5.1.2	High-Level Radioactive Waste 1.5.1-29
1.5.1.3	DOE SNF. 1.5.1-33
1.5.1.4	Naval SNF 1.5.1-62
1.5.1.5	General References 1.5.1-80
1.5.2	Waste Packages and Their Components. 1.5.2-1
1.5.2.1	Waste Package Description 1.5.2-1
1.5.2.2	Operational Processes and Procedures 1.5.2-6
1.5.2.3	Considerations Important to Safety and Important to Waste Isolation 1.5.2-7
1.5.2.4	Design Bases and Design Criteria 1.5.2-7
1.5.2.5	Procedural Safety Controls to Prevent Event Sequences or Mitigate Their Effects 1.5.2-8
1.5.2.6	Design Methodologies. 1.5.2-8
1.5.2.7	Consistency of Materials with Design Methodologies 1.5.2-17
1.5.2.8	Design Codes and Standards 1.5.2-21
1.5.2.9	General References 1.5.2-21
1.6	IDENTIFICATION OF HAZARDS AND INITIATING EVENTS 1.6-1
1.6.1	Overview of Preclosure Safety Analysis 1.6-2
1.6.1.1	Internal and External Event Identification. 1.6-4
1.6.1.2	Internal and External Initiating Event Screening 1.6-5

CONTENTS (Continued)

	Page
1.6.1.3	Event Sequence Development 1.6-6
1.6.1.4	Event Sequence Quantification and Categorization 1.6-6
1.6.1.5	Dose Consequence Analysis 1.6-8
1.6.1.6	Criticality Safety Analysis 1.6-10
1.6.1.7	Identification of Structures, Systems, and Components Important to Safety and Waste Isolation and Nuclear Safety Design Bases 1.6-11
1.6.2	Applications of Preclosure Safety Analyses 1.6-12
1.6.3	Identification and Screening of Initiating Events 1.6-12
1.6.3.1	Identification of Internal Initiating Events 1.6-13
1.6.3.2	Identification of External Initiating Events 1.6-18
1.6.3.3	Results of Internal and External Initiating Event Identification 1.6-20
1.6.3.4	Methodology and Results of External Initiating Event Screening 1.6-20
1.6.3.5	Construction Hazard Event Screening 1.6-38
1.6.4	Summary of Initiating Events Included in Event Sequence Analysis 1.6-44
1.6.5	General References 1.6-44
1.7	EVENT SEQUENCE ANALYSIS 1.7-1
1.7.1	Event Sequence Development and Categorization Methodology 1.7-3
1.7.1.1	Event Sequence Diagrams and Event Trees 1.7-8
1.7.1.2	Internal Events 1.7-14
1.7.1.3	External Events 1.7-18
1.7.1.4	Seismic Events 1.7-18
1.7.2	Reliability Methods 1.7-21
1.7.2.1	Fault Tree Analysis 1.7-21
1.7.2.2	Active System or Component Reliability 1.7-25
1.7.2.3	Passive Structure, System, or Component Reliability 1.7-27
1.7.2.4	Seismic Fragilities 1.7-34
1.7.2.5	Human Reliability Analysis 1.7-35
1.7.3	Event Sequence Quantification 1.7-39
1.7.4	Event Sequence Grouping 1.7-40
1.7.5	Event Sequence Categorization 1.7-42
1.7.5.1	Initial Handling Facility 1.7-46
1.7.5.2	Receipt Facility 1.7-46
1.7.5.3	Canister Receipt and Closure Facility 1.7-47
1.7.5.4	Wet Handling Facility 1.7-47
1.7.5.5	Intrasite Operations and Balance of Plant 1.7-48
1.7.5.6	Subsurface 1.7-49

CONTENTS (Continued)

	Page
1.7.6 General References	1.7-49
1.8 CONSEQUENCE ANALYSIS	1.8-1
1.8.1 Methodology for Dose Estimates	1.8-3
1.8.1.1 Dose Estimate Methodology	1.8-4
1.8.1.2 Dose Aggregation	1.8-9
1.8.1.3 Source-Term Released Inputs	1.8-9
1.8.1.4 Other Dose Estimate Inputs	1.8-25
1.8.2 Potential Releases and Direct Radiation from Normal Operations and Category 1 and Category 2 Event Sequences	1.8-32
1.8.2.1 Repository Operations	1.8-33
1.8.2.2 Normal Operations	1.8-33
1.8.2.3 Description of Category 1 Event Sequences	1.8-38
1.8.2.4 Description of Category 2 Event Sequences	1.8-38
1.8.3 Potential Dose to Members of the Public from Normal Operations and Category 1 and Category 2 Event Sequences	1.8-39
1.8.3.1 Public Dose Methodology	1.8-39
1.8.3.2 Potential Public Dose Results	1.8-42
1.8.4 Potential Doses to Radiation Workers from Normal Operations and Category 1 Event Sequences	1.8-44
1.8.4.1 Radiation Worker Dose Methodology	1.8-44
1.8.4.2 Potential Worker Dose Results	1.8-50
1.8.5 Uncertainty Analysis	1.8-52
1.8.5.1 Use of Conservative or Bounding Input Parameters	1.8-52
1.8.5.2 Uncertainty Analysis with GENII	1.8-55
1.8.5.3 Radionuclide and Input Parameter Screening	1.8-56
1.8.5.4 Uncertainty Analysis for a Chronic Release	1.8-58
1.8.5.5 Uncertainty Analysis for an Acute Release	1.8-59
1.8.5.6 Conclusions	1.8-61
1.8.6 Summary of Potential Public and Worker Dose Consequences and Compliance Confirmation	1.8-62
1.8.7 General References	1.8-62
1.9 STRUCTURES, SYSTEMS, AND COMPONENTS IMPORTANT TO SAFETY; NATURAL AND ENGINEERED BARRIERS IMPORTANT TO WASTE ISOLATION; SAFETY CONTROLS; AND MEASURES TO ENSURE AVAILABILITY OF THE SAFETY SYSTEMS	1.9-1
1.9.1 Structures, Systems, and Components Classified as Important to Safety	1.9-3
1.9.1.1 Means to Limit Concentration of Radioactive Material in Air	1.9-8

CONTENTS (Continued)

	Page
1.9.1.2 Means to Limit Time Required to Perform Work in Radiological Areas	1.9-9
1.9.1.3 Suitable Shielding	1.9-9
1.9.1.4 Means to Monitor and Control Dispersal of Radioactive Contamination	1.9-9
1.9.1.5 Means to Control Access to High Radiation Areas or Airborne Radioactivity Areas	1.9-10
1.9.1.6 Means to Prevent and Control Criticality	1.9-10
1.9.1.7 Radiation Alarm System	1.9-10
1.9.1.8 Ability of Structures, Systems, and Components to Perform Their Intended Safety Functions	1.9-11
1.9.1.9 Explosion and Fire Detection and Suppression Systems	1.9-11
1.9.1.10 Means to Control Radioactive Waste and Effluents and to Permit Prompt Termination of Operations and Evacuation of Personnel during an Emergency	1.9-12
1.9.1.11 Electrical Power	1.9-12
1.9.1.12 Redundant Systems and Inherent Reliability	1.9-13
1.9.1.13 Inspection, Test, and Maintenance Programs	1.9-15
1.9.1.14 ITS Structure, System, or Component/Non-ITS Structure, System, or Component Interactions	1.9-16
1.9.2 Identifying Postclosure Performance Assessment Design Control Parameters and Classifying ITWI Structures, Systems, and Components	1.9-17
1.9.3 Procedural Safety Controls	1.9-19
1.9.4 Risk Significance Categorization	1.9-20
1.9.5 General References	1.9-20
1.10 MEETING THE AS LOW AS IS REASONABLY ACHIEVABLE REQUIREMENTS FOR NORMAL OPERATIONS AND CATEGORY 1 EVENT SEQUENCES	1.10-1
1.10.1 Management Commitment to Maintain Doses As Low As Is Reasonably Achievable	1.10-2
1.10.1.1 Design and Construction	1.10-3
1.10.1.2 Operation	1.10-4
1.10.1.3 Decommissioning	1.10-4
1.10.2 As Low As Is Reasonably Achievable Principles in Design	1.10-5
1.10.2.1 General Considerations	1.10-7
1.10.2.2 Facility Layout Considerations	1.10-10
1.10.2.3 Equipment Design Considerations	1.10-13
1.10.2.4 Access Control Considerations	1.10-16
1.10.2.5 Radiation Zones	1.10-16
1.10.2.6 Contamination Control	1.10-16

CONTENTS (Continued)

	Page
1.10.2.7 Ventilation Considerations	1.10-17
1.10.2.8 Radiation and Airborne Radioactivity Monitoring Instrumentation	1.10-18
1.10.2.9 Event Sequence Considerations.	1.10-19
1.10.2.10 Decommissioning	1.10-19
1.10.2.11 Dose Assessment Considerations	1.10-19
1.10.3 Surface and Subsurface Shielding Design	1.10-22
1.10.3.1 Shielding Design Objectives	1.10-22
1.10.3.2 Calculation Methodology and Computer Codes	1.10-24
1.10.3.3 Radiation Sources	1.10-25
1.10.3.4 Source Terms.	1.10-32
1.10.3.5 Shielding Evaluation of Surface Repository Areas	1.10-34
1.10.3.6 Shielding Evaluation of Subsurface Repository Areas	1.10-39
1.10.3.7 Event Sequence Considerations.	1.10-40
1.10.4 As Low As Is Reasonably Achievable Principles in Operations	1.10-40
1.10.4.1 Operational ALARA Considerations.	1.10-41
1.10.4.2 Operational Radiation Protection Program	1.10-46
1.10.4.3 Recovery from Event Sequences.	1.10-46
1.10.4.4 Decommissioning	1.10-46
1.10.5 General References.	1.10-46
1.11 PLANS FOR RETRIEVAL AND ALTERNATE STORAGE OF RADIOACTIVE WASTES	1.11-1
1.11.1 Retrieval Plans	1.11-2
1.11.1.1 Operational Equipment and Processes	1.11-3
1.11.1.2 Identification of Design and Operational Conditions for Retrieval.	1.11-5
1.11.1.3 Compliance with Preclosure Performance Objectives	1.11-10
1.11.2 Alternate Storage Plans	1.11-11
1.11.2.1 Alternate Storage Facility Location.	1.11-11
1.11.2.2 Alternate Storage Facility Size and Operations.	1.11-12
1.11.2.3 Public and Repository Worker Safety	1.11-13
1.11.3 Retrieval Operations Schedule	1.11-13
1.11.4 General References.	1.11-13
1.12 PLANS FOR PERMANENT CLOSURE, DECONTAMINATION, AND DISMANTLEMENT OF SURFACE FACILITIES.	1.12-1
1.12.1 Design Considerations to Facilitate Permanent Closure and Dismantlement	1.12-2
1.12.2 Plans for Permanent Closure	1.12-3
1.12.3 Plans for Decontamination and Dismantlement of Surface Facilities	1.12-4

CONTENTS (Continued)

	Page
1.12.3.1 Facility Operating History	1.12-7
1.12.3.2 Facility Description	1.12-8
1.12.3.3 Radiological Status of the Facility.	1.12-8
1.12.3.4 Dose Modeling Evaluations.	1.12-12
1.12.3.5 Alternatives for Decontamination and Dismantlement	1.12-12
1.12.3.6 As Low As Is Reasonably Achievable Analyses.	1.12-13
1.12.3.7 Planned Decontamination and Dismantlement Activities	1.12-13
1.12.3.8 Project Management and Organization	1.12-16
1.12.3.9 Radiological Health and Safety Program during Decontamination and Dismantlement	1.12-18
1.12.3.10 Environmental Monitoring and Control Program	1.12-19
1.12.3.11 Low-Level Radioactive Waste Management Program	1.12-19
1.12.3.12 Quality Assurance Program.	1.12-21
1.12.3.13 Facility Radiation Surveys.	1.12-21
1.12.3.14 Development of a Decontamination and Dismantlement Plan	1.12-21
1.12.4 General References.	1.12-22
1.13 EQUIPMENT QUALIFICATION PROGRAM	1.13-1
1.13.1 Functions of the Equipment Qualification Program.	1.13-1
1.13.2 Equipment Qualification Program Requirements	1.13-2
1.13.2.1 Harsh and Mild Environments.	1.13-3
1.13.2.2 Equipment Qualification Records	1.13-4
1.13.2.3 Environmental Qualification Lists.	1.13-4
1.13.2.4 Testing and Analyses.	1.13-4
1.13.2.5 Procurement, Installation, Maintenance, Surveillance, and Monitoring	1.13-4
1.13.2.6 Corrective Action Program Evaluation	1.13-4
1.13.2.7 Equipment Qualification Margin.	1.13-5
1.13.3 Environmental Qualification Process.	1.13-5
1.13.3.1 Harsh Environment Qualification	1.13-5
1.13.3.2 Qualification Methods	1.13-5
1.13.3.3 Qualified Life	1.13-6
1.13.3.4 Environmental Qualification Documentation	1.13-7
1.13.4 Seismic Qualification Process	1.13-7
1.13.4.1 Methods	1.13-7
1.13.4.2 Acceptance Criteria	1.13-8
1.13.4.3 Process	1.13-8
1.13.4.4 Qualification Methods	1.13-8

CONTENTS (Continued)

	Page
1.13.4.5 Qualified Life	1.13-8
1.13.4.6 Seismic Qualification Documentation.....	1.13-9
1.13.5 General References	1.13-9
1.14 NUCLEAR CRITICALITY SAFETY.....	1.14-1
1.14.1 Nuclear Criticality Safety Organization and Administration.....	1.14-2
1.14.2 Nuclear Criticality Safety Technical Program.....	1.14-2
1.14.2.1 Nuclear Criticality Safety Requirements.....	1.14-3
1.14.2.2 Nuclear Criticality Analysis Process.....	1.14-3
1.14.2.3 Nuclear Criticality Safety Evaluation	1.14-6
1.14.2.4 Example of the Criticality Safety Analysis	1.14-31
1.14.3 Nuclear Criticality Safety Regulations, Codes, and Standards	1.14-35
1.14.3.1 Applicable Standards Documents	1.14-35
1.14.4 General References.....	1.14-36


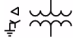



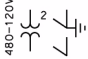


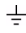

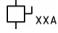

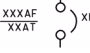


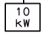


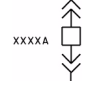




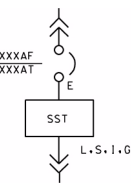




CHAPTER 1 ACRONYMS

ALARA	as low as is reasonably achievable
BWR	boiling water reactor
CCCF	Central Control Center Facility
CRCF	Canister Receipt and Closure Facility
DPC	dual-purpose canister
DBGM	design basis ground motion
DCMIS	digital control and management information system
DOE	U.S. Department of Energy
EBS	Engineered Barrier System
ECRB	Enhanced Characterization of the Repository Block
EDGF	Emergency Diesel Generator Facility
ESF	Exploratory Studies Facility
ES&H	Environmental, Safety and Health
FEP	feature, event, or process
GROA	geologic repository operations area
HAZOP	hazard and operability
HEPA	high-efficiency particulate air
HLW	high-level radioactive waste
HVAC	heating, ventilation, and air-conditioning
IHF	Initial Handling Facility
ITS	important to safety
ITWI	important to waste isolation
LLWF	Low-Level Waste Facility
MCO	multicanister overpack
MLD	master logic diagram
NRC	U.S. Nuclear Regulatory Commission
PCSA	preclosure safety analysis
PLC	programmable logic controller
PSHA	probabilistic seismic hazard analysis
PVHA	probabilistic volcanic hazard analysis
PWR	pressurized water reactor
RF	Receipt Facility

SNF	spent nuclear fuel
SSC	structure, system, or component
TAD	transportation, aging, and disposal
TEV	transport and emplacement vehicle
TSPA	total system performance assessment
WHF	Wet Handling Facility
WNNRF	Warehouse and Non-Nuclear Receipt Facility

SYMBOLS AND LEGENDS

Electrical Symbols

Single Line Diagrams	Single Line Diagrams (Continued)
 <p>Regulating transformer</p>	<p>Electric instrument/meter</p> <p>A = ammeter</p> <p>F = frequency meter</p> <p>VA = volt-ampere</p> <p>PF = power factor</p> <p>S = synchroscope</p> <p>VAR = reactive power</p> <p>V = volt meter</p> <p>W = watt meter</p>
 <p>Power transformer, delta-wye winding connection, solidly grounded</p>	
 <p>Potential transformer</p>	 <p>Space heater/heater element</p>
 <p>Potential transformer (PT) ratio, open delta-winding connection, and number of transformers</p>	 <p>Battery</p>
 <p>Current transformer: Number of current transformers, current transformer ratio, and polarity multiratio (MR)</p>	 <p>Ground</p>
 <p>Bushing-type current transformer Polarity marking</p>	 <p>Low-voltage disconnect switch</p>
 <p>Ground fault current transformer Current transformer ratio</p>	 <p>Molded case circuit breaker, amp frame, amp trip, and number of poles</p>
 <p>Diesel engine generator rating and grounding method</p>	 <p>Molded case circuit breaker, plug-in type, frame and trip</p>
 <p>Static or package load, kW or kVA, with rating</p>	 <p>Low-voltage air circuit breaker, drawout-type, frame and trip</p>
 <p>Synchronous motor HP</p>	 <p>Medium-voltage circuit breaker, drawout-type, continuous current rating</p>
 <p>DC motor, separately excited HP</p>	 <p>High-voltage circuit breaker, rating</p>
 <p>Wound rotor induction motor HP as shown</p>	<p>Power circuit breaker low-voltage drawout type, frame and trip with solid-state trip unit</p> <p>E = electrically operated</p> <p>M = manually operated</p> <p>(L) = long-time delay</p> <p>(S) = short-time delay</p> <p>(I) = instantaneous</p> <p>(G) = ground fault</p> <p>SST = solid-state trip unit</p>
 <p>Squirrel cage induction motor HP as shown</p>	
 <p>Diode</p>	
 <p>Battery charger</p>	
 <p>Rectifier</p>	
 <p>Inverter</p>	

Single Line Diagrams (Continued)



Medium-voltage, fused contactor, drawout-type with ratings



Current limiting fuse, rating



Fused load interruptor switch, medium-voltage ratings



Disconnect switch



Motor-operated disc switch



Capacitor



Selector switch; number of positions shown



Lightning arrestor



Surge arrestor, rating



Automatic transfer switch



Manual transfer switch



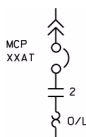
Uninterruptible power supply (UPS) maintenance bypass switch (make before break)



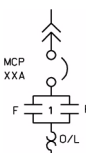
Grounding resistor
Rating



DC shunt
Rating

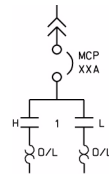


Combination motor starter, full voltage, nonreversing, plug-in type, contactor size, motor circuit protector rating and overload



Combination motor starter, full voltage, reversing, plug-in type, contactor size, motor circuit protector rating and thermal overload

Single Line Diagrams (Continued)



Combination motor starter, two speed, plug-in type, contactor size, motor circuit protector rating and thermal overloads



Transducer
A = current
V = volt
W = watt



Switch
AS = ammeter
VS = voltmeter
CS = control
SS = synchronizing
TS = test



Adjustable speed drive



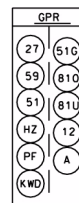
Rotary switch



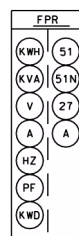
Motor thermal overload device



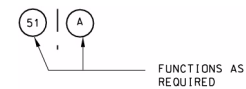
Relay
ANSI device number



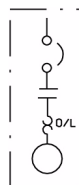
Solid state generator protection relay



Multifunction relay/metering
MPR/FPR/TPR/GPR

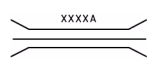


MPR = motor protection relay
FPR = feeder protection relay
TPR = transformer protection relay
GPR = generator protection relay



Package equipment (motor-starting device supplied by vendor)

Single Line Diagrams (Continued)



Bus duct
Rating



480 V welding receptacle

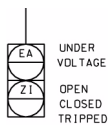


480 V power receptacle



Interlock
E = electrical
K = Kirk-key type
M = manual

Instrumentation



Digital control and management information system (DCMIS) communication input (not limited to functions indicated)
EA = voltage alarm
ZI = position indication



DCMIS control or monitoring function
XA = alarm

Schematic Diagrams



Operating coil
M = motor starter
CR = control relay
TD = timer, delay
C = contactor
SV = valve solenoid



Electronic relay (programmable logic controller (PLC)/data control system (DCS) input)



Electronic output (i.e., TRIAC)



Normally open contact
Operating coil designation



Normally closed contact
Operating coil designation



Open contact, time-delay close after coil is energized
Operating coil designation



Closed contact, time-delay open after coil is energized
Operating coil designation

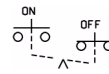


Push button, normally open, momentary contact

Schematic Diagrams (Continued)



Push button, normally closed, momentary contact



Maintained on-off push button



Limit switch, normally open



Limit switch, normally closed



Liquid level switch, normally open; closes on rising level



Liquid level switch, normally closed; opens on rising level



Pressure switch, normally open; closes on rising pressure



Pressure switch, normally closed; opens on rising pressure



Flow switch, normally open; closes on increasing flow



Flow switch, normally closed; opens on increasing flow



Torque switch, normally closed; opens on increasing torque



Torque switch, normally open; closes on increasing torque



Switch (general)
Single pole, single throw (SPST)



Switch (general)
Single pole, double throw (SPDT)



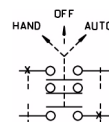
Temperature switch, normally open; closes on rising temperature



Temperature switch, normally closed; opens on rising temperature

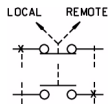


Cable shield
2-conductor cable with shield grounded shown, quantity or number of conductors



Hand-Off-Auto
Three-position selector switch

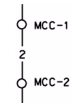
Schematic Diagrams (Continued)



Local-Remote
Two-position selector switch



Mushroom head push button,
two-position, maintained contact
Pull to reset



Pulled wire between locations
(motor control center (MCC)-1 and
MCC-2)
Wire number



Jumper wire between two cubicles
(MCC-2-1 and MCC-2-2)
Jumper number



Alarm, annunciation



Indicating light
A = amber
G = green
R = red
W = white



Alarm horn

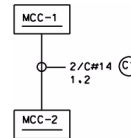
Schematic Diagrams (Continued)



Circuit terminal (for MCC,
switchgear (SWGR), or load center
(LC)) (external terminal—wired to
an interfacing terminal block and
available for external wiring)



Circuit terminal (internal terminal—
not wired to interfacing terminal
block and may not be available for
external wiring)



Block diagram
“from” and “to” locations
Cable size and cable identification
with wire numbers



Male contact


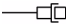



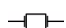
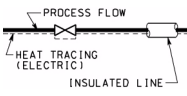
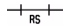
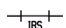


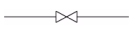

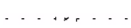

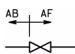

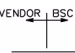










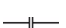










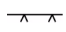
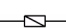
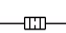
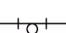


Female contact


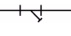
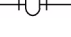

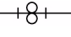





Separable connectors

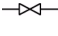



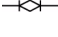

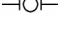

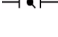

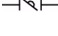
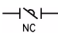
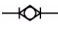

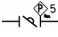



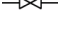
Mechanical Symbols

Process Flow		Connections (Continued)	
	Main process flow		Mechanical coupling
	Secondary process flow		Hose connection
	Flex hose		Shear spool
	Example of process flow		Removable spool
Construction Status			Insulating removable spool
	New		Open drain hub
	Existing		Manway (manhole)
	Future	Inline Items	
Specification Break/Boundaries			Expansion joint
	System change		Inline mixing tee
	BSC-vendor interface		Inline mixer
	Multiple changes can be grouped together. Values shown only for example (aboveground and underground, piping material)		Loop seal or P-trap
	Safety and seismic boundary flag (example shown as "non-ITS")		T-type strainer
Connections			Downward slope
	Flexible connection		Upward slope
	Blind flange		Flame arrestor
	Flanges, insulating flanges (IF)/dielectric union (DU)		Water hammer arrester
	Circular/hammer blind		Desiccant dryer
	Spectacle blind (open)		Atmospheric (J hook) vent
	Spectacle blind (closed)		Atmospheric (J hook) vent with bird screen (accessory when vendor supplied)
	Blind spacer		Atmospheric vent
	Dry break connection		Spray header (two heads shown)
			Strainer
			Screen-type strainer
			Automatic self-cleaning strainer


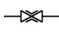
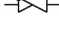
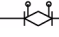
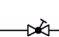




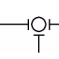
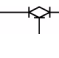
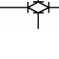
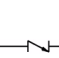
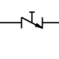
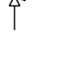


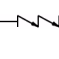


Inline Items (Continued)

	Refrigerant strainer
	Y-type strainer
	Basket strainer
	Breather
	Double basket strainer
	Steam trap
	Vent silencer
	Inline silencer

Valve Symbols

	Gate valve (open)
	Gate valve (closed)
	Globe valve (open)
	Globe valve (closed)
	Plug valve (open)
	Plug valve (closed)
	Ball valve (open)
	Ball valve (closed)
	Butterfly valve (open)
	Butterfly valve (closed)
	Rotating disc butterfly valve (open)
	Rotating disc butterfly valve (closed)
	Orbit valve (open)
	Orbit valve (closed)
	Preferred pressure end
	Throttle ("L" used when locked in throttling position)
	Needle valve (open)
	Needle valve (closed)
	Diaphragm

Valve Symbols (Continued)

	Knife gate valve
	Pinch valve
	Triple duty valve
	Circuit setter (balancing)
	Y-pattern globe (where only Y-pattern is acceptable)
	Globe valve packless
	Angle gate valve
	Angle globe valve—manual
	Three-way valve
	Three-way ball valve
	Three-way plug valve
	Four-way plug valve
	Hose valve
	Check valve
	Stop check valve
	Angle stop check
	Wafer check
	Combined recirculation and check valve
	Flow limiting check
	Backflow preventer

Actuator

G = gear (shown)

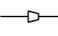
A = air wrench

CH = chain

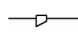
X = extension stem

S = special type

Reducer/Increases

	Concentric diameter change
---	----------------------------

Reducer/Increasesers (Continued)

 Eccentric diameter change

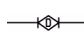
Caps

 Welded cap

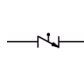
 Screwed cap

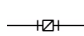
 Breather cap

Fire and Safety

 Deluge valve

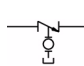
 Preaction valve


 Alarm check valve with retard chamber

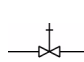
 Dry pipe valve


 Ball drip valve


 Siamese connection

 Check valve with integral automatic drain ball drip valve

 Post indicator valve

 Outside screw and yoke (OS&Y) valve


 Fire hydrant with key valve

 Fire hydrant with hose house

 Hose reel


 Hose rack

 Spray nozzles

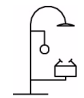
 Sprinkler heads

 Foam injector

 Eye wash

 Safety shower

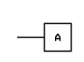
Fire and Safety (Continued)

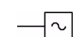
 Eye wash and safety shower

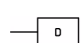
 Automatic air relief valve

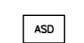
Drivers and Connectors

 Electric motor

 Air motor (separate from driver unit)

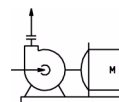
 Electric generator


 Diesel engine

 Adjustable speed drive (ASD) unit

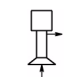
Pumps

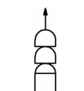
 Hand pump

 Centrifugal pump (shown horizontal with motor)

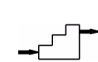
 Sump or dry pit vertical pump


 Diaphragm pump

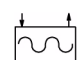
 Vertical wet pit pump

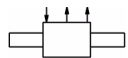
 Submersible vertical pump (stages may vary; three shown)

 Air diaphragm pump

 Positive displacement or metering pump

 Vertical inline pump

 Rotary screw pump

Pumps (Continued)

Boiler feed pump (barrel)



Vacuum pump



Gear pump



Screw pump



Reciprocating pump

Compressors

Air compressor package



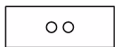
Vertical inline centrifugal compressor



Centrifugal compressor



Reciprocating compressor



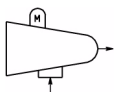
Rotary compressor



Rotary screw service air compressor



Screw compressor



Vapor compressor



Liquid seal

Liquid Separation Equipment

Waste water separator



Skimmer



Floating skimmer

Mixing Components

Propeller



Dust collector

Equipment Filters

Air intake filter



Inlet air filter with hood



Centridge or bag filter



Plate filter



Packed filter



Solid/liquid filter



Solid/gas filter

Tanks

Pressure vessels (vertical shown) or horizontal (e.g., tanks, receivers, dryers, separators)

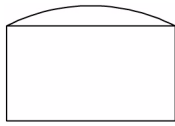


Pressurized gas bottle

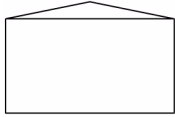
Storage Tanks

Open top tank

Storage Tanks (Continued)



Dome roof tank

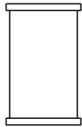


Cone fixed roof tank

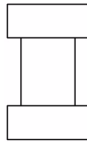


Flat roof tank

Waste Forms

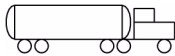


Waste package

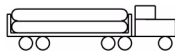


Transportation cask with impact limiters

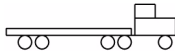
Transportation Equipment



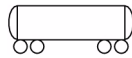
Liquid tanker truck



Gaseous tube tanker truck



Flatbed truck



Railcar



Flatbed railcar

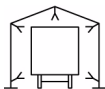


Muck rail cart



55 gal drum

Vehicle Cleaning



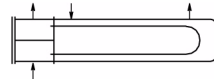
Railcar wash station

Vehicle Cleaning (Continued)

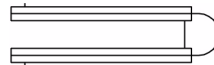


Truck wash station

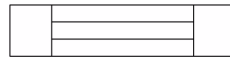
Heat Exchangers



U-tube heat exchanger



Double pipe exchanger



Straight tube heat exchanger



Coil exchanger

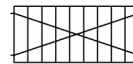
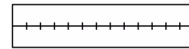


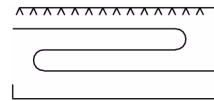
Plate-type heat exchanger



Sample cooler



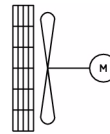
Finned tube exchanger/vaporizer



Spray cooler exchanger



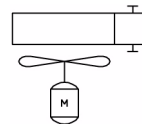
Oil cooler



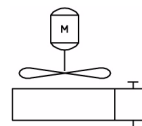
Induced draft cooler with straight coil



Air cooler

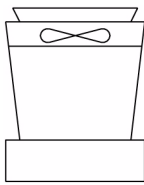


Forced draft air cooler

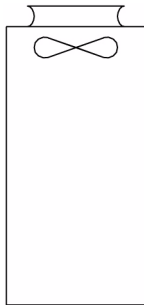


Induced draft air cooler

Heat Exchangers (Continued)

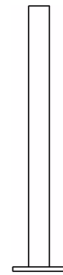


Mechanical draft cooling tower

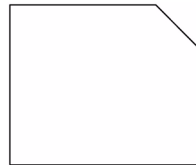


Cooling tower package

Heating and Cooling Element (Continued)

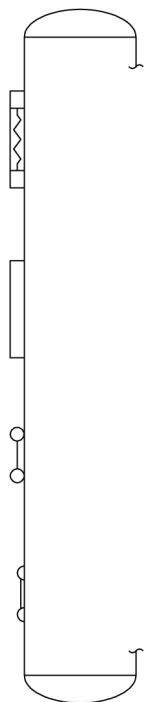


Self-supporting stack

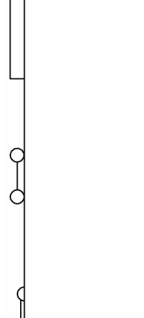


Boiler

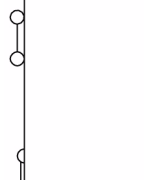
Heating and Cooling Element



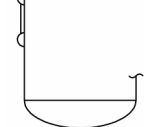
Electric jacket



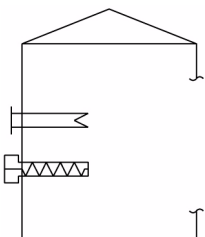
Jacket



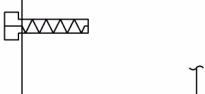
Full coil



Half coil

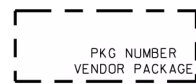


Internal heating coil



Electric bayonet

Definitions of Boundary Line Types



Vendor system break. Placed around piping and/or equipment to show scope of vendor responsibility



Generic black box. Used to show packaged systems or equipment (both BSC and vendor)



Building or facility boundary. Used to represent building limits.

Duct and Line Work



Ducted air flow



Cascade air movement (nonducted)



Direction of flow arrow



Flow arrow (from inleakage/outleakage)



Flow arrow ducted supply (room details)



Flow arrow ducted exhaust (room details)



Long line break flag

Louvers



Fixed louver

Louvers (Continued)



Adjustable louver



Security bars (large shown)

Air Devices



Tornado damper



Back draft damper



Opposed blade damper



Parallel blade damper, regulator



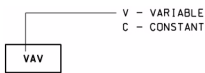
Slide gate damper



Butterfly damper



Sound attenuator



Variable air volume



Moisture separator/demister



Low efficiency prefilter (25%–35% efficiency)



Medium efficiency roughing filter, cartridge type (65%–90% efficiency). Used before high efficiency particulate air (HEPA) filter



High efficiency filter (80%–95% efficiency) cartridge type or bag type. Used in air handling unit



HEPA filter (99.97% efficiency).

Air Devices (Continued)



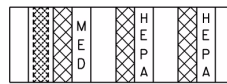
Humidifier or spray



Charcoal filter (if required)

NOTE: Blade configurations shown in graphic representations of air devices are not depictions of actual configurations.

Filter Plenum

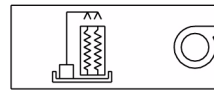


Filter plenum

Air Handling Equipment



Air handling unit (AHU)



AHU with evaporative cooler



Air-cooled condensing unit

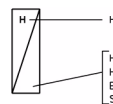


Air-cooled chiller

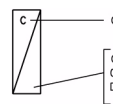


Air ejector

Coils

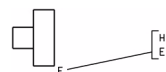


H = heating coil (shown)
HW = hot water
HR = heat recovery
E = electric
S = steam










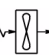


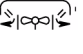
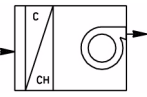
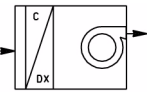
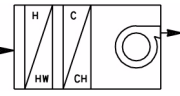
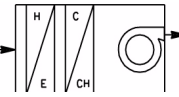
C = cooling coil (shown)
CH = chilled water
CW = cooling water
DX = refrigerant direct expansion

Unit Heaters

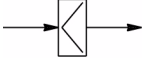
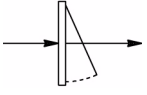


Unit heater
HW = hot water
E = electric (shown)

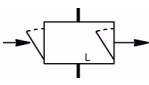
Fans and Blowers

	Centrifugal blower
	Centrifugal fan
	Centrifugal fan with inlet vanes
	Rotary fan
	Vane axial fan
	Centrifugal inline fan
	Plug fan/plenum fan
	Axial fan
	Propeller
	Centrifugal roof exhaust fan
	Axial fan (roof or wall mount)
	Fan coil unit (FCU) with chilled water (CH) cooling coil
	FCU with refrigerant direct expansion (DX) cooling coil
	FCU with hot water (HW) heating and chilled water (CH) cooling coil
	FCU with electric (E) heating and chilled water (CH) cooling coil

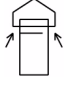
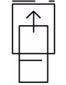
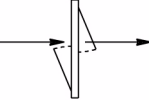
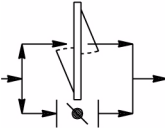
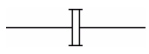
Subsurface Symbology

	Air duct backflow preventer
	Access hatch/emergency egress door



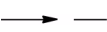
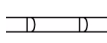
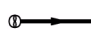
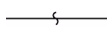
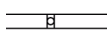
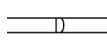


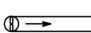
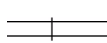

Subsurface Symbology (Continued)

	Isolation barrier with emergency egress door L = locked isolation barrier with restricted access door
--	--

Exhaust and Intake Hood

	Intake hood with bird screen
	Stacked head with bird screen
	Access door
	Emplacement access door with butterfly damper regulator
	Bulkhead seal

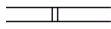

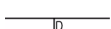
Subsurface Ventilation Components

	Airflow (intake)
	Airflow (return)
	Airflow (leakage)
	Airlock (double-door system)
	Auxiliary fan and vent pipe or tubing
	Brattice
	Box check
	Door
	Escapeway with direction of escape
	Escapeway with direction of escape opposite to airflow
	Fan with flow direction indicated
	Fire door (normally open)
	Regulator

Subsurface Ventilation Components (Continued)








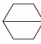

- Ⓢ Self-contained self-rescuer cache location
- Ⓣ Shaft with downcast flow of air
- ⓐ Shaft with upcast flow of air

Subsurface Ventilation Components (Continued)




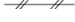


-  Stopping (permanent impermeable)
-  Stopping (temporary impermeable)
-  Stopping (temporary impermeable with small door)

Instrumentation Symbols


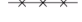

General Instruments

	Instrument for single measured variable. Instrument is field mounted. "XX" is instrument function identification (general to all.)
	Instrument for single measured variable, performing two functions, or instrument for two measured variables
	Central Control Center/facility operations room panel, front-mounted instrument. Location of panel identified outside of instrument circle.
	Field panel front mounted instrument
	Central Control Center shared control, shared display function, accessible to the operator
	Facility operations room shared control, shared display function, normally accessible to the operator
	Programmable logic function, normally accessible to the operator
	Data acquisition function accessible to the operator at primary location
	Pilot light

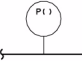
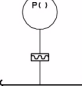
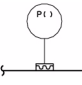
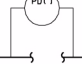
Signals and Lines

	Connection to process or mechanical link, or instrument input supply
	Electrical signal (hardwired)
	Internal system link (software, datalink)
	Pneumatic signal
	Electromagnetic or sonic signal (guided)
	Electromagnetic or sonic signal (unguided)


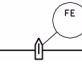

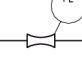



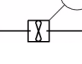
Signals and Lines (Continued)

	Hydraulic signal
	Capillary tubing (filled system)
	Mechanical link

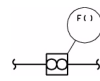

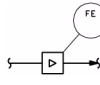
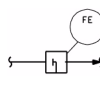
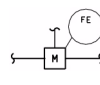
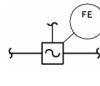
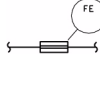

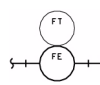
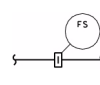
Pressure Sensors

	Direct connected pressure sensor
	Pressure sensor with diaphragm seal, piped
	Pressure sensor with diaphragm seal, line saddle or equipment mounted
	Direct-connected, differential pressure sensor


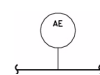
Flow Sensors

	Flow sensor FE = orifice plate for measurement FO = restriction orifice
	Flow sensor with orifice plate in quick-change fitting
	Flow nozzle
	Venturi/flow tube
	Single-port pitot or pitot-venturi tube
	Averaging pitot tube
	Flume
	Turbine or propeller

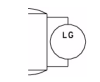
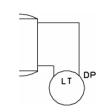
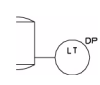
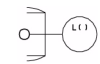
Flow Sensors (Continued)

	Positive displacement
	Variable area flowmeter
	Vortex
	Target
	Magnetic flowmeter
	Sonic flowmeter
	Flow straightening vanes
	Flow sight glass, plain or with paddle wheel, etc.
	Integral flow orifice
	Flow switch

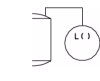
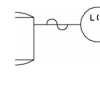
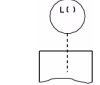
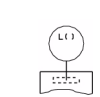
Analysis Sensors

	Flow-through type
	Nonflow-through type

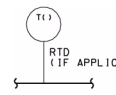
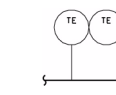
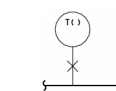
Level Sensors

	Gage glass or float or displacement-type level instrument
	Differential pressure-- (pressurized tank)
	Differential pressure-- (atmospheric tank)
	Internal ball-float type






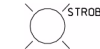
Level Sensors (Continued)

	Gage board type
	Electromagnetic or sonic (guided) type
	Capacitance or dielectric type
	Paddle or lever


Temperature Sensors

	TI = bimetallic thermometer TW = thermowell (not shown separately if associated with a primary element) TE = temperature element (e.g., thermocouple, RTD (resistance temperature detector))
	Dual or duplex temperature elements in one well when both elements are connected to instruments
	Filled system

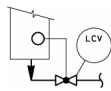
Fire Protection/Suppression

	System actuation panel
	Facility fire alarm panel
	Main fire alarm panel
	Horn
	Manual fire alarm
	Strobe light

Self-Actuated Flow Devices

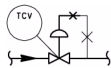
	Self-contained flow regulator
---	-------------------------------

Self-Actuated Level Devices



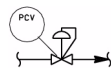
Level regulator, with mechanical linkage

Self-Actuated Temperature Devices

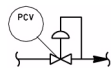


Temperature regulator (filled-system type)

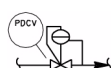
Self-Actuated Pressure Devices



Pressure-reducing regulator, self contained



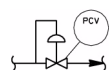
Pressure-reducing regulator with external pressure tap



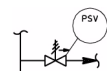
Differential pressure-reducing regulator with internal and external pressure taps



Backpressure regulator, self-contained



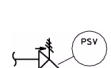
Backpressure regulator with external pressure tap



Pressure relief or safety valve, straight-through pattern, spring or weight loaded, or with integral pilot



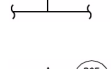
Pressure relief or safety valve general symbol



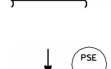
Vacuum relief valve general symbol



Pressure and vacuum safety relief valve

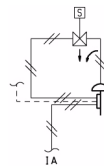


Pressure relief rupture disk or safety head for pressure relief



Pressure relief rupture disk or safety head for vacuum relief

Valve/Damper Actuators



Spring-opposed diaphragm (shown with positioner and overriding pilot valve)



Pressure-balanced diaphragm



Rotary motor (on/off) (shown typically with electric signal; may be hydraulic or pneumatic)



Rotary motor (modulating)



Pneumatic cylinder, single-acting



Pneumatic cylinder, double-acting



Single-acting cylinder assembled with actuating pilot valve



Pneumatic cylinder, double-acting, with pilot valve



Single solenoid reset after latch (optional). A double solenoid is shown with two single solenoids.



Electrohydraulic



Hand actuator mounted top, side, or bottom of valve or actuator

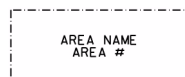


Unclassified (type of actuator written next to the symbol)

HVAC System Room/Area Boundary


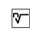


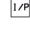
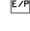





Room boundary within facility


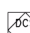


Area definition within room or facility

Miscellaneous Devices Symbols

	Volume booster (shown)
	Root extractor
	High selector
	Low selector
	Current to pneumatic converter
	Voltage to pneumatic converter
	Current to current converter
	Difference
	Average

Interlocks

	Hardwired interlock
	DCMIS logic interlock

Interlocks (Continued)

	PLC logic interlock
---	---------------------

Pneumatic Purge Devices

Purge device (means of regulating purge may be shown in place of the symbol); purge fluid and power supplies are:

- AS = air supply
- GS = gas supply
- HS = hydraulic fluid supply
- NS = nitrogen supply
- SS = steam supply
- WS = water supply



Function Blocks









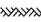


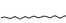
Function blocks—The description of the function of the relay, converter or computer “Y” may be shown outside the instrument circle, except when used with distinctive symbols such as a solenoid valve.



Instrument Function Identification		Instrument Function Identification (Continued)	
Measured or Initiating Variable	First Letters ()	Function	Succeeding Letters
Analysis ^a	A	Sensing device primary element	()E
Burner/Combustion	B	Sensing device transmitter, blind	()T
Conductivity	C	Sensing device transmitter, indicating	()IT
Density (Mass)	D	Display device indicator	()I
Voltage (EMF (electromotive force))	E	Display device recorder	()R
Flow	F	Display device integrator	()O
Flow ratio	FF	Display device alarm ^a	()A
Gaging (Dimensional)	G	Control device control station, manual/auto	()K
Hand (Manual)	H	Control device controller, blind	()C
Current	I	Control device controller, indicating	()IC
Power	J	Control device controller, recording	()RC
Time	K	Control device controller, pressure relief or safety valve	PSV
Level	L	Control device, control valve or damper	()V
Moisture	M	Control device, self-actuating, control valve	()CV
Video	N	Control device, other final control element	()Z
Pressure/vacuum	P	Control device switch ^a	()S
Pressure differential	PD	Well or probe	()W
Quantity	Q	Local observation glass	()G
Radiation	R	Light	()L
Speed or frequency	S	Test point connection	()P
Temperature	T	Relay, computing device	()Y
Temperature differential	TD	User choice	()O
Multivariable	U	Unclassified	()X
Vibration	V		
Weight	W		
Event/state	Y		
Position ^b	Z		

NOTE: ^aTerm placed outside of instrument circle denotes specific variable being analyzed.
^bSwitch conventions include, but are not limited to the following: ZSH = engaged, raised, extended, forward slowdown/stop, forward/stop, upper limit, unlocked, forward travel limit, counterclockwise, vertical; and ZSL = disengaged, lowered, retracted, reverse slowdown/stop, reverse/stop, lower limit, locked, reverse travel limit, clockwise, horizontal.
^dHIGH-HIGH-HIGH, HIGH-HIGH, HIGH, LOW, LOW-LOW, and LOW-LOW-LOW alarms or switches are designated by the modifying letters "HHH," "HH," "H," "L," "LL," "LLL." Letters may be placed outside the instrument circle or shared control, shared display functions.



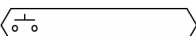
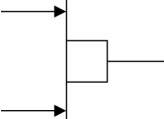
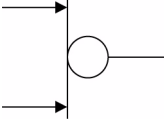
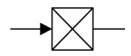
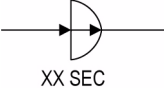

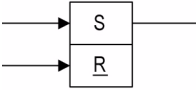

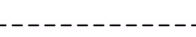
Structural Symbols

Structural		Structural (Continued)	
	Direction of grating span		Metal decking (section)
	Checkered plate		Direction of metal deck span
	Concrete		Work point
	Compacted soil		Opening
	Grade		Slab depression
	Handrail		Construction joint




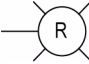

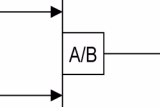
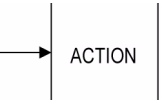
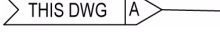


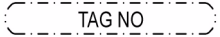
Digital Logic and Functional Control Diagram Symbols

NOTE: DCMIS and associated symbols and legends are non-ITS and non-ITWI. DCMIS and PLC hardwired input and output point names follow as closely to actual physical device tags as possible. Internal point names are based on hardwired input and output point names as closely as possible. Multiple inputs and outputs associated with the same device are named using the same loop number, with the function code identifying the particular point. No dash, space, or underbar characters are included in the DCMIS or PLC point name. It is a direct concatenation of the area code, system designator, function, loop number, loop number suffix, and component suffix. However, the loop number is padded with preceding zeros so that it is always four characters long. Some of the characters used as modifiers in the function codes are not actual ISA letters; for example, "S" for "START." Since no ISA equivalent is available, they have been assigned for clarity and consistency.

Logic and Control Symbols

	DCMIS momentary handswitch
	DCMIS maintained handswitch
	DCMIS handswitch datalink output to PLC (momentary shown)
	And: Output exists only when all inputs exist
	Or: Output exists only when one or more inputs exist
	Not: Output exists only when input does not exist
	On Delay: Output exists only when input has been continuously present for a preset time (XX sec) and remains present
	Off Delay: Output exists only when input exists and for a preset time (XX sec) after the input does not exist
	Memory: Set output exists only when set input exists (even momentarily) and continues until the reset input exists. Underline indicates which input overrides.
	Denotes standard logic algorithm (software)
	Denotes boundary between hardwired logic and software logic

Logic and Control Symbols (Continued)

	DCMIS alarm message on HMI console
	DCMIS indication on HMI console, such as a status indication or message
	Input to an annunciator separate from the DCMIS
	Hardwired indicator light: R = Red G = Green W = White A = Amber Y = Yellow
	Pulse or One Shot: The presence of a logic input, regardless of its subsequent state, causes logic output to exist immediately. Output exists for a preset time (XX sec) and then terminates
	Coincidence Matrix: Output exists only when "A" out of "B" inputs exist
	Action statement to describe logic output action such as stop, start, open, close, energize, etc.
	Continuation from/to point :A: on same logic drawing
	DCMIS input/output
	PLC input/output
	DCMIS software point not developed on the logic drawing

Logic and Control Symbols (Continued)

TAG NO	PLC software point not developed on the logic drawing
DCMIS DATALINK	Datalink output from PLC to DCMIS
OPEN (START) (DEFAULT 0)	Commands that require open or start permissives to be present in order for a command signal to open or start the device. Inputs to this block are process requirements that require the device to open or start provided that all of the permissives are met. If no logic open or start commands are required, then a zero is used as the default for the block. ^a
OPEN (START) PERMISSIVES (DEFAULT 1)	Logic permissives developed from process requirements are inputs to this block. If no logic permissives are required, then a one is used as the default for the block. ^a
OVERRIDE OPEN (START) (DEFAULT 0)	Commands that automatically bypass the logic to open or start the device. If no logic override commands are required, then a zero is used as the default for the block. ^a
CLOSE (STOP) (DEFAULT 0)	Commands that require the close or stop permissives to be present in order for a command signal to close or stop the device. Inputs to this block are process requirements that require the device to close or stop provided that all of the permissives are met. If no logic close commands are required, then a zero is used as the default for the block. ^b
CLOSE (STOP) PERMISSIVE (DEFAULT 1)	Logic permissives developed from process requirements are inputs to this block. If no logic permissives are required, then a one is used as the default for the block. ^b
OVERRIDE CLOSE (STOP) (DEFAULT 0)	Commands that automatically bypass the logic to close or stop the device. If no logic override commands are required, then a zero is used as the default for the block. ^b
OPEN FEEDBACK	Logic input for the switch is set up for a device with a fully open limit (position) switch. ^a
CLOSED FEEDBACK	Logic input for the switch is set up for a device with a fully closed limit (position) switch. ^b

Logic and Control Symbols (Continued)

RUNNING FEEDBACK	Logic input is set up for a motor running position. When a motor not running position is present. The input will need to be “inverted” (by adding a “not” function after the input).
NOT HIGH TORQUE	Logic input is set up to accept a normally closed contact opening on high closing torque switch.
AUTO OPEN (START) (DEFAULT 0)	Commands that require the open or start permissives to be present and the device to be in auto mode in order for a command signal to open or start the device. Inputs to the block are process requirements that require the device to open or start provided that all of the permissives are met. ^a
AUTO CLOSE (STOP) (DEFAULT 0)	Commands that require the close or stop permissives to be present and the device to be in auto mode in order for a command signal to close or stop the device. Inputs to this block are process requirements that require the device to close or stop provided that all of the permissives are met. ^b
START COMMAND	Logic point provided for DCMIS/PLC output to energize a relay to start the device. ^a
STOP COMMAND	Logic point provided for DCMIS/PLC output to stop the device. ^b
OPEN COMMAND	Logic point provided for DCMIS/PLC output to energize either a solenoid or relay to open the device. ^a
CLOSE COMMAND	Logic point provided for DCMIS/PLC output to energize either a solenoid or relay to close the device. ^b

NOTE: ^aThe open (start) inputs, feedback, and outputs could also represent other actions. For example: Engage; Raise; Extend; Unlock; Forward; Rotate CCW; and Vertical.

DCMIS and associated symbols and legends are non-ITS and non-ITWI.

^bThe close (stop) inputs, feedback, and outputs could also represent other actions. For example: disengage; lower; retract; lock; reverse; rotate clockwise; and horizontal.

Typical DCMIS/PLC Point Name

UUUSSSSXXXXX####YZ (18 character maximum)

UUU Area code

SSSS System designator

Typical DCMIS/PLC Point Name (Continued)

XXXXX Function, see extra codes below

Loop number

Y Loop number suffix (if required)

Z Component suffix (if required)

Hardwired Digital Inputs

Function ^a	Description	Onestate	Zerostate
HS	Handswitch (various functions) (used for single-function switches, e.g., pushbutton)	FUNCTION	NA
HSO	Open handswitch position ^b	OPEN	NA
HSC	Close handswitch position ^b	CLOSE	NA
HSS	Start handswitch position	START	NA
HSP	Stop handswitch position	STOP	NA
HSR	Remote handswitch position	REMOTE	NA
HSL	Local handswitch position	LOCAL	NA
HSA	Auto handswitch position	AUTO	NA
LSH	Level switch high	NORMAL	ALARM
LSHH	Level switch high high	NORMAL	ALARM
LSHHH	Level switch high high high	NORMAL	ALARM
LSL	Level switch low	NORMAL	ALARM
LSLL	Level switch low low	NORMAL	ALARM
LSLLL	Level switch low low low	NORMAL	ALARM
PSH	Pressure switch high	NORMAL	ALARM
PSHH	Pressure switch high high	NORMAL	ALARM
PSHHH	Pressure switch high high high	NORMAL	ALARM
PSL	Pressure switch low	NORMAL	ALARM
PSLL	Pressure switch low low	NORMAL	ALARM
PSLLL	Pressure switch low low low	NORMAL	ALARM
VSH	Vibration switch high	NORMAL	ALARM
VSHH	Vibration switch high high	NORMAL	ALARM
VSHHH	Vibration switch high high high	NORMAL	ALARM
XA	Trouble alarm	NORMAL	TROUBL
YIR	Motor running indicationg	RUNNG	STOPPD
YIH	Motor running high speed	RUNNG	NRUN
YIL	Motor running low speed	RUNNG	NRUN
ZSH	Position switch/breaker open ^c	OPEN	NOPEL
ZSL	Position switch/breaker closed ^c	CLOSED	NCLOSD

NOTE: ^aSome of the characters used as modifiers in the function codes are not actual ISA letters; for example “S” for “START.” Since no ISA equivalent is available, they have been assigned for clarity and consistency.

^bThe OPEN/CLOSE functions could also represent other actions. For example: ENGAGED/DISENGAGE; FWD/REV; RAISE/LOWER; UNLOCK/LOCK; EXTEND/RETRACT; and ROTATE CCW/ROTATE CW.

^cSwitch conventions include, but are not limited to the following: ZSH—ENGAGED, RAISED, EXTENDED, FWD SLOWDOWN/STOP, UPPER LIMIT, UNLOCKED, FWD TRAVEL LIMIT, COUNTERCLOCKWISE, VERTICAL and ZSL—DISENGAGED, LOWERED, RETRACTED, REV SLOWDOWN/STOP, REV/STOP, LOWER LIMIT, LOCKED, REV TRAVEL LIMIT, CLOCKWISE, HORIZONTAL.

NA = not applicable

Hardwired Digital Outputs

Function ^a	Description	Onestate	Zerostate
JYO	Power relay/solenoid energize to open ^b	OPEN	NOPEN
JYC	Power relay/solenoid energize to close ^b	CLOSE	NCLOSE
JYH	Power relay start high speed	RUN	NRUN
JYL	Power relay start low speed	RUN	NRUN
JYS	Power relay start or start/stop command	START	NSTART
JYP	Power relay stop command	STOP	NSTOP

NOTE: ^aSome of the characters used as modifiers in the function codes are not actual ISA letters; for example “S” for “START.” Since no ISA equivalent is available, they have been assigned for clarity and consistency.

^bThe OPEN/CLOSE functions could also represent other actions. For example: ENGAGED/DISENGAGE; FWD/REV; RAISE/LOWER; UNLOCK/LOCK; EXTEND/RETRACT; and ROTATE CCW/ROTATE CW.

Example DCMIS/PLC Points Naming Convention

First Letter (Process Variable)	Succeeding Letters (Function IDs and Modifiers)				
	S ^a	A ^b	T ^c	I ^d	V ^e
F	SL	AL	T	I	V
L	SLL	ALL			
	SLLL	ALLL			
P	SH	AH			
	SHH	AHH			
T	SHHH	AHHH			

NOTE: ^aThe “S” function points are either hardwired points or soft event points. Generally these points are multifunction, used for control, interlock, and/or alarm.

^bThe “A” represents internal alarms which are generated from analog input signals or logic.

^cThe “T” is a hardwired analog input point and is maintained throughout the DCMIS/PLC data highway unless the value is modified in the DCMIS/PLC logic, then it typically becomes an “I” point.

^dThe “I” represents a computed analog value or a modified (compensated) analog input point “T”

^eThe “V” represents an analog output point, typically associated with the modulating control valve or damper (for example, FV, LV, PV, TV, etc.).

GLOSSARY

aging. Placing commercial spent nuclear fuel in an aging overpack on an aging pad for a long period of time (years) for radioactive decay. Radioactive decay results in a cooler waste form that ensures thermal limits are met.

barrier. Any material, structure, or feature that, for a period to be determined by the NRC, prevents or substantially reduces the rate of movement of water or radionuclides from the Yucca Mountain repository to the accessible environment, or prevents the release of radionuclides from the waste. For preclosure safety considerations, a barrier is any device or measure that decreases the likelihood of occurrence or adverse effects of a threat to safety or quality.

buffer. Short-term holding area for loaded or unloaded transportation casks prior to movement into a handling facility for processing or prior to removal from the geologic repository operations area.

confinement. A building, building space, room, cell, or other enclosed volume in which air supply and exhaust are controlled, and typically filtered.

containment. A leak-tight enclosure designed to prevent fission products from escaping to the atmosphere.

controlled access area. Any temporarily or permanently established area, which is clearly demarcated, to which access is controlled and that affords isolation of the material or persons within it.

event sequence. A series of actions and/or occurrences within the natural and engineered components of a geologic repository operations area that could potentially lead to exposure of individuals to radiation. An event sequence includes one or more initiating events and associated combinations of repository system component failures, including those produced by the action or inaction of operating personnel. Those event sequences that are expected to occur one or more times before permanent closure of the geologic repository operations area are referred to as Category 1 event sequences. Other event sequences that have at least one chance in 10,000 of occurring before permanent closure are referred to as Category 2 event sequences.

feature. A physical, chemical, thermal, or temporal characteristic of the site or potential repository system. For the purposes of screening features, events, and processes for the total system performance assessment, a feature is defined to be an object, structure, or condition that has a potential to affect repository system performance.

geologic repository operations area. A HLW facility that is part of a geologic repository, including both surface and subsurface areas, where waste handling activities are conducted.

important to safety. With reference to structures, systems, and components, those engineered features of the geologic repository operations area whose function is: (1) to provide reasonable assurance that HLW can be received, handled, packaged, stored, emplaced, and retrieved without exceeding the requirements of 10 CFR 63.111(b)(1) for Category 1 event sequences; or (2) to prevent or mitigate Category 2 event sequences that could result in radiological exposures exceeding the values specified at 10 CFR 63.111(b)(2) to any individual located on or beyond any point on the boundary of the site.

important to waste isolation. With reference to design of the Engineered Barrier System and characterization of natural barriers, those natural and engineered barriers whose function is to provide a reasonable expectation that HLW can be disposed of without exceeding the requirements of 10 CFR 63.113(b) and (c).

initiating event. A natural or human-induced event that causes an event sequence.

land ownership area. Lands that are either acquired lands under the jurisdiction and control of the DOE or lands permanently withdrawn and reserved for its use.

licensing bases. The set of NRC requirements applicable to the Yucca Mountain site and the licensee's written commitments for ensuring compliance with and operation within applicable NRC requirements and the Yucca Mountain site design basis (including all modifications and additions to such commitments over the life of the license) that are docketed and in effect. The licensing bases include the NRC regulations, orders, license conditions, exemptions, and license specifications. It also includes the Yucca Mountain site design basis information defined in 10 CFR 63.2 as documented in the most recent SAR as required by 10 CFR 63.21, 63.24, or 63.44 and the licensee's commitments remaining in effect that were made in docketed licensing correspondence such as licensee responses to NRC bulletins, generic letters, and enforcement actions, as well as licensee commitments documented in NRC safety evaluations or licensee event reports.

license condition. Any requirement or restriction imposed by the NRC as part of construction authorization or the license to receive and possess source, special nuclear, or byproduct material at Yucca Mountain. A license condition may be in the form of a condition in the body of the license or in the form of a license specification, derived from analyses and evaluations in the license application and appended to the license, that outlines the operational limits of the facility.

license specifications. A set of license conditions appended to the license to receive and possess radioactive material that outline specific operational limits of the facility. License conditions are derived from analyses and evaluations in the license application. The term "license specifications" in 10 CFR Part 63 is equivalent to the term "technical specifications" in 10 CFR Parts 50 and 72.

member of the public. Any individual except when that individual is receiving an occupational dose.

normal operations. Planned, routine activities in which closely monitored exposures are expected from the high-level radioactive waste or spent nuclear fuel processed at the geologic repository operations area.

nuclear safety design basis. Information that identifies the specific nuclear safety functions to be performed by an SSC of a facility and the specific nuclear safety values or ranges of values chosen for controlling parameters as reference bounds for design. These values may be constraints derived from generally accepted state-of-the-art practices for achieving functional goals, or they may be requirements derived from the analyses (based on calculations or experiments) of the effects of a postulated event under which an SSC must meet the functional goals. The values of controlling parameters for external events include (10 CFR 63.2): estimates of severe natural events used for deriving design bases that are based on the consideration of historical data, physical data, and analysis of the upper limits of the physical processes involved; estimates of severe external human-induced events used for deriving design bases that are based on the analysis of human activity in the region, taking into account site characteristics and risks associated with the event.

occupational dose limits. Limits on allowed occupational dose to individual adults promulgated in 10 CFR 20.1201.

off-normal events. Deviations from procedures and equipment failures that do not lead to significantly elevated exposures to occupationally exposed individuals. Off-normal events are not Category 1 events.

onsite public. Any individual within the preclosure controlled area who is not receiving an occupational dose.

other design information. All other design information not included in the nuclear safety design basis or supporting design information. Other design information includes design information necessary to achieve certain economies of operation, maintenance, procurement, installation, or construction. Other design information may be presented in the SAR (as design descriptions) or other documents docketed with the NRC or retained by the applicant or licensee.

performance confirmation. The program of tests, experiments and analysis that is conducted to evaluate the adequacy of the information used to demonstrate compliance with identified performance objectives of 10 CFR Part 63, Subpart E.

postclosure. The period of time after permanent closure of the repository system.

postclosure controlled area. (1) The surface area, identified by passive institutional controls, that encompasses no more than 300 km². It must not extend: (i) farther south than 36°40'13.6661" North latitude, in the predominant direction of groundwater flow; and (ii) farther than 5 km from the repository footprint in any other direction; and (2) the subsurface underlying the surface area.

preclosure. The period of time before permanent closure of the geologic repository operations area.

preclosure controlled area. Area inside the site boundary, access to which can be limited by the licensee for any reason.

preclosure safety analysis. A systematic examination of the site; the design; and the potential hazards, initiating events, and event sequences and their consequences (e.g., radiological exposures to workers and the public). The analysis identifies structures, systems, and components important to safety.

procedural safety control. Procedures, training, maintenance, configuration control, human factor evaluations, audits and self-assessments, emergency planning, and investigation requirements, and other activities performed by personnel to ensure that operations are within analyzed condition.

protected area. An area encompassed by physical barriers and to which access is controlled.

reasonably maximally exposed individual. A hypothetical person meeting the criteria specified in 10 CFR 63.312. Criteria includes being an adult, living in the accessible environment above the highest concentration of radionuclides in the plume of contamination, having a diet and lifestyle representative of the people in the surrounding community, and using a specified amount of well water.

recovery. Actions taken after termination of the event sequence to safely recover materials or place the facility back into a safe condition.

relocation. The act of temporarily or permanently moving a waste package from one emplacement drift to another emplacement drift, or to a different emplacement location within the same drift.

removal. The act of temporarily moving a waste package from the subsurface facility to a surface facility for the purposes of inspecting, testing, or remediation. A removed waste package is put back in its intended emplacement location after the reason for its removal has been satisfied.

repository footprint. The outline of the outermost locations of where the waste is emplaced in the repository.

restricted area. Area within the controlled area, access to which is limited by the licensee for the purpose of protecting individuals against undue risks from exposure to radiation and radioactive materials.

retrieval. The act of permanently removing radioactive waste from the underground location at which the waste had been previously emplaced for disposal.

site. Area surrounding the geologic repository operations area for which the DOE exercises authority over its use in accordance with the provisions of 10 CFR Part 63.

site boundary. The line beyond which the land or property is not owned, leased, or otherwise controlled by the licensee.

staging. Short-term storage of waste forms within a facility to accommodate thermal blending or other operational needs.

supporting design information. The set of detailed design information underlying (supporting) nuclear safety design bases, including other design inputs, design analyses, and design output documents. Supporting design information may be presented in the SAR (as design description) or other documents docketed with the NRC or retained by the applicant or licensee.

termination of the event sequence. The condition at which elevated exposure conditions to persons have ended (e.g., by evacuation of personnel or physical mitigation), and the affected systems are no longer reasonably vulnerable to additional failure progression or additional failures related to the event sequence.

total system performance assessment. A risk assessment that quantitatively estimates how the proposed Yucca Mountain disposal system will perform in the future under the influence of specific features, events, and processes, incorporating uncertainty in the models and data.

unrestricted area. An area, access to which is neither limited nor controlled by the licensee.

INTENTIONALLY LEFT BLANK

CONTENTS

	Page
1. REPOSITORY SAFETY BEFORE PERMANENT CLOSURE.....	1-1

INTENTIONALLY LEFT BLANK

1. REPOSITORY SAFETY BEFORE PERMANENT CLOSURE

Introduction—Repository safety before permanent closure is described in [Chapter 1](#) of the SAR. This includes a description of the design, analyses, operations, preclosure safety analysis (PCSA), and procedural safety controls that demonstrate the preclosure safety and compliance with the preclosure performance objectives in 10 CFR Part 63.

Preclosure Safety—Preclosure safety is ensured by the application of numerous safety principles that contribute to the protection of public health and safety, the environment, and worker safety. The attributes of the repository site combine with the design of the repository structures, systems, and components (SSCs) to achieve safety by maximizing the prevention of events and minimizing the reliance on immediate automatic or human actions.

The Yucca Mountain repository site is located on federal land with the site boundary approximately 5 mi away from the waste handling facilities and currently with no permanent residents within approximately 14 mi of the geologic repository operations area. This remoteness from the general public reduces the potential effects of the events considered in the safety analysis. Even though the site is remote, the prevention and mitigation features of the design and operation are consistent with those of facilities with more radioactive material at risk and closer proximity to the general public.

To the extent practicable, the repository design is based on proven nuclear industry precedent and utilizes primarily canistered spent nuclear fuel (SNF) to minimize handling of individual fuel assemblies. Facility components are designed with robust margins and utilize diverse and redundant systems. Mechanical handling, shielding, and related safety equipment are based on proven technology. The safety philosophy includes design approaches where (1) prevention is preferable to mitigation, (2) design features are preferable to administrative features, (3) passive features are preferable to active features, and (4) automatic features are preferable to manual features. SSCs that are important to safety (ITS) are designed with sufficient margin and reliability that an event sequence resulting in the exposure of workers or the public to radiation is maintained at a low probability.

The PCSA provides a framework for risk-informed, performance-based decision making that is applied to identify SSCs that are ITS; to identify measures for providing defense in depth; and to identify license specifications to ensure operation consistent with the SAR. The PCSA identifies the potential natural and operational hazards for the preclosure period; assesses potential initiating events and event sequences and their consequences; and identifies the SSCs and procedural safety controls intended to prevent or reduce the probability of an event sequence or mitigate the consequences of an event sequence, should it occur. Specific design features that perform these functions are identified. The design information and analyses must be sufficient to demonstrate that the design features will perform their intended safety functions. Initiating event and event sequence identification and analysis comprise an iterative process integrally tied to repository design. The results of the PCSA (see [Sections 1.6 to 1.9](#)) confirm that the site characteristics combined with the repository design provide an inherently safe facility that meets the regulatory preclosure performance objectives with substantial margin.

The repository surface and subsurface facilities are designed to safely handle and dispose of commercial SNF; U.S. Department of Energy (DOE) SNF, including naval SNF; and vitrified high-level radioactive waste (HLW). HLW is generated from commercial as well as DOE applications; however, the characteristics are similar enough to consider HLW uniformly throughout the SAR, irrespective of origin. Commercial SNF comprises approximately 63,000 MTHM of the anticipated maximum repository inventory of 70,000 MTHM. DOE SNF comprises approximately 2,268 MTHM, naval SNF comprises approximately 65 MTHM (for a total DOE allotment of 2,333 MTHM), and HLW comprises the balance of approximately 4,667 MTHM.

Surface Facility Design—The principal surface facilities used to receive, buffer, stage, age, and package waste and to support transport to the subsurface facilities for disposal are the Initial Handling Facility (IHF), Canister Receipt and Closure Facility (CRCF), Wet Handling Facility (WHF), Receipt Facility (RF), Emergency Diesel Generator Facility (EDGF), Aging Facility, and the surface transportation system and buffer areas. Waste enters the geologic repository operations area by road or rail in transportation casks certified by the U.S. Nuclear Regulatory Commission (NRC) and is transferred to the handling facilities for packaging. The structures for the waste handling facilities are designed to withstand the effects of initiating events. Inside each waste handling facility, shielding and remote operations are used to protect workers from exposure to direct radiation. Heating, ventilation, and air-conditioning (HVAC) systems with confinement zones and high-efficiency particulate air filtration protect the workers and the public from exposure to airborne radioactivity. The mechanical handling equipment is designed to reliably lift and move loaded canisters, loaded waste packages, and uncanistered commercial SNF in a manner that minimizes the likelihood of drop or collision event sequences involving SNF or HLW. A redundant set of diesel generators is provided to ensure the reliable distribution of electrical power to HVAC components that are designed to mitigate releases of airborne radioactivity. In those instances in which design features alone cannot achieve the desired reliability, procedural safety controls are used. The decay heat load from the waste forms is sufficiently low that even with an extended loss of normal HVAC, no waste form exceeds a thermal limit. The Aging Facility is used for cooling of commercial SNF to meet thermal management goals and for management of the received commercial SNF to ensure efficient use of the handling facilities and waste packages. The loading of transportation, aging, and disposal (TAD) canisters and waste packages is controlled by loading plans that ensure the applicable thermal, criticality, and shielding criteria are satisfied.

The repository surface facilities are based on the concept of a canistered approach for handling commercial SNF. For this approach, TAD canisters are used to minimize handling of uncanistered commercial SNF at the repository by sealing commercial SNF in TAD canisters at utility sites. The uncanistered commercial SNF that arrives at the repository will be packaged into TAD canisters at the repository. The TAD canister is a component of the canister systems to be certified by the NRC for transportation of commercial SNF under 10 CFR Part 71, and potentially certified for dry storage at utility sites under 10 CFR Part 72. This license application seeks authorization to use TAD canisters for onsite transfer, aging, and geologic disposal at Yucca Mountain under 10 CFR Part 63. In all three modes, the TAD canister is placed inside another vessel that provides other functions (e.g., radiological shielding, decay heat removal, containment, corrosion resistance) as needed for each mode. These vessels include transportation casks, shielded transfer casks, aging overpacks, and waste packages when TAD canisters are used in onsite transfer, aging, or geologic

disposal modes, respectively. DOE SNF, naval SNF, and HLW also employ a canistered approach to minimize handling and the spread of contamination.

Subsurface Facility Design—The subsurface facilities include the access mains and ramps, emplacement drifts, performance confirmation test and observation drifts, and ventilation shafts. The description of the subsurface facilities also includes a description of the waste package emplacement pallet and the transport and emplacement vehicle (TEV), which is used to safely position the emplacement pallet with its waste package in the appropriate emplacement drift. The drip shields that are installed as part of the closure activities are also considered to be part of the subsurface facilities. The orientation, shape, and spacing of the emplacement drifts facilitate postclosure performance of the repository. The dimensions of the emplacement drift are selected such that no credible rockfall during the preclosure period causes a failure of the waste package. The emplacement drift layout includes a turnout that protects the worker in the normally occupied access mains from direct radiation exposure. Each emplacement drift is equipped with an access barrier that controls personnel access and regulates ventilation to each drift. The heat load in each drift is sufficiently low such that an extended loss of normal ventilation does not cause the waste form, waste package, or emplacement drift wall to exceed temperature limits. The loading of the waste packages in the emplacement drifts is controlled by loading plans that satisfy applicable spacing and thermal criteria.

The surface and subsurface facilities are planned to be constructed in phases. The construction of all of the surface waste handling facilities and all of the emplacement drifts will not be completed before the initiation of handling and emplacement operations. The initial handling capability of the repository will be provided by the IHF, CRCF-1, and WHF. Subsequently, CRCF-2, CRCF-3, and the RF will be constructed. Aging pads with a total capacity of 21,000 MTHM will also be constructed as the receipt rate is increased. The initial operating condition of the subsurface facilities is planned to include three drifts, which will serve both emplacement and performance confirmation functions. The development of the subsurface facility will proceed while emplacement operations are conducted in the completed drifts and will be done in a manner that safely accommodates waste package emplacement. The layout of the surface and subsurface facilities includes adequate space for spatial separation or for the erection of barriers to protect the operating portions of the repository from initiating events and to maintain appropriate radiation protection and security for both the operating portions and those portions of the repository that are still under construction.

Preclosure Safety Analysis—10 CFR 63.21(c)(5) requires a PCSA of the geologic repository operations area for the period before permanent closure to ensure compliance with the preclosure performance objectives. The anticipated length of time before permanent closure of the repository is 100 years from the time of initial emplacement. For the purposes of the PCSA, the duration of the preclosure period varies depending on the facilities being evaluated. For the surface facilities, the anticipated duration of operations involving SNF and HLW is 50 years; for the subsurface facilities, the anticipated length of time from initial placement until the conditions for closure are satisfied is expected to be 100 years. The time periods are used to determine the likelihood of initiating events and to categorize event sequences. The PCSA is a systematic examination of the site, the design, and the potential hazards, initiating events, resulting event sequences, and potential radiological exposures to workers and the public. The PCSA considers the probability of potential hazards, taking into account the range of uncertainty associated with the data that support

the probability calculations. Initiating events are reasonable human-induced and natural events that cause an event sequence. An event sequence includes one or more initiating events and associated combinations of repository SSC failures. The consequences of event sequences are calculated in terms of doses to workers and the public. 10 CFR 63.111 sets out two preclosure performance objectives that are defined based on the anticipated frequency of occurrence of the event sequences. The calculated doses are compared to the applicable preclosure standards to determine compliance with the performance objectives. The SSCs that must be functional to ensure compliance with the preclosure performance objectives are identified as ITS. The ITS SSCs and the associated nuclear safety design bases are listed in [Section 1.9](#). Procedural safety controls that must be implemented to ensure compliance with the preclosure performance objectives are also listed in [Section 1.9](#). The nuclear safety design bases and the design criteria for implementation of the safety functions are presented in [Sections 1.2 to 1.5](#), where the facilities and contained SSCs are described. Sufficient general and specific information is included in these design sections to support the PCSA. The PCSA is presented in [Sections 1.6 to 1.9](#).

The surface and subsurface facilities have been demonstrated to be safe for handling SNF and HLW based upon the following characteristics of the design and safety analysis:

- The structures are designed to reduce the likelihood that external hazards or internal hazards could initiate event sequences leading to damage to the waste forms.
- The mechanical handling equipment is designed to reduce the occurrence of initiating events that could cause damage to the waste forms.
- Some of the facilities are equipped with confinement and filtration SSCs to mitigate potential radioactive releases from damaged waste forms.
- The design and analysis of SSCs utilize approaches, materials, methods, and codes and standards typical of the nuclear industry that result in robust and reliable SSCs to perform the required safety functions.
- The analysis of the radiological consequences to the worker and public for Category 1 and Category 2 event sequences uses nuclear-industry practices and established regulatory guidance that yield a conservatively high calculation of potential doses.
- Even with a conservative approach to the calculation of the potential consequences, the calculated exposures to the worker and public for normal operations, Category 1 event sequences, and Category 2 event sequences are below the regulatory performance objectives in 10 CFR 63.111(a) and (b).

Content and Format of Chapter 1—[Chapter 1](#) focuses on SSCs that safety analyses have determined to be ITS or important to waste isolation (ITWI). Limited prescriptive design requirements are imposed because 10 CFR Part 63 allows the DOE to develop the nuclear safety design bases and demonstrate their appropriateness. Therefore, [Chapter 1](#) describes the ITS/ITWI SSCs; identifies operating processes; states the safety category classification; identifies procedural safety controls; presents the design bases and design criteria; discusses design methodologies; identifies materials of construction; provides the selection of codes and standards along with any

clarifications; and lists the load combinations, as applicable. This specific information for ITS and ITWI SSCs identifies the safety functions and demonstrates the ability to perform the safety functions when required with the necessary reliability. General information is provided for SSCs that are neither ITS nor ITWI to complete the description of the repository and its operations.

In compliance with 10 CFR Part 63 and the guidance in NUREG-1804, the descriptions of SSCs and operational processes in [Chapter 1](#) have been developed to provide an understanding of the design and function of the repository. The information provided in [Chapter 1](#) addresses the dimensions, material properties, specifications, and design methods used along with the applicable codes and standards to demonstrate that SNF and HLW can be received, handled, packaged, aged, emplaced, and retrieved (if necessary) in a safe manner. In those cases in which specific, detailed information about components is unavailable to support a quantitative demonstration of capability, sufficient performance-specification or representative information regarding safety function, nuclear safety design basis, design approach, and codes and standards are provided to define the safety envelope for the SSCs and to enable a technical review and a safety finding. The detailed design for construction of the surface and subsurface facilities is ongoing and will implement the nuclear safety design bases and SSCs, as described in the license application.

The PCSA and the total system performance assessment (TSPA) will be maintained throughout the design, construction, and operational periods of the repository. The detailed design for construction will be evaluated for effects on the ITS and ITWI SSCs, effects on the safety strategies, and the potential identification of additional hazards, initiating events, and event sequences. The PCSA and TSPA will continue to demonstrate that the ITS and ITWI SSCs can perform their intended safety functions when required to satisfy the performance objectives of 10 CFR Part 63.

After a construction authorization is issued, configuration control is used to ensure that proposed safety-significant changes to the repository design, the PCSA, the TSPA, and procedural safety controls are evaluated for their impact on safety. Changes to the design and analyses presented in the license application will be made in accordance with 10 CFR 63.32 or 10 CFR 63.44, as applicable. Additionally, the license application will be updated in accordance with 10 CFR 63.24.

[Chapter 1](#) describes the repository SSCs and the nuclear safety design bases for ITS and ITWI SSCs. Both ITS and ITWI and non-ITS and non-ITWI SSCs are discussed. In addition, the chapter provides design, operational, and process flow information to support the PCSA and to assist in the understanding of the overall design and function of the repository. [Chapter 1](#) is divided into the following sections:

- **Section 1.1: Site Description as It Pertains to the PCSA**—This section describes the Yucca Mountain site and the surrounding region. Information is presented that addresses site geology, regional demography, local meteorology, regional climatology, surface and groundwater hydrology, seismology, igneous activity, site geomorphology, site geochemistry, and land use in the land withdrawal area.
- **Section 1.2: Surface Facility Structures, Systems, and Components and Operational Process Activities**—The design and operation of surface SSCs are described in this section. It includes an overview of surface operations and a discussion of design considerations, including criteria, methodology, and loads considered in the design of the

surface SSCs. Specific surface facilities and SSCs contained within each facility are discussed. These include the IHF, CRCF, EDGF, WHF, RF, Aging Facility, and balance of plant facilities.

- **Section 1.3: Subsurface Structures, Systems, and Components and Operational Process Activities**—The design and operation of subsurface SSCs are described in this section. It includes an overview of the subsurface operations and a discussion of subsurface design criteria, methodology, and loads considered in the design of the subsurface SSCs. The layout, ground support, and ventilation of the subsurface facility are addressed. The TEV and its operations are described.
- **Section 1.4: Infrastructure Structures, Systems, Components, Equipment, and Operational Process Activities**—This section covers those SSCs that are common to the surface and subsurface. It includes electric power, controls and monitoring, fire protection, plant services, and radioactive waste management.
- **Section 1.5: Waste Form and Waste Package**—This section describes the waste forms to be permanently disposed and the waste package configurations that contain the waste forms. The canisters for commercial SNF, DOE SNF, naval SNF, and HLW are addressed in [Section 1.5.1](#). The waste package configurations are addressed in [Section 1.5.2](#).
- **Section 1.6: Identification of Hazards and Initiating Events**—This section discusses the identification of those external and internal hazards that are applicable to the repository and the screening analyses of those hazards that could initiate an event sequence with a potential radioactive release or direct exposure to radiation during preclosure operations.
- **Section 1.7: Event Sequence Analysis**—This section presents the methodology for identifying, quantifying, and categorizing the internal and external hazards and initiating events identified in [Section 1.6](#) into Category 1 and Category 2 event sequences. The reliability of SSCs and operator actions that are evaluated in event sequences are assessed in this section.
- **Section 1.8: Consequence Analysis**—This section discusses potential surface and subsurface releases during normal operations and Category 1 and Category 2 event sequences that could lead to radiological consequences, including controls used to prevent or mitigate event sequences. The results of calculating potential public and worker doses are summarized.
- **Section 1.9: Structures, Systems, and Components Important to Safety; Natural and Engineered Barriers Important to Waste Isolation; Safety Controls; and Measures to Ensure Availability of the Safety Systems**—The classification of SSCs is an integral part of the design process and is the final step in the PCSA. This section identifies ITS SSCs and the nuclear safety design bases from the PCSA. The procedural safety controls that prevent or mitigate event sequences are identified. Similar information is provided for ITWI SSCs and features based upon the postclosure performance assessment.

- **Section 1.10: Meeting the As Low As is Reasonably Achievable Requirements for Normal Operations and Category 1 Event Sequences**—This section describes the commitment to as low as is reasonably achievable (ALARA) principles, shielding design, and the implementation of ALARA principles in design and operations.
- **Section 1.11: Plans for Retrieval and Alternate Storage of Radioactive Wastes**—This section discusses approaches for retrieval and alternate radioactive waste storage that will be developed should a decision to retrieve be made.
- **Section 1.12: Plans for Permanent Closure, Decontamination, and Dismantlement of Surface Facilities**—This section discusses plans for permanent closure. It also discusses the preliminary plans for decontamination and dismantlement of the handling facilities and discusses key elements of such plans to be included in the application for permanent closure.
- **Section 1.13: Equipment Qualification Program**—This section describes the equipment qualification program.
- **Section 1.14: Nuclear Criticality Safety**—This section describes the nuclear criticality safety program and how the repository is designed, constructed, and operated to prevent a nuclear criticality event.

NUREG-1804 Acceptance Criteria—NUREG-1804 and Division of High-Level Waste Repository Safety—Interim Staff Guidance (HLWRS-ISG) includes acceptance criteria to be used by the NRC staff in its review of the license application. The format of Chapter 1 generally follows the format and sequence of NUREG-1804 acceptance criteria. Many of the license application section and subsection headings directly correlate to the various NUREG-1804 acceptance criteria.

At the beginning of each license application section, a table is provided that lists the NUREG-1804 and HLWRS-ISG-01 through -04 acceptance criteria applicable to the specific license application section and the applicable 10 CFR Part 63 requirements. The tables illustrate the relationship between the format and content of the license application sections and NUREG-1804.

In addition, the major license application subsection headings include parenthetical references to the applicable NUREG-1804 and HLWRS-ISG-01 through -04 acceptance criteria. This provides a general correlation between the information presented in a license application subsection and the corresponding acceptance criteria. Many of the acceptance criteria are addressed in more than one license application subsection, and it may be necessary to consider the information contained in those license application sections or chapters for a thorough understanding of the repository design, the PCSA, and the TSPA.

INTENTIONALLY LEFT BLANK

CONTENTS

	Page
1.1 SITE DESCRIPTION AS IT PERTAINS TO PRECLOSURE SAFETY ANALYSIS	1.1-1
1.1.1 Site Geography	1.1-1
1.1.1.1 Repository Boundaries	1.1-2
1.1.1.2 Natural Features	1.1-3
1.1.1.3 Man-Made Features	1.1-4
1.1.2 Regional Demography	1.1-23
1.1.2.1 Demographic Study Area	1.1-23
1.1.2.2 Population Centers	1.1-24
1.1.2.3 Population Projections	1.1-25
1.1.3 Local Meteorology and Regional Climatology	1.1-25
1.1.3.1 Meteorological Monitoring	1.1-26
1.1.3.2 Data Summary	1.1-36
1.1.3.3 Atmospheric Dispersion Characteristics	1.1-41
1.1.3.4 Atmospheric Stability	1.1-42
1.1.3.5 Meteorological Summary	1.1-44
1.1.3.6 Severe Weather Characteristics	1.1-45
1.1.4 Regional and Local Surface and Groundwater Hydrology	1.1-48
1.1.4.1 Surface Water Hydrology	1.1-49
1.1.4.2 Groundwater Hydrology	1.1-50
1.1.4.3 Hydrologic Engineering Studies for Surface Facilities	1.1-53
1.1.5 Site Geology and Seismology	1.1-55
1.1.5.1 Site Geology	1.1-55
1.1.5.2 Site Seismology	1.1-65
1.1.5.3 Geotechnical Properties and Conditions	1.1-101
1.1.6 Igneous Activity	1.1-134
1.1.6.1 Location of Volcanism in the Yucca Mountain Region	1.1-135
1.1.6.2 Probabilistic Volcanic Hazard Analysis	1.1-137
1.1.6.3 Potential Hazard from Ash Fall	1.1-138
1.1.7 Site Geomorphology	1.1-139
1.1.7.1 Geomorphic Information and Tectonic Activity	1.1-139
1.1.7.2 Variability in Quaternary Processes	1.1-140
1.1.8 Geochemistry	1.1-142
1.1.8.1 Introduction	1.1-142
1.1.8.2 Geochemical Composition of Subsurface Waters	1.1-143
1.1.8.3 Geochemical Conditions in the Preclosure Emplacement Drift Environment	1.1-144

CONTENTS (Continued)

	Page
1.1.8.4 Geochemical Alteration to Host-Rock Properties Environment	1.1-145
1.1.9 Land Use, Structures and Facilities, and Residual Radioactivity.....	1.1-148
1.1.9.1 Previous Land Uses within the Land Withdrawal Area	1.1-149
1.1.9.2 Previous Land Uses in the Vicinity of the Proposed Land Withdrawal Area	1.1-152
1.1.9.3 Location and Description of Existing Man-Made Structures or Facilities.....	1.1-156
1.1.9.4 Identification of Residual Radiation	1.1-161
1.1.10 General References.....	1.1-164

TABLES

		Page
1.1-1.	Federal Airways	1.1-183
1.1-2.	Estimates of the Resident Population Located within the 84-km Radiological Monitoring Grid	1.1-184
1.1-3.	Projected Population within the 84-km Grid, 2003 – 2017 ^a	1.1-186
1.1-4.	Projections of Population for Preclosure Operations Period ^a	1.1-190
1.1-5.	Projected Distribution by Age Groups for Preclosure Operations Midpoint in 2042, Including Repository-Induced Changes	1.1-192
1.1-6.	Geographic Coordinates of the Meteorological Monitoring Sites	1.1-194
1.1-7.	Parameters Measured at Each Meteorological Monitoring Station (1994 to 2006)	1.1-195
1.1-8.	Sensor Descriptions and Requirements	1.1-197
1.1-9.	System Accuracy Requirements	1.1-199
1.1-10.	Site 1 Climatic Summary for 1994 to 2006	1.1-200
1.1-11.	Site 2 Climatic Summary for 1994 to 2006	1.1-202
1.1-12.	Site 3 Climatic Summary for 1994 to 2006	1.1-204
1.1-13.	Site 4 Climatic Summary for 1994 to 2006	1.1-206
1.1-14.	Site 5 Climatic Summary for 1994 to 2006	1.1-208
1.1-15.	Site 6 Climatic Summary for 1994 to 2006	1.1-210
1.1-16.	Site 7 Climatic Summary for 1994 to 2006	1.1-212
1.1-17.	Site 8 Climatic Summary for 1994 to 2006	1.1-214
1.1-18.	Site 9 Climatic Summary for 1994 to 2006	1.1-216
1.1-19.	Average Annual Total Precipitation	1.1-218
1.1-20.	Annual Total Precipitation at Site 1 from 1994 through 2006	1.1-218
1.1-21.	Annual Average Total Precipitation Ranked by Total Amount for 1999 to 2006	1.1-218
1.1-22.	Precipitation Rate and Frequency Results	1.1-219
1.1-23.	Comparison of 24-Hour Maximum Precipitation from September 21 through 22, 2007, Storm to Values of Previous Maximum Events	1.1-220
1.1-24.	Summary of Mean and Maximum Wind Speeds	1.1-221
1.1-25.	Pasquill Stability Categories Based on Vertical Temperature Differences	1.1-221
1.1-26.	Joint Frequency Distribution of Wind Speed and Direction for All Hours (1994 to 2006) at Site 1 at 10 m above Ground Level	1.1-222
1.1-27.	Joint Frequency Distribution of Wind Speed and Direction (Decimal Fractions) for All Hours (1994 to 2006) at Site 1 at 60 m above Ground Level	1.1-224
1.1-28.	Joint Frequency Distribution of Wind Speed and Direction (Decimal Fractions) for All Hours (1994 to 2006) at Site 2 at 10 m above Ground Level	1.1-226

TABLES (Continued)

	Page
1.1-29. Joint Frequency Distribution of Wind Speed and Direction (Decimal Fractions) for All Hours (1994 to 1998) at Site 3 at 10 m above Ground Level	1.1-228
1.1-30. Joint Frequency Distribution of Wind Speed and Direction (Decimal Fractions) for All Hours (1994 to 2006) at Site 4 at 10 m above Ground Level	1.1-230
1.1-31. Joint Frequency Distribution of Wind Speed and Direction (Decimal Fractions) for All Hours (1994 to 1998) at Site 5 at 10 m above Ground Level	1.1-232
1.1-32. Joint Frequency Distribution of Wind Speed and Direction (Decimal Fractions) for All Hours (1994 to 1998) at Site 7 at 10 m above Ground Level	1.1-234
1.1-33. Joint Frequency Distribution of Wind Speed and Direction (Decimal Fractions) for All Hours (1994 to 2006) at Site 9 at 10 m above Ground Level	1.1-236
1.1-34. Joint Frequency Distribution of Wind Speed and Direction (Decimal Fractions) for Daytime Hours (1994 to 2006) at Site 1 at 10 m above Ground Level	1.1-238
1.1-35. Joint Frequency Distribution of Wind Speed and Direction (Decimal Fractions) for Night Hours (1994 to 2006) at Site 1 at 10 m above Ground Level	1.1-240
1.1-36. Joint Frequency Distribution of Wind Speed and Direction (Decimal Fractions) for Daytime Hours (1994 to 2006) at Site 1 at 60 m above Ground Level	1.1-242
1.1-37. Joint Frequency Distribution of Wind Speed and Direction (Decimal Fractions) for Night Hours (1994 to 2006) at Site 1 at 60 m above Ground Level	1.1-244
1.1-38. Joint Frequency Distribution of Wind Speed and Direction (Decimal Fractions) for Daytime Hours (1994 to 2006) at Site 2 at 10 m above Ground Level	1.1-246
1.1-39. Joint Frequency Distribution of Wind Speed and Direction (Decimal Fractions) for Night Hours (1994 to 2006) at Site 2 at 10 m above Ground Level	1.1-248
1.1-40. Joint Frequency Distribution of Wind Speed and Direction (Decimal Fractions) for Daytime Hours (1994 to 1998) at Site 3 at 10 m above Ground Level	1.1-250
1.1-41. Joint Frequency Distribution of Wind Speed and Direction (Decimal Fractions) for Night Hours (1994 to 1998) at Site 3 at 10 m above Ground Level	1.1-252
1.1-42. Joint Frequency Distribution of Wind Speed and Direction (Decimal Fractions) for Daytime Hours (1994 to 2006) at Site 4 at 10 m above Ground Level	1.1-254

TABLES (Continued)

	Page
1.1-43. Joint Frequency Distribution of Wind Speed and Direction (Decimal Fractions) for Night Hours (1994 to 2006) at Site 4 at 10 m above Ground Level	1.1-256
1.1-44. Joint Frequency Distribution of Wind Speed and Direction (Decimal Fractions) for Daytime Hours (1994 to 1998) at Site 5 at 10 m above Ground Level	1.1-258
1.1-45. Joint Frequency Distribution of Wind Speed and Direction (Decimal Fractions) for Night Hours (1994 to 1998) at Site 5 at 10 m above Ground Level	1.1-260
1.1-46. Joint Frequency Distribution of Wind Speed and Direction (Decimal Fractions) for Daytime Hours (1994 to 1998) at Site 7 at 10 m above Ground Level	1.1-262
1.1-47. Joint Frequency Distribution of Wind Speed and Direction (Decimal Fractions) for Night Hours (1994 to 1998) at Site 7 at 10 m above Ground Level	1.1-264
1.1-48. Joint Frequency Distribution of Wind Speed and Direction (Decimal Fractions) for Daytime Hours (1994 to 2006) at Site 9 at 10 m above Ground Level	1.1-266
1.1-49. Joint Frequency Distribution of Wind Speed and Direction (Decimal Fractions) for Night Hours (1994 to 2006) at Site 9 at 10 m above Ground Level	1.1-268
1.1-50. Joint Frequency Distribution of Wind Speed and Direction (Decimal Fractions) for Stability Category A (Extremely Unstable) (1994 to 2006) at Site 1 at 10 m above Ground Level	1.1-270
1.1-51. Joint Frequency Distribution of Wind Speed and Direction (Decimal Fractions) for Stability Category A (Extremely Unstable) (1994 to 2006) at Site 1 at 60 m above Ground Level	1.1-272
1.1-52. Joint Frequency Distribution of Wind Speed and Direction (Decimal Fractions) for Stability Category B (Moderately Unstable) (1994 to 2006) at Site 1 at 10 m above Ground Level	1.1-274
1.1-53. Joint Frequency Distribution of Wind Speed and Direction (Decimal Fractions) for Stability Category B (Moderately Unstable) (1994 to 2006) at Site 1 at 60 m above Ground Level	1.1-276
1.1-54. Joint Frequency Distribution of Wind Speed and Direction (Decimal Fractions) for Stability Category C (Slightly Unstable) (1994 to 2006) at Site 1 at 10 m above Ground Level	1.1-278
1.1-55. Joint Frequency Distribution of Wind Speed and Direction (Decimal Fractions) for Stability Category C (Slightly Unstable) (1994 to 2006) at Site 1 at 60 m above Ground Level	1.1-280
1.1-56. Joint Frequency Distribution of Wind Speed and Direction (Decimal Fractions) for Stability Category D (Neutral) (1994 to 2006) at Site 1 at 10 m above Ground Level	1.1-282

TABLES (Continued)

	Page
1.1-57. Joint Frequency Distribution of Wind Speed and Direction (Decimal Fractions) for Stability Category D (Neutral) (1994 to 2006) at Site 1 at 60 m above Ground Level.	1.1-284
1.1-58. Joint Frequency Distribution of Wind Speed and Direction (Decimal Fractions) for Stability Category E (Slightly Stable) (1994 to 2006) at Site 1 at 10 m above Ground Level	1.1-286
1.1-59. Joint Frequency Distribution of Wind Speed and Direction (Decimal Fractions) for Stability Category E (Slightly Stable) (1994 to 2006) at Site 1 at 60 m above Ground Level	1.1-288
1.1-60. Joint Frequency Distribution of Wind Speed and Direction (Decimal Fractions) for Stability Category F (Moderately Stable) (1994 to 2006) at Site 1 at 10 m above Ground Level	1.1-290
1.1-61. Joint Frequency Distribution of Wind Speed and Direction (Decimal Fractions) for Stability Category F (Moderately Stable) (1994 to 2006) at Site 1 at 60 m above Ground Level	1.1-292
1.1-62. Joint Frequency Distribution of Wind Speed and Direction (Decimal Fractions) for Stability Category G (Extremely Stable) (1994 to 2006) at Site 1 at 10 m above Ground Level	1.1-294
1.1-63. Joint Frequency Distribution of Wind Speed and Direction (Decimal Fractions) for Stability Category G (Extremely Stable) (1994 to 2006) at Site 1 at 60 m above Ground Level	1.1-296
1.1-64. Summary of Pasquill Stability Category Occurrences	1.1-298
1.1-65. Earthquakes with M_w Greater than 5.0 within 300 km of Yucca Mountain.	1.1-299
1.1-66. Summary of Fault Parameters from Probabilistic Seismic Hazard Assessment Seismic Source Characterization	1.1-301
1.1-67. Mean Fault Displacement Hazard at Nine Demonstration Sites	1.1-304
1.1-68. Summary of Deaggregation Results and Reference Earthquakes.	1.1-305
1.1-69. Preclosure Seismic Ground Motions for Design Analyses.	1.1-306
1.1-70. UE-25 RF#1	1.1-307
1.1-71. UE-25 RF#2	1.1-307
1.1-72. UE-25 RF#3	1.1-308
1.1-73. UE-25 RF#3b	1.1-312
1.1-74. UE-25 RF#4	1.1-313
1.1-75. UE-25 RF#5	1.1-314
1.1-76. UE-25 RF#7	1.1-314
1.1-77. UE-25 RF#7A.	1.1-315
1.1-78. UE-25 RF#8	1.1-316
1.1-79. UE-25 RF#9	1.1-317
1.1-80. UE-25 RF#10	1.1-318
1.1-81. UE-25 RF#11	1.1-319

TABLES (Continued)

	Page
1.1-82. Rock Mass Parameters for Nonlithophysal Repository Host Horizon Units Calculated using RocLab	1.1-320
1.1-83. Summary of In Situ Stresses at the Repository Host Horizon	1.1-322
1.1-84. Summary of Laboratory Physical Properties Testing of Alluvium from Boreholes UE-25 RF#47 and UE-25 RF#52	1.1-323
1.1-85. Summary of In-Place Soil Density Tests and Relative Density	1.1-325
1.1-86. Median, 16th Percentile, and 84th Percentile of Seismic Wave Velocities in Each Stratigraphic Unit from Free-Free Resonant Column Tests	1.1-326
1.1-87. Median, 16th Percentile and 84th Percentile of Material Damping Ratios in Each Stratigraphic Unit.	1.1-328
1.1-88. Measured Radionuclide Concentrations at Gate 510 Air Sampling Station	1.1-330

INTENTIONALLY LEFT BLANK

FIGURES

		Page
1.1-1.	Site Boundary	1.1-331
1.1-2.	Boundaries of Surface Geologic Repository Operations Area at Maximum Extent of the Restricted Area	1.1-333
1.1-3.	Surface Geologic Repository Operations Area Showing Changes of Restricted Area and Protected Area during Phased Repository Development.	1.1-335
1.1-4.	Map Showing the Location of Yucca Mountain Site	1.1-337
1.1-5.	Topography and Drainage System in the Vicinity of the Repository.	1.1-338
1.1-6.	Nevada Test Site Regional Location Map	1.1-339
1.1-7.	100-mi Regional Airspace Setting Surrounding Yucca Mountain	1.1-341
1.1-8.	Military Airports, Military Training Routes, and Navigation Aids in the Regional Setting	1.1-343
1.1-9.	Civilian Airports, Airways, and Navigation Aids in the Regional Setting.	1.1-345
1.1-10.	Transmission Lines in the Vicinity of the Repository	1.1-347
1.1-11.	Population Distribution within the Demographic Study Area (84-km Radiological Monitoring Grid).	1.1-348
1.1-12.	Yucca Mountain Meteorological Stations	1.1-349
1.1-13.	Locations of the Regional Meteorological Stations	1.1-350
1.1-14.	Wind Rose for Site 1 at 10 m above Ground Level for All Hours (1994 to 2006).	1.1-351
1.1-15.	Wind Rose for Site 1 at 60 m above Ground Level for All Hours (1994 to 2006).	1.1-352
1.1-16.	Wind Rose for Site 2 at 10 m above Ground Level for All Hours (1994 to 2006).	1.1-353
1.1-17.	Wind Rose for Site 3 at 10 m above Ground Level for All Hours (1994 to 1998).	1.1-354
1.1-18.	Wind Rose for Site 4 at 10 m above Ground Level for All Hours (1994 to 2006).	1.1-355
1.1-19.	Wind Rose for Site 5 at 10 m above Ground Level for All Hours (1994 to 1998).	1.1-356
1.1-20.	Wind Rose for Site 7 at 10 m above Ground Level for All Hours (1994 to 1998).	1.1-357
1.1-21.	Wind Rose for Site 9 at 10 m above Ground Level for All Hours (1994 to 2006).	1.1-358
1.1-22.	Wind Rose for Site 1 at 10 m above Ground Level for Daylight Hours (1994 to 2006).	1.1-359
1.1-23.	Wind Rose for Site 1 at 10 m above Ground Level for Night Hours (1994 to 2006).	1.1-360
1.1-24.	Wind Rose for Site 1 at 60 m above Ground Level for Daylight Hours (1994 to 2006).	1.1-361
1.1-25.	Wind Rose for Site 1 at 60 m above Ground Level for Night Hours (1994 to 2006).	1.1-362

FIGURES (Continued)

	Page
1.1-26. Wind Rose for Site 2 at 10 m above Ground Level for Daylight Hours (1994 to 2006).	1.1-363
1.1-27. Wind Rose for Site 2 at 10 m above Ground Level for Night Hours (1994 to 2006).	1.1-364
1.1-28. Wind Rose for Site 3 at 10 m above Ground Level for Daylight Hours (1994 to 1998).	1.1-365
1.1-29. Wind Rose for Site 3 at 10 m above Ground Level for Night Hours (1994 to 1998).	1.1-366
1.1-30. Wind Rose for Site 4 at 10 m above Ground Level for Daylight Hours (1994 to 2006).	1.1-367
1.1-31. Wind Rose for Site 4 at 10 m above Ground Level for Night Hours (1994 to 2006).	1.1-368
1.1-32. Wind Rose for Site 5 at 10 m above Ground Level for Daylight Hours (1994 to 1998).	1.1-369
1.1-33. Wind Rose for Site 5 at 10 m above Ground Level for Night Hours (1994 to 1998).	1.1-370
1.1-34. Wind Rose for Site 7 at 10 m above Ground Level for Daylight Hours (1994 to 1998).	1.1-371
1.1-35. Wind Rose for Site 7 at 10 m above Ground Level for Night Hours (1994 to 1998).	1.1-372
1.1-36. Wind Rose for Site 9 at 10 m above Ground Level for Daylight Hours (1994 to 2006).	1.1-373
1.1-37. Wind Rose for Site 9 at 10 m above Ground Level for Night Hours (1994 to 2006).	1.1-374
1.1-38. Wind Rose for Stability Category A at Site 1 at 10 m above Ground Level (1994 to 2006).	1.1-375
1.1-39. Wind Rose for Stability Category A at Site 1 at 60 m above Ground Level (1994 to 2006).	1.1-376
1.1-40. Wind Rose for Stability Category B at Site 1 at 10 m above Ground Level (1994 to 2006).	1.1-377
1.1-41. Wind Rose for Stability Category B at Site 1 at 60 m above Ground Level (1994 to 2006).	1.1-378
1.1-42. Wind Rose for Stability Category C at Site 1 at 10 m above Ground Level (1994 to 2006).	1.1-379
1.1-43. Wind Rose for Stability Category C at Site 1 at 60 m above Ground Level (1994 to 2006).	1.1-380
1.1-44. Wind Rose for Stability Category D at Site 1 at 10 m above Ground Level (1994 to 2006).	1.1-381
1.1-45. Wind Rose for Stability Category D at Site 1 at 60 m above Ground Level (1994 to 2006).	1.1-382
1.1-46. Wind Rose for Stability Category E at Site 1 at 10 m above Ground Level (1994 to 2006).	1.1-383
1.1-47. Wind Rose for Stability Category E at Site 1 at 60 m above Ground Level (1994 to 2006).	1.1-384

FIGURES (Continued)

	Page
1.1-48. Wind Rose for Stability Category F at Site 1 at 10 m above Ground Level (1994 to 2006).	1.1-385
1.1-49. Wind Rose for Stability Category F at Site 1 at 60 m above Ground Level (1994 to 2006).	1.1-386
1.1-50. Wind Rose for Stability Category G at Site 1 at 10 m above Ground Level (1994 to 2006).	1.1-387
1.1-51. Wind Rose for Stability Category G at Site 1 at 60 m above Ground Level (1994 to 2006).	1.1-388
1.1-52. Surface Water Features in the Yucca Mountain Region.	1.1-389
1.1-53. Surface Water Data Collection Sites Near Yucca Mountain	1.1-390
1.1-54. Surface Water Data Collection Sites in the Yucca Mountain Vicinity.	1.1-391
1.1-55. Inferred Groundwater Flow Paths in the Central Death Valley Subregion	1.1-392
1.1-56. Locations of Pre-2004 Exploration Relative to Exploratory Studies Facility and Repository.	1.1-393
1.1-57. Inundation Surface for No-Mitigation Scenario	1.1-395
1.1-58. Inundation Surface around South Portal.	1.1-397
1.1-59. Generalized Geologic Map of Yucca Mountain Repository Area	1.1-398
1.1-60. Stratigraphic Column with Lithostratigraphic Detail for the Repository Host Horizon.	1.1-399
1.1-61. Fault Traces Used in the Geologic Framework Model.	1.1-400
1.1-62. Locations of Boreholes	1.1-401
1.1-63. Locations of Measured Sections, Gravity Profiles, and Seismic Profiles	1.1-402
1.1-64. Generalized Geologic Map of the Surface Geologic Repository Operations Area, Including Exile Hill	1.1-403
1.1-65. Surface Geologic Repository Operations Area Geologic Cross Section G-G', Looking Northwest	1.1-404
1.1-66. Surface Geologic Repository Operations Area Geologic Cross Section A-A', Looking South	1.1-405
1.1-67. Surface Geologic Repository Operations Area Geologic Cross Section C-C', Looking West.	1.1-406
1.1-68. Historical Earthquake Epicenters within 300 km of Yucca Mountain	1.1-407
1.1-69. Historical Earthquake Epicenters within 100 km of Yucca Mountain	1.1-408
1.1-70. Focal Depth Distribution of Earthquakes in the Yucca Mountain Vicinity for the Period October 1, 1999, to September 30, 2000	1.1-409
1.1-71. Focal Mechanisms for Earthquakes in the Vicinity of Yucca Mountain	1.1-410
1.1-72. Seismicity at Yucca Mountain from October 1, 1995, to September 30, 2002	1.1-411
1.1-73. Known or Suspected Quaternary Faults and Other Notable Faults in the Yucca Mountain Region	1.1-412
1.1-74. Hazard Curves at Reference Rock Outcrop for Peak Horizontal Ground Acceleration and 1 Hz Horizontal Spectral Acceleration	1.1-413

FIGURES (Continued)

	Page
1.1-75. Deaggregation of Mean Seismic Hazard for Horizontal Spectral Acceleration at 10^{-4} Annual Exceedance Probability for the Reference Rock Outcrop	1.1-414
1.1-76. Example Summary Fault Displacement Hazard Curves for Yucca Mountain.	1.1-415
1.1-77. Schematic Representation of Development of Supplemental Ground Motions	1.1-416
1.1-78. Schematic Representation of the Locations for Which Seismic Input Ground Motions are Developed	1.1-417
1.1-79. Conditioned and Unconditioned Reference Rock Outcrop Mean Horizontal Peak Ground Velocity Hazard Curves	1.1-418
1.1-80. Conditioned and Unconditioned Reference Rock Outcrop Mean Horizontal Peak Ground Acceleration Hazard Curves	1.1-419
1.1-81. Reference Rock Outcrop Uniform Hazard Spectra Based on the Extreme-Stress-Drop and Shear-Strain-Threshold Conditioned and Unconditioned Hazard for an Annual Probability of Exceedance of 10^{-3}	1.1-420
1.1-82. Reference Rock Outcrop Uniform Hazard Spectra Based on the Extreme-Stress-Drop and Shear-Strain-Threshold Conditioned and Unconditioned Hazard for an Annual Probability of Exceedance of 10^{-4}	1.1-421
1.1-83. Reference Rock Outcrop Uniform Hazard Spectra Based on the Extreme-Stress-Drop and Shear-Strain-Threshold Conditioned and Unconditioned Hazard for an Annual Probability of Exceedance of 10^{-5}	1.1-422
1.1-84. Reference Rock Outcrop Uniform Hazard Spectra Based on the Extreme-Stress-Drop and Shear-Strain-Threshold Conditioned and Unconditioned Hazard for an Annual Probability of Exceedance of 10^{-6}	1.1-423
1.1-85. Reference Rock Outcrop Uniform Hazard Spectra Based on the Extreme-Stress-Drop and Shear-Strain-Threshold Conditioned and Unconditioned Hazard for an Annual Probability of Exceedance of 10^{-7}	1.1-424
1.1-86. Reference Rock Outcrop Uniform Hazard Spectra Based on the Extreme-Stress-Drop and Shear-Strain-Threshold Conditioned and Unconditioned Hazard for an Annual Probability of Exceedance of 10^{-8}	1.1-425
1.1-87. Representative Control Motion Response Spectra for Site Response Modeling.	1.1-426
1.1-88. Mean Horizontal and Vertical Seismic Hazard Curves for Peak Ground Acceleration at the Surface Geologic Repository Operations Area	1.1-427
1.1-89. Mean Horizontal Seismic Hazard Curve for Peak Ground Velocity at the Surface Geologic Repository Operations Area.	1.1-428
1.1-90. Surface Geologic Repository Operations Area 5%-Damped Horizontal Design Spectra for 10^{-3} , 5×10^{-4} , and 10^{-4} Annual Probabilities of Exceedance	1.1-429
1.1-91. Surface Geologic Repository Operations Area 5%-Damped Vertical Design Spectra for 10^{-3} , 5×10^{-4} , and 10^{-4} Annual Probabilities of Exceedance	1.1-430

FIGURES (Continued)

	Page
1.1-92. Horizontal and Vertical 5%-Damped Design Spectra at 10^{-3} Annual Probability of Exceedance at the Repository Block	1.1-431
1.1-93. Horizontal and Vertical 5%-Damped Design Spectra at 5×10^{-4} Annual Probability of Exceedance at the Repository Block	1.1-432
1.1-94. Horizontal and Vertical 5%-Damped Design Spectra at 10^{-4} Annual Probability of Exceedance at the Repository Block	1.1-433
1.1-95. Geologic Log of Drill Hole UE-25 RF#13 (Sheet 1 of 8)	1.1-434
1.1-95. Geologic Log of Drill Hole UE-25 RF#13 (Sheet 2 of 8)	1.1-435
1.1-95. Geologic Log of Drill Hole UE-25 RF#13 (Sheet 3 of 8)	1.1-436
1.1-95. Geologic Log of Drill Hole UE-25 RF#13 (Sheet 4 of 8)	1.1-437
1.1-95. Geologic Log of Drill Hole UE-25 RF#13 (Sheet 5 of 8)	1.1-438
1.1-95. Geologic Log of Drill Hole UE-25 RF#13 (Sheet 6 of 8)	1.1-439
1.1-95. Geologic Log of Drill Hole UE-25 RF#13 (Sheet 7 of 8)	1.1-440
1.1-95. Geologic Log of Drill Hole UE-25 RF#13 (Sheet 8 of 8)	1.1-441
1.1-96. Geologic Log of Drill Hole UE-25 RF#14 (Sheet 1 of 11)	1.1-442
1.1-96. Geologic Log of Drill Hole UE-25 RF#14 (Sheet 2 of 11)	1.1-443
1.1-96. Geologic Log of Drill Hole UE-25 RF#14 (Sheet 3 of 11)	1.1-444
1.1-96. Geologic Log of Drill Hole UE-25 RF#14 (Sheet 4 of 11)	1.1-445
1.1-96. Geologic Log of Drill Hole UE-25 RF#14 (Sheet 5 of 11)	1.1-446
1.1-96. Geologic Log of Drill Hole UE-25 RF#14 (Sheet 6 of 11)	1.1-447
1.1-96. Geologic Log of Drill Hole UE-25 RF#14 (Sheet 7 of 11)	1.1-448
1.1-96. Geologic Log of Drill Hole UE-25 RF#14 (Sheet 8 of 11)	1.1-449
1.1-96. Geologic Log of Drill Hole UE-25 RF#14 (Sheet 9 of 11)	1.1-450
1.1-96. Geologic Log of Drill Hole UE-25 RF#14 (Sheet 10 of 11)	1.1-451
1.1-96. Geologic Log of Drill Hole UE-25 RF#14 (Sheet 11 of 11)	1.1-452
1.1-97. Geologic Log of Drill Hole UE-25 RF#15 (Sheet 1 of 7)	1.1-453
1.1-97. Geologic Log of Drill Hole UE-25 RF#15 (Sheet 2 of 7)	1.1-454
1.1-97. Geologic Log of Drill Hole UE-25 RF#15 (Sheet 3 of 7)	1.1-455
1.1-97. Geologic Log of Drill Hole UE-25 RF#15 (Sheet 4 of 7)	1.1-456
1.1-97. Geologic Log of Drill Hole UE-25 RF#15 (Sheet 5 of 7)	1.1-457
1.1-97. Geologic Log of Drill Hole UE-25 RF#15 (Sheet 6 of 7)	1.1-458
1.1-97. Geologic Log of Drill Hole UE-25 RF#15 (Sheet 7 of 7)	1.1-459
1.1-98. Geologic Log of Drill Hole UE-25 RF#16 (Sheet 1 of 9)	1.1-460
1.1-98. Geologic Log of Drill Hole UE-25 RF#16 (Sheet 2 of 9)	1.1-461
1.1-98. Geologic Log of Drill Hole UE-25 RF#16 (Sheet 3 of 9)	1.1-462
1.1-98. Geologic Log of Drill Hole UE-25 RF#16 (Sheet 4 of 9)	1.1-463
1.1-98. Geologic Log of Drill Hole UE-25 RF#16 (Sheet 5 of 9)	1.1-464
1.1-98. Geologic Log of Drill Hole UE-25 RF#16 (Sheet 6 of 9)	1.1-465
1.1-98. Geologic Log of Drill Hole UE-25 RF#16 (Sheet 7 of 9)	1.1-466
1.1-98. Geologic Log of Drill Hole UE-25 RF#16 (Sheet 8 of 9)	1.1-467
1.1-98. Geologic Log of Drill Hole UE-25 RF#16 (Sheet 9 of 9)	1.1-468
1.1-99. Geologic Log of Drill Hole UE-25 RF#17 (Sheet 1 of 13)	1.1-469
1.1-99. Geologic Log of Drill Hole UE-25 RF#17 (Sheet 2 of 13)	1.1-470
1.1-99. Geologic Log of Drill Hole UE-25 RF#17 (Sheet 3 of 13)	1.1-471

FIGURES (Continued)

	Page
1.1-99. Geologic Log of Drill Hole UE-25 RF#17 (Sheet 4 of 13)	1.1-472
1.1-99. Geologic Log of Drill Hole UE-25 RF#17 (Sheet 5 of 13)	1.1-473
1.1-99. Geologic Log of Drill Hole UE-25 RF#17 (Sheet 6 of 13)	1.1-474
1.1-99. Geologic Log of Drill Hole UE-25 RF#17 (Sheet 7 of 13)	1.1-475
1.1-99. Geologic Log of Drill Hole UE-25 RF#17 (Sheet 8 of 13)	1.1-476
1.1-99. Geologic Log of Drill Hole UE-25 RF#17 (Sheet 9 of 13)	1.1-477
1.1-99. Geologic Log of Drill Hole UE-25 RF#17 (Sheet 10 of 13)	1.1-478
1.1-99. Geologic Log of Drill Hole UE-25 RF#17 (Sheet 11 of 13)	1.1-479
1.1-99. Geologic Log of Drill Hole UE-25 RF#17 (Sheet 12 of 13)	1.1-480
1.1-99. Geologic Log of Drill Hole UE-25 RF#17 (Sheet 13 of 13)	1.1-481
1.1-100. Geologic Log of Drill Hole UE-25 RF#18 (Sheet 1 of 6)	1.1-482
1.1-100. Geologic Log of Drill Hole UE-25 RF#18 (Sheet 2 of 6)	1.1-483
1.1-100. Geologic Log of Drill Hole UE-25 RF#18 (Sheet 3 of 6)	1.1-484
1.1-100. Geologic Log of Drill Hole UE-25 RF#18 (Sheet 4 of 6)	1.1-485
1.1-100. Geologic Log of Drill Hole UE-25 RF#18 (Sheet 5 of 6)	1.1-486
1.1-100. Geologic Log of Drill Hole UE-25 RF#18 (Sheet 6 of 6)	1.1-487
1.1-101. Geologic Log of Drill Hole UE-25 RF#19 (Sheet 1 of 7)	1.1-488
1.1-101. Geologic Log of Drill Hole UE-25 RF#19 (Sheet 2 of 7)	1.1-489
1.1-101. Geologic Log of Drill Hole UE-25 RF#19 (Sheet 3 of 7)	1.1-490
1.1-101. Geologic Log of Drill Hole UE-25 RF#19 (Sheet 4 of 7)	1.1-491
1.1-101. Geologic Log of Drill Hole UE-25 RF#19 (Sheet 5 of 7)	1.1-492
1.1-101. Geologic Log of Drill Hole UE-25 RF#19 (Sheet 6 of 7)	1.1-493
1.1-101. Geologic Log of Drill Hole UE-25 RF#19 (Sheet 7 of 7)	1.1-494
1.1-102. Geologic Log of Drill Hole UE-25 RF#20 (Sheet 1 of 3)	1.1-495
1.1-102. Geologic Log of Drill Hole UE-25 RF#20 (Sheet 2 of 3)	1.1-496
1.1-102. Geologic Log of Drill Hole UE-25 RF#20 (Sheet 3 of 3)	1.1-497
1.1-103. Geologic Log of Drill Hole UE-25 RF#21 (Sheet 1 of 3)	1.1-498
1.1-103. Geologic Log of Drill Hole UE-25 RF#21 (Sheet 2 of 3)	1.1-499
1.1-103. Geologic Log of Drill Hole UE-25 RF#21 (Sheet 3 of 3)	1.1-500
1.1-104. Geologic Log of Drill Hole UE-25 RF#22 (Sheet 1 of 6)	1.1-501
1.1-104. Geologic Log of Drill Hole UE-25 RF#22 (Sheet 2 of 6)	1.1-502
1.1-104. Geologic Log of Drill Hole UE-25 RF#22 (Sheet 3 of 6)	1.1-503
1.1-104. Geologic Log of Drill Hole UE-25 RF#22 (Sheet 4 of 6)	1.1-504
1.1-104. Geologic Log of Drill Hole UE-25 RF#22 (Sheet 5 of 6)	1.1-505
1.1-104. Geologic Log of Drill Hole UE-25 RF#22 (Sheet 6 of 6)	1.1-506
1.1-105. Geologic Log of Drill Hole UE-25 RF#23 (Sheet 1 of 3)	1.1-507
1.1-105. Geologic Log of Drill Hole UE-25 RF#23 (Sheet 2 of 3)	1.1-508
1.1-105. Geologic Log of Drill Hole UE-25 RF#23 (Sheet 3 of 3)	1.1-509
1.1-106. Geologic Log of Drill Hole UE-25 RF#24 (Sheet 1 of 4)	1.1-510
1.1-106. Geologic Log of Drill Hole UE-25 RF#24 (Sheet 2 of 4)	1.1-511
1.1-106. Geologic Log of Drill Hole UE-25 RF#24 (Sheet 3 of 4)	1.1-512
1.1-106. Geologic Log of Drill Hole UE-25 RF#24 (Sheet 4 of 4)	1.1-513
1.1-107. Geologic Log of Drill Hole UE-25 RF#25 (Sheet 1 of 3)	1.1-514
1.1-107. Geologic Log of Drill Hole UE-25 RF#25 (Sheet 2 of 3)	1.1-515

FIGURES (Continued)

	Page
1.1-107. Geologic Log of Drill Hole UE-25 RF#25 (Sheet 3 of 3)	1.1-516
1.1-108. Geologic Log of Drill Hole UE-25 RF#26 (Sheet 1 of 4)	1.1-517
1.1-108. Geologic Log of Drill Hole UE-25 RF#26 (Sheet 2 of 4)	1.1-518
1.1-108. Geologic Log of Drill Hole UE-25 RF#26 (Sheet 3 of 4)	1.1-519
1.1-108. Geologic Log of Drill Hole UE-25 RF#26 (Sheet 4 of 4)	1.1-520
1.1-109. Geologic Log of Drill Hole UE-25 RF#28 (Sheet 1 of 2)	1.1-521
1.1-109. Geologic Log of Drill Hole UE-25 RF#28 (Sheet 2 of 2)	1.1-522
1.1-110. Geologic Log of Drill Hole UE-25 RF#29 (Sheet 1 of 5)	1.1-523
1.1-110. Geologic Log of Drill Hole UE-25 RF#29 (Sheet 2 of 5)	1.1-524
1.1-110. Geologic Log of Drill Hole UE-25 RF#29 (Sheet 3 of 5)	1.1-525
1.1-110. Geologic Log of Drill Hole UE-25 RF#29 (Sheet 4 of 5)	1.1-526
1.1-110. Geologic Log of Drill Hole UE-25 RF#29 (Sheet 5 of 5)	1.1-527
1.1-111. Geologic Log of Drill Hole UE-25 RF#42 (Sheet 1 of 3)	1.1-528
1.1-111. Geologic Log of Drill Hole UE-25 RF#42 (Sheet 2 of 3)	1.1-529
1.1-111. Geologic Log of Drill Hole UE-25 RF#42 (Sheet 3 of 3)	1.1-530
1.1-112. Geologic Log of Drill Hole UE-25 RF#43 (Sheet 1 of 2)	1.1-531
1.1-112. Geologic Log of Drill Hole UE-25 RF#43 (Sheet 2 of 2)	1.1-532
1.1-113. Geologic Log of Drill Hole UE-25 RF#44 (Sheet 1 of 3)	1.1-533
1.1-113. Geologic Log of Drill Hole UE-25 RF#44 (Sheet 2 of 3)	1.1-534
1.1-113. Geologic Log of Drill Hole UE-25 RF#44 (Sheet 3 of 3)	1.1-535
1.1-114. Geologic Log of Drill Hole UE-25 RF#45 (Sheet 1 of 3)	1.1-536
1.1-114. Geologic Log of Drill Hole UE-25 RF#45 (Sheet 2 of 3)	1.1-537
1.1-114. Geologic Log of Drill Hole UE-25 RF#45 (Sheet 3 of 3)	1.1-538
1.1-115. Geologic Log of Drill Hole UE-25 RF#46 (Sheet 1 of 2)	1.1-539
1.1-115. Geologic Log of Drill Hole UE-25 RF#46 (Sheet 2 of 2)	1.1-540
1.1-116. Geologic Log of Drill Hole UE-25 RF#47 (Sheet 1 of 3)	1.1-541
1.1-116. Geologic Log of Drill Hole UE-25 RF#47 (Sheet 2 of 3)	1.1-542
1.1-116. Geologic Log of Drill Hole UE-25 RF#47 (Sheet 3 of 3)	1.1-543
1.1-117. Geologic Log of Drill Hole UE-25 RF#48 (Sheet 1 of 3)	1.1-544
1.1-117. Geologic Log of Drill Hole UE-25 RF#48 (Sheet 2 of 3)	1.1-545
1.1-117. Geologic Log of Drill Hole UE-25 RF#48 (Sheet 3 of 3)	1.1-546
1.1-118. Geologic Log of Drill Hole UE-25 RF#49 (Sheet 1 of 3)	1.1-547
1.1-118. Geologic Log of Drill Hole UE-25 RF#49 (Sheet 2 of 3)	1.1-548
1.1-118. Geologic Log of Drill Hole UE-25 RF#49 (Sheet 3 of 3)	1.1-549
1.1-119. Geologic Log of Drill Hole UE-25 RF#50 (Sheet 1 of 3)	1.1-550
1.1-119. Geologic Log of Drill Hole UE-25 RF#50 (Sheet 2 of 3)	1.1-551
1.1-119. Geologic Log of Drill Hole UE-25 RF#50 (Sheet 3 of 3)	1.1-552
1.1-120. Geologic Log of Drill Hole UE-25 RF#51 (Sheet 1 of 3)	1.1-553
1.1-120. Geologic Log of Drill Hole UE-25 RF#51 (Sheet 2 of 3)	1.1-554
1.1-120. Geologic Log of Drill Hole UE-25 RF#51 (Sheet 3 of 3)	1.1-555
1.1-121. Geologic Log of Drill Hole UE-25 RF#52 (Sheet 1 of 3)	1.1-556
1.1-121. Geologic Log of Drill Hole UE-25 RF#52 (Sheet 2 of 3)	1.1-557
1.1-121. Geologic Log of Drill Hole UE-25 RF#52 (Sheet 3 of 3)	1.1-558
1.1-122. Geologic Log of Drill Hole UE-25 RF#53 (Sheet 1 of 3)	1.1-559

FIGURES (Continued)

	Page
1.1-122. Geologic Log of Drill Hole UE-25 RF#53 (Sheet 2 of 3)	1.1-560
1.1-122. Geologic Log of Drill Hole UE-25 RF#53 (Sheet 3 of 3)	1.1-561
1.1-123. Geologic Log of Drill Hole UE-25 RF#54 (Sheet 1 of 4)	1.1-562
1.1-123. Geologic Log of Drill Hole UE-25 RF#54 (Sheet 2 of 4)	1.1-563
1.1-123. Geologic Log of Drill Hole UE-25 RF#54 (Sheet 3 of 4)	1.1-564
1.1-123. Geologic Log of Drill Hole UE-25 RF#54 (Sheet 4 of 4)	1.1-565
1.1-124. Geologic Log of Drill Hole UE-25 RF#55 (Sheet 1 of 3)	1.1-566
1.1-124. Geologic Log of Drill Hole UE-25 RF#55 (Sheet 2 of 3)	1.1-567
1.1-124. Geologic Log of Drill Hole UE-25 RF#55 (Sheet 3 of 3)	1.1-568
1.1-125. Geologic Log of Drill Hole UE-25 RF#56 (Sheet 1 of 5)	1.1-569
1.1-125. Geologic Log of Drill Hole UE-25 RF#56 (Sheet 2 of 5)	1.1-570
1.1-125. Geologic Log of Drill Hole UE-25 RF#56 (Sheet 3 of 5)	1.1-571
1.1-125. Geologic Log of Drill Hole UE-25 RF#56 (Sheet 4 of 5)	1.1-572
1.1-125. Geologic Log of Drill Hole UE-25 RF#56 (Sheet 5 of 5)	1.1-573
1.1-126. Geologic Log of Drill Hole UE-25 RF#58 (Sheet 1 of 3)	1.1-574
1.1-126. Geologic Log of Drill Hole UE-25 RF#58 (Sheet 2 of 3)	1.1-575
1.1-126. Geologic Log of Drill Hole UE-25 RF#58 (Sheet 3 of 3)	1.1-576
1.1-127. Geologic Log of Drill Hole UE-25 RF#59 (Sheet 1 of 4)	1.1-577
1.1-127. Geologic Log of Drill Hole UE-25 RF#59 (Sheet 2 of 4)	1.1-578
1.1-127. Geologic Log of Drill Hole UE-25 RF#59 (Sheet 3 of 4)	1.1-579
1.1-127. Geologic Log of Drill Hole UE-25 RF#59 (Sheet 4 of 4)	1.1-580
1.1-128. Geologic Log of Drill Hole UE-25 RF#60 (Sheet 1 of 4)	1.1-581
1.1-128. Geologic Log of Drill Hole UE-25 RF#60 (Sheet 2 of 4)	1.1-582
1.1-128. Geologic Log of Drill Hole UE-25 RF#60 (Sheet 3 of 4)	1.1-583
1.1-128. Geologic Log of Drill Hole UE-25 RF#60 (Sheet 4 of 4)	1.1-584
1.1-129. Repository Facilities Borehole and Test Pit Locations	1.1-585
1.1-130. Alluvium Thickness Contour Map of Midway Valley	1.1-586
1.1-131. Comparison of Original and Updated Shear Modulus and Hysteretic Damping Curves for Tuff	1.1-587
1.1-132. Comparison of Original and Updated Shear Modulus and Hysteretic Damping Curves for Surface GROA Alluvium	1.1-588
1.1-133. 2004 and 2007 Smoothed Surface GROA Base Case V_s Profiles for Tuff	1.1-589
1.1-134. Spectral Analysis of Surface Waves Surveys in the Vicinity of the Repository Block	1.1-590
1.1-135. Comparison of 2004 and 2007 Smoothed Repository Block Base Case V_s Profiles	1.1-591
1.1-136. Individual Profiles and Statistical Analysis of 24 Spectral Analysis of Surface Wave Tests Performed Around the Mountain Area	1.1-592
1.1-137. Individual Profiles and Statistical Analysis of 18 Spectral Analysis of Surface Wave Tests Performed Around the Mountain Area	1.1-593
1.1-138. Distribution of V_s Velocities from Spectral Analysis of Surface Wave Testing by Geologic Unit	1.1-594

FIGURES (Continued)

	Page
1.1-139. Distribution of Spectral Analysis Of Surface Wave Velocities by Underground Geologic Units	1.1-595
1.1-140. Comparison of V_S Ranges between Surface and Tunnel Spectral Analysis of Surface Wave Test Sites Based on Geologic Units.	1.1-596
1.1-141. Location of Pre-2004 Geophysical Surveys Relative to the Surface Geologic Repository Operations Area	1.1-597
1.1-142. Spectral Analysis of Surface Waves Testing in the Vicinity of the Surface GROA in 2004 and 2005	1.1-599
1.1-143. Individual Profiles and Statistical Analyses of 18 Spectral Analysis of Surface Waves Tests Performed in the Vicinity of the Surface GROA	1.1-600
1.1-144. Individual Profiles and Statistical Analyses of Spectral Analysis of Surface Waves Tests Performed at Surface GROA Without Site NPF 28 and Without Bottom Portions of V_S profiles for Sites NPF 2 and 14 and NPF 3 and 9 below 900 ft.	1.1-601
1.1-145. Locations of Pre-2004 Boreholes and Test Pits Relative to the Surface Geologic Repository Operations Area	1.1-603
1.1-146. Variation of Shear Wave Velocity with Total Unit Weight of the Thirty-Three Tuff Specimens from Stratigraphic Units below Tiva Canyon Tuff; V_S Measured at the Unconfined State in the Resonant Column Test	1.1-605
1.1-147. Summary Profile of Shear Wave Velocity versus Depth from Free-Free Resonant Column Tests	1.1-606
1.1-148. Summary Profile of Unconstrained Compression Wave Velocity versus Depth from Free-Free Resonant Column Tests	1.1-607
1.1-149. Summary Profile of Constrained Compression Wave Velocity versus Depth from Free-Free Resonant Column Tests	1.1-608
1.1-150. Summary Profile of Material Damping Ratio in Shear versus Depth from Free-Free Resonant Column Tests.	1.1-609
1.1-151. Summary Profile of Material Damping Ratio in Unconstrained Compression versus Depth from Free-Free Resonant Column Tests.	1.1-610
1.1-152. Miocene and Post-Miocene Basaltic Vent Locations in the Yucca Mountain Region	1.1-611
1.1-153. Locations of Boreholes Used for Characterizing Subsurface Mineralogy	1.1-612
1.1-154. Yucca Mountain Repository Proposed Land Withdrawal Area	1.1-613
1.1-155. Yucca Mountain Structures and Facilities	1.1-615

INTENTIONALLY LEFT BLANK

1.1 SITE DESCRIPTION AS IT PERTAINS TO PRECLOSURE SAFETY ANALYSIS

The information presented in this section addresses the requirements of 10 CFR 63.21(c)(1) by providing a general description of the geologic repository operations area (GROA) and vicinity, thereby addressing the requirements of 10 CFR 63.112(c). This section also provides information that addresses specific acceptance criteria in Section 2.1.1.1.3 of NUREG-1804. The following table lists the categories of information provided in this section, as well as the corresponding regulatory requirements and the acceptance criteria from NUREG-1804.

SAR Section	Information Category	10 CFR 63 Reference	NUREG-1804 Reference
1.1.1	Site Geography	63.21(c)(1)(i) 63.112(c)	Section 2.1.1.1.3: Acceptance Criterion 1 Section 2.1.1.2.3: Acceptance Criterion 1(1)
1.1.2	Regional Demography	63.21(c)(1)(i) 63.112(c)	Section 2.1.1.1.3: Acceptance Criterion 2
1.1.3	Local Meteorology and Regional Climatology	63.21(c)(1)(iii) 63.112(c)	Section 2.1.1.1.3: Acceptance Criterion 3
1.1.4	Regional and Local Surface and Groundwater Hydrology	63.21(c)(1)(ii) 63.112(c)	Section 2.1.1.1.3: Acceptance Criterion 4
1.1.5	Site Geology and Seismology	63.21(c)(1)(ii) 63.112(c)	Section 2.1.1.1.3: Acceptance Criterion 5 Section 2.1.1.7.3.2: Acceptance Criterion 1
1.1.6	Igneous Activity	63.21(c)(1) 63.112(c)	Section 2.1.1.1.3: Acceptance Criterion 6
1.1.7	Site Geomorphology	63.21(c)(1) 63.112(c)	Section 2.1.1.1.3: Acceptance Criterion 7
1.1.8	Geochemistry	63.21(c)(1)(ii) 63.112(c)	Section 2.1.1.1.3: Acceptance Criterion 8
1.1.9	Land Use, Structures and Facilities, and Residual Radioactivity	63.21(c)(1) 63.112(c)	Section 2.1.1.1.3: Acceptance Criterion 9

1.1.1 Site Geography

[NUREG-1804, Section 2.1.1.1.3: AC 1; Section 2.1.1.2.3: AC 1(1)]

This section describes geographic information relevant to development of the design, as well as potential hazards and initiating events that are important to safety (ITS) during the preclosure period. It summarizes site-specific and regional geographic data that have been used to quantify the expected magnitude, frequency, and duration of these potential hazards and initiating events. Section 1.6 evaluates the potential hazards and initiating events. This section provides a description of the site location relative to prominent natural and man-made features and to potentially hazardous

commercial operations and manufacturing centers that may be relevant to the preclosure safety analysis (PCSA) and to the design of the GROA.

[Section 1.1.1.1](#) provides information on the locations of surface facilities; boundaries of the GROA, site, and controlled area; and distances from these boundaries to features of the repository that are used in the PCSA.

[Section 1.1.1.2](#) includes a description of natural features that may be relevant for evaluation in the PCSA and to the design of the GROA.

[Section 1.1.1.3](#) includes a description of man-made features that may be relevant to the PCSA and for the design of the GROA.

1.1.1.1 Repository Boundaries

[NUREG-1804, Section 2.1.1.1.3: AC 1(3)]

1.1.1.1.1 Site

The site is located within the boundary of the proposed land withdrawal area and includes the GROA. The U.S. Department of Energy (DOE) exercises authority over land use within the boundary of the proposed land withdrawal area. [Figure 1.1-1](#) shows the site boundary, which encloses the proposed land withdrawal area. The land withdrawal area is intended to be the site at licensing. The relationship of site boundaries to preclosure performance objectives is discussed in [Section 1.8](#).

1.1.1.1.2 Controlled Area

The controlled area differs between the preclosure and postclosure periods. 10 CFR 63.302 provides a definition of controlled area for the postclosure period. For the preclosure period, and in accordance with the definition of 10 CFR 20.1003, the controlled area is the area outside of a restricted area inside the site boundary. [Figure 1.1-1](#) shows the site boundary and the preclosure controlled area. [Section 2.4](#) discusses the postclosure controlled area.

1.1.1.1.3 General Environment

10 CFR 63.202 defines the general environment as “everywhere outside the Yucca Mountain site, the Nellis Air Force Range, and the Nevada Test Site.” The Nellis Air Force Range has been renamed as the Nevada Test and Training Range. For the purpose of this SAR, the general environment is considered everywhere outside of the Yucca Mountain site, the Nevada Test and Training Range, and the Nevada Test Site ([Figure 1.1-1](#)).

1.1.1.1.4 Geologic Repository Operations Area

The GROA is the high-level radioactive waste facility that is part of a geologic repository, including both surface and subsurface areas, where waste-handling activities are conducted. A protected area is an area encompassed by physical barriers and to which access is controlled. The boundary of the

protected area will be a physical barrier as defined in 10 CFR 73.2. Waste handling will occur only within the protected area of the GROA.

A restricted area is an area to which access is limited by the licensee for the purpose of protecting individuals against undue risks from exposure to radiation and radioactive materials. The boundary of the restricted area will encompass not only the protected area but also will extend beyond the protected area barrier in the vicinity of the aging pads. The boundary of the surface GROA will encompass both the protected area and the restricted area.

The size of the GROA will change over time, coincident with the phased development of the surface and subsurface facilities. [Figure 1.1-2](#) shows the boundaries of the maximum expected extent of the GROA and locations of surface facilities. [Figure 1.1-3](#) illustrates the phased development and the associated changes of the protected area, the restricted area, and the surface GROA. Phased development of the subsurface facility is discussed in [Section 1.3.1.2.7](#) and illustrated in [Figure 1.3.1-1](#). Descriptions of surface facilities and their functions are provided in [Section 1.2.1](#).

1.1.1.1.5 Control Points

The DOE, as described in [Section 5.8](#), has the authority to determine activities within the preclosure controlled area, including exclusion or removal of personnel and property from the area. The preclosure controlled area will be demarcated but does not require physical barriers at the boundaries. There are three access control points planned for the restricted area, shown as facilities 30A, B, and C in [Figure 1.1-2](#).

1.1.1.2 Natural Features

[NUREG-1804, Section 2.1.1.1.3: AC 1(1), (2), (3)]

Yucca Mountain is located on federal land in a remote area of Nye County in southern Nevada. The Yucca Mountain site is approximately 130 km northwest of Las Vegas ([Figure 1.1-4](#)). Yucca Mountain is an irregularly shaped upland area 3 to 8 km wide and about 35 km long (BSC 2004a, Section 3.2.1.1). Above the repository, the crest of Yucca Mountain is 1,400 to 1,500 m above sea level. The western part of the repository vicinity is a steep slope that rises approximately 300 m above the base of Solitario Canyon. On the eastern side, the mountain slopes gently to the east and is incised by a series of east- to southeast-trending stream channels. The elevation at the base of the eastern slope is approximately 350 to 450 m below the ridge crest (DOE 2002a, Section 1.3.2.1).

The surface facilities located on the GROA are situated on the east side of Exile Hill in Midway Valley at the eastern margin of Yucca Mountain. [Figure 1.1-5](#) shows the topography in the immediate vicinity of the repository. Elevations of the Midway Valley floor range from about 1,070 m at its low point between Alice Hill and Fran Ridge in the east to about 1,220 m in the northwestern part of the valley. To the west and northwest, along the east slope of Yucca Mountain, drainage basins heading in Antler, Split, Drill Hole, Pagany, Sever, and Yucca washes channel flow eastward across Midway Valley into Fortymile Wash ([Figure 1.1-5](#)). Antler Wash drains into Midway Valley through a gap between Bow Ridge and Opal Hill. Split Wash and Drill Hole Wash drain into Midway Valley through a gap to the south of Exile Hill between Exile Hill and Opal Hill. Pagany Wash and Sever Wash drain into Midway Valley to the north of Exile Hill. These washes, and an unnamed drainage exiting the southern part of the canyon containing Yucca Wash, merge and

drain into Fortymile Wash through a gap between Fran Ridge and Alice Hill. Yucca Wash crosses the northern end of Midway Valley to drain into Fortymile Wash through a gap north of Alice Hill.

No perennial streams, natural bodies of water, or naturally occurring wetlands occur on the Yucca Mountain site (DOE 2002b, Sections 3.1.4.1.2 and 3.1.5.1.4). There are no navigable waterways and no potential for commercial water-based transportation.

1.1.1.3 Man-Made Features

[NUREG-1804, Section 2.1.1.1.3: AC 1(1), (2), (3)]

This section provides information relative to the locations and activities at prominent man-made features, such as federal facilities, military facilities, civilian airports, military airports, roads, railroads, and potentially hazardous commercial operations and manufacturing centers that may be relevant to the PCSA and to the design of the GROA. Sections 1.2 through 1.4 discuss planned man-made features within the controlled area. Section 1.1.2.2 discusses population centers. Section 1.1.9.3 discusses existing man-made structures and facilities within the proposed land withdrawal area.

The land withdrawal for the repository establishes a buffer zone that provides a minimum standoff distance from activities on the Nevada Test Site. It is approximately 5 mi from the North Portal to the closest point on the site boundary with the Nevada Test Site, and the surface GROA is more than 4 mi from the site boundary with the Nevada Test Site (Figure 1.1-6). Section 5.8 discusses controls to restrict access to the GROA and regulate land use.

1.1.1.3.1 Nevada Test Site

The Nevada Test Site (Figure 1.1-6) is approximately 1,375 mi² and is one of the largest restricted access areas in the United States. The Nevada Test Site was established as the Atomic Energy Commission on-continent proving ground. Nuclear weapons have been tested there for more than four decades. These nuclear detonations were conducted in Areas 1, 2, 3, 4, 5, 6, 7, 8, 9, 10, 11, 12, 15, 16, 18, 19, 20, and 30. The closest point of these areas to the surface GROA is approximately 9 mi away at Area 30 (Figure 1.1-6). A single test, Project Buggy, was conducted in Area 30. This was an experiment in the Plowshare Program designed to demonstrate cratering effects of nuclear explosions. The most common method of weapons testing was either in vertical drill holes or in underground tunnels (DOE 1996, Section 4.1.1.2). Since the nuclear weapons testing moratorium in 1992, and under the direction of the DOE National Nuclear Security Administration, use of the Nevada Test Site has diversified into many other programs, such as chemical-spill testing, emergency-response training, conventional-weapons testing, waste management, and environmental-technology studies (BSC 2008a, Section 6.3.1).

1.1.1.3.1.1 Defense Program

Stockpile Stewardship—Stockpile stewardship includes experimentation that ensures the safety, reliability, and performance of the nation's nuclear stockpile. There is a possibility, at the direction of the President of the United States, of a limited return to underground nuclear testing. Yucca Flat (Area 6) and Pahute Mesa (Areas 19 and 20) are the locations considered for these tests (DOE 1996, Section 3.1.1.1). The potential effect from underground nuclear weapons testing includes

ground motions imparted to the repository during such a test. Evaluation of nuclear weapons testing data demonstrated that ground motions at Yucca Mountain from nuclear tests have been at levels lower than would be expected from moderate to large earthquakes in the region. Thus, nuclear tests would not be the controlling seismic criteria (BSC 2008a, Section 6.3.1).

In addition to direct ground-motion effects of underground nuclear explosions, there is also a potential hazard from secondary seismic effects. However, such effects have not been seen at distances greater than 6 mi (BSC 2008a, Section 6.3.1).

The Device Assembly Facility in Area 6, located more than 20 mi from the repository, is a facility designed to allow nuclear devices, experimental components, and high explosives to be safely assembled, disassembled or modified, staged, and component tested (Figure 1.1-6). This facility is constructed primarily of heavy steel-reinforced concrete. The facility has a minimum of 5 ft of compacted earth overlay, leaving only one exterior wall. Assembly cells are designed to absorb the energy of an explosive blast to prevent propagation of the explosion into other structures within the facility. Each assembly cell design was tested to undergo an explosion from a maximum high-explosive device without injury to personnel outside of the cell. This design reduces the potential effects that could occur during an accident (BSC 2008a, Section 6.3.1).

The Nevada Test Site was one of five candidate sites considered for construction of a plutonium pit facility when the National Nuclear Security Administration announced its intention to prepare a supplement to the programmatic environmental impact statement for a Modern Pit Facility (DOE 2003a). On January 28, 2004, the DOE National Nuclear Security Administration announced that it was indefinitely postponing any decision on how it would obtain a large capacity pit manufacturing facility. The DOE National Nuclear Security Administration is now planning to prepare a *Supplement to the Stockpile Stewardship and Management Programmatic Environmental Impact Statement—Complex 2030*. Because this supplement will analyze alternatives for plutonium-related activities that include pit production, the DOE canceled the Modern Pit Facility Programmatic Environmental Impact Statement (71 FR 61731).

The Nevada Test Site was selected for relocation of materials and equipment from Technical Area 18 of the Los Alamos National Laboratory. Principal activities conducted at Technical Area 18 involve research in and the design, development, construction, and application of experiments on nuclear criticality (67 FR 79906). The western section of the Device Assembly Facility located in Area 6 is now designated the Criticality Experiments Facility (Figure 1.1-6) and is being retrofitted and reconfigured to accommodate the materials and equipment from Technical Area 18 (DOE 2005a).

The Big Explosives Experimental Facility is located in Area 4 (Figure 1.1-6), more than 20 mi from the repository. It consists of two underground bunkers, one aboveground structure containing primary diagnostic facilities (including radiography), and three blast-protective enclosures allowing for diagnostic assessment equipment. The facility is capable of up to a 70,000 lb TNT-equivalent physics experiment, providing for the study and investigation of explosive characteristics, impacted materials, and high-explosives pulsed power (DOE 2002c, Section 3.1.1.2).

The JASPER (“Joint Actinide Shock Physics Experimental Research”) facility is located at the former nuclear explosives assembly facility in Area 27 (DOE 2002c, Section 3.1.1.2) (Figure 1.1-6), about 20 mi from the repository. The JASPER facility conducts shock physics experiments on special nuclear materials and other actinide materials using a two-stage, light-gas gun to shoot projectiles at target materials. A high-energy electrical pulse ignites a propellant in the breech of the gun. Hot gases from the burning propellant drive a piston down a pump tube, compressing the low-molecular-weight gas. At a predetermined pressure, the gas breaks a rupture valve and enters the narrow barrel, propelling a projectile housed in the barrel toward the target. The projectile impacts the target, producing a high-pressure shock wave that excites and propagates through the target. Diagnostic equipment measures properties of the shocked material inside the target. The JASPER facility is categorized as a radiological facility because of radionuclides used as target materials in experiments (BSC 2008a, Section 6.3.1).

The Nevada Energetic Materials Operations Facility is a staging and storage facility for explosives used at the Big Explosives Experimental Facility and the JASPER facility. The Nevada Energetic Materials Operations Facility is located at Baker Site (Figure 1.1-6) of the former nuclear explosives assembly facility in Area 27 (DOE 2002c, Section 3.1.1.2), about 20 mi from the repository.

The U1a complex, located west of the Mercury Highway in Yucca Flat in Area 1, is more than 20 mi from the repository (Figure 1.1-6). The U1a complex consists of shafts approximately 960 ft deep and connecting mined tunnels. Dynamic experiments performed in this facility may include the use of special nuclear materials, but the experiments remain subcritical, meaning that no self-sustaining nuclear reaction occurs (BSC 2008a, Section 6.3.1).

The Atlas pulsed power facility is located in a building within Area 6 (Figure 1.1-6), more than 20 mi from the repository, and was successfully tested on July 27, 2005 (NNSA 2005). The Atlas pulsed-power system is designed to deliver a pulse of very high electrical current through a high-precision cylindrical metal liner that surrounds the sample of interest. The current produces a brief but powerful magnetic force on the liner, which implodes upon the sample. The behavior of the target material is observed by the use of diagnostic x-rays and lasers beamed through line-of-sight, evacuated tubes that connect to ports on the target chamber (DOE 2002c, Section 3.1.1.2).

Nuclear Emergency Response—The nuclear emergency response activities include (DOE 2002c, Table 3-1):

- Nuclear Emergency Support Team
- Consequence management
- Aerial measuring system
- Accident response group
- Radiological assistance program
- Internal emergency management program.

These nuclear emergency response activities are principally performed in response to accidents or nuclear emergencies (DOE 1996, Section A.1.1.3). Activities involving aircraft are discussed in the aircraft hazard analysis (Section 1.6).

Nuclear Weapons Disposition Program in G-Tunnel—The U-12g Tunnel, also known as G-Tunnel, is located about 25 mi from the repository in Area 12 of the Nevada Test Site (Figure 1.1-6). For the nuclear weapons disposition program, G-Tunnel is being rehabilitated to make the tunnel safe for the programs and infrastructure necessary to safely dispose of a damaged nuclear weapon or improvised nuclear device (DOE 2002c, Section 3.1.1.2).

1.1.1.3.1.2 Waste Management Program

Area 3 Radioactive Waste Management Site—Area 3 waste management operations consist of subsidence craters created from underground nuclear weapons tests (Figure 1.1-6) more than 20 mi from the repository. Bulk and large-packaged low-level radioactive waste is disposed of in these subsidence craters (BSC 2008a, Section 6.3.1).

Area 5 Radioactive Waste Management Complex—The Area 5 waste management facilities, which are more than 20 mi from the repository (Figure 1.1-6), dispose of low-level radioactive waste by burial in excavated pits and trenches and process transuranic waste to ensure it is compliant with waste acceptance criteria prior to shipment to the Waste Isolation Pilot Plant for disposal. The transuranic waste is stored in the transuranic pad cover building in metal drums, boxes, and other metal containers (DOE 2002c, Section 3.1.2). Transport vehicles will be at least 7 miles from the repository surface facilities (BSC 2008a, Section 6.3.5).

Area 5 Hazardous Waste Storage Unit—The Area 5 Hazardous Waste Storage Unit is located adjacent to the Area 5 Radioactive Waste Management Complex more than 20 mi from the repository. It is a prefabricated, rigid steel-framed, roofed shelter on a concrete pad used to store hazardous nonradioactive waste generated on the Nevada Test Site. Hazardous waste remains at this facility prior to shipment to an offsite, permitted treatment or disposal facility. Explosives are not permitted to be stored at this facility (Nevada Division of Environmental Protection 2000a; DOE 2002c, Section 3.1.2). Transport vehicles will be at least 7 mi from the repository surface facilities (BSC 2008a, Section 6.3.5).

Area 6 Waste-Management Operations—Waste-management operations occur at various areas in Area 6, more than 20 mi from the repository. The hydrocarbon landfill is a Class II disposal site permitted by the State of Nevada (BSC 2008a, Section 6.3.1).

Area 11 Explosive Ordnance Disposal Unit—The Area 11 Explosive Ordnance Disposal Unit is a thermal treatment unit (Figure 1.1-6) located more than 20 mi from the repository. Explosive ordnance wastes, regulated as characteristic reactive hazardous wastes under the Resource Conservation and Recovery Act of 1976, are detonated at the Explosive Ordnance Disposal Unit. The Explosive Ordnance Disposal Unit was first used in 1965 and continues to operate as a permitted Resource Conservation and Recovery Act treatment unit (BSC 2008a, Section 6.3.1).

The Explosive Ordnance Disposal Unit consists of a detonation pit surrounded by an earthen pad, approximately 25 by 100 ft, and ancillary equipment, including a bunker and an electric shock box. The Explosive Ordnance Disposal Unit has a maximum operating capacity to treat 45 kg/hr or an annual capacity of 1,873 kg (DOE 1996, Section A.2.1.4).

1.1.1.3.1.3 Environmental Restoration Program

Environmental restoration is the process by which contaminated DOE sites and facilities are identified and characterized, and how existing contamination is contained or removed and disposed to allow beneficial reuse of the property. Toxic materials from this program are not transported in the vicinity of the repository (DOE 1996, Section A.3). Controlled explosive demolition has been used in the demolition of part of Test Cell A (Figure 1.1-6) and is being considered for use in demolition of other facilities that were part of the nuclear rocket development program (Kruzic et al. 2007). As discussed in Section 1.1.9.2.2, these facilities are located outside of the proposed land withdrawal area and are more than 5 mi from the GROA.

1.1.1.3.1.4 Nondefense Research and Development Program

Alternative Energy—A solar energy enterprise facility has been proposed by a consortium of federal, state, and local entities and the solar power industry. Proposed technologies for the facility include photovoltaic systems, parabolic trough solar thermal systems, power tower systems, and parabolic dish systems (BSC 2008a, Section 6.3.1).

Nonproliferation Test and Evaluation Complex—The DOE Nonproliferation Test and Evaluation Complex (formerly known as the Hazardous Materials Spill Center and, before that, as the Spill Test Facility) is located approximately 25 mi from the repository in Area 5 on the eastern edge of the Nevada Test Site (Figure 1.1-6). This facility is designed to test large- and small-scale releases of hazardous and toxic materials and biological simulants in a controlled environment. The facility is available to private companies to conduct experiments. Most of the tests are performed when wind is blowing to the northeast, from a bearing of 225°. This bearing is allowed to vary up to 90° for small tests (DOE 1994, Section 1.2.4.1; DOE 2004a).

The release of biological simulants and low concentrations of chemicals is also permitted at various locations within the Nevada Test Site. Releases are also conducted at Test Cell C in Area 25 (Figure 1.1-6) in addition to releases at the Nonproliferation Test and Evaluation Complex (Wills 2005, Section 3.2.4; Wills 2006, Section 3.2.5).

Test plans for proposed releases are reviewed by the Nonproliferation Test and Evaluation Complex Project Advisory Panel. Only after review and approval of the test plan by the panel is the customer allowed to conduct a release (DOE 2004a).

Six biological species have been approved as simulants for biological agents. These organisms are not typically classified as human pathogens and were selected based on their documented lack of toxicity to healthy humans. Releases are conducted in areas and under conditions that preclude exposure of noninvolved workers and the public. Sufficient time is allowed between biological simulant releases conducted in the same area for the recovery of natural resources. Suspended aerosols of biological simulants could be released and could disperse beyond Nevada Test Site boundaries. However, given the low concentrations that would be released and rapid dispersion, the biological simulants would not be expected to be detected or differentiated from concentrations of naturally occurring organisms outside of the Nevada Test Site boundaries (DOE 2004a).

Exclusion and buffer areas are established for the chemical tests conducted outside of the Nonproliferation Test and Evaluation Complex. Access and administrative controls for personnel entering these areas during tests provide protective measures for worker exposure control. No impacts are expected to involved and noninvolved workers and members of the public (DOE 2004a).

Environmental Management and Technology Development Project—Five major remediation and waste management areas are the focus of the Environmental Management and Technology Development Project (BSC 2008a, Section 6.3.1):

- Contamination plume control and remediation
- Mixed waste characterization, treatment, and disposal
- High-level tank remediation
- Landfill stabilization
- Facility transitioning, decommissioning, and final disposition.

1.1.1.3.1.5 Work for Others Program

Treaty Verification—Treaty verification projects include (DOE 1996, Section A.5.1.1):

- The Threshold Test Ban Treaty verification project
- The Peaceful Nuclear Explosion Treaty verification project
- The Chemical Weapons Convention verification project
- The Treaty on Open Skies verification project.

There are no explosives or hazardous materials associated with the treaty verification projects (DOE 1996, Section A.5.1.1).

Nonproliferation—The policy of the United States is to resist the proliferation of weapons of mass destruction, such as nuclear, biological, and chemical weapons. In the past, seismic signatures and ground disturbances produced from underground nuclear weapons tests at the Nevada Test Site were analyzed to develop techniques and methods for detecting and evaluating underground nuclear tests worldwide. Additional nonproliferation-related experiments are currently using the unique capabilities of the Nonproliferation Test and Evaluation Complex for the development, characterization, and testing of remote sensors of chemical effluent (BSC 2008a, Section 6.3.1).

Counterproliferation Research and Development—Counterproliferation refers to the U.S. Department of Defense efforts to combat the international proliferation of weapons of mass destruction. Because facilities for the development, production, and storage of these weapons are located belowground, much of the research and development involves detection, monitoring, and neutralization of belowground targets. The tunnels and bunkers at the Nevada Test Site provide testing environments for these research activities.

Experiments for counterproliferation research and development can involve the surface and belowground detonation of conventional explosives in the vicinity of the Nevada Test Site bunkers and tunnels. Many of these activities will be performed at the Big Explosives Experimental Facility.

The activities associated with conventional high-explosives testing, surface dynamic experiments, and hydrodynamic tests are not expected to affect facilities surrounding these tests. The activities associated with conventional high-explosives testing, surface dynamic experiments, and hydrodynamic tests are located 20 or more miles away from the repository facilities (BSC 2008a, Section 6.3.1).

Conventional Weapons Demilitarization—The purpose of this program is to provide a demonstration of technologies to destroy obsolete conventional munitions. Underground tunnels and facilities at the Nevada Test Site provide the opportunity to demonstrate environmentally sound methods of destruction or treatment of weapons. Such methods include using specially designed pollution-abatement systems that remove the gaseous combustion products from the air before release to the atmosphere and provide for containment and treatment of residual debris (BSC 2008a, Section 6.3.1). X-Tunnel, about 10 mi from the GROA (Figure 1.1-6), has been used to demonstrate technologies involving destruction or treatment of solid-rocket motors and conventional munitions (Velsko et al. 1999).

Tactical Demilitarization Development Complex—The Tactical Demilitarization Development Complex is located more than 25 mi from the repository in Area 11 of the Nevada Test Site (Figure 1.1-6). This facility was developed as a prototype of a portable burn facility to dispose of unneeded tactical military rocket motors. The prototype consists of a firing chamber, an exhaust gas holder, and an emission scrubber. Emissions are controlled by a baghouse, high-efficiency particulate air filters, and ultra high-efficiency filters. This facility has not been used during 2004 and 2005 and is not intended to be used as it is expected to be removed from the Nevada Test Site air quality operating permit (Nevada Division of Environmental Protection 2000b; Wills 2005, Section 3.2.5; and Wills 2006, Section 3.2.6).

Defense-Related Research and Development—Defense-related research and development activities have included tests and training exercises employing a wide variety of weaponry, such as small arms, artillery, and guns (BSC 2008a, Section 6.3.1). These activities are located at various places in the Nevada Test Site. Some activities were located in Jackass Flats at the Army Ballistics Research Laboratory Test Range (Section 1.1.9.1.3), about 11 mi from the GROA, and at X-Tunnel (Section 1.1.9.2.1), about 10 mi from the GROA.

Weapons of Mass Destruction Work for the U.S. Department of Justice—The Nevada Test Site has been established as a U.S. Department of Justice/Office of State and Local Domestic Preparedness Support Center of Excellence for Training and Exercises. The mission is to develop and implement a national program to enhance the capacity of state and local agencies to respond to weapons of mass destruction terrorist incidents through coordinated training, equipment acquisition, technical assistance, and support for state and local exercise planning. As a result, Nevada Test Site personnel have been involved in providing training to state and local first responders at the Nevada Test Site (DOE 2002c, Section 3.1.5.2).

Defense Threat Reduction Agency Hard Target Defeat Tunnel Program—The purpose of this program is to develop and demonstrate capabilities and technologies to hold at risk and defeat military missions protected in tunnels and other deeply buried hardened facilities. The testing program demonstrates the capability to detect, identify, and characterize the target and then disrupt, neutralize, or destroy the tunnel target. The Defense Threat Reduction Agency evaluates

alternative capabilities with various platforms against a variety of different tunnel complexes constructed at the Nevada Test Site representing different geologic compositions (DOE 2002c, Section 3.1.5.2). The Defense Threat Reduction Agency tunnels are located in Area 16, about 15 mi from the repository (Figure 1.1-6).

U.S. Military Development and Training in Tactics and Procedures for Counterterrorism Threats and National Security Defense—U.S. Department of Defense organizations take advantage of the Nevada Test Site restricted access and remote high desert terrain in the west and northwest for developing realistic scenarios expected to be encountered in specific mission profiles, including (DOE 2002c, Section 3.1.5.2):

- Direct action live-fire takedown of high-fidelity target test beds
- Low-altitude fixed and rotary wing desert flight training and technique development
- Remote area advanced personnel overland navigation techniques
- Development and field testing of special-use military hardware, including new ordnance and vehicles
- Development and field testing of unmanned air vehicles
- Overland movement through rugged terrain to assess fatigue and war-fighter capability.

Aerial Operations Facility—An Aerial Operations Facility has been constructed on the southeast side of Yucca Lake in Area 6. The purpose of this facility is to construct, operate, and test a variety of unmanned aerial vehicles. Tests include, but are not limited to, airframe modifications, sensor operation, and on-board computer development. A small, manned chase plane is used to track the unmanned aerial vehicles. The facility includes an asphalt runway that is approximately 1.6 km long (DOE 2001a, Section 2.1).

1.1.1.3.1.6 Miscellaneous New Missions and Facilities

National Center for Combating Terrorism—The National Center for Combating Terrorism provides a comprehensive, coordinated, and integrated venue for combating terrorism, including research, development, testing, and evaluation exercises; training; intelligence support; and a comprehensive, fully integrated system of facilities and capabilities to meet a wide range of requirements for combating terrorism. Users include federal, state, and local agencies; institutions; and private entities involved in aspects of combating terrorism. The National Center for Combating Terrorism uses the unique capabilities of the Nevada Test Site to provide (DOE 2002c, Section 3.1.6; DOE 2003b):

- Comprehensive capabilities to support a broad range of user needs for combating terrorism
- A variety of test beds for research, development, testing, and evaluation

- A variety of facilities and scenarios for training and exercises
- The technology to capture data and develop lessons learned
- High-technology, field-ready products and services
- A remote location with restricted access.

Radiological/Nuclear Countermeasures Test and Evaluation Complex—Construction of a Radiological/Nuclear Countermeasures Test and Evaluation Complex is ongoing at the Nevada Test Site. The complex is located about 20 mi from the repository in Area 6 (Figure 1.1-6), south of the Device Assembly Facility. The purpose of the complex is to conduct testing and evaluation activities related to combating terrorism. Specifically, the complex would encompass (DOE 2004b):

- Prototype detector testing and evaluation
- Systems testing and evaluation
- Performance standards validation
- Demonstration of prototype detectors, systems, and performance standards
- Verified threat demonstration
- Concept of operations evaluation and verification
- Training.

As currently conceived, the Radiological/Nuclear Countermeasures Test and Evaluation Complex would include up to eight venues (DOE 2004b):

- Port of Entry–Primary
- Port of Entry–Secondary
- Airport Inspections Facility
- Active Interrogation Facility
- Environmental Test Facility
- Sensor Test Track
- High-Speed Road
- Training Facility.

Radioactive materials that could be used at these facilities could include up to 50 kg of highly enriched uranium and other special nuclear material components in various shapes and sizes up to several kilograms each. The special nuclear material would be solid metal and encased in nonradioactive metal cladding. Nonspecial-nuclear-material radioactive sources (also referred to as by-product material) would be in either solid or liquid form. Short half-life isotope forms of nonspecial-nuclear-material are typically used for medical purposes but would not be used for those purposes at the complex (i.e., they would not be administered to people or animals). All radioactive materials would be sealed or encased in metal cladding. None of the activities at the complex would involve the release of radioactive materials (DOE 2004b).

A source vault consisting of two portable steel armor storage magazines would be required to support operations. It is expected that the source vault would house a variety of

nonspecial-nuclear-material radioactive sealed sources. The majority of those would be small quantities of sources such as ^{60}Co , ^{137}Cs , ^{152}Eu , ^{133}Ba , ^{90}Sr , and ^{241}Am that are exempt from management under 10 CFR Part 835. In addition, accountable quantities of these sources and small quantities of uranium and plutonium would be held in the source vault. These sources would need to be readily available to personnel for checking the operation of and calibrating instruments in the complex. Special nuclear material would be stored at the Device Assembly Facility, transported to the Radiological/Nuclear Countermeasures Test and Evaluation Complex when needed, and returned to storage at the Device Assembly Facility at the completion of the activities (DOE 2004b).

The Active Interrogation Facility would provide a realistic test environment for development of active interrogation systems for the detection of highly enriched uranium, special nuclear material, or fissile materials. In addition to accelerator-produced radiation fields, a vertical shaft would be located in the middle of the integral roadway, allowing the emplacement of a high-activity neutron-emitting radionuclide. The neutron beam would be able to sweep across moving containers on the integral roadway. Shielding and exclusion areas would be established to protect personnel from receiving unsafe radiation doses. In addition, the very high radiation area would be surrounded with a chain link fence with an active interlock system for immediate accelerator shutdown if the gate is opened during operation. All radiation areas would be posted and marked. Warning lights would be active when accelerators are in operation (DOE 2004b).

Although not part of the current proposed project, future additions to the facilities could include venues such as a short length of full-scale railroad line, which would run parallel to the high-speed road; a seaport facility including transportation containers, a gantry crane, and a mock cargo ship; and a mock urban area (DOE 2004b).

1.1.1.3.1.7 Missile Launches

The last Army Tactical Missile System launch at the Nevada Test Site was conducted in Area 26 (Figure 1.1-6) in June 2000. No launches are expected in the near future, and, because this launch was the last for the program, there are no forecasts for future ground-to-ground missile testing (BSC 2007a, Section 6.5).

1.1.1.3.2 Airspace and Related Facilities and Activities

This section provides details regarding the location of and activities at airspace and related facilities in the region. A 100-mi regional area depicted in Figure 1.1-7 covers the airspace within 100 mi of the North Portal at Yucca Mountain (BSC 2007a, Section 6). Section 1.6 provides a discussion of the hazard assessment for the activities at the military and federal airspace-related facilities described in the following sections.

1.1.1.3.2.1 Nevada Test Site Airspace

With regard to airspace, a restricted area is airspace in which the flight of aircraft, while not prohibited, is subject to restrictions during scheduled periods when hazardous activities are being performed. Restricted airspace may be designated as joint use, allowing nonparticipating civil or military aircraft to be routed through this airspace by air traffic control when there is no conflict with scheduled activities. If not designated as joint use, nonparticipating aircraft are not permitted at any

time (BSC 2007a, Section 6.2.1.1). The Nevada Test Site airspace is protected by restricted areas R-4808N and R-4808S (Figure 1.1-7), known jointly as R-4808. R-4808N is designated nonjoint use by the Federal Aviation Administration, and the DOE retains exclusive, continuous control. R-4808S is a joint-use area that permits joint use by the Nevada Test Site, the Nellis Air Traffic Control Facility, and the Federal Aviation Administration Los Angeles Air Route Traffic Control Center. The Nevada Test Site airspace is controlled by the DOE for Nevada Test Site activities and is not part of the Nevada Test and Training Range. However, agreements with the U.S. Air Force and the Federal Aviation Administration allow specific uses by military and civilian aircraft as described below (BSC 2007a, Section 6.1).

R-4808S—Restricted area R-4808S is used jointly by the Nevada Test Site, Nellis Air Force Base, and the Federal Aviation Administration Los Angeles Air Route Traffic Control Center for military and civilian aircraft to overfly the southwest corner of R-4808S on an as-needed basis. Clearance for any aircraft entry into R-4808S is required. The closest boundary of R-4808S to a repository surface facility is about 6 mi (BSC 2007a, Section 6.1.1).

R-4808N—R-4808N is divided into R-4808A, R-4808B, R-4808C, R-4808D, and R-4808E and is controlled by the DOE. The repository surface facility is located in R-4808E. The DOE allows military aircraft to transit R-4808N over R-4808B, R-4808C, R-4808D, and R-4808E. Overflight with live or hung ordnance is prohibited except for critical in-flight emergencies. Overflights of R-4808A are restricted to United States emergency aircraft and other DOE approved missions. In addition, no-fly, flight-restricted areas exist over the Device Assembly Facility and BREN (“Bare Reactor Experiment-Nevada”) Tower (Figure 1.1-6) (BSC 2007a, Section 6.1.2). Proposed flight-restricted airspace and operational constraints over the repository are discussed in Section 1.6.3.

1.1.1.3.2.2 Nevada Test and Training Range

This section discusses existing operations on the Nevada Test and Training Range, which includes airspace, land, and infrastructure dedicated to military uses. The airspace of the Nevada Test and Training Range shown in Figure 1.1-7 is composed of the Reville and Desert military operations areas and restricted areas: R-4806, R-4807, and R-4809 (BSC 2007a, Section C.1).

Military Operations Areas—A military operations area is airspace established to separate or segregate certain military activities from civilian air traffic. The Reville and Desert military operations areas shown in Figure 1.1-7 are used for conducting air-to-air intercept training, which consists of high-altitude operations, abrupt maneuvers, and supersonic flight at and above 5,000 ft above ground level with a ceiling of 18,000 ft above mean sea level. However, air traffic control assigned airspace can be provided on an as-needed basis by the Federal Aviation Administration to higher altitudes needed to accommodate flight training requirements (BSC 2007a, Section 6.2.1.1).

The Reville military operations area airspace includes the northern portion of the Nevada Test and Training Range. The closest boundary of the Reville military operations area is about 71 mi from the North Portal at Yucca Mountain (BSC 2007a, Section C.1.2).

The Desert military operations area is the eastern half of the Nevada Test and Training Range. It is divided into the following areas (Figure 1.1-7) (BSC 2007a, Section C.1.3):

- The Sally Corridor is a transition route between Nellis Air Force Base and portions of the Nevada Test and Training Range. The closest boundary of the Sally Corridor to a repository surface facility is greater than 60 mi.
- Elgin is primarily an air-to-air training area and contains a training range. Elgin is normally entered and exited via the Sally Corridor. The closest boundary of Elgin to a repository surface facility is greater than 80 mi.
- Caliente is primarily an air-to-air training area with west entry and exit via the Sally Corridor and east entry and exit via military training routes or the Sally Corridor. The closest boundary of Caliente to a repository surface facility is greater than 80 mi.
- Coyote provides airspace for tactical training maneuvers. The closest boundary of Coyote to a repository surface facility is greater than 50 mi.

Restricted Areas and Range Subsections—The restricted areas of the Nevada Test and Training Range are divided into the North Range and the South Range. These two ranges are separated by the Nevada Test Site. Within the Nevada Test and Training Range airspace, restricted areas R-4806, R-4807, and R-4809 are joint use; within the Nevada Test Site airspace, R-4808S is joint use and R-4808N is not joint use (BSC 2007a, Section C.2).

The North Range is approximately 1.8 million acres of withdrawn land. It contains unmanned weapons delivery subranges, electronic combat ranges, the Tonopah Test Range (R-4809), and Pahute Mesa, which is used by the DOE (BSC 2007a, Sections C.2.1 and C.2.1.2).

- R-4807 includes the 70-series ranges (Figure 1.1-7) and is divided into several subsections that are used for electronic combat training. The closest boundary to a repository surface facility is about 5 mi (BSC 2007a, Section C.2.1.1).
- The land at Pahute Mesa (Figure 1.1-7) is used by the DOE as an annex to the Nevada Test Site in support of the nation's nuclear weapons test program, and the U.S. Air Force uses the airspace for overflights. Helicopter traffic extends up to 500 ft above ground level. The closest boundary to a repository surface facility is greater than 30 mi (BSC 2007a, Section C.2.1.2).
- R-4809 (Tonopah Test Range) (Figure 1.1-7) contains electronic-combat-threat simulators and equipment used by the Sandia Corporation for the DOE. The Tonopah Test Range Airfield, located within R-4809, can be used as a diversion base for in-flight emergencies. The closest boundary to a repository surface facility is greater than 50 mi (BSC 2007a, Section C.2.1.3).

The South Range is approximately 1.2 million acres of withdrawn land and contains weapons-delivery areas (Figure 1.1-7) (BSC 2007a, Section C.2.2).

- Alamo, located in the eastern part of R-4806, is primarily an air-to-air training area with entry and exit via the Sally Corridor. The closest boundary to a repository surface facility is greater than 60 mi (BSC 2007a, Section C.2.2.1).
- The 60-series ranges are in the western portion of R-4806 and are used for conventional bombing and gunnery testing and training. The closest boundary to a repository surface facility is greater than 20 mi (BSC 2007a, Section C.2.2.2).

1.1.1.3.2.3 Military Training Routes and Areas

Military training routes and areas include low-altitude tactical navigation areas and military training routes.

Low-Altitude Tactical Navigation Areas—The low-altitude tactical navigation areas associated with the Nevada Test and Training Range are unrestricted airspace established for A-10s and helicopters to practice random selection of navigation points and low-altitude tactical formations between 100 and 1,500 ft above ground level and at speeds below 250 knots. These areas are used when no airspace is available for this type of training within the Nevada Test and Training Range complex (BSC 2007a, Section 6.2.2). Low-altitude tactical navigation areas are not depicted on aeronautical charts; however, local airports and aviation groups have been advised of their existence and associated operations. Three low-altitude tactical navigation areas are associated with the Nevada Test and Training Range: east, central, and west. The east low-altitude tactical navigation area is greater than 100 mi from the repository surface facilities. No estimate of the number of flights is available. The central low-altitude tactical navigation area is greater than 40 mi from the repository surface facilities. No estimate of the number of flights is available. The west low-altitude tactical navigation area is generally between the R-2508 Range Complex, the Nevada Test and Training Range restricted areas, and the southwestern side of the Nevada Test Site in an area known as the Beatty Corridor (BSC 2007a, Section C.3.1; BSC 2007b, Figure 2). About 30 to 38 sorties are conducted weekly in the west low-altitude tactical navigation area by Nellis Air Force Base A-10s and helicopters. The nearest boundary of the west low-altitude tactical navigation area is approximately 1 mi from the surface GROA (BSC 2007a, Section C.3.1).

Military Training Routes—Military training routes permit military flight training at airspeeds in excess of 250 knots below 10,000 ft above mean sea level while providing training in low-altitude tactics and navigation. Military training routes are established as instrument flight rule routes or visual flight rule routes. Military training routes in the region have floor segments as low as 100 ft above ground level, but they are normally flown between 500 and 1,000 ft above ground level (BSC 2007a, Section C.3.2). Section 3.5.1.6 of NUREG-0800 indicates that a military training route at least 5 statute miles beyond the site presents an acceptably low risk for a light water reactor nuclear power plant. For the purpose of assessing hazard to the surface facilities, it is concluded that airways greater than 30 mi from the North Portal will not pose a hazard to the

repository (BSC 2007a, Section 7.1.3). Three military training routes are within 30 mi (Figure 1.1-8). These routes and their closest distance are (BSC 2007a, Table 6-3):

- IR-286 15 mi
- VR-222 11 mi
- VR-1214 18 mi.

The section of VR-222 due west of the North Portal is limited to a maximum altitude of 1,500 ft above ground level, which represents a deviation from normal maximum altitude (BSC 2007a, Section C.3.2). A discussion of the hazard assessment is provided in Section 1.6.

1.1.1.3.2.4 **R-2508 Complex**

A large area of airspace, referred to as the R-2508 complex, exists to the west and southwest of Yucca Mountain (Figure 1.1-8). The R-2508 complex includes the airspace and associated land presently used and managed by Edwards Air Force Base; the National Training Center, Fort Irwin; and the Naval Air Warfare Center Weapons Division, China Lake. The airspace is divided both horizontally and vertically, with military operations areas being overlapped by air-traffic-control assigned airspaces and restricted areas (e.g., R-2505, R-2524, and R-2502). The military operations areas and air-traffic-control assigned airspaces combine with R-2508 to form four major work areas. Peripheral areas containing military operations areas and air-traffic-control assigned airspaces increase the size of the usable airspace. Typical operations within the R-2508 Complex include (BSC 2007a, Section C.4):

- Aircraft research and development
- Operational weapons test and evaluation flights
- Student pilot training
- Air combat maneuvering and proficiency flights
- Civilian test aircraft in direct support of the U.S. Department of Defense or defense training.

R-2508 Complex Military Operations Areas—The four major military operations areas within the lateral boundaries of the R-2508 complex (Figure 1.1-8) include Isabella, Owens, Saline, and Panamint. The Saline military operations area is the closest to the repository surface facilities at a distance of greater than 30 mi (BSC 2007a, Section C.4.1).

R-2505—R-2505 airspace (Figure 1.1-8) is restricted on a continuous basis and is subdivided into five primary ranges. The primary mission of these ranges is the research, development, testing, and evaluation of weapons and weapon systems. The closest boundary is about 70 mi from the repository surface facilities (BSC 2007a, Section C.4.2).

R-2524—R-2524 airspace (Figure 1.1-8) is restricted on a continuous basis. This area includes an electronic combat range that provides a simulated hostile land and sea surface-to-air weapons

installation. The closest boundary is greater than 70 mi from the repository surface facilities (BSC 2007a, Section C.4.3).

R-2502—R-2502 airspace ([Figure 1.1-8](#)) is restricted on a continuous basis. R-2502 includes force-on-force battle simulation areas, a live-fire exercise area, and a deep space tracking facility (Porter 2002). The closest edge is greater than 80 mi from the repository surface facilities ([Figure 1.1-8](#)).

1.1.1.3.2.5 R-2508 Complex Peripheral Areas

Two peripheral areas within the R-2508 complex ([Figure 1.1-8](#)) are located within the 100 mi regional setting of Yucca Mountain. The Deep Springs area provides additional work areas for segregation of military operations from instrument flight-rule traffic. The closest edge is located greater than 50 mi from the repository. The Shoshone military operations area activities include operational testing and evaluation, air-combat maneuvering, low-altitude training, and large-scale exercises. Shoshone north and south air traffic control assigned airspaces, located above the Shoshone military operations area, provide airspace for segregation of military operations from instrument flight-rule traffic. The closest edge is greater than 30 mi from the repository surface facility (BSC 2007a, Section C.5).

1.1.1.3.2.6 Low- and High-Altitude Routes and Area Navigation Routes

Low-altitude airways (Victor airways) are used by both visual and instrument flight-rule traffic. These airways are 8 nautical mi wide and, generally, are established from 1,200 ft above ground level up to but not including 18,000 ft above mean sea level (BSC 2007a, Appendix E). Generally, instrument flight-rule, en-route, high-altitude routes overlie those low-altitude federal airways bordering the Nevada Test and Training Range. The majority of instrument flight-rule air traffic conducts flights on these high-altitude jet routes at or above 18,000 ft above mean sea level. Aircraft flying these routes include airliners, air cargo, corporate jets, and other high-performance aircraft (BSC 2007a, Section 6-4). [Table 1.1-1](#) lists the federal airways and jet routes in the regional setting of Yucca Mountain, as well as distances from the North Portal at Yucca Mountain.

1.1.1.3.3 Military, Federal, and Civilian Airports and Airfields

This section provides details regarding the location of and activities at airports and airfields located within the regional setting of Yucca Mountain, as shown in [Figures 1.1-8](#) and [1.1-9](#). Included are military, DOE, and civilian airports and airfields. A discussion of the hazard assessment related to activities at airports is provided in [Section 1.6](#).

1.1.1.3.3.1 Military Airports and Airfields

There are three military airports within 100 mi of Yucca Mountain.

Crech Air Force Base—Crech Air Force Base, formerly known as Indian Springs Air Force Auxiliary Field airfield ([Figure 1.1-8](#)), is greater than 40 mi from the surface facilities at Yucca Mountain. It is located on the southern boundary of R-4806. There were about 4,000 operations at this airfield during 2003 (BSC 2007a, Section D.1.1).

Tonopah Test Range Airfield—The Tonopah Test Range Airfield (Figure 1.1-8) is located more than 60 mi from the surface facilities at Yucca Mountain. There were about 200 flight operations for the Tonopah Test Range Airfield during 2003 (BSC 2007a, Section D.1.2).

Nellis Air Force Base—Nellis Air Force Base (Figure 1.1-8) is greater than 85 mi from the surface facilities at Yucca Mountain. Nellis Air Force Base is surrounded by Las Vegas airspace. There were 32,400 operations for Nellis Air Force Base during 2003 (BSC 2007a, Section D.1.3).

1.1.1.3.3.2 Federal Airports and Airfields

There are three DOE airports within the 100 mi regional setting of Yucca Mountain.

Desert Rock Airport—The Desert Rock Airport (Figure 1.1-8) is greater than 25 mi from the surface facilities at Yucca Mountain. Small commuter aircraft that fly staff and equipment to and from various national laboratories and the Nevada Test Site use the Desert Rock Airport. Helicopters based on the Nevada Test Site also use this airfield. Aircraft operations at this field are estimated at about 4,700 per year (BSC 2007a, Section D.2.1).

Pahute Mesa Airstrip—The Pahute Mesa Airstrip (Figure 1.1-8) is greater than 15 mi from the surface facilities at Yucca Mountain. There were no reported operations at this airstrip in 2003 (BSC 2007a, Table 6-4).

Yucca Strip—The Yucca Strip (Figure 1.1-8) is greater than 20 mi from the surface facilities at Yucca Mountain and has not been used since 1995 (BSC 2007a, Section 6.3). An asphalt runway has been constructed approximately 1 mi east of Yucca Airstrip for the purpose of testing unmanned aerial vehicles (Section 1.1.1.3.1.5).

Helipads—Helicopter operations are conducted from helipads at Mercury, Area 6, Area 29, Area 12, and Area 25 (Figure 1.1-6), as well as Desert Rock Airport and Pahute Mesa Airstrip (Figure 1.1-8). The helipad in Area 25 is the closest helipad and is located outside of the land withdrawal area, greater than 8 mi from the surface facilities. Most of the helicopter operations to these areas are out of the Desert Rock Airport (BSC 2007a, Section 6.3). The North Portal heliport is discussed in Section 1.1.9.3.2.11.

1.1.1.3.3.3 Civilian Airports and Airfields

Several civilian airports and airfields are within 100 mi of the North Portal at Yucca Mountain (Figure 1.1-9). Many of the high-volume facilities are located near Las Vegas. Aircraft activity ranges from 0 to more than 500,000 operations per year (BSC 2007a, Section D.3). The following text provides a discussion of airports or airfields with high operational volume or in close proximity to Yucca Mountain.

Beatty Airport—The Beatty Airport (Figure 1.1-9), located on the outskirts of the town of Beatty, Nevada, is a public facility owned by Nye County, Nevada. The airport serves few locally owned single-engine aircraft, as well as air taxi service for Beatty and Death Valley National Park. The Beatty Airport does not have a control tower and is unattended. Pilots are expected to maintain radio contact with other aircraft in the area and use visual flight rules during takeoffs and

landings. The Beatty Airport is greater than 20 mi west of the surface facilities at Yucca Mountain (BSC 2007a, Section D.3.1). This airport has about 1,000 operations per year (BSC 2007a, Table 6-4).

Jackass Aeropark—The Jackass Aeropark (Figure 1.1-9) is about 15 mi south of the surface facilities at Yucca Mountain (BSC 2007a, Table 6-4). The Jackass Aeropark was shut down in June 2004 (BSC 2007a, Table 6-4).

Furnace Creek Airport—The Furnace Creek Airport (Figure 1.1-9), located in Death Valley National Park, California, is a public facility owned by the U.S. Department of the Interior, National Park Service. The airport serves approximately two locally owned single-engine aircraft. Single-wheel weight limitation is 4,000 lb. The runway is 3,065 ft long, limiting operations to small aircraft. The Furnace Creek Airport does not have a control tower and is unattended. Pilots are expected to maintain radio contact with other aircraft in the area and use visual flight rules during takeoffs and landings. The Furnace Creek Airport is greater than 35 mi southwest of the surface facilities at Yucca Mountain (BSC 2007a, Section D.3.2). This airport has about 10,000 operations per year (BSC 2007a, Table 6-4).

Imvite Airfield—The Imvite Airfield (Figure 1.1-9), located in Amargosa Valley, Nevada, is a private facility owned by IMV, a division of the Floridin Company. The airport serves a small number of locally owned single-engine aircraft. The airfield is not paved and is 2,600 ft long. The Imvite Airfield is greater than 25 mi south of the surface facilities at Yucca Mountain (BSC 2007a, Section D.3.3). Annual operations are listed as zero (BSC 2007a, Table 6-4).

McCarran International Airport—McCarran International Airport (Figure 1.1-9) is located in Las Vegas, Nevada, greater than 85 mi east-southeast of the surface facilities at Yucca Mountain. It is a public facility owned by Clark County, Nevada. McCarran International Airport has a control tower that is attended at all times and is surrounded by Las Vegas airspace, which is a class of airspace that is characteristic of any airport environment having a high volume of air traffic. Aircraft entering or transiting through this charted airspace must be in contact with and under the positive control of either Nellis Air Force Base or McCarran International Airport radar approach control facilities. The positive protective nature of this airspace enhances flight safety of civilian aviation transiting through this high-density air traffic area (BSC 2007a, Section D.3.4). Annual operations are about 540,000 per year (BSC 2007a, Table 6-4).

North Las Vegas Airport—The North Las Vegas Airport (Figure 1.1-9), located greater than 80 mi east-southeast of the surface facilities at Yucca Mountain in North Las Vegas, Nevada, is a public facility owned by Clark County, Nevada. The North Las Vegas Airport has a control tower that is attended between 5:30 a.m. and 9:30 p.m. This airport is surrounded by Las Vegas airspace (BSC 2007a, Section D.3.5). Annual operations are about 200,000 per year (BSC 2007a, Table 6-4).

1.1.1.3.4 Roads

U.S. Highway 95, Nevada State Route 373, and roads on the Nevada Test Site (Figure 1.1-6) are used to haul quantities of explosives, munitions, propellants, and hazardous and radioactive materials. U.S. Highway 95 is the closest major highway and is approximately 13 mi from the

surface GROA. Of the primary paved roads in the southern part of the Nevada Test Site, Lathrop Wells Road is approximately 7 mi from and the closest to the surface GROA. The Lathrop Wells Road, which traverses the southeastern area of the Yucca Mountain site, is used to support activities discussed in [Section 1.1.1.3.1](#). Even though some hazardous materials are transported onto the Nevada Test Site via the Lathrop Wells Road for these activities, the transport vehicles will be at least 7 mi from the surface GROA ([Figure 1.1-6](#)) (BSC 2008a, Section 6.3.5).

1.1.1.3.5 Railroads

There are no passenger or freight railroad lines within 20 mi of the surface GROA (BSC 2008a, Section 6.3.5).

The DOE will construct a new rail line to connect the GROA to commercial rail lines within the State of Nevada. Construction of this rail line is outside the scope of this license application. The DOE will construct rail facilities to support repository operations. Two facilities are planned to be on, or in the immediate vicinity of, the site. The first facility, the rail equipment maintenance yard (also referred to as the end-of-line facility), will be for the maintenance, repair, staging, storage, and operations of railroad equipment and will be located on the site, south of the GROA (Nevada Rail Partners 2007, Section 6.1). The second facility, the cask maintenance facility (also known as the fleet management facility), will be for the maintenance, repair, storage, and staging of the transportation casks for spent nuclear fuel and high-level radioactive waste. This facility will be collocated with the rail equipment maintenance yard. Power and water utility feed connections to the rail equipment maintenance yard and the cask maintenance facility will be provided by the GROA (DOE 2007a, Section 3.1.16). Diesel fuel for locomotive use will be approximately 50,000 gal and will be located at the southern end of the rail equipment maintenance yard (Hamilton-Ray 2007). Evaluations of hazards to the repository resulting from these facilities are discussed in [Section 1.6](#).

1.1.1.3.6 Potentially Hazardous Commercial Operations and Manufacturing Centers

This section provides details regarding the location of and activities at commercial operations in the vicinity of Yucca Mountain that could present potential hazards.

1.1.1.3.6.1 Commercial Rocket Launch and Retrieval

Kistler Aerospace Corporation proposed to launch low-earth-orbit satellites using a reusable two-stage vehicle. A potential launch site and landing and recovery area are proposed to be located in Areas 18 and 19 at the Nevada Test Site ([Figure 1.1-6](#)). This space vehicle launch project at the Nevada Test Site is in the formative stages; there are no constructed and operational facilities. The Federal Aviation Administration prepared and issued an Environmental Assessment evaluating launches from the Nevada Test Site (FAA 2002) and the Federal Aviation Administration Associate Administrator for Commercial Space Transportation issued a Finding of No Significant Impact (67 FR 22479). In July 2003, Kistler voluntarily filed to reorganize under Chapter 11 bankruptcy (Kistler Aerospace 2003). In 2006, Rocketplane Limited, Inc. and Kistler Aerospace merged to form Rocketplane Kistler. NASA selected Rocketplane Kistler to receive partial funding to provide delivery services to the International Space Station under the Commercial Orbital Transportation Services initiative (FAA 2007, p. 4).

Rocketplane Kistler expects to operate the K-1 reusable launch vehicle from two launch sites: Spaceport Woomera in South Australia and a site in the United States that is yet to be determined. Kistler Aerospace received authorization from the Australian government to begin construction of launch facilities in April 1998 and held a ground-breaking ceremony at the site several months later. The launch pad design is complete and Rocketplane Kistler will conduct its initial K-1 flights and commercial operations from Woomera. Although an agreement was signed with the Nevada Test Site Development Corporation to permit Kistler to occupy a segment of the Nevada Test Site for its launch operations, and the environmental review process was completed for the project in 2002, the company is currently examining other options for a domestic launch site, including Cape Canaveral Air Force Station (FAA 2007, p. 24). Hazards that could occur during the preclosure period are assessed in [Section 1.6](#).

1.1.1.3.6.2 Bureau of Land Management Activities

There were no hazards identified on Bureau of Land Management land within a 5-mi radius from the repository (BSC 2008a, Section 6.3.2).

1.1.1.3.6.3 Mining Activities

There are no mining claims within the repository footprint. Public Land Order 6802 was granted by the Bureau of Land Management with an expiration date of 1990 and extended until 2010 by Public Land Order 7534. These public land orders preclude the staking of mining claims within an area that includes the repository footprint (BSC 2008a, Section 6.3.3).

The IMV Nevada Mine is the only major mine operating in Nye County in southern Amargosa Valley in the vicinity of Yucca Mountain (Driesner and Coyner 2006, Section VI). The mine is not within a 5-mi radius of the repository but contributes to truck traffic along U.S. Highway 95 and Nevada State Route 373 because mine supplies are provided by truck. These transportation corridors are greater than 10 mi from the surface GROA (BSC 2008a, Section 6.3.3).

Patent 27-83-0002 comprises about 200 acres within the site in T.14S. R.48E., Section 36 (BLM 1982). The Cind-R-Lite Block Company is mining the cinder cone at that location ([Figure 1.1-6](#)) for aggregates used in the manufacture of cinder blocks (DOE 2002b, Section 3.1.1.2). This property is the only private property within the proposed site. Rights-of-way and other encumbrances on the site are discussed in [Section 5.8](#).

There are currently unpatented mining claims at the southern edge of the site that are located outside of a 5-mi radius from the repository (BSC 2008a, Section 6.3.3). These are discussed in [Section 5.8](#).

1.1.1.3.7 Transmission Lines

The repository does not generate electrical power for offsite use. There are no transmission lines emanating from the repository. A map of power supply transmission lines is provided in [Figure 1.1-10](#). There are no transmission line rights-of-way within about 7 mi of the repository ([Section 5.8](#)).

1.1.2 Regional Demography

[NUREG-1804, Section 2.1.1.1.3: AC 2]

This section provides regional demographic information based on current census (2000) and supplemental data and presents the population distribution as a function of distance from the GROA. The demographic information identifies the locations of the members of the public. Population projections are provided for the preclosure operations period. A discussion of regional population centers is also provided.

Section 1.1.2.1 describes the demographic study area and population distribution within the area.

Section 1.1.2.2 provides a discussion of population centers in the Yucca Mountain vicinity.

Section 1.1.2.3 provides population projections for the demographic study area.

1.1.2.1 Demographic Study Area

[NUREG-1804, Section 2.1.1.1.3: AC 2(1)]

An area of population analysis, known as the demographic study area, has been established consistent with Regulatory Guide 4.2. The demographic study area is an 84-km-radius, radial grid (Figure 1.1-11; also known as the radiological monitoring grid) centered on Nevada State Plane coordinates Northing 765621.5 and Easting 570433.6, which is on the eastern side of Exile Hill at the Yucca Mountain site. The surface GROA is located over this point. The demographic study area consists of a grid formed by 10 concentric rings, each 8 km wide, radiating from an 8-km-diameter circular central cell. The rings are divided into 16 evenly spaced sections of 22.5°, each centered on 16 compass points beginning with north. The cell labels in the concentric rings are derived from a concatenation of the numbering system of the rings and sections. The rings are labeled from 1 to 10 moving outward from the circular central cell. The 16 sections are numbered counterclockwise beginning with the section directly north.

This demographic study area surrounding the Yucca Mountain site includes five counties within 84 km of the repository: four counties in Nevada and Inyo County, California. There are no permanent residents within about 22 km. Estimates of the resident population located within the 84-km grid for the years 2001 through 2003 are presented in Table 1.1-2. The housing unit method was used to calculate population estimates for each grid cell. The basis for this method is that the population of any given geographic area is equal to the number of households multiplied by the average number of people per household, plus the number of people living in group quarters (BSC 2003a, Section 4.3). Information on population by grid cell is based on census data, electric utility data, and surveys. Data are organized in Table 1.1-2 by the state, county, area, and grid cell in which the resident population is located. Figure 1.1-11 shows the population distribution within the 84-km grid for 2003 (BSC 2003a, Figure 1). This information provides a baseline for population projection estimates discussed in Section 1.1.2.3.

The nearest resident population to the repository is located in the unincorporated Town of Amargosa Valley. The closest year-round housing is at the intersection of U.S. Highway 95 and Nevada State Route 373 (Figure 1.1-11 and Table 1.1-2). For 2008, the population for the entire Amargosa Valley

area is estimated as 1,844 (Table 1.1-3); details on the population distribution are provided in Figure 1.1-11 and Tables 1.1-2 and 1.1-3.

Most of the other counties surrounding Yucca Mountain, including Lincoln and Esmeralda counties in Nevada and Inyo County in California, have low population densities. The nearest large populations reside in Pahrump in Nye County, Nevada, and in Clark County, Nevada, southeast of Yucca Mountain (Section 1.1.2.2).

1.1.2.2 Population Centers

[NUREG-1804, Section 2.1.1.1.3: AC 2(1)]

Population and related economic activity in southern Nevada are concentrated in Clark County (Figure 1.1-4) in the incorporated cities and in the unincorporated areas of the Las Vegas Valley. Population figures for Clark County for 2006, based on estimates by the Clark County Department of Comprehensive Planning, are provided in the following text. The incorporated cities include Boulder City (15,790), Henderson (256,390), Las Vegas (591,536), Mesquite (18,012), and North Las Vegas (202,520), which in 2006 contained about 57% of Clark County's 1,912,654 residents. 33,802 of these people reside in the incorporated cities of Mesquite and Boulder City, which are outlying from the Las Vegas Valley. Most of the remainder of the Clark County population resides in the unincorporated areas in the Las Vegas Valley, which together total 797,049 residents. Residents in unincorporated outlying areas total 31,357 people (Clark County Department of Comprehensive Planning 2006).

Lincoln County (Figure 1.1-4) had an estimated total population in 2006 of 3,987 residents, 2,695 (approximately 68%) of whom live in the incorporated town of Caliente (1,002) or in the unincorporated towns of Alamo (432), Panaca (558), and Pioche (703) (Nevada Department of Taxation and Nevada State Demographer 2007). The area of Lincoln County within the demographic study area does not contain any residents (Figure 1.1-11 and Table 1.1-2) (BSC 2003a, Table 1).

In 2006, Nye County (Figure 1.1-4) had an estimated population of 44,795 residents. Of this population, 42,927 residents (96%) live in the unincorporated towns of Beatty (1,025), Gabbs (313), Manhattan (122), Pahrump (36,645), Round Mountain (787), Tonopah (2,600), and the Town of Amargosa Valley (1,435). The largest population concentration is in Pahrump, with 36,645 residents or approximately 82% of the total county population (Nevada Department of Taxation and Nevada State Demographer 2007).

Esmeralda County (Figure 1.1-4) had an estimated 2006 population of 1,262. Of this population, 547 residents (43%) live in the unincorporated towns of Goldfield (430) and Silver Peak (117) (Nevada Department of Taxation and Nevada State Demographer 2007). However, only a small portion of the county is within the repository demographic study area (Section 1.1.2.1). This small area of Esmeralda County does not contain any residents (Figure 1.1-11 and Table 1.1-2) (BSC 2003a, Table 1).

Inyo County, California (Figure 1.1-4), is about 36 km from the repository at its closest boundary. Inyo County has an estimated population of 18,383 as of January 1, 2007. Of this population, 3,585 residents (approximately 20%) live in the city of Bishop (California Department of Finance 2007).

However, the area of Inyo County within the demographic study area is almost entirely within Death Valley National Park. Population and employment within the national park are primarily related to park activities (BSC 2003a). Population information for the area within the demographic study area is presented in [Tables 1.1-2](#) and [1.1-3](#).

1.1.2.3 Population Projections

[NUREG-1804, Section 2.1.1.1.3: AC 2(1)]

Population projections are provided consistent with the format described in Regulatory Guide 4.2. Population estimates for 2003 ([Table 1.1-2](#)), developed using the housing unit method and based on the year 2000 census ([Section 1.1.2.1](#)), provide a baseline for population projections. From the starting point of population by grid cell in 2003, population by year in each grid cell is calculated through application of the same annual rate of growth or declination as the baseline projections for the county in which each respective cell lies (BSC 2007c, Section 4.3.1). The resident population within the demographic study area is projected to the expected first year of operation of the repository ([Table 1.1-3](#)), and then, by census decade through the expected completion of spent nuclear fuel and high-level radioactive waste handling operations ([Table 1.1-4](#)). Changes in population because of repository and rail corridor construction and operation are included in these projections. Projections are also provided for the year 2042 ([Table 1.1-4](#)), which is the midpoint year between 2017 and 2067. These midpoint population projections for the year 2042 are used to furnish age distributions of the projected population for the midpoint year ([Table 1.1-5](#)).

1.1.3 Local Meteorology and Regional Climatology

[NUREG-1804, Section 2.1.1.1.3: AC 3]

Climatic and meteorological conditions in the Yucca Mountain region are one subset of natural phenomena that could pose hazards to repository safety during the preclosure period. This section summarizes site-specific and regional climatic and meteorological data that have been used to quantify the expected magnitude, frequency, and duration of climatological phenomena occurring in the Yucca Mountain region and repository vicinity. This section also provides a basis to evaluate climate-related hazards and events for their potential to affect repository safety during the preclosure period. Design bases are developed for structures, systems, and components (SSCs) based upon the information provided in this section and are discussed in [Sections 1.2.2](#) and [1.3.2](#).

Atmospheric stability categories determined from temperature gradient data and wind speed and wind direction data are used for developing atmospheric dispersion factors for use in evaluating airborne radionuclide concentrations from hypothetical radioactivity release scenarios. Meteorological data are also incorporated into the event consequence analyses performed to evaluate the safety of the repository ([Section 1.8](#)).

[Section 1.1.3.1](#) describes the meteorological monitoring program and addresses data collection techniques and instruments.

[Section 1.1.3.2](#) includes descriptions of the precipitation, wind speed temperature, atmospheric humidity, solar radiation, and barometric pressure characteristics of the repository site.

[Section 1.1.3.3](#) includes descriptions of atmospheric dispersion characteristics of the repository site.

[Section 1.1.3.4](#) includes a discussion of atmospheric stability characteristics in the Yucca Mountain vicinity.

[Section 1.1.3.5](#) provides a summary of the meteorological characteristics of the Yucca Mountain site.

[Section 1.1.3.6](#) addresses the characteristics of severe weather that are considered for their potential applicability to the repository site and the design of the GROA.

Additional information regarding the regional climate is provided in [Section 2.3.1](#) and [GI Section 5.2.5](#).

1.1.3.1 Meteorological Monitoring

[*NUREG-1804, Section 2.1.1.1.3: AC 3(2), (5)*]

Meteorological monitoring stations installed in the vicinity of Yucca Mountain to support site characterization activities, and regional meteorological monitoring stations installed in central and southern Nevada by the National Weather Service provide data on historical temperatures and temperature extremes occurring at Yucca Mountain and in the surrounding region. [Figure 1.1-12](#) shows the twelve locations of the nine meteorological monitoring Sites 1 through 9 and the three precipitation monitoring Sites 401, 405, and 415, which are operated by the DOE. [Figure 1.1-13](#) shows the locations of meteorological monitoring sites operated by the regional National Weather Service.

The Yucca Mountain meteorological monitoring program was designed and operated to comply with U.S. Nuclear Regulatory Commission (NRC) monitoring guidance. Through 2006, NRC monitoring guidance was from *Onsite Meteorological Programs*, the original Atomic Energy Commission Safety Guide 23, also known as Regulatory Guide 1.23, Section C. Draft revisions were proposed as Revision 1, but were not finalized until March 2007. In the interim, voluntary consensus standards ANSI/ANS 3.11-2000, *American National Standard for Determining Meteorological Information at Nuclear Facilities*, and ANSI/ANS-3.11-2005, *American National Standard for Determining Meteorological Information at Nuclear Facilities*, were used for guidance on modern equipment not contained in Regulatory Guide 1.23. The new guidance in Regulatory Guide 1.23, Rev. 1, promulgated in March 2007, did not significantly change measurement requirements. More information was included on monitoring in complex terrain and for instrument exposures.

The Yucca Mountain meteorological monitoring program has been performed in accordance with:

- Regulatory Guide 1.23, *Onsite Meteorological Programs*, Section C
- Regulatory Guide 1.23, Rev. 1, *Meteorological Monitoring Programs for Nuclear Power Plants*, Section C

- *Meteorological Monitoring Guidance for Regulatory Modeling Applications* (EPA 2000, Section 2-8).

In addition, the program has been performed in accordance with voluntary consensus standards from:

- ASTM D 5741-96, *Standard Practice for Characterizing Surface Wind Using a Wind Vane and Rotating Anemometer*
- ANSI/ANS-3.11-2000, *American National Standard for Determining Meteorological Information at Nuclear Facilities*
- ANSI/ANS-3.11-2005, *American National Standard for Determining Meteorological Information at Nuclear Facilities*.

The monitoring program has also been performed in accordance with a hierarchy of quality assurance documents and project procedures. Specifically, the program is subject to the requirements of the two quality documents, as follows; primary field and data processing procedures are also listed:

- *Quality Management Directive* (BSC 2007d)
- *Quality Assurance Requirements and Description* (DOE 2007b)
- EV-PRO-5001, *Tests and Checks of Meteorological Measuring and Test Equipment*
- EV-PRO-5002, *Tests, Checks, and Performance Audits of Meteorological Equipment*
- EV-PRO-5003, *Routine Operations and Maintenance of Meteorological Equipment*
- EV-PRO-5004, *Meteorological Data Processing*.

1.1.3.1.1 General Site Exposure and Monitoring Stations

The primary surface facility area for the GROA is the west side of Midway Valley, east of the Yucca Mountain ridge. The area comprises complex terrain (Figures 1.1-5 and 1.1-12). Midway Valley slopes generally toward the east; the hydrologic drainage is between Alice Hill and Fran Ridge. The elevation of the ridgeline crest is more than 330 m higher than the west side of Midway Valley. This area is south of higher elevation mesas of the Nevada Test Site. The larger broad valley of Jackass Flats, east of Midway Valley, includes Fortymile Wash. The terrain of Jackass Flats slopes toward the south and opens into the Town of Amargosa Valley along U.S. Highway 95 (BSC 2007e, Section 2.2).

The typically clear skies and arid conditions of the Yucca Mountain site promotes a wide range of surface temperatures between day and night periods. This temperature cycle, in turn, produces upslope and downslope airflow, respectively, on a range of spatial scales. Terrain features also tend to steer airflow along the axis of valleys, particularly during nighttime hours when the air is thermally stable and is less likely to flow over obstacles. Local airflow is a complex product of terrain-generated airflow mechanisms interacting with regional-scale weather system forces. The general exposures of the monitoring sites were chosen to characterize the influence of terrain on local airflow and atmospheric dispersion (BSC 2007e, Section 2.2).

Meteorological monitoring Sites 1 through 5 (Figure 1.1-12) were established in 1985 for environmental monitoring. During the planning of site characterization activities, these five sites were determined to be adequate to support site characterization. To better understand airflow and local meteorological conditions, Sites 6, 7, 8, and 9 (Figure 1.1-12) were added to the meteorological monitoring network in 1992. Precipitation monitoring Sites 401, 405, and 415 have had storage gauges since 1999 (BSC 2007e, Section 2.2).

The instrument configuration of the sites was changed in 1993. The data since 1994 provide a consistent data set for analysis. The wind, solar radiation, and barometric pressure measurements were discontinued at Sites 3, 6, 7, and 8 during 1999. The wind and solar radiation measurements were discontinued at Site 5 during 1999. These data are summarized through 1998. Precipitation is reported from storage gauges at Sites 401, 405, and 415 since 1999 (BSC 2007e, Section 2.2).

Meteorological monitoring site locations and instruments were chosen to characterize airflow and atmospheric dispersion near potential future emission sources from the GROA in Midway Valley along potential airflow pathways toward the populated area of Amargosa Valley south of Yucca Mountain. Monitoring sites were located in a variety of topographic positions such as hill slopes, ridge tops, and valleys over a wide area because of topographic influences on local airflow and related atmospheric dispersion characteristics. The variation in topography and elevation among the sites also provided useful information regarding meteorological conditions for geohydrologic studies (BSC 2007e, Section 2.2).

General exposure characteristics of the sites in the monitoring network are described in the following text. The quantity and size of nearby vegetation cover can influence meteorological conditions near the monitoring sites. Vegetation at the lower-elevation sites (e.g., Sites 5 and 9), is typical of the Mojave Desert. Vegetation at the crest of Yucca Mountain and upper slopes is transitional to Great Basin Desert flora. Vegetation near the monitoring stations is sparse (generally less than 20% ground cover) and average shrub height ranges from about 0.3 to 0.5 m. The small-sized and sparse vegetation near the meteorological monitoring sites do not interfere with the meteorological measurements being representative of their surrounding area (BSC 2007e, Section 2.2).

General descriptions of the measurements made at each site are included to show how the data contribute to characterizing the airflow and meteorological conditions of the area. More detailed descriptions of the measurements are provided Section 1.1.3.1.2.

Site 1 (NTS-60)—Site 1 is located in western Midway Valley at an elevation of 1,144 m above mean sea level (Figure 1.1-12; Table 1.1-6). The site exposure is an open area in the west-central portion of the valley floor, approximately 1 km south of the GROA, and 3.3 km east of the crest of Yucca Mountain. Site 1 is the network station most representative of ambient weather conditions of the GROA. The site has a 60-m-tall, multilevel meteorological tower instrumented at the 2-, 10-, and 60-m levels with wind, temperature, and humidity measurement instrumentation. Precipitation and barometric pressure instruments are mounted near ground level, and the solar pyranometer is at 2 m above ground (BSC 2007e, Section 2.2).

Site 2 (Yucca Mountain)—Site 2 (Figure 1.1-12; Table 1.1-6) is located on the Yucca Mountain ridge crest at an elevation of 1,478 m above mean sea level, approximately 3.3 km west-northwest

of Site 1 (Figure 1.1-12). This site was selected to provide meteorological conditions on the ridge crest and information on airflow above Midway Valley. Site 2 has a 10-m tower with the same measurement instrumentation as Site 1, except for the measurements at the 60-m level (BSC 2007e, Section 2.2).

Site 3 (Coyote Wash)—Site 3 (Figure 1.1-12; Table 1.1-6) is located in a narrow wash oriented east–west along the east side of Yucca Mountain at an elevation of 1,278 m above mean sea level, approximately 2.3 km west-northwest of Site 1. This site is representative of the many drainages that dominate the eastern slope of Yucca Mountain. Site 3 represents a mid-elevation location between Sites 1 and 2. From 1985 through 1998, Site 3 was instrumented the same as Site 2. The wind, solar radiation, and barometric pressure measurements were discontinued in July 1999 (BSC 2007e, Section 2.2).

Site 4 (Alice Hill)—Site 4 (Figure 1.1-12; Table 1.1-6) is located on Alice Hill at an elevation of 1,234 m above mean sea level, approximately 3.4 km northeast of Site 1. Site 4 was selected to provide meteorological conditions on an exposed hilltop location that could be compared with Sites 1 and 7 in the floor of Midway Valley to evaluate the vertical structure of the airflow in this region. Site 4 is fully instrumented at the 2- and 10-m levels, the same as Site 2 (BSC 2007e, Section 2.2).

Site 5 (Fortymile Wash)—Site 5 (Figure 1.1-12; Table 1.1-6) is in the broad valley of lower Jackass Flats on the east bank of Fortymile Wash. This site is 9.4 km southeast of Site 1 at an elevation of 952 m above mean sea level. This site was selected to help study airflow between Midway Valley and Amargosa Valley. The measurement periods and instrumentation at Site 5 correspond with those at Site 3, except that barometric pressure was continued at Site 5 (BSC 2007e, Section 2.2).

Site 6 (WT-6)—Site 6 (Figure 1.1-12; Table 1.1-6) is the northern-most monitoring site; it is located at the pad for UE-25 WT#6 adjacent to Yucca Wash. Site 6 is at an elevation of 1,315 m above mean sea level, approximately 6.1 km north-northwest of Site 1. This site was located to monitor the daytime airflow from the south exiting the northern end of Midway Valley, and the nocturnal airflow into Midway Valley from the northwest. The measurement period and instrumentation at Site 6 correspond with those at Site 3 (BSC 2007e, Section 2.2).

Site 7 (Sever Wash)—Site 7 (Figure 1.1-12; Table 1.1-6) is located on the east side of Midway Valley near the gap between Fran Ridge and Alice Hill, near the hydrologic outflow from Midway Valley. Site 7 is at an elevation of 1,081 m above mean sea level, approximately 2.1 km east-northeast of Site 1. This site is near the lowest elevation in Midway Valley, about 60 m below the elevation of Site 1. Site 7 is on the surface pathway for nocturnal airflow that exits Midway Valley through the topographic gap between Fran Ridge and Alice Hill. The measurement period and instrumentation at Site 7 correspond with those at Site 3 (BSC 2007e, Section 2.2).

Site 8 (Knothead Gap)—Site 8 (Figure 1.1-12; Table 1.1-6) is in the southern portion of Midway Valley in the saddle between Yucca Mountain and Fran Ridge. Site 8 is at an elevation of 1,123 m above mean sea level, approximately 1.7 km south of Site 1. This site is east of the South Portal. Site 8 was chosen to study airflow in this region of Midway Valley, partly because of the

proximity to the South Portal. The measurement period and instrumentation at Site 8 correspond with the instrumentation at Site 3 (BSC 2007e, Section 2.2).

Site 9 (Gate 510)—Site 9 is located along the southern border of the site (Figure 1.1-12; Table 1.1-6) at an elevation of 839 m above mean sea level, approximately 19.2 km south of Site 1. The site was moved about 130 m to the north on May 2, 2006, to accommodate local construction work. This site is located between Jackass Flats and Amargosa Valley along the Lathrop Wells Road and was selected to provide information on near-surface airflow between Yucca Mountain and the Town of Amargosa Valley; the nearest populated area to the repository location. Site 9 is fully instrumented at the 2- and 10-m levels, the same as Sites 2 and 4 (BSC 2007e, Section 2.2).

Site 401 (Bleach Bone Ridge)—Site 401 (Figure 1.1-12; Table 1.1-6) is on the northern end of the ridge on top of Yucca Mountain at an elevation of 1,563 m above mean sea level. It is about 5.7 km northwest of Site 1, overlooking upper Yucca Wash. This is the highest elevation site in the network. The only measurement at Site 401 is precipitation (BSC 2007e, Sections 2.2 and 2.3).

Site 405 (Yucca Mtn)—Site 405 (Figure 1.1-12; Table 1.1-6) is about the center of the ridge on top of Yucca Mountain at an elevation of 1,489 m above mean sea level. It is about 2.2 km west-southwest of Site 1. The only measurement at Site 405 is precipitation (BSC 2007e, Section 2.2).

Site 415 (Yucca Mtn)—Site 415 (Figure 1.1-12; Table 1.1-6) is further south than Site 405 along the ridge on top of Yucca Mountain, east of a small saddle separating the ridge top from the hill overlooking Abandoned Wash. It is at an elevation of 1,442 m above mean sea level and is about 2.7 km southwest of Site 1. The only measurement at Site 415 is precipitation (BSC 2007e, Section 2.2).

1.1.3.1.2 Local Instrument Exposure

The 12 monitoring sites were configured as three basic types, with negligible variation within a type. The types are 60-m tower (Site 1), 10-m towers (Sites 2, 3, 4, 5, 6, 7, 8, and 9), and precipitation measurement sites (401, 405, and 415). Table 1.1-7 lists the years in which different meteorological parameters were measured at Sites 1 through 9 from 1994 through 2006. The three types of sites are described in the following text.

60-m Tower (Site 1)—The 60-m tower of Site 1 is a Rohn 55G guyed triangular-lattice tower, 0.46 m on each side. There are instrument carriages at the 10- and 60-m levels for wind and temperature sensors. The carriages are connected to an electric winch to readily bring the sensors to near ground level for servicing. The wind crossarms on the carriages are 1.88 m from the west side of the tower, which is approximately four times the side dimension. Prevailing winds at the 10-m level are from the south during the day, and the northwest at night. Thus, the wind sensors are seldom influenced by the tower lattice structure. The mechanically aspirated temperature sensor shield inlets are 1.32 m from the tower, which is more than twice the side dimension. The 2-m temperature and humidity sensors are in a mechanically aspirated temperature sensor shield mounted on an extension arm with the shield inlet 1.32 m from the side of the tower. All shields have horizontal inlets that face north to minimize direct solar influence on the sensors

(BSC 2007e, Section 2.3). Thus, the wind, temperature, and atmospheric moisture measurements meet the local exposure criteria of Regulatory Guide 1.23, Rev. 1.

Two precipitation gauges, a recording tipping-bucket gauge and a manually measured storage gauge, are mounted with the gauge inlets about 1 m above ground level. At Site 1, the gauges are about 55 m southwest of the tower. The tipping-bucket gauge has an Alter wind shield. The solar radiation sensor is 3.4 m further west of the precipitation gauges (BSC 2007e, Section 2.3).

The signal conditioners and dataloggers are housed in an environmentally controlled shelter that is 20 m southwest of the tower. The shelter is approximately 3.0 by 4.9 m on a side and 3.0 m tall. The barometric pressure sensor inlet is outside this shelter, near the surface. For much of the 1994 through 2006 period, all instruments and dataloggers have operated on a 12-volt DC battery system on continuous recharge by commercial power. This power source minimizes data losses during commercial power interruptions. Two other shelters are located at this site; both are west of the tower. One is a concrete building located 12.8 m from the tower, measuring 3.4 by 4.3 m on a side, and 3.0 m tall. The other is a metal trailer, measuring 3.7 by 18.3 m on a side, and 3.7 m tall. This trailer is about 3 m further from the tower beyond the concrete building, about 20 m from the tower. These heights are less than one-half the 10-m height of the wind measurement, thereby meeting the obstruction criteria for wind sensors (BSC 2007e, Section 2.3).

10-m Towers (Sites 2, 4, and 9 (1994–2006) and Sites 3, 5, 6, 7, and 8 (1994–1998))—The 10-m towers are free-standing aluminum triangular-lattice towers that are 0.46 m on each side at the base. These towers are hinged at the base plate and are lowered for servicing the wind and temperature sensors at the top. The wind crossarm is mounted on a central shaft extending from the top tower section, with the sensors 10 m above ground level. With few exceptions, there are no obstructions near these towers. At Site 3, the canyon walls extend well above the top of the tower within about 100 ft north and south of the tower. This site was purposely located in this setting to characterize the airflow in the terrain typical of the east side of Yucca Mountain. Typical airflow is along the axis of the narrow wash, so the walls did not adversely impact wind measurements. At Site 9, a small guard shack about 1.8 by 3.0 m on a side and about 2.4 m tall was located about 30 m west of the tower much of the time that this site has been in operation. This direction is not in either prevailing wind direction for that site, and the height is within the obstruction criteria in Regulatory Guide 1.23, Rev. 1. Wind measurements were discontinued in 1999 at Sites 3, 5, 6, 7, and 8 (BSC 2007e, Section 2.3) (Table 1.1-7).

At all sites, the upper mechanically aspirated temperature shield is mounted immediately below the crossarm on the central shaft. The lower mechanically aspirated temperature and humidity shield is mounted 2 m above ground level on the side of the tower. The shield inlet is 1.14 m from the side of the tower, which is 2.5 tower-widths from the side. Both shields have horizontal inlets that face north. In late 2006, the horizontally mounted temperature shields were replaced by mechanically aspirated, circular, layered-plate shields with very similar temperature and humidity sensors at Sites 3, 5, 6, 7, and 8 (BSC 2007e, Section 2.3). Thus, the wind, temperature, and atmospheric moisture measurements meet the NRC criteria for local exposures in accordance with Regulatory Guide 1.23, Rev. 1, Section C.2-3.

At all sites, the data recording equipment is housed in a protected enclosure about 1.2 m above the ground, within about 1.5 m of the tower base. This enclosure includes the barometric pressure

sensor. The enclosure is ventilated with an opening to allow the sensor to measure ambient conditions. The solar radiation sensor is about 2.1 m above ground level either mounted on the enclosure structure or the tower; depending on the site. It is above all enclosure and solar panel components (BSC 2007e, Section 2.3).

At Sites 2 through 9, a recording tipping-bucket gauge and a manually measured storage gauge are mounted with the gauge inlets about 1 m above ground level within about 9.1 m from the tower and enclosure. The tipping-bucket gauges at Sites 2 and 6 have Alter wind shields (BSC 2007e, Section 2.3).

Precipitation Sites—In addition to the precipitation measurements at Sites 1 through 9, three precipitation measurement sites (Sites 401, 405, and 415) with storage gauges were added in 1999 along the crest of Yucca Mountain (Figure 1.1-12 and Table 1.1-6). These storage gauges are also mounted the same way as at Sites 1 through 9 (BSC 2007e, Section 2.3).

1.1.3.1.3 Meteorological Sensors

The meteorological sensors are standard types from companies that supply equipment to nuclear facilities. The instruments are reliable and result in high data recovery. The equipment was selected based on Regulatory Guide 1.23, Rev. 1, Section C.4, and other performance guidance in *Meteorological Monitoring Guidance for Regulatory Modeling Applications* (EPA-454/R-99-005) (EPA 2000, Section 3.2.2). Procurement of equipment and any equipment services (e.g., calibration or equipment repair) are made through vendors meeting quality assurance requirements in accordance with *Quality Assurance Requirements and Description* (DOE 2007b, Section 7). Trained quality assurance auditors conducted periodic supplier audits of the vendors (BSC 2007e, Section 2.4).

Table 1.1-8 lists the sensors used, the measurement method, and the instrument specifications from manufacturer sources. Table 1.1-9 lists the NRC accuracy limits and other performance criteria. The required accuracy and performance limits imposed on operational checks and calibrations meet the guidance of Regulatory Guide 1.23, Rev. 1. Table 1.1-9 shows that the project criteria meet the NRC criteria per Regulatory Guide 1.23, Rev. 1. Detailed descriptions of individual sensors with rationale for their suitability for the monitoring program are described in *Local Meteorology of Yucca Mountain, Nevada, 1994–2006* (BSC 2007e, Section 2.4).

1.1.3.1.4 Onsite Data Recording

The sensors described in Table 1.1-8 were connected to onsite electronic data processing and recording systems (dataloggers). The Campbell Scientific, Inc. model CR10 datalogger was used at Sites 2 through 9 throughout the period. The Odessa Engineering model DSM-3260 was used at Site 1 during 1994 and 1995. A Campbell Scientific, Inc. model CR21X datalogger was used during 1996 and 1997. A Campbell Scientific, Inc. model CR23X datalogger was used for the remainder of the period. Campbell Scientific dataloggers are used throughout the meteorological monitoring community and in industrial applications, including work in nuclear facilities. All the dataloggers were equipped with visual displays that can be read during site visits. Some sites have radio communication capability so that current conditions and recently recorded data can be polled between site visits to ensure continued correct operation. Analog strip charts were utilized at some

sites as a source of diagnostic information during site checks and data validation. The chart data were not used for backup data (BSC 2007e, Section 2.5).

The onsite data recording process included three steps: (1) sensor output signals were input to the datalogger and values were calculated in engineering units, (2) intermediate calculations were performed on the input for extreme values, summary statistics, and additional variables, and (3) output data arrays were stored. The actions performed by the dataloggers were controlled and documented by the procedures (Section 1.1.3.1) governing operation of the field equipment (BSC 2007e, Section 2.5).

Datalogger inputs were electronic output from the sensors, such as analog DC voltages and pulse counting. The input signal sampling rate was once every second. The engineering units of the measurements were metric, except for the tipping-bucket precipitation gauge that recorded in inches. Following a conversion of the precipitation data, the metric units were maintained throughout the data processing steps (BSC 2007e, Section 2.5).

The primary data output variables are based on guidance of Regulatory Guide 1.23, Rev. 1. Some additional output variables were based on ASTM D 5741-96, *Standard Practice for Characterizing Surface Wind Using a Wind Vane and Rotating Anemometer* (Section 4.3), which is a consensus standard for characterizing surface wind. Other information on battery status, datalogger condition, and self-check results identifying outlier values were also stored in output arrays. This information was used during data validation and was stored in the full database files, but was generally not included in the final meteorological database files (BSC 2007e, Section 2.5).

The primary data output is the hourly arrays. The daily arrays contain select data summaries. The data recorded onsite in solid-state storage modules were collected monthly and transferred to the project computer network for further storage and data validation (BSC 2007e, Section 2.5).

Horizontal wind speed measurements were processed and recorded as scalar values in meters per second. The primary output was 10-minute and hourly averages, both with corresponding directions. The maximum 3-second gust and maximum 1-minute average speed, with associated average direction, were recorded for engineering design applications. In addition, the standard deviation of the horizontal wind speed was calculated and recorded as an indication of atmospheric turbulence for dispersion or other applications (BSC 2007e, Section 2.5).

Vertical wind speed measurements were processed and recorded as scalar values in meters per second. Positive values indicate updrafts and negative values indicate downdrafts. The primary output was the 10-minute average. Also, the standard deviation of vertical wind speed was calculated and recorded as another indication of atmospheric turbulence for dispersion or other applications (BSC 2007e, Section 2.5).

Wind direction measurements were processed and recorded as scalar values in degrees with 0° and 360° as wind from true north, 90° as wind from the east, and so forth. The scalar value of direction was calculated by the unit vector method to allow for the circular distribution of wind data. The primary output was 10-minute and hourly averages, with corresponding speeds. The 1-minute average direction, associated with the maximum 1-minute average speed values, was recorded for engineering design applications. In addition, the standard deviation of the wind direction was

calculated and recorded as an indication of atmospheric turbulence for dispersion or other applications. The hourly standard deviation values are the root mean square of standard deviation values computed for 15-minute periods (BSC 2007e, Section 2.5).

Air temperature measurements were recorded in degrees Celsius. The primary output is 10-minute and hourly averages. Maximum and minimum 1-minute average air temperatures were recorded daily. This averaging time was chosen for comparability with data from climatic stations using glass thermometer or slow response electric sensors (BSC 2007e, Section 2.5).

Vertical temperature difference between the 2-, 10-, and 60-m heights were calculated by the onsite dataloggers as the upper-level temperature minus the lower-level temperature. The sensors were matched for nearly identical linearity characteristics to meet the tight accuracy limits shown in Tables 1.1-8 and 1.1-9. The vertical temperature difference data can be used as an indicator of atmospheric stability (BSC 2007e, Section 2.5).

Relative humidity, dew point, barometric pressure, and solar radiation data output were average values reported for the 10-minute and hourly periods (BSC 2007e, Section 2.5).

Precipitation was measured by two methods. The recording gauges have tipping-bucket mechanisms that register increments of 0.01 in. Hourly totals of the measurements were recorded for all years. Ten-minute and daily period data were recorded beginning in mid-1995, except for Site 1, which began in 1996. The storage gauges required manual measurements of precipitation depth, which were recorded on the site checklist forms. The readings were entered into an Excel database, generally for annual periods. Storage gauge data are considered the most reliable and accurate for precipitation totals because they lack the equipment failure modes and potential uncertainties inherent with the tipping-bucket mechanism. The tipping bucket data are an acceptable source of total precipitation data, but the primary use is for precipitation rate information (BSC 2007e, Section 2.5).

1.1.3.1.5 Instrument Surveillance

The frequency of site visits and tests were established to ensure an annual data recovery rate of at least 90%. Actual data recovery rates typically exceed 98%, with missing periods when the instruments were off-line for testing and routine maintenance. The fully instrumented sites are inspected at least weekly; the other sites are inspected at least twice monthly. The visits enable the site technician to visually confirm the physical integrity of the external sensors, and check that the results being recorded are reasonable given the present and recent conditions. The routine site inspections include periodic quality control tests of the tipping-bucket precipitation gauges to ensure that tips of the bucket mechanism were correctly counted by the datalogger. The results of the visits were documented on site checklist forms (BSC 2007e, Section 2.6).

The operating sensors are calibrated at least annually using measuring and test equipment standards traceable to nationally recognized standard bodies, such as the National Institute of Standards and Technology. The project procedures controlling measuring and test equipment (e.g., CO-PRO-1001, *Control of Measuring and Test Equipment*), have requirements that are implemented by the field procedures. The wind sensors are sent to the manufacturers for testing in a wind tunnel of the starting threshold speed and the accuracy of the sensor output when operating.

The measuring and test equipment used as working standards was sent to qualified suppliers to perform the traceable calibrations after one year of operation or sooner (BSC 2007e, Section 2.6).

Checks of the full measurement system that amount to limited field calibrations, from sensors through dataloggers, were performed using measuring and test equipment. The wind sensor outputs are checked by placing the vanes in known directions, checking crossarm and sensor orientation, and by rotating the anemometer shaft at known rates. The starting speed thresholds are checked by rotating the wind sensor shafts with torque watches. The temperature, humidity, pressure, and solar sensors and the recording precipitation gauges were calibrated and checked by comparison with either known input conditions, such as a set volume of water in the precipitation gauges, or the output of a collocated measurement from a measuring and test equipment standard (BSC 2007e, Section 2.6).

Periodic field checks are performed by technicians independent of the Yucca Mountain staff using independent measuring and test equipment. These independent checks satisfy U.S. Environmental Protection Agency requirements for “performance audits” (EPA 2000, Section 8.4). The original frequency of the periodic checks and performance audits was each calendar quarter. Based on instrument performance, the frequency of both tests was reduced in 1997 to twice yearly, in alternating calendar quarters (BSC 2007e, Section 2.6).

Preventive and corrective maintenance tasks are also controlled by procedures. The wind sensors are given routine preventive maintenance by the manufacturers when sent for periodic wind tunnel calibration tests. The preventive maintenance activities and frequencies are based on operating experience to balance interference with the equipment and measurements with the need to minimize downtimes due to equipment failure. Equipment failures, operator errors, and periods of suspect data were tracked through the Corrective Action Program (BSC 2007e, Section 2.6).

1.1.3.1.6 Data Acquisition and Reduction

Output data are stored onsite in solid-state storage modules. At least monthly, data were copied from the site storage modules to transfer storage modules, and the site checklists and diagnostic strip charts were collected. Data from the transfer storage modules were copied to computer files using the Campbell Scientific software PC208W. These raw data text files are comma-delimited strings, with data stored in the engineering units that were displayed in the dataloggers (BSC 2007e, Section 2.7).

The raw data text files were then imported to Microsoft Access database files using the quality-affecting software program called EFPData. Precipitation data from the recording tipping-bucket gauges were recorded in inches in increments of 0.01 in.; the imported data were converted to millimeters by multiplying the data in inches by 25.4. The importing program recognizes the output array identifiers that distinguish the monitoring site and time period of the records, and sorts the data into appropriate database tables. Limited screening checks for missing time periods, ranges and rates of change were performed on the imported data. Periods that exceed range or rate of change criteria were noted in a separate listing of edits. No data were changed without examination by data validation staff. Periods that do not meet acceptable data recovery criteria were invalidated, with notation made in the edits file (BSC 2007e, Section 2.7).

The imported data were reviewed and edited in accordance with project procedures. Edits were documented in the edits lists that are included in the database files in the Records Processing Center. The data processing and validation included examining results of import screening, listings of the “outlier” results recorded during site checks, the site checklists, and graphical data summaries. Edits were made to the data to account for equipment testing, periods when sensors were adversely affected by ice, or other adverse influences (BSC 2007e, Section 2.7).

Validated data from a calendar year were technically reviewed. After review comments were resolved, the data were submitted to the Technical Data Management Systems database for archival purposes and access by users. Each data set was assigned a unique data tracking number. The data sets in the Technical Data Management Systems database are the controlled meteorological data for the project. Metadata files were included with the controlled data in the Technical Data Management Systems database. The metadata provides an explanation of the column headings for measured or calculated meteorological parameters (BSC 2007e, Section 2.7).

Quality assurance audits, surveillances, and assessments were performed on the different aspects of the meteorological monitoring program. Meteorology staff members performed self assessments of different aspects of the program each year. Program areas typically reviewed include meteorological site operations; data evaluation and review; measuring and test equipment; and records, training, and document control. The Management and Operating Contractor quality assurance organization routinely performed surveillance and audits on the meteorology program as either part of larger quality assurance audits or surveillances of specific aspects of the program. On a less frequent basis, the Office of Civilian Radioactive Waste Management quality assurance organization included aspects (e.g., measuring and test equipment) of the meteorology program in oversight quality assurance audits. Findings from all audits, surveillances, and assessments were entered into the Corrective Action Program system and tracked to resolution (BSC 2007e, Section 2.7).

1.1.3.2 Data Summary

[NUREG-1804, Section 2.1.1.1.3: AC 3(1), (3), (5)]

Summaries of the meteorological data collected during 1994 through 2006 are presented in this section. [Tables 1.1-10](#) through [1.1-18](#) contain the data summaries for 1994 through 2006 for Sites 1 through 9. The full set of summary tables for each annual period for Sites 1 through 9 is provided in *Local Meteorology of Yucca Mountain, Nevada, 1994–2006* (BSC 2007e, Appendices H through T). The listing of available data by time period and site is shown in [Table 1.1-7](#). This information is relevant to understanding relationships between results from various sites, as some periods of record are not the same among sites. The results from Site 1 are frequently discussed because Site 1 is the most representative site of the conditions in the immediate vicinity of the GROA. Other sites are included as appropriate in some parameter discussions to identify trends or extremes.

1.1.3.2.1 Precipitation

Four precipitation variables are presented in the climatic data tables ([Tables 1.1-10](#) through [1.1-18](#)) for the monthly and annual periods by site: total precipitation, maximum one-hour and daily precipitation rates, and the number of days with measurable precipitation (daily total greater than or equal to 0.254 mm).

The average monthly and annual total precipitation data (mm) are included in [Tables 1.1-10](#) through [1.1-18](#). These tables show that February had the highest average monthly total precipitation at all sites. For Site 1 ([Table 1.1-10](#)), the February average precipitation total was 50.7 mm, which was more than twice the average monthly total during any other month and about one-fourth of the average annual total. The next two wettest months at all sites were January and March; the average totals for the three-month period (January through March) were about one-half the annual average totals. Except for Sites 6 and 9, the monthly average total showed a secondary maximum seasonal period in July, which typically coincides with the southwestern monsoon period (BSC 2007e, Section 5.1.1).

The average annual precipitation totals for all sites are summarized in [Table 1.1-19](#). The range of annual averages differed by nearly a factor of 2: across the sites with 116.0 mm at Site 9 and 225.3 mm at Site 6. The averages at Sites 1, 2, 4, 7, 8, and 401 were within a few millimeters of 200 mm. The average annual total precipitation varied considerably from year to year. For example, the Site 1 annual totals for the period from 1994 through 2006 ranged from 39.6 mm in 2002 to 366.5 mm in 1998 ([Table 1.1-20](#)), a factor of more than 9 (BSC 2007e, Section 5.1.1).

[Table 1.1-21](#) shows annual average total precipitation data in increasing order for all 12 sites for the period from 1999 through 2006. The site elevations are included. This period was selected for this analysis because it included data from all 12 sites to investigate the geographic distribution of total precipitation using data from common years. The 1999 through 2006 average annual precipitation totals include both wet and dry years relative to the averages from 1994 through 2006 shown in [Table 1.1-19](#). The average annual totals in [Table 1.1-21](#) ranged from 113.4 mm at Site 9 to 223.2 mm at Site 3, which are very close to the 1994 through 2006 averages in [Table 1.1-19](#) (BSC 2007e, Section 5.1.1).

The two greatest annual average precipitation totals occurred at Sites 3 and 6 ([Table 1.1-21](#)). The four sites on the crest of Yucca Mountain (Sites 2, 401, 405, and 415) have higher elevations than Sites 3 and 6 but lesser average annual precipitation totals. Average annual totals of Sites 1, 4, 7 and 8 in Midway Valley ([Figure 1.1-12](#)), were very near 200 mm. Finally, the two lowest elevation sites (Sites 5 and 9) had the least amount of precipitation. Thus, higher site elevation corresponded to higher total precipitation to some extent, but other factors seem to also influence the average annual total precipitation (BSC 2007e, Section 5.1.1).

Another factor apparently related to average annual total precipitation is the north and south positions relative to the Yucca Mountain ridge line. Site 6 is the furthest north, and it had a high average annual total precipitation of 212.2 mm ([Table 1.1-21](#)). Sites 2 and 401 are the furthest north on the crest; they have virtually identical average totals about 201 mm. The further south locations on the crest (Sites 405 and 415) also had identical average totals about 180 mm, indicating a decreasing pattern from north to south. This pattern of decreasing average annual total precipitation for sites further south is also evident when comparing the annual averages for the sites in Midway Valley (Sites 1, 4, 7, and 8) to sites further south in Jackass Flats (Sites 5 and 9) (BSC 2007e, Section 5.1.1).

The climatic data tables include maximum one-hour and daily precipitation rates, and the number of days with measurable precipitation occurrences. [Table 1.1-22](#) is a summary of the precipitation rate and occurrences for Sites 1 through 9 for the period 1994 through 2006 that are listed in

Tables 1.1-10 through 1.1-18. The calendar months during which the maximum values occurred are included.

The two sites in Jackass Flats (Sites 5 and 9) had the fewest days with measurable precipitation occurrences with averages of 30 and 26, respectively. The highest average number of days with measurable precipitation was 34, which occurred at both Sites 1 and 3.

The maximum 1-hr precipitation rate ranged from 13.72 mm/hr at Site 9 to 31.50 mm/hr at Site 7; both occurred during the month of July (Table 1.1-22). The maximum 1-hr amounts occurred during July or August, when convective storms may cause isolated but heavy rainfall events. The maximum daily precipitation amounts for the period 1994 through 2006 ranged from 44.70 mm/day at Site 6 to 64.77 mm/day at Site 7. With one exception, the highest daily values for the period 1994 through 2006 occurred during February, the month with the highest total precipitation. Site 7 had the highest daily rainfall event occur during July (Table 1.1-22) (BSC 2007e, Section 5.1.1).

While Table 1.1-22 documents maximum daily precipitation values from 1994 through 2006, a storm that occurred between 1000 PST on September 21, 2007, and 0400 PST September 22, 2007, resulted in the highest 24-hr precipitation totals ever reported from the monitoring network. The new maximum value, 87.12 mm at Site 4, is an increase of 22.35 mm (34.5% greater) compared to the previous maximum value of 64.77 mm at Site 7. The new maximum precipitation values for each of the monitoring sites are provided in Table 1.1-23.

As described in Section 1.1.4, the primary flooding hazard at and near Yucca Mountain occurs as a result of flash flooding resulting from intense rainfall, which is evaluated as a probable maximum precipitation event and runoff. The procedure used for determining the probable maximum precipitation (13.2 in. over a 6-hour duration for the basins containing the North Portal pad and 12.9 in. over a 6 hour duration for the basins containing the South Portal pad) is discussed in Section 1.1.4.3.1. These values can be compared to maximum recorded precipitation values for the site. Review of Appendices H through T in *Local Meteorology of Yucca Mountain, Nevada, 1994–2006* (BSC 2007e) and Table 1.1-23 indicates that the maximum observed hourly precipitation event was 1.24 in. at Site 7 in 1999 and that the maximum 24-hr precipitation value was 3.43 in., which occurred at Site 4 on September 21 through 22, 2007.

1.1.3.2.2 Wind Speed

Monthly and annual mean and maximum wind speeds are summarized for the 1994 through 2006 period in Tables 1.1-10 through 1.1-18. Maximum wind speeds are described as the “fastest” when applied to one-minute average speed, and the “peak gust” when applied to the maximum three-second average speed. Table 1.1-24 is a summary of the annual mean and extreme speeds that appear in Tables 1.1-10 through 1.1-18. The available wind data periods are 1994 through 2006 for Sites 1, 2, 4, and 9, and 1994 through 1998 for the remaining five sites. The discussion is focused on Sites 1, 2, 4, and 9 because they cover the longer period with wind data.

The mean monthly speeds at the 10 m level at Site 1 ranged from 3.0 m/s in January to 4.2 m/s in April, and the annual average was 3.5 m/s (Table 1.1-10). On the ridge top location of Site 2, the mean monthly speeds ranged from 3.9 m/s in the winter months to 5.4 m/s in April, and the annual average was 4.4 m/s (Table 1.1-11). The consistent occurrence of drainage winds at night at Site 9

kept the mean speed higher than it might otherwise experience. The mean monthly speeds ranged from 4.0 m/s in the winter months to 4.9 m/s in April, and the annual average was 4.4 m/s (Table 1.1-18) (BSC 2007e, Section 5.1.2).

The peak three-second gust was 27.6 m/s, and the fastest one-minute average speed was 23.3 m/s at Site 1 (Table 1.1-24). The data from Sites 2 and 4 show the influence of terrain on maximum wind speeds. The peak three-second gust was 38.7 m/s and the fastest one-minute average speed was 33.1 m/s on the ridge top location of Site 2. The hilltop location of Site 4 on Alice Hill in the northeast portion of Midway Valley experienced yet higher speeds. The peak three-second gust at Site 4 was 39.9 m/s, and the fastest one-minute average speed was 35.8 m/s. The valley floor location of Site 9 experienced unusually high maximum speeds during July with the peak three-second gust of 33.1 m/s and the fastest one-minute average speed of 27.5 m/s (BSC 2007e, Section 5.1.2).

The annual highest peak gusts and fastest one-minute average speeds occurred throughout the year, with some tendency toward the fall and winter months (Table 1.1-24). The directions of the fastest one-minute wind speeds were from northwesterly directions, except for the east-northeast direction at Site 9 (Table 1.1-24) (BSC 2007e, Section 5.1.2).

1.1.3.2.3 Temperature

The monthly and annual temperature data summaries across the years are shown in Tables 1.1-10 through 1.1-18. The one-minute average extreme temperature data were not available from Site 1 for 1994 and 1995 because the datalogger in use then did not record these values. Thus, the summaries of extreme temperatures at Site 1 are based on 11 years of data. The extremes, means of extremes, overall means, and the number of days per month and year when the maximum temperature reached at least 32.2°C and the minimum temperature dipped to 0°C or less are provided in the summary tables by monthly and annual periods.

The 11 years of daily extreme one-minute average data at Site 1 show the annual mean maximum and extreme maximum values to be 23.6°C and 43.3°C, respectively (Table 1.1-10). The annual cycle of monthly mean maximum values varies seasonally from 12.2°C to 37.0°C. The annual mean minimum and extreme minimum values are 9.3°C and -10.9°C, respectively. The annual cycle of monthly mean minimum values seasonally ranges from 0.4°C to 20.5°C, respectively. These mean maximum and minimum monthly averages show a large diurnal change, ranging from about 12°C in winter to nearly 17°C in summer. The overall annual mean temperature at Site 1 was 16.6°C. On the average, Site 1 had 99 days each year with maximum temperatures reaching 32.2°C; virtually all of July and August met this criterion. Also, Site 1 also had an average of 43.8 days each year when the minimum temperature dropped to 0°C or less (BSC 2007e, Section 5.1.3).

In contrast to the valley location of Site 1, the ridge-top location of Site 2 had a lower annual mean temperature of 15.8°C (Table 1.1-11). The annual mean maximum and extreme maximum temperatures were 21.4°C and 42.7°C, respectively. The annual cycle of monthly mean maximum values ranged seasonally from 9.7°C to 35.3°C. The annual mean minimum and extreme minimum values were 11.3°C and -10.4°C, respectively. The average diurnal range in temperature was 7°C in winter and 13°C in summer. The daily temperature range was less than at Site 1, due to the differences in terrain exposure at the two sites. Site 2 averaged 78 days each year with maximum

temperatures reaching 32.2°C, and 30.8 days when the minimum temperature drops to 0°C or less (BSC 2007e, Section 5.1.3).

The site with the lowest elevation is Site 9; it is located in the large, open valley area of Jackass Flats near Gate 510 and the Town of Amargosa Valley. While the highest temperatures were recorded at this site, the minimum temperatures were as low as those at other sites. The annual mean was 18.3°C, the highest in the network (Tables 1.1-10 through 1.1-18). The annual mean maximum and extreme maximum temperatures were also the highest in the network (Tables 1.1-10 through 1.1-18) at 26.2°C and 45.7°C, respectively. The annual cycle of monthly mean maximum values ranged seasonally from 14.2°C to 39.9°C. The annual mean minimum and extreme minimum temperatures were 9.9°C and -10.8°C, respectively. The average diurnal change in temperature ranges from about 7°C in winter to over 18°C. Site 9 averaged 127 days each year when maximum temperatures reached 32.2°C or higher, and 42 days when the minimum temperature dropped to 0°C or less (BSC 2007e, Section 5.1.3).

Site 7 is located in the hydrologic outflow area for much of Midway Valley. Drainage winds typically occur during the nocturnal period at this site and the lowest temperatures in the network often occurred at this site. The annual mean minimum and extreme minimum values were 6.3°C and -16.4°C, respectively (Table 1.1-16). This extreme is the lowest value recorded throughout the network. Site 7 had an average of 87.7 days when the minimum temperature dropped to 0°C or less and an average of 110 days per year when the maximum temperature was 32.2°C or higher. (BSC 2007e, Section 5.1.3).

Evaluating this site data with a survey of meteorological records from three regional National Weather Service stations (Beatty, for the period 1984 through 2000; Amargosa Farms, for the period 1965 through 2000; and Mercury Desert Rock Airport Weather Station, for the period 1984 through 2000; Table 1.1-13) indicates that recorded outside temperatures at these sites fall between -16°C and 47°C. The design basis temperatures are established as -17°C and 47°C.

1.1.3.2.4 Atmospheric Humidity

Summaries of atmospheric humidity data were made as averages by month for four specific hours of the day typical of climatic data analyses: 0400, 1000, 1600, and 2200 PST. The 0400 and 1600 results tend to be the maximum and minimum extreme values of relative humidity because these times are near the minimum and maximum air temperature occurrences. The results show the overall dry conditions that occur in this arid region. The annual average relative humidity ranged from 21.1% at 1600 PST to 40.5% at 0400 PST. The average afternoon (1600 PST) value during June was 9.5% (BSC 2007e, Section 5.1.4). The results for all sites are shown in Tables 1.1-10 through 1.1-18.

1.1.3.2.5 Solar Radiation

Summaries of solar radiation data were made as monthly averages of the daily maximum one-hour values, and are shown in Tables 1.1-10 through 1.1-18. Site 9, located in the open, exposed Jackass Flats area, had the highest maximum monthly values ranging from about 0.75 cal/cm²/min in winter to just over 1.5 cal/cm²/min in summer. The other eight sites had similar, but slightly lower, solar

radiation results ranging from about 0.7 cal/cm²/min in winter to between 1.4 and 1.5 cal/cm²/min in summer (BSC 2007e, Section 5.1.5).

1.1.3.2.6 Barometric Pressure

Monthly and annual average barometric pressure data are summarized in [Tables 1.1-10 through 1.1-18](#). The monthly averages showed a small tendency for an annual cycle, with lower values occurring in April through June. The average annual barometric pressure ranged from 851.1 mb on the ridge crest at Site 2 ([Table 1.1-11](#)) to 917.2 mb at the low elevation of Site 9 ([Table 1.1-18](#)). At Site 1, the annual average was 886.4 mb ([Table 1.1-10](#)) (BSC 2007e, Section 5.1.6).

1.1.3.3 Atmospheric Dispersion Characteristics

[NUREG-1804, Section 2.1.1.1.3: AC 3(1)]

The wind speed and direction joint frequency distribution is useful for summarizing atmospheric dispersion characteristics; including wind speed, direction, and seven Pasquill stability categories based on vertical temperature differences ([Table 1.1-25](#)). The joint frequency distribution of wind speed and direction for each of the seven Pasquill stability categories is used to describe wind characteristics and to evaluate the potential for atmospheric dispersion. The joint frequency distribution is expressed as a table of decimal fractions that represents a proportion of time that the wind is blowing from a specific direction and at a specific speed. In the tables, the wind direction categories are shown in the furthest left column and the wind speed categories in the upper row. The body of the table is cells showing the fraction of the hours in the given time (all hours, day or night) or atmospheric stability category that the wind direction and speed were in the ranges corresponding to the given cell. Wind speed is divided into ten speed categories plus calms. Wind direction uses sixteen categories from the same reference source, evenly spaced at 22.5-degree arc intervals centered on standard compass points (e.g., north, north-northeast, northeast). Wind roses are graphical representations of joint frequency distributions and show the percent of time that the wind is blowing from a particular direction and the percent time for each wind speed category. The wind rose figures are circular histograms, with segmented legs pointing from a central hub on the direction from which the wind blew. The leg segment lengths are proportional to the occurrences of winds within given speed categories from that direction. For clarity, only six wind speed categories are used in the wind rose figures. The speed category segments are color-coded according to the legend on the figures to facilitate visualizing occurrences of the various speeds in each direction category (BSC 2007e, Section 4.2).

Data were selected from seven of the monitoring sites to characterize joint frequency distributions of wind direction and speed. Sites 1, 2, 4, and 9 were fully instrumented for wind data for 1994 to 2006. Site 1 best represents wind flows in Midway Valley where the majority of repository surface facilities are located. Site 2 characterizes wind flow on the crest of Yucca Mountain and above Midway Valley. Site 4 is located on an exposed hilltop east-northeast of the repository surface facilities and provides information on the vertical structure of airflow above Midway Valley. Site 9 is located in flat terrain southeast of Midway Valley and characterizes airflow near the community of Amargosa Valley (BSC 2007e, Section 4.2). Three additional sites (Sites 3, 5, and 7) were instrumented for wind data from 1994 to 1998. Site 3 characterizes the wind flow in the valleys and ravines on the east side of Yucca Mountain. Site 5 is located along Fortymile Wash and characterizes winds along the pathway to Amargosa Valley (i.e., between Sites 7 and 9). Site 7 is

located in the southeast corner of Midway Valley (south-southeast of the repository surface facilities) in the hydrologic outflow area from Midway Valley and characterizes airflow into and out of this area toward Fortymile Wash. Joint frequency distributions and wind roses were also developed by Pasquill stability categories for Site 1 as it was equipped to record temperature measurements at both 10 and 60 m (BSC 2007e, Section 4.2).

Tabular summaries of joint frequency distributions are provided for wind speed and direction for all hours (Tables 1.1-26 through 1.1-33), for wind speed and direction for the daytime and nighttime hours (Tables 1.1-34 through 1.1-49), and for wind speed and direction for the Pasquill stability categories at Site 1 (Tables 1.1-50 through 1.1-63). Graphical wind rose presentations for wind speed and direction for all hours are provided in Figures 1.1-14 through 1.1-21; for wind speed and direction for the daytime and nighttime hours are provided in Figures 1.1-22 through 1.1-37, and for wind speed and direction for the Pasquill stability categories are provided in Figures 1.1-38 through 1.1-51. The all hours analysis characterizes the overall airflow patterns for the specific monitoring station. The daylight and night hours analysis examined the influence of diurnal cycles (heating and cooling) and local topography on wind flow patterns in the Yucca Mountain area. Evaluation of joint frequency distributions for different atmospheric stability categories characterized wind flows under varying atmospheric conditions that can influence atmospheric dispersion (BSC 2007e, Section 4.2).

1.1.3.4 Atmospheric Stability

[NUREG-1804, Section 2.1.1.1.3: AC 3(1), (5)]

Atmospheric stability is incorporated into the event consequence analyses performed to evaluate the safety of the repository (Section 1.8). Information on atmospheric stability provides an indication of the potential strength of horizontal and vertical atmospheric mixing processes. Atmospheric stability categories are used for developing atmospheric dispersion factors for use in evaluating hypothetical airborne radioactivity release scenarios.

Atmospheric stability is an indication of the dispersion potential of the atmosphere. The temperature difference between 10 and 60 m was measured at Site 1 and was used to assign Pasquill stability categories (BSC 2007e, Section 4.2). The categories are: extremely unstable (A), moderately unstable (B), slightly unstable (C), neutral (D), slightly stable (E), moderately stable (F), and extremely stable (G). The stability data are summarized by hour of the day (1 to 24) and for all hours in Table 1.1-64. The unstable categories (A through C) occurred during 28.5% of the total hours, mostly during daytime hours. The stable categories occurred during 56.7% of the total hours, mostly during nighttime hours and some transition periods. The neutral category (D) occurred during 14.9% of the total hours, mostly during the day portion of the transition between daytime and nighttime (BSC 2007e, Section 5.2.1).

Joint frequency distributions tables for the Pasquill atmospheric stability categories at Site 1 at the 10- and 60-m above ground levels for the period 1994 through 2006 are provided in Tables 1.1-50 to 1.1-63. The wind and stability conditions follow a very regular diurnal (day) and nocturnal (night) cycle and are influenced by local terrain.

The trend of the atmospheric stability cycle is closely tied to the diurnal and nocturnal cycle. The following text discusses this trend. The wind roses from the unstable and neutral (classes A

through D; Figures 1.1-38 through 1.1-45) and stable (stability classes E through G; Figures 1.1-46 through 1.1-51) distributions are similar to the diurnal (Figures 1.1-22 and 1.1-24) and nocturnal periods (Figures 1.1-23 and 1.1-25), respectively. The similarities are directly related to the close association between time of day and stability categories (Table 1.1-64). The most unstable (classes A and B) and most stable (classes F and G) distributions are associated more with the lower speed winds compared to the moderately stable or unstable and neutral (C, D, and E) class times showing occurrences of all wind speeds (BSC 2007e, Section 5.2.2).

Most of the diurnal hours had winds from the southerly directions, with some differences associated with local terrain features that apparently channel the winds along the axis of main hill and valley features of Midway Valley and Jackass Flats. At the 10-m level at Site 1, nearly 37% of the daytime winds are from the south or south-southeast directions with speeds between 2.1 and 8.1 m/s; about 40% of the daytime hours had speeds at least 4.1 m/s (Table 1.1-34 and Figure 1.1-22). Winds at the 60-m level at Site 1 are similar, with a tendency toward higher speeds (Table 1.1-36 and Figure 1.1-24). The open exposure of Site 2 on top of Yucca Mountain showed a wider distribution of directions (Figure 1.1-16) than were seen at the remaining sites at the lower elevations that showed higher occurrences of wind directions along the corresponding valley axis directions. Nearly 50% of the diurnal hours had speeds at least 4.1 m/s at Site 2 (Table 1.1-38 and Figure 1.1-26) (BSC 2007e, Section 5.2.2).

Winds during nocturnal hours were mostly from the northerly directions with greater indications of direction channeling by terrain than was evident in the diurnal periods. These patterns are typical of “drainage” winds that occur in valleys with clear sky conditions at night. Winds at the 10-m level at Site 1 were from the west to north quadrant during 74% of the nocturnal hours; most of these winds were from the northwest to north-northwest directions from 1.6 to 4.1 m/s (Table 1.1-35 and Figure 1.1-23). Virtually all of the winds at Site 1 at the 10-m level during the most stable periods (categories F and G) were from the northwest and north-northwest directions with speeds between 1.6 and 3.1 m/s (Tables 1.1-60 and 1.1-62, Figures 1.1-48 and 1.1-50). This direction is aligned with the Drill Hole Wash feature on the east side of Yucca Mountain (BSC 2007e, Section 5.2.2).

At Site 3 the nocturnal winds were from the west to northwest directions for 73% of the hours in Coyote Wash on the east side of Yucca Mountain; 47% of the hours were from the single west-northwest direction category, and the majority of those winds were in the 1.6 to 3.1 m/s speed categories (Table 1.1-41 and Figure 1.1-29).

Nocturnal drainage winds occurred at Site 7, which is near the Sever Wash hydrologic outflow feature of Midway Valley. Winds were from the west to north-northwest drainage direction at speeds below 3.1 m/s during 64% of the hours. A related grouping of stronger winds with a more northerly component was seen with 13% of the nocturnal hours having speeds above 3.1 m/s from the north-northwest to north directions (Table 1.1-47 and Figure 1.1-35).

Winds in the Jackass Flats area showed larger scale, down-valley airflow characteristics. Winds at Site 5, which is along Fortymile Wash, were from the north to north-northeast with speeds of 2.1 to 8.1 m/s during 64% of the nocturnal hours (Table 1.1-45 and Figure 1.1-33). The winds at Site 9 on the southern boundary of the Nevada Test Site near the Town of Amargosa Valley, were from the north to north-northeast during 63% of the nocturnal hours with speeds below 6.1 m/s (Table 1.1-49 and Figure 1.1-37).

While similar to joint frequency distributions from Sites 3, 5, and 9 and from the 10-m level at Site 1; nocturnal data from the ridge and hill tops (Sites 2 and 4) and the 60-m level at Site 1 showed another significant feature of dispersion conditions in the vicinity of Yucca Mountain. The stable atmospheric structure that occurs at night allows for winds at the 10-m level to be quite different from winds at higher levels. Winds at the Site 1 60-m level were from the northwest to northeast quadrant during 60% of the time, generally with speeds less than 3.1 m/s, though the north directions showed relatively frequent occurrences of winds up to 8.1 m/s (Table 1.1-49 and Figure 1.1-37). These directions are related to the overall features of Midway Valley, rather than the specific terrain feature, Drill Hole Wash, that appears to influence winds at the 10-m level at Site 1 (Figure 1.1-23). The winds at the 60-m level with category G stability were mostly from the north-northwest to north directions, with speeds less than 3.1 m/s (Table 1.1-63 and Figure 1.1-51). The winds during category F stability shifted to include the north-northwest to north-northeast directions, with some speeds from 3.1 to 8.1 m/s (Table 1.1-61 and Figure 1.1-49).

In a similar way to the Site 1 winds at the 60-m level, winds at Site 4 on Alice Hill were from the north-northwest to northeast directions during 70% of the nocturnal hours (Table 1.1-43 and Figure 1.1-31). As evidence of terrain features affecting the nocturnal winds in a different way, winds at Site 2 were from the northeast to south-southeast directions for over 60% of the nocturnal hours (Table 1.1-39 and Figure 1.1-27). These directions tend to show large-scale airflow from the higher terrain well northeast of Yucca Mountain, as well as periods with winds from the south that are not affected by the local terrain influences at times (BSC 2007e, Section 5.2.2).

Winds from southerly directions occurred during a small portion of the nocturnal hours, apparently associated with larger-scale wind systems overwhelming the locally generated winds. For example, only about 12% of the nocturnal hours at the 10-m level at Site 1 were from the south-southeast to south-southwest (Table 1.1-35 and Figure 1.1-23). Also, the higher-speed winds from the northwesterly and northerly directions evident at most of the sites are associated with larger-scale wind systems rather than the drainage-type winds (BSC 2007e, Section 5.2.2).

1.1.3.5 Meteorological Summary

[NUREG-1804, Section 2.1.1.1.3: AC 3(1), (3), (5)]

The thirteen years of meteorological monitoring data collected from the meteorological network operating in the vicinity of Yucca Mountain show the local climate is typical of the southwestern United States high desert region, with some local variations due to complex terrain in the area.

- The area is arid to semi-arid, that is, precipitation is adequate only to support sparse desert vegetation. Annual total precipitation varied significantly from year to year, and to a lesser extent according to the elevation and location relative to terrain features. The annual average at Site 1 was 200.8 mm (Table 1.1-10). Precipitation was infrequent, so short-term large amounts influenced the long-term totals (BSC 2007e, Section 5.3).
- Wind speed varied by diurnal and seasonal cycles. Daytime speeds were generally higher than nighttime, though the persistent nocturnal downslope winds at the valley floor sites kept the nighttime averages higher than would occur otherwise. The highest monthly average speeds occurred in April. The extreme three-second gust speed at Site 1 was 27.6 m/s (i.e., about 62 mph), while the hilltop location of Site 4 on Alice Hill

experienced a gust of 39.9 m/s (i.e., almost 90 mph). With one exception, the maximum one-minute average wind speeds occurred from a northwesterly direction (BSC 2007e, Section 5.3).

- Daytime air temperature generally varied by elevation with higher temperatures at lower elevations, but nighttime temperatures varied considerably by terrain exposure. The cold air drainage dropped minimum temperatures more, and more often, at valley floor sites than on the higher slopes and on the hilltop locations. The temperature data also show seasonal cycles. The monthly mean maximum and minimum temperatures varied by over 20°C between summer and winter at Site 1 (BSC 2007e, Section 5.3).
- Relative humidity reflected the arid climate with overall low values and a diurnal cycle matching the diurnal temperature cycle (BSC 2007e, Section 5.3).
- High mean maximum solar radiation values were due to the clear-sky conditions typical of the southwestern desert region (BSC 2007e, Section 5.3).
- Barometric pressure showed seasonal variations of the mean monthly averages of 4 to 7 mb, with lower values occurring during the period from April through June. This cycle was associated with seasonal cycles in synoptic weather patterns (BSC 2007e, Section 5.3).
- Atmospheric stability, one factor in determining the dispersion potential of the atmosphere, typically underwent a diurnal cycle with stable (low dispersion) conditions occurring during the nighttime hours and neutral (moderate dispersion) to unstable (high dispersion) conditions in the daytime hours (BSC 2007e, Section 5.3).
- Joint frequency distributions of wind speed and wind direction by time of day and stability categories showed regular cycles influenced by local terrain. Unless large-scale weather systems overrode the local-scale wind dynamics related to terrain, daytime unstable conditions occurred with winds from southerly directions. Terrain features tended to channel airflow in directions along the axis of valleys during the daytime periods. Surface cooling in the clear-sky environment led to stable periods with cold air flowing down local slopes and large valley areas at night, particularly in the valley floor locations. The downslope directions were generally from the west to north on the east side of Yucca Mountain and in Jackass Flats (BSC 2007e, Section 5.3).

1.1.3.6 Severe Weather Characteristics

[NUREG-1804, Section 2.1.1.1.3: AC 3(4), (5)]

1.1.3.6.1 Tornadoes

Tornadoes represent a special case of extreme winds where localized wind forces cause pressure drops and exert wind loading. Such tornado-induced pressure and wind loading, if sufficiently intense, may result in physical disruption of one or more repository operations.

Tornadoes are infrequent and weak in the Yucca Mountain region because of the generally dry weather conditions occurring most of the time and the unfavorable terrain conditions for tornado generation (CRWMS M&O 1997a, Section 4.2.2.5). Data on reported tornado occurrences within counties lying within the Great Basin region, encompassing most of Nevada and portions of Utah, Arizona, and California, indicate that during the period between January 1, 1950, and September 30, 2003, the following tornadoes occurred (Deng 2004a, Deng 2004b, Deng 2004c, Deng 2004d):

- 84 tornadoes that were classified as Fujita-scale category F0 (wind speeds from 40 to 72 mph)
- 27 tornadoes that were in the F1 category (wind speeds from 73 to 112 mph)
- Two category F2 tornadoes (wind speeds from 113 to 157 mph)
- No category F3 or greater tornadoes (wind speeds greater than 157 mph)
- 27 unclassified tornadoes.

There were no category F2 or greater tornadoes reported in the State of Nevada during this period. The tornadoes reported closest to Yucca Mountain were three category F0 tornadoes in Nye County (Deng 2004a).

Although the probability of a tornado occurring in the region is low, the requisite conditions for tornado formation, including a moist atmosphere, atmospheric instability from near the ground surface to several thousand meters above the surface, and the existence of vertical wind shear, might occur within the region on rare occasions. Such conditions might exist when a cold, closed low-pressure system migrates from the eastern Pacific Ocean to Nevada or when thick layers of subtropical moisture move into the region from the Gulf of Mexico or the Gulf of California (CRWMS M&O 1997a, Section 4.2.2.5).

The design basis tornado wind speed is 189 mph, which corresponds to a frequency of occurrence of 10^{-6} per year. The corresponding pressure drop is 0.81 psi and the rate of pressure drop is 0.3 psi/s (BSC 2007f, Section 6.1.4). The extreme wind, tornado, and tornado missile hazard analysis is reported in [Section 1.6.3](#).

1.1.3.6.2 Thunderstorms and Lightning Strikes

Lightning data are collected by an automated lightning-detection system installed on the Nevada Test Site as part of the Air Resources Laboratory and Special Operations and Research Division of the National Oceanic and Atmospheric Administration. Lightning-strike data are limited to cloud-to-ground strikes only. The data collected from 1991 through 1996 were analyzed. Data characteristics for each lightning strike documented include latitude, longitude, date and time of occurrence, and signal sign, which is positive or negative (CRWMS M&O 1997a, Section 2.6). Positive (positively charged) lightning strikes are characterized by longer duration and are generally more intense current flows than the more commonly occurring negative lightning strikes (CRWMS M&O 1997b, Section 7.2.4.3).

The data show that for a 3,600-km² area around Yucca Mountain, lightning strikes occurred most frequently during August, with a secondary strike maximum occurring in May. The months of May through September exhibited the most strikes, and few or no lightning strikes occurred in other months. The annual flash density ranged from approximately 0.06 to 0.4 strikes/km² per year. Of that strike frequency, the fraction of positive strikes is 2% to 3% of the total number of strikes (CRWMS M&O 1997a, Section 4.2.2.4).

A similar analysis of lightning occurrences, based on data collected from 1991 through 1996, was performed for a 100-km² area centered on western Midway Valley. Results of the analysis indicate that the strike maximum for the area occurs in August, with no observable pronounced secondary maximum. The density of flashes ranged from 0.07 to 0.4 strikes/km² per year, which is similar to the 3,600 km² area analysis. No positive strikes occurred for the 100-km² area during the years the data were collected (CRWMS M&O 1997a, Section 4.2.2.4).

Warm-season, cloud-to-ground lightning data in the vicinity of the Nevada Test Site were summarized and analyzed for the 8 year period of 1993 through 2000 by Randerson and Sanders (2002). Thunderstorm activity and the accompanying cloud-to-ground lightning are both primarily summertime phenomena in this vicinity. Consequently, the study focused on warm-season lightning defined as occurring in June through September.

A total of 9,596 cloud-to-ground lightning flashes were detected on the Nevada Test Site for the period of record. Of these flashes, 9,346 lowered negative charge to the ground (negative flashes) and 250 lowered positive charge to the ground (positive flashes). The data illustrate large inter-annual variability in thunderstorm activity in a desert environment. Measured total warm-season cloud-to-ground lightning flashes on the Nevada Test Site range from only 409 flashes in 1993 to 2,532 flashes in 1999. The most active lightning season was the one following the 1998 to 1999 El Nino event (Randerson and Sanders 2002, Table 1). There is not only a great inter-annual variability in negative flashes on the Nevada Test Site, but also in positive flashes. The annual percentage of positive cloud-to-ground flashes on the Nevada Test Site ranges from 1.0% in 1993 to 6.2% in 1997 (Randerson and Sanders 2002, Table 1). An annual average of 6.2% is large for the summer months for the continental United States. However, the average warm-season positive flash percentage of the 8 year sample is 2.6%, which is similar to values reported in other studies for the northern Rocky Mountains and for southern Nevada (Randerson and Sanders 2002, p. 7).

Based on the total number of cloud-to-ground flashes detected on the 3,500-km² Nevada Test Site, the mean annual warm-season cloud-to-ground flash density for the analysis area is 0.34 flashes/km² during the eight years of record. This number is smaller than calculations of the annual average of 2.0 flashes/km² for the contiguous United States that include an adjustment for a 70% detection efficiency (flash-density counts are multiplied by 1.4). If the average Nevada Test Site warm-season flash density of 0.34 flashes/km² is multiplied by 1.4, the resulting average Nevada Test Site flash density of 0.48 flashes/km² is very similar to other flash density estimates for southern Nevada (Randerson and Sanders 2002, pp. 7 to 8).

Cloud-to-ground lightning occurs throughout the Nevada Test Site. However, Area 25 in the southwestern section of the Nevada Test Site has experienced the least number of flashes. The total flash count in this area is ≤ 4.0 flashes/km² for the eight warm seasons, 1993 through 2000. Frenchman Flat has also experienced a similar low flash count. By contrast, widespread

thunderstorm and cloud-to-ground lightning flash activity has occurred in the northwest quarter of the Nevada Test Site. Total flash counts of 10 to 13 flashes/km² have been detected along the northern border of the Nevada Test Site for the period of record. In addition, another active area appears in the northeastern part of the Nevada Test Site, in Areas 8 and 15. The largest total flash count on the Nevada Test Site was measured approximately 5 km south of Mercury, where 13 flashes/km² occurred. Another active area of 12 flashes/km² is located nearly 10 km southwest of Mercury. These two areas appear to be associated with thunderstorms that develop over the Spring Mountain Range and move northeastward onto the Nevada Test Site (Randerson and Sanders 2002, p. 8 and Figure 8).

Site-specific, warm-season (1993 through 2000) cloud-to-ground lightning information was compiled for a circular area, centered on Yucca Crest, with a 10-mi radius that includes most of the northern part of the land withdrawal area and encompasses the GROA. This area experienced 1,313 total cloud-to-ground flashes within the 10-mi radius and had a flash density of 0.20 flashes/km²/warm season. Thirty-four positive flashes occurred, resulting in a 2.6% positive flash ratio. The maximum flash amperage detected within the 10-mi radius was +122 KA (Randerson and Sanders 2002, Table 3 and Figure 17). In comparison, the maximum flash current detected on the Nevada Test Site is -167 KA and the maximum positive-flash current detected on the Nevada Test Site is +152 KA (Randerson and Sanders 2002, p. 17).

1.1.3.6.3 Sandstorms

Although sandstorms have not been documented at the Yucca Mountain site, it has long been recognized that the southern Nevada desert region experiences the highest incidence of dust storms in the state. However, the relatively strong winds, typically greater than 25 mph, needed for sand or dust storms occur only a fraction of the time (Eglington and Dreicer 1984, Section 2.2.2). Evaluations of sand and dust storm hazards are discussed in [Section 1.6.3](#).

1.1.3.6.4 Snowfall

Snowfall and snow depth measurements were not part of the meteorological monitoring program at Yucca Mountain. Therefore, reasonable estimates of the Yucca Mountain snowfall environment are based upon climatological records from the Desert Rock Airport Weather Service Meteorological Observatory, Nevada, which is located approximately 45 km southeast of the repository at an elevation of 3,301 ft above mean sea level. The period of record is January 1, 1983, through February 28, 2005, and indicates a maximum daily snowfall at 6 in. and a maximum monthly snowfall of 6.6 in.

1.1.4 Regional and Local Surface and Groundwater Hydrology

[NUREG-1804, Section 2.1.1.1.3: AC 4]

Surface and groundwater hydrology in the Yucca Mountain region are a subset of natural conditions that are relevant in the development of a repository design and that could pose hazards to safety during the preclosure period. This section describes hydrologic information relevant to the development of a design. It also describes potential hydrologic hazards and initiating events that could affect the safety of the repository during the preclosure period. Additionally, it summarizes

site-specific and regional hydrologic data that have been used to quantify the expected magnitude, frequency, and duration of these hazards and events.

[Section 1.1.4.1](#) provides a description of the Yucca Mountain regional and local surface water hydrology and hydrologic features relevant to the PCSA and to the repository design.

[Section 1.1.4.2](#) provides a description of the Yucca Mountain regional and local groundwater hydrology and hydrologic features relevant to the PCSA and to the repository design.

[Section 1.1.4.3](#) provides a description of the Yucca Mountain flooding potential, including the probable maximum flood and its characteristics.

1.1.4.1 Surface Water Hydrology *[NUREG-1804, Section 2.1.1.1.3: AC 4(1)]*

1.1.4.1.1 Regional Surface Water Hydrology

The Yucca Mountain region is characterized by a dry, semiarid climate, low annual precipitation with a mean of 125 mm/yr at about 1,500 m elevation, and infrequent rainstorms (BSC 2004a, Section 3.4.2). Stream flow is a result of regional storms that occur mostly during the winter and localized thunderstorms that occur mostly during the summer. No perennial streams, natural bodies of water, or naturally occurring wetlands occur on the Yucca Mountain site (DOE 2002b, Sections 3.1.4.1.2 and 3.1.5.1.4). As a result of the dry climate, even the larger streams are ephemeral, which means they flow only in immediate response to precipitation and are dry most of the time. Throughout the Death Valley drainage basin, perennial flow is only observed downgradient of spring discharges and around the margins of playas and salt pans where the land surface and water table converge (BSC 2004a, Section 7.1.1.2).

Fortymile Wash is the main drainage channel on the Yucca Mountain site. It originates on Pahute Mesa ([Figure 1.1-52](#)) and flows southward. The eastern slope of Yucca Mountain drains via Yucca Wash, Drill Hole Wash, and Dune Wash to Fortymile Wash ([Figure 1.1-53](#)). Fortymile Wash spreads out into a distributary system in the Amargosa Desert and during floods joins the Amargosa River about 13 mi northwest of Death Valley Junction, California ([Figures 1.1-53](#) and [1.1-54](#)). An unnamed ephemeral stream channel drains the western slope of Yucca Mountain via Solitario Canyon ([Figure 1.1-53](#)). This channel also collects drainage from the southern slope of Yucca Mountain, then drains to the Amargosa River near its confluence with Fortymile Wash. Topopah Wash drains Jackass Flats ([Figure 1.1-53](#)). During floods, water from Topopah Wash flows into the Amargosa River in the Amargosa Desert (BSC 2004a, Section 7.1.1).

The only permanent bodies of surface water in the vicinity of Yucca Mountain are Crystal Reservoir, Lower Crystal Marsh, Horseshoe Reservoir, and Peterson Reservoir. These artificial impoundments store discharge of springs in Ash Meadows ([Figure 1.1-54](#)) about 50 km southeast of Yucca Mountain. Like the streams in the area, the playas shown in [Figures 1.1-52](#) and [1.1-54](#) contain water only after periods of heavy precipitation. However, some, like Badwater Basin in Death Valley and Franklin Lake playa (also known as Alkali Flat) in the Amargosa Desert, represent sumps for groundwater discharge and can be wet for extended periods as the water evaporates (BSC 2004a, Section 7.1.1).

1.1.4.1.2 Local Surface Water Hydrology

The surface facilities are situated on the east side of Exile Hill in Midway Valley at the eastern margin of Yucca Mountain. [Figure 1.1-5](#) shows the topography of the Midway Valley drainage system and surrounding area. To the west and northwest of Midway Valley, along the east slope of Yucca Mountain, drainage basins that form Antler, Split, Drill Hole, Pagany, Sever, and Yucca washes, channel flow eastward across Midway Valley into Fortymile Wash ([Figure 1.1-5](#)). Antler Wash drains into Midway Valley through a gap between Bow Ridge and Opal Hill. Split Wash and Drill Hole Wash drain into Midway Valley through a gap between Exile Hill and Opal Hill. Pagany Wash and Sever Wash drain into Midway Valley to the north of Exile Hill. These washes, and an unnamed drainage exiting the southern part of the canyon containing Yucca Wash, merge and drain into Fortymile Wash through a gap between Fran Ridge and Alice Hill. Yucca Wash crosses the northern end of Midway Valley to drain into Fortymile Wash through a gap north of Alice Hill ([Figure 1.1-5](#)).

The pooling or ponding of large quantities of water on the surface is limited by the arid-to-semiarid climate and geologic conditions, such as permeable surficial materials and a deep groundwater table. Pads are graded to prevent the pooling of water.

1.1.4.1.2.1 Flooding Potential

The current major flood hazard at and near Yucca Mountain is flash flooding resulting from intense rainfall and runoff from localized convective storms or from high-intensity precipitation cells within regional storm systems (BSC 2004a, Section 3.4.3). [Section 1.1.4.3](#) discusses the evaluation of the probable maximum flood.

1.1.4.1.2.2 Potential Water and Debris Flows from Slopes above the North Portal

Two stormwater drainage diversion channels, the north diversion ditch and the south diversion ditch, are planned to protect the North Portal and the surface GROA from runoff and debris flows that could emanate from the eastern slopes of Exile Hill that lie to the west of the North Portal pad). These man-made channels shall be sized to transport the probable maximum flood (BSC 2007f, Section 6.1.9).

1.1.4.2 Groundwater Hydrology *[NUREG-1804, Section 2.1.1.1.3: AC 4(1)]*

1.1.4.2.1 Regional Groundwater Flow System

Yucca Mountain is located within the Death Valley regional groundwater flow system, in the southern part of the Great Basin. The Death Valley regional groundwater flow system includes an area of approximately 70,000 km². The area encompassed by this flow system is contained entirely within Nevada and California. Groundwater movement within this regional flow system occurs in an asymmetric radial-flow pattern from recharge areas in mountains and other highlands, which are located principally along the periphery of the basin, toward the regional hydraulic sink in the bottom of Death Valley (BSC 2004a, Section 8.2.2).

The repository is located in the Alkali Flat–Furnace Creek groundwater basin, which is part of the central Death Valley subregion of the Death Valley regional groundwater flow system (Figure 1.1-55). This basin is bordered on the north and northwest by the Pahute Mesa–Oasis Valley groundwater basin and on the east by the Ash Meadows groundwater basin (BSC 2004a, Section 8.2.7.3).

Potentiometric data indicate that groundwater generally flows south from upland recharge areas in the volcanic terrain of Pahute Mesa, beneath Timber Mountain, and continues to flow southward toward the Yucca Mountain area (Figure 1.1-55). The groundwater flows through the aquifers of the Tertiary volcanic and volcanoclastic sequence beneath Crater Flat, Yucca Mountain, and Jackass Flats, eventually entering into the valley-fill sedimentary deposits of the Amargosa Desert.

Natural discharge does not occur within the immediate vicinity of Yucca Mountain. The nearest natural discharge areas connected to the saturated zone flow system beneath Yucca Mountain are Franklin Lake playa (Alkali Flat) and possibly the major springs at Furnace Creek and the valley floor of Death Valley (Figure 1.1-55).

1.1.4.2.2 Water Use in the Region

Throughout the Death Valley region, groundwater is the principal source of water for agricultural, mining, industrial, municipal, and domestic uses. Surface water is sparsely distributed, and it occurs generally at small and unreliable rates of flow; it is a minor component of the region's water resource. In contrast, groundwater is widely available and has been sufficient to satisfy most of the historically modest demand. Most of the groundwater resource development in the central Death Valley subregion has occurred in Nevada, although minor development has taken place in the extreme southwestern Amargosa Desert near Death Valley Junction, California. In the Furnace Creek area of Death Valley National Park, spring discharge supplies the domestic and commercial use.

Generally, groundwater can be obtained in sufficient amounts to cover existing needs throughout the region. In the lowland valleys, including the Amargosa Desert, thick alluvial deposits in the valley-fill aquifer supply water to wells sufficient to irrigate the soils of the area. Wells at selected locations on the Nevada Test Site tapping volcanic aquifers and the deep carbonate aquifer have furnished adequate water for the industrial needs of the Nevada Test Site. The carbonate aquifer, along with the alluvial aquifers, is widely viewed as a major water supply source in southern Nevada (BSC 2004a, Section 8.5.3).

1.1.4.2.3 Local Groundwater Hydrology

The combination of aridity, large topographic relief, and transmissive rocks results in a thick unsaturated zone, which is a principal hydrologic attribute of the site. The water table is deep beneath the land surface. At the surface GROA, the land surface is at an elevation of about 1,120 m, and the water table is at about 730 m above mean sea level and about 390 m below the land surface of the surface GROA. The minimum distance from the floor of the emplacement area to the top of the current water table is about 210 m in the northwestern part of the repository. The maximum distance to the water table is about 375 m in the southern part of the repository (BSC 2007g, Figure 11 and Tables 12 and 15; BSC 2004c, Figure 6-2).

The unsaturated zone rock units include Quaternary surficial deposits and Tertiary volcanic tuffs. The principal hydrogeologic units defined in the unsaturated zone at the repository are unconsolidated alluvium, Tiva Canyon welded, Paintbrush nonwelded, Topopah Spring welded, Calico Hills nonwelded, and Crater Flat undifferentiated (GI [Figure 5-30](#)). These hydrogeologic units, together with natural hydrologic processes, control water movement in the unsaturated zone, including net infiltration, percolation, fracture–matrix interaction, accumulation of perched water, lateral flow, and deep percolation to the water table (BSC 2004a, Section 7).

Within the saturated zone, the geologic strata at Yucca Mountain form a series of alternating, intercalated volcanic aquifers and confining units above the regional Paleozoic carbonate aquifer. The volcanic rocks generally thin and pinch out toward the south, away from their eruptive sources in the vicinity of Timber Mountain. Downgradient, the undifferentiated valley fill and the valley-fill aquifer to the south and southeast of Yucca Mountain replace or overlie the volcanics. Generally, only a small number of intervals within the aquifers, usually associated with fractures or faults, produce water. The confining units also may transmit water but to a lesser extent than the aquifers. For the volcanic tuff units, groundwater flow is considered to occur primarily through fractures, while flow in the alluvium is through the porous matrix (BSC 2004a, Section 8.3.8.1.1; Luckey et al. 1996).

Potentiometric data indicate the potential for groundwater flow toward the repository from the area of the large hydraulic gradient to the north, from the moderate hydraulic gradient to the west, and from the repository toward Fortymile Wash to the east. The flow path from beneath the repository initially appears to be eastward to southeastward toward Jackass Flats, then south-southwest. Beneath the crest of Yucca Mountain, flow is entirely in the lower volcanic aquifer and deeper units. However, near Fortymile Wash, the rock units composing the upper volcanic aquifer dip beneath the water table and dominate the flow system. That portion of flow reaching the Fortymile Wash area from beneath Yucca Mountain then generally flows south-southwestward where it enters and flows through valley-fill sedimentary deposits to the Amargosa Desert (BSC 2004a, pp. ES-7 and ES-8).

Discharge nearest to Yucca Mountain occurs through groundwater withdrawals from pumpage at wells UE-25 J-12 and UE-25 J-13, both of which penetrate volcanic rock east of Yucca Mountain ([Figure 1.1-53](#)). Withdrawals from wells UE-25 J-13 and UE-25 J-12 were about 16.3 Mgal and 12.9 Mgal, respectively, during 2000; about 27.6 Mgal and 8.6 Mgal, respectively, during 2001; and about 10.2 Mgal and 7.5 Mgal, respectively, during 2002 (Locke and La Camera 2003, p. 23). Groundwater withdrawals from well UE-25 J-13 decreased to about 0.7 Mgal in 2003. Groundwater withdrawals from well UE-25 J-12 increased to about 12.8 Mgal in 2003 (La Camera et al. 2005, p. 13). In 2004, withdrawals from wells UE-25 J-13 and UE-25 J-12 were about 14 Mgal, with UE-25 J-12 accounting for about 84% of the total (La Camera et al. 2006, p. 13).

Perched water has been identified below the repository horizon in seven boreholes in the Yucca Mountain area (BSC 2004a, Section 7.4.2): USW UZ-1, USW UZ-14, and USW NRG-7a in Drill Hole Wash; USW SD-9, USW SD-12, and USW SD-7 along the Exploratory Studies Facility (ESF) main drift; and USW WT-24, north of the repository area ([Figure 1.1-56](#)). The accumulation of perched water seems to be caused by either the basal vitrophyre of the Topopah Spring Tuff or the vitric–zeolitic boundary in the Calico Hills Formation acting in concert with a lateral structural barrier formed by a fault (Rousseau et al. 1999, pp. 171 and 172). The stratigraphic horizons and the perched-water bodies identified are at elevations of 100 to 200 m below the repository horizon and

at least 381 m belowground surface; therefore, they do not represent obstacles to repository design or construction (BSC 2004a, Section 7.4.2).

1.1.4.3 Hydrologic Engineering Studies for Surface Facilities

[NUREG-1804, Section 2.1.1.1.3: AC 4(2), (3)]

Hydrologic engineering studies have been completed to evaluate flood hazards to the surface facilities discussed in [Section 1](#), including the effects on existing and planned modifications of surface features (BSC 2004b; BSC 2007h).

1.1.4.3.1 Probable Maximum Precipitation Determination

Section 2.4.3 of NUREG-0800 (NRC 1987) sets forth the acceptance criteria for determining the extent of flood protection required. It indicates that publications of the National Oceanic and Atmospheric Administration may be used for large and small basin probable maximum precipitation estimates, and models of the U.S. Army Corps of Engineers may be used to estimate the probable maximum flood discharge and water level condition at the site. The probable maximum precipitation was determined using the National Oceanic and Atmospheric Administration procedures, and U.S. Army Corps of Engineers computer programs were used to evaluate the peak discharges and flooding conditions at the site. These usages are also consistent with ANSI/ANS-2.8-1992, *American National Standard for Determining Design Basis Flooding at Power Reactor Sites*.

The probable maximum precipitation was determined using procedures described in *Probable Maximum Precipitation Estimates, Colorado River and Great Basin Drainages* (Hansen et al. 1977) by the National Oceanic and Atmospheric Administration. These procedures provide the best estimate of probable maximum precipitation potential (BSC 2002a, Section 6.2.1) for this region. The method takes into account meteorological conditions and atmospheric processes in a region, moisture-maximized rains of record, and broad-scale terrain features, among other factors, to determine a theoretical maximum amount of precipitation for a region or a local watershed. Using the watershed size and geographical location, the estimated local storm probable maximum precipitation is determined to be 13.2 in. over a 6-hour duration for the basins containing the North Portal pad and 12.9 in. over a 6-hour duration for the basins containing the South Portal pad. The local storm precipitation intensity is calculated to be greater than that determined for the general storm probable maximum precipitation and is, therefore, used in the probable maximum flood determination (BSC 2004b, Section 4.2.2).

As a comparison to these estimates of 13.2 and 12.9 in. of precipitation in 6 hours in Midway Valley, precipitation records at Yucca Mountain indicate that the maximum 24-hr precipitation amount measured is 3.43 in. at the Alice Hill site (Meteorological Monitoring Site 4) on the east side of Midway Valley. This amount was also the maximum 24-hr precipitation amount observed for all nine of the Yucca Mountain stations. The maximum 24-hr precipitation amount for the drainage basin that includes the surface GROA (Sever Wash; Meteorological Monitoring Site 7) is 3.30 in. ([Section 1.1.3.2.1](#) and [Table 1.1-23](#)).

1.1.4.3.2 Probable Maximum Flood Flow Characteristics

Probable maximum flood inundation studies completed in 2004 encompass the North Portal pad and vicinity; the South Portal pad; and alternative layouts for the surface facilities GROA, muck storage, and aging pads. The alternatives also considered different configurations for the buildings of the surface GROA. The calculations determined the magnitude and duration of runoff that would occur during a probable maximum flood event and determined flow characteristics, including the maximum lateral extent of inundation, flow depths, and velocities (BSC 2004b).

The U.S. Army Corps of Engineers HECRAS software, version 2.1 was used for the flood inundation analyses. This program is designed for flood inundation studies and flood risk analysis. HECRAS is a Federal Emergency Management Agency nationally accepted computer software that can be used to estimate flood elevations (BSC 2004b, Section 3.2).

A no-mitigation scenario was evaluated to assess the flooding potential at the North Portal pad modified for a previously planned surface facilities layout. This scenario assumed that the planned facilities upstream are not constructed and that flood control measures, such as diversion channels or floodwalls, are not implemented. Peak discharges were used with a bulking factor of 10% as inputs to the HECRAS software (BSC 2004b, Section 6). A bulking factor in discharge is included to account for increased flow depths caused by the presence of entrained air, debris, and sediment load relative to clear water flow. A literature review suggests that bulking may not be a significant factor affecting probable maximum flood flows at Yucca Mountain. A probable maximum flood will have too much water for bulking to be significant. The use of a bulking factor of 10% is conservative (BSC 2002a, pp. 29 to 30).

It was determined that without flood control measures, runoff from the probable maximum flood would inundate part of the North Portal pad with the modifications for previously planned surface facilities ([Figure 1.1-57](#)) (BSC 2004b, Section 6.2.1). Water depths across the North Portal pad would range between approximately 2 and 11 ft. The North Portal would remain above the inundation surface (BSC 2004b, Section 6.2.3). As it was determined that ITS facilities in the vicinity of the North Portal would be inundated by the probable maximum flood without mitigation (BSC 2004b), a new calculation was completed to evaluate mitigation needed to protect the current surface GROA configuration from inundation (BSC 2007h). The results of this new study and the design features planned for mitigation are discussed in [Section 1.2.2](#).

Calculations were performed to determine the limits of inundation in three channels in the vicinity of the South Portal pad during a probable maximum flood event: Antler Wash, a small unnamed channel to the north between the South Portal pad and Antler Wash, and a small unnamed channel to the southeast of the South Portal pad, referred to as sportal1, sportal3, and sportal2, respectively, in [Figure 1.1-58](#) (BSC 2004b, Section 6.10.1). Peak discharges were used as inputs to the HECRAS software and were increased by a bulking factor of 10% (BSC 2004b, Section 6.10.1). In these calculations, water levels in Antler Wash (sportal1) and the unnamed channel to the southeast (sportal2) do not rise to the level of the South Portal pad. The water level in the unnamed channel to the north of the South Portal pad (sportal3) rises to the northern edge of the elevated South Portal pad ([Figure 1.1-58](#)). The depth of water along the northern edge of the elevated South Portal pad is estimated to be less than 1 ft (BSC 2004b, Section 6.10.3). The water would not overflow the South Portal pad surface because the water surface elevation is calculated to be 3,785 ft (BSC 2004b,

Table 6-11) and the South Portal pad surface elevation is greater than 3,793 ft (CRWMS M&O 1999a).

The North Construction Portal has not been built. It is planned to be excavated on a ridge with the bottom of the boxcut at an elevation of 3,891 ft above mean sea level (BSC 2003b, Table 7). The probable maximum flood study indicates that the portal will be outside of the probable maximum flood inundation area and that the flood waters would reach an elevation of about 3,885 ft above mean sea level in the channel to the southwest of the portal (BSC 2004b, Figure 7-4 and Table 7-4).

Any potential effect from coincident wind waves was not included in the probable maximum flood calculation. The transitory nature of the flooding, short fetch distance, and relatively shallow water depth were judged to make any additional height of water because of coincident wind waves minimal (BSC 2004b, Section 8.2).

1.1.5 Site Geology and Seismology

[NUREG-1804, Section 2.1.1.1.3: AC 5; Section 2.1.1.7.3.2: AC 1]

This section presents a description of the geologic, geotechnical, geomechanical, and seismic setting characteristics of Yucca Mountain as they pertain to the PCSA and the design of the GROA.

[Section 1.1.5.1](#) provides a description of the stratigraphy, lithology, and structural geology at the repository site. The rock units underlying the repository site are described. The structural framework of the site area is described, including the characteristics of the various types of faults and fractures.

[Section 1.1.5.2](#) provides information on the known seismic sources in the Yucca Mountain region. Earthquake (vibratory ground motion) and fault displacement hazards are described. This section also discusses the development of seismic design data for the preclosure period.

[Section 1.1.5.3](#) addresses the in situ and laboratory testing performed for design purposes and the principal geotechnical properties of the surface and subsurface soils and rocks important to design of facilities at the site. There are two main parts to this discussion: the geotechnical properties of materials in the underground facilities area and in the surface facilities area. The underground facilities area includes the emplacement drifts and access mains. The surface facilities area includes ITS facilities located at grade elevation.

1.1.5.1 Site Geology

[NUREG-1804, Section 2.1.1.1.3: AC 5(1) to (5)]

The geology of the repository site, including the stratigraphy and structural geology of the site, provides the framework for assessing the preclosure behavior of the repository. In this section, information on both the bedrock and surficial deposits at the GROA and the structural features of the area, including local faults and fractures, are described.

1.1.5.1.1 Site Stratigraphy

Yucca Mountain consists of successive layers of volcanic tuffs, which were formed approximately 14 to 11.4 million years ago by eruptions of volcanic ash from calderas to the north. Tertiary volcanic rocks dominate the exposed and near-subsurface bedrock at Yucca Mountain, which is shown in map view in [Figure 1.1-59](#). These rocks consist mostly of pyroclastic flow (ash flow) and fallout tephra deposits with minor lava flows and reworked materials. Where present, the thick series of volcanic rocks and older Tertiary rocks that form Yucca Mountain overlie Paleozoic sedimentary strata along a pronounced unconformity. The volcanic rocks are covered in many areas by a variety of late Tertiary and Quaternary surficial deposits (BSC 2004a, Section 2.3.5).

The physical properties of the tuff and lava units that make up Yucca Mountain often contrast greatly across depositional contacts but tend to be relatively uniform laterally over broad areas. This characteristic results from several causes. First, large batches of homogenized material were laid down quickly as ash flows over large areas. Second, there were differences in the composition of each eruptive batch, and sometimes there were differences in the composition of first-erupted and last-erupted material in a single eruptive batch. Finally, the postdepositional processes of welding, vapor phase crystallization, alteration, and gas dispersion were different for each unit. These genetic causes have resulted in differences in lithology, rock properties, mineralogy, and geochemistry that are used as characteristics or criteria to develop a detailed stratigraphic subdivision of the major lithostratigraphic units (BSC 2004a, Sections 2.3 and 3.3).

At Yucca Mountain, the Prow Pass Tuff of the Crater Flat Group, the Calico Hills Formation, and the formations of the Paintbrush Group have been studied sufficiently to allow for the subdivision of the formations into members; zones; subzones; and, in some cases, intervals. Most of the surface of Yucca Mountain is composed of the volcanic rocks of the Paintbrush Group ([Figure 1.1-59](#)), which consists of four formations, each primarily composed of pyroclastic flow deposits interstratified with small-volume pyroclastic flow and fallout tephra deposits. In ascending order, these formations are the Topopah Spring (which includes the repository host horizon), Pah Canyon, Yucca Mountain, and Tiva Canyon tuffs ([Figure 1.1-60](#)). This group is one of the most widespread and voluminous caldera-related assemblages in the southwestern Nevada volcanic field. The Topopah Spring Tuff forms the host rock for the repository. The Paintbrush Group is dominated volumetrically by the Topopah Spring and Tiva Canyon tuffs. The Pah Canyon and Yucca Mountain tuffs are volumetrically minor but are of potential hydrologic importance because of their high matrix porosity compared to the Topopah Spring and Tiva Canyon tuffs, which are densely welded and fractured with low matrix porosity. The Topopah Spring and Tiva Canyon tuffs are classic examples of compositional zonation: from a first-erupted, more voluminous, crystal-poor (less than 5% crystal fragments), high-silica, rhyolitic lower part to a last-erupted, crystal-rich (greater than 10% crystal fragments), quartz-latic upper part. Contacts of several lithostratigraphic units correspond with hydrogeologic and thermal-mechanical unit boundaries throughout Yucca Mountain and have been used in the development of three-dimensional geologic and hydrogeologic models (BSC 2004a, Sections 3.3.2 and 3.3.4.7).

The Topopah Spring Tuff (12.8 million years old) (Sawyer et al. 1994, Table 1) includes the repository host-rock units. The Topopah Spring Tuff has a maximum thickness of about 380 m in the Yucca Mountain vicinity. The unit is compositionally zoned and is divided into a lower crystal-poor rhyolitic member (Tptp) and an upper crystal-rich quartz-latic member (Tptr), with an

upward chemical change from high-silica rhyolite in the Tptp to quartz latite in the Tptr. Each member is divided into numerous zones, subzones, and intervals, based on variations in characteristics such as lithophysal content, crystal content and assemblage, size and abundance of pumice and lithic clasts, distribution of welding and crystallization zones, and fracture characteristics. As shown in Figure 1.3.4-2, the repository will be located in the four lithostratigraphic units known as the upper lithophysal (Ttpul), middle nonlithophysal (Ttpmn), lower lithophysal (Ttpll), and lower nonlithophysal (Ttpln) zones of the Tptp (BSC 2004a, Section 3.3.4.7).

The Pah Canyon Tuff (between 12.8 and 12.7 million years old) (Sawyer et al. 1994, Table 1) is a simple cooling unit composed of multiple flow units. The formation reaches its maximum thickness of about 80 m in the northern part of Yucca Mountain and thins southward to 0 m. The Pah Canyon Tuff varies from moderately welded in the north to nonwelded toward the south. A bedded-tuff unit intervenes between the Pah Canyon Tuff and the overlying Yucca Mountain Tuff, where these two formations are present at Yucca Mountain. In addition, in the northern part of the Yucca Mountain area, rhyolite lava flows and related tephra deposits occur locally between the Pah Canyon and Yucca Mountain tuffs. These include the rhyolites of Black Glass Canyon, Delirium Canyon, and Zig Zag Hill (BSC 2004a, Section 3.3.4.7).

The Yucca Mountain Tuff (between 12.8 and 12.7 million years old) (Sawyer et al. 1994, Table 1) is a relatively thin, simple cooling unit that is nonwelded throughout much of Yucca Mountain but is partially to densely welded where it thickens in the northern and western parts of Yucca Mountain. Although typically vitric, the tuff is increasingly devitrified where it is thick. The formation is nonlithophysal throughout Yucca Mountain but contains lithophysae where it is densely welded in northern Crater Flat. A bedded-tuff sequence overlies the Yucca Mountain Tuff and separates it from the overlying Tiva Canyon Tuff. This sequence is characterized by thin beds of pyroclastic fallout tephra deposits that upwardly grade into a thin, oxidized, weathered zone (BSC 2004a, Section 3.3.4.7; Moyer et al. 1996, pp. 18 to 26).

The Tiva Canyon Tuff (12.7 million years old) (Sawyer et al. 1994, Table 1) forms most of the rocks exposed at the surface of Yucca Mountain. It is a large-volume, regionally extensive tuff sequence that is compositionally zoned from lower crystal-poor rhyolite to upper crystal-rich quartz latite. The formation ranges in thickness from less than 50 m to as much as 175 m at Yucca Mountain. Separation of the formation into a lower crystal-poor member and an upper crystal-rich member, and into zones, subzones, and intervals within each of these members, is based on variations in characteristics similar to those discussed for the Topopah Spring Tuff (BSC 2004a, Section 3.3.4.7).

Beneath the Paintbrush Group, the Calico Hills Formation (12.9 million years old) is a complex series of rhyolite tuffs and lavas. Five pyroclastic units, overlying a bedded-tuff unit and a locally occurring basal sandstone unit, are present in the Yucca Mountain area. The formation thins southward across the area, from composite thicknesses of about 460 m to about 15 m. The unit outcrops in the northern part of the site area; its type section is in the Calico Hills to the east of Yucca Mountain (BSC 2004a, Section 3.3.4.6).

The basal volcanoclastic sandstone unit of the Calico Hills Formation is interbedded with locally reworked pyroclastic flow deposits. The overlying bedded tuff is composed primarily of pyroclastic

fall deposits with subordinate, primary, and reworked pyroclastic-flow deposits. Each of the five pyroclastic units forming the bulk of the Calico Hills Formation consists of one or more pyroclastic flow deposits with similar macroscopic characteristics. The flow deposits are separated by locally preserved fall horizons. Ash-fall and ash-flow deposits beneath the repository block give way to lava flows to the north and east (BSC 2004a, Section 3.3.4.6).

The Crater Flat Group, which is located stratigraphically below the Calico Hills Formation, consists of three formations of moderate- to large-volume pyroclastic flow deposits and interstratified bedded tuffs. In ascending order, these formations are the Tram, Bullfrog, and Prow Pass tuffs, ranging in age from 13.25 to 12.9 million years old, respectively (BSC 2004a, Section 2.3.5.1).

Surficial deposits of late Tertiary and Quaternary ages are widespread in the Yucca Mountain area. They include:

- Alluvium that underlies alluvial fan and fluvial terrace surfaces and is deposited along active washes
- Colluvium and debris-flow deposits that occur along the base and that mantle the lower parts of the hillslopes
- Eolian deposits
- Pedogenic calcite and opaline silica deposits.

The relative ages of the surficial deposits are well established, but there is only limited direct numerical age control (BSC 2004a, Section 3.3.7).

1.1.5.1.2 Site Structural Geology

The dominant element of the structural framework of the site area consists of the major block-bounding faults. Block-bounding faults are spaced 1 to 5 km apart and separate large, more-or-less intact blocks of generally east-dipping volcanic strata. As shown in [Figures 1.1-59 and 2.3.4-21](#), from west to east these faults include the Windy Wash, Fatigue Wash, Solitario Canyon, Bow Ridge, and the Paintbrush Canyon faults. Fault scarps generally dip 50° to 80° to the west. A subordinate component of left-lateral displacement is commonly associated with these faults, as determined from slickenside orientations (BSC 2004a, Section 3.5).

Displacement was transferred between block-bounding faults along relay faults. Relay faults intersect block-bounding faults at oblique angles and provide a kinematic link between the bounding structures ([Figure 1.1-61](#)). As such, the relay faults and related structures that constitute relay fault zones are significant components of the block-bounding fault systems, particularly in the southern half of Yucca Mountain. Throughout most of the site area, block-bounding faults strike to the north, and relay faults strike to the northwest. South of Bow Ridge, the Paintbrush Canyon Fault becomes a major fault system as it merges with Dune Wash Fault and Bow Ridge Fault. The Paintbrush Canyon Fault system collects the aggregate displacement of all of these faults. The area in which these faults intersect is concealed beneath surficial deposits northwest of Busted Butte (BSC 2004a, Section 3.5). Considered in the context of relay faults, the northwest-striking

segments of Dune Wash Fault and Bow Ridge Fault transfer displacement between their north-striking segments to the north and the north-striking Paintbrush Canyon Fault system to the south. In the southern part of Yucca Mountain, northwest-striking narrow grabens, such as the Dune Wash graben, are commonly associated with relay faults.

Within structural blocks, small strains were accommodated along intrablock faults. Intrablock faults represent local structural adjustments in response to displacements along the block-bounding faults. In some cases, intrablock faults are expressions of hanging-wall or footwall deformation within a few hundred meters of block-bounding faults. Some intrablock faults, such as the Sundance Fault, lack the vertical continuity of individual fault strands through different stratigraphic levels. This lack of vertical continuity requires a mechanism for accommodation of strain within and between different stratigraphic units. In cases like this, strain likely occurs as distributed deformation within breccia zones and through incremental, small offsets along numerous tectonic fractures that are probably reactivated cooling joints (BSC 2004a, Section 3.5).

In contrast to the deformation observed near block-bounding faults, deformation near small displacement intrablock faults is minimal. The Ghost Dance Fault is an intrablock fault in the GROA vicinity (Figure 1.1-61). It is a north-striking normal fault zone that dips steeply west with down-to-the-west offset. The offset, amount of brecciation, and number of associated splays vary considerably along its trace (Day, Dickerson et al. 1998, p. 11).

The Ghost Dance Fault zone can be divided into three segments based on the amount of offset and brecciation. In the north, it is a relatively narrow zone (2 to 4 m wide) with up to 6 m of offset. In the central part, the zone widens to approximately 100 to 150 m and is made up of several splays with a cumulative offset of approximately 30 m. To the south, the amount of offset is less than 6 m, and brecciation in the hanging wall extends about 15 m to the west. In the southern segment, the fault bifurcates into the Abandoned Wash Fault and towards, but not into, the Dune Wash Fault. Offset on the fault increases to the southwest from Ghost Dance Wash, becoming about 17 m in Abandoned Wash. In the Ghost Dance Wash area (Figure 1.1-5), offset on the fault is less than approximately 3 m and deformation is about 2 m. (Day, Potter et al. 1998, pp. 9 to 10).

1.1.5.1.2.1 Extension

Evaluating the amount and location of extensional faulting at Yucca Mountain aids in developing an understanding of the structural framework of the site. In a brittle deformation regime such as Yucca Mountain, the amount of extension is determined by the number of faults present across an area, the amount of displacement on those faults, and the dip of the faults. (Day, Dickerson et al. 1998, p. 14).

The amount of extension varies across Yucca Mountain. The least extended part of Yucca Mountain is located in the northern part of the site area between Drill Hole Wash and Yucca Wash. The transition from the less-extended northern part of Yucca Mountain to the more-extended southern part is generally expressed on geologic maps by numerous fault splays that fan southward from block-bounding faults in the north. Changes in strike, dip, and displacement of faults indicate increasing crustal extension toward the south. Increased east–west extension is accompanied by the southward splaying of the Solitario Canyon Fault and the development of a broad, complexly faulted graben between Dune Wash and the unnamed ridge between Dune Wash and Abandoned Wash. The Paintbrush Canyon Fault increases in displacement and has a shallower dip toward the

south. The southward increase in the amount of extension and intensity of deformation is accompanied by an increase in the amount of vertical-axis rotation. Clockwise vertical-axis rotations of Paintbrush Group strata increase from north to south, from no rotation at The Prow (Figure 1.1-5), to about 5° at the latitude of Busted Butte in the southern part of the Yucca Mountain site area, to 30° at the extreme south end of Yucca Mountain, 10 km south of the repository vicinity (Day, Dickerson et al. 1998, p. 17; BSC 2004a, Section 3.5.3).

1.1.5.1.2.2 Timing of Deformation

Stratigraphic relations across faults and angular relations across unconformities demonstrate that block-bounding faults were active at Yucca Mountain during eruption of the Paintbrush Group (12.8 to 12.7 million years ago), and significant motion on these faults continued after the Rainier Mesa Tuff was deposited 11.6 million years ago (BSC 2004a, Section 3.5).

1.1.5.1.3 Fractures

1.1.5.1.3.1 Fracture Characteristics of Lithostratigraphic Units of the Repository Horizon

The timing of fracture formation fundamentally determines the geometry of the fracture network by controlling the truncations and thereby the lengths of each subsequent fracture generation. The first fractures to form are those associated with the cooling process. During cooling of the pyroclastic flow deposits, the sequence of fracture formation guides the sequence of fracture truncation and the lengths of each subsequent fracture generation. Two types of fractures formed early during the period of cooling of the pyroclastic flow deposits: (1) vapor-phase partings, which are long and low-angle discontinuities (i.e., dips less than 20°) with vapor-phase mineralization; and (2) long, smooth, high-angle discontinuities with vapor-phase mineralization. These fractures tend to be long and only slightly truncated. As cooling progressed, smaller truncated fractures were formed. These smaller fractures are typically moderate to high angle, commonly exhibit similar orientations as the longer high-angle fractures, and may or may not exhibit vapor-phase mineralization (BSC 2004d, Section 6.1.6).

Based on the relative proportion of lithophysal cavities, the repository host rock can be characterized as alternating nonlithophysal (lower and middle nonlithophysal) zones and lithophysal (lower and upper lithophysal) zones. Within the host rock, fracture formation appears to have been significantly affected by the presence and intensity of lithophysae formation. The lithophysal and nonlithophysal zones within the welded tuffs of the repository horizon exhibit distinctive fracturing patterns and characteristics. In general, the nonlithophysal units are hard, strong, fractured rocks with low matrix and lithophysal porosities. Fractures that formed during the cooling process are the primary structural features in these units. In contrast, the lithophysal units have significantly fewer fractures of significant continuous length (i.e., trace length greater than 1 m) but the matrix-groundmass material is heavily fractured with small-scale (lengths of less than 1 m) fractures in the lower lithophysal zone and is relatively fracture-free in the upper lithophysal zone. Lithophysal porosity in the lower and upper lithophysal zones is generally on the order of less than 10% to about 30% by volume. The matrix-groundmass that makes up the rock material between lithophysae in the lithophysal units is mineralogically the same as the matrix-groundmass of the nonlithophysal units (BSC 2004d, Section 6.1 and Appendix O).

Topopah Spring Tuff—The Topopah Spring Tuff includes the host-rock units for the repository and is of direct importance to repository design. Vitric rocks form zones at the top and bottom of the formation; alternating lithophysal and nonlithophysal zones characterize the remaining parts of the two members (Ttp and Tptr). The repository horizon is within the lower, crystal-poor member of the formation and, in descending order, is composed of the upper lithophysal (Ttpul), middle nonlithophysal (Ttpmn), lower lithophysal (Ttppl), and lower nonlithophysal (Ttpln) zones (Figure 1.1-60) (BSC 2004a, Section 3.3.4.7.1).

There are differing fracture characteristics in various zones of the Topopah Spring Tuff. Many fractures within the densely welded, crystal-rich vitrophyre near the top of the Topopah Spring Tuff terminate upward within the overlying, moderately welded pumiceous material (Sweetkind et al. 1997, p. 65), which is part of the Paintbrush nonwelded unit. The crystal-rich vitrophyre is underlain by the crystal-rich nonlithophysal zone; the upper subzone of the nonlithophysal zone is a thin (2 to 3 m) interval of devitrified tuff that contains argillically altered pumice clasts. Below this subzone, pumice clasts are replaced with coarsely crystalline vapor-phase minerals (Buesch et al. 1996, pp. 7 and 19). The population of fractures within the upper, crystal-rich member of the Topopah Spring Tuff is dominated by steeply dipping cooling joints of various orientations (Sweetkind et al. 1997, pp. 38 to 42). Lengths of cooling joints in surface exposures range from 1 to 4 m. Tectonic joints are mostly less than 1 m, although some are as long as 5 m (Throckmorton and Verbeek 1995, pp. A-11 to A-21). Within the ESF, vapor-phase crystallization is intense in the subzone between Stations 12+75 and 13+36 (ESF station numbers represent the distance from the North Portal in meters (for example, Station 12+75 would indicate a location in the ESF that is 1,275 m from the North Portal); station numbers are shown on Figure 2.3.3-7), where pumice fragments are corroded and the rock matrix contains pockets of vapor-phase minerals. The fracture intensity in this vapor-phase-altered interval is high. At Station 13+37 and beyond, fracture frequency decreases, and interfracture distance increases. This change corresponds to a vapor-phase alteration boundary within the Topopah Spring Tuff crystal-rich member and indicates a change in the brittleness of the units (Sweetkind et al. 1997, p. 65).

In the ESF, fracture density of fractures greater than 1 m decreases again at the contact with the crystal-poor member of the Topopah Spring Tuff, specifically the upper lithophysal zone of the crystal-poor member, in which fracturing is infrequent and discontinuous. In contrast to the overlying crystal-rich member, steeply dipping cooling joints are rare in the upper lithophysal zone of the crystal-poor member. The predominant fractures are north- and northwest-striking tectonic joints, which have spacings that typically range from 0.5 to 3 m. Tectonic fractures in the highly lithophysal rock are short, and most cannot be followed continuously for more than 3 m. Joint surfaces are rough and pockmarked by abundant lithophysal cavities, and their traces are irregular. These properties reflect the difficulty of propagating a smooth, continuous fracture through a rock containing numerous large voids, resulting in a network of relatively short, widely spaced, discontinuous tectonic fractures with a high proportion of blind fracture terminations (Sweetkind et al. 1997, pp. 65 and 66).

A network of long, relatively closely spaced joints generally characterizes the underlying middle nonlithophysal zone of the crystal-poor member of the Topopah Spring Tuff. At least four joint sets are interpreted to be present in this unit in the ESF, including two subvertical sets that strike northwest and northeast, a northwest-striking set with moderate dips (50°), and a northwest-striking set with about 20° dips (Albin et al. 1997, pp. 26 to 28, Table 1; Sweetkind et al. 1997, pp. 47 to 48).

Northwest-striking joints are the most prevalent set throughout the unit, followed in abundance by northeast-striking joints. An intensely fractured zone is present in the main drift of the ESF from Stations 42+00 to 51+50, where the overall fracture frequency is more than twice the frequency observed in other areas. Within the intensely fractured zone, a northwest-striking set, oriented 80°W to 35°W, dominates all other joint sets. These joints are smooth, with manganese-oxide coatings and some vapor-phase mineralization (Albin et al. 1997, pp. 28 to 62).

Fracture intensity drops sharply and fracture character changes markedly at the contact between the middle nonlithophysal and the lower lithophysal zones of the Topopah Spring Tuff. Fractures within the middle nonlithophysal zone tend to be planar or arcuate, with low surface roughness. Fractures within the lower lithophysal zone are subplanar and extremely rough. On average, fractures in the middle nonlithophysal zone are significantly longer than fractures in the lower lithophysal zone. The numerous large fractures that characterize the middle nonlithophysal zone typically terminate abruptly at the contact with the lower lithophysal zone of the crystal-poor member of the Topopah Spring Tuff (Sweetkind et al. 1997, pp. 65 to 66). Below this contact, fractures greater than 1 m are infrequent, with an average apparent spacing of 3.3 m (Sweetkind et al. 1997, pp. 48 to 49).

The Enhanced Characterization of the Repository Block (ECRB) Cross-Drift exposes about 260 m of the lower nonlithophysal zone of the crystal-poor member of the Topopah Spring Tuff. The most prominent of the three steeply dipping joint sets in this unit, which includes almost half the fractures, strikes northwest. There is also a northwest-striking set with a relatively shallow dip of about 17° (Mongano et al. 1999, pp. 72 and 74). Fracture frequency from borehole core measurements for this unit typically range from 19.4 to 23.7 fractures per 10-ft interval (Sweetkind et al. 1997, p. 49). These fracture frequencies are high, relative to the lithophysal-bearing units in the crystal-poor member of the Topopah Spring Tuff, but are similar to fracture frequencies obtained from the middle nonlithophysal zone (Sweetkind et al. 1997, Figure 3).

Three sets of steeply dipping cooling joints form an incipient columnar network of joints within the vitrophyre of the crystal-poor member of the Topopah Spring Tuff in exposures at Busted Butte. Also present are distinct, subhorizontal discontinuities that separate column intervals. Mean fracture spacing is 0.5 m, which is smaller than that observed in most of the welded, devitrified units encountered in the ESF (Sweetkind et al. 1997, p. 49).

1.1.5.1.3.2 Fractures Associated with Faults

The total width of a fault zone includes a zone of influence around the principal fault plane in which fracture intensity is higher or in which some other parameter, such as orientation, changes in response to the presence of the fault. In the ESF, overall variability in the frequency of fractures 1 m long or longer is primarily a function of lithology, not proximity to faults (Sweetkind et al. 1997, p. 68). At the scale used for detailed mapping in the ESF, there are no abrupt increases in the number of fractures longer than 1 m in proximity to faults. The relationship of the proximity of fractures shorter than 1 m to faults, which could be correlated with a fault mapped at the surface, was evaluated by visual examination of faults in the ESF. Four principal conclusions were reached (Sweetkind et al. 1997, pp. 68 to 71):

- The width of the zone of influence on fracture frequency in the immediate vicinity of a fault is quite narrow, ranging from less than 1 m up to 7 m from the fault.

- The width of the zone of influence in the immediate vicinity of a fault correlates with the amount of fault offset. Faults with small amounts of offset (1 to 5 m) have zones of influence that are 1 to 2 m wide. Faults with tens of meters of offset (e.g., faults at ESF Stations 11+20 and 70+58) have zones of influence that range up to 6 to 7 m wide.
- The width of the zone of influence around a fault is not related to depth. The width of the zones of influence for small faults observed along the North Ramp, where overburden is 50 to 60 m thick, is similar to those of small faults observed elsewhere in the ESF, where overburden thickness is two to three times greater. However, upward-splaying faults can result in apparent broad zones of influence at the surface because of the overlap of fractured zones surrounding individual fault splays, such as the closely fractured area associated with the Ghost Dance Fault on the south-facing slope of Antler Ridge.
- The amount of deformation associated with faults depends on which lithologic unit is involved in the faulting. Faults within nonwelded to partly welded portions of the crystal-poor vitric zone of the Tiva Canyon Tuff or stratigraphically lower-bedded tuffs are generally sharp, discrete breaks with minimal fault gouge or secondary shear surfaces. Individual pumice clasts along some faults can be traced to the fault surface without visible sign of breakage, and wall rocks show little evidence of deformation. In comparison to brittle, welded rocks, nonwelded units accommodate a greater amount of extensional strain before failing by fracture.

The repository area contains small, discontinuous faults that interact with fracture networks. The fracture network acts as a preexisting weakness in the rock mass that can distribute strain in the form of small amounts of shear along many fractures. Evidence for distributed shear along fractures includes thin selvages of tectonic breccia along cooling joints and slip lineations along joint surfaces (Sweetkind et al. 1996).

Lithology plays a role in the interaction between discontinuous faults and the fracture network. Because each lithostratigraphic zone at Yucca Mountain has characteristic fracture attributes, including preferred orientations, spacing, trace length, and joint type (Sweetkind et al. 1997, pp. 62 to 67), each unit is unique in its ability to deform by distributed slip along fractures. The result is stratigraphic control of structural geometry; thus, what may be a discrete break in one lithostratigraphic unit may be a broad zone of distributed deformation in another. The northwest-striking Sundance Fault has as much as 12 m of dip-slip offset where it displaces the crystal-rich member of the Tiva Canyon Tuff. Within the underlying crystal-poor member, however, displacement is distributed across numerous discontinuous fault segments over a maximum width of about 70 m (Potter et al. 1999, pp. 5 to 6). The trend of each fault segment corresponds to one of the dominant orientations of cooling joints exposed on this portion of the mountain. This trend implies that the discontinuous faults are likely to be reactivated cooling joints (Potter et al. 1996; Sweetkind et al. 1996).

1.1.5.1.3.3 Fracture Hazard Summary

Fractures are ubiquitous at Yucca Mountain. Fracture orientation, length, smoothness, connectivity, and other attributes are variable and strongly dependent on stratigraphic position. Compared to lithostratigraphy, faulting has a secondary influence on the fracture network. The hazard from

fractures and associated rockfall are location-specific, depending both on the lithostratigraphic unit that the access tunnel or emplacement drift encounters and the orientation and size of the tunnel or drift in each lithostratigraphic unit. The hazard from fractures and rockfall under static conditions is bounded or enveloped by the hazard from drift degradation under seismic loading conditions. The drift degradation hazard under seismic loading conditions is discussed in [Sections 1.6](#) and [1.7](#).

1.1.5.1.4 Subsurface Conditions at the Surface Geologic Repository Operations Area

Subsurface conditions are established through geologic mapping, boreholes, test pits, geologic trenches, and geophysical investigations, as shown in [Figures 1.1-62](#) and [1.1-63](#). Geologic mapping has been conducted at natural and excavated ground surface and in trenches, pits, and washes. A geologic map of the surface GROA vicinity is shown in [Figure 1.1-64](#). Age dating has been performed to assess the age of the Midway Valley alluvial deposits. Geophysical investigations include seismic (i.e., downhole, suspension logger, spectral analysis of surface waves, reflection, and refraction), gamma-gamma, gravity, and magnetic and magnetotelluric surveys. The results of the field exploration are used to develop an understanding of the subsurface conditions (BSC 2002b, Section 6.6).

The surface GROA is characterized as being underlain in ascending order by densely welded, rhyolitic to quartz latitic, pyroclastic flow deposits of the Tiva Canyon Tuff (Tpc); pre-Tuff unit “x” bedded tuffs (Tpbt5 (also referred to as post-Tiva Canyon Tuff bedded tuff)); Tuff unit “x” (Tpki); pre-Rainier Mesa Tuff bedded tuffs (Tmbt1); Rainier Mesa Tuff (Tmr); and by Quaternary alluvium (Qal) (SNL 2008a, Table 6.2-1). Alluvium thickness is zero at the base of Exile Hill and increases in thickness to about halfway across the valley. Alluvium reaches a maximum thickness of about 200 ft and then begins to thin east toward Alice Point (SNL 2008a, Section 6.2.2). Structurally, the area is crisscrossed with mostly high-angle normal faults of various offsets. These faults offset the bedrock, but there is no evidence of offset in the Quaternary deposits (BSC 2002b, Section 6.6). The Exile Hill Fault splay has produced significant down-to-the-northeast offset of the volcanic stratigraphy. As a result, the area to the northeast of the Exile Hill Fault splay is characterized by a significantly thicker sequence of nonwelded bedded tuffs overlying the Tiva Canyon Tuff, and the area to the southwest of the Exile Hill Fault splay is typically characterized by a relatively thin to nonexistent sequence of nonwelded tuffs overlying the Tiva Canyon Tuff (BSC 2002b, Section 6.6).

The surface facilities located on the GROA extend from the eastern toe of Exile Hill out into Midway Valley. Exile Hill is a horst, bounded on its west side by the Bow Ridge Fault and on its east side by the Exile Hill Fault. Exile Hill consists of Tiva Canyon Tuff that is surrounded and partially covered by Quaternary alluvium and colluvium. The sediments ([Figure 1.1-59](#)) that fill Midway Valley consist mostly of alluvium and colluvium and some thin eolian deposits (BSC 2002b, Section 6.6).

There is a north-northwest-trending fault that offsets the volcanic rocks that underlie the surface GROA that is referred to as the Exile Hill Fault splay. [Figure 1.1-64](#) also shows several other interpreted faults with smaller vertical offsets that offset the volcanic rocks that underlie the surface GROA and do not displace Quaternary alluvial deposits. Cross sections through the surface GROA are shown in [Figures 1.1-65](#) to [1.1-67](#) (BSC 2002b, Section 6.6).

The Midway Valley Fault underlies northeastern facilities on the surface GROA (Figure 1.1-64). It is exposed for about 1 km in Tiva Canyon Tuff bedrock at the southeast end of Bow Ridge (Figure 1.1-5). The fault is covered by the surficial deposits of Midway Valley for a distance of about 9 km north from Bow Ridge. North of Yucca Wash, it continues northward for at least another 3 km as a west-dipping normal fault with an exposed bedrock offset of about 120 m down to the west in the upper part of the Paintbrush Group. Displacements of buried bedrock within Midway Valley are interpreted from gravity and magnetic surveys to be 40 to 60 m, and the fault dips 70° W. The Midway Valley Fault does not displace Quaternary alluvial deposits (Keefer et al. 2004, p. 27 and Table 5).

1.1.5.2 Site Seismology

[NUREG-1804, Section 2.1.1.1.3: AC 5(6), (7); Section 2.1.1.7.3.2: AC 1(3)]

The Yucca Mountain area is located in a region that is tectonically active. The seismic activity that presently characterizes this region is expected to continue well beyond the preclosure period. In this section, information on the known seismic sources in the Yucca Mountain region and the results of the probabilistic seismic hazard analyses (PSHAs) as they relate to the design of the repository SSCs and PCSA are presented (BSC 2004a, Section 4).

Specific seismic-related hazards considered during screening-level preclosure safety evaluations include earthquake (vibratory ground motion), surface fault displacement, and subsurface fault displacement (BSC 2008b, Section 6.1). These seismic-related events are considered as potential hazards during the preclosure period because their probability of occurrence is greater than one in 10,000 during the 100 year preclosure period for the subsurface facilities and during the 50 year preclosure period for surface facilities. The assessment of seismic hazards at Yucca Mountain is founded on the evaluation of a large database that incorporates information on seismic sources in the Yucca Mountain region, including maximum earthquakes, source geometry, and earthquake recurrence of those sources. The probabilistic seismic hazard analysis (PSHA) explicitly incorporates uncertainties in the characterization of seismic sources, fault displacement, and ground motion (BSC 2004a, Section 4.3). The PSHA process and results are described in Section 2.2.2.

1.1.5.2.1 Historical Seismicity of the Yucca Mountain Region

The historical and instrumental earthquake record within 300 km of Yucca Mountain includes the reported earthquakes of the southern Basin and Range Province and portions of the southern Sierra Nevada and Mojave Desert in California. Compiled as part of the PSHA, the catalog of historical and instrumentally recorded earthquakes for this region contains 271,223 earthquakes of magnitude approximately 0.5 and greater from 1868 to 1996 (CRWMS M&O 1998a, Appendix G). The known magnitudes for each earthquake are listed in the catalog. (When referring to earthquake magnitudes, the following scales are cited and abbreviated as follows: M_L indicates Richter local, M_w indicates moment, M_S indicates surface wave, m_b indicates body wave, M_c or M_d indicates coda duration, M_I indicates intensity-based, and M indicates unspecified.) For use in the PSHA, a moment magnitude (M_w) was determined for each event based on the available magnitude data. Catalog completeness for the region within 100 km of Yucca Mountain was assessed as part of the PSHA and varies as a function of magnitude (CRWMS M&O 1998a, Appendix E). The catalog includes a few events of greater than M_w 5 that are located slightly outside of the 300 km radius. These events are included because they are associated with surface ruptures that form historical analogues for assessing fault

displacement hazards at the site. [Figure 1.1-68](#) shows events in the catalog with moment magnitudes greater than 3.5. [Figure 1.1-69](#) shows historical seismicity within 100 km of Yucca Mountain with moment magnitudes greater than or equal to 2.5. Significant historical earthquakes (moment magnitudes greater than or equal to 5) in the 300 km Yucca Mountain region are listed in [Table 1.1-65](#) (BSC 2004a, Section 4.3.1.2).

The larger earthquakes documented in the historical catalog occurred to the northwest, west, southwest, and south of Yucca Mountain. These earthquakes include the 1872 Owens Valley, California, earthquake (M_w 7.8); the 1932 Cedar Mountain, Nevada, earthquake (M_w 6.8); the 1954 Fairview Peak and Dixie Valley, Nevada, earthquakes (M_w 7.1 and M_w 6.8, respectively); and the 1992 Landers, California, earthquake (M_w 7.3) ([Figure 1.1-68](#)).

Rupture zones for these events range in length from about 50 to 100 km. They exhibit primarily right-lateral strike-slip faulting, with the exception of the Dixie Valley earthquake, which is primarily a normal faulting event (BSC 2004a, Section 4.3.1.3). The 1999 Hector Mine, California, earthquake (M_w 7.1) also occurred in this region but after the time period shown on [Figure 1.1-68](#).

Three events during the historical period with moment magnitudes greater than 5.5 are located within 100 km of Yucca Mountain. The largest event is the 1916 M_w 6.1 earthquake that occurred in Death Valley. Other events include the 1992 M_w 5.6 earthquake that occurred near Little Skull Mountain, about 15 km southeast of Yucca Mountain, and an event in 1910 about 85 km to the northwest (BSC 2004a, Section 4.3.1.3). Many earthquakes of M_w 4 and greater within 100 km occur near the Furnace Creek Fault system, the most active tectonic feature in this region ([Figure 1.1-69](#)).

The northern region of the Nevada Test Site has experienced considerable vibratory ground motion associated with nuclear testing, in contrast to seismicity that is tectonic in origin in the southern part of the Nevada Test Site. Discriminating between naturally occurring earthquake activity and events associated with underground nuclear explosions is problematic. The relative number of artificial and induced earthquakes in the areas where nuclear testing has occurred suggests that the natural seismicity of the region is close to the background seismic activity of the southern Basin and Range Province. In 1979 and 1983, several swarms of microearthquakes occurred in the region, which were apparently unrelated to the underground nuclear explosions (BSC 2004a, Section 4.3.1.3).

1.1.5.2.1.1 Characteristics of the Recorded Seismicity in the Southern Great Basin

Instrumentally recorded seismicity over about the past 20 years provides information on the characteristics of earthquakes that occur in the southern Great Basin. In addition to helping to define the extent and rate of recurrence for seismic source zones, the data are used to understand the thickness of the seismogenic crust in the Yucca Mountain vicinity. Crustal thickness is a factor in evaluating the maximum magnitude for a seismic source. For some events, the data allow focal mechanisms to be determined. Focal mechanisms provide information on the state of stress in the region, which can be useful in assessments of the potential activity of faults (BSC 2004a, Section 4.3.1.4).

Earthquake Depths—Various analyses have shown that earthquakes in the southern Great Basin occur predominantly between depths of 2 and 12 km (BSC 2004a, Section 4.3.1.4). The Little

Skull Mountain earthquake of 1992, one of the best-documented recent earthquakes in the region, occurred at a calculated depth of 11.8 km (BSC 2004a, Section 4.3.1.5). It is recognized, however, that focal depth determinations are uncertain to within several kilometers even for well recorded events because of velocity model limitations and trade-off between origin time and depth. Evaluations of data since 1992 are dominated by the aftershock sequence following the Little Skull Mountain earthquake. To address this situation, recent evaluations of data from the Southern Great Basin Digital Seismic Network segregate the catalog into earthquakes that occurred within the Little Skull Mountain aftershock zone and those that did not. Earthquakes that are not part of the Little Skull Mountain sequence have depths primarily within a range of 4 to 12 km (Figure 1.1-70). Earthquakes within the Little Skull Mountain aftershock zone are more narrowly distributed, between 8 and 12 km. The estimated number of earthquakes with depths less than 4 km is probably biased by a significant number of events whose depths were not well determined. However, many earthquakes in the Rock Valley area, south of Little Skull Mountain, do have reliable shallow focal depths (BSC 2004a, Section 4.3.1.4.1).

The depths of larger earthquakes that have occurred in the Basin and Range Province are not well characterized because most of these events occurred during periods of less dense seismic network coverage. Several larger magnitude earthquakes are reported to have nucleated deeper than 15 km. Nucleation depths ranging from 10 to 20 km have been determined from waveform modeling for several major earthquakes in the Basin and Range Province, including the 1954 Dixie Valley earthquake; the 1959 Hebgen Lake, Montana, earthquake; and the 1983 Borah Peak, Idaho, earthquake. Each of these three earthquakes is associated with surface faulting on range-bounding normal faults (BSC 2004a, Section 4.3.1.4.1).

Focal Mechanisms—Focal mechanisms of recent earthquakes within the southern Great Basin indicate that right-lateral slip on north-trending faults is the predominant mode of stress release near the site. Normal and oblique-slip faulting is also observed. Focal mechanisms for the period 1971 through 1992 indicate roughly equal proportions of strike-slip and normal faulting. The principal extensional (minimum compression or elongation) stress axes inferred from earthquake mechanisms trend northwest and plunge approximately horizontally (Figure 1.1-71). The principal compressional (shortening) stress axes from earthquake mechanisms are concentrated along a belt that sweeps from vertical (normal faulting) to northeast and horizontal (strike-slip faulting). Regional stress orientations indicate north–south and east–west orientations for high-angle fault planes, with right-lateral slip on the north-striking and left-lateral slip on the east-striking surfaces. Normal and oblique slips are indicated on fault surfaces with orientations intermediate to these directions. The style of faulting determined from the focal mechanisms does not appear to vary as a function of depth (BSC 2004a, Section 4.3.1.4.2).

In an analysis of the stress field, based upon a set of regional earthquake focal mechanisms, the presence of both strike-slip and dip-slip mechanisms in particular localities indicates an axially symmetric stress field in which the intermediate and maximum compressive stresses are nearly equal. Because no large earthquakes are present in the data set, it is interpreted that movement along a variety of fault plane orientations is accommodated by multiple small preferentially oriented faults (BSC 2004a, Section 4.3.1.4.2).

1.1.5.2.1.2 Seismicity in the Vicinity of Yucca Mountain

Although the southern portion of the Nevada Test Site, southeast of Yucca Mountain, is one of the more seismically active regions in the southern Great Basin (Figure 1.1-69), the area immediately beneath Yucca Mountain and its immediate surroundings (Figure 1.1-72) have been nearly aseismic since local monitoring began in the late 1970s. The zone of quiescence surrounding Yucca Mountain has been studied and is a real feature of the seismicity and not an artifact of network design or detection capability. Earthquakes located in the immediate vicinity of Yucca Mountain are shown in Figure 1.1-72 (BSC 2004a, Section 4.3.1.5).

Microearthquakes have been recorded in the immediate vicinity of Yucca Mountain (Figure 1.1-72). The events range from about magnitude -1 to 1. These microearthquakes occur throughout the Yucca Mountain block and have focal depths between approximately 3 and 13 km. Short-period focal mechanisms are determined for some of the events and are consistent with normal to normal-oblique slip on faults with orientations similar to several Quaternary faults mapped at the surface (BSC 2004a, Section 4.3.1.5).

While the immediate Yucca Mountain area has been quiescent during the historical period, the paleoseismic evidence (Section 1.1.5.2.2) indicates active Quaternary faults exist near the site. Paleoseismic events exhibit very long times between events (from many thousands of years to more than 100,000 years). Little or no microseismicity may occur on the faults during this long time period between events. Many faults in the Great Basin with paleoseismic evidence for prehistoric surface-rupture earthquakes have little or no associated historical seismicity (BSC 2004a, Section 4.3.1.5).

Seismicity to the east and southeast of Yucca Mountain is spatially associated with the Rock Valley, Mine Mountain, and Cane Spring fault zones. This activity forms a wide, northeast-trending zone that includes the 1973 Ranger Mountain sequence, the 1992 Little Skull Mountain sequence, the 1993 Rock Valley sequence, the 1999 Frenchman Flat sequence, and other earthquake clusters (Figure 1.1-69). The main shocks from the Little Skull Mountain and Frenchman Flat sequences, near the ends of the seismicity zone, exhibit normal faulting on northeasterly striking planes. The Rock Valley sequence in the middle of the zone exhibits strike-slip faulting. Some seismicity in the Yucca Mountain area is also spatially associated with the southern boundary of the Timber Mountain caldera (BSC 2004a, Section 4.3.1.5).

1.1.5.2.2 Quaternary Paleoseismic Data

The presence of faults that have experienced recurrent motion during the Quaternary Period suggests the potential for producing earthquakes during the preclosure period. Initially, reconnaissance studies identified approximately 100 faults with known or suspected Quaternary activity within a 100-km radius of the repository site at Yucca Mountain (Figure 1.1-73). Subsequently, more detailed studies identified and documented specific physiographic and structural evidence for Quaternary displacements (BSC 2004a, Section 4.3.2).

Prehistoric earthquakes are interpreted on the basis of displacement of Quaternary deposits and timing of surface ruptures at specific locations. A total of 52 exploratory trenches and natural exposures have been excavated, cleaned, and logged as part of seismotectonic investigations in the

Yucca Mountain site and environs. Forty of these trenches and exposures are located across nine local Quaternary faults. These faults include the Crater Flat (northern segment), Crater Flat (southern segment), Windy Wash, Fatigue Wash, Solitario Canyon, Iron Ridge, Stagecoach Road, Bow Ridge, and Paintbrush Canyon faults (Figure 1.1-73(b)). Twenty-eight of the 40 trenches display evidence for displacement of Quaternary deposits across the fault traces. The other trenches lack evidence of Quaternary displacement, either because the trench did not intersect a fault in surficial deposits or because undisturbed deposits were found to overlie a bedrock fault. The remaining 12 trenches were excavated across bedrock faults in the central repository block, and no evidence for Quaternary activity on these faults was observed (BSC 2004a, Section 4.3.2).

An additional 11 trenches were excavated across the nearby Bare Mountain Fault and Rock Valley Fault, located within a 20 km radius of the site. These trenches exposed displaced Quaternary deposits (BSC 2004a, Section 4.3.2).

Evidence exists for recurrent middle to late Quaternary fault displacement activity on the block-bounding Quaternary faults in the Yucca Mountain site area: the Windy Wash, Fatigue Wash, Solitario Canyon, Bow Ridge, and Paintbrush Canyon faults. At least two and as many as eight individual displacement events per fault are evident. Events that produced fracturing and fissuring with no detectable offset are nearly as common as displacement events. The fracturing events, if tectonic in origin, record relatively frequent earthquakes of small to moderate magnitude that do not produce measurable rupture at the surface. Alternatively, these events are a record of distributed faulting and fracturing produced by rarer surface-rupture earthquakes of larger magnitude on one of several nearby faults or of large, distant earthquakes (BSC 2004a, Section 3.5.1).

1.1.5.2.3 Vibratory Ground Motion Information

In a seismic hazard analysis, assessments are made of the size and recurrence rate of earthquakes that seismic sources might generate, as well as the propagation of earthquake energy from the source. The level of ground motion that is experienced at the site for any given earthquake location and magnitude is assessed and is described by attenuation relations. The vibratory ground motions adopted for the seismic design of the repository facilities and analysis of the postclosure performance incorporate the effects of the seismic sources, propagation path, and local site geology specific to the Yucca Mountain region and site. Ideally, recorded ground motions from earthquakes in the Yucca Mountain region or Basin and Range Province would be used directly to develop attenuation relations for application at Yucca Mountain. However, no large earthquakes have occurred in the region during the period of strong-motion instrumentation. The data recorded in the Yucca Mountain region and the Basin and Range Province, along with the geophysical and seismological properties derived for the region, provide information for estimating ground motions at the repository site. This information forms part of the basis for the expert interpretation and assessments of uncertainty that are part of the PSHA for Yucca Mountain (BSC 2004a, Section 4.3.3).

Characterizing ground motions at Yucca Mountain using existing attenuation relations involves resolving the extent to which these relations for the western United States are applicable to the Basin and Range Province in general and to Yucca Mountain in particular. The seismological questions include whether differences in the factors that influence ground motions in the Yucca Mountain region and in the western United States would lead to significant differences in ground motion

estimates for the two regions. These factors include seismic source properties, regional crustal properties, and shallow geologic site properties at the repository (BSC 2004a, Section 4.3.3).

To address these issues, multiple ground-motion studies were carried out as part of site characterization activities. The first study was an empirical analysis of worldwide ground-motion data from extensional regimes. The second study comprised numerical modeling of selected scenario earthquakes near Yucca Mountain in which ground motions were estimated using seismological models of the source, path, and site effects. The numerical modeling allowed the region-specific crustal structure and site-specific rock properties to be incorporated in the ground-motion estimates. The third study used weak-motion recordings to characterize the near-surface seismic wave attenuation at Yucca Mountain. The fourth study examined earthquake stress drops in extensional regimes to compare them to those for earthquakes used to develop western U.S. ground-motion attenuation relations. Stress drop is a factor in determining the level of high-frequency ground motion. The fifth study investigated the possible constraint that precariously balanced rocks can indicate on the levels of ground motion that have occurred in the past. The sixth study is the ground motion characterization performed as part of the PSHA; it is the most comprehensive of the studies and incorporated results from the previous five studies. The PSHA study is a formal elicitation of a panel of ground-motion experts that resulted in ground-motion attenuation relations specific to Yucca Mountain (Section 2.2.2.1). For the PSHA, both a vertical component and a random horizontal component of ground motion were addressed (CRWMS M&O 1998a, Appendix F).

1.1.5.2.4 Probabilistic Seismic Hazard Analysis

The PSHA provides quantitative hazard results to support an assessment of the long-term performance of the repository with respect to waste containment and isolation and to form the basis for developing seismic design criteria. The methodology used for the Yucca Mountain PSHA is generally consistent with NUREG-1563 (Kotra et al. 1996) and follows *Methodology to Assess Fault Displacement and Vibratory Ground Motion Hazards at Yucca Mountain* (YMP 1997). This methodology is consistent with guidance provided by the Senior Seismic Hazard Analysis Committee in a study sponsored by the DOE, the NRC, and the Electric Power Research Institute (Budnitz et al. 1997).

The PSHA incorporates and quantifies uncertainty due to randomness and diversity of data interpretation and displays this uncertainty in the final hazard results. Formal expert elicitation, described in Section 5.4, was used to obtain interpretations of seismic sources and earthquake ground-motion relationships that capture the range of interpretations that are supported by the data. The hazard analysis produces a distribution of hazard curves showing the annual frequency with which various levels of ground motion or fault displacement are exceeded (CRWMS M&O 1998a, Sections 7 and 8).

Seismic sources that contribute to vibratory ground motion and fault displacement hazards at Yucca Mountain are identified and characterized. There are three principal components of seismic source characterization: source location and geometry, maximum earthquake magnitude, and earthquake recurrence. Seismic sources can be characterized into two types: fault sources and areal sources. Two types of fault sources are considered in the development of the vibratory ground motion for the design of the surface facilities located on the GROA: regional faults and local faults. Regional faults

are those within 100 km of Yucca Mountain but outside the local vicinity of the site that are judged to be capable of generating earthquakes of M_w 5 and greater. Local faults are those located within about 15 km of Yucca Mountain. The specific faults that required characterization were determined based on factors including but not limited to fault length and location relative to Yucca Mountain, displacement of Quaternary deposits, direct relationship with seismicity, structural relationship to other Quaternary faults, orientation within the contemporary stress regime, and considerations of alternative tectonic models. The faults are listed in [Table 1.1-66](#). Faults are considered but judged not to be relevant to the hazard analysis if they had short lengths or no significant Quaternary displacement (BSC 2004a, Section 4.3.4.1.1).

Areal sources represent areas of distributed seismicity that are not apparently associated with specific, known faults. Areal sources can be divided into three types: sources whose boundaries enclose a concentrated zone of seismicity, sources defined by regional seismotectonic characteristics, and sources with regional backgrounds, typically applying to larger regions than are defined by the other types of areal sources. Alternative zones were defined for the PSHA (BSC 2004a, Section 4.3.4.1.1).

For each seismic source included in the PSHA, the maximum earthquake magnitude (M_{max}) was determined to represent the largest earthquake the source is capable of generating. Two basic approaches are used to assess maximum magnitude. The primary approach, which is used for faults, is based on estimates of the maximum dimensions of fault rupture. Multiple sources of uncertainties were considered in estimating physical dimensions of maximum rupture on faults, including uncertainties in rupture length, rupture area, and displacement per event. The second approach considered historical data on the seismicity of the region. This approach is used primarily for areal source zones. For each of the sources included in the PSHA, the uncertainty in M_{max} is expressed as a probability distribution. The range of maximum magnitude values is indicated in [Table 1.1-66](#) (BSC 2004a, Section 4.3.4.1.1).

Earthquake recurrence relationships express the rate or annual probability of different magnitude earthquakes occurring on a seismic source. Methods for developing these relationships are usually different for fault sources than for areal sources. For areal sources, earthquake recurrence relationships are determined from the catalog of historical and instrumentally recorded earthquakes within a 300 km radius of Yucca Mountain. For faults, earthquake recurrence rates are derived from paleoseismic data on the number and timing of coseismic surface rupture events. The ranges of slip rate and recurrence rate values are indicated in [Table 1.1-66](#) (BSC 2004a, Section 4.3.4.1.1).

1.1.5.2.4.1 Results of the Probabilistic Seismic Hazard Analysis

Vibratory Ground Motion Hazard—The final ground motion products of the PSHA are hazard curves of the annual rate of exceeding a particular measure of vibratory ground motion (e.g., spectral acceleration at selected oscillator frequencies, peak ground velocity). The hazard results are determined for a hypothetical reference rock outcrop with a defined set of seismic velocity and site attenuation properties typical of those beneath the waste emplacement level. Ground motion computed at this reference location serves as the basis for site-response modeling. The site-response model incorporates the effects of the site-specific tuff and alluvium properties at Yucca Mountain to determine seismic inputs at the surface and subsurface for use in analyses supporting design and performance assessment (BSC 2004a, Section 4.3.4.2.1).

The ground-motion hazard is determined for horizontal and vertical components of peak ground acceleration (defined at 100 Hz); 5% damped response spectral accelerations at frequencies of 0.3, 0.5, 1, 2, 5, 10, and 20 Hz; and peak ground velocity. The ground motion hazard is expressed in terms of hazard curves (Figure 1.1-74). Peak ground acceleration (100 Hz); 0.3, 1.0, and 10 Hz spectral values; and peak ground velocity for the reference rock outcrop conditions are summarized in Table 2.2-16 for the mean annual probabilities of exceedance of 5×10^{-4} , 10^{-4} , 10^{-5} , 10^{-6} , and 10^{-7} .

An understanding of the contributions to seismic hazard at a particular annual probability of exceedance and for a given ground-motion measure can be obtained by deaggregating the hazard. This process shows which magnitude and distance combinations characterize the earthquakes contributing to the hazard. The process also highlights how ground motion uncertainty contributes to the hazard in terms of the difference between the logarithm of ground motion and the mean logarithm of ground motion for that magnitude and distance, measured in units of standard deviation (ϵ). Deaggregation of the mean hazard for an annual probability of exceedance of 10^{-4} shows that, at 5 to 10 Hz, ground motion is dominated by earthquakes smaller than M_w 6.5 occurring at distances less than 15 km from Yucca Mountain (Figure 1.1-75). Dominant events for low-frequency ground motion, such as at frequencies of 1 to 2 Hz, display a bimodal distribution that includes moderate nearby events and M_w 7 and larger earthquakes beyond distances of 45 km (Figure 1.1-75). The latter contribution is mainly because of the relatively higher activity rates for the Death Valley Fault and Furnace Creek Fault (BSC 2004a, Section 4.3.4.2.1).

The primary contributor to uncertainty in ground-motion hazard is the uncertainty in ground motion amplitude that was expressed by each ground motion expert (i.e., within expert epistemic uncertainty). With respect to seismic source characterization uncertainty, the recurrence approach used (either slip rates or recurrence interval) and the recurrence model used are the factors that contribute the most to uncertainty for annual probabilities of exceedance of 10^{-3} and 10^{-4} . Maximum magnitude has a small effect on uncertainty, especially for 10 Hz spectral acceleration because a large fraction of the hazard at this frequency comes from more frequent, moderate-magnitude events. Geometric fault parameters, such as rupture lengths, dips, and maximum depths, are minor contributors to uncertainty. These parameters have a moderate effect on the locations of earthquakes and on maximum magnitude but do not affect earthquake recurrence.

The dominant sources for seismic hazard at 10 Hz ground motion for mean annual probabilities of exceedance of 10^{-3} and 10^{-4} are the Paintbrush Canyon–Stagecoach Road Fault and the Solitario Canyon Fault (or coalesced fault systems including these two faults) and the host areal seismic source zone. For 1 Hz ground motion, the dominant seismic sources are the Death Valley Fault and Furnace Creek Fault, as well as the Paintbrush Canyon–Stagecoach Road Fault and the Solitario Canyon Fault. Multiple-rupture interpretations of the type with comparable seismic moment release on more than one fault (i.e., those requiring modification of the attenuation equations) make a small contribution to the total hazard. Buried strike-slip faults, volcanic seismicity, and seismogenic detachments contribute negligibly to the total hazard (BSC 2004a, Section 4.3.4.2.1).

Fault Displacement Hazard—The final fault displacement products of the PSHA are hazard curves showing the annual rate of exceeding particular fault-displacement levels, given faulting at a specific site. The probabilistic fault displacement hazard is calculated for nine demonstration

sites located at or near Yucca Mountain (Table 1.1-67). Two of the sites have four hypothetical conditions representative of the features encountered within the ESF and expected at the repository, ranging from intact rock to the presence of existing small faults with 2 m of cumulative offset. Figure 1.1-76 shows sample results of summary hazard curves for three of the nine demonstration sites. The integrated results provide a representation of fault displacement hazard and its uncertainty at the nine sites. Separate results are obtained for each site in the form of summary hazard curves (BSC 2004a, Section 4.3.4.2.2).

With the exception of the block-bounding Bow Ridge Fault and Solitario Canyon Fault (Sites 1 and 2, respectively), the mean displacements are 0.1 cm or less at 10^{-5} annual probability of exceedance. At 10^{-5} annual probability of exceedance, the mean displacements are 7.8 and 32 cm, respectively, for these two faults (Table 1.1-67).

The fault displacement hazard results display significant uncertainty. Sites with the highest fault displacement hazard show uncertainties comparable to those obtained in ground-motion PSHA. Sites with low hazard show much higher uncertainties (e.g., a large spread between the 15th and 85th percentile of the hazard distribution) (Figure 1.1-76). This situation largely reflects the data available to characterize fault displacement at the different demonstration locations. For locations with fewer data available, the uncertainties in assessed fault displacement hazard are greater (BSC 2004a, Section 4.3.4.2.2).

1.1.5.2.5 Ground Motion Input Evaluation

Ground motion inputs for design and preclosure safety analyses are based on results of the PSHA. Several steps are involved in developing appropriate ground motion inputs (Figure 1.1-77):

1. Results of the PSHA are conditioned to reflect information on the level of extreme ground motion that is consistent with the geologic setting of Yucca Mountain.
2. Site-response modeling is carried out to account for the effects on ground motion of the local tuff and alluvium.
3. The conditioned PSHA results are combined with the site-response modeling results to produce location-specific hazard curves and uniform hazard spectra for the surface GROA and the repository block.
4. Location-specific design response spectra are developed from the uniform hazard spectra for mean annual probabilities of exceedance corresponding to design basis ground motion (DBGM) levels. DBGM-1 has a mean annual probability of exceedance of 1×10^{-3} , while DBGM-2 has a mean annual probability of exceedance of 5×10^{-4} . For beyond DBGM analyses and fragility analyses, a mean annual probability of exceedance of 1×10^{-4} is used.

5. Three-component time histories are determined by modifying recorded strong motion accelerograms such that their response spectra match the design response spectra for a given mean annual probability of exceedance.
6. Strain-compatible material properties are computed for the surface GROA based on the site-response modeling results for a given mean annual probability of exceedance.

These steps are discussed in more detail in [Sections 1.1.5.2.5.1](#) through [1.1.5.2.5.6](#).

1.1.5.2.5.1 Conditioning of Ground Motion Hazard at the Reference Rock Outcrop

Two approaches are used to condition ground motion hazard at the reference rock outcrop such that it is consistent with the geologic setting of Yucca Mountain. One approach, the shear-strain-threshold approach, expands the method described in [Section 2.3.4.3.3](#), which estimates a ground motion level that has not been exceeded at Yucca Mountain. The second approach, the extreme-stress-drop approach, is based on characterization of the upper range of stress drop that is consistent with the geologic setting of Yucca Mountain (BSC 2008c, Section 6.5.1).

The first approach uses geologic observations at the repository level to develop a limiting distribution on shear-strains experienced at Yucca Mountain ([Section 2.3.4.3.3](#)). In this approach, laboratory rock mechanics data, corroborated by numerical modeling, are used to derive the shear-strain levels required to initiate stress-induced failure of the weaker lithophysal zones. Because these seismic-related failures in the lithophysal units are not observed, it is concluded that the derived threshold shear strains have not occurred since deposition of the Topopah Spring Tuff 12.8 M years ago. A distribution for shear strain threshold was developed (BSC 2005a, Section 6.4.3) and the corresponding distribution of horizontal peak ground velocity was developed using results of ground motion site-response modeling (BSC 2004e, Section 6.3.4). The site-response model incorporates uncertainty and variability in modeling the lithophysal unit and uncertainties in the geotechnical model for the site. Consequently, distributions are developed for both the shear strain threshold and horizontal peak ground velocity that are consistent with the site-response model. With distributions developed for peak ground velocity, operators in the form of complementary cumulative distribution functions were developed that were applied to an unbounded horizontal peak ground velocity hazard curve for the repository block to develop a conditioned hazard curve consistent with geologic observations (BSC 2005a, Section 6.8).

Although the fundamental assessment that a shear-strain threshold has not been exceeded within the Topopah Spring Tuff lithophysal units remains the same, other aspects of the approach are generalized, refined, and updated in developing supplemental ground motions. First, the approach is generalized to deal with ground motion parameters other than horizontal peak ground velocity. Response spectral acceleration at 0.3, 0.5, 1, 2, 5, 10, 20 Hz and peak ground acceleration are now addressed. Second, the approach is modified to use the inferred shear-strain threshold at the repository waste emplacement level to determine the level of ground motion not experienced at the reference rock outcrop, rather than at the waste emplacement level. This allows the approach to be used in analyzing conditioned ground motions at the surface GROA as well as the repository block. Third, implementation of the conditioning is refined to include variability in shear strain levels and integration over the entire hazard curve. Finally, the site-response component of the approach is

updated to incorporate additional geotechnical data on site tuff and alluvium properties. As a result of these changes, the previously developed strain-based complementary cumulative distribution function hazard operators (BSC 2005a, Section 6.8) are revised (BSC 2008c, Section 6.5.1.1 and Appendix A, Sections A2.2 and A4.5.2).

In the second approach, a distribution of extreme stress drop in the Yucca Mountain vicinity is developed. An extreme stress drop is defined as one that results in strong ground motion far in excess of that instrumentally recorded. The distribution is based on available data and interpretations and is informed by discussions with ground motion experts during a series of workshops that were held to evaluate the issue (BSC 2008c, Appendix A, Section A.3.2.1.3). The distribution on extreme stress drop is used in the stochastic point-source ground motion model to develop a distribution on peak ground acceleration and peak ground velocity at the reference rock outcrop (Figure 1.1-78) that are used as operators to condition seismic hazard (BSC 2008c, Section 6.5.1.2). The conditioned peak ground acceleration hazard is then used to scale uniform hazard spectra from the PSHA for a given annual probability of exceedance. This approach preserves the spectral shape from the PSHA for the reference rock outcrop. Preservation of this shape is desirable as it is a key output of the PSHA and represents the interpretations developed through a formal expert elicitation process (Sections 1.1.5.2.4 and 2.2.2.1.1).

Extreme stress drop is characterized by a log-normal distribution with a value of 400 bars and σ_{\ln} of 0.6 (mean of 480 bars) (BSC 2008c, Appendix A, Section A3.2.1.3). In using this distribution to condition extreme ground motions, the distribution is approximated by three values: 150 bars, 400 bars, and 1100 bars, with weighting factors of 0.2, 0.6, and 0.2, respectively. Data and interpretations considered in developing the distribution include measurements of stress drop and apparent stress from laboratory experiments, stress drop and apparent stress determinations from earthquakes occurring globally, implications of alternate source representations, and regulatory requirements. These approaches were discussed during the workshops with ground motion experts and the extreme stress drop distribution is informed by those discussions.

Conditioned hazard using combined shear-strain-threshold and extreme-stress-drop approaches is illustrated in Figures 1.1-79 and 1.1-80 for peak ground velocity and peak ground acceleration, respectively. The shear-strain-threshold-conditioning has a marginal impact on the unconditioned hazard as compared to the extreme-stress-drop approach (BSC 2008c, Section 6.5.1.3).

The reference rock outcrop horizontal uniform hazard spectra based on the conditioned hazard are illustrated in Figures 1.1-81 through 1.1-86 for annual probabilities of exceedance of 10^{-3} , 10^{-4} , 10^{-5} , 10^{-6} , 10^{-7} , and 10^{-8} , respectively. For annual probabilities of exceedance of 10^{-3} and 10^{-4} , spanning the range of annual probabilities of exceedance used for design analyses (DBGM-1, DBGM-2, and beyond DBGM) (Figures 1.1-81 and 1.1-82), the uniform hazard spectra using conditioned and unconditioned hazard are approximately equal. For the decreasing annual probabilities of exceedance of 10^{-5} , 10^{-6} , 10^{-7} , and 10^{-8} (Figures 1.1-83 through 1.1-86), uniform hazard spectra using the conditioned hazard are increasingly lower than the unconditioned uniform hazard spectra.

1.1.5.2.5.2 Site-Response Modeling

A site-response analysis was performed to develop earthquake ground motion input for preclosure assessment of the repository. The purpose of the ground motion site-response model is to incorporate the effects of the upper rock and soil layers at Yucca Mountain on earthquake ground motions. Incorporation of these effects was decoupled from the PSHA, which provided ground motion for a reference rock outcrop (Figure 1.1-78 and Section 2.2.2.1.3.2) (CRWMS M&O 1998a, Section 5.3.1.2; BSC 2004e, Section 1). The site-response model determines, for specific locations of interest such as at the surface GROA and the repository block, how ground motion propagation through the site tuff and alluvium modifies an input control motion based on the PSHA results. Site-response modeling supports the development of transfer functions consisting of both site amplification factors and vertical-to-horizontal response spectral ratios.

In evaluating potential preclosure and postclosure effects of ground motion, incorporation of site-response effects on ground motion at Yucca Mountain has followed two approaches. Both approaches are designed to produce site-specific response spectra that maintain the hazard level (probability of exceedance) of the conditioned PSHA reference rock outcrop spectra used as the basis for input to the site-response modeling (BSC 2008c, Section 6.1). The approaches used are described in *Technical Basis for Revision of Regulatory Guidance on Design Ground Motions: Hazard- and Risk-Consistent Ground Motion Spectra Guidelines* (NUREG/CR-6728) (McGuire et al. 2001, Section 6.1).

One approach (labeled Approach 2B in NUREG/CR-6728) (McGuire et al. 2001, Section 6.1) uses scaling of an input ground motion to obtain a site-specific uniform hazard spectrum with the same annual probability of exceedance. The input ground motion is derived from a rock uniform hazard spectrum for a probability of exceedance of interest. Scaling of the input motion is based on results of site-response modeling that determines the effect of the site tuff and alluvium on the input motion. The site response modeling takes into account the distributions of earthquake magnitudes contributing to the hazard at high and low oscillator response frequencies for the probability of exceedance of interest and also the variability and uncertainty in site tuff and alluvium properties. Site response results for the low and high oscillator frequency ranges and for different site tuff and alluvium property base cases are enveloped to obtain the overall site response. The result is a site specific uniform hazard spectrum reflecting the effects of the site tuff and alluvium. This approach is used to develop the ground motions for the postclosure analyses described in Section 2.3.4.3.

A second approach (labeled Approach 3 in NUREG/CR-6728) (McGuire et al. 2001, Section 6.1) uses integration over multiple rock ground motion amplitude levels with the site-response dependent on the amplitude level and the associated contributing magnitude and distance distribution. As in Approach 2B, site-response modeling takes into account high and low oscillator frequency ranges and the variability and uncertainty in site properties. This approach results directly in a site-specific hazard curve. Uncertainty in site properties leads to hazard curves for each combination of base-case properties. The overall hazard curve is determined by averaging, using weighting factors if appropriate, the hazard curves for the different base-case property combinations. When implemented for a suite of ground motion parameters (e.g., spectral acceleration at a suite of response oscillator frequencies), the approach provides the results needed to construct a site specific uniform hazard curve for a probability of exceedance of interest. This

approach is used to develop ground motions that, for preclosure design and probabilistic seismic safety analyses, supplement those developed using Approach 2B.

A key aspect of Approach 3 is that it facilitates averaging the results of different cases that represent epistemic uncertainty in site-response model inputs. With Approach 2B, site-specific response spectra or site-response transfer functions for different cases are enveloped. The enveloping is carried out without regard to the assessed relative likelihood that the different cases reflect the true nature of the site. With Approach 3, the site response results for different cases yield a set of hazard curves. The probabilities of the ground motions for the different cases can thus be averaged, using weighting factors that reflect assessments of their relative likelihood, if appropriate, to produce the final site-specific hazard. To develop ground motions for probabilistic preclosure seismic safety analyses, it was decided to move beyond the possible conservatism of enveloping and to use the approach that facilitates appropriate weighting of cases representing epistemic uncertainty (BSC 2008c, Sections 6.1.3 and 6.4.5).

1.1.5.2.5.2.1 Site Amplification Factors

The site-response model for Yucca Mountain addresses seismic wave propagation through the site tuff and alluvium and takes dynamic behavior of those materials into account (BSC 2004e, Section 6). Key inputs to the model consist of earthquake response spectra derived from the conditioned PSHA hazard results, profiles of seismic velocity as a function of depth, and curves that represent the dynamic properties of the site tuff and alluvium as a function of shear strain. At higher levels of ground motion, strains induced in the site tuff and alluvium alter the shear modulus and damping properties of the material, which in turn affect ground motion propagation.

The response of the site tuff and alluvium is modeled using a one-dimensional equivalent-linear formulation (BSC 2004e, Section 6.1.1). That is, nonlinear behavior of the site tuff and alluvium under ground-motion loading is approximated with a linear equation over a limited range of its variables. The effective strain produced in the site tuff and alluvium by the ground motion is used to adjust the material dynamic properties, and the process is iterated to achieve a solution that is compatible with the induced strains. Random vibration theory is used to determine peak strains from which the effective strains are calculated. Thus, the site-response model is referred to as a random vibration theory-based equivalent-linear model.

The overall approach for developing location-specific ground motions (i.e., for the surface GROA or for the repository block) aims to produce a response spectrum that preserves the annual probability of exceedance corresponding to the input ground motion derived from the PSHA and conditioning. To reach this goal, uncertainty and variability in site tuff and alluvium properties are taken into account (McGuire et al. 2001, Section 6). Uncertainty and variability in the ground motion that forms the basis for input into the site-response model are accounted for in the PSHA process.

One role of site-response modeling is to produce amplification factor transfer functions. Amplification factors reflect the ratio between the location-specific 5%-damped response spectrum determined from site-response modeling and the 5%-damped response spectrum of the control motion input representing ground motion at the PSHA reference rock outcrop. The amplification

factors are integrated with appropriate hazard curves to determine probabilistic site-specific ground motions.

Ground motion inputs to site-response modeling consist of appropriate reference earthquake response spectra scaled to a peak ground acceleration in the range of 0.1 to 10 g. These reference earthquake response spectra are based on results of the PSHA. The uniform hazard spectra are determined from the PSHA results for mean annual probabilities of exceedance of 10^{-3} , 5×10^{-4} , 10^{-4} , 10^{-5} , 10^{-6} , and 10^{-7} (BSC 2004e, Section 6.2.2.3). Because the uniform hazard spectra are broad-band response spectra, reflecting contributions to ground motion hazard from earthquakes with a range of magnitudes and distances, reference earthquake response spectra were developed to represent the uniform hazard spectra in site-response analyses (BSC 2004e, Section 6.2.2.4). For each annual probability of exceedance, two reference earthquakes, characterized by a modal magnitude and modal distance, were determined. One was based on deaggregation of the seismic hazard for spectral response at 1 and 2 Hz (BSC 2008c, Figures 6.4.1-5 through 6.4.1-10) and the other on deaggregation of the seismic hazard for spectral response at 5 and 10 Hz (BSC 2008c, Figures 6.4.1-11 through 6.4.1-16).

In developing a suite of site-response amplification factors for use in integrating over ground-motion, site-response modeling is carried out for a range of ground motion levels (peak ground acceleration from 0.01 to 10 g). This range of motions provides amplification factors appropriate for the ground motion levels observed in the reference rock outcrop hazard curves, conditioned or unconditioned, for annual probabilities of exceedance ranging from 10^{-2} to below 10^{-8} . The control motion response spectrum for each level of ground motion is determined by scaling an appropriate reference earthquake response spectrum to the peak ground acceleration level of interest. The appropriate reference earthquake for each ground motion level is chosen by comparing the peak ground acceleration level of interest to the peak ground acceleration level of the reference earthquake spectrum (BSC 2008c, Table 6.4-3). These control motion response spectra (Figure 1.1-87) are used as input for site-response modeling to develop the suite of amplification factors for the range of ground motion considered (BSC 2008c, Section 6.4).

Velocity profile inputs to the site response model are based on available geotechnical information (BSC 2008c, Section 6.4.2). In developing ground motion inputs, the goal is to produce inputs that are applicable for the entire surface GROA. Similarly, for the repository block, the goal is to produce ground motion inputs that apply throughout the waste emplacement area footprint. To achieve this goal, in cases in which there is observed variability in velocity profiles across a site, site-response modeling is carried out for the different profiles.

For the surface GROA, velocity characteristics vary across the Exile Hill Fault splay. Thus, different velocity profiles are developed for the area to the northeast of the fault splay and to the south of the fault splay (Section 1.1.5.2.6.1). For the surface GROA there is also observed variability in the thickness of alluvium. For the area northeast of the fault splay, site-response modeling is carried out for four alluvium thickness values: 30, 70, 100, and 200 ft. For the area south of the fault splay, alluvium thickness is less and only three thickness values are modeled: 30, 70, and 100 ft. For the area south of the Exile Hill Fault splay there is also epistemic uncertainty in the velocity profile. Three alternate interpretations are used in site-response modeling for each thickness of alluvium.

For the repository block, velocity characteristics vary spatially. To represent this observed variability, two velocity profiles are developed (Section 1.1.5.2.6.2).

Dynamic material property curves providing input to site-response modeling are subject to epistemic uncertainty. For both tuff and alluvium, two alternate sets of curves are developed to represent the uncertainty in site properties (Section 1.1.5.2.6.1).

Amplification factors are developed for the various combinations of velocity profile, dynamic material property curves, and alluvium thickness (for the surface GROA) representing observed variability and epistemic uncertainty across the surface GROA and repository block. For each combination, aleatory variability is incorporated in the amplification factors by carrying out site-response modeling for 60 randomized velocity profiles and sets of dynamic material property curves, based on the corresponding base cases, and then averaging the resulting amplification factors (BSC 2008c, Section 6.5.2).

1.1.5.2.5.2.2 Vertical-to-Horizontal Ratios

Site-specific vertical motions are determined from site-specific horizontal motions using transfer functions consisting of ratios of vertical-to-horizontal 5%-damped response spectra. Two methods are used to evaluate the vertical-to-horizontal ratios. First, a stochastic point-source ground motion model is used in conjunction with the random-vibration-theory-based equivalent-linear site-response model to numerically simulate ratios appropriate for the Yucca Mountain site. Second, empirical ratios determined for western North America are also used for surface motions. For the surface facilities area, for which both approaches are used, the approaches are given equal weight.

A stochastic point-source ground motion model has been developed and validated (BSC 2008c, Sections 6.3 and 7). The model uses an ω -squared source model with a single-corner frequency and a constant stress drop. Random vibration theory is used to relate root-mean-square values to peak values of acceleration and oscillator response computed from the power spectra to expected peak time domain values (BSC 2008c, Section 6.3.1). For this approach to developing vertical-to-horizontal ratios, first the point-source model is run for three moment magnitude values (5, 6, 7). For each magnitude, the distance and depth of the point-source are adjusted to produce a target peak ground acceleration at the PSHA reference rock outcrop. The same suite of target peak ground acceleration values, ranging from 0.1 to 10 g, as was used in developing amplification factors is used for development of vertical-to-horizontal ratios. The point-source model is used for both the horizontal and vertical component analyses to ensure a cancellation of source processes in computing the vertical to horizontal ratio.

Next, the output of the point-source model is used as the input control motion to the site-response model to develop site-specific horizontal and vertical response spectra. The horizontal component analyses are performed using the equivalent-linear formulation, while the vertical component analyses are performed linearly (BSC 2008c, Section 6.1.4.1.3). Ratios are developed for the various combinations of velocity profile, dynamic material property curves, and alluvium thickness (for the surface GROA) representing observed variability and epistemic uncertainty across the surface GROA and repository block (BSC 2008c, Sections 6.5.2.1.2 and 6.5.3.1). The product of these analyses for each combination of velocity profile, dynamic material property curves, and, for the surface GROA, alluvium thickness is a suite of vertical-to-horizontal response spectral ratios for

peak ground acceleration values from 0.1 to 10 g for three magnitudes with associated distant and depth combinations.

To complement the numerical approach for determining vertical-to-horizontal response spectral ratios, an approach employing empirical relations is also used. As empirical relations are only available for surface motions, this approach applies only to the development of ground motions for the surface GROA. The empirical relations of Abrahamson and Silva (1997) and Campbell and Bozorgnia (2003) were both used and are given equal weight (BSC 2008c, Section 6.5.2.1.2). Because the alluvium at Yucca Mountain is quite stiff, relations for both rock (soft) and soil (deep firm) conditions were considered. Results for the two material classes are weighted based on the average shear-wave velocity in the upper 30 m (V_{S30}). Comparison of the V_{S30} associated with the rock and soil classes used in deriving the empirical relations to corresponding velocities for the surface GROA led to the judgment that weighting factors of 0.8 (rock) and 0.2 (soil) are appropriate. Both empirical relations also provide predictions of ground motion for hanging wall and foot wall locations. Because the surface GROA is in the foot wall of the Bow Ridge Fault and the hanging wall of the Paintbrush Canyon Fault, results for both conditions are considered. Based on seismic source characterization (recurrence relation, maximum magnitude) for these two faults during the PSHA the Paintbrush Canyon Fault has a stronger contribution to overall ground motion hazard (BSC 2004f, Section 6.5.4). Therefore, weighting factors of 0.75 (hanging wall) and 0.25 (foot wall) are adopted.

In integrating over ground-motion to develop site-specific vertical hazard curves using Approach 3, appropriate vertical-to-horizontal ratio values are determined from the suite of values through interpolation. Deaggregation of the seismic hazard is used to determine the appropriate vertical-to-horizontal ratio values (magnitude-distance-depth combination) to use for interpolation (BSC 2008c, Section 6.5.2.1.2).

1.1.5.2.5.3 Development of Site-Specific Hazard Curves

The supplemental ground motions developed for preclosure analyses (BSC 2008c) are computed using Approach 3 of NUREG/CR-6728 (McGuire et al. 2001, Section 6.1). This approach is a fully probabilistic analysis procedure that moves the site response into the hazard integral (BSC 2008c, Section 6.1.3). In this approach, the hazard for a specific location (e.g., surface GROA or repository block) is computed by integrating the hazard curve at the PSHA reference rock outcrop with the probability distribution of appropriate amplification factors. The site-specific amplification is characterized by a suite of frequency-dependent amplification factors that account for nonlinearity in tuff and alluvium response. Approach 3 involves approximations to the hazard integration using suites of transfer functions, or, for vertical motions, vertical-to-horizontal ratios, that result in complete site-specific hazard curves.

A distinct advantage of Approach 3 is the proper incorporation of site epistemic uncertainty. Multiple hazard curves may be developed reflecting multiple site representations (e.g., velocity profiles, normalized shear modulus and hysteretic damping curves as a function of shear strain) that are then averaged over probability to develop mean, median, and fractile estimates. Additionally, vertical hazard curves may also be developed that are consistent with the horizontal by applying distributions of vertical-to-horizontal 5%-damped response spectral ratios to the site specific horizontal hazard curves. Also, Approach 3 results in a full hazard curve for a given location of

interest, rather than location-specific ground motion at a limited number of annual probabilities of exceedance, as with Approach 2B.

A weighted contribution of the factors developed from the low- and high-frequency reference earthquakes is used in applying the amplification factors during the Approach 3 analyses for horizontal motions, based on the reference rock outcrop hazard deaggregations. Because distance is a controlling factor as well as magnitude, the vertical-to-horizontal ratios are weighted based on distance deaggregations of the reference rock outcrop hazard. As a result, the transfer functions (amplification factors and vertical to horizontal ratios) change with annual probability of exceedance (BSC 2008c, Section 6.1.4.1).

Hazard-consistent site-specific supplemental ground motion inputs for preclosure analyses were determined for the surface GROA and for the repository block based on Approach 3 for DBGGM-1, DBGGM-2, and beyond DBGGMs. In developing hazard-consistent site-specific ground motion inputs for the two locations of interest, hazard curves were developed for the various combinations of velocity profile, dynamic material property curves, and alluvium thickness. For the various cases representing epistemic uncertainty in velocity south of the Exile Hill Fault splay, the hazard results were averaged using weighting factors based on the assessed degree to which each alternate profile reflects actual site conditions. Hazard results for different base case sets of dynamic material property curves were also combined using a weighted average because these base cases represent epistemic uncertainty. Hazard results for different cases representing observed variability in site properties are combined by enveloping. For the surface GROA, hazard results for the velocity profiles northeast and south of the Exile Hill Fault splay and for the various depths of alluvium were enveloped. For the repository block, hazard results for the two velocity profiles were enveloped. This process results in hazard curves for the surface GROA and the repository block that appropriately incorporate epistemic uncertainty, observed variability, and aleatory variability (randomness) (BSC 2008c, Section 6.4.2).

1.1.5.2.5.4 Development of Design Response Spectra

Design response spectra (5%-damped) for the surface GROA and repository block are developed from the location-specific uniform hazard spectra (BSC 2008c, Sections 6.5.2.3 and 6.5.3.3). The uniform hazard spectra are generally followed, but if spectral holes exist they are eliminated by smoothing. The uniform hazard spectra extend to periods as long as 3.3 s; beyond that period extrapolation using the logarithm of period and spectral acceleration is used.

In addition to 5%-damped seismic design spectra, surface GROA spectra at other damping values were calculated for the annual probabilities of exceedance of 10^{-3} , 5×10^{-4} , and 10^{-4} . Design spectra for damping values of 0.5%, 1%, 2%, 3%, 7%, 10%, 15%, and 20% are determined for the surface GROA by developing scaling factors to adjust the 5%-damped spectra (BSC 2008c, Section 6.5.2.3.3). To develop site-specific scaling factors, time histories that are spectrally matched to the 5%-damped design spectrum are used to determine response spectra at other damping values. By using time histories that are spectrally matched to the 5%-damped design spectra, employment of the resulting scaling factors leads to response spectra at other damping values that are consistent with the time histories for design analyses.

1.1.5.2.5.5 Development of Design Time Histories

Time histories are developed such that their response spectra closely match the design spectrum at the appropriate mean annual probability of exceedance (BSC 2008c, Sections 6.5.2.5 and 6.5.3.6). To develop each set of time histories, strong ground motion recordings from past earthquakes are used as input in the spectral matching process to provide time histories with phase and duration characteristics of observed ground motion. The seed strong ground motion recordings are chosen from the NUREG/CR-6728 (McGuire et al. 2001, Appendix B) analysis time history database. The seed time histories are chosen based on the deaggregated hazard at Yucca Mountain such that their magnitude and distance characteristics are similar to those of earthquakes that dominate seismic hazard at the site.

Development of design time histories follows applicable recommendations in NUREG/CR-6728 (McGuire et al. 2001, Section 5.3) as outlined below (BSC 2008c, Section 6.5.2):

- The artificial accelerogram achieves approximately a mean-based fit to the target spectrum. The average ratio of the spectral acceleration calculated from the accelerogram to the target, calculated frequency by frequency, is only slightly greater than one to ensure there are no significant gaps and the result is not biased high with respect to the target.
- Records have a sufficiently small frequency increment and sufficiently high maximum frequency (or alternatively time increment and maximum duration). The total duration of the record can be increased by zero packing to satisfy these frequency requirements. It is recommended that records have a maximum frequency increment of 0.05 Hz with a Nyquist frequency of at least 50 Hz or a time increment of at most 0.01 s for a total duration of 20 s. A time increment at 0.005 is used for all cases.
- Spectral accelerations at 5% damping are computed at a minimum of 100 points per frequency decade, uniformly spaced over the log frequency scale from 0.1 Hz to 50 Hz or the Nyquist frequency. The computed 5%-damped response spectrum of the accelerogram (if one artificial motion is used for analysis) or the average of all accelerograms (if a suite of motions is used for analysis) does not fall more than 10% below the target spectrum at any one frequency point. No more than nine adjacent spectral points are allowed to fall below the target spectrum at any frequency. This corresponds to a moving frequency window of $\pm 10\%$ centered on the frequency.
- The computed 5%-damped response spectrum of the artificial ground motion (if one motion is used for analysis) or the average of the 5%-damped response spectra (if a suite of motions is used for analysis) does not exceed the target spectrum by more than 30% in the frequency range between 0.2 Hz and 50 Hz.
- The upper limit for the zero-lag cross-correlation coefficient between any two design ground motions (acceleration time histories) is 0.3.

These criteria ensure that no gaps in the power spectral density or Fourier amplitude spectrum will occur over a significant frequency range (BSC 2008c, Section 6.5.2).

For the surface GROA, 5 sets of three-component time histories are developed each for mean annual probabilities of exceedance of 10^{-3} , 5×10^{-4} , and 10^{-4} . For the repository block, one single three-component set of time histories is developed for the same three mean annual probabilities of exceedance.

1.1.5.2.5.6 Development of Strain-Compatible Material Properties

Strain-compatible soil properties are determined for the surface GROA that are consistent with the design spectra and time histories for a given mean annual probability of exceedance. The approach adopts a lognormal distribution for strain-compatible properties and makes use of the strain-compatible properties determined during development of the site response amplification factors. For each case representing epistemic uncertainty, the site-specific horizontal and vertical hazard curves are examined to determine the ground motion level for a given mean annual probability of exceedance. Strain-compatible properties calculated for ground motion levels that bracket the ground motion at the mean annual probability of interest are then used as the basis to compute median and sigma values (over aleatory variability). To combine the results for the various cases representing epistemic uncertainty in site-specific properties, the same weighting factors used in developing location-specific hazard curves are applied to the corresponding strain-compatible properties. The approach accommodates median estimates as well as epistemic uncertainty and aleatory variability in strain-compatible properties that are consistent with the site-specific horizontal and vertical hazard used for design. The calculation is carried out for peak ground acceleration and for response spectral acceleration at an oscillator period of 1 s. The final results average the values obtained for these two periods (BSC 2008c, Section 6.5.2).

In soil-structure interaction analyses, best-estimate, upper-bound, and lower-bound properties are used. For Yucca Mountain, best-estimate properties are taken as the median (mean log) properties. Upper-bound and lower-bound properties are determined by taking the best-estimate plus and minus one standard deviation (σ_{ln}). Such an approach is recommended in NUREG-0800 (NRC 2007, Section 3.7.2). For Yucca Mountain, use of the σ_{ln} to determine upper- and lower-bounds for shear-wave velocity is modified to impose a minimum σ_{ln} consistent with a coefficient of variation on shear modulus of 0.5. Use of this constraint is recommended in NUREG-0800 (NRC 2007, Section 3.7.2) for well-investigated sites for which only a single site-response calculation is available. While 60 site-response calculations are carried out for Yucca Mountain for each case representing epistemic uncertainty, this constraint is incorporated for conservatism. The same minimum value of σ_{ln} was also applied in determining the upper and lower bounds for shear-wave damping, compressional-wave velocity, and compressional-wave damping. The minimum value of σ_{ln} consistent with a coefficient of variation on shear modulus of 0.5 is 0.203 (BSC 2008c, Section 6.5.2.6). Finally, the value of σ_{ln} was adjusted to account for an assumed lower-bound strain-compatible shear-wave velocity of 500 ft/s (BSC 2008c, Sections 6.5.2.6 and 5.5).

1.1.5.2.6 Ground Motion Inputs

Ground motion inputs are developed for the surface GROA and repository block following the process described in Sections 1.1.5.2.5.1 through 1.1.5.2.5.6. These inputs are discussed in more detail in Sections 1.1.5.2.6.1 and 1.1.5.2.6.2. A summary of ground motion inputs is provided in

[Section 1.1.5.2.6.3](#). The adequacy of the inputs for the site response model is discussed in [Section 1.1.5.2.6.4](#).

1.1.5.2.6.1 Surface Geologic Repository Operations Area Ground Motion Inputs

The first phase in developing site-specific ground motions consists of determining transfer functions. Transfer functions include both amplification factors for horizontal motions and vertical-to-horizontal ratios of response spectral acceleration. Amplification factors reflect the ratio between the site-specific 5%-damped response spectrum determined from site-response modeling and the 5%-damped response spectrum of the control motion input representing ground motion at the PSHA reference rock outcrop. Vertical-to-horizontal ratios reflect the ratio between vertical and horizontal 5%-damped response spectra; both are determined using a combined stochastic point-source model and site-response model. Both types of transfer functions are ultimately integrated with appropriate hazard curves to determine probabilistic site-specific ground motions (BSC 2008c, Section 6.5.2).

For the amplification factors, reference earthquake spectra computed from the PSHA attenuation relations and scaled to peak ground acceleration values ranging from 0.01 to 10 g are used as control motions in site-response modeling. Following Regulatory Guide 1.165, both 1-to-2 Hz and 5-to-10 Hz reference earthquake spectra were used. Reference earthquakes are summarized in [Table 1.1-68](#). This approach is intended to produce amplification factors appropriate for specific earthquakes (magnitude and distance combinations) dominating the hazard at low- and high-structural frequency, as well as reflecting site- and region-specific spectral shapes. The range of peak ground acceleration used to scale the reference earthquake spectra to obtain control motion inputs provides amplification factors appropriate for ground motion levels observed in the reference rock outcrop hazard curves, conditioned or unconditioned, for annual probabilities of exceedance ranging from 10^{-2} to below 10^{-8} (BSC 2008c, Section 6.5.2).

The amplification factor is determined by taking the ratio between the site-specific 5%-damped response spectrum, calculated using the site-response model, and the corresponding control motion input spectrum. Amplification factors for peak ground velocity are computed in a similar fashion. Amplification factors are developed for combinations of base-case velocity profiles, base-case dynamic material property curves, and alluvium thickness representing known variability and epistemic uncertainty across the surface GROA (BSC 2008c, Section 6.5.2).

As discussed in [Section 1.1.5.2.7.2](#), complete characterization of the surface GROA involves two base-case velocity profiles (south of the Exile Hill Fault splay and northeast of the Exile Hill Fault splay) representing observed variability; two base-case sets of dynamic material property curves for tuff (upper mean tuff and lower mean tuff) and two base-case sets of dynamic material property curves for alluvium (upper mean alluvium and lower mean alluvium) representing epistemic uncertainty; and four values of alluvium thickness (30, 70, 100, and 200 ft) representing known variability. For the south of the Exile Hill Fault splay velocity profile, there are three interpretations representing epistemic uncertainty (A, B, and C). With respect to alluvium thickness, three values (30, 70, and 100 ft) are used to characterize the area in which the south of the Exile Hill Fault splay velocity profile applies, while all four values are used for the northeast of the Exile Hill Fault splay velocity profile area. This results in a total of 52 combinations of site properties that are evaluated in the site-response modeling. For each combination, aleatory variability is incorporated in the amplification factors by carrying out site-response modeling for 60 randomized velocity profiles

and sets of dynamic material property curves, based on the corresponding base cases, and then averaging the resulting amplification factors (BSC 2008c, Section 6.5.2).

In the development of site-wide hazard curves for the surface GROA, separate sets of hazard curves are first developed for each combination. Then, for each combination of velocity profile and alluvium thickness, the hazard curves for the different combinations of dynamic material property curves are averaged using weighting factors that represent an assessment of the degree to which each combination reflects the actual site conditions at the surface GROA. Next, for each value of alluvium thickness, the hazard curves for the three alternate interpretations of the south of the Exile Hill Fault splay velocity profile are averaged using weighting factors. This results in seven sets of hazard curves for the seven combinations of velocity profile and alluvium thickness: south of the Exile Hill Fault splay and alluvium thickness values of 30, 70, and 100 ft; and northeast of the Exile Hill Fault splay and alluvium thickness values of 30, 70, 100, and 200 ft (BSC 2008c, Figures 6.5.2-7 to 6.5.2-27). The vertical seismic hazard curves are calculated using vertical-to-horizontal ratios (BSC 2008c, Section 6.5.2.).

The seven combinations of alluvium and tuff hazard curves are then combined to make two sets of curves, one for northeast of the Exile Hill Fault splay and one for south of the Exile Hill Fault splay. The hazard curves for the four combinations of alluvium thickness for northeast of the Exile Hill Fault splay are enveloped. Similarly, hazard curves for the three values of alluvium thickness for south of the Exile Hill Fault splay are enveloped (BSC 2008c, Figures 6.5.2-28 to 6.5.2-33).

Finally, these two sets of hazard curves were enveloped to produce a set of mean horizontal and vertical seismic hazard curves for the entire surface GROA (BSC 2008c, Figures 6.5.2-34 to 6.5.2-41). As an example, the mean horizontal and vertical peak ground acceleration hazard curves for the surface GROA are shown in [Figure 1.1-88](#). Also, the mean horizontal peak ground velocity hazard curve for the surface GROA is shown in [Figure 1.1-89](#).

Horizontal and vertical uniform hazard spectra for the surface GROA are calculated from the hazard curves. Uniform hazard spectra for 5%-damping are determined for annual probabilities of exceedance of 10^{-3} , 5×10^{-4} , 10^{-4} , 10^{-5} , 2×10^{-6} , 10^{-6} , and 10^{-7} (BSC 2008c, Section 6.5.2.2 and Figures 6.5.2-43 to 6.5.2-49).

As the annual probability of exceedance decreases, the vertical-to-horizontal ratio generally increases at short periods. For annual probabilities of exceedance of 10^{-4} and smaller, this results in the vertical uniform hazard spectra exceeding slightly the horizontal uniform hazard spectra at short periods (about 0.02 to 0.1 s). This trend is consistent with the hazard deaggregation that shows large nearby events dominate the hazard at annual probabilities of exceedance less than about 10^{-4} . For nearby events, short-period vertical motions are observed to exceed horizontal motions (BSC 2008c, Section 6.5.2).

The mean horizontal and vertical uniform hazard spectra form the basis for the horizontal and vertical design spectra (BSC 2008c, Figures 6.5.2-50 to 6.5.2-57), respectively. For the horizontal design spectra, the corresponding uniform hazard spectra is taken and extrapolated to a response spectral period of 10 seconds, based on the linear trend in log (period) and log (spectral acceleration) between 2 and 3.3 sec. Each of these spectra is then digitized and interpolated to 298 points. Following an analysis to determine design spectra for damping values other than 5%, all design

response spectra are interpolated to 28 points. For the vertical design spectra, the process is the same, except that the vertical uniform hazard spectra were smoothed slightly at their peaks during the step to extend them to a response spectral period of 10 seconds (BSC 2008c, Section 6.5.2).

In addition to 5%-damped seismic design spectra, surface GROA spectra at other damping values were calculated for the annual probabilities of exceedance of 10^{-3} , 5×10^{-4} , and 10^{-4} ; spectra were also determined for damping values of 0.5%, 1%, 2%, 3%, 7%, 10%, 15%, and 20%. To determine the spectra for other damping values, an analysis was carried out to evaluate the spectral ratio, as a function of frequency and damping value, between the 5%-damped design spectra and the design spectra at other damping values. Five sets of three-component time histories that had been spectrally matched to the 5%-damped design spectra form the data set for the analysis. These time histories were developed using recorded accelerograms (seed time histories) that have magnitude and distance characteristics consistent with those shown by seismic hazard deaggregation to control the hazard at Yucca Mountain for a given annual frequency of exceedance. Response spectra at the required damping values are computed for the time histories, and the resulting suite of spectra is used to develop the scaling factors. One analysis is done for the spectra with damping values less than 5% (i.e., 0.5%, 1%, 2%, and 3%), and another analysis is done for the spectra with damping values greater than 5% (i.e., 7%, 10%, 15%, and 20%). For a given frequency, the 5%-damped spectral value, when multiplied by the spectral ratio determined from the analyses, yields the spectral value for the damping value of interest. Separate analyses are carried out for horizontal and vertical spectra (BSC 2008c, Section 6.5.2.3). These design response spectra are illustrated in [Figures 1.2.2-8 through 1.2.2-13](#) and further discussed in [Section 1.2.2](#).

The supplemental horizontal and vertical design spectra differ from those calculated in 2004 (BSC 2004e) in several ways. The methods used to develop the 2004 design spectra included the following (BSC 2008c, Section 6.5.2.3):

- They were based on velocity data collected from the area southwest of the Exile Hill Fault splay.
- They were developed using Approach 2B from NUREG/CR-6728 (McGuire et al. 2001, Section 6.1), rather than Approach 3.
- The site-response control motions were not conditioned to reflect updated characterization of extreme ground motion at Yucca Mountain.

At annual probabilities of exceedance of 10^{-3} and 5×10^{-4} , the new supplemental surface GROA horizontal design spectra are lower at short periods (< about 0.1 s), comparable at intermediate periods (about 0.1 to 1 seconds), and slightly higher at longer periods (> about 1 s) (BSC 2008c, Figures 6.5.2-50 and 6.5.2-51). At 10^{-4} annual probability of exceedance, the supplemental horizontal design spectrum is lower at all periods except in the range of about 1.5 to 2.5 seconds, for which it is negligibly higher (BSC 2008c, Figure 6.5.2-52). In a similar fashion, the supplemental vertical design spectra at annual probabilities of exceedance of 10^{-3} and 5×10^{-4} are lower than the 2004 spectrum at short periods (< 0.2 to 0.3 s) and long periods (> 2 s) and higher at periods between about 0.3 and 2 seconds (BSC 2008c, Figures 6.5.2-53 and 6.5.2-54). At 10^{-4} annual probability of exceedance, the supplemental vertical design spectrum is lower than the 2004 spectrum at short periods (BSC 2008c, Figure 6.5.2-55). The difference at peak ground acceleration is more than a

factor of 2. The surface GROA 5%-damped horizontal and vertical design spectra are summarized in [Figures 1.1-90](#) and [1.1-91](#), respectively (BSC 2008c, Section 6.5.2).

Five sets of three-component time histories were developed for the surface GROA at 10^{-3} , 5×10^{-4} , and 10^{-4} annual probability of exceedance, resulting in a total of 15 sets. Each set of time histories is developed to closely match the design spectrum at the appropriate annual probability of exceedance. This approach is consistent with how the time histories are to be used in design analyses (BSC 2008c, Section 6.5.2).

Seed strong ground-motion recordings are chosen from the NUREG/CR-6728 (McGuire et al. 2001, Appendix B) analysis time history database and used as input in the spectral matching process to provide time histories with phase and duration characteristics of observed ground motion. Acceleration plots of the seed time histories are used to match the design spectra at 10^{-3} and 5×10^{-4} annual probability of exceedance (BSC 2008c, Figures 6.5.2-86 to 6.5.2-90). Corresponding seed plots are used to match the beyond design basis spectra at 10^{-4} annual probability of exceedance (BSC 2008c, Figures 6.5.2-91 to 6.5.2-95).

For preclosure design at the surface GROA for an annual probability of exceedance of 10^{-3} , five sets of three-component time histories were developed by spectrally matching to the surface GROA seismic design spectra (BSC 2008c, Figures 6.5.2-96 to 6.5.2-140).

Two of the five input strong ground motions are rock sites: the 1994 Northridge earthquake, Wrightwood Jackson Flat station recording, and the 1994 Northridge earthquake, Rancho Cucamonga Deer Canyon station recording. These records, (M 6.7, R 68.4 km and R 80.0 km, respectively) were selected from the M: 6.5, D: 50 to 100 km bin of the NUREG/CR-6728 (McGuire et al. 2001, Appendix B) analysis time history database (BSC 2008c, Section 6.5.2).

The next two of the five input strong ground motions are the 1987 Whittier Narrows earthquake, Calabasas North Las Virgenes station recording, a rock site; and the 1987 Whittier Narrows earthquake, Pasadena–California Boulevard station recording, a soil site. These records, (M 6.0, R 53.3 km and R 15.5 km, respectively), were selected from the M: 6.0, D: 0 to 50 km and D: 50 to 100 km bins of the NUREG/CR-6728 (McGuire et al. 2001, Appendix B) analysis time history database (BSC 2008c, Section 6.5.2).

The last of the five input strong motions is a rock site, the 1999 Chi-Chi, Taiwan earthquake, Tap 036 station recording. This record (M 7.6, R 95.6 km) was selected from the M: 7.5, D: 50 to 100 km bin of the NUREG/CR-6728 (McGuire et al. 2001, Appendix B) analysis time history database.

The modal magnitude and distance determined from the joint deaggregation of the hazard at 10^{-3} annual probability of exceedance gives a M 7.4 event at 51 km in the 1 to 2 Hz frequency range and a M 5.2 event at 9 km in the 5 to 10 Hz frequency range ([Table 1.1-68](#)). Following NUREG/CR-6728 (McGuire et al. 2001, Section 5), when matching to a uniform hazard spectrum (one spectrum instead of the two deaggregated reference events), it is recommended that the strong ground motion duration be the longer duration associated with the low-frequency event. Thus, four of the five seed strong motion records are for larger more distant earthquakes; one is from a smaller less distant earthquake (BSC 2008c, Section 6.5.2).

For preclosure design at the surface GROA at 5×10^{-4} annual probability of exceedance, five sets of three-component time histories were developed by spectrally matching to the surface GROA seismic design spectrum (BSC 2008c, Figures 6.5.2-141 to 6.5.2-185). Because deaggregation of the seismic hazard at 5×10^{-4} annual probability of exceedance shows that earthquakes dominating the hazard are similar to those at 1×10^{-3} annual probability of exceedance (Table 1.1-68), the input time histories used to match the 10^{-3} annual probability of exceedance seismic design spectra are also used for the time histories with a 5×10^{-4} annual probability of exceedance (BSC 2008c, Section 6.5.2).

Five sets of three-component time histories were developed for surface GROA preclosure design analyses at 10^{-4} annual probability of exceedance by spectrally matching to the surface GROA seismic design spectra (BSC 2008c, Figures 6.5.2-186 to 6.5.2-230). The modal magnitude and distance determined from the joint deaggregation of the hazard at 10^{-4} annual probability of exceedance gives a M 7.7 event at 51 km in the 1 to 2 Hz frequency range and a M 6.2 event at 4 km in the 5 to 10 Hz frequency range (Table 1.1-68). Based on these results, five sets of seed strong motion recordings were selected (BSC 2008c, Section 6.5.2).

Three of the five input strong ground motions are: (1) the 1999 Kocaeli earthquake, Iznik station recording; (2) the 1992 Landers earthquake, Twentynine Palms station recording; and (3) the 1992 Cape Mendocino earthquake, Shelter Cove station recording. These records (M 7.4, R 29.7 km, M 7.3, R 42.2 km, M 7.1, R 33.8 km, respectively) were selected from the M: 7.5, D: 10 to 50 km bin of the NUREG/CR-6728 (McGuire et al. 2001, Appendix B) analysis time history database. These recordings are on rock (BSC 2008c, Section 6.5.2).

The last two of the five input strong ground motions are also rock sites: the 1992 Landers earthquake, Silent Valley station recording, and the 1999 Kocaeli earthquake, Mecidiyekoy station recording. These records (M 7.3, R 51.7 km and M 7.4, R 62.3 km, respectively) were selected from the M: 7.5, D: 50 to 100 km bin of the NUREG/CR-6728 (McGuire et al. 2001, Appendix B) analysis time history database (BSC 2008c, Section 6.5.2).

Strain-compatible soil properties were generated for the seven combinations of alluvium thickness over tuff velocity profiles (BSC 2008c, Table 6.5-8) following the approach described in Section 1.1.5.2.5.6.

For the northeast of the Exile Hill Fault splay velocity profile, strain-compatible material properties are developed for alluvium thickness values of 30, 70, 100, and 200 ft. For the south of the Exile Hill Fault splay velocity profile, strain-compatible material properties are developed for alluvium thickness values of 30, 70, and 100 ft. Depending on the location of an ITS building that is to be analyzed, an appropriate set or sets of strain-compatible properties are selected (BSC 2008c, Section 6.5.2 and Figures 6.5.2-231 through Figures 6.5.2-314).

1.1.5.2.6.2 Repository Block Ground Motion Inputs

Modeling and analyses are used to develop seismic hazard curves and design parameters with annual probabilities of exceedance of 10^{-3} , 5×10^{-4} , and 10^{-4} for the repository block waste emplacement level. Site-response modeling results in horizontal and vertical hazard curves, uniform hazard spectra, and 5%-damped seismic design response spectra and expected peak ground

velocities at each annual probability of exceedance. Design-time histories are also developed for the three annual probabilities of exceedance. Results are also used for comparison with repository block waste emplacement level ground motions previously developed (BSC 2004e) using alternate modeling inputs and an alternate analysis approach (BSC 2008c, Section 6.5.3)

Horizontal amplification factors and vertical-to-horizontal ratios were computed for the waste emplacement area following the same process as described for the surface GROA. However, because empirical relations are not available for at-depth motions, only numerical modeling was used for site-specific vertical-to-horizontal ratios. In terms of reference earthquake and point-source magnitude contributions varying with structural frequency and exceedance probability, the distributions used for the surface GROA were also used for the repository block (BSC 2008c, Section 6.5.3; and Tables 6.5-1, 6.5-3, and 6.5-4).

Hazard curves were calculated for the repository block for horizontal and vertical ground motions. Two base-case velocity profiles for the repository block, a soft zone and a stiff zone, were used in the site response model calculations (BSC 2008c, Section 6.5.3).

In the final step to develop hazard curves for the repository block, the hazard curves based on the two velocity profiles are enveloped. Mean horizontal and vertical seismic hazard curves for the repository block and peak ground acceleration, 0.05, 0.1, 0.2, 0.5, 1.0, 2.0, and 3.3 s spectral acceleration have been developed (BSC 2008c, Figures 6.5.3-9 to 6.5.3-16). For horizontal and vertical peak ground velocity, the mean, median and fractile (5th, 15th, 85th, and 95th percentiles) hazard curves are also developed by enveloping the hazard curves for the two repository block base-case velocity profiles (BSC 2008c, Figures 6.5.3-17 and 6.5.3-18). Based on the resulting repository block hazard curves, mean uniform hazard spectra are determined for annual probabilities of exceedance of 10^{-3} , 5×10^{-4} , 10^{-4} , 10^{-5} , 10^{-6} , 10^{-7} , and 10^{-8} (BSC 2008c, Figures 6.5.3-19 to 6.5.3-25)

Design spectra for annual probabilities of exceedance of 10^{-3} , 5×10^{-4} , and 10^{-4} are based on the corresponding uniform hazard spectra for the repository block. For the design spectra, the uniform hazard spectra are smoothed and extrapolated to 10 s spectral acceleration. In smoothing, a decrease in spectral acceleration at 1 Hz for the uniform hazard spectra is eliminated. Extrapolation beyond 3.0 seconds is based on the slope between 2 and 3.0 seconds. In developing the design spectra, a spectral acceleration value at 0.02 seconds is estimated that results in a divergence from a straight-line log-log interpolation between the uniform hazard spectra values at 0.05 and 0.01 seconds. Horizontal and vertical design spectra for the repository block with annual probabilities of exceedance of 10^{-3} , 5×10^{-4} , and 10^{-4} are shown in [Figures 1.1-92](#), [1.1-93](#), and [1.1-94](#), respectively (BSC 2008c, Section 6.5.3). Seismic design and loads applicable to preclosure for the subsurface SSCs are discussed in [Section 1.3.2.5.1](#). Ground response spectral acceleration plots corresponding to annual probability of exceedance events of 1×10^{-3} , 5×10^{-4} , and 1×10^{-4} for 2003–2004 and 2007–2008 data sets for 5% damping ratios are illustrated in [Figures 1.3.2-7](#) through [1.3.2-12](#).

Design spectra developed in *Supplemental Earthquake Ground Motion Input for a Geologic Repository at Yucca Mountain, NV* (BSC 2008c) for the repository block waste emplacement level differ from those developed in *Development of Earthquake Ground Motion Input for Preclosure Seismic Design and Postclosure Performance Assessment of a Geologic Repository at Yucca Mountain, NV* (BSC 2004e) in several ways. The following are shown in the 2004 report:

- Site-response model inputs were based on geotechnical data described in *Geotechnical Data for a Potential Waste Handling Building and for Ground Motion Analyses for the Yucca Mountain Site Characterization Project* (BSC 2002b).
- Site-response model results were used to determine site-specific, hazard-consistent ground motion inputs using Approach 2B of NUREG/CR-6728 (McGuire et al. 2001).
- Control motion inputs to the site-response model were not conditioned to reflect new information on extreme ground motion at Yucca Mountain.

The 2004 design spectra exceed the 2008 spectra at most spectral periods and particularly for vertical ground motions. The differences may be attributed to similar factors as for the surface GROA (BSC 2008c, Section 6.5.3).

The approach used to develop time histories for repository block preclosure analyses is identical to the approach for the surface GROA. One set of time histories each was developed for the repository block at 10^{-3} , 5×10^{-4} , and 10^{-4} annual probabilities of exceedance, resulting in a total of three sets. Strong ground motion recordings from past earthquakes are used in the spectral matching process to provide realistic time histories with characteristics of observed ground motion. The seed strong ground motion recordings are chosen from the NUREG/CR-6728 (McGuire et al. 2001, Appendix B) analysis time history database. Acceleration plots of the seed time histories are used to match the design spectra at 10^{-3} and 5×10^{-4} annual probabilities of exceedance (BSC 2008c, Figure 6.5.3-49) and at 10^{-4} annual probability of exceedance (BSC 2008c, Figure 6.5.3-50).

For repository block preclosure design for a annual probability of exceedance of 10^{-3} , one set of three-component time histories were developed by spectrally matching to the repository block seismic design spectrum. The input strong motion is a rock site, the 1994 Northridge, California, earthquake, Duarte-Mel Canyon station recording (BSC 2008c, Table 6.5-22). This record (M 6.7, R 52.0 km) was selected from the M: 6.5, D: 50 to 100 km bin of the NUREG/CR-6728 (McGuire et al. 2001, Appendix B) analysis time history database (BSC 2008c, Section 6.5.3).

The deaggregation of the hazard at 10^{-3} annual probability of exceedance shows that the hazard is dominated by a M 6.9 event at 52 km at the 1 to 2 Hz frequency range and a M 6.3 event at 5 km at the 5 to 10 Hz frequency range (Table 1.1-68). Following NUREG/CR-6728 (McGuire et al. 2001, Section 5), when matching to uniform hazard spectra (one spectrum instead of the two deaggregated reference event spectra), it is recommended that the strong ground motion duration be the longer duration associated with the low-frequency event. The matching criteria presented in NUREG/CR-6728 (McGuire et al. 2001) were followed for time history spectral matching (BSC 2008c, Section 6.5.3).

The spectral matches to the target (design) spectra, plots of the ratios between the spectra of the matched time history and the target spectra, and the spectrally matched time histories for acceleration, velocity, and displacement for 10^{-3} annual probability of exceedance and horizontal and vertical ground motions are illustrated in *Supplemental Earthquake Ground Motion Input for a Geologic Repository at Yucca Mountain, NV* (BSC 2008c, Figures 6.5.3-51 to 6.5.3-59).

For repository block preclosure design at 5×10^{-4} annual probability of exceedance, the same set of three-component seed time histories as used for 10^{-3} annual probability of exceedance were used to spectrally match to the seismic design spectra. The spectral matches to the target (design) spectra, plots of the ratios between the spectra of the matched time history and the target spectra, and the spectrally matched time histories for acceleration, velocity, and displacement for 5×10^{-4} annual probability of exceedance and horizontal and vertical ground motions are illustrated in *Supplemental Earthquake Ground Motion Input for a Geologic Repository at Yucca Mountain, NV* (BSC 2008c, Figures 6.5.3-60 to 6.5.3-68).

For repository block preclosure design at 10^{-4} annual probability of exceedance, one set of three-component time histories was developed by spectrally matching to the repository block seismic design spectrum. The input strong ground-motion site is a rock site, the 1999 Chi Chi, Taiwan earthquake, TCU015 station recording (BSC 2008c, Table 6.5-22). This record, (M 7.6, R 47.3 km) was selected from the M: 7.5, D: 0 to 50 km bin of the NUREG/CR-6728 (McGuire et al. 2001, Appendix B) analysis time history database. It was selected in light of the deaggregation of the hazard at 10^{-4} annual probability of exceedance, which is dominated by a M 7.7 event at 52 km at the 1 to 2 Hz frequency range and a M 6.3 event at 5 km at the 5 to 10 Hz frequency range (Table 1.1-68) (BSC 2008c, Section 6.5.3).

The spectral matches to the target (design) spectra, plots of the ratios between the spectra of the matched time history and the target spectra, and the spectrally matched time histories for acceleration, velocity, and displacement for 10^{-4} annual probability of exceedance and horizontal and vertical ground motions are illustrated in *Supplemental Earthquake Ground Motion Input for a Geologic Repository at Yucca Mountain, NV* (BSC 2008c, Figures 6.5.3-69 to 6.5.3-77).

Repository block time histories developed for postclosure analyses in *Development of Earthquake Ground Motion Input for Preclosure Seismic Design and Postclosure Performance Assessment of a Geologic Repository at Yucca Mountain, NV* (BSC 2004e, Section 6.3.2.3) differ from the updated time histories for corresponding annual probabilities of exceedance. Section 6.3.2.3 of the report shows the following:

- Suites of 17 sets of three-component time histories were developed for three annual probabilities of exceedance: 10^{-5} , 10^{-6} , and 10^{-7} .
- For each annual probability of exceedance, seed time histories were selected based on deaggregation of the PSHA results.
- The H1 component of each seed time history was then scaled according to the horizontal peak ground velocity determined from site-response modeling.
- The other two components were scaled to maintain the inter-component variability of the original seed time history.
- Control motion inputs to the site-response modeling were not conditioned to reflect new information on extreme ground motion.

For an annual probability of exceedance of 10^{-5} , the median response spectrum of the horizontal components of the 17 suites of time histories is similar to the updated horizontal uniform hazard spectrum for oscillator frequencies of about 1 to 10 Hz. At lower frequencies, the updated results are slightly higher; at higher frequencies the updated results are slightly lower (BSC 2008c, Figure 6.5.3-78). For an annual probability of exceedance of 10^{-6} , the updated uniform hazard spectra are significantly lower than the median for the 2004 time histories at all oscillator frequencies above about 0.6 Hz. Above about 3 Hz, the updated results are comparable to or lower than the -1 sigma spectrum (BSC 2008c, Figure 6.5.3-79). For an annual probability of exceedance of 10^{-7} (BSC 2008c, Figure 6.5.3-80), the current results are significantly lower than the -1 sigma spectrum for oscillator frequencies above about 2 Hz and below the median for the 2004 time histories at all oscillator frequencies (BSC 2008c, Section 6.5.3).

1.1.5.2.6.3 Summary of Ground Motions

Preclosure seismic ground motions for design analyses are listed in [Table 1.1-69](#). Both horizontal and vertical surface facilities design response spectra at 10^{-3} , 5×10^{-4} , and 10^{-4} annual probabilities of exceedance were computed for additional damping values of 0.5%, 1.0%, 2.0%, 3.0%, 7.0%, 10.0%, 15.0%, and 20.0%. These response spectra are illustrated in [Figures 1.2.2-8](#) through [1.2.2-13](#) and discussed in [Section 1.2.2](#). Seismic design and loads applicable to preclosure for the subsurface SSCs are discussed in [Section 1.3.2.5.1](#). Ground response spectral acceleration plots corresponding to annual probability of exceedance events of 1×10^{-3} , 5×10^{-4} , and 1×10^{-4} for 2003–2004 and 2007–2008 data sets for 5% damping ratios are illustrated in [Figures 1.3.2-7](#) through [1.3.2-12](#). For periods greater than 2.0 seconds (frequencies less than 0.5 Hz), the spectral acceleration amplitude is lower than appropriate for the nominal uniform hazard spectra annual probability of exceedance (BSC 2008c). The applicability of the uniform hazard spectra for periods greater than 2 seconds is, therefore, limited. Because design response spectra are based on the uniform hazard spectra, and design time histories are spectrally matched to the design response spectra, these outputs are similarly limited. Analyses conducted that utilize spectral accelerations for periods greater than 2 seconds have been performed with estimated spectral accelerations. The structural analyses discussed in [Section 1.2.2](#) conclude that the response of ITS facilities are not affected by the limitation. Analyses discussed in [Section 1.3.2](#) contain sensitivity evaluations that indicate subsurface facilities are not sensitive to the limitation. Event sequences associated with seismic initiating events and the overall approach to the probabilistic seismic analysis is discussed in [Section 1.7.1.4](#). The mean seismic hazard curve used in the preclosure safety analysis for the surface facilities is shown in [Figure 1.7-7](#). Seismic fragilities and development of seismic fragility curves is discussed in [Section 1.7.2.4](#).

1.1.5.2.6.4 Adequacy of Site-Response Model Inputs

Seismic and geotechnical data that form inputs to the random-vibration-theory-based equivalent-linear site-response model are adequate to develop ground motions for preclosure and postclosure analyses. The results of the Yucca Mountain PSHA, conditioned by recent evaluations of the level of extreme ground motion that is consistent with the geologic setting, are used for control motion inputs (BSC 2008c, Section 6.4.1). These results incorporate epistemic uncertainty and aleatory variability in the characterization of seismic sources and ground motion attenuation relationships for the Yucca Mountain vicinity, as determined through a formal expert elicitation process (BSC 2008c, Section 6.4.1). As part of the PSHA, the experts considered an extensive database of geologic, geophysical, tectonic, and seismic information pertinent to the Yucca Mountain site. Control motion inputs to site-response modeling also incorporate uncertainty in the level of extreme ground motion that Yucca Mountain can experience (BSC 2008c, Section 6.4.6).

Seismic velocity profiles are determined on the basis of seismic data collected in boreholes and through spectral analysis of surface wave surveys at the surface and within the ESF and ECRB Cross-Drift (BSC 2008c, Section 6.4.2). The velocity characteristics are adequately determined using knowledge of the subsurface geology at the site and the combination of borehole and spectral analysis of surface wave data. While not used as direct basis for velocity profiles, laboratory determinations of velocity differ from the in situ data in expected ways and corroborate the profiles of in situ velocity (BSC 2008c, Figure 6.4.4-7 and Section 6.4.4.2).

Uncertainty and variability in velocity characteristics at Yucca Mountain are appropriately accounted for in site-response modeling through the use of multiple velocity profiles. Results from different profiles representing epistemic uncertainty are weighted according to the degree that they are supported by the data. Results from different profiles representing spatial variability for the repository block and surface GROA are enveloped to provide ground motions that apply to the entire repository block and entire surface GROA, respectively. For example, for the surface GROA, the developed ground motions incorporate uncertainty and variability across the entire area, not just beneath any individual ITS structure. Aleatory (random) variability in velocity is also incorporated in the development of site-specific ground motion through site response modeling that employs a suite of randomized velocity profiles determined from a given mean base-case profile (BSC 2008c, Section 6.4.6).

Dynamic material property curves are determined on the basis of laboratory testing of site materials, consideration of results in the literature for other materials, and judgment on how those data relate to in situ conditions at Yucca Mountain (BSC 2008c, Section 6.4.4). Consideration of this technical basis indicates that there is epistemic uncertainty in the characterization of dynamic properties for tuff and alluvium. Because of this uncertainty, multiple sets of curves for the variation of normalized shear modulus and material damping as a function of shearing strain are incorporated into the site-response modeling. Site-response modeling also incorporates aleatory variability in dynamic properties to provide ground motions appropriate for the entire site of interest. Uncertainty and variability in dynamic properties are appropriately incorporated into site-response modeling and the development of site-specific ground motions (BSC 2008c, Section 6.4.6).

1.1.5.2.7 Seismic Design Data for Preclosure Facilities

1.1.5.2.7.1 Design Methodology for Preclosure Facilities

The seismic design strategy for Yucca Mountain provides the methodology for assigning DBGGM levels. The strategy for prevention of preclosure seismic event sequences is to design ITS SSCs to withstand a specified level of DBGGM in accordance with the seismic event sequence analysis as described in [Section 1.7.2.4](#).

For fault displacement, the repository is located to avoid Quaternary faults with a potential for significant displacement. In cases for which avoidance is not practical, appropriate mean annual probabilities of exceedance for design basis fault displacement are identified as 10^{-4} and 5×10^{-5} (DBFD-1 and DBFD-2, respectively) (DOE 2007c, Section 5.2.1). Based on results from the PSHA, fault displacement hazard values at these levels are less than 0.1 cm within the surface facilities and repository waste-emplacement areas ([Table 1.1-67](#)).

1.1.5.2.7.2 Development of Seismic Design Data

A ground motion site-response analysis is used in developing the earthquake ground-motion input for preclosure design and safety analysis. The ground motion site-response model uses the reference rock outcrop ground motion developed in PSHA, conditions it to reflect constraints on extreme motions consistent with the geologic setting, and incorporates the effects of the overlying tuff and alluvium at Yucca Mountain on earthquake ground motions. The site-response model determines the propagation of ground motion through the site materials for specific locations of interest such as at the surface GROA or at the depth of the repository block waste emplacement area. Incorporation of site-response effects is carried out in a manner that maintains the hazard level (annual probability of exceedance) of the motion at the PSHA reference rock outcrop. Output of the site-response model consists of seismic design response spectra and strain-compatible soil properties. The seismic design response spectra are then used to develop time histories (seismograms) representing ground motion for a given annual probability of exceedance. The time histories provide input to analyses of rockfall and structural response of repository SSCs under seismic loads.

The ground motion site-response model for preclosure design and analyses is described in [Section 1.1.5.2.5](#). The discussion addresses the conceptual approach of the model, the implementation of the model, and model results. In this section, the model description in [Section 1.1.5.2.5](#) is supplemented with a discussion of model data for the surface GROA and repository block.

The discussion in [Section 2.3.4](#) focuses on ground motions for postclosure analyses and ground motions for the waste emplacement level with an annual probability of exceedance of less than 10^{-4} . [Section 2.3.4](#) also describes the development of time histories on the basis of model results for postclosure analyses. Development of time histories for preclosure analyses follows a different approach, which is described in [Section 1.1.5.2.5](#).

Geotechnical Investigations—Geotechnical investigations have been carried out to collect information on the material properties of the site (BSC 2002b; BSC 2004e, Sections 6.2.3 and 6.2.4; SNL 2008a). The studies focused on the two primary sites of interest: the surface GROA and the area above the repository footprint. The surface GROA is of interest for preclosure design; the area above the repository footprint is characterized to allow determination of subsurface ground motion for analyses supporting both preclosure design and postclosure performance assessment. Studies consisted of drilling and logging boreholes, velocity surveys, and laboratory testing of rock and soil samples to determine the dynamic response properties of the materials (i.e., the shear modulus and damping behavior as a function of imposed dynamic strain level). This discussion focuses on the investigations to characterize the surface facilities area and the repository block to support preclosure analyses. Investigations to characterize the repository block for postclosure analyses are discussed in [Section 2.3.4](#).

Exploratory drilling has been performed in the vicinity of the surface GROA since the mid-1980s. The earliest repository facility boreholes (UE-25 RF#1, UE-25 RF#2, UE-25 RF#3, UE-25 RF#3b, UE-25 RF#4, UE-25 RF#5, UE-25 RF#7, UE-25 RF#7A, UE-25 RF#8, UE-25 RF#9, UE-25 RF#10, and UE-25 RF#11) were drilled to collect data on potential sites for repository surface facilities. Descriptive borehole logs are provide in [Tables 1.1-70](#) through [1.1-81](#). Beginning in

1998, additional repository facility boreholes were drilled to gather geotechnical information supporting foundation design of surface facilities and development of inputs for seismic ground motion analyses. Repository facility boreholes drilled from 1998 through 2000 focused on an area in the vicinity of the North Portal of the ESF. Graphical logs for these boreholes are provided in [Figures 1.1-95](#) through [1.1-110](#). At that time, conceptual surface facilities for the Site Recommendation consisted of a limited number of buildings near the North Portal. Following approval of the Site Recommendation, the surface facilities layout evolved to consist of a larger number of ITS facilities that extended to the northeast, away from the North Portal. Consequently, a new phase of drilling was initiated in 2005 to collect relevant geotechnical information on the materials underlying the new layout. The 2005 program of repository facility exploratory drilling in the vicinity of the surface GROA began in March 2005 and concluded in July 2005. The drilling program was developed to gain an understanding of subsurface geologic conditions. The boreholes were drilled to penetrate the top of bedrock to determine the thickness of the alluvium (SNL 2008a, Section 6.2.2). Geologic data acquired in the boreholes included depth of lithostratigraphic subzone contacts, welding, and percent core recovery. Detailed geologic borehole logs for the holes drilled in 2005 are shown in [Figures 1.1-111](#) through [1.1-128](#). Locations of these boreholes are shown on [Figure 1.1-129](#). Along with plans for transportation, aging, and disposal canister system for packaging of commercial spent nuclear fuel, a further evolution of the layout of repository surface facilities ensued. In response, a new program of drilling was initiated to collect additional geotechnical data for confirmation of inputs used in analyses and modeling supporting a license application. This drilling program began in 2006 and continued through the fall of 2007 (SNL 2008a, Section 6.2.2).

The sonic coring method has been used in the drilling program since 2005 to collect as much useful information as possible regarding geotechnical properties in alluvial material with substantial gravel-, cobble-, and boulder-size material. This method provides improved recovery of alluvial materials over other drilling methods. The sonic coring method, similar to other methods of sample recovery, recovers a disturbed sample. When coring through cobble- or boulder-size particles, this method may produce a rock flour, which can increase the apparent fines content (i.e., material capable of passing a No. 200 sieve) in the sample recovered. The drilling processes can also break down oversize material (greater than 3 in.) and increase the apparent percentage of gravel-size material. As a result, descriptions of the alluvial materials may not reflect in situ geologic conditions due to mechanical degradation of the sample. However, using the Unified Soil Classification System visual method provides consistent material classifications. For the types of material recovered by the drilling, it does not appear that the sonic method affects the material to the point that major changes in the gradation occur (SNL 2008a, Section 6.2.2).

During 2006 and 2007, 43 additional repository facility boreholes were drilled. These boreholes are shown on [Figure 1.1-129](#) (Buesch and Lung 2008). A thickness of alluvium contour map was developed ([Figure 1.1-130](#)) using data from boreholes from pre-2005, 2005, and depth of alluvium information available from 23 boreholes from the 2006 to 2007 drilling program. This map is a computer-generated interpretation based on a 100-ft grid. Although the contour lines are depicted as solid, they represent an approximation of alluvium thickness and are not meant to depict an exact thickness at any given location (SNL 2008a, Section 6.2.2).

Although drilling, geologic, and geophysical logs are still being processed for the 43 boreholes drilled during 2006 and 2007; initial examinations have been made for many of the boreholes and

several boreholes have been examined in more detail. Boreholes examined in more detail include (Buesch and Lung 2008):

- An angled borehole that was designed to penetrate the Exile Hill Fault splay (UE-25 RF#40)
- Boreholes within or near the boundaries of planned ITS facilities (UE-25 RF#30, UE-25 RF#81, UE-25 RF#82, UE-25 RF#85, UE-25 RF#86, and UE-25 RF#92)
- Boreholes within or near the boundaries of the aging pads (UE-25 RF#67, UE-25 RF#69, UE-25 RF#71, UE-25 RF#94, and UE-25 RF#102).

Initial examination of the cores, geologic logs, and geophysical logs from boreholes drilled and test pits excavated in 2006 and 2007 (especially the 12 boreholes listed above) indicate that they are consistent with expected results from geologic observations of boreholes drilled and test pits excavated previously. These observations are consistent with expected geologic conditions relative to the distribution and characteristics of the (1) alluvium, (2) Miocene tuffaceous rocks, (3) correlations of lithostratigraphic features and units with properties determined from geophysical logs, (4) locations of faults, and (5) nonwelded-tuff-filled fractures in some of the Miocene rocks (Buesch and Lung 2008).

Geologic cross sections have been developed based on drilling results through 2000. These cross sections show the base of the alluvium in Midway Valley as relatively flat in each section (Figures 1.1-65 through 1.1-67). Results from the 2005 through 2007 drilling not only confirm this but also extend the interpretation of a smooth, relatively flat top of bedrock contact across two-thirds of Midway Valley from west to east. Alluvium thickness is zero at the base of Exile Hill and increases in thickness to almost 200 ft about halfway across the valley, and then begins to thin eastward towards Alice Point (Figure 1.1-130) (SNL 2008a, Section 6.2.2).

Material Dynamic Properties Data—Dynamic properties of the site materials form input to the site-response model. These properties are the following:

- Shear modulus, normalized to its small-strain value, as a function of shearing strain
- Material damping as a function of shearing strain
- Seismic velocity as a function of depth.

Shear modulus reduction and variation in material damping as a function of shear strain are parameters that characterize the response of site materials to dynamic strains caused by seismic wave propagation through them.

Geotechnical investigations have been carried out to characterize these inputs (Section 1.1.5.3). Results of the investigations are used to determine geometric mean values and to assess uncertainties. In addition, the properties vary about their geometric mean values when the spatial extent of a location of interest is considered. To determine site-specific ground motion that is consistent with the results of the PSHA, these uncertainties and variability are incorporated into the site response analysis, just as uncertainties and variability are explicitly incorporated in the PSHA.

Shear Modulus and Material Damping Properties—To characterize the normalized shear modulus reduction and damping properties of the repository block and surface GROA, laboratory tests were conducted on rock and soil samples. Resonant column and torsional shear tests were performed to examine the nonlinear behavior of the materials as a function of shearing strain. (BSC 2002b, Sections 6.2.10 and 6.3.3). To accommodate uncertainty in mean normalized shear modulus reduction and material damping curves for tuff, two sets of base-case curves were developed (Figure 1.1-131). For alluvium, two sets of curves were also developed (Figure 1.1-132). Development of these curves is discussed in Section 1.1.5.3.2.6.3.

Seismic Velocity as a Function of Depth— V_S and V_P profiles for the surface GROA and the repository block are major inputs into the site response model. The goal is to develop velocity profiles that appropriately represent the uncertainty and variability in velocities for the surface GROA and the repository block. Profiles are developed for the surface GROA and the repository block such that, in terms of final ground motions, a single set of site-specific ground motion hazard curves and related ground motion inputs are developed for the surface GROA and repository block. To the extent that different base case velocity profiles characterize different portions of the surface GROA and repository block, site response calculations are made using each base case profile and the results are enveloped. In the case in which there is epistemic uncertainty in a given base case velocity profile, alternative interpretations are used in site response calculations and the results are combined in a weighted average based on the assessed degree to which each interpretation is supported by the available data. Aleatory variability (randomness) in velocity profiles is also incorporated into the site response calculations. Each base case profile forms the basis for developing a suite of 60 randomized profiles that are used in site response calculations (BSC 2008c, Section 6.4.2).

The velocity profiles are developed on the basis of available velocity data and an understanding of the geologic framework of the surface GROA and repository block. Velocity data for the site were acquired using a range of techniques: spectral analysis of surface waves, downhole seismic velocity surveys, suspension logging surveys, sonic velocity logging, and vertical seismic profiling. Borehole-based techniques provide information on velocities in the immediate vicinity of the borehole. Spectral analysis of surface waves surveys complement the borehole-based measurements and provide information on the average velocity along the length of the survey line. Spectral analysis of surface waves surveys were also carried out in the subsurface within the ESF and the ECRB Cross-Drift. Geologic data are used to provide insights on the areas or zones in which various representative velocity profiles apply (BSC 2008c, Section 6.4.2).

Surface GROA V_S Base-Case Profiles—For the surface GROA, base-case velocity profiles for alluvium and tuffs of the Timber Mountain and Paintbrush groups are based on a combination of surface-based spectral analysis of surface waves surveys, downhole seismic, and suspension logging data. For the repository block, surface-based spectral analysis of surface waves surveys data form the basis for developing profiles for the tuffs of the Paintbrush Group. For both the surface GROA and repository block, sonic logging data provide the technical basis for an assumption of V_S values for the Calico Hills Formation and the Prow Pass Tuff. Vertical seismic profiling data, downhole velocity data from shallow (< 200 ft) boreholes on the repository block, and subsurface-based spectral analysis of surface waves survey data are used to compare to and corroborate the developed base-case profiles, but are not relied on directly. Final profiles for site response modeling are developed by combining, as appropriate, the component profiles for

alluvium, the tuffs of the Timber Mountain and Paintbrush groups, and the V_S values for the Calico Hills Formation and Prow Pass Tuff. V_p profiles are determined from the V_S profiles based on an analysis of Poisson's ratio (BSC 2008c, Section 6.4.2).

Velocities corresponding to alluvium and tuff units were evaluated separately when developing the base-case V_S profiles. Figure 1.1-133 shows a base-case V_S profile for tuff units for the zone northeast of the Exile Hill Fault splay and three base-case V_S profiles for the zone south of the Exile Hill Fault splay, and provides a comparison to the base-case V_S profile used in the 2004 evaluation of ground motions. In 2004, there was a single base-case tuff V_S profile for the surface GROA south of Exile Hill Fault splay, which went to a depth of 500 ft because the available data indicated that a V_S of 1,900 m/s (about 6,000 ft/s) was reached at that depth (BSC 2004e, Section 6.2; Figure 1.1-133).

Four base-case tuff V_S profiles are now used in site response modeling. Three base-case tuff V_S profiles are used for the area south of Exile Hill Fault splay to represent the differences in the data acquired using different measurement techniques at depths shallower than 500 ft and the epistemic uncertainty in the V_S profile at depths greater than 500 ft. An additional tuff V_S profile represents the surface GROA northeast of the Exile Hill Fault splay (Figure 1.1-133). The current profiles incorporate additional spectral analysis of surface waves profiles that are interpreted to depths of over 1,000 ft (Section 1.1.5.3.2). The south of Exile Hill Fault splay base-case tuff V_S profiles are similar to the 2004 base case profiles at least to a depth of 400 ft with Base Case C (Figure 1.1-133) resembling the 2004 base case to 500 ft depth (BSC 2008c, Section 6.4.2).

A single mean V_S profile was developed for alluvium (BSC 2008c, Section 6.4.2.5 and Figure 6.4.2-42). The alluvium postdates movement on the Exile Hill Fault and its splays, so the alluvium is the same on both sides of the fault (BSC 2008c, Section 6.4.2.5 and Figure 6.4.2-43). The thickness of the alluvium, however, varies across the surface GROA.

Alluvium thickens from zero at the base of Exile Hill to about 200 ft at the eastern boundary of the surface GROA (Figure 1.1-130). Depending on the foundation design and layout of the surface GROA structures, the thickness of alluvium varies significantly. Ground motion inputs are developed to provide a set of ground motions applicable to the entire surface GROA. To accommodate the effect of the varying thickness of alluvium, site-response modeling was carried out for multiple values of alluvium thickness. For the area northeast of the Exile Hill Fault splay, four alluvium thickness values of 30, 70, 100, and 200 ft were used. For the area south of the Exile Hill Fault splay, three alluvium thickness values of 30, 70, and 100 ft were used for each velocity profile representing epistemic uncertainty (BSC 2008c, Section 6.4.2). These thickness values span the range found under ITS facilities for the areas represented by the various tuff velocity profiles (Figure 1.1-130). The result of these variations is a total of 13 V_S profiles (BSC 2008c, Figures 6.4.2-44 through 6.4.2-56).

Smoothed and extrapolated Poisson's ratios were used for development of V_p profiles. For alluvium, depth-dependent Poisson's ratios range from about 0.25 to 0.34 (BSC 2008c, Figure 6.4.2-63). For tuff, a Poisson's ratio of 0.29 was used to a depth of 1,300 ft. Below 1,300 ft, for the Calico Hills Formation and the Prow Pass Tuff, a Poisson's ratio of 0.25 was used (BSC 2008c, Section 6.4.2).

As was done for the V_S profiles, the average V_P profiles were combined for various alluvium thicknesses and different velocity zones across the surface GROA to obtain the final 13 V_P base-case profiles (BSC 2008c, Figures 6.4.2-64 to 6.4.2-76) corresponding to the 13 base-case V_S profiles (BSC 2008c, Section 6.4.2).

Repository Block V_S Base-Case Profiles—Twenty-one spectral analysis of surface waves velocity profiles from 2004 to 2005 were used together with the 2000 to 2001 spectral analysis of surface waves profiles to develop V_S base case profiles for the repository block. Figure 1.1-134 shows the spectral analysis of surface waves profiles available in the vicinity of the repository block collected during 2000 to 2001 and 2004 to 2005 field investigations (BSC 2008c, Section 6.4.2.6).

Due to the large variability in the V_S values, the V_S profiles at individual locations were examined to see whether there was a spatial component to the variability. The V_S profiles showing higher velocities at depths ranging from about 600 to 1,000 ft (e.g., YM-8, YM-10, YM-12, YM-13, YM-14A, YM-14B, YM-21, and YM-15B) were observed to cluster spatially. These sites are classified as “stiff” sites. The remaining V_S profiles that do not show this velocity increase were classified as “soft” profiles; the locations where these soft V_S profiles were measured were classified as “soft” sites (BSC 2008c, Section 6.4.2.6).

Geologic cross sections at each of the spectral analysis of surface waves locations were reviewed to evaluate whether they could be grouped based on similarities in the occurrence of the various lithostratigraphic units and their thicknesses. It was concluded that the repository block could be subdivided into four zones based on similarities in lithology (BSC 2008c, Section 6.4.2.6). The four zones, consisting of a central stiff zone and three soft zones, and the spectral analysis of surface waves profiles that are included in each of the four zones, are shown on Figure 1.1-134.

The mean V_S profiles for the three soft zones (northern, central, and southern) were calculated by averaging the V_S profiles for the spectral analysis of surface waves surveys in each zone (BSC 2008c, Figure 6.4.2-79). The mean of the three soft zones were also calculated based on: (1) computing the mean of each zone and (2) averaging over all spectral analysis of surface waves velocity profiles. These two means for the soft zones are very similar (BSC 2008c, Figure 6.4.2-79). To avoid a bias towards a zone that had more V_S measurements, the mean V_S profile based on the three zone means is used as the base case V_S profile for the soft zones. To accommodate the variability in tuff V_S data, two base-case profiles were developed for use as input to the site response model. One base case represents the soft zones and the second the central stiff zone (BSC 2008c, Section 6.4.2).

V_S values obtained for the specific Topopah Spring Tuff units in the ESF and ECRB Cross-Drift tunnels (SNL 2008a, Section 6.4.5) were also compared to V_S values obtained from surface studies (BSC 2008c, Figures 6.4.2-81 through 6.4.2-83). The tunnel spectral analysis of surface waves measurements were separated into stiff and soft measurements based on their occurrence in each of the four zones (BSC 2008c, Table 6.4-14).

The tunnel measurements in Tptpmn were found to be consistently higher than the spectral analysis of surface waves measurements from the surface, which can be explained on the basis of sampling bias. In the tunnel, an equal number of test locations had been selected in the high fracture and the

low fracture zones. In the field, the volume of high fracture material may be more than the low fracture material. The tunnel measurements for the other two units, Ttpul and Ttppl, agree well with the spectral analysis of surface waves from the surface (BSC 2008c, Figures 6.4.2-81 to 6.4.2-84).

The final base case (Figure 1.1-135) used for the soft zones is a smoothed version of the mean soft profile (BSC 2008c, Figure 6.4.2-79). The base case hits the Calico Hills V_S of 5,600 ft/s at a depth of 1,300 ft and the Prow Pass (reference rock outcrop, Figure 1.1-78) V_S of 6,000 ft/s at 1,700 ft depth. The base case developed for the central stiff zone (Figure 1.1-135) was developed using the mean V_S profile developed for the central stiff zone (BSC 2008c, Figure 6.4.2-80).

Although the vertical seismic profile measurements were not included in the base case calculations, a comparison of the base case profiles and the vertical seismic profile measurements illustrates that the two are in reasonable agreement given the large spatial variability across the repository block (BSC 2008c, Figure 6.4.2-90).

V_p profiles for the repository block tuff (BSC 2008c, Figures 6.4.2-91 and 6.4.2-92) were estimated using the V_S profiles developed and the Poisson's ratios computed for the repository block. A constant Poisson's ratio of 0.30 was used throughout the tuff units in the repository block (BSC 2008c, Section 6.4.2.6).

1.1.5.2.7.3 Depth to the Reference Rock Outcrop Conditions and Comparison of the 2004 and Current Base-Case V_S Profiles

The PSHA reference rock outcrop V_S , which determines the depth of the control motion input to the site response model, was defined as 1,900 m/s (approximately 6,000 ft/s). Based on available data in 2002, the depth at which this velocity was obtained beneath the repository block was determined to be 1,100 ft (Figure 1.1-135; BSC 2004e, Figure 6.2-116). At the surface GROA, available data led to identification of the reference rock outcrop V_S at a depth of 500 ft (Figure 1.1-133; BSC 2004e, Figure 6.2-119). Recognizing that the depth to the reference rock outcrop V_S varied spatially for site response modeling in 2004, it was randomly varied from 700 to 1,500 ft for the repository block and from 400 to 600 ft for the surface GROA (BSC 2004e, Section 6.2.3.5).

The depth at which the reference rock outcrop V_S is obtained has been revised. It is now associated with the Prow Pass Tuff. Using the geologic framework model, the upper contact of the Prow Pass Tuff is taken at 1,500 ft for repository block base case profiles and 1,700 ft for the surface GROA base case profiles (BSC 2008c, Section 6.4.2.4.3).

Newer spectral analysis of surface waves-based velocity profiles that extend to greater depth than those from 2000 to 2001 and that provide greater spatial coverage of the repository footprint have reduced uncertainty in characterization of V_S for the repository block. Whereas in 2004 differences in velocity profiles based on spectral analysis of surface waves and vertical seismic profile data were treated as epistemic uncertainty (BSC 2004e, Section 6.2.3), the available data now support an interpretation that the velocity of the repository block varies spatially. To develop site-specific ground motions that apply to the entire repository block, site response modeling is carried out for two base-case profiles (Figure 1.1-135) and the results are enveloped (BSC 2008c, Section 6.5.3).

Comparison of the repository block base case profiles from 2004 (BSC 2004e, Section 6.2.3.3.1) and those determined in this analysis shows similarities and differences. The 2004 Base Case 1 and base case soft zones profiles agree fairly well with each other (Figure 1.1-135). Both show a rapid increase in velocity in the upper 50 ft and then a gradual increase to a depth of about 700 ft. From 700 to 1,100 ft below the ground surface, the 2004 Base Case 1 profile used a linear increase in velocity between the velocities interpreted from surface-based spectral analysis of surface waves measurements at 700 ft to the value determined at about 1,100 ft from subsurface-based spectral analysis of surface waves measurements in the ESF (Figure 1.1-135). For the base-case soft-zones profiles, additional surface-based spectral analysis of surface waves data allow velocity interpretations to greater depths. The surface-based measurements are corroborated by subsurface-based measurements covering a wider range of units than in the 2004 study (BSC 2008c, Section 6.4.2.4.2).

Comparison of 2004 Base Case 2 profiles and the Base Case stiff zones profiles shows significant differences. The Base Case 2 profile was based on vertical seismic profile data from areas in and near the repository block for which spectral analysis of surface waves data were not available. These data suggested that a profile with higher velocities characterized the repository block. Additional spectral analysis of surface waves data gathered since 2001 have clarified that the higher velocities do not represent epistemic uncertainty, but rather that different velocity profiles characterize different areas of the repository block (BSC 2008c, Figure 6.4.2-77). The base case stiff zone exhibits a moderate rate of increase in velocity from about 1,000 ft/s at the surface to about 6,800 ft/s at a depth of 750 ft (Figure 1.1-135). This contrasts with a more gradual increase based on the vertical seismic profile data in the 2004 study (2004 Base Case 2 profile, Figure 1.1-135). For the base case stiff zone profile, the vertical seismic profile data are not included because spectral analysis of surface waves data are now available and are considered more reliable.

1.1.5.3 Geotechnical Properties and Conditions

[NUREG-1804, Section 2.1.1.1.3: AC 5(2), (3), (4), (5), (8)]

This section summarizes the principal geotechnical properties of the subsurface soils and rocks important to design of facilities at the site. The GROA is divided into two main areas: the underground facilities area and the surface facilities area. The underground facilities are the emplacement drifts, as well as the access ramps, ventilation shafts, and auxiliary excavations. The surface facilities are the structures and other facilities. This section is divided into two main parts, addressing the geotechnical properties of materials in the underground facilities area and the surface facilities area, respectively.

The geotechnical properties discussed are static properties (strength and deformation characteristics), dynamic properties (seismic velocity profiles, shear modulus and material damping ratio as functions of shear strain), and thermal properties (thermal conductivity, specific heat, and coefficient of thermal expansion). The thermal properties are important for the emplacement drifts, where large temperature changes occur due to waste heat. In addition, the shear-wave velocity profile of the site is an important input to ground-motion analysis. Physical properties such as density and porosity are also discussed, in part because other properties are found to be dependent on them and also because total density is often a direct analysis input. This section discusses primarily results from field observations and field and laboratory testing; in some cases, properties were developed through simulations and numerical analysis or the data were further analyzed to

develop parameters. [Section 2.3.4](#) gives additional discussion of rock geomechanical and thermal properties.

1.1.5.3.1 Underground Facilities

1.1.5.3.1.1 Subsurface Conditions

The repository emplacement areas are located at a depth of approximately 300 to 400 m belowground surface within several subunits of the crystal-poor member of the Topopah Spring Tuff (Ttp). In descending order, the host-rock subunits include the Ttpul, the Ttpmn, the Ttppl, and the Ttppln. The internal geologic texture of these units is shown schematically in [Figure 2.3.4-22](#).

The Topopah Spring Tuff includes both lithophysal and nonlithophysal rock units. The nonlithophysal rocks (the Ttpmn and Ttppln units) comprise roughly 15% of the emplacement area and are hard, strong, fractured rock masses. The lithophysal rocks (the Ttppl and Ttpul units) comprise approximately 85% of the emplacement area. About 80% of emplacement is within the Ttppl. These rocks contain macroscopic voids (lithophysae) resulting from trapping of gas during the cooling process and are relatively more deformable with lower compressive strength than the nonlithophysal units. The lithophysal units have fewer fractures of significant continuous length (i.e., trace length greater than about 1 m). Lithophysal porosity in the Ttpul and Ttppl ranges from less than about 10% to approximately 30% by volume. The groundmass that makes up the rock matrix in the lithophysal units is mineralogically the same as the matrix of the nonlithophysal units, but it is heavily fractured with small-scale (lengths of less than 1 m) fractures in the Ttppl and is relatively free of fractures in the Ttpul (BSC 2004d, Section 6.1.4.1). [Figure 1.3.4-2](#) shows a plan view of the Topopah Spring Tuff subunits at the repository horizon with a superimposed repository subsurface layout.

The primary subsurface design-related activities that require geotechnical rock properties are (1) determination of the stability response of the various emplacement and nonemplacement excavations to thermal and mechanical loading, and (2) specification of ground support methods to ensure personnel safety. These design activities account for the nonlithophysal and lithophysal rocks separately. These two rock types, while compositionally similar, have different physical, thermal, and mechanical properties because of the difference in their internal geologic structure (i.e., longer fracture sets in nonlithophysal rock and lithophysae and widespread, short fractures in lithophysal rock) and have different modes of mechanical response, particularly failure under applied loading. The nonlithophysal rock mass strength and yield are controlled by the natural fracturing, whereas the lithophysal rock mass strength and yield are controlled by the degree of lithophysal porosity, as well as the small-scale fracture fabric (particularly in the Ttppl). The rock properties and structural parameters that are significant for the subsurface design are different in lithophysal and nonlithophysal units. In nonlithophysal units, the thermal properties of the intact rock, the fracture geometry, and fracture surface properties are of greatest importance for excavation and ground support design because of the relatively high strength of the intact rock. In lithophysal rock, the thermal and mechanical properties of the rock mass, which includes the effect of lithophysal porosity and the small-scale fracture fabric, are of greatest importance. The

following properties and geotechnical characteristics of the nonlithophysal and lithophysal rock masses are input to subsurface design analyses:

- Intact rock
 - Mechanical properties, including elastic moduli, unconfined and triaxial compressive strength (and associated shear strength properties), and tensile strength
 - Thermal properties, including thermal conductivity, thermal expansion coefficient, and heat capacity
 - Physical properties, including density and porosity
- Rock fractures
 - Mechanical properties, including normal and shear stiffness and shear strength properties
 - Geometric properties of fracture sets, including orientation (dip and dip direction), spacing, length, and surface characteristics (roughness, planarity, infilling materials)
 - Surface properties, including normal and shear stiffness, shear strength properties, and surface roughness and associated dilation angle
- Rock mass
 - Mechanical properties, including in situ compressive strength (shear strength properties), deformation modulus, and surface roughness and associated dilation angle
 - Geotechnical characterization, including engineering classification (Q, RMR, Geological Strength Index) and geologic characterization of lithophysae porosity, size, shape, and distribution.

These rock properties and geotechnical parameters have been determined using different exploration and testing activities at Yucca Mountain, including:

- Geologic mapping of the repository host-rock mass lithology and structure on surface outcrops and within the ESF and ECRB Cross-Drift
- Geotechnical rock mass characterization for ground support analysis
- Laboratory thermal and mechanical rock properties determination from cores obtained from surface and from underground diamond drilling
- In situ testing within the ESF and ECRB Cross-Drift to obtain rock mass thermal and mechanical properties

- Instrumentation for stability monitoring and observation of rock mass response within the ESF and ECRB Cross-Drift
- In situ stress state measurement
- Geophysical investigations, including downhole, spectral analysis of surface waves, vertical seismic profiling, seismic reflection, seismic refraction, and gamma-gamma surveys.

The locations of the exploration boreholes are shown in [Figure 1.1-56](#). The results of the field exploration are used to characterize the subsurface conditions for use in analyses of underground facilities before closure (BSC 2007i, Section 6).

Subsurface Models—For subsurface excavation stability and ground support design analyses, both empirical and numerical design approaches are used ([Section 1.3.4](#)). Empirical methods utilize the results of geotechnical characterization performed in the repository host horizon in the ESF and ECRB Cross-Drift to specify ground support methods based on mining and tunneling experience. Two- and three-dimensional numerical modeling stress analysis methods are then used to examine the detailed effects of in situ stress and preclosure thermal and preclosure seismic loading on excavation stability and ground support response. These analyses are used to establish design safety margins for preclosure drift stability and ground support design (BSC 2007j). Design bases and criteria for ground support can be found in [Section 1.3.2](#). The stability analyses for emplacement and nonemplacement drifts in nonlithophysal and lithophysal rocks are discussed in [Section 1.3.2.4](#).

1.1.5.3.1.2 Rock Properties Used in Subsurface Design Analyses

1.1.5.3.1.2.1 Geotechnical Characterization of Nonlithophysal and Lithophysal Rock Masses

Geologic and geotechnical mapping studies have been conducted in the ESF and ECRB Cross-Drift that provide the basis for development of rock mass properties and stochastic rock fracturing models for the nonlithophysal rocks. The geometric and surface characteristics of fractures in nonlithophysal rocks were determined from detailed line surveys and full periphery geologic mapping that was conducted in conjunction with construction of the ESF and ECRB Cross-Drift. The geometric characteristics derived include fracture dip, dip direction, trace length, end terminations, and spacing. Surface characteristics include planarity and roughness, fracture filling, and offset. These field-mapping studies are supplemented by laboratory determination of fracture properties using direct shear and rotary shear tests. The fracture mechanical properties include shear and normal stiffness, cohesion, and friction angle. The fracture characterization and properties measurements are described in [Section 2.3.4](#).

In addition to the detailed fracture mapping, geotechnical engineering classification using the Q and RMR systems was performed. These methods (e.g., Hoek 2000) involve use of the fracture mapping in combination with intact rock mass strength and groundwater conditions to provide a measure of the engineering rock mass quality index (Q or RMR) and its variability within the nonlithophysal rock. This quality index is related to case histories of tunneling in rock with similar

quality for empirical estimation of stability and ground support requirements. Additionally, widely used methodologies have been developed (e.g., Hoek 2000) for estimating rock mechanical properties from the intact rock properties and the quality index. These methodologies are used to establish the design properties for the nonlithophysal rock mass. A similar approach is not possible for the lithophysal rock mass as the presence of lithophysae is not accommodated in existing rock mass quality classification methods.

The field characteristics of lithophysae, including the size, shape, distribution, and porosity have been determined through panel mapping studies conducted in the Tptpl in the ECRB Cross-Drift (Section 2.3.4). These data are used to define the variability of lithophysal porosity within the repository host horizon and are used as a basis for estimating the variability of rock mass strength in the lithophysal units.

1.1.5.3.1.2.2 Mechanical Properties of Nonlithophysal and Lithophysal Rocks

The mechanical properties of the nonlithophysal and lithophysal subunits of the repository host rock are subdivided into intact properties and rock mass properties. The intact properties are determined from laboratory testing on rock cores obtained from surface- or subsurface-based drilling. For nonlithophysal rocks, the rock mass properties are estimated through the use of industry-standard, in situ geotechnical classification within the repository host horizon of the ESF and ECRB Cross-Drift. The geotechnical classification and intact rock properties are used to provide estimates of the range of rock mass properties for use in preclosure design studies of excavation stability and ground support design. For lithophysal rock, large-core sampling and testing are used, coupled with extrapolation using calibrated numerical models to provide the range of rock mass properties and their relationship to lithophysal porosity. The range of these rock mass properties is used in preclosure design studies of excavation stability and ground support design.

1.1.5.3.1.2.2.1 Intact Rock Properties

Intact rock (i.e., the rock blocks of the nonlithophysal rock and the matrix of the lithophysal rock) mechanical properties required for design include Young's modulus, Poisson's ratio, compressive strength, tensile strength, and the internal angle of friction. Laboratory testing on 25 to 50 mm diameter cores in unconfined and triaxial compression is used to define the mechanical properties and their relationship to porosity in the repository host horizon subunits. A description of the intact mechanical properties is provided in Section 2.3.4. A summary of the intact mechanical properties of the rock matrix used in design analyses is given in *Drift Degradation Analysis* (BSC 2004d, Appendix E, Tables E-6 to E-8).

1.1.5.3.1.2.2.2 Rock Mass Strength of Nonlithophysal Rock

Rock mass properties for the fractured nonlithophysal rock for subsurface design analyses are derived from the estimation method developed from the "Hoek-Brown Failure Criterion—2002 Edition" (Hoek et al. 2002). This method involves deriving rock mass mechanical properties from engineering geotechnical rock mass classification, along with results from laboratory mechanical strength testing of intact rock samples.

The rock mass modulus, rock mass strength, and failure properties (derived from the common rock mass failure criteria of Hoek-Brown and Mohr-Coulomb) are derived from the rock mass quality classification, intact rock strength, and Young's modulus. The results of these calculations show that the Geological Strength Index for the Tptpmn follows a typical normal distribution with a mean value of 62, an average rock mass modulus of approximately 20 GPa, and an average rock mass compressive strength of approximately 34 MPa. The Geological Strength Index for the Tptpln also follows a typical normal distribution with a mean value of 65, an average rock mass modulus of approximately 24 GPa, and an average rock mass compressive strength of approximately 58 MPa. [Table 1.1-82](#) provides a summary of the rock mass properties. For the parametric numerical modeling evaluation of emplacement drift stability in nonlithophysal rock, the variability of rock mass quality derived from field characterization is divided into five categories at 5%, 20%, 40%, 70%, and 90% of the cumulative probability of occurrence within the nonlithophysal units.

Emplacement and nonemplacement drift stability assessments and ground support design studies are performed for the full range of expected in situ mechanical properties for nonlithophysal rock, as described above. These design analyses are discussed in [Section 1.3.4](#), and the results of the preclosure rockfall hazard assessment are described in [Section 1.6](#).

1.1.5.3.1.2.2.3 Rock Mass Strength of Lithophysal Rocks

The mechanical properties (elastic modulus and strength properties) of the lithophysal rocks are a function of lithophysal porosity, as discussed in [Section 2.3.4](#). Because of the size of lithophysal cavities (average around 10 cm in diameter), mechanical testing of small diameter cores (e.g., 25 to 50 mm) does not give a proper representation of the rock mass properties. Therefore, testing in the lithophysal rocks has been oriented toward sampling and compression testing of large diameter (150 to 300 mm) cores, as well as in situ compression testing of large blocks (approximately 1 m) to provide estimates of actual rock mass size effects. Testing on these large cores has been conducted at room dry and saturated conditions. This testing has been supplemented by calibration of discontinuum numerical models that simulate the basic mechanics of the lithophysal rock. These models have been used to explore the effect of the variability of lithophysae size, shape, distribution, and overall porosity on the range of elastic and strength properties. The entire range of lithophysal rock mass properties has been divided into five classifications that are functions of lithophysal porosity as described in [Section 2.3.4.4](#) and shown on [Table 2.3.4-16](#) and [Figure 2.3.4-29](#). The abundance of each of these five classifications in the repository host horizon has been further estimated by relating the approximate lithophysal porosity that each classification represents to the abundance of that porosity level observed in geologic mapping studies within the ECRB Cross-Drift ([Figure 2.3.4-29](#)). Emplacement and nonemplacement drift stability assessments and ground support design studies have been performed for the full range of expected in situ mechanical properties of lithophysal rock, as described above. Discussion of these design analyses can be found in [Section 1.3.2](#), and a description of the results of preclosure drift degradation hazard assessment can be found in [Section 1.6](#).

1.1.5.3.1.2.3 Thermal Properties of the Rock Mass

The thermal properties of nonlithophysal and lithophysal rock required for subsurface design include the thermal conductivity, thermal expansion coefficient, and heat capacity. An extensive laboratory database exists for thermal property measurements as functions of saturation and

temperature as performed on core samples taken from the matrix material from the four subunits of the Topopah Spring Tuff. The matrix thermal conductivity, heat capacity, and thermal expansion coefficient for these subunits are summarized in [Tables 2.3.4-10](#), [2.3.4-12](#), and [2.3.4-15](#), respectively. Rock mass thermal properties, which take into account the effect of rock structure, such as fracturing and lithophysae, have been determined from in situ heater testing and from analytical extrapolations. The rock mass thermal conductivity, heat capacity, and thermal expansion coefficient are summarized in [Tables 2.3.4-11](#), [2.3.4-13](#), and [2.3.4-14](#), respectively. A detailed description of the thermal properties testing can be found in [Section 2.3.4](#). Thermal-mechanical analysis of emplacement drift stability and ground support design for lithophysal and nonlithophysal rock masses is summarized in [Section 1.3.4](#). Design bases for these analyses are given in [Section 1.3.2](#).

1.1.5.3.1.2.4 In Situ Stress Conditions

Design of the repository requires knowledge of the magnitude, direction, and variability of the preconstruction in situ state of stress for the analysis and design of stable underground openings, as well as for the prediction of short-term and long-term rock-mass deformation. Hydraulic fracturing tests performed for ambient characterization of the Drift Scale Test block measured in situ stresses in the Topopah Spring welded lithophysae-poor (TSw2) unit. The results are summarized in [Table 1.1-83](#). Tests results for borehole ESF-AOD-HDFR#1, drilled from the ESF in the Thermal Test Facility in Alcove 5 ([Figure 1.1-56](#)), at depths approximately 240 to 249 m belowground surface, are summarized in [Table 1.1-83](#). The table also includes results from a second borehole where the vertical stress was not measured but is approximated from the weight of the overburden at the depth of the tests to be 3.7 MPa (BSC 2004a, Section 3.7.5).

Although the measured horizontal stresses differ, both are smaller than the vertical stress. This measured stress regime is consistent with the late Quaternary normal slip observed on faults in the vicinity of Yucca Mountain. The north-northeast direction of the maximum horizontal stress is subparallel to the average strike of these faults and is supported by previous measurements in the Yucca Mountain area (BSC 2004a, Section 3.7.5).

1.1.5.3.1.3 Dynamic Properties

Dynamic properties include seismic velocity profiles and dynamic shear modulus and damping ratios. Dynamic properties are used for seismic design, including development of earthquake ground motions and site response. Dynamic properties are based on interpretation and evaluation of in situ and laboratory tests conducted and analyzed using accepted industry techniques. Subsurface conditions for the underground facilities are known through exploration activities undertaken at Yucca Mountain, including geologic mapping, borehole logging, and geophysical surveys. Geologic mapping has been done in the ESF and ECRB Cross-Drift. Geophysical investigations include downhole, spectral analysis of surface waves, vertical seismic profiling, reflection, refraction, and gamma-gamma surveys. The locations of these explorations are shown in [Figure 1.1-56](#). The results of the field exploration are used to characterize the subsurface conditions for use in analyses of underground facilities before closure (BSC 2007i, Section 6).

1.1.5.3.1.3.1 Seismic Velocity Profiles

At the repository site, shear-wave velocity profiles, which are needed for site response analyses, are interpreted from spectral analysis of surface waves, downhole seismic, and vertical seismic profiling surveys. Compression-wave, seismic velocity profiles at the repository site are sampled by vertical seismic profiling surveys only. Spectral analysis of surface wave surveys are performed both from the ground surface near the crest of Yucca Mountain and in the ESF and ECRB Cross-Drift.

The depth-dependent distributions of shear-wave and compression-wave velocities are derived from the survey data, assessed statistically, and used to interpret shear-wave and compression-wave velocity profiles. Velocity profile results from the different methods, which are summarized in the following paragraphs, are used to derive seismic velocity profiles for surface facility design, as discussed in [Section 1.1.5.3.2.2](#).

1.1.5.3.1.3.1.1 Seismic Velocities from Spectral Analysis of Surface Wave Surveys near the Crest of Yucca Mountain

Spectral analysis of surface wave surveys were performed at Yucca Mountain from 2000 through 2001 at the 33 locations shown in [Figure 1.1-56](#). Many of these survey locations show a velocity inversion, where lower-velocity rock underlies higher-velocity rock. Velocity inversions are consistent with limited downhole shear-wave velocity data from shallow depths at locations near the crest of Yucca Mountain (BSC 2002b, Section 6.4.2).

Of the 33 survey locations, 13 were oriented approximately parallel to the crest and 9 were oriented approximately perpendicular to and downslope of the crest. The data, which are concentrated in the upper 150 ft but extend to 750 ft for some surveys, show a mean shear-wave velocity profile oriented parallel to the crest that is about 600 ft/s faster than the profile oriented perpendicular to the crest. The lower velocities perpendicular to the crest are consistent with the parallel-to-the-crest fracturing in the near-surface volcanic units of Yucca Mountain (BSC 2002b, Section 6.4.2).

A total of 24 spectral analysis of surface wave surveys were performed on the surface outside the vicinity of the surface GROA in 2004 and 2005. These spectral analysis of surface wave surveys augment the 33 sites that were surveyed from 2000 through 2001 (SNL 2008a, Section 6.3.1).

The 24 spectral analysis of surface wave surveys from 2004 and 2005 are identified with the prefix "YM." Eighteen of these spectral analysis of surface wave surveys were performed in areas that are near the waste emplacement area. [Figure 1.1-134](#) shows the locations of the 18 surveys that were performed for the purposes of obtaining velocities above or near the waste emplacement areas. Six of the spectral analysis of surface wave survey sites were selected because their locations represented areas where a specific geologic unit, such as the Calico Hills Formation, would be at a depth such that its velocity could be characterized using the spectral analysis of surface wave method. This testing at these six locations allowed measurements of the velocity of geologic units that occur below the waste emplacement area but that are too deep to be reached by spectral analysis of surface wave surveys within the repository footprint (SNL 2008a, Section 6.3.1).

The method for performing the statistical analysis of the spectral analysis of surface wave measurements is provided in *Technical Report: Geotechnical Data for a Geologic Repository at Yucca Mountain, Nevada* (SNL 2008a, Section 6.2.5). Figure 1.1-136 shows the 24 V_S profiles of YM sites and their statistical analysis. Among the 24 YM sites, the shallowest spectral analysis of surface wave V_S profile is 451 ft at Site YM 24 and the deepest one is 1,496 ft at Site YM 5. The maximum depth is almost twice the maximum profiling depth as the spectral analysis of surface wave surveys from this area done in 2000 and 2001. Most of the 24 spectral analysis of surface wave V_S profiles are deeper than 750 ft. As observed in Figure 1.1-136, some profiles are stiffer with V_S values greater than 5,800 ft/s at the bottom of the profiles or softer with V_S values that never exceed 5,800 ft/s in the profile. Possible causes of this variability include variability in the geology related to the distribution of fractures, consolidation of the material, and the deposition mechanisms in the area tested. These factors would affect the transfer of seismic energy through the tested area. As a result, the coefficient of variation profile has a wide range of values from 0.05 to 0.35 at various depths below about 25 ft.

Figure 1.1-137 presents the V_S profiles of the 18 YM sites that are either over or near the repository footprint (Figure 1.1-134). There is not much difference between the results in Figure 1.1-136 and 1.1-137. The velocity profiles can be separated into several velocity groups below 600 ft. This grouping is not observed in the spectral analysis of surface wave surveys from 2000 and 2001 because these spectral analysis of surface wave profiles did not extend to these depths (SNL 2008a, Section 6.3.2).

Because of the large variation in the V_S profiles determined at the YM sites, the 24 sites are divided into three generalized groups based on their V_S profiles. The first group is “stiffer” sites. This group exhibits V_S values larger than 5,800 ft/s at the bottom of the profiles (SNL 2008a, Figure 6.3-4). The sites are YM 8, YM 10, YM 12, YM 13, YM 14A, YM 14B, YM 15B, YM 21, and YM 25. These nine sites are around the planned repository area, except for Site YM 25 which is located along the southern tip of Fran Ridge, to the southeast of the repository footprint (see Figure 1.1-5). The second group is “softer” sites. This group exhibits V_S values that never exceed 5,800 ft/s in the profile (SNL 2008a, Figure 6.3-5). The sites are YM 1, YM 2, YM 3, YM 4, YM 5, YM 6, YM 16, YM 17, YM 23, and YM 26. Site YM 26 is the only site not around the repository area and is located near Rainier Ridge (Figure 1.1-5). The remaining five sites, YM15A, YM19, YM20, YM22, and YM24 are “neutral” sites whose V_S profiles in the 750 ft to 1,000 ft range do not extend to a sufficient depth of greater than 1,200 ft to allow them to be grouped into “stiffer” or “softer” categories or they have V_S profiles which are distributed between the first two groups (SNL 2008a, Figure 6.3-6).

Comparisons of the results of spectral analysis of surface wave tests to geologic units are presented in Figure 1.1-138. The alluvium has the lowest median V_S value at about 1,600 ft/s. In contrast, the Tptpln has the highest median V_S value of about 5,500 ft/s. The Tptpmn has the largest variation in the V_S value which could be attributed to variation in density or fracturing of the formation (SNL 2008a, Section 6.3.3).

1.1.5.3.1.3.1.2 Seismic Velocities from Spectral Analysis of Surface Wave Surveys in the ESF Main Drift

Spectral analysis of surface wave surveys were performed in 2001 at five locations selected to represent a range in materials exposed along the ESF main drift. The five locations are on the west wall at a height of about 4 to 5 ft above the tunnel invert and are designated T-1 through T-5 (Figure 1.1-56) (BSC 2002b, Section 6.3.2).

Highly fractured tuff is exposed at the locations of surveys T-3 and T-1, where the rock also sounded hollow at many places along the wall. Results at survey T-1 show an average shear velocity of 3,500 ft/s and the lowest velocities at distances of 3 ft and greater into the tunnel wall, with fractured tuff extending at least 20 ft into the tunnel wall. Survey T-1 also shows the most scatter in the experimental dispersion curve, which is attributed to severe fracturing (BSC 2002b, Section 6.3.2).

Much less fracturing is apparent at surveys T-2, T-4, and T-5. Survey T-2, which has the least apparent fracturing, and survey T-5 show the highest shear-wave velocities: from 6,000 to 7,000 ft/s, beginning within 0.5 ft of the exposed surface. Surveys T-3 and T-4 show a transitioning of shear-wave velocities from about 2,000 ft/s at the tunnel wall to 5,100 to 6,250 ft/s at distances of 3 ft and greater into the tunnel wall. For surveys T-3, T-4, and T-5, the low velocities close to the tunnel wall are due to the effects of fracturing from the tunneling process (BSC 2002b, Section 6.3.2).

Interpretation of the results yield the following approximate shear-wave velocities (BSC 2002b, Section 6.3.2):

- Intact tuff with few fractures: 6,000 to 7,000 ft/s
- Fractured tuff near the tunnel walls: 3,000 to 4,000 ft/s.

However, it is unlikely that the velocities of either the softest (highly fractured) tuff or the stiffest (unfractured) tuff were measured, partly because there are locations where the rock is more fractured than at surveys T-1 and T-3. In particular, no area was surveyed where metal ground support was installed. Such sites along the tunnel exhibited considerably more fracturing than any of the five spectral analysis of surface wave sites, which is consistent with the need for support (BSC 2002b, Section 6.3.2).

Forty-five additional spectral analysis of surface wave surveys were performed in the ESF main drift tunnel and the ECRB Cross-Drift during 2004 and 2005. The locations (SNL 2008a, Figures 6.4-2 and 6.4-3) were selected to represent a range of the exposed geologic units that comprise both the waste emplacement area as well as the geologic units above the waste emplacement area. To accommodate the configuration of the spectral analysis of surface wave sensors, at least 40 to 50 ft of the geologic unit was required to be exposed in the tunnel before a survey could be performed. In several test locations, 40 to 50 ft of exposed geologic unit was not available, but testing was performed seeking to characterize the tuff unit. For example, Site ESF 14 was sampled across the Tpcpmn-Tpcpll contact. Such sampling can create variabilities in the measured shear wave velocities that is referred to as a boundary effect (SNL 2008a, Section 6.4.2).

A large percentage of testing was concentrated on measuring the Tptpll and Tptpmn units, as these two units represent the majority of the waste emplacement horizon. In the underground, these two units are predominately available in the ECRB Cross-Drift. For the ESF, the spectral analysis of surface wave surveys were performed at a height of roughly 3 to 6 ft from the bottom of the tunnel invert, but none of them reached the spring line height of the tunnel. The majority of the ESF spectral analysis of surface wave surveys were performed on the wall that was on the outside of the ESF tunnel. Looking in from the North Portal, this would be the right-hand side of the tunnel, and from the South Portal this would be the left-hand side of the tunnel. For the ECRB Cross-Drift the spectral analysis of surface wave surveys were performed at approximately the spring line (center) of the tunnel wall. When looking into the ECRB Cross-Drift from the ESF tunnel, the spectral analysis of surface wave surveys were performed on the left-hand rib of the tunnel, with the exception of the ECRB Cross-Drift 16 + 41 test location, which was located on the right rib at a break in the conveyor belt assembly (SNL 2008a, Section 6.4.2).

The center points of 29 sites were surveyed. The remaining 16 sites were not surveyed prior to suspension of operations in the tunnel. The locations of these sites are based on a distance measurement using a tape measure to record the distance to the nearest tunnel survey marker. For the 2004 and 2005 underground spectral analysis of surface wave surveys, receiver spacings of 2, 4, 8, 16 and 32 ft were generally used. The 6 in. and 1 ft spacings used in the 2001 testing were removed from the testing procedure. Testing at these shorter spacings resulted in highly variable and noisy data that were affected by the fractures and lithophysal cavities that exist near the tunnel wall. Two impact hammers of 1 and 8 lbs were used to excite the surface wave energy along the tunnel wall (SNL 2008a, Section 6.4.2).

Nine tuff units were tested in the tunnel sites by the spectral analysis of surface wave method. The shear wave velocity at depths of 10 ft to 15 ft behind the tunnel face in each V_S profile should represent the V_S of the tuff without the influence of stress release due to the tunnel excavation. Profiles not reaching a depth of 10 ft or more were not included in the statistical analysis. Therefore, the median and 16th and 84th percentile boundaries are based on the bottom portion of the profiles for the spectral analysis of surface wave measurements in each type of tuff. The spectral analysis of surface wave V_S profiles are divided into seven groups as discussed below (SNL 2008a, Section 6.4.3).

V_S profiles were obtained from a single site for each of the following tuff units: Tpcpmn-Tpcpll (the survey transected the contact between the Tpcpmn and Tpcpll (Tiva Canyon crystal poor, middle nonlithophysal zone and Tiva Canyon crystal poor, lower lithophysal zone)), Tpcrn2 (Tiva Canyon crystal-rich, mixed-pumice subzone) and Tptrn (Topopah Spring crystal-rich, nonlithophysal zone). Even though these represent different types of tuffs, Sites ESF 14 (Tpcpmn-Tpcpll) and ESF 15 (Tpcrn2), which are next to each other, have similar velocities of about 2,800 ft/s at the bottom of the shear wave velocity profiles (SNL 2008a, Section 6.4.3).

For the Tmbt1 (pre-Rainier Mesa Tuff bedded tuffs), all V_S profiles agree closely except profile 1 of ESF 02 + 12 below 12-ft deep (SNL 2008a, Figure 6.4-5). The ESF 02 + 12 site is close to the contact between two different tuff units, Tmbt1 and Tpcpmn, which could explain the difference, especially when the V_S profiles of ESF 02 + 12 are compared with the profiles for ESF 14 (Tpcpmn-Tpcpll) (SNL 2008a, Section 6.4.3).

The V_S profiles of the Tpk1 (Tuff unit “X”) are consistent, except for Site ESF 03 + 15, which is near the boundary between Tpk1 and Tpcr tuffs, and the latter seems stiffer than the former based on the comparison of V_S profiles of Tpk1 and Tpcr2. The boundary effect may be the reason for the inconsistency (SNL 2008a, Section 6.4.3).

The Tptpul (Topopah Spring crystal-poor, upper lithophysal zone) V_S profiles are inconsistent above the top 12 ft, but they reach similar V_S values below that depth. In general, the deeper V_S values agree with each other, ranging from about 4,000 to 5,000 ft/s (SNL 2008a, Section 6.4.3).

There is a large variation in the spectral analysis of surface wave V_S profiles of the Tptpmn (Topopah Spring crystal-poor, middle nonlithophysal zone). This same variability was observed in the 2001 spectral analysis of surface wave tunnel tests. By combining the spectral analysis of surface wave measurements on the Tptpmn from 2001 and 2005, there are 14 spectral analysis of surface wave V_S profiles for the Tptpmn for evaluation. The median and 16th and 84th percentile boundaries were obtained based on the V_S values in the deepest parts of these 14 profiles. Although there is a large variation in the 14 spectral analysis of surface wave profiles, they can be divided into two groups based on their deeper (bottom) V_S profiles. This division is a V_S value of 5,800 ft/s which separates the “stiffer” and “softer” velocity groups in the mountain area (SNL 2008a, Section 6.4.3 and Figures 6.4-10 and 6.4-11).

The Tptpll (Topopah Spring crystal-poor, lower lithophysal zone) is the most sampled tuff group. Most V_S profiles come reasonably close together below 13 ft, except for sites ECRB Cross-Drift 21 + 63 and ECRB Cross-Drift 22 + 94. The boundary effect may explain what happens at site ECRB 22 + 94 (SNL 2008a, Section 6.4.3).

The last type of tuff evaluated is the Tptpln (Topopah Spring crystal-poor, lower nonlithophysal zone). All V_S profiles converge to the range of 5,000 to 6,000 ft/s below about 10 ft (SNL 2008a, Section 6.4.3 and Figure 6.4-13).

A comparison was conducted among the shear wave velocity values for six different tuffs units sampled in the ESF and ECRB Cross-Drift that have three or more V_S profiles (Figure 1.1-139). The Tmbt1 has the lowest median V_S value which is about 2,300 ft/s. In contrast, the Tptpln has the highest median V_S value of about 5,500 ft/s (SNL 2008a, Section 6.4.4).

Because the spectral analysis of surface wave tests that were carried out on the surface in the Yucca Mountain area in 2004 and 2005 allowed V_S profiles to be determined to depths near 1,000 ft, a comparison can be made between these V_S profiles at about 1,000 ft depth with V_S values measured in the tunnel by spectral analysis of surface wave testing. The spectral analysis of surface wave V_S profiles of 18 YM sites over the repository displayed in Figure 1.1-134 and whose data are plotted in Figure 1.1-138, were chosen for comparison with all the tunnel spectral analysis of surface wave results. Very good consistency is shown among these measurements (SNL 2008a, Figure 6.4-15). Furthermore, if the V_S ranges of the high and low velocity (“stiffer” and “softer”) groups of the Tptpmn are used instead of their overall V_S range, the high and low velocity groups at the mountain area match the high and low velocity groups of the Tptpmn (SNL 2008a, Figures 6.4-16 and 6.4-17). This comparison shows that the same geologic unit may have large variations in the stiffness due to geologic variations (e.g., fracturing or voids) in the tuff (SNL 2008a, Section 6.4.5).

A comparison based on the geologic material type between surface and tunnel spectral analysis of surface wave test results is shown in [Figure 1.1-140](#). This comparison shows the same type of consistency and general overlap between the surface and tunnel spectral analysis of surface wave test results for Tptpul, Tptpmn, Tptpll, and Tptpln. In addition, both surface and tunnel results show the Tptpln has the highest median V_S value (over 5,500 ft/s) compared to the other tuff units (SNL 2008a, Section 6.4.5).

In general, the median V_S values obtained from the tunnel spectral analysis of surface wave tests are higher than from the surface spectral analysis of surface wave tests. This difference is probably impacted by the sample size, with the surface spectral analysis of surface wave tests sampling a much larger volume of material than the tunnel spectral analysis of surface wave test combined with the fact that the poorest material in the tunnel could not be tested due to the large number and size of the flaws. As a result, more flaws (cracks, lithophysae, fissures, etc.) were sampled in the surface spectral analysis of surface wave tests, which likely resulted in the somewhat lower median shear wave velocities. The only exception is the Tptpll tuff. The reason or reasons for this difference are unknown at this time (SNL 2008a, Section 6.4.5).

1.1.5.3.1.3.1.3 Seismic Velocities from Downhole Seismic Surveys

Eight downhole seismic surveys were performed along or near the crest of Yucca Mountain in the few open existing boreholes above the emplacement area. These boreholes contained hanging (ungROUTED) steel casings that obscured the compression waves (BSC 2002b, Section 6.4.3). The velocity data from these downhole seismic surveys were not used in developing the base-case velocity profiles for the repository block because these measurements were too shallow and were not considered to impact the base-case velocity profile developed for the repository block (BSC 2008c, Section 6.4.2).

1.1.5.3.1.3.1.4 Seismic Velocities from Vertical Seismic Profiling Surveys

Vertical seismic profiling and velocity surveys were performed at boreholes USW SD-12, USW G-2, USW G-4, USW NRG-6, USW WT-2, and UE-25 UZ#16 (Majer et al. 1996, pp. 26 to 33). These borehole locations are shown in [Figure 1.1-56](#). The results show generally increasing shear-wave and compression-wave velocities with depth increases from 25 ft belowground surface to depths greater than 1,000 ft belowground surface. Although the vertical seismic profile measurements were not included in the repository block base-case seismic profiles calculations, a comparison of the base-case profiles and the vertical seismic profile measurements illustrates that the two are in reasonable agreement (BSC 2008c, Figure 6.4.2-90).

1.1.5.3.2 Surface Facilities

The surface facilities will be built on the Midway Valley alluvium. Although some facilities located near Exile Hill may be built on welded tuff, this material is much stronger than the native alluvium and poses no particular constraints on development. This section covers the native materials, mainly alluvium. The existing nonengineered fill placed to construct the North Portal pad is planned to be removed prior to construction of the surface GROA and to be replaced with an engineered fill (BSC 2007k, Section 6.1.4.1). Requirements for engineered fill are discussed in [Section 1.2.2.1.7](#).

The geotechnical properties discussed in this section include seismic velocity profiles, density, shear strength, Poisson's ratio, and dynamic shear modulus and damping ratio, as well as a brief discussion of liquefaction potential. The properties are based on the interpretation and evaluation of detailed soil testing data and results obtained from laboratory and in situ tests conducted and analyzed using accepted industry techniques.

The dynamic shear modulus and damping ratio discussion includes curves for rock (tuff) and soil (alluvium) (Figure 1.1-131 and 1.1-132, respectively) that are input to the design and analysis methodologies described in Section 1.2.2 for the stability and safety of surface structures.

1.1.5.3.2.1 Surface Conditions

The surface GROA is characterized as being underlain in ascending order by densely welded, rhyolitic, pyroclastic flows of the Tiva Canyon Tuff (Tpc); pre-Tuff unit "x" bedded tuffs (Tpbt5 (also referred to as post-Tiva Canyon Tuff bedded tuff)); Tuff unit "x" (Tpki); pre-Rainier Mesa Tuff bedded tuffs (Tmbt1); Rainier Mesa Tuff (Tmr); and by Quaternary alluvium (Qal). Alluvium thickness is zero at the base of Exile Hill and increases in thickness to about half way across the valley. Alluvium reaches a maximum thickness of almost 200 ft, and then begins to thin east toward Alice Point (SNL 2008a, Table 6.2-1). Structurally, the area is crisscrossed with mostly high-angle normal faults of various offsets. The Exile Hill Fault splay, a northwest-trending normal fault, has produced significant offset of the volcanic stratigraphy in the northeast portion of the surface GROA. As a result, the area to the northeast of the Exile Hill Fault splay is characterized by a significantly thicker sequence of nonwelded bedded tuffs overlying the Tiva Canyon Tuff, and the area to the southwest of the Exile Hill Fault splay is typically characterized by no or a relatively thin sequence of nonwelded tuffs overlying the Tiva Canyon Tuff. The westernmost extent of the nonwelded bedded tuffs occurs midway across the surface GROA. From this line, the nonwelded bedded tuffs generally thicken to the east. The exception to this trend is the result of an elongated graben that trends to the southeast beginning just north of borehole UE-25 RF#26 (BSC 2002b, Section 6).

The static and dynamic soil properties in the vicinity of the surface GROA have been evaluated (BSC 2007k). Exile Hill is immediately west of the surface GROA and slopes at about 2.5H:1V (horizontal: vertical), or flatter, in its upper portion and flattens to about 6H:1V, or flatter, near its base adjacent to the west corner of the surface GROA. The steeper, upper portions of Exile Hill, west of the surface GROA, are composed of bedrock at the surface. Alluvium and colluvium constitute the flatter lower portion (Figures 1.1-64 and 1.1-66). Due the flatness of the adjacent alluvial and colluvial portions and the presence of bedrock in the upper portions, slope stability of Exile Hill is not a significant concern for the surface GROA. Temporary cuts in the alluvium should be no steeper than 1.5H:1V. Permanent fill slopes should be no steeper than 2H:1V. Permanent cut and fill slopes should be provided with erosion protection by placement of at least 3 in. of coarse aggregate shouldering material (BSC 2007k, Section 7.1.7).

1.1.5.3.2.2 Seismic Velocity Profiles

Shear-wave and compression-wave velocity profiles are needed for site response analyses. The velocity profiles are obtained by analyzing data from three seismic methods: downhole seismic, suspension seismic, and spectral analysis of surface waves (shear-wave velocity only).

Downhole and suspension seismic surveys were performed in 16 boreholes designated UE-25 RF#13 to UE-25 RF#29 (UE-25 RF#27 was not drilled) at the surface GROA. The borehole locations are shown in [Figure 1.1-141](#). The depths of surveys ranged from 96 to 640 ft belowground surface, with seven of the surveys extending to more than 400 ft belowground surface.

Spectral analysis of surface wave surveys were performed in 2000 and 2001 on 40 locations, shown in [Figure 1.1-141](#), at the surface GROA. Five of the surveys were combined with other adjacent surveys resulting in 35 experimental dispersion curves. A total of 20 profiles extend to depths of 150 ft or greater, and five extend to depths of 300 ft or greater (SASW-3, -24, -26, -32+35, and -34+36 Profile 1) (BSC 2002b, Section 6.2.7).

Additional reflection and refraction seismic surveys were performed in early Midway Valley studies ([Figure 1.1-141](#)), but the useful information is limited to the general geologic insight that was obtained. Results from the seismic profiling methods are used to derive seismic velocity profiles for surface facility design, as discussed in this section.

Additional spectral analysis of surface wave testing in the vicinity of the surface GROA was performed in 2004 and 2005. This testing consisted of 20 spectral analysis of surface wave surveys resulting in 18 shear wave velocity profiles as displayed in [Figure 1.1-142](#) with the designator “NPF” (note that the “AP” surveys displayed in [Figure 1.1-142](#) were done in an area that is no longer being considered for use as an aging pad site). This testing was also performed using a new vibroseis truck, which was capable of generating more energy than previous sources at low frequencies that allowed profiling to depths greater than 1,000 ft. For these tests, the energy source was either an 8-lb sledgehammer for sensor spacings less than 50 ft or the vibroseis truck for receiver spacings greater than or equal to 50 ft. The spectral analysis of surface wave surveys performed with the vibroseis truck used a swept-sine mode in which the truck source signal was swept over the frequency of interest. A built-in source output of the analyzer is utilized to control the vibroseis truck to perform a stepped-sine vibration (vibrating at each frequency for several seconds from high-to-low frequencies) or other sine wave vibrations (SNL 2008a, Section 6.2.5).

The spectral analysis of surface waves measurements were performed using a sequence of increasing spacings. Distances between receivers generally started at 6 ft and progressed to 12, 25, 50, 100, 200, 400, 800, and 1,600 ft. These distances represent a typical receiver spacing, but variations in the spacings would occur in the field to accommodate specific site conditions or the target profile depth. For each sensor spacing, typically five measurements were averaged for each survey when a hammer was used as the source. For the vibroseis truck the spectral functions were determined one frequency at a time in a swept-sine fashion. Successful implementation of the spectral analysis of surface waves method requires that multiple receiver spacings are used at one site. Multiple spacings are not used in creating the theoretical dispersion curve that matches the experimental dispersion curve. Rather, the theoretical dispersion curve is calculated assuming that

the receivers are located 2λ and 4λ (λ being wavelength) from the source (SNL 2008a, Section 6.2.5).

The distribution of V_S profiles is assumed to be a log-normal distribution. The median and corresponding 16th and 84th percentile boundaries are three important indices used as a standard to evaluate the V_S profiles acquired at this area. Also, the coefficient of variation (the ratio of one standard deviation to the mean) of a test site is investigated. The coefficient of variation may be used as an index of the uniformity of a site. The calculations of these four parameters only apply to three or more V_S profiles at the same area. It is preferable to have five or more profiles whenever possible. Before conducting the statistical analysis, if there is more than one profile at the same site, these profiles are averaged to calculate the representative profile of this site. This avoids putting too much weight on the same site where multiple profiles have been acquired (SNL 2008a, Section 6.2.5).

Among the 18 spectral analysis of surface waves V_S profiles in the vicinity of the surface GROA, the shortest profile was acquired at Site NPF 1. There are three possible profiles at this site. However, these three profiles are only consistent in the top 40 ft. Geologic variability at Site NPF 1 below 40 ft results in the top 40 ft being the only representative profile that can be used. The deepest spectral analysis of surface waves V_S profile obtained in the vicinity of the surface GROA is 1,472 ft at Site NPF 3 and 9. The depths of most profiles are in the range from 500 to 1,450 ft. Spectral analysis of surface waves surveys NPF 2 and 14 were combined into a single velocity profile as were NPF 3 and 9. These surveys were combined as they represent the same physical location in vicinity of the surface GROA. NPF 2 and NPF 3 were performed in early summer of 2004. Following modifications to the vibroseis truck which improved the signal source quality at low frequencies, the sites were repeated as NPF 14 and NPF 9 to achieve deeper profile depths (SNL 2008a, Section 6.2.5).

The 18 V_S profiles and the statistical analysis results are shown in [Figure 1.1-143](#). The coefficient of variation profile is quite constant (about 0.10) from 30 to 930 ft. However, below 930 ft the coefficient of variation value becomes three times larger because of the significant variability in the velocities in the lower parts of the V_S profiles, especially the higher velocities at Sites NPF 2 and 14 and NPF 3 and 9. Some variability in profiles can be observed in the depth range of 280 to 430 ft ([Figure 1.1-143](#)). These profiles are from Site NPF 28 which is located near Exile Hill in an area with minimal overlying alluvium and the alluvium directly overlies Tiva Canyon Tuff without any intervening nonwelded units such as are found on the other (northeast) side of the Exile Hill Fault splay. For NPF 28 at these depths, it is likely that the velocities are associated with the welded Tiva Canyon Tuff ([Figure 1.1-65](#)). For the other sites, these depths are associated with the nonwelded tuff units below the alluvium. These welded and nonwelded units have distinctly different velocity characteristics. NPF 2 and 14 are south of the Exile Hill Fault splay where there is Tpki and some Tpbt5 between the Tiva Canyon Tuff and the alluvium but these bedded units are not as thick as the Tpbt5, Tpki, and Tmbt1 bedded units found on the other side of the Exile Hill Fault splay. At the bottom of the V_S profiles for Sites NPF 3 and 9, the V_S values increase abruptly. These SASW surveys were performed almost directly on or near the Exile Hill Fault splay and they may even cross the fault at the southern end of the survey line. This created a complex shear wave velocity measurement. To avoid the uncertainty associated with the lack of lateral uniformity in the tuff at the bottom of these V_S profiles, these V_S data were removed at deeper depths in computing profile statistics (SNL 2008a, Section 6.2.5).

Figure 1.1-144 excludes the V_S profiles from the bottom of Sites NPF 2 and 14, NPF 3 and 9, and NPF 28. The coefficient of variation profile has a constant value of 0.10 from about 30 to 1,100 ft and small coefficient of variation values below 1,100 ft (SNL 2008a, Section 6.2.5).

1.1.5.3.2.3 Density and Relative Density

Prior to 2005, the total density of subsurface materials at the surface GROA has been measured by gamma-gamma logging in boreholes UE-25 RF#16, UE-25 RF#18, UE-25 RF#20, UE-25 RF#21, UE-25 RF#22, UE-25 RF#24, and UE-25 RF#28. The processes established in AP-SIII.5Q, *Yucca Mountain Site Characterization Project Field Verification of Geophysical Operations*, and AP-SIII.6Q, *Geophysical Logging Programs for Surface-Based Testing Program Boreholes*, were followed for the gamma-gamma wireline surveys (BSC 2002b, Section 6.2.8). In addition, density tests have been performed in the alluvial deposits at the surface GROA by water replacement and sand-cone methods in test pits TP-WHB-1 through TP-WHB-4 (BSC 2002b, Section 6.2.4). Sand-cone tests were performed in accordance with USBR 7205-89, *Procedure for Determining Unit Weight of Soils In-Place by the Sand-Cone Method*. Six-foot ring-density tests were performed using USBR 7221-89, *Procedure for Determining Unit Weight of Soils In-Place by the Water Replacement Method in a Test Pit*. Earlier tests were done in the vicinity but the data quality are questionable (BSC 2002b, Section 6.8.3) and are not used in design analyses (discussed below).

Based on the trends of total density versus depth, the alluvium was divided into two units. The first unit was from 0 to 8 ft below the top of the alluvium, and the second unit was from 8 to 70 ft below the top of the alluvium. The average density values from these depth ranges are 114 and 117 lb/ft³, respectively (BSC 2002c, p. I-19).

Thirty-one in situ density tests have been made at the surface GROA prior to 2005; 9 in 7 test pits (McKeown 1992, Appendix 1, Table 26), and 22 in 4 test pits (BSC 2002b, Table 6). Overall, the first investigation averaged lower relative density values than the second investigation. There is no clear trend of relative density with depth. Taking the results together, the mean value of relative density is 64% and the mean $\pm 1\sigma$ are 84% and 44%, respectively. These values indicate that the sandy gravel soil is medium dense to dense.

At the completion of the 2005 drilling program, alluvium samples from two boreholes were selected for static geotechnical laboratory testing. The testing consisted of standard physical properties tests on the alluvium from boreholes UE-25 RF#47 and UE-25 RF#52. The alluvium samples were separated based on the field classifications (Unified Soil Classification System Visual Method) completed on site using technical procedures YMP-USGS-GP-57, R0 and YMPB-USGS-GP-57, R0, *Determining Unified Soil Classification (Visual Method)*, (SNL 2008a, Section 6.2.3). The samples were analyzed in the laboratory using procedures in scientific notebook SN-USGS-SCI-144-V1 (Strauss 2007). Unified Soil Classification System group classifications determined in the laboratory also used USBR 5000-86, *Procedure for Determining Unified Soil Classification (Laboratory Method)*. A summary of the laboratory Unified Soil Classification System classifications, gradation test results (particle size distribution), specific gravity, and average absorption is provided in Table 1.1-84. Detailed laboratory test results and gradation curve plots for the sonic cores are provided in *Technical Report: Geotechnical Data for a Geologic Repository at Yucca Mountain, Nevada* (SNL 2008a, Attachment III).

Beginning in August 2006, three additional test pits were excavated to further analyze engineering properties of the alluvium in the vicinity of the surface GROA. The test pits, designated TP-WHB-5 through TP-WHB-7, are located as shown on [Figure 1.1-129](#). The test pits were excavated to approximately 19 ft belowground surface, with side slopes formed by a series of five horizontal benches with vertical sides. The pits were square, approximately 75 ft on a side (at ground surface), with one of the four side slopes excavated to provide a ramp to the bottom of the pit. All test pits were sprayed with water during excavation to control dust; as a result, the measured water contents may not be representative of in situ conditions.

The alluvium in the three exposed walls of each test pit was mapped and logged according to the Unified Soil Classification System using technical procedures YMP-USGS-GP-57, R0 and YMPB-USGS-GP-57, R0, *Determining Unified Soil Classification (Visual Method)* (SNL 2008a, Section 6.2.4). Nine 6-ft-diameter water replacement ring density tests were performed within the test pits, where greater than 20% of the particles (on a weight basis) were retained on the 1.5-in. (37.5-mm) sieve. Samples of alluvium were collected for physical properties testing and laboratory classification (SNL 2008a, Section 6.2.4). The detailed results of mapping are provided on the test pit logs and on the photomosaic test pit maps (SNL 2008a, Attachment III).

Three soil units were mapped and field-classified within test pit TP-WHB-5 down the approximate center of the east wall of the pit. The Unified Soil Classification System group classifications for the mapped units are poorly graded sand with clay and cobbles (SP-SC)c, poorly graded sand with gravel and cobbles (SP)gc, and poorly graded gravel with sand and cobbles (GP)sc. The lowest measured dry density value, from 6-foot-diameter ring density tests at 19-foot depth, expressed as mass per unit volume, was 109.2 lbm/ft³, and the highest measured dry density value, at the 4-foot depth, was 114.3 lbm/ft³ (SNL 2008a, Section 6.2.4).

Five soil units were mapped and field-classified within test pit TP-WHB-6, down the approximate center of the east wall of the pit. All of the soil units in this test pit were classified as poorly graded sand (SP) with varying amounts of gravel and cobbles or poorly graded gravel (GP) with varying amounts of sand and cobbles. The lowest measured dry density value, from 6-ft-diameter ring density tests at 12-ft depth, was 105.1 lbm/ft³, and the highest measured dry density value, at the 4-ft depth, was 111.8 lbm/ft³ (SNL 2008a, Section 6.2.4).

Seven soil units were mapped and field-classified within test pit TP-WHB-7 down the approximate center of the east wall of the pit. All of the soil units in this test pit were classified as poorly graded sand (SP) with varying amounts of gravel and cobbles; or poorly graded gravel (GP) with varying amounts of sand, cobbles, and boulders. One soil unit received a group symbol of (GP/SP)c because the gravel and sand components were about equal. The lowest measured dry density value, from 6-ft-diameter ring density tests at 4-ft depth, was 108.2 lbm/ft³, and the highest measured dry density value, at the 12-ft depth, was 114.8 lbm/ft³ (SNL 2008a, Section 6.2.4).

The results of the in-place density tests, including moisture content and relative density, are summarized in [Table 1.1-85](#). Unified Soil Classification System group classifications indicated in [Table 1.1-85](#) are based on laboratory classifications performed using scientific notebook SN-USGS-SCI-144-V1 (Strauss 2007) and USBR 5000-86, *Procedure for Determining Unified Soil Classification (Laboratory Method)* and not on field classifications (SNL 2008a,

Section 6.2.4). Detailed testing results and the laboratory gradation curve plots for each sample are provided (SNL 2008a, Attachment II).

Density Used in Design Analyses—Densities are required input in the site-response modeling but the resulting ground motions have a negligible sensitivity to the parameter since they vary little throughout the profiles. Because of the lack of ground motion sensitivity to the range of material densities, a single uniform density is used for alluvium, for tuff of the Timber Mountain and Paintbrush groups, and for tuff of the Calico Hills Formation and Prow Pass Tuff. Alluvium is assumed to have a uniform bulk density of 1.8 g/cm^3 (112 pcf). Tuffs of the Timber Mountain and Paintbrush groups are assumed to have a uniform bulk density of 2.2 g/cm^3 (137 pcf). Tuff of the Calico Hills Formation and the Prow Pass Tuff are assumed to have a uniform bulk density of 2.4 g/cm^3 (150 pcf) (BSC 2008c, Section 5.6).

The value for alluvium is based on gamma-gamma density measurements in two boreholes at the surface GROA. The value for tuff is based on gamma-gamma measurements from the Tiva Canyon Tuff and on dry bulk density for core samples from the Topopah Spring Tuff middle-nonlithophysal (Ttptmn) and lower-lithophysal (Ttptll) units (BSC 2008c, Section 5.6). More recent measurements of density for core samples from the Topopah Spring Tuff (SNL 2008a, Table 6.5-3) are consistent with the assumed value (BSC 2008c, Section 5.6).

For tuff underlying the Paintbrush Group, an increase in density is assumed to 2.4 g/cm^3 (150 pcf). The increase is to reflect an assumed effect of increasing confining pressure. However, dynamic properties of small samples from the Calico Hills Formation and Prow Pass Tuff show little effect of confining pressures up to about 3 MPa. Mean densities for core samples from the Calico Hills Formation and Prow Pass Tuff range from about 1.5 to 2.0 g/cm^3 (94 to 125 pcf). While the assumed value for in situ conditions is high relative to laboratory measured values, given the lack of ground motion sensitivity to the value of density used, an assumed value of 2.4 g/cm^3 is acceptable (BSC 2008c, Section 5.6).

1.1.5.3.2.4 Shear Strength of Alluvium

Based on consideration of several correlations, a friction angle on the order of 39° is used as the value for the upper alluvium. Based on the beneficial effects of aging, the shear strength may tend to increase with depth (BSC 2002c, Section I.2.2.1).

1.1.5.3.2.5 Poisson's Ratio

The shear-wave and compression-wave velocities were used to calculate small-strain Poisson's ratio using the theory of elasticity. This calculation is done using the downhole seismic and suspension seismic logging results for each survey. In addition, profiles of median, mean, and mean $\pm 1\sigma$ are computed for the suspension seismic data following the same approach outlined for shear-wave velocity in [Section 1.1.5.3.2.2](#) (BSC 2002b, Sections 6.2.5 and 6.2.6).

Poisson's ratio values obtained from downhole data mostly range from about 0.11 to 0.43 (BSC 2002b, Figure 28, Table 10). The suspension seismic data indicate a similar range in Poisson's ratio. The mean value of Poisson's ratio is near 0.3 for most of the younger lithostratigraphic units surveyed but is about 0.22 for the older Ttptmn and Ttptll zones of the Tiva

Canyon Tuff crystal-poor member and 0.17 for the Tpcpln zones of the Tiva Canyon Tuff crystal-poor member (BSC 2002b, Table VII-4).

Plate load tests have been completed on the alluvium in Midway Valley at or near the surface GROA for the muck conveyor and at the booster pump station near the south end of Exile Hill. For tests performed in a shallow trench with a 13.5-in. diameter plate at the booster pump station, the load-deflection ranges from 640 to 1,330 tsf/ft. Two similar tests performed nearby at existing grade yielded load-deflection values of 1,220 and 1,370 tsf/ft. Nine tests performed with a 30-in. diameter plate at existing grade yielded load-deflection values of 70 to 290 tsf/ft (Riggins 1994a; Riggins 1994b; Riggins 1995).

The unadjusted load per unit deflection values are higher at the booster pump station than at the surface GROA. After multiplying the values obtained along the muck conveyor alignment with the larger diameter plate by a factor of approximately 2 to adjust for scale effects due to the different plate diameters, the difference is reduced but is still substantial (Riggins 1994a; Riggins 1994b; Riggins 1995).

1.1.5.3.2.6 Dynamic Shear Modulus and Damping Ratio

1.1.5.3.2.6.1 Test Program from 2000 and 2001 on Specimens from Boreholes at the Surface Geologic Repository Operations Area

Laboratory tests using combined resonant column and torsional shear equipment were performed in 2000 and 2001 to evaluate the dynamic properties of both rock (tuff) and surficial soil (alluvium) samples obtained from boreholes UE-25 RF#13 through UE-25 RF#17 (Figure 1.1-145). The tests were performed in accordance with NWI-SPO-004Q, *Laboratory Dynamic Rock/Soil Testing* or LP-GEO-002Q-BSC, *Laboratory Dynamic Rock/Soil Testing*. Twenty-four test specimens were trimmed from tuff core and five specimens were reconstituted from alluvial samples. The dynamic characteristics that were measured were the shear modulus and the material damping ratio in shear as functions of shear strain. Dry unit weight was also measured (CRWMS M&O 1999b, Appendix Q; BSC 2002b, Section 6.2.10).

Alluvium—At small strain (less than 10^{-5}), the small-strain shear modulus ranges from 2,000 to 2,200 ksf and from 5,600 to 6,000 ksf under effective confining pressures of 30 and 120 psi for the alluvial specimens from 57.3 to 57.5 ft depth in borehole UE-25 RF#13 and from 2,000 to 2,600 ksf and 5,500 to 7,400 ksf under effective confining pressures of 36 and 144 psi for the alluvial specimens from 66.9 to 67.0 ft depth in borehole UE-25 RF#13 (CRWMS M&O 1999b, Figures Q-8 and Q-16). Small-strain shear modulus is measured at 1,100, 1,880, and 2,850 ksf under effective confining pressures of 8, 16, and 32 psi, respectively, for the alluvial specimen from 59.0 ft depth in borehole UE-25 RF#17 (BSC 2002b, Table XII-19a).

Small-strain shear modulus increases linearly with confining pressure, and material damping ratio decreases fairly linearly with confining pressure (CRWMS M&O 1999b, Appendix Q; BSC 2002b, Section 6.2.10).

The relation for normalized shear modulus versus shear strain lies generally within the upper half of the range for sands (Seed et al. 1986, Figure 2), with some values lying above the range. The

material damping ratio versus shear strain relation lies within or near the range for sands (Seed et al. 1986, Figure 6) but tends to be more linear, so that the material damping ratio in some cases is slightly above the range for sands at a shear strain of 0.0001% and below the range at shear strains above 0.03% (CRWMS M&O 1999b, Appendix Q; BSC 2002b, Section 6.2.10).

Tuff—At in situ confining pressures, shear-wave velocities in tuff increase with increasing dry densities. At a dry density of 80 pcf, shear-wave velocity is about 3,400 to 3,800 ft/s, and, at 145 pcf, it is about 7,300 to 8,800 ft/s (CRWMS M&O 1999b, Appendix Q; BSC 2002b, Section 6.2.10).

The variations in normalized small-strain shear modulus with normalized confining pressure that are measured by resonant column testing indicate that the intact tuff specimens exhibited only small increases in small-strain shear modulus as confining pressure increased from 0.25 to 4 times in situ total stress. The small increases in small-strain shear modulus that do occur with increasing confining pressure occur mainly at confining pressures less than the in situ total stress. This behavior is due to the closing of microcracks in the specimens in this pressure range (BSC 2002b, Section 6.2.10).

The variations in small-strain material damping ratio with normalized confining pressure that are measured by resonant column testing show little effect of confining pressure. The values of small-strain material damping ratio range from about 0.2% to 2.0% at in situ total stress and are not correlated with dry unit weight (BSC 2002b, Section 6.2.10).

The effects of time of confinement at a constant isotropic stress state and excitation frequency on small-strain shear modulus and small-strain damping ratio were also studied. The effect of time of confinement on small-strain shear modulus and small-strain material damping ratio is less than 1% over the range of time of confinement (BSC 2002b, Section 6.2.10).

The effect of excitation frequency is investigated in two ways. First, in torsional shear testing at the in situ total stress, small-strain shear modulus and small-strain material damping ratio are measured over a frequency range of 0.1 to about 10 Hz. The effect of frequency on small-strain shear modulus over this range is less than 2%. Second, the effect of changing the excitation frequency from 1 Hz in the torsional shear test to the range of several hundred hertz in the resonant column test is evaluated. In this case, small-strain shear modulus increased about 11% for the 18 intact tuff specimens. This increase is attributed to both excitation frequency and limitations in each testing technique. An average increase in small-strain shear modulus of 11% is approximately equivalent to a 5.4% increase in shear-wave velocity over this frequency range. This variation in values is considered small and within the range of typical variability to be expected in such measurements (BSC 2002b, Section 6.2.10).

The test results indicate that the normalized shear modulus of tuff decreases less with shear strain than that of the alluvium. The normalized shear modulus of the welded tuff shows less decrease than that of the nonwelded tuff (BSC 2002b, Section 6.2.10).

The variation in material damping ratio for the nonwelded specimens indicates a more linear behavior than the alluvium at shear strain less than 0.01%. The results for the welded specimens indicate a relatively constant and high value (0.5% to 1.5%) of material damping ratio at shear strain

less than 0.003%. The material damping ratio for welded specimens increases rapidly at larger shear strain (BSC 2002b, Section 6.2.10).

In terms of the variation in material damping ratio with shear strain, the intact tuff specimens exhibit a linear response with material damping ratio at shear strain equal to 0.01% being generally less than twice the small-strain damping ratio. This response is more linear than the response typically exhibited by sands, as represented by the range for sands (Seed et al. 1986, Figure 6). There are, however, three exceptions, one in each of groups 1, 2, and 3. These specimens exhibited significant increases in material damping ratio as shear strain increased above 0.0001% (BSC 2002b, Section 6.2.10).

1.1.5.3.2.6.2 Test Program on ESF Specimens

Laboratory tests using combined resonant column and torsional shear equipment were performed in 2000 and 2001 to evaluate the dynamic properties of tuff samples obtained by drilling into the wall of the North Ramp tunnel (BSC 2002b, Sections 6.1 and 6.3.3). The tests were performed in accordance with NWI-SPO-004Q or LP-GEO-002Q-BSC. Five specimens of tuff were trimmed from the tunnel wall samples. The specimens were of nonwelded tuff, three being from the Tuff unit “x” (Tpki) zone (dry unit weights from 70 to 77 pcf), one from the pre-Rainier Mesa Tuff bedded tuff (Tmbt1) (dry unit weight of 106 pcf), and one from the vitric (Tpcrv) zone of the Tiva Canyon Tuff crystal-rich member (dry unit weight of 126 pcf) (BSC 2002b, Table 23).

The small-strain shear modulus is approximately 2.3 GPa for the pre-Rainier Mesa Tuff bedded tuff specimen, 1.7 GPa for two of the Tuff unit “x” specimens, and 1.0 GPa for the specimen of the nonlithophysal zone of the Tiva Canyon Tuff crystal-rich member and the remaining Tuff unit “x” specimen (BSC 2002b, Figure 154).

The main differences between the ESF specimens and those from the surface GROA boreholes (Section 1.1.5.3.2.6) are that two of the ESF specimens show more nonlinearity in their normalized shear modulus versus logarithm of shear strain relationship (BSC 2002b, UTA-20-I and UTA-20-L in Figure 155), and one specimen (BSC 2002b, UTA-20-I in Figure 156) shows relatively large values of material damping ratio at shear strain less than 0.001%. These differences are attributable to the shallow depths behind the tunnel wall from which the specimens in the ESF were taken, where disturbance from the tunnel boring process was likely to have been significant and to have resulted in microcracking in the specimens (BSC 2002b, Section 6.3.3). The results of these tests have not been used in developing the dynamic properties for tuff used in the site-response model (Section 1.1.5.3.2.6.3).

Additional dynamic properties testing on a total of 168 specimens of tuff was done from 2004 through 2006 to augment the 2000 through 2001 laboratory testing. The specimens were selected to dynamically test tuffs from most of the major geologic units above, at the level of, and below the waste emplacement level. This laboratory testing started in 2004 and initially consisted of 33 samples subjected to fixed-free testing using the resonant column and torsional shear system. The resonant column and torsional shear testing method is described briefly in Section 1.1.5.3.2.6.2.1 and in more detail in *Technical Report: Geotechnical Data for a Geologic Repository at Yucca Mountain, Nevada* (SNL 2008a, Section 6.5.2). From 2004 through 2006, 135 specimens were also tested using the unconfined resonant column (free-free) method. The

135 samples tested using free-free method, were selected so that approximately 6 to 8 samples could be tested from each major geologic unit above, at the level of, and below the waste emplacement horizon. The free-free testing method is described briefly in [Section 1.1.5.3.2.6.2.2](#) and in more detail in *Technical Report: Geotechnical Data for a Geologic Repository at Yucca Mountain, Nevada* (SNL 2008a, Section 6.5.3).

1.1.5.3.2.6.2.1 2004 through 2006 Resonant Column and Torsional Shear (Fixed-Free) Testing of Tuff Samples

The resonant column and torsional shear apparatus can be idealized as a fixed-free system in which the bottom of the specimen is fixed against rotation at the base pedestal and the top of the specimen is connected to the driving system. The driving system can rotate freely to excite the specimen in torsional motion. The basic operational principle of the fixed-free resonant column test is to vibrate the cylindrical specimen in first-mode torsional motion. Harmonic torsional excitation is applied to the top of the specimen over a range in frequencies and the variation of the acceleration amplitude of the specimen with frequency is obtained. Once first-mode resonance is established, measurements of the resonant frequency and amplitude of vibration are made. These measurements are then combined with equipment characteristics and specimen size to calculate shear-wave velocity and shear modulus based on stress wave propagation. Material damping is determined either from the width of the frequency response curve or from the free-vibration decay curve (SNL 2008a, Section 6.5.2). A more detailed description of the test procedure and the method of analysis is provided in *Geotechnical Data for a Potential Waste Handling Building and for Ground Motion Analyses for the Yucca Mountain Site Characterization Project* (BSC 2002b, Section 6.2.10).

The torsional shear test is another method of determining shear modulus and material damping using the same resonant column and torsional shear equipment but operating it in a different manner. A cyclic torsional force with a given frequency, generally below 10 Hz, is applied at the top of the specimen. Instead of determining the resonant frequency, the stress-strain hysteresis loop is determined from measuring the torque-twist response of the specimen. Proximitors are used to measure the angle of twist while the voltage applied to the coil is calibrated to yield torque. Shear modulus is calculated from the slope of a line through the end points of the hysteresis loop and material damping is obtained from the area of the hysteresis loop (SNL 2008a, Section 6.5.2).

The tuff specimens that were tested were collected from boreholes from various locations around Yucca Mountain, near the North Portal pad and surrounding area, in the ESF, and in the ECRB Cross-Drift. Thirty-three tuff specimens were tested using the resonant column and torsional shear device. Thirty-one specimens were cored from Yucca Mountain borehole samples. Two other specimens were cored from larger test specimens. In all cases, the dimensions were measured to determine the volume, and they were weighed to determine the specimen mass. The specimens were inspected for defects and a free-free resonant column test was performed on each specimen prior to resonant column and torsional shear testing. The dimensions of the original cores changed through the coring, cutting, or trimming processes. Free-free resonant column tests were performed whenever these processes were done (SNL 2008a, Section 6.5.2). Free-free results are discussed in [Section 1.1.5.3.2.6.2.2](#).

Following preparation, the specimens were affixed in the resonant column and torsional shear device. Some specimens were tested under additional conditions with an exterior membrane or with an epoxy membrane. The epoxy membrane resulted in filling the lithophysae exposed on the specimen surface. Dynamic testing of each specimen involved the evaluation of shear modulus (G) and the material damping ratio in shear (D) over a range of isotropic confining pressures. Three or more isotropic confining pressures were used in a loading sequence, with the isotropic confining pressure (σ_0) doubled upon completion of the required tests at the lower pressure. Low-amplitude resonant column testing was performed at each σ_0 to determine the effects of magnitude of confinement and time of confinement on the small-strain shear modulus (G_{\max}) and small-strain material damping ratio (D_{Smin}). Low-amplitude dynamic tests are defined as those tests in which the resonant amplitude did not exceed 0.001% and was often below that level (SNL 2008a, Section 6.5.2).

All specimens were tested at small strains at the different confining pressures in an increasing confining pressure sequence. High-amplitude resonant column and torsional shear tests were performed during this loading path at one or more pressures below or at the estimated in situ mean effective stress (σ_m) and often at $4\sigma_m$. In cases where $4\sigma_m$ was greater than 400 psi, these tests were performed at 400 psi following tests at 100 psi or σ_m (SNL 2008a, Section 6.5.2).

High-amplitude testing was composed of two series of tests. The first involved cyclic torsional shear testing. Torsional shear tests were conducted with the drainage line opened at all times. The shearing strains (γ) that were attained were those that could be generated within the limit of power applied in torsion. The majority of the measurements were performed at an excitation frequency of 0.5 Hz. However, torsional shear tests at two or three different levels of were also conducted to evaluate the effect of excitation frequency on G and D at these strains. In these tests, ten cycles of loading were applied at four different frequencies ranging from 0.1 to 5 Hz (SNL 2008a, Section 6.5.2).

After the torsional shear tests were completed, confinement of the specimen was continued at the given pressure. A series of high-amplitude resonant column tests was performed following the torsional shear tests. Before the high-amplitude resonant column tests commenced, small-strain resonant column tests were performed to determine if any changes in the coupling of the rock specimen with the top cap or base pedestal might have occurred from the torsional shear tests. No significant changes were measured in any of the tests. Significant changes are defined as a change of 5% in G_{\max} and 10% in D_{Smin} (SNL 2008a, Section 6.5.2).

High-amplitude resonant column testing was conducted to evaluate the influence of shear strain amplitude on G and D . A complete set of resonant column tests took about two hours to perform and these tests were performed with the drainage line opened as in the case of the torsional shear tests. In these tests, about 1,000 cycles of loading were applied at each strain amplitude. Upon completion of the high-amplitude resonant column tests, low-amplitude resonant column tests were again performed to determine if any changes in the coupling of tuff core with the top cap or base pedestal occurred from the high-amplitude tests. If no significant changes were measured in G_{\max} and D_{Smin} after a short rest period, the next stage of testing (low-amplitude tests at a higher confining pressure) was undertaken. In two cases (Specimens 7C-2 and 1G-1), testing was stopped after the first set of high-amplitude resonant column tests at the lower confining pressure due to failure at the top-cap-specimen interface. Otherwise, no significant changes were measured due to the high-amplitude resonant column tests (SNL 2008a, Section 6.5.2).

1.1.5.3.2.6.2.1.1 Dynamic Properties in the Small-Strain Range ($\gamma < 0.001\%$)

Tuff specimens were selected to represent a range of lithostratigraphic units below the Tiva Canyon Tuff. A total of 33 specimens were selected for testing. The 33 specimens are divided into four groups based on their total unit weight (γ_t):

- Group 1 (very low density) = γ_t from 60 pcf to 92 pcf
- Group 2 (low density) = γ_t from 93 pcf to 120 pcf
- Group 3 (medium density) = γ_t from 121 pcf to 140 pcf
- Group 4 (high density) = γ_t from 141 pcf to 150 pcf.

This grouping was chosen because of the relationship between the small-strain shear wave velocity (V_s) and γ_t as shown in [Figure 1.1-146](#).

None of the samples from Groups 2 through 4 exhibit any pressure dependency on G_{\max} . Two of the four specimens in Group 1 exhibit little to no increase in G_{\max} with increasing σ_o . The two specimens that exhibit moderate pressure dependency on G_{\max} are bedded tuffs: pre-Yucca Mountain Tuff bedded tuff (Tpbt3) and pre-Pah Canyon Tuff bedded tuff (Tpbt2). They have two of the lowest three γ_t values as well as the lowest G_{\max} values throughout the entire test pressure range compared with the other specimens. It is thought that micro-cracks in these weak and porous specimens were closing as the pressure was increased because their volume change associated with the increase in pressure (estimated from the height change combined with the approximation of isotropic straining) was negligible (SNL 2008a, Section 6.5.2). The shear-wave velocities, shear moduli, and material damping values from the resonant column and torsional shear tests are presented in tabular form (SNL 2008a, Attachment VII). The variations in G_{\max} with σ_o that were measured by resonant column testing for Groups 1 through 4 are presented in Figures 6.5-7 through 6.5-10 of the report (SNL 2008a).

Two specimens were recored from larger cores, specimen 2C-2 was recored from 2B-2 and specimen 3K-2 was cored from the piece of core next to 3C-2. These specimens have an average diameter and height of 0.83 and 1.89 in, respectively. Based on visual inspection, 2C-2 had fewer surface lithophysae than 2B-3. In addition, the total unit weight of 2C-2 was 6 pcf larger. These two factors resulted in an increase in G_{\max} . The G_{\max} of 2C-2 was 94% higher than value of the larger parent specimen at the highest confining pressure. Specimen 3K-2 had a slightly higher total unit weight than 3C-2 (higher by 3 pcf). The higher unit weight and the slightly different location resulted in an increase in G_{\max} of 39% for 3K-2 at the highest confining pressure (SNL 2008a, Section 6.5.2 and Figures 6.5-9 and 6.5-10).

As with G_{\max} , D_{\min} shows only a small effect of σ_o for the specimens for Groups 1 through 4. The values of D_{\min} range from about 0.2% to 1.4% at the highest confining pressures at which the specimens were tested. With exception of the two bedded tuff specimens discussed above (Tpbt3 and Tpbt2), the γ_t values do not correlate with V_s (and hence G_{\max}). The two recored small specimens (2C-2 and 3K-2) exhibit lower D_{\min} values (with ΔD_{\min} equal to 0.64% and 0.12%) compared with the larger specimens (Specimens 2B-3 and 3C-2, respectively) at their highest test pressures (SNL 2008a, Section 6.5.2). The variations in D_{\min} with σ_o that were measured by resonant column testing for Groups 1 through 4 are shown in Figures 6.5-11 through 6.5-14 of the report (SNL 2008a).

The effects of time of confinement at a constant isotropic stress state (t) and excitation frequency (f) on G_{\max} and D_{\min} of the intact tuff specimens were also studied. The effect of t on G_{\max} and D_{\min} was negligible in these tests; less than a 1% change over the testing time that ranged from about 30 to 60 minutes at each σ_o . The effect of f was investigated by performing small-strain torsional shear tests using 10 cycles of loading at four different frequencies ranging from 0.1 to 5 Hz. Exciting slow-cyclic motion in pure torsion was more difficult than exciting resonance in torsion (resonant column testing) due to the impact of flaws (cracks, lithophysae, etc.) in the specimens. The flaws create non-uniformities within a specimen that result, to varying degrees, in bending and torsional motions occurring when torque is applied to the top of the specimen. When this complex motion occurs, it occurs together in slow-cyclic loading (torsional shear testing). This motion distorts the values of G_{\max} and D_{Smin} in torsional shear testing, with a larger impact on D_{Smin} . However, the two motions (bending and torsion) generally have different resonant frequencies, which allow them to be separated and measurements in torsional resonance (resonant column testing) to be performed with little distortion. Therefore, one set of G_{\max} measurements (specimen 10A-2) in torsional shear testing was discarded and about one-half of the D_{Smin} data in torsional shear testing were also discarded due to complication caused by bending. No values in the resonant column data set were discarded. With the remaining data, the average change in G_{\max} as excitation frequency changes from 1 to 400 Hz is less than 8%, with G_{\max} decreasing slightly at the highest frequencies (SNL 2008a, Section 6.5.2 and Figures 6.5-15 and 6.5-16). The scatter in the D_{Smin} data is much more than in the G_{\max} data (SNL 2008a, Section 6.5.2 and Figures 6.5-17 and 6.5-18). Values of normalized material damping ratio vary from about 1.65 to 0.5 times D_{Smin} at 1 Hz when the excitation frequency increases to about 400 Hz. The lack of consistent trends combined with the complexity of making torsional shear measurements in specimens with varying flaws makes determining a correlation in G_{\max} and D_{Smin} with frequency unclear so that a frequency independent approximation is suggested (SNL 2008a, Section 6.5.2).

1.1.5.3.2.6.2.1.2 Dynamic Properties in the Large-Strain Range ($\gamma > 0.001\%$)

The influence of shearing strain (γ) on shear modulus (G), normalized shear modulus (G/G_{\max}), and material damping ratio (D) has been measured by resonant column testing for 33 intact tuff specimens (SNL 2008a, Figures 6.5-20 through 6.5-22). For values measured at the highest test pressure of each specimen both G and D exhibit linear ranges where they are constant and equal to G_{\max} and D_{Smin} , respectively. This linear range is followed by a nonlinear range where G decreases and D increases as γ increases. D is affected more in the nonlinear range than G (SNL 2008a, Section 6.5.2).

Test results of the four density groups indicate that σ_o shows a small effect on the $G/G_{\max} - \log \gamma$ relationships of most specimens (SNL 2008a, Figures 6.5-24 through 6.5-27). The material that shows the most effect, although a small effect, is the bedded tuff (specimens 24C and 28E; Tpbt3 and Tpbt2, respectively), which displays a slight increase in G/G_{\max} values in the nonlinear range as σ_o increases (SNL 2008a, Figure 6.5-24). These trends may be the result of the variability in the material (SNL 2008a, Section 6.5.2).

In general, the $G/G_{\max} - \log \gamma$ relationships of the 33 specimens follow the trend of a hyperbolic line based on a relationship proposed by Darendeli (2001). There is some variability which is likely due to natural material property scatter (SNL 2008a, Section 6.5.2).

1.1.5.3.2.6.2.2 2004 through 2006 Free-Free Laboratory Testing of Tuff Samples

Free-free testing is a laboratory testing method incorporated into the geotechnical investigations at Yucca Mountain starting in 2004. This free-free method involves an unconfined resonant column test set-up and is used to evaluate the stiffness and material damping ratios of soil and rock specimens at small strains. Measurements in both shear and compression can be performed on the same specimen to provide comparisons with measurements from the laboratory combined resonant column and torsional shear tests and the field spectral analysis of surface waves surveys, crosshole, downhole, and compression and shear wave suspension logging tests. The simplicity of the unconfined resonant column setup eliminates potential compliance problems such as fixity of the bottom platen in a fixed-free configuration and equipment-induced damping in the torsional electrical motor of the resonant column and torsional shear test (Stokoe et al. 1994). The method is briefly described below, and a more detailed discussion on the test methodology is contained in *Technical Report: Geotechnical Data for a Geologic Repository at Yucca Mountain, Nevada* (SNL 2008a, Section 6.5.3).

The free-free laboratory testing of tuff samples at Yucca Mountain started in 2004 and was completed in late 2006. Free-free testing was performed on a total of 135 samples from boreholes and cored from surface boulders (SNL 2008a, Tables 6.5-4 and 6.5-5). The intent was to assess the variability in a geologic unit across the footprint of the repository (SNL 2008a, Figure 6.5-32). If the geologic unit had several subunits, where possible, a representative number of samples were selected from each subunit. This especially applied to the Topopah Spring Tuff where the repository horizon is located. To increase the numbers of samples from the Topopah Spring Tuff, specimens were tested from boreholes from the ESF and ECRB Cross-Drift (SNL 2008a, Figure 6.5-34). If specimens existed in the inventory from boreholes drilled in the vicinity of the surface GROA, they were included in the testing program. Laboratory testing of specimens from boreholes that had downhole seismic testing or a surface spectral analysis of surface waves survey performed nearby provide additional insight into the velocity data collected by the various testing methods (SNL 2008a, Section 6.5.3).

The tests carried out in the unconfined resonant column set-up consist of two general types of small-strain seismic tests: (1) free-free resonance tests and (2) direct-travel-time tests. Shear wave velocity (V_S), shear modulus (G_{max}), and material damping ratio in shear (D_{Smin}) can be measured in free-free resonance tests in torsional motion. Unconstrained compression wave velocity (V_C), Young's modulus (E_{max}), and material damping ratio in unconstrained compression (D_{Cmin}) can be measured in free-free resonance tests in longitudinal motion. Direct-travel-time measurements of compression waves also provide the estimation of the constrained compression wave velocity (V_p), and constrained modulus (M_{max}) (SNL 2008a, Section 6.5.3).

Free-free resonance tests are performed by establishing longitudinal and torsional resonant vibrations to evaluate the dynamic properties of soil and rock specimens. Free-free boundary conditions are created by laying the rock specimens on soft cushions, to minimize the restriction of movements of the specimen. The excitation is created by different types of impact devices: (1) a small hand-held hammer for longitudinal vibration and (2) a scissors source or a tangential impact for torsional vibration. Resonant motions of the specimen created by the impacts are measured by accelerometers on the free end opposite the source (SNL 2008a, Figure 6.5-35). The outputs of the accelerometers are monitored with a dynamic signal analyzer that provides data acquisition and

signal processing operations. All time-domain and frequency-domain data are saved in a data logger that is connected to the analyzer (SNL 2008a, Section 6.5.3). The configuration of the equipment for the compressional (longitudinal) resonance test and direct-travel-time measurement is shown in Figure 6.5-36 of the SNL report (SNL 2008a). The configuration for the torsional resonance test is illustrated in Figure 6.5-37 of the SNL report (SNL 2008a).

Known-property metal specimens were used as reference specimens to evaluate the system compliance in the unconfined resonant column set-up. The tests of the metal specimens provide the proper selection of the wavelength-to-diameter ratio and resonance mode used to evaluate the stiffness of rock and soil samples. By increasing the frequency resolution of the analyzer, it will increase the digitization of the data at and around the resonant frequency which will increase the resolution of the measurement spectrum resulting in an improved measurement of the stiffness and material damping throughout the specimen (SNL 2008a, Section 6.5.3).

The small-strain material damping ratio could be overestimated when a large frequency bandwidth is used. For frequency bandwidths less than about 3 kHz, the damping ratios in both compression and shear become nearly constant (SNL 2008a, Figure 6.5-40). Values between 0.02 and 0.06% were accurately measured and agree well with values reported in the literature (SNL 2008a, Section 6.5.3).

As a continuation of the evaluation of the free-free method, test specimens were cut from Yucca Mountain borehole samples, dimensions were measured to determine the volume, and specimens were weighed to determine the mass. The specimens were inspected for defects and a free-free resonant column test was performed on each specimen. The results of the free-free resonant column tests on the cored specimens are compared with the results of the fixed-free resonant column and torsional shear tests on corresponding specimens (SNL 2008a, Section 6.5.3).

A total of 135 tuff cores were selected for free-free unconfined resonant column testing. These cores were selected to represent a wide range in the tuff materials at the Yucca Mountain site. Cores from a majority of the tuff stratigraphic units at the site were tested (SNL 2008a, Table 6.5-6). In addition to these 135 samples, the 33 specimens tested using the fixed-free approach discussed in [Section 1.1.5.3.2.6.2.1](#) were also tested using the free-free unconfined resonant column method.

The length of the specimens ranged from 2.8 to 12.3 in., and the diameter of the specimens ranged from 1.8 to 5.7 in. Total unit weights covered a wide range, from 65 to 148 pcf. The porosity of each specimen was calculated with the assumption that the specific gravity of the solid material is 2.55 and the water content of the tuff specimens was essentially zero. Based on these assumptions, the range in calculated porosity estimates is from 0.073 to 0.59 (SNL 2008a, Section 6.5.3 and Table 6.5-5).

The general trends investigated were between: (1) seismic wave velocities and total unit weights, and (2) seismic wave velocities and estimated porosity. Specimens FR1 through FR7 are non-Q data because they were tested before the accelerometers and the signal conditioners were calibrated. Specimens FR9, FR35, FR97, and FR102 were excluded from the data set as outliers in evaluating general trends determined with fitting lines because they had significant flaws. Flaws such as cracks, joints, and fractures can be clearly detected in the specimen and cause the specimens to have off-normal seismic wave velocities. Specimen FR97 is specified as an outlier in describing the

general trends of the shear wave velocity and unconstrained compressional wave velocity because the specimen broke after the V_p measurement and before V_s and V_c measurements. Specimens FR24, FR54, FR77, and FR100 were also excluded as outliers in evaluating general trends between material damping ratios and seismic wave velocities because of flaws in these specimens (SNL 2008a, Section 6.5.3; Figures 6.5-41 through 6.5-43 and 6.5-56 through 6.5-59).

There is a distinct trend in general relationship between shear wave velocity (V_s) and total unit weight (γ_t), with V_s increasing as γ_t increases (SNL 2008a, Figure 6.5-44). Much of variability in the trend is thought to arise from flaws (cracks, lithophysae, etc.) that affect the small strain-strain stiffness and therefore the shear wave velocity of the core (SNL 2008a, Section 6.5.3).

Similar relationships between unconstrained compression wave velocity (V_c) and γ_t and between constrained compression wave velocity (V_p) and γ_t occur with the similar trend of V_c and V_p increasing as γ_t increases (SNL 2008a, Figures 6.5-45 and 6.5-46).

Because the small-strain moduli are equal to the total unit weight times the square of the associated wave velocity, the small-strain moduli (shear, Young's modulus, and constrained modulus) show the same trend of increasing moduli with increasing total unit weight as exhibited by the seismic wave velocities (SNL 2008a, Section 6.5.3).

The seismic wave velocities have been compared with the variation of estimated porosity (n) because porosity is a more common property used to represent the physical state of rock specimens in rock mechanics (SNL 2008a, Figures 6.5-47 through 6.5-49). These comparisons have been made even though the uncertainties are greater because of the assumptions in calculating porosity, discussed below.

Porosity (n) is defined as the ratio of the void volume to the total volume of the specimen as: $n = \text{void volume}/\text{total volume}$. The void ratio (e) is defined as the ratio of the void volume to the solid volume of the specimen as: $e = \text{void volume}/\text{solid volume}$. The porosity and void ratio are related as follows:

$$n = \frac{e}{1+e} \quad (\text{Eq. 1.1-1})$$

The void ratio is related with the total unit weight (γ_t) of the specimen as follows:

$$\gamma_t = \frac{(1+w)G_s\gamma_w}{1+e} \quad (\text{Eq. 1.1-2})$$

where

$$\begin{aligned} w &= \text{water content (\%)} \\ G_s &= \text{specific gravity (\approx 2.55)} \end{aligned}$$

$$\gamma_w = \text{total unit weight of water (= 62.4 pcf).}$$

The porosity has been calculated from the total unit weight and two assumptions. The first assumption is that the specific gravity (G_s) of the solid part of the tuff specimen is 2.55. The second assumption is that the water contents (w) of all tuff specimens are zero for all of the tuff specimens from Yucca Mountain (SNL 2008a, Section 6.5.3).

The general relationship between V_s , V_c , and V_p and estimated porosity indicates that there is a strong trend in seismic wave velocity decreasing as porosity increases (SNL 2008a, Figures 6.5-47 through 6.5-49). The trends are opposite to those for total unit weight because γ_t and n are inversely proportional (SNL 2008a, Section 6.5.3).

Poisson's ratio can be computed by measuring shear modulus (G_{max}), unconstrained Young's modulus (E_{max}), and constrained modulus (M_{max}). For an isotropic material assumption, two out of the three moduli are necessary for the calculation of Poisson's ratio. Out of these three methods of calculating of Poisson's ratio, the method using M_{max} and G_{max} (which results in ν_{MG}) is selected to represent values of Poisson's ratio of tuff specimens because the values of ν_{MG} are more consistent, with values ranging between 0.1 and 0.4 (SNL 2008a, Section 6.5.3). There is a weak correlation between Poisson's ratio and V_s , with Poisson's ratio decreasing as the shear wave velocity increases (SNL 2008a, Figure 6.5-50). The constrained compression wave velocity and Poisson's ratio are poorly correlated, as indicated by the very low R^2 value (SNL 2008a, Figure 6.5-51).

The general relationship between material damping ratio in shear (D_{Smin}) and shear wave velocity (V_s) and the general relationship between the material damping ratio in unconstrained compression (D_{Cmin}) and unconstrained compression wave velocity (V_c) show similar trends. Material damping ratios decrease modestly with increases in wave velocity. (SNL 2008a, Figures 6.5-52 and 6.5-53).

The general relationship between material damping ratio in shear (D_{Smin}) and material damping ratio in unconstrained compression (D_{Cmin}) is that D_{Smin} increases as D_{Cmin} increases, with the values of D_{Smin} slightly greater than D_{Cmin} (SNL 2008a, Figure 6.5-54). The larger values of D_{Smin} and D_{Cmin} , defined as values greater than 1.0%, are believed to be mostly caused by flaws in the cores. Therefore, the relationship between D_{Smin} and D_{Cmin} was examined for those cores with material damping values less than 1.0%. The least square, best-fit relationship is given by:

$$D_{Cmin} = 0.87 D_{Smin} \quad (\text{Eq. 1.1-3})$$

with $R^2 = 0.627$ (SNL 2008a, Section 6.5.3 and Figure 6.5-55).

A total of eight specimens are specified as outlier in describing the general trend of material damping ratio. Four specimens (FR9, FR35, FR97, and FR102) are excluded because they are already outliers in describing the seismic wave velocities. Another four specimens (FR25, FR54, FR77, and FR100) are also excluded in describing the general trend of material damping ratio because of the flaws present in the specimens. Specimen FR25 displays large voids and lithophysae that impacted the measured results. FR54 displays small cracks that break through to the surface of the sample which also affect the measured properties for this sample. These flaws distort the

resonance motion of the specimens and produce the outlier material damping ratio values. Specimens FR77 and FR100 have very soft surfaces that crumble apart with the touch of finger. Although they do not show a detectable flaw in appearance, they have a high probability of internal flaws due to their softness. For all four of these samples, their material damping ratios were biased when compared with the material damping ratio of the similar tuff specimens from the same or similar geologic units. Therefore, they are excluded as outliers in representing the general trend of material damping ratio (SNL 2008a, Section 6.5.3).

The seismic wave velocities measured in the unconfined resonant column tests were compiled according to the geologic units present at Yucca Mountain and as a function of depth. This provides a means of viewing variations in seismic wave velocity with depth and geologic unit. The distribution of seismic wave velocity for each stratigraphic unit was assumed to have a lognormal distribution. Table 1.1-86 presents the median, 16th-percentile and 84th-percentile values of the seismic wave velocities of each stratigraphic unit. Using these values, profiles of seismic wave velocities versus depth from the cores were established. The V_S profile over the entire depth is shown in Figure 1.1-147. Expanded profiles of shear wave velocities are provided in *Technical Report: Geotechnical Data for a Geologic Repository at Yucca Mountain, Nevada* (SNL 2008a, Figures 6.5-61 through 6.5-63). The distribution of seismic wave velocities of the cores shows a reasonable trend with stratigraphic unit. The shear wave velocities decrease from highest to lowest for groups of lithologic units in the following order: nonlithophysal welded tuffs (Tpcrn, Tpcpmn, Tpcpln, Tptrn, Tptpmn, Tptpln), lithophysal welded tuffs (Tpcrl, Tpcpul, Tpcpll, Tptrl, Tptpul, Tptpll), moderately welded tuffs (Tcp, Tcb, Tct), and nonwelded tuffs (Tmr, Tпки, Tpp, Tpy, Tac). The variation of shear wave velocities among the subunits along the stratigraphic column for the Tiva Canyon Tuff and the Topopah Spring Tuff shows a similar pattern (SNL 2008a, Figure 6.5-64).

Similar presentations for the unconstrained compression wave velocity (V_C) and constrained compression wave velocity profile (V_P) over the stratigraphic column are shown in Figures 1.1-148 and 1.1-149, respectively. Expanded profiles for V_C are provided in *Technical Report: Geotechnical Data for a Geologic Repository at Yucca Mountain, Nevada* (SNL 2008a, Figures 6.5-66 through 6.5-68). Expanded profiles for V_P are provided in the report (SNL 2008a, Figures 6.5-69 through 6.5-72). As in the V_S profile (Figure 1.1-147), the V_C and V_P profiles in Figures 1.1-148 and 1.1-149 show the same trends with stratigraphic units.

Figure 1.1-147 also presents a comparison of the in situ shear wave velocity ranges determined with the spectral analysis of surface wave tests with the shear wave velocities measured in the free-free unconfined resonant column tests in the laboratory. The shear wave velocities in the field are generally less than the shear wave velocities measured in the laboratory. This is due to the presence of fractures, cracks, and other flaws that are sampled in the field measurements that do not occur in the intact cores tested in the laboratory. The overall variation of the shear wave velocities in field with the stratigraphic units show much less correlation than the variation of the shear wave velocities measured in the laboratory (SNL 2008a, Section 6.5.3).

Table 1.1-87 presents the median, 16th-percentile, and 84th-percentile values of the material damping ratios for stratigraphic units measured in the laboratory with core. The test results generally indicate large differences between stratigraphic units when the material damping ratios are used for making the comparisons as opposed to using seismic wave velocities for the

comparisons. This is likely an artifact of the material damping ratio being more sensitive to flaws in the specimens than the seismic wave velocities. The summary profiles of material damping ratios in shear (D_{Smin}) and material damping ratios in unconstrained compression (D_{Cmin}) are shown in Figures 1.1-150 and 1.1-151, respectively.

1.1.5.3.2.6.3 Normalized Shear Modulus and Damping for Design

Tuff—Dynamic laboratory test data were not available for the Topopah Spring Tuff nor some of the overlying bedded tuff units at the time the dynamic curves were developed for initiating site response calculations. Two sets of mean normalized shear modulus reduction and damping curves were developed in *Development of Earthquake Ground Motion Input for Preclosure Seismic Design and Postclosure Performance Assessment of a Geologic Repository at Yucca Mountain, NV* (BSC 2004e, Section 6.2.4) to represent the uncertainty in mean shear modulus reduction and hysteretic damping curves to be used for the tuff. One set of curves represented the case in which in situ conditions consist of unfractured rock. The second set was developed to represent in situ conditions that reflect fracturing and heterogeneity, the effects of which are not captured in laboratory testing. For the first case, referred to as the “upper mean tuff curves,” the normalized shear modulus reduction curve was developed by visually fitting a generic, cohesionless soil curve through the most linear tuff data (BSC 2008c, Figure 6.4.4-9). For the second case, termed the “lower mean tuff curves,” the normalized shear modulus reduction curve was developed by first visually fitting the generic, cohesionless soil curve shape through the middle of the laboratory testing data. Next, the reference strain for the curve is adjusted downward by a factor of 4 based on the ratio of G_{max} in the field and laboratory (determined from V_S) to account for in situ fracturing and heterogeneity. This adjustment assumed the presence of voids and fracture systems affects nonlinear dynamic material properties directly through reference strain and directly proportional to the differences (laboratory versus field) in shear moduli (BSC 2008c, Section 6.4.4).

In the tuff curves developed in 2004 (BSC 2004e, Section 6.2.4), no accommodation was made for the potential effects of confining pressure (depth) on the curves. The effects of confining pressure on shear modulus reduction and hysteretic damping curves were expected to be small, particularly for the upper mean tuff curves. More importantly, the 2004 analysis used a semi-deterministic approach (i.e., McGuire et al. 2001, Approach 2b) to develop ground motion inputs in which motions reflecting site epistemic variability were enveloped. With this enveloping approach, more nonlinear curves controlled the low frequencies while the more linear curves controlled high frequencies. In a fully probabilistic approach, to achieve desired exceedance probabilities in design and performance assessment spectra, site epistemic variability is treated in a manner analogous to earthquake source uncertainty, with weighted hypotheses. With a fully probabilistic approach, compared to a deterministic approach, in order to achieve unbiased results, more rigor is demanded in characterizing components of epistemic variability, including those associated with earthquake source characterization. In view of the increased rigor, anticipated effects of confining pressure have been included as an update to the original suite of tuff curves (BSC 2008c, Section 6.4.4).

For the upper mean tuff curves, expected to have a very moderate effect of confining pressure, the reference strain was increased 30% for depths of 500 ft and below (Figure 1.1-131). This roughly corresponds to a “step” (EPRI 1993) or increase in reference strain for a factor of 2 increase in depth. The “step” size is generally considered to reflect a significant difference in computed motions, depending on loading level and initial stiffness. The lower mean tuff curves, which are significantly

more nonlinear than the upper mean tuff curves, as they were intended to accommodate nonlinearity due to movement along existing fracture systems, may be expected to have a more pronounced effect of confining pressure due to increased friction along the fractures (BSC 2008c, Section 6.4.4). As a result the “steps” were adopted with the depth adjustments taken on the lower mean tuff curves and applied for the depth intervals as shown on [Figure 1.1-131](#). Comparisons between the curves used in *Development of Earthquake Ground Motion Input for Preclosure Seismic Design and Postclosure Performance Assessment of a Geologic Repository at Yucca Mountain, NV* (BSC 2004e, Section 6.2) and the updated curves used in site response modeling are also shown in [Figure 1.1-131](#). Damping curves reach a maximum of 15% in accordance with guidance from NUREG-0800, Section 3.7.2 (NRC 2007).

Data used as direct input in developing the nonlinear dynamic material property curves for tuff come from the vicinity of the surface GROA. The available repository block data for Tiva Canyon Tuff and Yucca Mountain Tuff samples from boreholes USW SD-9, USW SD-12, and USW NRG-7/7a is unqualified, but fall within the range of the data from the vicinity of the surface GROA (BSC 2008c, Figure 6.4.4-11). Although qualified data from the repository block were unavailable at the time that site response calculations were carried out, such data have recently become available ([Section 1.1.5.3.2.6.2](#) and SNL 2008a) and corroborate the curves developed (BSC 2008c, Section 6.4.4). Based on the range displayed by the two mean curves (upper mean tuff, lower mean tuff), the comparison of available data from the repository block, as well as the aleatory variability of the laboratory test data as a whole, application of the dynamic material property curves appropriately captures the uncertainty in dynamic material properties (BSC 2008c, Section 6.4.4).

Alluvium—Laboratory dynamic tests were performed on five reconstituted alluvium specimens recovered from boreholes at the surface GROA. Alluvial materials at the surface GROA consist of interbedded caliche-cemented and non-cemented, poorly sorted gravel with some fines, cobbles, and boulders. The depth to groundwater is approximately 1,270 ft, and the water content in the alluvium is estimated at less than 5%. Disturbed samples were collected and reconstituted in the laboratory to create test specimens. Sample reconstitution, including destruction of cementation present in the field, likely has a significant effect on the measured dynamic properties in the laboratory. The comparison of measured laboratory specimen V_S compared to field measurements for one of the reconstituted alluvial samples shows that, contrary to the intact tuff specimens where the laboratory values of V_S were greater than the field values, the reconstituted alluvial specimen exhibits more nonlinearity and more damping than the in situ material (BSC 2008c, Figure 6.4.4-12 and Section 6.4.4).

Five testing related factors were considered when developing the G/G_{\max} curves for alluvium based on the laboratory test specimens (BSC 2008c, Section 6.4.4):

1. Destruction of cementation
2. Decrease in coefficient of uniformity
3. Variation of confining pressure in the field
4. Variation of density in the field
5. Increase in mean particle size.

Ratios of laboratory to in situ shear moduli are about 0.25, suggesting in situ nonlinearity should be significantly less than that shown by laboratory test results. However, due to the effects of scalping

and loss of cementation, unambiguous adjustment of the reference strain associated with the laboratory test results was not possible. The development of two sets of mean shear modulus reduction and hysteretic damping curves, based primarily on anticipated effects of cementation loss and scalping on test results, is considered to adequately accommodate uncertainty in the properties of the alluvium. This uncertainty in mean properties is large, as it is intended to acknowledge the lack of experience of the geotechnical community in the dynamic response of these generally stiff, dry, and cemented soils, particularly at high loading levels (BSC 2008c, Section 6.4.4).

One set of curves, consisting of the upper mean normalized shear modulus curve and the lower mean material damping curve, is adjusted to be more linear than the data and accommodates the possibility of cementation not breaking during shearing, as well as acknowledges the lack of experience with this type of material, as reflected in the geotechnical literature. A second set, consisting of the lower mean normalized shear modulus curve and the upper mean material damping curve, represents the case in which cementation in the field breaks under ground-motion strains. These curves are developed taking into account the difference between reconstituted, scalped specimens and field conditions (BSC 2008c, Section 6.4.4).

As with the tuff curves, the initial alluvium curves were developed (BSC 2004e, Section 6.2.4) independent of confining pressure effects as their inclusion would not have materially impacted the deterministic enveloping process over site epistemic uncertainty. To accommodate potential effects of confining pressure as well as recently published testing on cemented materials (Camacho-Padron 2006), the initial depth-independent lower mean alluvium curve was adjusted to be more nonlinear, reflecting a reference strain of 0.01% (G/G_{\max} value of 0.5) from the initial reference strain of about 0.015%, a 50% change. The reference strain is defined as was done by Darendeli (2001) using a modified hyperbolic model (BSC 2008c, Section 6.4.4). Because recent test results on cemented sands show a weaker dependence on confining pressure than uncemented cohesionless materials (Camacho-Padron 2006), the updated curves were taken to be appropriate for the top 50 ft (Figure 1.1-132). Depth adjustments consisting of one-half Electric Power Research Institute “step” (EPRI 1993) were then taken for the 50 to 100 ft depth interval and again for 100 to 200 ft, the deepest alluvium encountered across the site (Figure 1.1-132).

1.1.5.3.2.7 Liquefaction Potential

The potential for liquefaction is a condition that results from several factors, including the potential for the soil deposit to be saturated during the time period under consideration, the ground motions anticipated over the time period under consideration, the stress state at the point under consideration, and the relative density and classification characteristics of the soil. In Midway Valley, the water table lies approximately 1,270 ft below the ground surface, a distance far below the base of the alluvium (Section 1.1.4.2.3). The conditions necessary for liquefaction at a scale needed to affect ITS facilities are not expected at the site (BSC 2007k, Section 7.1.12).

1.1.6 Igneous Activity

[NUREG-1804, Section 2.1.1.1.3: AC 6]

The Yucca Mountain area is located in a region that is tectonically active. The regional volcanic activity that has occurred in the past may continue into the future and could affect repository performance in the preclosure period. In this section, information on the known volcanic sources in

the Yucca Mountain region and the probabilistic volcanic hazard analysis (PVHA) conducted, as they pertain to PCSA and the design of the GROA, are summarized (BSC 2004a, Section 4.2).

[Section 1.1.6.1](#) includes descriptions of the late Tertiary and Quaternary history of igneous activity in the Yucca Mountain region, including the rates of basaltic volcanism in the area.

[Section 1.1.6.2](#) includes a discussion of the analysis conducted to produce a quantitative assessment of the probability of a basaltic dike intersecting the repository and the uncertainty associated with the assessment.

[Section 1.1.6.3](#) includes a discussion of the potential ash-fall hazard, including possible sources of ash and the potential effects on repository facilities.

1.1.6.1 Location of Volcanism in the Yucca Mountain Region

[NUREG-1804, Section 2.1.1.1.3: AC 6(1)]

The late Tertiary and Quaternary history of igneous activity in the Yucca Mountain region has been studied to evaluate the potential for future volcanic activity. As part of site characterization, investigations were performed to assess the ages and character of the volcanic episodes that have occurred in the region. Field studies, including trenching and geologic mapping, and age determinations using multiple dating methods have been conducted at volcanic centers in the Yucca Mountain region. The levels of detail of the studies vary with the age of the volcanic activity (BSC 2004a, Section 4.2). The most detailed studies are of the Pliocene and Pleistocene (about 4.0 to 0.1 million years ago; the Quaternary is the past 1.6 million years) basaltic volcanic centers because they record the most recent volcanic activity in the area and are considered the most likely analogues for future igneous activity near Yucca Mountain (BSC 2004g, Section 5.1).

Basalts erupted in the Yucca Mountain region during two major episodes. The first episode began during the Miocene about 11.3 million years ago. The second episode consisted of Pliocene and Pleistocene basalts formed during at least six volcanic events (based on age and spatial groupings) that occurred within 50 km of the repository ([Figure 1.1-152](#)). These six events, in order of decreasing age are: (1) basalt of Thirsty Mesa; (2) Pliocene basalts that are about 3.7 million years old in southwest Crater Flat and Anomaly B in Amargosa Valley, which is about 3.8 million years old; (3) Buckboard Mesa, (4) Pleistocene basalts located in Crater Flat at Makani Cone, Black Cone, Red Cone, and Little Cones; (5) Hidden Cone and Little Black Peak (the Sleeping Butte centers); and (6) Lathrop Wells. Three of these events are in or near Crater Flat, within 20 km of Yucca Mountain. The seven (or eight if Little Cones counts as two volcanoes) Quaternary volcanoes in the Yucca Mountain region occur to the south, west, and northwest of Yucca Mountain in a roughly linear zone defined as the Crater Flat volcanic zone ([Figure 1.1-152](#)). Models that attempt to relate volcanism and structural features in the Yucca Mountain region have emphasized the Crater Flat Basin because of the frequency of volcanic activity associated with Crater Flat and its proximity to the repository (BSC 2004a, Section 4.2.1.1).

Aeromagnetic data have been gathered at a variety of scales in the Yucca Mountain region. A number of the identified aeromagnetic anomalies have been interpreted as buried or partially buried basaltic centers. An anomaly in the northern Amargosa Valley (known as Anomaly B; [Figure 1.1-152](#)) has been drilled and confirmed to be buried basalt with an age of about 3.8 million

years. Fourteen selected aeromagnetic anomalies in the vicinity of the repository site were surveyed using ground magnetic surveys in 1996 and 1997. Of the 14 surveys, seven provide no evidence of buried basalt, and three are equivocal, since they were conducted over areas with known surface exposures of basalt. Four of the 14 surveys provide sound evidence of buried volcanic centers (BSC 2004a, Section 4.2.1.2).

An aeromagnetic survey conducted in 1999 recorded a number of small dipole anomalies in Crater Flat and the northern Amargosa Desert. Potential-field modeling provides an interpretation that isolated, small-volume magnetic bodies embedded within the alluvial deposits of both areas produce the anomalies (O'Leary et al. 2002, p. 19). The magnetic anomalies were modeled as bodies having volumes, forms, and magnetic susceptibilities comparable to those of the basaltic volcanoes exposed in the vicinity of Yucca Mountain. The physical characteristics of the modeled bodies and the fact that they tend to be aligned along major structural trends indicate that the anomalies could represent small-volume basaltic volcanic centers buried at depths between 150 and 350 m (BSC 2004a, Section 4.2.1.2). The most recent aeromagnetic survey was completed in June 2004, comprising over 15,000 flight-line mi covering a 333 mi² area. These data have been used to identify drilling targets to explore for potential buried basalt to increase confidence in assessments of the probability of igneous activity disrupting the repository. Additional information on the results of this drilling program is provided in [Section 2.3.11.2](#).

Basalts in the Yucca Mountain area appear to be products of partial melting of small volumes of lower lithospheric material. In the Yucca Mountain region, the exact mechanism of mantle melting is poorly understood. It may be controlled by a complex combination of processes, including the effect of residual heat in the lithospheric mantle from previous episodes of volcanism and the presence of a plate subduction system, local variations in volatile (water) content, variations in mantle mineralogy and chemistry, and the effect of regional lithospheric extension (BSC 2004a, Section 4.2.1.3).

1.1.6.1.1 Characteristics of Basaltic Volcanism in the Yucca Mountain Area

The volume of basalt erupted through time has decreased from approximately 3 km³ in the oldest cycle to 0.1 km³ at the youngest center, Lathrop Wells. The volume of individual episodes has decreased progressively through time, with the three Pliocene episodes having volumes of approximately 1 to 3 km³ each and the three Quaternary episodes having a total volume of less than 0.5 km³. The Quaternary volcanoes are similar in that they are of small volume, about 0.15 km³ or less ([Table 2.3.11-2](#); [Figure 2.3.11-3](#)). The total volume of the post-Miocene basalts is approximately 6 km³. The relatively long lifetime of the Crater Flat field, combined with the small volume of erupted material, results in one of the lowest eruptive rates of any basaltic volcanic field in the southwestern United States (BSC 2004a, Section 4.2.2.2).

Researchers who have analyzed magmatic processes in the Yucca Mountain region generally agree that the magnitude of mantle melting has drastically decreased since the middle Miocene and that melts in the past few million years have been generated within relatively cool (compared to asthenospheric mantle) ancient lithospheric mantle. This factor contributes to the relatively small volume of basaltic melt erupted in the Yucca Mountain region since the Miocene. The combination of decreasing eruptive volume through time and geochemical data indicates that the intensity of mantle melting processes beneath the Yucca Mountain region has waned over the past 5 million

years. It has been observed that the waning volcanism through time is also valid when the time frame is extended to include basalts of Miocene age (less than 11 million years old). A general decrease through time in the amount of partial melting of the mantle source is the most reasonable explanation (BSC 2004a, Section 4.2.2.2).

1.1.6.1.2 Simultaneous Seismic Activity and Volcanic Eruption

Magma ascending through the upper crust along fractures may release seismic energy in the form of earthquakes. Earthquakes that result from volcanic activity typically are smaller than about M 4.0 to 5.0; however, such earthquakes may trigger larger tectonic earthquakes on nearby faults that have sufficient strain accumulation. In the Yucca Mountain region, basaltic ash is present as a minor to dominant component in fissure fillings and alluvial horizons exposed by trenching of several faults. Characteristics of the ash indicate minimal abrasion from surface transportation. Correlation of these ashes (or ash) to the contemporary eruptive source has been used to constrain the age of the ash and, therefore, to provide information about the slip history of a fault. The most concentrated occurrence of ash in a trenched fault exposure is found in a trench across the trace of the Solitario Canyon Fault. This ash occurs at the bottom of the trench in a 65 cm wide fissure that represents the largest recorded Quaternary displacement event (more than 1 m) on the Solitario Canyon Fault (BSC 2004a, Section 4.2.2.3).

Pure ash separates from the trench exposures were analyzed for trace elements and compared to the composition of the Quaternary eruptive centers in the Yucca Mountain region. These geochemical comparisons indicate that the ash preserved in trenches across the Solitario Canyon Fault, Windy Wash Fault, Fatigue Wash Fault, and Stagecoach Road Fault originated from the eruption of the Lathrop Wells volcanic center, south of Yucca Mountain. Based on geochronology results from Lathrop Wells, the age of this ash is about 80,000 years old. This conclusion also is consistent with geochronology results from stratigraphic units exposed in Solitario Canyon Fault Trench 8 (BSC 2004a, Section 4.2.2.3).

1.1.6.2 Probabilistic Volcanic Hazard Analysis *[NUREG-1804, Section 2.1.1.1.3: AC 6(1)]*

To assess the probability of a future volcanic event intersecting the repository, a PVHA was conducted (CRWMS M&O 1996, Section 4.0). The product of the PVHA was a quantitative assessment of the probability of a basaltic dike intersecting the repository and of the uncertainty associated with the assessment (BSC 2004a, Section 4.2.4.2). Following completion of the PVHA, probability distributions were developed for the length and orientation of dikes intersecting with the repository footprint and for the number of eruptive centers located within the footprint, conditional on a dike intersecting the repository (BSC 2004g, Section 6.1). The PVHA and associated assessments to evaluate volcanic hazard are described in more detail in [Section 2.2.2](#).

The mean annual probability of future intersection of the repository footprint by an ascending basaltic dike is about 1.7×10^{-8} (BSC 2004g, Table 7-1). Alternative evaluations of the mean conditional annual frequency of occurrence of one or more eruptive centers within the subsurface facility range from about 4.8×10^{-9} to 1.3×10^{-8} ([Section 2.3.11](#)). The evaluation of hazards from volcanic activity is discussed in [Section 1.6.3](#).

1.1.6.3 Potential Hazard from Ash Fall

[NUREG-1804, Section 2.1.1.1.3: AC 6(1)]

Three volcanic areas within the western Great Basin have undergone recent silicic volcanism. These areas are the Coso, Long Valley–Mono-Inyo craters, and Big Pine areas, all located at distances about 150 to 250 km west of Yucca Mountain, in eastern California. In the last 10,000 years, at least 28 small-volume rhyolitic eruptions have occurred in the Mono and Inyo chains of the Long Valley volcanic area, and at least 48 eruptions have taken place within the past 100,000 years in the Coso and Long Valley volcanic areas. The amount of ash that could accumulate at the Yucca Mountain site from a silicic site in the western Great Basin depends on the volume of ash erupted, distance to the vent location, and wind direction at the time of eruption. The amount of ash that could be deposited in the Yucca Mountain area during the preclosure period has been assessed, based on two assumptions. These assumptions are: (1) a maximum volume of ash is erupted, based on consideration of the largest known volume of ash erupted in a single eruptive episode in the western Great Basin during the last 100,000 years, and (2) the location of Yucca Mountain is directly on the dispersal axis of the ash fall. Based on this assessment, up to 1 cm of ash could be deposited in the Yucca Mountain area (Perry and Crowe 1987, pp. 1 to 12).

In the southwestern Nevada volcanic field, within which Yucca Mountain is located, basaltic volcanism occurred approximately 80,000 years ago at Lathrop Wells and approximately 400,000 years ago at Sleeping Butte (Hidden Cone and Little Black Peak volcanoes). This information indicates that the probability of basaltic volcanism in this area is greater than one in 10,000 during the 100-year preclosure period, which is greater than or equal to 10^{-6} events per year (Section 1.6.3 and Figure 2.3.11-3). As is the case for silicic ash from a distal location, the amount of ash that would accumulate at the Yucca Mountain site from a nearby basaltic eruption depends on the volume of ash erupted, distance to the vent location, and wind direction at the time of eruption.

A design calculation provides an estimate of the ash-fall hazard at the surface GROA due to potential basaltic volcanism. This ash-fall hazard is assessed for a potential basaltic eruption because the estimated depth of ash fall from the basaltic eruption is substantially greater than the ash fall estimated from a silicic eruption. The ash-fall hazard is expressed as probability of deposition areal density. The resultant hazard curve (frequency versus areal density) will be used to guide building design to withstand potential ash fall from basaltic volcanism (BSC 2004h, Section 1). The results are calculated as the probability-weighted mean and in terms of percentiles of the frequency of exceeding various ash densities. The estimate of the thickness hazard at the surface GROA is suitable to be used in the building design to withstand potential ash fall from basaltic volcanism. For design consideration, the frequency calculations corresponding to the ash areal density of 10 g/cm^2 are particularly relevant. The current design for surface facilities corresponds to an ash areal density of about 10 g/cm^2 . The mean annual frequency of exceeding an ash areal density of 10 g/cm^2 is 6.4×10^{-8} . Because these results incorporate uncertainty, it is concluded that there is a 99% probability that the mean annual frequency of exceeding an areal density of 10 g/cm^2 will not exceed 6.8×10^{-7} (BSC 2004h, Section 6).

1.1.7 Site Geomorphology

[NUREG-1804, Section 2.1.1.1.3: AC 7]

Geomorphic processes could pose hazards to repository safety during the preclosure period. Surface process studies were conducted in the Yucca Mountain region as part of site characterization to evaluate erosional and depositional processes occurring during the Quaternary and to evaluate landscape response to Quaternary climate changes. This information provides a basis for evaluating whether site structures or operations could be affected by a geomorphic hazard, which means any natural or man-made landform change that adversely affects a site (BSC 2004a, Sections 3.2 and 3.4).

Section 1.1.7.1 provides information on erosional and depositional processes from tectonic features, such as fault scarps and volcanic cinder cones.

Section 1.1.7.2 discusses the processes that have been active during the Quaternary. These processes provide a basis for evaluating geomorphic processes that may occur during the repository preclosure period. Section 1.6 provides further discussion and evaluation of potential external hazards during the preclosure time frame, including those resulting from geomorphic processes.

1.1.7.1 Geomorphic Information and Tectonic Activity

[NUREG-1804, Section 2.1.1.1.3: AC 7(1)]

Observations of volcanic and tectonic features, such as volcanic cinder cones and fault scarps, provide information on erosional and depositional processes. Past and modern geomorphic processes have been investigated to estimate the long-term average rates of erosion on the ridge crests and hillslopes of Yucca Mountain (BSC 2004a, Section 3.4).

1.1.7.1.1 Geomorphic Information Related to Faulting

Yucca Mountain is one of a series of en echelon fault blocks formed by a series of parallel, north-striking, primarily dip-slip faults displacing a broad apron of Miocene ash-flow tuffs (Figures 1.1-59 and 2.3.4-21). Some faults have been active during the Quaternary, as shown by detailed mapping and by trenching studies (Section 1.1.5.2).

On the west side of Yucca Mountain, hillslopes are of nearly uniform gradients, decreasing gradually from 32° near ridge tops to about 15° near the base. This characteristic results from the homogeneous nature of the underlying volcanic tuff at the ridge crest and from the low rates of uplift, which means there are no overly steepened slopes or high relief. The formation of pediments by lateral planation is evident on the lower slopes of Yucca Mountain. Lateral planation of the lower hillslopes has been observed in trenches on both the eastern and western slopes of Yucca Mountain, where early and middle Pleistocene deposits are truncated and overlain by a thin veneer (less than 1 m thick) of late Pleistocene–Holocene alluvium (BSC 2004a, Section 3.2.2.1).

Fault scarps are commonly visible along the block-bounding faults. The scarps are generally located between the bedrock footwall and colluvium on the hanging wall. The scarps appear sharp, with fault dips up to 80°, because the volcanic bedrock or silica-cemented fault breccia weathers very slowly. A pattern of enhanced erosion at the base of the scarps in channels and rills indicates that the

scarps have been exposed by hillslope erosion (Harrington et al. 2000). The Stagecoach Road Fault also exhibits a prominent scarp where eolian sand has washed away from a scarp formed in a well-cemented, reworked tuff. Thus, most prominent scarps at Yucca Mountain appear to be fault-line scarps, which are tectonic in origin but significantly enhanced by erosion (BSC 2004a, Section 3.2.2.1).

1.1.7.1.2 Geomorphic Information Related to Volcanism

Compared to other cinder cones in Crater Flat, a limited amount of erosional modification has taken place on the Lathrop Wells cinder cone, the youngest volcanic center in the Yucca Mountain region with an estimated age of 70,000 to 90,000 years. The maximum cone slope is preserved, and there is only a small amount of erosional modification of the cone flanks and crater (BSC 2004a, Section 3.4.6.5).

The Quaternary cinder cones in Crater Flat, formed about 1 million years ago, are fairly well preserved. Several near-surface features, such as pressure ridges and bombs with original morphology, are preserved at these eruptive centers. In contrast, the original topography associated with the basaltic centers that formed 3.7 million years ago in southeast Crater Flat has been strongly modified by erosion. Erosional features on these older centers include deep gullies with inset fills, integrated channel networks, and aprons with well-developed soils. Erosion of the original volcanic cones has exposed dikes that formed along fissures from which the lava was extruded into these centers (Perry et al. 1998, pp. 2-23 and 2-24).

1.1.7.2 Variability in Quaternary Processes *[NUREG-1804, Section 2.1.1.1.3: AC 7(1)]*

The kinds and rates of geomorphic processes at Yucca Mountain have varied considerably during the Quaternary in response to cycles of climate change. At present, semiarid conditions prevail in the southern Great Basin. During much of the Quaternary, however, cooler and wetter conditions existed; most of the surficial deposits mapped on and around Yucca Mountain are the products of climatic conditions that are different from the present. Under the present climate, the landscape is dominated by warm temperatures and eolian processes, with infrequent storms producing localized runoff; during cooler and wetter climates, there were changes in the type and density of vegetation, increases in runoff and streamflow, and the potential for longer periods of freezing (BSC 2004a, Sections 3.2 and 3.4).

1.1.7.2.1 Erosion and Deposition in the Present Climate

Erosion on modern hillslopes in the Yucca Mountain region occurs during infrequent, intense, short-duration summer thunderstorms. This process takes place as the unconsolidated material on the midslopes is activated into debris flows that carry the material off the hillslopes and into an adjacent basin. Although debris flows are the primary mechanism for hillslope erosion in the Yucca Mountain region, they are infrequent events (BSC 2004a, Section 3.4).

Debris flows were triggered on the south hillslope of Jake Ridge (Figure 1.1-5), located about 6 km northeast of the Yucca Mountain crest during a 2-day storm that occurred in July 1984. Rainfall intensities ranged up to 73 mm/hr during this unusual El Niño storm that stalled over the south slope

of Jake Ridge. Digital elevation models from prestorm and poststorm aerial photographs were used to map hillslope erosion and downslope redistribution of debris. Volumetric calculations indicate that about 7,040 m³ of debris were redistributed during the 2-day storm. The maximum and mean depths of erosion were about 1.8 m and 5 cm, respectively. The mean depth of deposition on the lower hillslope was 16 cm. Data on precipitation intensity and duration, combined with field observations of the amount and stability of the remaining hillslope sediment, suggest this erosional event is related to a storm interval significantly larger than 500 years (BSC 2004a, Section 3.4).

Modern dust deposition has been studied by annual collection of dust samples from 1984 to 1989 from 55 sites in southern Nevada and southern California. The average silt and clay flux, which is the rate of deposition, ranges from 4.3 to 15.7 g/m² per year. Annual dust flux increases with mean annual temperature and appears to be more strongly affected by decreases in annual precipitation than by increases in temperature. Playa and alluvial sources produce about the same amount of dust per unit area; however, the total volume of dust produced from alluvial sources is much larger. The mineralogic and major oxide composition of dust samples indicates that sand and some silt is locally derived and deposited, whereas clay and some silt can be derived from distant sources. Eolian dust constitutes much of the pedogenic material in the Pleistocene and Holocene soils in desert regions. Modern and Holocene dust has been infiltrating and accumulating below desert pavements on alluvial and colluvial surfaces in the Yucca Mountain region (BSC 2004a, Section 3.4).

1.1.7.2.2 Potential for Future Erosion and Deposition at Yucca Mountain

In the present climatic regime, most of the valleys that drain eastward down the dip slope of Yucca Mountain and directly over the repository merge in Midway Valley, then discharge into Fortymile Wash. The true base level for these valleys is Fortymile Wash, but the effective base level is the floor of Midway Valley for the present and the foreseeable future. Midway Valley is currently undergoing aggradation. Since at least the beginning of the Holocene, storms have activated debris-flow stripping of the hillslopes around Midway Valley. The sediment is carried onto the valley floor, resulting in a rising base level in Midway Valley. If a period of incision ensues as a result of a change in climate to one of greater effective moisture, the main wash in Midway Valley would ultimately start to incise its valley floor and then erode headward, thereby initiating a period of downcutting in the tributary valleys and the removal of channel fill deposits (BSC 2004a, Section 3.4).

An examination of the fill in Coyote Wash demonstrates that such a complete emptying of the alluvium in these valleys did not occur during the last glacial cycle. Relict Pleistocene fill documents the incomplete stripping of the valley alluvium during the last two climatic cycles. The climate change approximately 28,000 years ago to a regime favoring sediment removal did not last long enough to allow complete sediment removal from these valleys. Since approximately 15,000 to 18,000 years ago, when the climate began to become drier, these valleys have been in an aggradational mode. The incomplete removal of hillslope and valley alluvium in the tributary valleys during the 10,000 to 13,000 wet years of the last climate cycle indicates that more than 10,000 years is needed to remove alluvium from these valleys, assuming that the climate for that time interval was favorable for erosion. Based on the best documented period of erosion in the valleys that overlie the repository, substantially more than 10,000 years would be required to effectively remove the alluvium and to begin to actively erode the bedrock floor of these valleys (BSC 2004a, Section 3.4).

The detailed middle and late Quaternary history of Fortymile Wash indicates that the wash has incised and aggraded within a limited vertical range as it has migrated across the head of its fan. Since such behavior can be documented as a response to regional climate changes, there is no evidence to suggest there was a major period of incision in the wash that initiated a lengthy head-cutting period with deep incision in the tributary valleys (BSC 2004a, Section 3.4).

1.1.8 Geochemistry

[NUREG-1804, Section 2.1.1.1.3: AC 8]

This section provides a description of the geochemical information for Yucca Mountain that is relevant to the PCSA and the design of the GROA.

[Section 1.1.8.1](#) provides an introduction to geochemical features and processes anticipated to occur during the preclosure period.

[Section 1.1.8.2](#) addresses the geochemical composition of the repository host-rock units and associated subsurface waters held within the host rock.

[Section 1.1.8.3](#) describes the geochemical conditions that are anticipated to be present in the repository emplacement drifts during the preclosure period.

[Section 1.1.8.4](#) evaluates the potential for geochemical alteration due to heating and other processes to alter host-rock properties during the preclosure period.

1.1.8.1 Introduction

[NUREG-1804, Section 2.1.1.1.3: AC 8(1) to (3)]

Geochemical features and processes operating during the preclosure period are unlikely to affect preclosure repository safety. They are determined by the geochemical characteristics of the host rock, as altered by excavation, waste emplacement, heating, and ventilation. Preclosure geochemical alteration of the near-field host rock, composition of host-rock waters, and interaction with the gas phase is included in modeling of the longer-term postclosure response ([Section 2.3.5.3](#)). Evaluation of dust accumulation during preclosure operations, its composition and deliquescence within the drifts, has been performed to support screening of features and processes that contribute to postclosure performance ([Section 2.2.1](#)). Other processes, such as radiolysis and microbial activity, have also been evaluated as discussed below and in [Section 2.2.1](#). Waste isolation performance during the postclosure period, including a description of effects of key features, events, and processes, is described in [Section 2.3](#).

Heat output from the waste packages is at a maximum during preclosure. After emplacement, waste package temperatures increase, reaching a peak within a few years (during ventilation, as the near-field rock temperature distribution approaches a steady state). Waste heat output declines with time, so the in-drift and near-field temperatures decline throughout the preclosure period, as modeled with constant ventilation (BSC 2004i, Sections 4.1.10 and 6.6.1). Simulations for an 800 m long drift show that temperatures for individual waste packages vary depending on the elapsed time, waste package type, distance from the ventilation inlet, and seasonal variation in ventilation inlet air temperature (SNL 2007a, Appendix A). Average annual peak temperatures of

the drift wall and drift air are approximately 85°C and 80°C, respectively (BSC 2004i, Section 8.1). For a typical waste package in the middle of a drift, the average seasonal peak temperature is approximately 90°C during the summer in the first few years after emplacement. The corresponding relative humidity for summer conditions is approximately 1%. The lowest average seasonal temperature of the same typical waste package is approximately 38°C during the winter, at the end of the 50 year ventilation period, with a corresponding relative humidity of 8.5%. This range of conditions is extended for waste packages at the upstream and downstream ends of the emplacement drifts (BSC 2004i, Section 6.6.2; SNL 2007a, Appendix A). The preclosure in-drift humidity is always less than that of the outside air, and for waste packages at elevated temperatures (e.g., 90°C or greater) the relative humidity is very low, on the order of 1% or less.

Forced ventilation effectively dries out the near-field host rock. This is observed for ambient temperature ventilation in the ESF, where the rock matrix is substantially dewatered for a distance of approximately 1.5 m into the drift walls (Section 2.3.3), and seepage into ventilated openings in the host-rock geologic units has not been observed. At elevated temperature during preclosure ventilation, the decreased relative humidity produces increased extent and intensity of host-rock dryout (SNL 2008b, Section 7.5.2), further decreasing the likelihood of seepage into ventilated repository emplacement drifts. The heat output of emplaced waste greatly exceeds that necessary to evaporate the natural host-rock percolation flux incident on the drift opening, and evaporates pore water from the near-field host rock (BSC 2004i, Section 6.9.1).

Evaporation of water in the near-field host rock will result in precipitation of minerals, such as amorphous silica, less-soluble salts (e.g., calcite, gypsum, fluorite), and more-soluble salts (e.g., halite, niter, soda niter). Precipitation will occur in the matrix pores from evaporation of pore water and potentially in the fractures from evaporation of percolating fracture water where it occurs. Evaporative precipitates are identified and included in the thermal-hydrologic-chemical seepage model (Section 2.3.5.3) and the in-drift seepage evaporation abstraction (Section 2.3.5.5) representing postclosure features and processes. The same processes will be in effect during preclosure ventilation with important differences: (1) the peak temperature and relative humidity are lower; (2) preclosure forced ventilation is produced by suction, which has the effect of drawing water vapor into the drift opening from the surrounding rock instead of allowing it to migrate outward and condense; and (3) with no condensation zone in the rock, mineral dissolution is minimal. These differences decrease the potential for preclosure geochemical alteration of the in-drift environment from evaporation in the host rock.

Leaching of host-rock minerals, and associated interactions with the gas phase, are processes included in the thermal-hydrologic-chemical seepage model (Section 2.3.5.3). These processes will not significantly impact preclosure geochemical conditions in the emplacement drifts, which are dominated by the effects of forced ventilation.

1.1.8.2 Geochemical Composition of Subsurface Waters *[NUREG-1804, Section 2.1.1.1.3: AC 8(1), (2)]*

The mineralogical makeup of the host-rock affects preclosure geochemical conditions within the repository emplacement drifts, and the chemical composition of waters in the rock. Dust that accumulates on the waste packages will be derived in part from the host rock during excavation and operations, as demonstrated by evaluation of dust collected in the ESF (SNL 2007a, Section 6.3.3).

The composition and distribution of minerals in the host rock have been evaluated (BSC 2004a, Section 3.3.5.1) and are represented in the mineral assemblages developed for input to the thermal-hydrologic-chemical seepage model (Section 2.3.5).

Mineralogical data used for developing the abstraction include mineral-abundance data (BSC 2004j) obtained from drillcore samples from boreholes UE-25 a#1, UE-25 b#1, USW G-1, USW G-2, USW G-3, USW G-4, and USW H-6 and rock cuttings from 16 additional boreholes shown in Figure 1.1-153. The host rock units are chemically very similar, containing principally feldspars, plus a variable combination of the silica polymorphs: tridymite, cristobalite, and quartz. Accessory minerals include magnetite, ilmenite, monazite, zircon, apatite, allanite, and perrierite, all present in amounts much less than 1 vol % (BSC 2004a, Section 3.3.5.1). The relative proportions of silica polymorphs vary with depth and between lithophysal and nonlithophysal zones. The host rock units are generally devoid of zeolites, except for minor occurrences along some fractures. However, samples recovered from drill hole USW UZ-16 contain up to 14% of the zeolite mineral stellerite, which is associated with smaller feldspar abundance (BSC 2004a, Section 3.3.5.1).

Minerals that may still be forming today include zeolites, clays, opal, and calcite. Ongoing diagenetic alteration typically produces clinoptilolite (as a precipitate) with possible mordenite, smectite, silica, iron-manganese oxides and hydroxides, and other minor phases (BSC 2004a, Section 3.3.5.1.2).

The chemical composition of waters present within the host rock is also a factor in the composition of waters that might seep into the repository drifts in the unlikely event that such seepage occurs. Sufficient flow has not been observed within fractures in the host rock units to allow collection of water samples for analysis. Therefore, characterization of waters in the unsaturated zone has focused on matrix pore water present in the host rock and overlying units (BSC 2004a, Section 5.2.2). Four representative water compositions are used in the thermal-hydrologic-chemical seepage model (Section 2.3.5.3) to simulate evolution of the near-field chemical environment during the postclosure period. These same compositions also represent the range of host-rock pore waters pertinent to host-rock preclosure conditions. The four representative compositions were obtained from core samples extracted from host rock units: samples are from the Tptpul unit, the Tptpll unit, and from the Tptpmn unit. The four input water compositions are described in Section 2.3.5.3 and tabulated in Table 2.3.5-5.

1.1.8.3 Geochemical Conditions in the Preclosure Emplacement Drift Environment *[NUREG-1804, Section 2.1.1.1.3: AC 8(2)]*

Chemical conditions within the repository drift during the preclosure period are influenced by dust, which is mainly derived from the host rock, from the outside atmosphere, and from anthropogenic sources (SNL 2007a, Section 6.1.2.4).

Preclosure thermal-hydrologic conditions in the near-field host rock within a few meters of the drift openings, impede the penetration of fracture flow. The potential evaporation from heat output of the waste forms greatly exceeds the percolation flux in the host rock that is incident on the drift opening (BSC 2004i, Section 6.9.1). The effectiveness of evaporation is accentuated during the preclosure period by the induction of formation air into the emplacement drifts by suction from ventilation. Forced ventilation is driven by suction fans, so the absolute pressure in the emplacement drifts is

less than that in the host rock, continuously drawing air from the fracture network into the drifts. For partially saturated hydrologic conditions, forced ventilation is combined with heating to ensure that evaporation takes place within the host rock rather than at the drift wall. Also, fracture walls dry out in the affected rock so that rock matrix dryout causes pore water to migrate toward nearby fractures rather than toward the drift wall. Thus, the salts produced from dryout accumulate within the host-rock fractures rather than as efflorescence on the drift wall. Even if fracture flow penetrates the affected dryout zone, the capillary diversion response remains effective (Section 2.3.3). Accordingly, the potential contribution of precipitated salts to dust on the waste packages is limited, and is represented to the extent that it is likely to occur, by dust samples collected in the ESF.

Dust Deliquescence—Dust deposits on waste packages consist of particulate matter suspended by preclosure ventilation. Dust will accumulate throughout the preclosure ventilation period, and the accumulation will be monitored (Chapter 4). The influence of introduced materials used in construction and operation of the repository on the soluble constituents of dust is represented by dust samples collected in the ESF. Evaporation of water used for dust control is a limited source of soluble salt content in dust that accumulates on waste packages during the preclosure period, as demonstrated for dust samples from the ESF. In addition, atmospheric salts will be brought into the repository by preclosure ventilation. The composition and behavior of dust that accumulates on the waste packages is addressed in a screening evaluation for postclosure features and processes that also considers preclosure effects. At preclosure waste package temperatures, the ammonium salts present in dust readily volatilize and are removed as gases in the ventilation air. The remaining salts do not deliquesce at preclosure temperature and humidity conditions; salts such as $MgCl_2$ and $CaCl_2$, which can deliquesce at these conditions, are either not present or present only in insignificant quantities (SNL 2007a, Chapter 6).

Potential Corrosion of Introduced Materials—The stainless steel ground support components do not corrode significantly under conditions more humid than the dry conditions extant in the preclosure emplacement drift environment (SNL 2007b, Section 6.5.1.5). In addition, low-alloy or carbon-steel components are used in the invert. With a relative lifetime of about 50 years/cm (SNL 2007b, Sections 6.5.1.6 and 6.8) these steels are more reactive than stainless steel. However, corrosion rates for these materials are correlated with relative humidity (SNL 2007b, Section 6.5.1.6). For example, the mean corrosion rate for low-alloy or carbon steel exposed to a rural atmosphere with relative humidity of 60% or less is approximately 13.9 $\mu\text{m}/\text{yr}$. The actual corrosion rate in the emplacement drift environment is smaller since the average relative humidity in the drift is much less than 60%, as discussed above. Thus, corrosion of structural steel in the invert may occur in the preclosure in-drift environment but will be of insignificant extent. Section 1.3.4.4 provides design considerations for ground support.

1.1.8.4 Geochemical Alteration to Host-Rock Properties Environment [NUREG-1804, Section 2.1.1.1.3: AC 8(3)]

1.1.8.4.1 Potential Geochemical Alteration Due to Heating

Thermal loading of the near-field host-rock units can produce geochemical alteration from dissolution or precipitation (in the presence of liquid water), mineral hydration and dehydration, and mineral phase-transitions. The potential effects of thermal loading have been evaluated through field and laboratory testing (Sections 2.3.3 and 2.3.5). Test results generally encompass

temperature ranges greater than those anticipated during the preclosure period and support understanding of both preclosure and postclosure behavior.

Results indicate that thermally driven changes in rock properties during the preclosure period are not significant in magnitude or extent. Dissolution reactions occur as host-rock fracture or matrix waters percolate into warmer rock; however, evaporation, as discussed above, makes such dissolution unlikely near the drift openings. Precipitation reactions occur as waters evaporate in the rock fractures and matrix and may occur closer to the drift openings, but precipitates act as cement that increases rock strength. If liquid water is not present, as in the dryout zone around drift openings, mineral dissolution and precipitation reactions do not occur. Mineral hydration and dehydration do not produce significant changes in host-rock properties because of the scarcity of water-sensitive materials lining the fractures or within the host-rock matrix (Section 2.3.5).

Mineral phase transitions may occur in tridymite and cristobalite (BSC 2004j, Section 6.3.5 and Appendices A and B). Tridymite and cristobalite are silica polymorphs that occur in spatially variable abundance throughout the host rock units, and the abundance rarely exceeds 20% for tridymite and 30% for cristobalite. These transitions are observed to cause volume increases in pure-mineral grains but are less evident in elevated-temperature measurements of whole-rock thermal and mechanical properties, which show moderate sensitivity to temperature and do not exhibit transitional behavior. The potential effects from tridymite and cristobalite phase transitions are, therefore, included in the characterization of temperature dependence for rock properties. Laboratory tests for temperature-dependence of key parameters were conducted at temperatures up to 325°C, while the upper limit for field testing was approximately 200°C (BSC 2007i, Section 6.5). These temperature ranges are consistent with the drift-wall temperature limit given in Table 1.3.1-2.

1.1.8.4.2 Potential Geochemical Alteration Due to Other Processes

Radiation Effects on Host Rock—Radiation levels at the waste package surfaces will be at their highest during the preclosure period (SNL 2008c, FEP 2.1.13.01.0A). The gamma-radiation field could affect the rock exposed at the drift wall and possibly penetrate up to a few centimeters into the rock (Blair et al. 1996, p. 13).

The effect of radiation on the geomechanical and geochemical properties of the welded Topopah Spring Tuff was investigated by irradiating samples of the nonlithophysal host rock unit (Ttptmn) obtained from Fran Ridge, and comparing mechanical properties with those of matched nonirradiated rock samples (Cikanek et al. 2004, Section 3.1.7; Blair et al. 1996). A gamma-ray dose of 950 ± 100 Mrad was used to irradiate the samples over a 47-day period.

A number of heterogeneous pairs of irradiated and nonirradiated samples, many of which contained preexisting, partially healed, vertical or nearly vertical cracks, showed that the irradiated samples had lower mean strengths and a lower Young's modulus (Blair et al. 1996, p. 11).

Several factors indicate that such radiolysis effects will be insignificant. First, ventilation during preclosure will reduce humidity and remove moisture from the drift wall, both of which reduce the potential for radiation-induced weakening of host rock by radiolytic reaction involving water. Second, the waste packages will provide shielding such that the drift wall will not receive the large dose used in the experiments. For 21-PWR packages, calculations indicate that for a 140-year

period the cumulative gamma dose on the drift wall surface is approximately 63.5 Mrad (BSC 2004k, Table 6.4-6), or 7% of the dose used in the experiments. Dose rates would be lower with a transportation, aging, and disposal canister because of attenuation by the stainless steel shell of the transportation, aging, and disposal canister (BSC 2006a, Section 7.2). Ground support for drifts is discussed in [Section 1.3.2](#) and drift stability is discussed in [Section 2.3.4](#).

Chemical Effects of Excavation and Construction Activities on the Host Rock—Excavation and construction of underground openings will not produce significant geochemical alteration of host-rock properties. The emplacement drifts will be excavated with limited use of chemical explosives. The limited volume of water used during excavation, for construction activities and dust control prior to waste emplacement, will not significantly alter the near-field host rock because any introduced water is expected to be removed by the repository ventilation system, which will operate during waste emplacement and for a minimum of 50 years after waste emplacement. Other potential impacts of excavation and construction will be avoided through appropriate controls on preclosure operations (SNL 2008c, FEP 1.1.02.00.0A).

1.1.8.4.3 Summary of Effects from Preclosure Geochemical Alteration on Host-Rock Properties

The geotechnical parameters developed to represent the host rock in subsurface design and performance evaluations ([Sections 1.1.5](#) and [2.3.4](#)) will not be significantly affected by geochemical features and processes operating during the preclosure period or else the characterization of these parameters already incorporates the effects. Geotechnical parameters in the following categories are considered ([Section 1.1.5](#)):

- Intact rock physical, mechanical, and thermal properties (i.e., density and porosity, deformation moduli and strength properties, thermal conductivity, thermal expansivity) are not significantly affected because such small quantities of minerals are dissolved, precipitated, or otherwise altered in the near-field host rock ([Section 1.1.8.4.1](#)). In addition, mineral phase-change effects are incorporated in the laboratory measurements of intact-rock properties at elevated temperature ([Section 1.1.8.4.1](#)). Rock fracture mechanical and geometrical properties (i.e., normal and shear stiffness, shear strength, fracture network geometry, fracture characteristics) are not deleteriously affected in the near-field host rock, principally because geochemical alteration is limited by the effects and extent of dryout ([Section 1.1.8.4.1](#)). The extent of preclosure dryout is comparable to the zone of increased shear stress and decreased normal stress perpendicular to the drift wall, where changes in fracture properties are potentially important. In addition, geochemical alteration does not create new fractures or change the geometry of the fracture network.
- Rock mass mechanical and geometrical properties (i.e., in situ compressive strength and shear strength, deformation modulus, dilation angle, geotechnical classification, lithophysal porosity characterization) are also not significantly affected by geochemical features and processes in the near-field host rock. This results from the limited changes in rock fracture properties and the rock matrix, proximal to the drift openings.

The above listed host-rock properties are used to analyze both the preclosure and postclosure geomechanical responses, whereby the thermal and mechanical loading are greater for postclosure than for preclosure. Importantly, the intact-rock mechanical data include laboratory measurements for dry rock conditions as well as in situ testing data collected in drifts dried by ventilation (Section 2.3.4).

The strength and deformability properties of fractures are most important to the preclosure geomechanical response of the host rock. While precipitation in some fractures is expected as percolating water contacts the ventilation-induced dryout zone around the drifts, significant deleterious changes in fracture properties are unlikely. Leaching is not important in the host rock proximal to drift openings because of the dry conditions. Other processes, including thermal alteration, radiolysis, and mineralogical phase transitions, are either insignificant or are already incorporated in temperature-dependent parameter descriptions.

1.1.9 Land Use, Structures and Facilities, and Residual Radioactivity

[NUREG-1804, Section 2.1.1.1.3: AC 9]

This section describes the previous uses of land within the proposed land withdrawal area, describes the locations and uses of man-made structures and facilities within the proposed land withdrawal area, and identifies any residual sources of radiation within the proposed land withdrawal area as they relate to the PCSA. Based on information provided in Sections 1.1.9.1 and 1.1.9.4, there are no indications of residual radioactivity from previous land uses within the GROA. Any residual radioactivity within the proposed land withdrawal area will make a negligible contribution to worker and public radiation exposure.

In accordance with 10 CFR 63.121(a)(1), the GROA will be located in and on lands that are either acquired lands under the jurisdiction and control of the DOE or lands permanently withdrawn and reserved for its use. Additional information regarding ownership of land is provided in Section 5.8.1.

The proposed land withdrawal area (Figure 1.1-154) includes about 600 km² of land currently under the control of the DOE, the U.S. Department of Defense, and the U.S. Department of the Interior (DOE 2002b, Section 1.4.1).

Section 1.1.9.1 discusses previous land uses within the proposed land withdrawal area.

Section 1.1.9.2 discusses previous land uses in the vicinity of the proposed land withdrawal area.

Section 1.1.9.3 discusses the location and description of existing man-made structures or facilities.

Section 1.1.9.4 provides information regarding the identification of residual radiation.

Section 5.8.1.1 identifies DOE land-use interests that exist within the proposed land withdrawal area.

Section 5.8.2.2 identifies the existing rights-of-way and other encumbrances in the proposed land withdrawal area.

1.1.9.1 Previous Land Uses within the Land Withdrawal Area

[NUREG-1804, Section 2.1.1.1.3: AC 9(1)]

1.1.9.1.1 Mining Claims

As shown in [Figure 5.8-1](#), unpatented mining claims are located in the southern part of the proposed land withdrawal area on Bureau of Land Management land. Additional information regarding these unpatented mining claims is provided in [Section 5.8.2.2.2](#).

1.1.9.1.2 MX Missile

A portion of Area 25 at the Nevada Test Site that is within the proposed withdrawal area was used for development and testing of the MX (missile experimental) support systems and programs by the Ballistic Missile Office of the U.S. Air Force from 1978 to 1983 ([Figure 1.1-154](#)). Some of the activities involved siting studies for 71-ft-long MX Peacekeeper missiles and canister ejection tests (DOE 2001b, Section 2.2.1).

One of the first MX projects was the Vertical Shelter Ground System Definition Program, which required construction of an 18-ft-diameter, 130-ft-deep vertical silo for missile loading and egress (exit) tests. The egress mechanism was built to thrust a 348,000-lb simulated missile and canister out of the silo to a height of 40 ft above ground, after it burst through a layer of soil weighing 50,000 lb. In other experiments, an extensive network of experimental roads was built to evaluate construction methods in native desert soils to ensure the roads could accommodate the heavy loads associated with transporting 200 MX missiles among 4,600 shelters. These tests were part of the Multiple Protective Shelter System (DOE 1999).

When the decision was made to use a horizontal shelter-basing mode, a program was started to develop this design and to evaluate precast construction versus a cast-in-place method. The shelter segments used about 220 yd³ of concrete per segment and weighed between 240 and 300 tons each. Studies into this basing mode were canceled in October 1981 (DOE 1999).

There is an ongoing program for environmental restoration of the Nevada Test Site, which involves identifying potentially contaminated sites and facilities, investigating contamination, and performing corrective actions. As part of this program, two corrective action sites at the MX site were identified and investigated for radioactive contamination, including a construction landfill ([Figure 1.1-154](#)). As part of the corrective action investigation, a total of 1,344 individual beta and gamma measurements were recorded by a drive-over survey. The survey indicated that no radioactive contamination above the established area background was detected in surface and near-surface soil (DOE 2001b, Section 2.5.7.1). A storage yard located on the west side of Lathrop Wells Road at the MX site was also identified as a corrective action site. This location was used to store heavy equipment and materials used during the MX program. The site later became the storage yard for materials and scrap prior to sale as salvage. Hazardous materials, such as paint, hydraulic fluid, and batteries, were found during inspections but were removed prior to an August 1996 material salvage auction. In June 1996, prior to the August 1996 material salvage auction, inventoried items in the yard were radiologically surveyed and were found to be free of radiation and contamination (DOE 2003c, Section 2.2.5 and Appendix A.1.1.5).

No impact on the repository is expected from the previous activities or facilities at the MX site because of its distance from the repository (greater than 10 mi) and the previous cleanup activities. Additional MX missile-testing information related to X-Tunnel is provided in [Section 1.1.9.2.1](#).

1.1.9.1.3 Army Ballistics Research Laboratory Test Range

The Army Ballistics Research Laboratory Test Range ([Figure 1.1-154](#)) site has been used for multiple, open-air tests of depleted-uranium munitions. This open-air site consisted of (DOE 1992, Section 1.1 and Figure 2):

- A steel target pad 17 by 17 m within a 100 m radius graded area, with a short-range firing station within the graded area
- A 100 by 100 m fenced compound approximately 1.7 km west of the target pad containing a maintenance building, observation tower, and instrumentation trailers
- A 120 by 120 m long-range firing station 2 km southwest of the target pad
- An environmental monitoring area with four 10 m wide bladed arcs spaced 100 m apart that arc from the west-northwest to the east around the target pad
- An ammunition bunker approximately 3 km to the west of the target pad.

Tests conducted at this site consisted of (DOE 1992, Sections 1.1.1 and 1.1.2):

- Firing depleted-uranium or nondepleted-uranium munitions at military targets that may also contain depleted-uranium armor on the target pad
- Detonation or burning of depleted-uranium ammunition packed in shipping containers on the target pad
- Detonation or burning of depleted-uranium ammunition in military vehicles on the target pad.

Operational guidelines to ensure minimal contamination included (DOE 1992, Section 1.0):

- Covering the steel target pad with several centimeters of soil under the test
- Removing the remains of the target after the test
- Establishing a movable structure around the test pad following testing until contaminated materials subject to wind dispersion could be removed
- Removing and disposing of the depleted-uranium contaminated soil at an approved low-level radioactive waste management site.

Recovery of depleted-uranium fragments and oxide was considered not only a cleanup activity but also part of the tests to study fragmentation patterns and chemical form of the oxides produced by the test (DOE 1992, Section 1.0).

A radiological survey of this site was conducted in June 1999 (DOE 2000, Volume 1, Appendix A) to assess compliance with 10 CFR Part 835. The site has been posted in accordance with 10 CFR Part 835, and appropriate fencing has been constructed. The target pad area of less than 2,000 ft² has been posted as a contamination area and is fenced with smooth wire. The 430,000 ft² graded area around the target pad has been posted as a radioactive material area. Additionally, the access road is fenced with a locked gate (DOE 2000, Volume 1, Appendix A).

No impact on the repository is expected from the previous Army Ballistics Research Laboratory Test Range activities or facilities because of the distance from the repository (greater than 10 mi), previous cleanup activities, and existing access controls and precautions. Additional information regarding the Army Ballistics Research Laboratory tests related to X-Tunnel is provided in [Section 1.1.9.2.1](#).

1.1.9.1.4 Borehole USW G-3

Borehole USW G-3 ([Figure 1.1-154](#)) is located on the crest of Yucca Mountain at an elevation of 4,856 ft above mean sea level. The borehole is located on Bureau of Land Management land that has been withdrawn from mining and mineral exploration outside of the Nevada Test Site boundary, west of Area 25. USW G-3 was drilled in 1982 to support the evaluation of the geologic, geophysical, and hydrologic potential of Yucca Mountain as an underground repository for high-level radioactive waste (DOE 2001b, Section 2.2.1.5).

The borehole was identified as a corrective action site because of a ¹³⁷Cs source lost on January 26, 1982, from a Birdwell Nuclear Annulus Investigation Logging tool during cementation activities in the hole. The source was lost at a depth interval of 1,247 to 1,250 ft belowground surface with a 45 ft³ volume of cement being used at this depth interval. The source was not detected by a gamma-ray logging tool that was run downhole to a depth of 1,247 ft belowground surface (DOE 2001b, Section 2.2.1.5).

Following the loss of the ¹³⁷Cs source, drilling was diverted to avoid debris left in the original shaft, and the drill hole was completed to a total depth of 5,031 ft belowground surface. Cuttings from USW G-3 were continually monitored for radioactivity until the drill team had successfully bypassed the cement plug. No elevated radiation was detected, and the source is judged to remain sealed in the concrete plug. The original receipt for the source (dated July 7, 1977) confirmed that it had an original activity level of 200 mCi of ¹³⁷Cs (DOE 2001b, Section 2.2.1.5).

At the ground surface, USW G-3 is capped and is situated in a fenced area that measures 20 by 20 ft. The area is marked with signs designating it as an underground radioactive material area, indicating that caution is required because of buried radioactive material, and any digging operations in the immediate area require precautions (DOE 2001b, Section 2.2.1.5).

No impact on the repository is expected from USW G-3 because of the small quantity of radioactivity, its underground location, and the existing access controls and precautions.

1.1.9.1.5 Concrete Batch Plant

A concrete batch plant was located within the proposed land withdrawal area about 5 km from the GROA, just northeast of water supply well UE-25 J-13 (Figure 1.1-154). The concrete batch plant provided construction concrete for Yucca Mountain Project site characterization activities. Dust control consisted of filtration and truck dust collection equipment (Dixon 1993). The concrete batch plant did not operate in 2001, 2002, 2003 (Wade 2002; Wade 2003, and Wade 2004) and has been removed from the site (Arthur 2004).

1.1.9.2 Previous Land Uses in the Vicinity of the Proposed Land Withdrawal Area [NUREG-1804, Section 2.1.1.1.3: AC 9(2)]

1.1.9.2.1 X-Tunnel

X-Tunnel and Y-Tunnel are underground test facilities mined out of volcanic ash-fall tuff within Little Skull Mountain in Area 25 of the Nevada Test Site. Both tunnels are outside the southeast border of the proposed withdrawal area (Figure 1.1-154). X-Tunnel and Y-Tunnel were originally developed as part of the MX missile-basing program. Tests in the early 1980s were completed to demonstrate the feasibility of excavating egress portals for the MX missile, with special attention to tunneling through rubblized rock (Voegelé 1993, p. 182; DOE 1982; DOE 1992, Appendix 2).

In the late 1980s and 1990s, X-Tunnel was used for testing the effectiveness of U.S. weapons against special military targets, and Y-Tunnel was placed on inactive status. Depleted-uranium and conventional munitions were used in live-fire tests against classified targets by the Army Ballistics Research Laboratory. The tests were conducted by firing depleted-uranium ammunition or nondepleted-uranium ammunition into X-Tunnel from a tank located on a firing pad outside of the portal. The targets were located on a steel target pad in an approximately 500 m² test room at the end of the 215 m tunnel. Operational guidelines similar to those discussed for the Army Ballistics Research Laboratory Test Range in Section 1.1.9.1.3 ensured minimal contamination (DOE 1992, Section 1.2 and Appendix 2).

Radiological surveys were completed in January 1996 after the depleted-uranium tests in X-Tunnel ended, and a cleanup was performed from May through July 1996. Radioactively contaminated equipment and materials, including an underground sump located in the test room for collecting spilled fluids from the targets and a large metal plate (target pad), were removed from the test chamber. The ceiling and walls in the main tunnel and test chamber from a side drift (approximately 150 m from the portal of the 215 m tunnel) to the end of the tunnel were cleaned and shotcreted to stabilize contamination. The invert (floor) of this same portion of the main tunnel and test chamber was removed (DOE 2002d, Section 2.5.2).

Subsequent to cleanup activities, the test chamber and main drift of the X-Tunnel were available for access with no radiological restrictions or postings. The side drift is posted as a controlled area; it contains ventilation piping with internal radioactive contamination and areas on the invert with radioactive contamination that has been fixed in place (DOE 2002d, Section 2.5.2).

More recently, the X-Tunnel complex has been used in a collaborative effort between the U.S. Department of Defense and the DOE for joint demilitarization tests, which included detonation tests

of high-explosive projectiles in 1996 and 1997 and low-pressure rocket-motor propellant burns in 1997 and 1999 (Velsko et al. 1999). These tests are intended for demonstrating and validating technologies for resource recovery, recycling, and alternative destruction and treatment technologies. During these tests, the test chamber was sealed off from the access drift by a steel and concrete containment barrier. This barrier was designed to withstand blast effects, such as shock, shrapnel impacts, and high-pressure and temperature environments, and to prevent the release of gases produced by munitions detonations and rocket-motor propellant burns (Velsko et al. 1999).

A location in the test chamber was identified as a corrective action site and an investigation was conducted. Investigation activities included inspection of the gravel and soil, and a total alpha and total beta radiological survey was conducted in March 2003. The radiological survey results were considered to be within the range of background (DOE 2003d, Sections A.9.0 to A.9.4).

1.1.9.2.2 Nevada Test Site Nuclear Testing

The Nevada Test Site was the primary location for the testing of nuclear explosives in the continental United States from 1951 to 1992. Historically, nuclear testing at the Nevada Test Site has included (Wills 2006, Section 1.3):

- Atmospheric nuclear explosion testing in the 1950s and early 1960s
- Underground nuclear explosion testing in drilled, vertical holes and horizontal tunnels
- Earth-cratering nuclear explosion experiments
- Open-air nuclear reactor and engine testing.

The nuclear explosion testing took place outside of both Area 25 and the proposed land withdrawal area (Wills 2006, Figure 1.3).

From 1959 through 1973, a series of open-air nuclear reactor, nuclear rocket engine, and nuclear furnace tests was conducted in Area 25, and a series of tests with a nuclear ramjet engine was conducted in Area 26 (Wills 2006, Section 1.3). Area 26 is more than 10 mi from the GROA and more than 7 mi outside of the proposed land withdrawal area (Figure 1.1-6). Facilities in Area 25 (Radioactive Materials Storage Facility, Engine Test Stand-1, Engine Maintenance, Assembly, and Disassembly (E-MAD), Reactor Maintenance, Assembly, and Disassembly (R-MAD), Test Cell A, and Test Cell C) related to these tests are located outside of the proposed land withdrawal area and are more than 5 mi from the GROA (Figure 1.1-154).

In most instances, the open-air nuclear reactor and nuclear rocket engine tests were conducted when the wind was blowing to the northeast. In the instances when tests were conducted with the wind blowing to the southwest or west, the radiological effluent plume could have passed over the proposed land withdrawal area. The effluent from a nuclear reactor run differs from a nuclear explosion (Friesen 1995). In the case of an atmospheric nuclear explosion, hundreds of radionuclides were produced almost instantly, some in large quantities, and interactions with the medium surrounding the detonation increased the number and size of radioactive particulates that could be spread over a wide area. In a rocket reactor run, small quantities of radioactive effluents were initially generated, with the quantity increasing as the power was increased. The hydrogen coolant and propellant exited the exhaust nozzle, straight up at high temperatures, and was burned. The very hot effluent cloud would rise to thousands of feet above the ground, reaching heights of

6,000 to 10,000 ft. The effluent was composed of water vapor and gases liberated by fission from the metal fuel elements. High temperatures and high flow rates in the propellant could erode and expel solid particles of nuclear fuel from the reactor; these heavy particles would drop out of the effluent within a few thousand feet of the test (Friesen 1995).

Although these open-air rocket reactor tests released large quantities of fission product activity through their exhaust plumes, the highest recorded aerial deposition of fallout in the vicinity of the Test Cell C site occurred during the Kiwi Transient Nuclear Test (Kiwi-TNT) and the Phoebus 1A Test (DOE 2003e, Section 2.4.2). The Kiwi-TNT excursion was conducted on a test pad located approximately 640 ft north of Test Cell C on January 12, 1965. The planned excursion produced sufficient energy to damage the reactor and disperse debris, such as fission products and core fuel, into the atmosphere (DOE 2003e, Section 2.4.1). During the Kiwi-TNT excursion, the fission rate was deliberately increased so that the resulting heat could not be transferred fast enough to avoid vaporizing significant amounts of the fissionable material and the surrounding graphite. The pressures resulting from this vaporization caused destruction of the reactor (Fultyn 1968, pp. 18 to 19). As the vapor cloud cooled, the fission products condensed on graphite or entrained desert dust particles in the cloud, accounting for particle activity as a surface phenomenon (Fultyn 1968, p. 20). The highest recorded deposition of fallout from the Kiwi-TNT occurred within two primary areas: within a 4,000-ft arc from the test location and over an estimated 90-acre area approximately 16,000 ft southwest of the Kiwi-TNT pad at a bearing of 215°. The explosion scattered reactor components and fuel over a 2,000-ft radius of the Kiwi-TNT pad; however, the majority of the debris was contained within a 500-ft radius (DOE 2003e, Section 2.4.1). On June 18, 1965, a loss-of-coolant accident occurred during a high-power test of the Phoebus 1A reactor at the Test Cell C test pad, which severely damaged the reactor core. Rapid overheating resulted in the ejection of approximately 5% to 8% of the core through the nozzle, scattering fuel fragments over the surrounding area. In addition, radioactive debris from fission products and core fuel was dispersed into the atmosphere. This material was carried north of the Test Cell C test pad with the highest recorded deposition of fallout occurring over an estimated 51-acre area approximately 8,000 ft northwest of Test Cell C at a bearing of 315° (DOE 2003e, Section 2.4.2).

Initial decontamination of the Kiwi-TNT site was performed in conjunction with collection of material to document the size distribution and geographic locations of the larger reactor fragments (Fultyn 1968, p. 15). Decontamination cleanup activities were conducted at the Test Cell C site after the Phoebus 1A accident (Sanders 1967). Additional cleanup activities at both sites were conducted from 1974 to 1983 (DOE 2003e, Section 2.5).

As part of the ongoing Nevada Test Site environmental remediation activities, areas around Test Cell C were identified for investigation and remediation. Due to the large area and complexity of previous operations, the site was subdivided into nine separate parcels based on the types of contaminants released (NNSA 2004, Section 1.0).

At four parcels (A, B, D, and F), no further action was recommended, because contaminants were not identified at these locations based on the results of the corrective action investigations (NNSA 2004, Section 2.3).

At two parcels where contaminants were identified (G and J), a risk assessment indicated that the level of contamination present does not pose an unacceptable risk to human health and the

environment; therefore, it was recommended that no further action be taken (NNSA 2004, Section 2.3).

At one parcel (C), ^{137}Cs was the only contaminant detected at concentrations that posed an unacceptable risk to human health and the environment based on the data results of the corrective action investigation and based on the results of a risk assessment. A corrective action was conducted to remove ^{137}Cs contaminated soil that exceeded the Nevada Department of Environmental Protection approved levels at four locations identified at the parcel. Approximately 12 yd³ of ^{137}Cs contaminated soil were removed, containerized, and disposed of at the Nevada Test Site Area 5 Radioactive Waste Management Site. After the soil removal, samples were taken to verify that the corrective action was effective. Based on the corrective action and the results of the verification and the risk assessment, it was determined that no further action is needed at this parcel (NNSA 2004, Section 2.3).

Samples at two parcels (E and H) exceeded contaminant limits and the recommended corrective action for these parcels is that they be closed in place with administrative controls. At Parcel E, ^{137}Cs sample concentrations exceeded the contaminant limit. However, the extent of contamination is bounded both laterally and vertically with concentrations less than the contaminant limit, and there is 6 ft of soil above the contamination that shields the contamination and reduces the exposure to a level below the acceptable risk threshold value. Therefore, the ^{137}Cs contamination is not an exposure risk and will remain within the fenced boundary of the radioactive materials area located at Test Cell C. At Parcel H, samples exceeded the contaminant limit for total petroleum hydrocarbons-diesel-range organics. Field investigation results show no significant contaminant transport mechanisms exist and contaminants have not migrated away from the parcels. In addition, the modeling results indicate that the downstream transport or vertical migration to groundwater of site contaminants does not pose an unacceptable risk to human health and the environment. Due to the infeasibility of removing the contaminants from Parcels E and H, it was determined that the close in place with administrative controls corrective action alternative is appropriate, because it will prevent inadvertent contact with the subsurface contaminants and meets all applicable state and federal regulations for closure of the site. A wire fence was installed around each parcel and use-restriction signs were posted in accordance with Federal Facility Agreement and Consent Order use-restriction guidelines. These use-restriction controls with fencing and posting limit access and prevent unauthorized intrusive activities. The future use is restricted from any activity that would alter or modify the containment control unless appropriate concurrence was obtained from the Nevada Department of Environmental Protection (NNSA 2004, Sections 2.2.1.2, 2.2.1.4, 2.3, and Appendix G).

None of these sites are within the proposed land withdrawal area. Based on information provided in [Sections 1.1.9.1](#) and [1.1.9.4](#), there are no indications that the previous land uses in the vicinity of the proposed land withdrawal area discussed in [Section 1.1.9.2](#) will contribute to worker and public radiation exposure within the land withdrawal area or in the general environment.

1.1.9.3 Location and Description of Existing Man-Made Structures or Facilities *[NUREG-1804, Section 2.1.1.1.3: AC 9(2)]*

1.1.9.3.1 Mining Facilities

Patent 27-83-0002 comprises about 200 acres within the proposed land withdrawal area in T.14S., R.48E., Section 36. The Cind-R-Lite Block Company is mining the cinder cone at that location for aggregates used in the manufacture of cinder blocks ([Figure 1.1-154](#)). There is no subsurface work at the mine, but the mine has a water well. The mine is located about 15 km from the GROA (DOE 2002b, Section 3.1.1.2; Jacobs 2004).

1.1.9.3.2 Yucca Mountain Facilities Within the Land Withdrawal Area

This section provides details on existing surface structures and facilities that were built to support the Yucca Mountain Project and occur within the proposed land withdrawal area. These existing structures or facilities are subject to being replaced. Surface disturbances, facilities, or structures that are the result of environmental monitoring or site characterization activities (e.g., meteorological monitoring sites, trenches, test pits, drill hole pads) are not included in this discussion. Planned repository structures and facilities are not discussed in detail in this section; these structures and facilities are discussed in [Section 1.2](#).

1.1.9.3.2.1 North Portal Pad

The North Portal pad ([Figure 1.1-155](#)) is located within the proposed land withdrawal area at a location that will be part of the surface GROA. It is about 800 to 1,200 ft by 600 to 700 ft in size and slopes roughly 2% to the east, from an elevation of about 3,683 ft at the base of Exile Hill to 3,670 ft above sea level. The North Portal pad consists of alluvium covered by fill that was added to support tunneling of the ESF in support of Yucca Mountain site characterization. The fill is composed of colluvium and bedrock from shallow excavations at the toe of Exile Hill and excavations for the North Portal of the ESF, alluvium from borrow pits, and tunnel muck (BSC 2002b, Section 6.6). Muck storage areas are located to the southeast and east of the North Portal pad ([Figure 1.1-155](#)) (CRWMS M&O 1998b, Attachment I). As discussed in [Section 5.8.2](#), these muck piles will be removed and used as fill for activities associated with construction.

Beneath the fill placed for the North Portal pad is a variable thickness of colluvial and alluvial material overlying Tertiary volcanic bedrock units. The North Portal pad is the surface at which the ESF tunnel portal was constructed. The pad supported the muck-handling facilities for the tunnel excavation, as well as offices, shops, and rail equipment supporting the boring of the ESF tunnel, and facilities for engineering and scientific testing in the ESF (CRWMS M&O 1999b, Section 1.2.2).

The fill covering the North Portal pad varies in thickness from 0 to 24.4 ft (BSC 2002b, Attachment I; BSC 2002c, Section 5, Assumption 10). It is considered nonengineered fill, as it does not meet the criteria for engineered fill. The existing nonengineered fill at the North Portal pad is planned to be removed prior to the construction of the surface GROA and to be replaced with an engineered fill (BSC 2007k, Section 6.1.4.1).

The offices, shops, and other equipment located on the North Portal pad are considered nonpermanent items. Such nonpermanent items associated with surface accommodations for the ESF are planned to be removed before the construction of the surface facilities described in [Section 1.2](#) (BSC 2005b, Section 13.5).

1.1.9.3.2.2 South Portal Pad

The South Portal pad ([Figure 1.1-155](#)) is located within the proposed land withdrawal area. It was developed beginning in late 1996 as the terminus for the 5-mi ESF tunnel. This pad provided a location for the tunnel boring machine to tunnel to the surface. The South Portal pad is not serviced by any surface utilities. The subsurface electrical power distribution system ends at the South Portal, powering two ventilation fans. Additionally, an emergency generator is located on the South Portal pad for backup power to one ventilation fan in the event of an emergency. The remaining sections of the tunnel boring machine are located on the South Portal pad. The tunnel boring machine is planned to be moved to the location of the Gate 510 area (DOE 2005b, Section 5.1.3). [Section 1.3.1](#) discusses plans to use the South Portal pad for construction of emplacement drifts.

1.1.9.3.2.3 Subdock Equipment Storage Area

The subdock equipment storage area ([Figure 1.1-155](#)) is located within the proposed land withdrawal area on the south side of H Road approximately 0.6 mi west of the North Portal. Facilities include unloading dock facilities and office trailers. The subdock equipment storage area provides space for the unloading of vehicles and the storage of material used for surface based testing and maintenance of facilities. Utilities provided are limited to electrical power (BSC 2005b, Section 6.2.10.1).

1.1.9.3.2.4 Rock Storage Area

The Rock Storage Area ([Figure 1.1-155](#)) is located within the proposed land withdrawal area south of the North Portal pad and west of the Topsoil Storage Area. It consists of approximately 1.3 acres of graded pad lined with a 40 mil polyvinyl chloride geomembrane liner. The Rock Storage Area is used to store rock originating from the ESF Starter Tunnel (BSC 2005b, Section 6.2.7).

1.1.9.3.2.5 Topsoil Storage Area

The Topsoil Storage Area ([Figure 1.1-155](#)) is located within the proposed land withdrawal area south of the North Portal pad and east of the Rock Storage Area. It is approximately 25 acres in size. The Topsoil Storage Area is unlined and is used to store topsoil originating from surface-disturbing activities that supported site characterization activities (BSC 2005b, Section 6.2.7). The stored soil is contoured to prevent erosion and excess runoff and stabilized by the presence of introduced plants and grasses. No structures, services, or utilities are present (BSC 2005c, Section 2.2.19).

1.1.9.3.2.6 Borrow Pit

The borrow pit ([Figure 1.1-155](#)) is located within the proposed land withdrawal area on the northeast side of Fran Ridge and occupies approximately 80 acres. The borrow pit has provided a source of aggregate for construction activities in support of ESF and surface based testing activities

and continues to provide a source of aggregate. The borrow pit is a standard aggregate production operation in keeping with industrial practice. No blasting is required to recover the aggregate from the borrow pit. A diesel generator provides power to the equipment and dust control water is drawn from an onsite tank. No outside service or utilities are available. Drinking water is provided in jugs, and portable toilet facilities are located nearby (BSC 2005b, Section 6.2.10.3; BSC 2005c, Section 2.5.2).

1.1.9.3.2.7 Water Supply System

The water supply system is located within the proposed land withdrawal area. It consists of wells UE-25 J-12 and UE-25 J-13, a groundwater distribution system, three nonpotable water storage tanks, a booster pump station and two booster tanks, a fire water storage tank, chlorination system, arsenic treatment system, a potable water storage tank, and connections to the water system on the North Portal pad. Water for the North Portal pad facilities originates from wells UE-25 J-12 and UE-25 J-13 (Figure 1.1-154), which are part of the Nevada Test Site water supply system, but are separately permitted for the Yucca Mountain public water system at the UE-25 J-13 pumphouse. Water is pumped from wells UE-25 J-12 or UE-25 J-13 into a 50,000 gal storage tank located at the pad for Well UE-25 J-13. Raw water is transferred from the storage tank at Well UE-25 J-13 to any of three 10,000-gal nonpotable water storage tanks (also referred to as baker tanks) located along H Road (Figure 1.1-155) or to two 20,000-gal booster tanks located at the Booster Pump Station south of the North Portal pad (Figure 1.1-155). Water in the nonpotable water storage tanks is transferred to trucks for dust suppression needs or other project-related activities. Water is pumped from the booster tanks to the 200,000-gal fire water storage tank atop Exile Hill (Figure 1.1-155) (BSC 2007l, Section 3).

Raw water in the public water distribution system is treated to produce potable water that meets federal and state regulatory requirements. Chlorination ensures that bacteriological contamination is not present in the potable water system. Arsenic treatment employing a fixed-bed system using granular ferric oxide reduces the arsenic content of the drinking water. The chlorination and arsenic treatment process to produce potable water occurs atop Exile Hill. Treated water is transferred to a 50,000 gal potable water storage tank on Exile Hill, which provides an on-demand supply of treated water to the North Portal pad facilities for restrooms, showers, and drinking water. The water storage area on Exile Hill is at an approximate elevation of 3,860 ft, providing adequate head pressure to the North Portal pad that is approximately 3,675 ft in elevation.

1.1.9.3.2.8 Surface Sanitation System

The surface sanitation system is made up of two major subsystems: a collection system, and a treatment system. The collection system is located at the North Portal pad and consists of piping and manholes. The collection system uses polyvinyl chloride piping designed to collect sanitary wastewater from each building on the North Portal pad. The main line piping is part of the buried utilities on the pad. The line is sloped to provide sufficient velocity to maintain solids in suspension. Manholes are provided as part of the collection system to allow access to the piping for maintenance. Each manhole is constructed of concrete approximately 48 in. in diameter with a watertight seal between the manhole and the sewer piping for leakage prevention. The treatment system is a below-ground septic tank and below-ground open leach field (Figure 1.1-155) located about 4,000 ft southeast of the North Portal on the northeast side of the Lower Muck Yard. The

treatment system is designed to accommodate the sewage from approximately 400 people per day. The septic tank is designed to contain 18,000 gal and is constructed of concrete. The dosing tank and dosing siphon, which are directly eastward from the septic tank, has the capacity to distribute sewage equally to all parts of the leach field at 3 to 4 hour intervals. The dosing tank feeds a set of distribution boxes, which in turn, distribute the sewage to the leach field. The leach field is constructed of 4-in. diameter, perforated and corrugated, polyvinyl chloride piping which disperses effluent into approximately 6 ft deep trenches containing clean aggregate (BSC 2005b, Section 6.2.3.5).

1.1.9.3.2.9 Waste Management Facility (Nonradioactive)

The Waste Management Facility (Figure 1.1-155) is located within the proposed land withdrawal area on the north side of H Road and approximately 0.6 mi west of the North Portal. The Waste Management Facility is the primary collection area and offsite shipment facility for nonhazardous and hazardous waste. Radioactive wastes are not handled at these facilities. The waste collection areas within the Waste Management Facility are divided into two distinct fenced areas, the Non-Hazardous Waste Management Area and the Project Accumulation Area. Electric power is provided to the offices, field lab, and yard. No water is piped to the yard. Drinking water is provided in jugs and portable toilet facilities are located nearby.

Waste types managed in the Non-Hazardous Waste Management Area include waste petroleum hydrocarbons, used batteries, oily rags, and oil-contaminated soil. The area also houses the oily water skimming system and the supply of barrels and tanks used to collect and store the various nonhazardous wastes. All fluid wastes are placed in secondary containment. The wastes are contained within a fenced area that is separate from the Project Accumulation Area (BSC 2005c, Section 2.5.5).

The Project Accumulation Area consists of four buildings, located inside a chain link fence, that are designed to house hazardous chemicals. The buildings are numbered 1 through 4 with signs displaying chemical hazard index ratings attached to each building (BSC 2005c, Section 2.5.5).

1.1.9.3.2.10 Terrestrial Ecosystems Yard

The Terrestrial Ecosystems Storage Yard (also known as the Environmental Storage Yard) (Figure 1.1-155) is located within the proposed land withdrawal area on the north side of H Road and approximately 0.9 mi west of the North Portal. This storage yard houses the reclamation materials, supplies, and equipment used to re-seed areas disturbed by testing, construction, and operations once they are no longer needed. Various farm implements, an office trailer, storage container, and hay storage are located at this site. Line power is provided to the office trailer. No water is piped to the yard. Drinking water is provided in jugs, and portable toilet facilities are located nearby (BSC 2005c, Section 2.5.6).

1.1.9.3.2.11 Heliport

The North Portal pad heliport (Figure 1.1-155) is located within the proposed land withdrawal area approximately 0.3 mi east of the North Portal. This facility is a concrete slab approximately 100 ft by 100 ft. A wheel-mounted fire extinguisher is present for emergencies. No outside service or

utilities are available (BSC 2005c, Section 2.5.9). It is intended to replace this facility with a new heliport located outside of the GROA as shown in [Figure 1.1-2](#).

1.1.9.3.2.12 Lower Muck Yard

An area originally known as the ESF Muck Storage Area, this area was designed as the primary storage location for tunnel muck. However, it was not used for this purpose (BSC 2005b, Section 6.1). The designed ESF Muck Storage Area was to be a triangular-shaped parcel of land located within the proposed land withdrawal area approximately 2,000 ft southeast of the North Portal pad and north of H Road. The southern portion of the ESF Muck Storage Area was cleared and partially graded (topsoil removed). This area has been used for parking and equipment storage (BSC 2005b, Section 6.2). It has since become known as the Lower Muck Yard ([Figure 1.1-155](#)). This area is the site for planned facilities to support DOE public outreach; the test coordination office; and the maintenance and repair of ESF SSCs, including the existing tunnel and ECRB Cross-Drift (BSC 2006b, Section 2.3).

1.1.9.3.2.13 Gate 510 (Guard Station 510)

Gate 510 (also known as Guard Station 510) provides the primary entrance point to proposed land withdrawal area for the Yucca Mountain Project. It was located at the southern boundary of proposed land withdrawal area along the Lathrop Wells Road ([Figure 1.1-154](#)). The guard station has been relocated temporarily to the north along the Lathrop Wells Road to allow for foundation and soils investigations and construction of a new facility at the original site on the southern boundary. A permanent 6-ft security fence extends for 1 mi in each direction from the Lathrop Wells Road along the proposed land withdrawal area border and a 4-ft temporary security fence runs parallel to the Lathrop Wells Road from the land withdrawal area boundary to within about 100 ft of the temporary guard station (BSC 2006c).

1.1.9.3.2.14 Communications System

Communication towers and associated equipment are located within the proposed land withdrawal area with separate towers at Gate 510 ([Figure 1.1-154](#)), on the Yucca Mountain crest ([Figure 1.1-155](#)), and on Exile Hill ([Figure 1.1-155](#)). This communication system supplies high-speed connectivity between the DOE facilities in Las Vegas and the North Portal pad. A fiber-optic line from the DOE facility in Las Vegas connects to the Gate 510 facility, which links to the Yucca Mountain crest tower via line-of-sight transmissions, which links to the Exile Hill tower via line-of-sight transmissions, which links to the North Portal pad via fiber-optic cable (DOE 2006; SNL 2007c).

Equipment at Gate 510 includes a prefabricated fiberglass shelter, a propane standby power generator, a 325-gal propane tank, and a 70-ft-tall galvanized steel tower mounted onto a concrete base. An electrical line provides power to the communications equipment with the propane generator supplying backup power. Equipment on the Yucca Mountain crest comprises a primary solar photovoltaic power system with storage batteries, a propane standby power generator, and a 250-gal propane fuel tank to supply the generator. The communications tower is 80 ft tall and is mounted on a concrete base. The facility is enclosed within chain-link fencing that is spaced away from the photovoltaic panels to eliminate shadows that would impact performance. Equipment on

Exile Hill consists of a prefabricated shelter, a 325-gal propane tank, a propane-powered generator, and a 70-ft-tall galvanized steel tower mounted onto a concrete base. A fiber-optic communications line runs from the top of Exile Hill to the North Portal pad in a conduit (DOE 2006; SNL 2007c; Spence 2006).

Agreements have been reached allowing DOE to install an antenna on an existing communications tower that is located offsite at the Nye County Sheriff's Office at Amargosa Valley. This antenna will provide a backup communications link with line-of-sight transmission to the tower on the Yucca Mountain crest in the event of in the event of any failure of the Gate 510 telecommunications system (DOE 2006).

1.1.9.4 Identification of Residual Radiation *[NUREG-1804, Section 2.1.1.1.3: AC 9(3)]*

The Nevada Test Site has been the subject of numerous aerial radiological surveys since 1962. Several of these covered portions of Area 25:

- A 1970 survey, by fixed-wing aircraft, reported a region of elevated activity in Fortymile Canyon (Hendricks and Riedhauser 2000, p. 35).
- A 1976 survey by helicopter did not detect any evidence of anomalous radioactivity—man-made activity—along Fortymile Canyon (Hendricks and Riedhauser 2000, p. 35; Tipton 1979, p. 9).
- A 1992 survey did not detect any regions of anomalous activity in Area 25 (Hendricks and Riedhauser 2000, p. 35).
- A 1994 survey did not detect any regions of anomalous activity within the proposed land withdrawal area in Area 25; however, two sites of man-made activity were detected in Area 25. Both of the sites were outside of the proposed land withdrawal area, at Test Cell A and Test Cell C ([Figure 1.1-154](#)) (Hendricks and Riedhauser 2000, p. 35).
- A 2006 radiological aerial survey was commissioned to examine the proposed land withdrawal area and the section of Area 25 where nuclear rocket testing activities were performed. The survey did not detect any regions of anomalous activity within the proposed land withdrawal area in Area 25. Five sites of man-made radiological activity were detected outside of the proposed land withdrawal area in Area 25 (Lyons and Hendricks 2006, Section 6.8). The locations of these sites ([Figure 1.1-154](#)) are:
 - Vicinity of Well UE-25 J-11
 - Radioactive material containers outside the Area 25 Radioactive Material Storage Facility storage yard
 - Nuclear furnace car within the Area 25 Radioactive Material Storage Facility storage yard

- Test Cell C Facility
- Test Cell A Facility.

Radiological preactivity surveys were routinely conducted prior to activities at Yucca Mountain. During a preactivity survey in 1991, an isolated piece of radioactive material that was believed to be present due to previous Nevada Test Site operational activities was recovered at reclamation trial area number 3, which is located within the proposed land withdrawal area on the east side of Fortymile Wash about 0.5 km north of well UE-25 J-13 (Sorensen 1991).

The Nevada Test Site has 19 onsite environmental sampling stations that include three that have only low-volume, air-particulate samplers, one that has only a tritium sampler, and 15 that have both air-particulate and tritium samplers. They are located throughout the Nevada Test Site in or near areas recognized as radiation sources. These include areas with radioactivity in surface soil that can be resuspended by the wind, tritium that transpires or evaporates from plants and soil at the sites of past nuclear cratering tests, and tritium that evaporates from ponds receiving tritiated water or from tunnels that cannot be sealed shut. Six of the 15 samplers that have both air-particulate and tritium samplers are located near the boundaries and the center of the Nevada Test Site and are approved by the Environmental Protection Agency as critical receptor samplers. Radionuclide concentrations measured at these six stations are used to assess compliance with the National Emission Standards For Hazardous Air Pollutants dose limit (Wills 2006, Section 3.1).

Monitoring is also performed on the Nevada Test Site with a surveillance network of thermoluminescent dosimeters. In 2005, there were 109 active environmental thermoluminescent dosimeter locations on the Nevada Test Site. These include the following types of locations (Wills 2006, Section 5.2):

- **Background**—10 locations where radiation effects from Nevada Test Site operations are negligible.
- **Environmental 1**—41 locations where there is no measurable radioactivity from past operations but which are of interest due to, either (1) the presence of personnel or the public in the area, or (2) the potential for receiving radiation exposure from a current operation.
- **Environmental 2**—35 locations where there is measurable added radioactivity from past operations and the locations are of interest due to (1) the potential for personnel to be in the area, and (2) the need to monitor exposure trends in the area.
- **Waste Operations**—17 locations in and around the Area 3 and Area 5 Radioactive Waste Management Sites.
- **Control**—6 locations in Mercury where control thermoluminescent dosimeters are kept in stable environments and are used as a quality check on the thermoluminescent dosimeters and the analysis process.

During calendar year 2005, sources of emissions on site at the Nevada Test Site were identified as (Wills 2006, Section 3.1.9):

- Tritium gas released from equipment calibrations
- Evaporation of tritiated water from containment ponds
- The evaporation and transpiration of tritiated water from soil and vegetation, respectively, at sites of past nuclear tests and from the Area 3 and Area 5 Radioactive Waste Management Sites
- The evaporation of tritiated water removed from the basement in the North Las Vegas Facility and transported to the Nevada Test Site for disposal in the Area 5 Sewage Lagoon
- Resuspension of plutonium and americium from soil contaminated by past nuclear testing.

The airborne emissions of tritiated water vapor from the containment ponds were conservatively reported as if the liquid discharges into the ponds had evaporated and become airborne. For tritiated water vapor diffusing from the Radioactive Waste Management Sites and nuclear explosion craters and for particulate resuspension of plutonium and americium from various areas on and near the Nevada Test Site, the airborne effluents were conservatively estimated from air sampling measurements. Total ^3H emissions from all sources was estimated to be 170 Ci in 2005, and those for $^{239+240}\text{Pu}$ and ^{241}Am were 0.29 and 0.047 Ci, respectively (Wills 2006, Table 3-13).

With regard to offsite releases, an oversight radiological air monitoring program is run by the Community Environmental Monitoring Program and is coordinated by the Desert Research Institute to provide monitoring for radionuclides that might be released from the Nevada Test Site. A network of 27 stations, located in selected towns and communities within 386 km from the Nevada Test Site, was operated during 2005. The stations monitored gross alpha and beta radioactivity in airborne particulates using low-volume particulate air samplers, penetrating gamma radiation using thermoluminescent dosimeters, gamma radiation exposure rates using pressurized ion chamber detectors, and meteorological parameters using automated weather instrumentation (Wills 2006, p. ii).

No airborne radioactivity related to historic or current Nevada Test Site operations was detected in any of the samples from the particulate air samplers during 2005. Gross alpha and gross beta radioactivity was detected at all stations at levels consistent with previous years and reflecting radioactivity from naturally occurring radioactive materials. The mean annual gross alpha activity across all sample locations was $1.80 \pm 0.54 \times 10^{-15} \mu\text{Ci/mL}$. The mean annual gross beta activity across all sample locations was $2.08 \pm 0.17 \times 10^{-14} \mu\text{Ci/mL}$. No man-made gamma-emitting radionuclides were detected (Wills 2006, p. iii).

An air sampling station that measures radionuclide air concentrations for the Nevada Test Site is located at the southern boundary of the proposed withdrawal area at Guard Station 510

(Figure 1.1-154). Average radionuclide concentrations for calendar years 2004 and 2005 were recorded and are shown in Table 1.1-88.

Each of these concentration averages are less than one-quarter of 1% of the compliance levels for the national emission standards for hazardous air pollutants (40 CFR 61, Appendix E).

There are no indications of residual radioactivity from previous land uses within the GROA. Locations of residual radioactivity from previous land uses within the proposed land withdrawal area and the existing access controls and precautions are discussed in Sections 1.1.9.1.3 and 1.1.9.1.4. Any residual radioactivity within the proposed land withdrawal area will make a negligible contribution to worker and public radiation exposure.

1.1.10 General References

55 FR 39152. Public Land Order 6802. Withdrawal of Public Land to Maintain the Physical Integrity of the Subsurface Environment, Yucca Mountain Project, Nevada.

67 FR 53359. Public Land Order No. 7534; Extension of Public Land Order No. 6802; Nevada.

Abrahamson, N.A. and Silva, W.J. 1997. "Empirical Response Spectral Attenuation Relations for Shallow Crustal Earthquakes." *Seismological Research Letters*, 68 (1), 94–127. El Cerrito, California: Seismological Society of America. TIC: 240553.

Albin, A.L.; Singleton, W.L.; Moyer, T.C.; Lee, A.C.; Lung, R.C.; Eatman, G.L.W.; and Barr, D.L. 1997. *Geology of the Main Drift—Station 28+00 to 55+00, Exploratory Studies Facility, Yucca Mountain Project, Yucca Mountain, Nevada*. Milestone SPG42AM3. Denver, Colorado: Bureau of Reclamation and U.S. Geological Survey. ACC: MOL.19970625.0096.

ANSI/ANS-2.8-1992. *American National Standard for Determining Design Basis Flooding at Power Reactor Sites*. La Grange Park, Illinois: American Nuclear Society. TIC: 236034.

ANSI/ANS-3.11-2000. *American National Standard for Determining Meteorological Information at Nuclear Facilities*. La Grange Park, Illinois: American Nuclear Society. TIC: 248540.

ANSI/ANS-3.11-2005. *American National Standard for Determining Meteorological Information at Nuclear Facilities*. La Grange Park, Illinois: American Nuclear Society. TIC: 258445.

Arthur, W.J., III 2004. "Air Quality Operating Permit AP9199-0573.01—Request to Delete Sources from the Permit." Letter from W.J. Arthur, III (DOE/ORD) to K. Regan (State of Nevada), May 17, 2004, 0518041627, MFR:OFO:MJC-1261. ACC: MOL.20040812.0036.

ASTM D 5741-96. 1998. *Standard Practice for Characterizing Surface Wind Using a Wind Vane and Rotating Anemometer*. West Conshohocken, Pennsylvania: American Society for Testing and Materials. TIC: 236772.

Belcher, W.R. 2004. *Death Valley Regional Ground-Water Flow System, Nevada and California—Hydrogeologic Framework and Transient Ground-Water Flow Model*. Scientific Investigations Report 2004-5205. Reston, Virginia: U.S. Geological Survey. ACC: MOL.20050323.0070.

Blair, S.C.; Kelly, J.M.; Pine, O.; Pletcher, R.; and Berge, P.A. 1996. *Effect of Radiation on the Mechanical Properties of Topopah Spring Tuff*. UCRL-ID-122899. Livermore, California: Lawrence Livermore National Laboratory. ACC: MOL.19961021.0132.

BLM (Bureau of Land Management) 1982. Patented Mining Claim Seal Date November 29, 1982. Patent Number: 27-83-0002. Reno, Nevada: Bureau of Land Management. ACC: MOL.20050913.0108.

BSC (Bechtel SAIC Company) 2002a. *Preliminary Hydrologic Engineering Studies for the North Portal Pad and Vicinity*. ANL-EBS-MD-000060 REV 00. Las Vegas, Nevada: Bechtel SAIC Company. ACC: MOL.20021028.0123.

BSC 2002b. *Geotechnical Data for a Potential Waste Handling Building and for Ground Motion Analyses for the Yucca Mountain Site Characterization Project*. ANL-MGR-GE-000003 REV 00. Las Vegas, Nevada: Bechtel SAIC Company. ACC: MOL.20021004.0078.

BSC 2002c. *Soils Report for North Portal Area, Yucca Mountain Project*. 100-00C-WRP0-00100-000-000. Las Vegas, Nevada: Bechtel SAIC Company. ACC: MOL.20021015.0323.

BSC 2003a. *Yucca Mountain Project Summary of Socioeconomic Data Analyses Conducted in Support of the Radiological Monitoring Program, During FY 2003*. TDR-MGR-EV-000040 REV 00. Las Vegas, Nevada: Bechtel SAIC Company. ACC: DOC.20031203.0003.

BSC 2003b. *Underground Layout Configuration*. 800-P0C-MGR0-00100-000-00E. Las Vegas, Nevada: Bechtel SAIC Company. ACC: ENG.20031002.0007.

BSC 2004a. *Yucca Mountain Site Description*. TDR-CRW-GS-000001 REV 02 ICN 01. Two volumes. Las Vegas, Nevada: Bechtel SAIC Company. ACC: DOC.20040504.0008.

BSC 2004b. *Hydrologic Engineering Studies for the North Portal Pad and Vicinity*. 000-00C-CD04-00100-000-00A. Las Vegas, Nevada: Bechtel SAIC Company. ACC: ENG.20040504.0005.

BSC 2004c. *Development of Numerical Grids for UZ Flow and Transport Modeling*. ANL-NBS-HS-000015 REV 02. Las Vegas, Nevada: Bechtel SAIC Company. ACC: DOC.20040901.0001.

BSC 2004d. *Drift Degradation Analysis*. ANL-EBS-MD-000027 REV 03. Las Vegas, Nevada: Bechtel SAIC Company. ACC: DOC.20040915.0010.

BSC 2004e. *Development of Earthquake Ground Motion Input for Preclosure Seismic Design and Postclosure Performance Assessment of a Geologic Repository at Yucca Mountain, NV.* MDL-MGR-GS-000003 REV 01. Las Vegas, Nevada: Bechtel SAIC Company. ACC: DOC.20041111.0006.

BSC 2004f. *Characterize Framework for Seismicity and Structural Deformation at Yucca Mountain, Nevada.* ANL-CRW-GS-000003 REV 00, with errata. Las Vegas, Nevada: Bechtel SAIC Company. ACC: MOL.20000510.0175; DOC.20040223.0007.

BSC 2004g. *Characterize Framework for Igneous Activity at Yucca Mountain, Nevada.* ANL-MGR-GS-000001 REV 02. Las Vegas, Nevada: Bechtel SAIC Company. ACC: DOC.20041015.0002.

BSC 2004h. *Ash Fall Hazard for North Portal Operations Area Facilities.* CAL-WHS-GS-000001 REV 00A. Las Vegas, Nevada: Bechtel SAIC Company. ACC: DOC.20041116.0001.

BSC 2004i. *Ventilation Model and Analysis Report.* ANL-EBS-MD-000030 REV 04. Las Vegas, Nevada: Bechtel SAIC Company. ACC: DOC.20041025.0002 .

BSC 2004j. *Mineralogic Model (MM3.0) Report.* MDL-NBS-GS-000003 REV 01. Las Vegas, Nevada: Bechtel SAIC Company. ACC: DOC.20040908.0006.

BSC 2004k. *Dose Rate Calculation for 21-PWR Waste Package.* 000-00C-DSU0-01800-000-00C. Las Vegas, Nevada: Bechtel SAIC Company. ACC: ENG.20041102.0003.

BSC 2004l. *Geologic Framework Model (GFM2000).* MDL-NBS-GS-000002 REV 02. Las Vegas, Nevada: Bechtel SAIC Company. ACC: DOC.20040827.0008.

BSC 2005a. *Peak Ground Velocities for Seismic Events at Yucca Mountain, Nevada.* ANL-MGR-GS-000004 REV 00. Las Vegas, Nevada: Bechtel SAIC Company. ACC: DOC.20050223.0002.

BSC 2005b. *Determination of Importance Evaluation for the Surface Exploratory Studies Facility.* BAB000000-01717-2200-00106 REV 03 ICN 03. Las Vegas, Nevada: Bechtel SAIC Company. ACC: DOC.20050822.0009.

BSC 2005c. *Safety Basis Report.* TDR-CRW-SE-000008 REV 01. Las Vegas, Nevada: Bechtel SAIC Company. ACC: SIT.20050919.0053.

BSC 2005d. *ESF As-Built Configuration.* 800-KMC-SSD0-00800-000-000. Las Vegas, Nevada: Bechtel SAIC Company. ACC: ENG.20050825.0005.

BSC 2006a. *TAD Source Term and Dose Rate Evaluation.* 000-30R-GGDE-00100-000-00A. Las Vegas, Nevada: Bechtel SAIC Company. ACC: ENG.20060831.0007.

BSC 2006b. *Lower Muck Yard Basis of Design.* 780-3DR-SB00-00100-000-001. Las Vegas, Nevada: Bechtel SAIC Company. ACC: ENG.20060830.0002.

BSC 2006c. *NTS Gate 510 Temporary Fencing & Guard Station Relocation Plan*. ESF-BSC-MISC-GENL-0011 REV 01. Las Vegas, Nevada: Bechtel SAIC Company. ACC: SIT.20060712.0039.

BSC 2007a. *Identification of Aircraft Hazards*. 000-30R-WHS0-00100-000-008. Las Vegas, Nevada: Bechtel SAIC Company. ACC: ENG.20070705.0002.

BSC 2007b. *Frequency Analysis of Aircraft Hazards for License Application*. 000-00C-WHS0-00200-000-00F. Las Vegas, Nevada: Bechtel SAIC Company. ACC: ENG.20070925.0012.

BSC 2007c. *Population Projections to 2075 for the Yucca Mountain Radiological Monitoring Grid*. 950-PSA-MGR0-00100-000 REV 000. Las Vegas, Nevada: Bechtel SAIC Company. ACC: ENG.20070905.0012.

BSC 2007d. *Quality Management Directive*. QA-DIR-10, Rev. 2. Las Vegas, Nevada: Bechtel SAIC Company. ACC: DOC.20080103.0002.

BSC 2007e. *Local Meteorology of Yucca Mountain, Nevada, 1994–2006*. TDR-MGR-MM-000002 REV 00. Las Vegas, Nevada: Bechtel SAIC Company. ACC: DOC.20070905.0008.

BSC 2007f. *Project Design Criteria Document*. 000-3DR-MGR0-00100-000-007. Las Vegas, Nevada: Bechtel SAIC Company. ACC: ENG.20071016.0005.

BSC 2007g. *Underground Layout Configuration for LA*. 800-KMC-SS00-00200-000-00B. Las Vegas, Nevada: Bechtel SAIC Company. ACC: ENG.20070727.0004.

BSC 2007h. *Yucca Mountain Project Drainage Report and Analysis*. 000-CDC-MGR0-00100-000-00A. Las Vegas, Nevada: Bechtel SAIC Company. ACC: ENG.20070924.0043.

BSC 2007i. *Subsurface Geotechnical Parameters Report*. ANL-SSD-GE-000001 REV 00. Las Vegas, Nevada: Bechtel SAIC Company. ACC: ENG.20070115.0006.

BSC 2007j. *Ground Control for Emplacement Drifts for LA*. 800-K0C-SSE0-00100-000-00C. Las Vegas, Nevada: Bechtel SAIC Company. ACC: ENG.20070925.0082.

BSC 2007k. *Supplemental Soils Report*. 100-S0C-CY00-00100-000-00D. Las Vegas, Nevada: Bechtel SAIC Company. ACC: ENG.20080102.0045.

BSC 2007l. *Public Water System Operations and Maintenance Manual*. MIS-PSP-OM-000001 REV. 0. Las Vegas, Nevada: Bechtel SAIC Company. ACC: DOC.20071024.0001.

BSC 2008a. *Industrial/Military Activity-Initiated Accident Screening Analysis*. 000-PSA-MGR0-01500-000-00A. Las Vegas, Nevada: Bechtel SAIC Company. ACC: ENG.20080204.0006.

BSC 2008b. *External Events Hazards Screening Analysis*. 000-00C-MGR0-00500-000-00C. Las Vegas, Nevada: Bechtel SAIC Company. ACC: ENG.20080219.0001.

BSC 2008c. *Supplemental Earthquake Ground Motion Input for a Geologic Repository at Yucca Mountain, NV*. MDL-MGR-GS-000007 REV 00. Las Vegas, Nevada: Bechtel SAIC Company. ACC: DOC.20080221.0001.

Budnitz, R.J.; Apostolakis, G.; Boore, D.M.; Cluff, L.S.; Coppersmith, K.J.; Cornell, C.A.; and Morris, P.A. 1997. *Recommendations for Probabilistic Seismic Hazard Analysis: Guidance on the Uncertainty and Use of Experts*. NUREG/CR-6372. Two volumes. Washington, D.C.: U.S. Nuclear Regulatory Commission. TIC: 235076.

Buesch, D.C. and Lung, R.C. 2008. *Update of Geotechnical Boreholes and Test Pit Program through 2007 in Midway Valley, Nevada*. Denver, Colorado: U.S. Geological Survey. ACC: LLR.20080121.0080.

Buesch, D.C.; Spengler, R.W.; Moyer, T.C.; and Geslin, J.K. 1996. *Proposed Stratigraphic Nomenclature and Macroscopic Identification of Lithostratigraphic Units of the Paintbrush Group Exposed at Yucca Mountain, Nevada*. Open-File Report 94-469. Denver, Colorado: U.S. Geological Survey. ACC: MOL.19970205.0061.

California Department of Finance 2007. "State Adds Almost 470,000 in 2006; 2007 Population Nears 37.7 Million." Sacramento, California: State of California Department of Finance, Demographic Research Unit. ACC: MOL.20070521.0095.

Camacho-Padrón, B.I. 2006. *Effect of Particle Cementation on the Stiffness of Uniform Sand as Measured with Stress Wave Velocities*. Ph.D. dissertation. Austin, Texas: University of Texas at Austin. TIC: 260003.

Campbell, K.W. and Bozorgnia, Y. 2003. "Updated Near-Source Ground Motion (Attenuation) Relations for the Horizontal and Vertical Components of Peak Ground Acceleration and Acceleration Response Spectra." *Bulletin of the Seismological Society of America*, 93 (1), 314–331. El Cerrito, California: Seismological Society of America. TIC: 259845.

Charles B. Reynolds & Associates. 1985. *Final Report, 1985 Repository Surface Facility Seismic Survey, Yucca Mountain Area, NTS, Nye County, Nevada*. Albuquerque, New Mexico: Charles B. Reynolds & Associates. ACC: MOL.19970415.0158.

Cikanek, E.M.; Grant, T.A.; and Blakely, R.J. 2004. *Data Qualification and Data Summary Report: Intact Rock Properties Data on Uniaxial Compressive Strength, Triaxial Compressive Strength, Friction Angle, and Cohesion*. TDR-MGR-GE-000003 REV 00, with errata. Las Vegas, Nevada: Bechtel SAIC Company. ACC: DOC.20040514.0003; DOC.20040506.0003; DOC.20031105.0007; DOC.20031007.0004; DOC.20030214.0007.

Clark County Department of Comprehensive Planning 2006. "Clark County, Nevada 2006 Resident Population Estimates." *Southern Nevada Consensus Population Estimate, July 2006*. Las Vegas, Nevada: Clark County Department for Comprehensive Planning. Accessed July 16, 2007. ACC: MOL.20070718.0163.

CO-PRO-1001, Rev. 2. *Control of Measuring and Test Equipment*. Las Vegas, Nevada: Bechtel SAIC Company. ACC: ENG.20070905.0001.

CRWMS M&O (Civilian Radioactive Waste Management System Management and Operating Contractor) 1996. *Probabilistic Volcanic Hazard Analysis for Yucca Mountain, Nevada*. BA0000000-01717-2200-00082 Rev 0. Las Vegas, Nevada: Civilian Radioactive Waste Management System Management and Operating Contractor. ACC: MOL.19971201.0221.

CRWMS M&O 1997a. *Engineering Design Climatology and Regional Meteorological Conditions Report*. B00000000-01717-5707-00066 REV 00. Las Vegas, Nevada: Civilian Radioactive Waste Management System Management and Operating Contractor. ACC: MOL.19980304.0028.

CRWMS M&O 1997b. *DBE/Scenario Analysis for Preclosure Repository Subsurface Facilities*. BCA000000-01717-0200-00017 REV 00. Las Vegas, Nevada: Civilian Radioactive Waste Management System Management and Operating Contractor. ACC: MOL.19980218.0237.

CRWMS M&O 1998a. *Probabilistic Seismic Hazard Analyses for Fault Displacement and Vibratory Ground Motion at Yucca Mountain, Nevada*. Milestone SP32IM3, September 23, 1998. Three volumes. Las Vegas, Nevada: Civilian Radioactive Waste Management System Management and Operating Contractor. ACC: MOL.19981207.0393.

CRWMS M&O 1998b. *Title III Evaluation for the North Portal Pad Drainage*. BABBB0000-01717-5705-00001 REV 00. Las Vegas, Nevada: Civilian Radioactive Waste Management and Operating Contractor. ACC: MOL.19981217.0063.

CRWMS M&O 1998c. *Off-Site Utilities Preliminary Assessment*. B00000000-01717-5705-00091 REV 00. Las Vegas, Nevada: Civilian Radioactive Waste Management System Management and Operating Contractor. ACC: MOL.19980519.0235.

CRWMS M&O 1999a. *Exploratory Studies Facility, South Portal Pad and Box-Cut Site and Grading Plan*. BAB000000-01717-2100-20210-01. Las Vegas, Nevada: Civilian Radioactive Waste Management System Management and Operating Contractor. ACC: MOL.19990817.0253.

CRWMS M&O 1999b. *Preliminary Geotechnical Investigation for Waste Handling Building, Yucca Mountain Site Characterization Project*. BCB000000-01717-5705-00016 Rev. 00. Las Vegas, Nevada: Civilian Radioactive Waste Management System Management and Operating Contractor. ACC: MOL.19990625.0182.

Darendeli, B.M. 2001. *Development of a New Family of Normalized Modulus Reduction and Material Damping Curves*. Ph.D. dissertation. Austin, TX: University of Texas at Austin. TIC: 259797.

Day, W.C.; Dickerson, R.P.; Potter, C.J.; Sweetkind, D.S.; San Juan, C.A.; Drake, R.M., II; and Fridrich, C.J. 1998. *Bedrock Geologic Map of the Yucca Mountain Area, Nye County, Nevada*. Geologic Investigations Series Map I-2627. Denver, Colorado: U.S. Geological Survey. ACC: MOL.19981014.0301.

Day, W.C.; Potter, C.J.; Sweetkind, D.S.; Dickerson, R.P.; and San Juan, C.A. 1998. *Bedrock Geologic Map of the Central Block Area, Yucca Mountain, Nye County, Nevada*. Miscellaneous Investigations Series Map I-2601. Washington, D.C.: U.S. Geological Survey. ACC: MOL.19980611.0339.

Deng, S.F.A. 2004a. "NOAA Tornado Data in Nevada (All Counties) between 01/01/1950 and 09/30/2003." Interoffice memorandum from S.F.A. Deng (BSC) to Record Processing Center, April 7, 2004, 0407041070, with attachment. ACC: MOL.20040407.0083; MOL.20040304.0081.

Deng, S.F.A. 2004b. "NOAA Tornado Data in California (Counties of Modoc, Lassen, Plumas, Sierra, Nevada, Placer, El Dorado, Alpine, Mono, Inyo, Amado, and San Bernardino) between 01/01/1950 and 09/30/2003." Interoffice memorandum from S.F.A. Deng (BSC) to Record Processing Center, April 7, 2004, 0407041067, with attachment. ACC: MOL.20040407.0082; MOL.20040304.0082.

Deng, S.F.A. 2004c. "NOAA Tornado Data in Mohave County of Arizona between 01/01/1950 and 09/30/2003." Interoffice memorandum from S.F.A. Deng (BSC) to Record Processing Center, April 7, 2004, 0407041072, with attachment. ACC: MOL.20040407.0085; MOL.20040304.0083.

Deng, S.F.A. 2004d. "NOAA Tornado Data in Utah (Counties of Box Elder, Tooele, Juab, Millard, Beaver, Iron and Washington) between 01/01/1950 and 09/30/2003." Interoffice memorandum from S.F.A. Deng (BSC) to Record Processing Center, April 7, 2004, 0407041071, with attachment. ACC: MOL.20040407.0084; MOL.20040304.0084.

Dixon, W.R. 1993. "Air Quality Permit Application for Concrete Batch Plant and Associated Radial Stacker Conveyer (SCP: N/A)." Letter from W.R. Dixon (DOE/YMSCO) to G. McCleary (State of Nevada), December 8, 1993, POCD:WRD-1090, with enclosures. ACC: NNA.19931222.0142.

DOE (U.S. Department of Energy) 1982. *Environmental Assessment for MX Experiment to Demonstrate Egress Feasibility, Little Skull Mountain, Area 25, Nevada Test Site*. DOE/EA-0189. Las Vegas, Nevada: U.S. Department of Energy. TIC: 210611.

DOE 1992. *Environmental Assessment for the Depleted Uranium Testing Program at the Nevada Test Site by the United States Army Ballistics Research Laboratory*. DOE/EA-0398. Las Vegas, Nevada: U.S. Department of Energy, Nevada Field Office. TIC: 206181.

DOE 1994. *Environmental Assessment for Hazardous Materials Testing at the Liquefied Gaseous Fuels Spill Test Facility, Frenchman Flat, Nevada Test Site*. DOE/EA-0864. Washington, D.C.: U.S. Department of Energy, Office of Fossil Energy. ACC: MOL.20040618.0207.

DOE 1996. *Final Environmental Impact Statement for the Nevada Test Site and Off-Site Locations in the State of Nevada*. DOE/EIS-0243. Las Vegas, Nevada: U.S. Department of Energy, Nevada Operations Office. ACC: MOL.20010727.0190; MOL.20010727.0191.

DOE 1999. "MX Missile, Shelter, Launch Methods Undergo Testing." Las Vegas, Nevada: U.S. Department of Energy. Accessed April 20, 2004. ACC: MOL.20040421.0046.

DOE 2000. *Nevada Test Site Contaminated Land Areas Report*. DOE/NV/11718-481. Two volumes. Las Vegas, Nevada: U.S. Department of Energy, Nevada Operations Office. TIC: 254345.

DOE 2001a. *Aerial Operations Facility, Nevada Test Site*. DOE/EA-1334. Las Vegas, Nevada: U.S. Department of Energy, Nevada Operations Office. ACC: MOL.20050418.0039.

DOE 2001b. *Corrective Action Investigation Plan for Corrective Action Unit 168: Areas 25 and 26 Contaminated Materials and Waste Dumps, Nevada Test Site, Nevada*. DOE/NV-780, Rev. 0. Las Vegas, Nevada: U.S. Department of Energy, National Nuclear Security Administration, Nevada Operations Office. ACC: MOL.20040426.0024.

DOE 2002a. *Yucca Mountain Science and Engineering Report*. DOE/RW-0539, Rev. 1. Washington, D.C.: U.S. Department of Energy, Office of Civilian Radioactive Waste Management. ACC: MOL.20020404.0042.

DOE 2002b. *Final Environmental Impact Statement for a Geologic Repository for the Disposal of Spent Nuclear Fuel and High-Level Radioactive Waste at Yucca Mountain, Nye County, Nevada*. DOE/EIS-0250. Washington, D.C.: U.S. Department of Energy, Office of Civilian Radioactive Waste Management. ACC: MOL.20020524.0314 through MOL.20020524.0320.

DOE 2002c. *Supplement Analysis for the Final Environmental Impact Statement for the Nevada Test Site and Off-Site Locations in the State of Nevada*. DOE/EIS-0243-SA-01. Las Vegas, Nevada: U.S. Department of Energy, National Nuclear Security Administration, Nevada Operations Office. ACC: MOL.20030409.0001.

DOE 2002d. *Corrective Action Investigation Plan for Corrective Action Unit 127: Areas 25 and 26 Storage Tanks Nevada Test Site, Nevada*. DOE/NV-833, Rev. 0. Las Vegas, Nevada: U.S. Department of Energy, National Nuclear Security Administration, Nevada Operations Office. ACC: MOL.20040401.0081.

DOE 2003a. *Draft Supplemental Programmatic Environmental Impact Statement on Stockpile Stewardship and Management for a Modern Pit Facility*. DOE/EIS-236-S2. Volume I. Washington, D.C.: U.S. Department of Energy, National Nuclear Security Administration. ACC: MOL.20041206.0114.

DOE 2003b. *National Center for Combating Terrorism Strategic Plan*. DOE/NV/11718-847. Las Vegas, Nevada: U.S. Department of Energy, National Nuclear Security Administration, Nevada Site Office. ACC: MOL.20070516.0138.

DOE 2003c. *Corrective Action Investigation Plan for Corrective Action Unit 214: Bunkers and Storage Areas Nevada Test Site, Nevada*. DOE/NV-893, Rev. 0. Las Vegas, Nevada: U.S. Department of Energy, National Nuclear Security Administration, Nevada Site Office. ACC: MOL.20040426.0025.

DOE 2003d. *Corrective Action Decision Document for Corrective Action Unit 127: Areas 25 and 26 Storage Tanks Nevada Test Site, Nevada*. DOE/NV-925, Rev. 0. Las Vegas, Nevada: U.S. Department of Energy, National Nuclear Security Administration, Nevada Site Office. ACC: MOL.20040426.0022.

DOE 2003e. *Corrective Action Investigation Plan for Corrective Action Unit 529: Area 25 Contaminated Materials Nevada Test Site, Nevada*. DOE/NV-870, Rev. 0. Las Vegas, Nevada: U.S. Department of Energy, National Nuclear Security Administration, Nevada Site Office. ACC: MOL.20040510.0204.

DOE 2004a. *Final Environmental Assessment for Activities Using Biological Simulants and Releases of Chemical at the Nevada Test Site*. DOE/EA-1494. Las Vegas, Nevada: U.S. Department of Energy, National Nuclear Security Administration, Nevada Site Office. ACC: MOL.20070517.0103.

DOE 2004b. *Radiological/Nuclear Countermeasures Test and Evaluation Complex, Nevada Test Site, Final Environmental Assessment*. DOE/EA-1499. Las Vegas, Nevada: U.S. Department of Energy, National Nuclear Security Administration, Nevada Site Office. ACC: MOL.20070516.0139.

DOE 2005a. *Criticality Experiments Facility Project*. DOE/NV-1063. Las Vegas, Nevada: U.S. Department of Energy, National Nuclear Security Administration, Nevada Site Office. ACC: MOL.20070516.0137.

DOE 2005b. *Office of Repository Development 10-Year Site Plan*. ORD 10-Year Site Plan, Rev. 0. Las Vegas, Nevada: U.S. Department of Energy, Office of Repository Development. ACC: MOL.20050509.0387.

DOE 2006. *Communication Site Plan of Development: U.S. Department of Energy, Office of Civilian Radioactive Waste Management Telecommunications Site at the Crest of Yucca Mountain*. Las Vegas, Nevada: U.S. Department of Energy, Office of Civilian Radioactive Waste Management. ACC: MOL.20070116.0003.

DOE 2007a. Waste Acceptance, Transportation, and Monitored Geologic Repository System Elements. Volume 2 of *Integrated Interface Control Document*. DOE/RW-0572, Rev. 0. Las Vegas, Nevada: U.S. Department of Energy, Office of Civilian Radioactive Waste Management. ACC: DOC.20070706.0001.

DOE 2007b. *Quality Assurance Requirements and Description*. DOE/RW-0333P, Rev. 19. Washington, D.C.: U.S. Department of Energy, Office of Civilian Radioactive Waste Management. ACC: DOC.20070717.0006.

DOE 2007c. *Preclosure Seismic Design and Performance Demonstration Methodology for a Geologic Repository at Yucca Mountain Topical Report*. YMP/TR-003-NP, Rev. 5. Las Vegas, Nevada: U.S. Department of Energy, Office of Civilian Radioactive Waste Management. ACC: DOC.20070625.0013.

Driesner, D. and Coyner, A. 2006. *Major Mines of Nevada 2005, Mineral Industries in Nevada's Economy*. Nevada Bureau of Mines and Geology Special Publication P-17. Reno, Nevada: University of Nevada, Reno, Mackay School of Mines. ACC: MOL.20070517.0101.

Eglinton, T.W. and Dreicer, R.J. 1984. *Meteorological Design Parameters for the Candidate Site of a Radioactive-Waste Repository at Yucca Mountain, Nevada*. SAND84-0440/2. Albuquerque, New Mexico: Sandia National Laboratories. ACC: NNA.19870407.0048.

EPA (U.S. Environmental Protection Agency) 2000. *Meteorological Monitoring Guidance for Regulatory Modeling Applications*. EPA-454/R-99-005. Research Triangle Park, North Carolina: U.S. Environmental Protection Agency. TIC: 253879.

EPRI (Electric Power Research Institute) 1993. *Appendices for Ground Motion Estimation*. Volume 2 of *Guidelines for Determining Design Basis Ground Motions*. EPRI TR-102293. Palo Alto, California: Electric Power Research Institute. TIC: 226496.

EV-PRO-5001, Rev. 3. *Tests and Checks of Meteorological Measuring and Test Equipment*. Las Vegas, Nevada: Bechtel SAIC Company. ACC: DOC.20070412.0012.

EV-PRO-5002, Rev. 4. *Tests, Checks, and Performance Audits of Meteorological Equipment*. Las Vegas, Nevada: Bechtel SAIC Company. ACC: DOC.20070412.0013.

EV-PRO-5003, Rev. 3. *Routine Operations and Maintenance of Meteorological Equipment*. Las Vegas, Nevada: Bechtel SAIC Company. ACC: DOC.20070412.0014.

EV-PRO-5004, Rev. 3. *Meteorological Data Processing*. Las Vegas, Nevada: Bechtel SAIC Company. ACC: DOC.20070412.0015.

FAA (Federal Aviation Administration) 2002. *Final Environmental Assessment for the Site, Launch, Reentry and Recovery Operations at the Kistler Launch Facility, Nevada Test Site (NTS)*. Volume 1. Washington, D.C.: U.S. Department of Transportation, Federal Aviation Administration. TIC: 252956.

FAA 2007. *2007 U.S. Commercial Space Transportation Developments and Concepts: Vehicles, Technologies, and Spaceports*. Washington, D.C.: Federal Aviation Administration. ACC: MOL.20070420.0560.

Fransioli, P. 2007. "Max 24-hr Precip." E-mail from P. Fransioli to A. Matthusen, December 18, 2007. ACC: MOL.20071228.0320.

Friesen, H. N. 1995. *Radiological Effluents Released from Nuclear Rocket and Ramjet Engine Tests at the Nevada Test Site, 1959 through 1969, Fact Book*. DOE/NV-401. Las Vegas, Nevada: U.S. Department of Energy, Nevada Operations Office. ACC: MOL.20040506.0038.

Fultyn, R.V. 1968. *Environmental Effects of the Kiwi-TNT Effluent: A Review and Evaluation*. LA-3449. Los Alamos, New Mexico: University of California, Los Alamos Scientific Laboratory. TIC: 226015.

Gibson, J.D.; Swan, F.H.; Wesling, J.R.; Bullard, T.F.; Perman, R.C.; Angell, M.M.; and DiSilvestro, L.A. 1992. *Summary and Evaluation of Existing Geological and Geophysical Data near Prospective Surface Facilities in Midway Valley, Yucca Mountain Project, Nye County, Nevada*. SAND90-2491. Albuquerque, New Mexico: Sandia National Laboratories. ACC: NNA.19910709.0001.

Grossman, R.F. 2005. *National Emission Standards for Hazardous Air Pollutants Calendar Year 2004*. DOE/NV/11718-1065. Las Vegas, Nevada: U.S. Department of Energy, National Nuclear Security Administration, Nevada Site Office. ACC: MOL.20070516.0136.

Grossman, R.F. 2006. *National Emission Standards for Hazardous Air Pollutants Calendar Year 2005*. DOE/NV/11718-1135. Las Vegas, Nevada: U.S. Department of Energy, National Nuclear Security Administration, Nevada Site Office. ACC: MOL.20070516.0074.

Hamilton-Ray, B.V. 2007. "Contracting Officer Authorization to Bechtel SAIC Company, LLC (BSC), Directing BSC to Consider Interface Requirements and Include Utility Feed Connections from the Monitored Geological Repository to the Transportation Facilities, Contract No. DE-AC28-01RW12101, LTR. No. 07-020." Letter from B.V. Hamilton-Ray (DOE/OCRWM) to T.C. Feigenbaum (BSC), May 9, 2007, 0509070891, OCE:SB-0992. ACC: CCU.20070509.0005.

Hansen, E.M.; Schwarz, F.K.; and Riedel, J.T. 1977. *Probable Maximum Precipitation Estimates, Colorado River and Great Basin Drainages*. Hydrometeorological Report No. 49. Silver Spring, Maryland: U.S. Department of Commerce, National Oceanic and Atmospheric Administration. TIC: 220224.

Harrington, C.D.; Whitney, J.W.; Jull, A.J.T.; and Phillips, W. 2000. "Cosmogenic Dating and Analysis of Scarps Along the Solitario Canyon and Windy Wash Faults, Yucca Mountain, Nevada." Chapter G of *Geologic and Geophysical Characterization Studies of Yucca Mountain, Nevada, A Potential High-Level Radioactive-Waste Repository*. Whitney, J.W., and Keefer, W.R., eds. Digital Data Series 058. Denver, Colorado: U.S. Geologic Survey. ACC: MOL.20010627.0275.

Hendricks, T.J. and Riedhauser, S.R. 2000. *An Aerial Radiological Survey of the Nevada Test Site*. DOE/NV/11718-324. Las Vegas, Nevada: U.S. Department of Energy, Nevada Operations Office. TIC: 255734.

Hoek, E. 2000. *Practical Rock Engineering*. Toronto, Ontario, Canada: RocScience. TIC: 253544.

- Hoek, E.; Carranza-Torres, C.; and Corkum, B. 2002. "Hoek-Brown Failure Criterion—2002 Edition." *5th North American Rock Mechanics Symposium and 17th Tunneling Association of Canada Conference: NARMS-TAC, July 7–10, 2002, University of Toronto*. 267-271. Toronto, Ontario, Canada: Rocscience. TIC: 253954.
- Jacobs, W.R. 2004. "Report on Decisions—Proposed Land Withdrawal." Interoffice memorandum from W.R. Jacobs (BSC) to E.W. McCann (BSC), April 20, 2004, 0420041227, with attachment. ACC: MOL.20040429.0082.
- Keefer, W.R.; Whitney, J.W.; and Taylor, E.M., eds. 2004. *Quaternary Paleoseismology and Stratigraphy of the Yucca Mountain Area, Nevada*. Professional Paper 1689. Reston, Virginia: U.S. Geological Survey. ACC: MOL.20050512.0077.
- Kistler Aerospace 2003. "Kistler Aerospace Corporation Restructures Its Finances to Achieve the Reusable Launch Vehicle's First Flight." News Release, July 15, 2003. Kirkland, Washington: Kistler Aerospace. Accessed April 21, 2004. TIC: 256006.
- Kotra, J.P.; Lee, M.P.; Eisenberg, N.A.; and DeWispelare, A.R. 1996. *Branch Technical Position on the Use of Expert Elicitation in the High-Level Radioactive Waste Program*. NUREG-1563. Washington, D.C.: U.S. Nuclear Regulatory Commission. TIC: 226832.
- Kruzic, M.; Nelson, J.; and Simonsen, R. 2007. *Nuclear Rocket Facility Decommissioning Project: Controlled Explosive Demolition of Neutron-Activated Shield Wall*. DOE/NV/25946–114. Washington, D.C.: U.S. Department of Energy. ACC: MOL.20070605.0062.
- La Camera, R.J.; Locke, G.L.; and Habte, A.M. 2005. *Selected Ground-Water Data for Yucca Mountain Region, Southern Nevada and Eastern California, January–December 2003*. Open-File Report 2005-1286. Carson City, Nevada: U.S. Geological Survey. ACC: MOL.20070517.0100.
- La Camera, R.J.; Locke, G.L.; Habte, A.M.; and Darnell, J.G. 2006. *Selected Ground-Water Data for Yucca Mountain Region, Southern Nevada and Eastern California, January–December 2004*. Open-File Report 2006-1285. Carson City, Nevada: U.S. Geological Survey. ACC: MOL.20070212.0119.
- Locke, G.L. and La Camera, R.J. 2003. *Selected Ground-Water Data for Yucca Mountain Region, Southern Nevada and Eastern California, January 2000–December 2002*. Open-File Report 03-387. Carson City, Nevada: U.S. Geological Survey. ACC: MOL.20040209.0318.
- LP-GEO-002Q-BSC, Rev. 0, ICN 1. *Laboratory Dynamic Rock/Soil Testing*. Washington, D.C.: U.S. Department of Energy, Office of Civilian Radioactive Waste Management. ACC: MOL.20010406.0165.
- Luckey, R.R.; Tucci, P.; Faunt, C.C.; Ervin, E.M.; Steinkampf, W.C.; D'Agnesse, F.A.; and Patterson, G.L. 1996. *Status of Understanding of the Saturated-Zone Ground-Water Flow System at Yucca Mountain, Nevada, as of 1995*. Water-Resources Investigations Report 96-4077. Denver, Colorado: U.S. Geological Survey. ACC: MOL.19970513.0209.

Lyons, C. and Hendricks, T. 2006. *An Aerial Radiological Survey of the Yucca Mountain Project Proposed Land Withdrawal and Adjacent Areas*. DOE/NV/11718-1258. Las Vegas, Nevada: U.S. Department of Energy, National Nuclear Security Administration. ACC: MOL.20061025.0035.

Majer, E.L.; Feighner, M.; Johnson, L.; Daley, T.; Karageorgi, E.; Lee, K.H.; Williams, K.; and McEvelly, T. 1996. *Surface Geophysics*. Volume 1 of *Synthesis of Borehole and Surface Geophysical Studies at Yucca Mountain, Nevada and Vicinity*. Milestone OB05M. Berkeley, California: Lawrence Berkeley National Laboratory. ACC: MOL.19970610.0150.

McGuire, R.K.; Silva, W.J.; and Costantino, C.J. 2001. *Technical Basis for Revision of Regulatory Guidance on Design Ground Motions: Hazard- and Risk-Consistent Ground Motion Spectra Guidelines*. NUREG/CR-6728. Washington, D.C.: U.S. Nuclear Regulatory Commission. TIC: 251294.

McKeown, M. 1992. *Soil and Rock Geotechnical Investigations Field and Laboratory Studies, North Ramp Surface Facility Exploratory Studies Facility, Yucca Mountain Project, Nevada*. Technical Memorandum 3610-92-35. Denver, Colorado: U.S. Department of Interior, Bureau of Reclamation. ACC: NNA.19930607.0020.

Mongano, G.S.; Singleton, W.L.; Moyer, T.C.; Beason, S.C.; Eatman, G.L.W.; Albin, A.L.; and Lung, R.C. 1999. *Geology of the ECRB Cross Drift—Exploratory Studies Facility, Yucca Mountain Project, Yucca Mountain, Nevada*. Deliverable SPG42GM3. Denver, Colorado: U.S. Geological Survey. ACC: MOL.20000324.0614.

Moyer, T.C.; Geslin, J.K.; and Flint, L.E. 1996. *Stratigraphic Relations and Hydrologic Properties of the Paintbrush Tuff Nonwelded (PTn) Hydrologic Unit, Yucca Mountain, Nevada*. Open-File Report 95-397. Denver, Colorado: U.S. Geological Survey. ACC: MOL.19970204.0216.

Nevada Department of Taxation and Nevada State Demographer 2007. *Governor Certified Population of Nevada's Counties, Cities and Towns 2000 to 2006*. Reno, Nevada: University of Nevada, Reno. ACC: MOL.20070824.0048.

Nevada Division of Environmental Protection 2000a. Permit for a Hazardous Waste Management Facility, United States Department of Energy, Nevada Operations Office. Permit Number: NEV HW009. Carson City, Nevada: Nevada Division of Environmental Protection. ACC: MOL.20041006.0266.

Nevada Division of Environmental Protection 2000b. Research, Development and Demonstration Permit for the Tactical Development and Demonstration Project for Demilitarization Activities. Permit Number: RD&D #1. Carson City, Nevada: Nevada Division of Environmental Protection Bureau of Federal Facilities. ACC: MOL.20041006.0265.

Nevada Rail Partners 2007. *Facilities Design Analysis Report Caliente Rail Corridor, Task 10: Facilities, Rev. 03*. Document No. NRP-R-SYSW-FA-0001-03. Las Vegas, Nevada: Nevada Rail Partners. ACC: ENG.20070606.0020.

- NNSA (National Nuclear Security Administration) 2004. *Corrective Action Decision Document/Closure Report for Corrective Action Unit 529: Area 25 Contaminated Materials, Nevada Test Site, Nevada*. DOE/NV-1000-Rev. 1. Las Vegas, Nevada: U.S. Department of Energy, National Nuclear Security Administration. ACC: MOL.20070618.0021.
- NNSA 2005. "Atlas Resumes Experimental Work at the Nevada Test Site." *Nevada Site Office News*. NV-05-22. Las Vegas, Nevada: National Nuclear Security Administration, Nevada Site Office. ACC: MOL.20070517.0099.
- NRC (U.S. Nuclear Regulatory Commission) 1987. *Standard Review Plan for the Review of Safety Analysis Reports for Nuclear Power Plants*. NUREG-0800. LWR Edition. Washington, D.C.: U.S. Nuclear Regulatory Commission. TIC: 203894.
- NRC 2007. "Seismic System Analysis." Section 3.7.2 of *Standard Review Plan*. NUREG-0800, Rev. 3. Washington, D.C.: U.S. Nuclear Regulatory Commission. ACC: MOL.20070521.0105.
- NWI-SPO-004Q, Rev. 0. *Laboratory Dynamic Rock/Soil Testing*. Las Vegas, Nevada: Civilian Radioactive Waste Management System Management and Operating Contractor. ACC: MOL.19990317.0325.
- O'Leary, D.W.; Mankinen, E.A.; Blakely, R.J.; Langenheim, V.E.; and Ponce, D.A. 2002. *Aeromagnetic Expression of Buried Basaltic Volcanoes Near Yucca Mountain, Nevada*. Open-File Report 02-020. Denver, Colorado: U.S. Geological Survey. ACC: MOL.20020627.0225.
- Orrell, S.A. 2007. "Preliminary 2007 Geotechnical Drilling Results from the U.S.G.S for the Waste Handling Buildings and Aging Pad Areas." Letter from S.A. Orrell (SNL) to R.J. Tosetti (BSC), May 29, 2007, 07_631_YMP-LL_05-29-2007, with enclosure. ACC: LLR.20070531.0001.
- Perry, F.V. and Crowe, B.M. 1987. *Preclosure Volcanic Effects: Evaluations for a Potential Repository Site at Yucca Mountain, Nevada*. Los Alamos, New Mexico: Los Alamos National Laboratory. ACC: NNA.19900112.0341.
- Perry, F.V.; Crowe, B.M.; Valentine, G.A.; and Bowker, L.M., eds. 1998. *Volcanism Studies: Final Report for the Yucca Mountain Project*. LA-13478. Los Alamos, New Mexico: Los Alamos National Laboratory. TIC: 247225.
- Porter, R.D. 2002. "FW: R-2502N/E AUR." E-mail from R.D. Porter to J. Ziegler (BSC), March 27, 2002, with attachments. ACC: MOL.20020515.0095.
- Potter, C.J.; Day, W.C.; Sweetkind, D.S.; and Dickerson, R.P. 1996. "Fault Styles and Strain Accommodation in the Tiva Canyon Tuff, Yucca Mountain, Nevada." *Eos, Transactions (Supplement)*, 77 (17), S265. Washington D.C.: American Geophysical Union. TIC: 234819.
- Potter, C.J.; Dickerson, R.P.; and Day, W.C. 1999. *Nature and Continuity of the Sundance Fault*. Open-File Report 98-266. Denver, Colorado: U.S. Geological Survey. TIC: 246609.

Potter, C.J.; Dickerson, R.P.; Sweetkind, D.S.; Drake, R.M., II; Taylor, E.M.; Fridrich, C.J.; San Juan, C.A.; and Day, W.C. 2002. *Geologic Map of the Yucca Mountain Region, Nye County, Nevada*. Geologic Investigations Series I-2755. Denver, Colorado: U.S. Geological Survey. TIC: 253945.

Randerson, D. and Sanders, J.B. 2002. *Characterization of Cloud-to-Ground Lightning Flashes on the Nevada Test Site*. NOAA Technical Memorandum OAR ARL-242. Silver Spring, Maryland: U.S. Dept. of Commerce, National Oceanic and Atmospheric Administration. ACC: MOL.20070227.0026.

Regulatory Guide 1.165. 1997. *Identification and Characterization of Seismic Sources and Determination of Safe Shutdown Earthquake Ground Motion*. Washington, D.C.: U.S. Nuclear Regulatory Commission. TIC: 233774.

Regulatory Guide 1.23. 1972. *Onsite Meteorological Programs*. Washington, D.C.: U.S. Atomic Energy Commission. TIC: 2937.

Regulatory Guide 1.23, Rev. 1. 2007. *Meteorological Monitoring Programs for Nuclear Power Plants*. Washington, D.C.: U.S. Nuclear Regulatory Commission. ACC: MOL.20070926.0187.

Regulatory Guide 4.2, Rev. 2. 1976. *Preparation of Environmental Reports for Nuclear Power Stations*. Washington, D.C.: U.S. Nuclear Regulatory Commission. ACC: HQS.19880517.2783.

Resource Conservation and Recovery Act of 1976. 42 U.S.C. 6901 et seq.

Riggins, M. 1994a. "Geotechnical Engineering Investigation for the Proposed Booster Pump Station." Letter from M. Riggins (SNL) to H. Montalvo (Fluor Daniel), September 16, 1994, with enclosures. ACC: MOL.19941116.0075.

Riggins, M. 1994b. "Geotechnical Engineering Investigation for the Proposed Water Storage Tanks at the Booster Pump Station and North Portal on Exile Hill." Letter from M. Riggins (SNL) to H. Montalvo (Fluor Daniel), November 3, 1994, with enclosures. ACC: MOL.19950208.0151.

Riggins, M. 1995. "Geotechnical Engineering Investigation for the Proposed Muck Conveyor Foundations at the ESF." Letter from M. Riggins (SNL) to M. Taylor (Morrison-Knudsen), April 18, 1995, with enclosures. ACC: MOL.19950815.0024 to MOL.19950815.0028.

Rousseau, J.P.; Kwicklis, E.M.; and Gillies, D.C., eds. 1999. *Hydrogeology of the Unsaturated Zone, North Ramp Area of the Exploratory Studies Facility, Yucca Mountain, Nevada*. Water-Resources Investigations Report 98-4050. Denver, Colorado: U.S. Geological Survey. ACC: MOL.19990419.0335.

Sanders, F.W. 1967. *Decontamination of Test Cell "C" at the Nuclear Rocket Development Station After a Reactor Accident*. LA-3633-MS. Los Alamos, New Mexico: University of California, Los Alamos Scientific Laboratory. ACC: MOL.20040511.0071.

Sawyer, D.A.; Fleck, R.J.; Lanphere, M.A.; Warren, R.G.; Broxton, D.E.; and Hudson, M.R. 1994. "Episodic Caldera Volcanism in the Miocene Southwestern Nevada Volcanic Field: Revised Stratigraphic Framework, $^{40}\text{Ar}/^{39}\text{Ar}$ Geochronology, and Implications for Magmatism and Extension." *Geological Society of America Bulletin*, 106 (10), 1304–1318. Boulder, Colorado: Geological Society of America. TIC: 222523.

Seed, H.B.; Wong, R.T.; Idriss, I.M.; and Tokimatsu, K. 1986. "Moduli and Damping Factors for Dynamic Analyses of Cohesionless Soils." *Journal of Geotechnical Engineering*, 112 (9), 1018–1033. New York, New York: American Society of Civil Engineers. TIC: 243355.

SNL (Sandia National Laboratories) 1997. *Hydraulic Fracturing Stress Measurements in Test Hole ESF-AOD-HDFR#1, Thermal Test Facility, Exploratory Studies Facility at Yucca Mountain*. WA-0065. Albuquerque, New Mexico: Sandia National Laboratories. TIC: 237818.

SNL 2007a. *Analysis of Dust Deliquescence for FEP Screening*. ANL-EBS-MD-000074 REV 01 ADD 01. Las Vegas, Nevada: Sandia National Laboratories. ACC: DOC.20070911.0004.

SNL 2007b. *Engineered Barrier System: Physical and Chemical Environment*. ANL-EBS-MD-000033 REV 06. Las Vegas, Nevada: Sandia National Laboratories. ACC: DOC.20070907.0003.

SNL 2007c. *Determination of Importance Evaluation for Communications Towers on the Crest of Yucca Mountain and on Exile Hill*. DIE-MGR-PA-000001 REV 00. Las Vegas, Nevada: Sandia National Laboratories. ACC: DOC.20070411.0001.

SNL 2008a. *Technical Report: Geotechnical Data for a Geologic Repository at Yucca Mountain, Nevada*. TDR-MGR-GE-000010 REV 00. Las Vegas, Nevada: Sandia National Laboratories. ACC: DOC.20080206.0001.

SNL 2008b. *Multiscale Thermohydrologic Model*. ANL-EBS-MD-000049 REV 03 ADD 02. Las Vegas, Nevada: Sandia National Laboratories. ACC: DOC.20080201.0003.

SNL 2008c. *Features, Events, and Processes for the Total System Performance Assessment: Analyses*. ANL-WIS-MD-000027 REV 00. Las Vegas, Nevada: Sandia National Laboratories. ACC: DOC.20080307.0003.

Sorensen, C.D. 1991. "Radiological Preactivity Survey for Proposed Activities by EG&G/EM for Conducting Reclamation Trials (Action Item TMSS-1991-00216), Contract #DE-AC08-87NV10576." Letter from C.D. Sorensen (SAIC) to C.P. Gertz (DOE/YMSCO), October 10, 1991, CDS:JKP;jh:L91-4375. ACC: NNA.19911021.0018.

Spence, R. E. 2006. "Second Partial Approval of Land Access And Environmental Compliance (EC) For Gate 510 Telecommunication Site (Case 06-002.00)." Letter from R. E. Spence (DOE/YMSOO) to L. I. Scanlan (Catapult Technology), August 15, 2006, 0816069225, YMSOO:MJC-1376, with enclosures. ACC: CCU.20060816.0012.

Stokoe, K.H., II.; Hwang, S-K.; Roesset, J.M.; and Sun, C.W. 1994. "Laboratory Measurement of Small-Strain Material Damping of Soil Using a Free-Free Resonant Column." *Earthquake Resistant Construction and Design, Proceedings of the Second International Conference on Earthquake Resistant Construction and Design, Berlin, 15-17 June 1994*. Savidis, S.A., ed. 195–202. Rotterdam, The Netherlands: A.A. Balkema. TIC: 251641.

Strauss, T. 2007. Geotechnical Laboratory Tests Performed on Sonic Tube Drill Core Samples. Scientific Notebook SN-USGS-SCI-144-V1. Pages 1-52. ACC: MOL.20070821.0128.

Sweetkind, D.S.; Potter, C.J.; and Verbeek, E.R. 1996. "Interaction Between Faults and the Fracture Network at Yucca Mountain, Nevada." *Eos, Transactions (Supplement)*, 77 (17), S266. Washington, D.C.: American Geophysical Union. TIC: 236789.

Sweetkind, D.S.; Barr, D.L.; Polacsek, D.K.; and Anna, L.O. 1997. *Administrative Report: Integrated Fracture Data in Support of Process Models, Yucca Mountain, Nevada*. Milestone SPG32M3. Denver, Colorado: U.S. Geological Survey. ACC: MOL.19990825.0109.

Throckmorton, C.K. and Verbeek, E.R. 1995. *Joint Networks in the Tiva Canyon and Topopah Spring Tuffs of the Paintbrush Group, Southwestern Nevada*. Open-File Report 95-2. Denver, Colorado: U.S. Geological Survey. TIC: 235000.

Tipton, W.J. 1979. *An Aerial Radiological Survey of Areas 25 and 26, Nevada Test Site*. EGG-1183-1745. Las Vegas, Nevada: EG&G, Energy Measurements Group. TIC: 206237.

USBR 5000-86. *Procedure for Determining Unified Soil Classification (Laboratory Method)*. Denver, Colorado: U.S. Department of the Interior, Bureau of Reclamation. TIC: 232041.

USBR 5005-86. *Procedure for Determining Unified Soil Classification (Visual Method)*. Denver, Colorado: U.S. Department of the Interior, Bureau of Reclamation. TIC: 232041.

USBR 7205-89. *Procedure for Determining Unit Weight of Soils In-Place by the Sand-Cone Method*. Denver, Colorado: U.S. Department of the Interior, Bureau of Reclamation. TIC: 232041.

USBR 7221-89. 1990. *Procedure for Determining Unit Weight of Soils In-Place by the Water Replacement Method in a Test Pit*. Denver, Colorado: U.S. Department of the Interior, Bureau of Reclamation. TIC: 232041.

Velsko, C.A.; Watkins, B.E.; Pruneda, C.O.; Stephens, J.R.; and Lipkin, J. 1999. *Emissions Characterization in the Contained Underground Demilitarization Laboratory at the Nevada Test Site*. UCRL-JC-126887. Livermore, California: Lawrence Livermore National Laboratory. ACC: MOL.20040426.0026.

Voegele, M.D. 1993. "Photogeologic Reconnaissance of X-Tunnel at Little Skull Mountain." *High Level Radioactive Waste Management: Proceedings of the Fourth Annual International Conference, Las Vegas, Nevada, April 26–30, 1993, 1*, 182–187. La Grange Park, Illinois: American Nuclear Society. TIC: 208542.

Wade, S.A. 2002. "2001 Actual Production/Emissions Reporting Form for the Yucca Mountain Site Characterization Project Air Quality Operating Permit AP9199-0573.01." Letter from S.A. Wade (DOE/YMSCO) to M.J. Elges (State of Nevada), February 27, 2002, OPE:MJC-0683, with enclosure. ACC: MOL.20020430.0298.

Wade, S.A. 2003. "2002 Actual Production/Emissions Reporting Form for Air Quality Operating Permit AP9199-0573.01." Letter from S.A. Wade (DOE/ORD) to M. Moghimi (State of Nevada), February 24, 2003, 0225036219, OFO:MJC-0727, with enclosure. ACC: MOL.20030401.0020.

Wade, S.A. 2004. "2003 Actual Production/Emissions Reporting Form for Class II Air Quality Operating Permit AP9199-0573.01." Letter from S.A. Wade (DOE/ORD) to M.J. Elges (State of Nevada), February 23, 2004, 0225040563, MFR:OFO:MJC-0765, with enclosure. ACC: MOL.20040322.0436.

Wills, C.A. 2005. *Nevada Test Site Environmental Report 2004*. DOE/NV/11718-1080. Las Vegas, Nevada: U.S. Department of Energy, National Nuclear Security Administration, Nevada Site Office. ACC: MOL.20060417.0025.

Wills, C.A. 2006. *Nevada Test Site Environmental Report 2005*. DOE/NV/11718-1214-ATT A. Las Vegas, Nevada: U.S. Department of Energy, National Nuclear Security Administration. ACC: MOL.20070718.0188.

YMP (Yucca Mountain Site Characterization Project) 1997. *Methodology to Assess Fault Displacement and Vibratory Ground Motion Hazards at Yucca Mountain*. Topical Report YMP/TR-002-NP, Rev. 1. Las Vegas, Nevada: Yucca Mountain Site Characterization Office. ACC: MOL.19971016.0777.

YMP-USGS-GP-57, R0. *Determining Unified Soil Classification (Visual Method)*. Denver, Colorado: U.S. Geological Survey. ACC: MOL.20050303.0107.

YMPB-USGS-GP-57, R0. *Determining Unified Soil Classification (Visual Method)*. Denver, Colorado: U.S. Geological Survey. ACC: MOL.20070418.0120.

INTENTIONALLY LEFT BLANK

Table 1.1-1. Federal Airways

Federal Airways	Approximate Closest Distance from Airway Centerline to North Portal (mi)	Approximate Distance from Airway Edge to North Portal (mi) ^a	Flights per Year ^b
J-9	86	68	143
J-58/J-80	82	71	561
J-72	88	88	3,454
J-76	88	68	209
J-86	14	6	3,806
J-92	11	6	79,753
J-100	86	68	52
J-110	41	36	3,415
J-146	86	68	65
J-148	95	71	0
V-105	16	11	1,017
V-135	16	11	534
V-244	85	80	13
V-394	88	83	196
V-538	89	83	0
Q-13 ^c	61	61	0

NOTE: ^aJet routes (routes that begin with the letter J) do not have defined widths. Ground controllers continually monitor aircraft flights on jet routes and may divert flights from the centerline as needed to maintain adequate aircraft separation and to not intrude in unauthorized or conflicting airspace. Edge distances are measured to the closest restricted airspace location.

^bFlight activities for Victor routes (routes that begin with the letter V) are only associated with instrument flight rule flight operations. Visual flight rule flights are neither reported nor known.

^cRoute was not established until November 2003 and terminates at the LIDAT fix. Aircraft at this point join J-92 en route to southeast locations.

Table 1.1-2. Estimates of the Resident Population Located within the 84-km Radiological Monitoring Grid

	Population		
	2001	2002	2003
NEVADA			
Nye County			
Amargosa Valley area			
Grid Cell 309 (Lathrop Wells)	14	14	11
Grid Cell 408 (Amargosa Valley)	310	301	310
Grid Cell 409 (Amargosa Valley)	282	274	279
Grid Cell 508 (Amargosa Valley)	60	63	69
Grid Cell 509 (Amargosa Valley)	463	477	471
Grid Cell 510 (Crystal)	23	23	21
Grid Cell 609 (Stateline)	104	104	112
Grid Cell 610 (Crystal)	122	125	120
Grid Cell 710 (Ash Meadows)	16	16	19
Amargosa Valley area subtotal	1,395	1,397	1,412
Beatty area			
Grid Cell 304 (Hot Springs)	43	34	34
Grid Cell 403 (Hot Springs)	26	22	19
Grid Cell 404 (Beatty)	684	718	690
Grid Cell 405 (Beatty)	411	426	417
Grid Cell 505 (Rhyolite)	9	9	9
Grid Cell 903 (Scotty's Junction)	24	26	24
Beatty area subtotal	1,195	1,234	1,193
Pahrump area			
Grid Cell 711 (Johnnie)	21	23	25
Grid Cell 810 (Pahrump)	50	46	48
Grid Cell 811 (Pahrump)	2	2	2
Grid Cell 910 (Pahrump)	5,667	5,849	5,951
Grid Cell 911 (Pahrump)	2	5	5
Grid Cell 1010 (Pahrump)	11,780	12,218	12,581
Pahrump area subtotal	17,522	18,142	18,611
Mercury			
Mercury subtotal	0	0	0
Clark County			
Indian Springs area			
Grid Cell 912 (Indian Springs and Cactus Springs)	1,319	1,359	1,325
Grid Cell 1011 (Cold Creek)	162	153	170
Indian Springs area subtotal	1,481	1,512	1,494
Esmeralda County			
Esmeralda County subtotal	0	0	0
Lincoln County			
Lincoln County subtotal	0	0	0
NEVADA SUBTOTAL	21,594	22,285	22,711

Table 1.1-2. Estimates of the Resident Population Located within the 84-km Radiological Monitoring Grid (Continued)

	Population		
	2001	2002	2003
CALIFORNIA			
Inyo County			
Death Valley area			
Grid Cell 707 (Furnace Creek)	462	418	361
Grid Cell 807 (Timbisha)	18	18	16
Grid Cell 808 (Ryan)	2	2	2
Grid Cell 809 (Death Valley Junction)	2	4	2
Grid Cell 906 (Stovepipe Wells)	68	66	62
Grid Cell 1004 (Scotty's Castle)	7	8	12
Grid Cell 1010 (Stewart Valley)	13	15	15
CALIFORNIA SUBTOTAL	572	531	469
GRAND TOTAL IN THE 84-KM GRID	22,166	22,816	23,180

NOTE: Columns may not sum precisely because of rounding in calculations.

Table 1.1-3. Projected Population within the 84-km Grid, 2003 – 2017^a

	2003	2004	2005	2006	2007	2008	2009	2010	2011	2012	2013	2014	2015	2016	2017
Nye County, Nevada															
Amargosa Valley Area															
Grid Cell 309 (Lathrop Wells)	11	11	12	13	14	14	15	16	16	17	17	18	18	19	19
Grid Cell 408 (Amargosa Valley)	310	323	349	368	386	404	422	440	456	472	488	502	516	529	542
Grid Cell 409 (Amargosa Valley)	279	291	315	332	349	365	381	397	412	426	440	453	466	478	489
Grid Cell 508 (Amargosa Valley)	69	71	77	81	85	89	93	97	101	104	108	111	114	117	120
Grid Cell 509 (Amargosa Valley)	471	491	531	560	588	616	642	669	694	719	742	764	785	805	825
Grid Cell 510 (Crystal)	21	21	23	25	26	27	28	29	30	31	32	33	34	35	36
Grid Cell 609 (Stateline)	112	117	127	134	140	147	153	159	165	171	177	182	187	192	197
Grid Cell 610 (Crystal)	120	125	135	142	149	156	163	170	176	182	188	194	199	204	209
Grid Cell 710 (Ash Meadows)	19	20	22	23	24	25	26	27	28	29	30	31	32	33	34
Total Amargosa Valley within the 84-km Grid	1,412	1,470	1,591	1,678	1,761	1,844	1,924	2,004	2,079	2,152	2,223	2,289	2,352	2,412	2,471

Table 1.1-3. Projected Population within the 84-km Grid, 2003 – 2017^a (Continued)

	2003	2004	2005	2006	2007	2008	2009	2010	2011	2012	2013	2014	2015	2016	2017
Beatty Area															
Grid Cell 304 (Hot Springs)	34	36	39	41	43	45	47	49	51	52	54	56	57	59	60
Grid Cell 403 (Hot Springs)	19	20	22	23	24	25	26	27	28	30	30	31	32	33	34
Grid Cell 404 (Beatty)	690	719	778	820	861	902	941	980	1,016	1,052	1,087	1,119	1,150	1,179	1,208
Grid Cell 405 (Beatty)	417	435	470	496	521	545	568	592	614	636	657	676	695	713	730
Grid Cell 505 (Rhyolite)	9	9	10	10	11	11	12	12	13	13	14	14	14	15	15
Grid Cell 903 (Scotty's Junction)	24	25	27	28	30	31	32	34	35	36	37	38	39	40	41
Total Beatty within the 84-km Grid	1,193	1,243	1,345	1,419	1,489	1,559	1,626	1,694	1,757	1,820	1,879	1,935	1,988	2,039	2,089
Pahrump Area															
Grid Cell 711 (Johnnie)	25	26	28	30	31	33	34	36	37	38	40	41	42	43	44
Grid Cell 810 (Pahrump)	48	50	54	57	60	63	66	68	71	73	76	78	80	82	84
Grid Cell 811 (Pahrump)	2	2	3	3	3	3	3	3	3	3	4	4	4	4	4
Grid Cell 910 (Pahrump)	5,951	6,199	6,706	7,074	7,426	7,773	8,109	8,448	8,764	9,074	9,371	9,651	9,915	10,168	10,416
Grid Cell 911 (Pahrump)	5	5	5	5	6	6	6	7	7	7	7	7	8	8	8

Table 1.1-3. Projected Population within the 84-km Grid, 2003 – 2017^a (Continued)

	2003	2004	2005	2006	2007	2008	2009	2010	2011	2012	2013	2014	2015	2016	2017
Grid Cell 1010 (Pahrump)	12,581	13,106	14,177	14,956	15,700	16,433	17,145	17,861	18,529	19,185	19,813	20,404	20,963	21,497	22,021
Total Pahrump within the 84-km Grid	18,611	19,388	20,973	22,125	23,225	24,311	25,364	26,422	27,412	28,381	29,311	30,184	31,012	31,802	32,577
Total Nye County within the 84-km Grid	21,216	22,102	23,908	25,221	26,476	27,713	28,913	30,120	31,248	32,353	33,413	34,409	35,352	36,253	37,137
Clark County, Nevada															
Grid Cell 912 (Indian Springs and Cactus Springs)	1,325	1,410	1,465	1,537	1,607	1,679	1,751	1,823	1,893	1,961	2,025	2,085	2,142	2,195	2,245
Grid Cell 1011 (Cold Creek)	170	180	188	197	206	215	224	233	242	251	259	267	274	281	287
Total Clark County within the 84-km Grid	1,494	1,591	1,653	1,734	1,812	1,894	1,975	2,057	2,136	2,212	2,284	2,352	2,416	2,476	2,533
Total Nevada within the 84-km Grid	22,711	23,692	25,561	26,955	28,288	29,607	30,888	32,177	33,384	34,565	35,697	36,760	37,768	38,729	39,670
Inyo County, California															
Grid Cell 707 (Furnace Creek)	361	361	361	361	362	362	362	362	362	363	363	363	363	363	363
Grid Cell 807 (Timbisha)	16	16	16	16	16	16	16	16	16	16	16	16	16	16	16
Grid Cell 808 (Ryan)	2	2	2	2	2	2	2	2	2	2	2	2	2	2	2

Table 1.1-3. Projected Population within the 84-km Grid, 2003 – 2017^a (Continued)

	2003	2004	2005	2006	2007	2008	2009	2010	2011	2012	2013	2014	2015	2016	2017
Grid Cell 809 (Death Valley Junction)	2	2	2	2	2	2	2	2	2	2	2	2	2	2	2
Grid Cell 906 (Stovepipe Wells)	62	62	62	62	62	62	62	62	62	62	62	62	62	62	62
Grid Cell 1004 (Scotty's Castle)	12	12	12	12	12	12	12	12	12	12	12	12	12	12	12
Grid Cell 1010 (Stewart Valley, CA)	15	15	15	15	15	15	15	15	15	15	15	15	15	15	15
Total Inyo County within the 84-km Grid	469	470	470	470	471	471	471	472	472	472	472	472	472	472	472
Total population within the 84-km Grid	23,180	24,162	26,031	27,425	28,759	30,078	31,360	32,649	33,855	35,037	36,168	37,232	38,240	39,201	40,141

NOTE: ^aProjected population, including repository- and rail transportation-induced changes.
Totals may not sum precisely because of rounding in calculations.

Source: BSC 2007c, Table II-1.

Table 1.1-4. Projections of Population for Preclosure Operations Period^a

	2017	2020	2030	2040	2042	2050	2060	2067
Nye County, Nevada								
Amargosa Valley Area								
Grid Cell 309 (Lathrop Wells)	19	20	24	27	28	31	36	39
Grid Cell 408 (Amargosa Valley)	542	577	671	771	792	881	1,012	1,115
Grid Cell 409 (Amargosa Valley)	489	521	606	696	715	796	914	1,007
Grid Cell 508 (Amargosa Valley)	120	128	149	171	175	195	224	247
Grid Cell 509 (Amargosa Valley)	825	878	1,022	1,174	1,205	1,341	1,541	1,698
Grid Cell 510 (Crystal)	36	38	45	51	53	59	67	74
Grid Cell 609 (Stateline)	197	209	244	280	287	320	367	405
Grid Cell 610 (Crystal)	209	223	259	298	306	340	391	431
Grid Cell 710 (Ash Meadows)	34	36	42	48	49	55	63	69
Total Amargosa Valley within the 84-km Grid	2,471	2,631	3,061	3,515	3,609	4,018	4,615	5,085
Beatty Area								
Grid Cell 304 (Hot Springs)	60	64	75	86	88	98	112	124
Grid Cell 403 (Hot Springs)	34	36	42	48	49	55	63	70
Grid Cell 404 (Beatty)	1,208	1,286	1,496	1,719	1,765	1,964	2,256	2,486
Grid Cell 405 (Beatty)	730	777	904	1,039	1,067	1,187	1,364	1,503
Grid Cell 505 (Rhyolite)	15	16	19	21	22	24	28	31
Grid Cell 903 (Scotty's Junction)	41	44	51	59	60	67	77	85
Total Beatty within the 84-km Grid	2,089	2,224	2,587	2,971	3,051	3,397	3,901	4,299
Pahrump Area								
Grid Cell 711 (Johnnie)	44	47	55	63	64	72	82	91
Grid Cell 810 (Pahrump)	84	90	104	120	123	137	157	173
Grid Cell 811 (Pahrump)	4	4	5	6	6	7	7	8
Grid Cell 910 (Pahrump)	10,416	11,091	12,902	14,818	15,217	16,938	19,455	21,437
Grid Cell 911 (Pahrump)	8	9	10	11	12	13	15	16
Grid Cell 1010 (Pahrump)	22,021	23,449	27,278	31,329	32,171	35,810	41,132	45,322

Table 1.1-4. Projections of Population for Preclosure Operations Period^a (Continued)

	2017	2020	2030	2040	2042	2050	2060	2067
Total Pahrump within the 84-km Grid	32,577	34,690	40,354	46,346	47,592	52,976	60,850	67,048
Total Nye County within the 84-km Grid	37,137	39,545	46,002	52,833	54,253	60,390	69,366	76,431
Clark County, Nevada								
Grid Cell 912 (Indian Springs and Cactus Springs)	2,245	2,379	2,712	3,020	3,085	3,361	3,742	4,034
Grid Cell 1011 (Cold Creek)	287	305	347	386	395	430	479	516
Total Clark County within the 84-km Grid	2,533	2,684	3,059	3,406	3,480	3,791	4,221	4,550
Total Nevada within the 84-km Grid	39,670	42,229	49,061	56,239	57,733	64,181	73,587	80,982
Inyo County, California								
Death Valley Area								
Grid Cell 707 (Furnace Creek)	363	363	360	353	352	349	347	347
Grid Cell 807 (Timbisha)	16	16	16	16	16	16	16	16
Grid Cell 808 (Ryan)	2	2	2	2	2	2	2	2
Grid Cell 809 (Death Valley Junction)	2	2	2	2	2	2	2	2
Grid Cell 906 (Stovepipe Wells)	62	62	62	61	61	60	60	60
Grid Cell 1004 (Scotty's Castle)	12	12	12	12	12	12	12	12
Grid Cell 1010 (Stewart Valley,)	15	15	15	14	14	14	14	14
Total Inyo County within the 84-km Grid	472	472	468	459	458	454	451	451
Total population within the 84-km Grid	40,141	42,701	49,529	56,698	58,191	64,635	74,038	81,433

NOTE: ^aProjected population, including repository- and rail transportation-induced changes.
Totals may not sum precisely because of rounding in calculations.

Source: BSC 2007c, Table 11.

Table 1.1-5. Projected Distribution by Age Groups for Preclosure Operations Midpoint in 2042, Including Repository-Induced Changes

	Total	Ages 0–11	Ages 12–18	Ages 19 +
Nye County, Nevada				
Amargosa Valley Area				
Grid Cell 309 (Lathrop Wells)	28	4	2	21
Grid Cell 408 (Amargosa Valley)	792	125	70	596
Grid Cell 409 (Amargosa Valley)	715	113	64	538
Grid Cell 508 (Amargosa Valley)	175	28	16	132
Grid Cell 509 (Amargosa Valley)	1,205	190	107	907
Grid Cell 510 (Crystal)	53	8	5	40
Grid Cell 609 (Stateline)	287	45	26	216
Grid Cell 610 (Crystal)	306	48	27	230
Grid Cell 710 (Ash Meadows)	49	8	4	37
Total Amargosa Valley within the 84-km Grid	3,609	570	321	2,718
Beatty Area				
Grid Cell 304 (Hot Springs)	88	14	8	66
Grid Cell 403 (Hot Springs)	49	8	4	37
Grid Cell 404 (Beatty)	1,765	279	157	1,329
Grid Cell 405 (Beatty)	1,067	169	95	803
Grid Cell 505 (Rhyolite)	22	3	2	17
Grid Cell 903 (Scotty's Junction)	60	10	5	46
Total Beatty within the 84-km Grid	3,051	482	272	2,298
Pahrump Area				
Grid Cell 711 (Johnnie)	64	10	6	49
Grid Cell 810 (Pahrump)	123	19	11	93
Grid Cell 811 (Pahrump)	6	1	1	4
Grid Cell 910 (Pahrump)	15,217	2,404	1,354	11,458
Grid Cell 911 (Pahrump)	12	2	1	9
Grid Cell 1010 (Pahrump)	32,171	5,083	2,863	24,225
Total Pahrump within the 84-km Grid	47,592	7,520	4,236	35,837
Total Nye County within the 84-km Grid	54,253	8,572	4,829	40,853

Table 1.1-5. Projected Distribution by Age Groups for Preclosure Operations Midpoint in 2042, Including Repository-Induced Changes (Continued)

	Total	Ages 0–11	Ages 12–18	Ages 19 +
Clark County, Nevada				
Grid Cell 912 (Indian Springs and Cactus Springs)	3,085	487	275	2,323
Grid Cell 1011 (Cold Creek)	395	62	35	297
Total Clark County within the 84-km Grid	3,480	550	310	2,620
Total Nevada within the 84-km Grid	57,733	9,122	5,138	43,473
Inyo County, California				
Death Valley Area				
Grid Cell 707 (Furnace Creek)	352	56	31	265
Grid Cell 807 (Timbisha)	16	3	1	12
Grid Cell 808 (Ryan)	2	0	0	1
Grid Cell 809 (Death Valley Junction)	2	0	0	1
Grid Cell 906 (Stovepipe Wells)	61	10	5	46
Grid Cell 1004 (Scotty's Castle)	12	2	1	9
Grid Cell 1010 (Stewart Valley)	14	2	1	11
Total Inyo County within the 84-km Grid	458	72	41	345
Total population within the 84-km Grid	58,191	9,194	5,179	43,818

NOTE: Totals may not sum precisely because of rounding in calculations.

Source: BSC 2007c, Table 16.

Table 1.1-6. Geographic Coordinates of the Meteorological Monitoring Sites

Site	UTM Coordinates Zone 11N (m)	State Plane Nevada Central (ft)	Latitude–Longitude (deg° min' sec")	Elevation ^a
Site 1 (NTS-60)	550784E 4077374N	569127E 761796N	36° 50' 34"N 116° 25' 50"W	3,752 ft 1,144 m
Site 2 (Yucca Mountain)	547646E 4078753N	558844E 766356N	36° 51' 19"N 116° 27' 56"W	4,850 ft 1,478 m
Site 3 (Coyote Wash)	548875E 4078708N	562876E 766195N	36° 51' 17"N 116° 27' 06"W	4,194 ft 1,278 m
Site 4 (Alice Hill)	553117E 4079779N	576811E 769661N	36° 51' 51"N 116° 24' 15"W	4,049 ft 1,234 m
Site 5 (Fortymile Wash)	554397E 4068682N	580883E 733230N	36° 45' 51"N 116° 23' 26"W	3,125 ft 952 m
Site 6 (WT-6)	549390E 4083084N	564618E 780550N	36° 53' 40"N 116° 26' 45"W	4,313 ft 1,315 m
Site 7 (Sever Wash)	552800E 4077847N	575747E 763325N	36° 50' 49"N 116° 24' 28"W	3,546 ft 1,081 m
Site 8 (Knothead Gap)	551161E 4075773N	570344E 756537N	36° 49' 42"N 116° 25' 35"W	3,684 ft 1,123 m
Site 9 (Gate 510) prior to 5/2/06	553418E 4058398N	577554E 699491N	36° 40' 17"N 116° 24' 08"W	2,750 ft 838 m
Site 9 (Gate 510) as of 5/2/06	553486E 4058477N	577778E 699750N	36° 40' 20"N 116° 24' 05"W	2,754 ft 839 m
Site 401 (Bleach Bone Ridge)	547967E 4082373N	559940E 778231N	36° 53' 17"N 116° 27' 42"W	5,129 ft 1,563 m
Site 405 (Yucca Mtn–WX4b)	547482E 4075997N	558274E 757315N	36° 49' 50"N 116° 28' 03"W	4,884 ft 1,489 m
Site 415 (Yucca Mtn SE)	548094E 4074073N	560261E 750992N	36° 48' 47"N 116° 27' 39"W	4,730 ft 1,442 m

NOTE: ^aAbove mean sea level.

All coordinates are based on NAD27 (North American Datum of 1927) horizontal and NGVD29 (National Geodetic Vertical Datum of 1929) vertical.

UTM = Universal Transverse Mercator.

Source: BSC 2007e, Table 2-1.

Table 1.1-7. Parameters Measured at Each Meteorological Monitoring Station (1994 to 2006)

Parameter	Height (m ^a)	Site								
		1 (NTS-60)	2 (Yucca Crest)	3 ^b (Coyote Wash)	4 (Alice Hill)	5 ^b (Fortymile Wash)	6 ^b (WT-6)	7 ^b (Sever Wash)	8 ^b (Knothead Gap)	9 (Gate 510)
Wind speed	10	1994–2006	1994–2006	1994–1998	1994–2006	1994–1998	1994–1998	1994–1998	1994–1998	1994–2006
	60	1994–2006	—	—	—	—	—	—	—	—
Wind direction	10	1994–2006	1994–2006	1994–1998	1994–2006	1994–1998	1994–1998	1994–1998	1994–1998	1994–2006
	60	1994–2006	—	—	—	—	—	—	—	—
Vertical wind speed	10	1994–2006	1994–2006	1994–1998	1994–2006	1994–1998	1994–1998	1994–1998	1994–1998	1994–2006
Temperature	2	1994–2006	1994–2006	1994–2006	1994–2006	1994–2006	1994–2006	1994–2006	1994–2006	1994–2006
	10	1994–2006	1994–2006	1994–1998	1994–2006	1994–1998	1994–1998	1994–1998	1994–1998	1994–2006
	60	1994–2006	—	—	—	—	—	—	—	—
Vertical temperature difference	2 to 10	1994–2006	1994–2006	1994–1998	1994–2006	1994–1998	1994–1998	1994–1998	1994–1998	1994–2006
	10 to 60	1994–2006	—	—	—	—	—	—	—	—
Precipitation (tipping bucket)	1	1994–2006	1994–2006	1994–2006	1994–2006	1994–2006	1994–2006	1994–2006	1994–2006	1994–2006
Precipitation ^c (storage gauge)	1	1996–2006	1996–2006	1996–2006	1996–2006	1996–2006	1996–2006	1996–2006	1996–2006	1996–2006
Relative humidity	2	1999–2006 ^d	1994–2006	1994–2006	1994–2006	1994–2006	1994–2006	1994–2006	1994–2006	1994–2006
Dew-Point	2	1994–1998 ^d	—	—	—	—	—	—	—	—
Barometric pressure	2	1994–2006	1994–2006	1994–1998	1994–2006	1994–2006	1994–1998	1994–1998	1994–1998	1994–2006

Table 1.1-7. Parameters Measured at Each Meteorological Monitoring Station (1994 to 2006) (Continued)

Parameter	Height (m ^a)	Site								
		1 (NTS-60)	2 (Yucca Crest)	3 ^b (Coyote Wash)	4 (Alice Hill)	5 ^b (Fortymile Wash)	6 ^b (WT-6)	7 ^b (Sever Wash)	8 ^b (Knothead Gap)	9 (Gate 510)
Solar radiation	2	1994–2006	1994–2006	1994–1998	1994–2006	1994–1998	1994–1998	1994–1998	1994–1998	1994–2006

NOTE: ^aMeters above ground level.

^bAt Sites 3, 6, 7, and 8, wind speed and direction, vertical wind speed, vertical temperature difference, barometric pressure, and solar radiation were recorded from 1994 to 1998, and discontinued in 1999. At Site 5, wind speed and direction, vertical wind speed, vertical temperature difference, and solar radiation were recorded from 1994 to 1998, and discontinued in 1999.

^cStorage gauge precipitation measurements were started in October 1995.

^dDew-point temperature was recorded from 1994 to 1998, and relative humidity was recorded from 1999 to 2006 at Site 1.

Blank cells indicate that the parameter was never measured at that site.

Source: BSC 2007e, Table 2-2.

Table 1.1-8. Sensor Descriptions and Requirements

Measurements	Sensors	Methods	System Requirements
Wind speed (horizontal)	Climatronics 100075	Three-cup anemometer with photochopper	Accuracy: greater of ± 0.2 m/s or 5% of observed speed
			Starting speed: < 0.45 m/s (1 mph)
	Met One 1564B	Three-cup anemometer with photochopper	Accuracy: greater of ± 0.2 m/s or 5% of observed speed
			Starting speed: < 0.45 m/s (1 mph)
Wind direction	Climatronics 100076	Vane with potentiometer	Accuracy: ± 5 degrees
			Starting speed: < 0.45 m/s (1 mph)
	Met One 1565C	Vane with resolver	Accuracy: ± 5 degrees
			Starting speed: < 0.45 m/s (1 mph)
Temperature and vertical difference	Climatronics 100093	Three-bead thermistor	$\pm 0.5^\circ\text{C}$ (absolute, for temperature), also $\pm 0.1^\circ\text{C}$ (relative, for vertical difference)
	Met One T-200	Platinum wire	$\pm 0.5^\circ\text{C}$ (absolute, for temperature), also $\pm 0.1^\circ\text{C}$ (relative, for vertical difference)
Relative humidity	Climatronics 101812-G0	Capacitance film	$\pm 4\%$ (for $\leq 40\%$ RH, else: $\pm 1.5^\circ\text{C}$ dew point)
Dew point	General Eastern 700	Chilled mirror	$\pm 1.5^\circ\text{C}$ dew point
Precipitation	Climatronics 100097 and 100097-2	Tipping bucket, 203.2-m (8-in.) orifice, 0.254-mm (0.01-in.) resolution	$\pm 10\%$ volume
	Qualimetrics 6011A	Same tipping bucket	$\pm 10\%$ volume
	Belfort 302 and Weather Measure P511E	Same tipping bucket	$\pm 10\%$ volume
	Nova Lynx 260-2510 Storage gauge	Manual, 203.2-mm (8-in.) orifice, 0.254-mm (0.01-in.) resolution	

Table 1.1-8. Sensor Descriptions and Requirements (Continued)

Measurements	Sensors	Methods	System Requirements
Barometric pressure	Climatronics 101448	Aneroid wafer	(± 3 mb)
Solar radiation	Climatronics 100848	Pyranometer, 0.3 to 3 μ	($\pm 5\%$, zero < ± 10 W/m ²)
Vertical wind speed	Climatronics 101284	Propeller anemometer with generator	Accuracy: greater of ± 0.2 m/s or 5% of observed speed
	Climatronics 102236	Propeller anemometer with optical chopper	Accuracy: greater of ± 0.2 m/s or 5% of observed speed

Source: BSC 2007e, Table 2-3.

Table 1.1-9. System Accuracy Requirements

Measurement	Calibration Tolerance	Performance Check and Performance Audit Tolerance	Instrument Accuracy Guidance from NRC ^a	System Accuracy Guidance from NRC ^b
Wind direction Starting threshold	±3 degrees < 0.45 m/s at 10 degrees	±5 degrees Torque limits (gm-cm): Climatronics 100076: 6.0 Met One 1564B: 2.5	±5 degrees	±5 degrees < 0.45 m/s
Wind speed (horizontal and vertical) Starting threshold	≤ 5 m/s: ± 0.25 m/s > 5 m/s: ± 5% of observed < 0.45 m/s	Same accuracy as calibration; Torque limits (gm-cm): Climatronics 100075: 0.3 Met One 1565C: 0.25 Climatronics 102236: 0.75	±0.5 mph < 1 mph	±0.2 m/s or 5% of observed wind speed < 0.45 m/s
Temperature	±0.5°C	±0.5°C	±0.5°C	±0.5°C (±0.9°F)
Vertical temperature difference	±0.1°C	±0.1°C	±0.1°C	±0.1°C (±0.18°F)
Precipitation Recording gauge Manual storage gauge	Orifice: 8 ± 0.75 in. diameter Volume: ±10%, count: exact Volume: ±10%	Recording: same as calibration Manual: NA	None specified	±10% for a volume equivalent to 2.54 mm (0.1 in.) of precipitation at a rate < 50 mm/hr (< 2 in./hr)
Barometric pressure	±3 mb	±3 mb	None specified	None specified
Relative humidity	< ±1.5°C dew point	RH ≤ 40%: ±4% RH > 40%: see calibration	None specified	±4%
Solar radiation Zero check Measurement	±10 W/m ² ±5%	Zero check; same as calibration	None specified	None specified

NOTE: ^aRegulatory Guide 1.23.^bRegulatory Guide 1.23, Rev. 1.

NA = not applicable; RH = relative humidity.

Source: BSC 2007e, Table 2-4.

Table 1.1-10. Site 1 Climatic Summary for 1994 to 2006

Parameter	Jan	Feb	Mar	Apr	May	Jun	Jul	Aug	Sep	Oct	Nov	Dec	1994–2006
Temperature (°C)													
Extreme maximum	24.0	23.8	29.7	32.1	40.0	42.1	43.3	42.1	37.7	34.7	26.8	21.9	43.3
Mean maximum	12.8	13.3	18.0	21.2	28.3	33.3	37.0	35.8	31.0	23.9	16.5	12.2	23.6
Mean temperature	6.8	7.7	11.2	14.1	20.4	25.5	29.2	28.1	23.6	16.9	10.1	6.2	16.6
Mean minimum	1.1	1.8	4.1	6.6	12.1	16.5	20.5	19.6	15.6	9.7	3.9	0.4	9.3
Extreme minimum	-10.2	-10.1	-7.2	-3.9	2.4	6.3	13.6	12.8	6.6	-0.3	-8.4	-10.9	-10.9
Average Number of Days													
Precipitation													
0.01 in. or more	4	6	3	4	2	1	3	2	2	3	3	3	34
Temperature													
32°C (90°F) and above	0	0	0	0	8	20	29	29	13	1	0	0	99
0°C (32°F) and below	11	8	4	2	0	0	0	0	0	0	4	14	44
Barometric Pressure (mb)													
Mean barometric pressure	888.9	886.9	885.6	884.4	884.1	884.1	886.4	886.6	885.9	886.5	888.3	889.3	886.4
Mean Relative Humidity (%)													
Hour 0400 PST	52.3	55.2	47.7	46.5	32.9	25.3	31.2	33.2	30.9	37.6	44.9	48.8	40.5
Hour 1000 PST	38.8	42.1	32.0	28.7	19.2	14.6	18.5	19.9	18.7	25.2	30.3	35.9	27.0
Hour 1600 PST	32.9	35.0	24.5	21.3	13.1	9.5	13.4	13.4	12.9	20.3	25.8	31.6	21.1
Hour 2200 PST	48.0	51.0	40.2	37.7	24.1	17.4	23.5	24.5	24.0	33.1	39.8	45.0	34.0

Table 1.1-10. Site 1 Climatic Summary for 1994 to 2006 (Continued)

Parameter	Jan	Feb	Mar	Apr	May	Jun	Jul	Aug	Sep	Oct	Nov	Dec	1994–2006
Precipitation (mm)													
Maximum one-hour total	4.57	8.64	6.10	5.84	13.97	6.60	19.30	21.34	10.67	6.35	10.16	5.84	21.34
Maximum daily total	26.16	54.10	29.97	28.70	16.76	17.02	36.58	25.40	28.96	26.16	22.61	24.64	54.10
Average total	24.40	50.70	21.70	12.40	8.50	6.80	16.50	9.20	11.20	10.60	13.70	15.10	200.80
Wind													
Mean speed (m/s)	3.0	3.3	3.8	4.2	3.9	4.0	3.6	3.5	3.5	3.3	3.1	3.1	3.5
Fastest one-minute													
Speed (m/s)	17.5	20.8	17.4	21.0	21.7	20.5	17.3	20.2	19.3	23.3	17.5	21.6	23.3
Direction (degree)	183.3	330.5	341.3	167.1	169.2	337.8	157.3	338.1	012.8	338.1	175.3	343.1	338.1
Peak three-second gust													
Speed (m/s)	21.9	24.8	21.9	27.1	27.6	24.6	22.7	24.1	24.6	27.1	22.2	27.6	27.6
Solar Radiation (cal/cm ² /min)													
Mean maximum	0.71	0.85	1.11	1.28	1.38	1.43	1.40	1.35	1.21	1.01	0.79	0.68	1.10

Source: BSC 2007e, Table 5-1.

Table 1.1-11. Site 2 Climatic Summary for 1994 to 2006

Parameter	Jan	Feb	Mar	Apr	May	Jun	Jul	Aug	Sep	Oct	Nov	Dec	1994–2006
Temperature (°C)													
Extreme maximum	21.2	21.7	27.7	30.0	38.2	39.9	41.4	42.7	36.1	33.5	25.0	19.5	42.7
Mean maximum	10.0	11.0	15.7	18.9	25.9	31.4	35.3	34.1	29.0	21.6	14.0	9.7	21.4
Mean temperature	6.3	6.6	10.2	12.7	19.2	24.5	28.3	27.3	22.8	16.4	9.6	5.9	15.8
Mean minimum	3.2	3.2	5.8	7.5	13.5	18.5	22.5	21.8	17.9	12.3	6.2	2.7	11.3
Extreme minimum	-10.4	-6.8	-4.6	-3.2	0.8	3.4	13.6	13.0	5.9	-0.4	-7.3	-9.7	-10.4
Average Number of Days													
Precipitation													
0.01 in. or more	4	6	3	3	2	2	2	2	2	2	2	3	33
Temperature													
32°C (90°F) and above	0	0	0	0	4	16	27	25	7	0	0	0	78
0°C (32°F) and below	7	7	3	2	0	0	0	0	0	0	4	8	31
Barometric Pressure (mb)													
Mean barometric pressure	851.8	850.1	849.3	848.5	849.3	850.2	853.2	853.2	851.7	851.4	852.0	852.3	851.1
Mean Relative Humidity (%)													
Hour 0400 PST	47.9	49.5	41.1	40.3	31.5	23.8	24.7	26.2	28.3	31.3	38.6	41.9	35.4
Hour 1000 PST	44.6	46.7	36.5	31.4	23.5	17.8	18.9	20.0	22.5	26.4	34.0	38.0	30.0
Hour 1600 PST	39.5	37.7	26.8	21.9	15.4	10.9	12.3	12.8	15.1	20.5	28.8	33.7	23.0
Hour 2200 PST	45.7	46.3	35.3	32.8	24.2	17.1	19.4	20.1	22.9	28.2	35.6	39.4	30.6

Table 1.1-11. Site 2 Climatic Summary for 1994 to 2006 (Continued)

Parameter	Jan	Feb	Mar	Apr	May	Jun	Jul	Aug	Sep	Oct	Nov	Dec	1994–2006
Precipitation (mm)													
Maximum one-hour total	7.87	10.16	8.89	6.35	20.07	9.14	30.23	13.97	10.41	5.33	6.60	5.84	30.23
Maximum daily total	30.99	50.04	24.13	20.07	20.07	21.34	49.02	17.78	29.21	29.97	22.86	23.88	50.04
Average total	25.20	48.30	22.30	12.70	6.50	7.10	14.80	9.70	11.80	13.20	12.50	14.40	198.50
Wind													
Mean speed (m/s)	3.9	4.4	4.8	5.4	4.8	4.7	4.3	4.3	4.3	4.1	3.9	3.9	4.4
Fastest one-minute													
Speed (m/s)	29.1	33.1	28.7	28.9	26.4	30.0	26.4	27.8	32.0	29.4	26.9	31.4	33.1
Direction (degree)	300.0	309.7	309.7	309.7	229.4	229.4	283.9	314.1	262.0	262.0	302.0	300.7	309.7
Peak three-second gust													
Speed (m/s)	33.8	37.6	34.8	38.2	29.7	33.4	28.8	33.7	38.7	33.3	31.9	36.8	38.7
Solar Radiation (cal/cm ² /min)													
Mean maximum	0.70	0.85	1.11	1.29	1.38	1.43	1.40	1.34	1.22	1.00	0.79	0.67	1.10

Source: BSC 2007e, Table 5-2.

Table 1.1-12. Site 3 Climatic Summary for 1994 to 2006

Parameter	Jan	Feb	Mar	Apr	May	Jun	Jul	Aug	Sep	Oct	Nov	Dec	1994–2006
Temperature (°C)													
Extreme maximum	22.5	22.6	28.6	30.9	38.1	40.9	42.2	40.7	36.6	33.5	25.6	20.3	42.2
Mean maximum	11.2	12.2	16.5	19.6	26.3	31.8	35.6	34.4	29.6	22.5	15.1	10.8	22.1
Mean temperature	6.7	7.5	11.0	13.7	20.0	25.2	28.9	27.8	23.3	16.8	10.1	6.2	16.4
Mean minimum	2.5	2.9	5.4	7.4	12.9	17.6	21.5	20.8	17.0	11.4	5.3	2.1	10.6
Extreme minimum	-10.1	-7.6	-4.3	-2.5	2.0	4.6	12.7	13.3	6.2	0.3	-6.6	-8.6	-10.1
Average Number of Days													
Precipitation													
0.01 in. or more	4	6	3	3	2	2	3	3	2	2	2	3	34
Temperature													
32°C (90°F) and above	0	0	0	0	5	17	27	25	8	0	0	0	81
0°C (32°F) and below	7	6	3	1	0	0	0	0	0	0	4	9	30
Barometric Pressure (mb)													
Mean barometric pressure	872.3	871.3	870.1	869.5	868.9	869.6	872.2	872.6	871.3	871.6	872.3	873.1	871.2
Mean Relative Humidity (%)													
Hour 0400 PST	51.5	52.1	44.4	42.2	34.2	26.1	27.3	29.0	31.2	34.0	43.0	46.0	38.4
Hour 1000 PST	41.6	42.7	32.9	28.3	21.3	16.3	17.3	18.1	20.6	24.1	31.7	36.3	27.6
Hour 1600 PST	37.8	35.0	25.0	20.5	14.4	10.3	11.6	12.1	14.4	19.7	28.6	33.7	21.9
Hour 2200 PST	48.2	48.2	37.1	33.7	24.7	17.6	19.5	20.9	24.2	30.0	38.7	42.5	32.1

Table 1.1-12. Site 3 Climatic Summary for 1994 to 2006 (Continued)

Parameter	Jan	Feb	Mar	Apr	May	Jun	Jul	Aug	Sep	Oct	Nov	Dec	1994–2006
Precipitation (mm)													
Maximum one-hour total	6.86	11.43	7.37	5.84	18.80	5.59	22.35	16.51	10.41	5.33	14.48	8.89	22.35
Maximum daily total	30.73	54.36	29.46	28.19	19.56	19.30	47.50	18.80	28.96	28.45	25.91	27.43	54.36
Average total	29.10	55.80	25.50	13.50	9.10	6.90	16.10	9.70	13.50	10.20	18.00	16.40	223.80
Wind													
Mean speed (m/s)	2.4	2.7	2.9	3.1	2.9	2.9	2.7	2.6	2.6	2.7	2.4	2.5	2.7
Fastest one-minute													
Speed (m/s)	16.3	16.9	16.0	17.0	13.7	20.1	18.6	18.5	13.9	18.0	15.6	14.9	20.1
Direction (degree)	— ^a	308.2	309.2	309.2	309.2	302.3	302.3	297.7	297.7	307.4	303.2	303.8	302.3
Peak three-second gust													
Speed (m/s)	23.3	23.2	25.2	24.5	19.6	27.3	21.0	26.4	19.5	26.2	21.5	22.0	27.3
Solar Radiation (cal/cm ² /min)													
Mean maximum	0.67	0.87	1.11	1.28	1.36	1.43	1.40	1.38	1.23	1.04	0.79	0.67	1.10

NOTE: ^aFastest one-minute speed direction was not recorded at Site 3 until 1996; fastest January one-minute speed occurred in 1994.

Source: BSC 2007e, Table 5-3.

Table 1.1-13. Site 4 Climatic Summary for 1994 to 2006

Parameter	Jan	Feb	Mar	Apr	May	Jun	Jul	Aug	Sep	Oct	Nov	Dec	1994–2006
Temperature (°C)													
Extreme maximum	23.5	23.7	29.9	32.3	40.1	42.3	43.8	42.0	38.0	34.8	26.5	21.1	43.8
Mean maximum	12.0	13.0	17.5	20.9	27.8	33.2	37.0	35.9	30.9	23.6	15.9	11.5	23.3
Mean temperature	7.1	7.8	11.4	14.1	20.6	25.8	29.6	28.6	23.9	17.2	10.4	6.7	16.9
Mean minimum	2.5	2.9	5.5	7.6	13.3	18.1	22.1	21.4	17.1	11.0	5.3	2.1	10.7
Extreme minimum	-8.5	-7.9	-4.1	-2.0	2.0	4.1	14.5	14.1	8.3	0.0	-6.0	-9.5	-9.5
Average Number of Days													
Precipitation													
0.01 in. or more	3	6	3	3	1	2	2	2	2	2	2	3	31
Temperature													
32°C (90°F) and above	0	0	0	0	7	20	29	29	13	1	0	0	98
0°C (32°F) and below	7	6	3	1	0	0	0	0	0	0	3	9	29
Barometric Pressure (mb)													
Mean barometric pressure	878.2	876.5	875.2	874.0	873.9	874.3	876.8	877.0	876.0	876.4	877.9	878.7	876.2
Mean Relative Humidity (%)													
Hour 0400 PST	50.5	51.8	43.1	41.3	32.7	23.9	25.5	26.3	29.6	33.1	41.2	44.3	36.9
Hour 1000 PST	44.0	44.5	33.6	28.4	20.9	15.9	17.2	18.1	20.5	24.4	32.5	37.6	28.1
Hour 1600 PST	36.5	35.1	25.1	20.1	13.6	9.5	11.2	11.5	13.7	18.7	26.8	31.3	21.1
Hour 2200 PST	46.8	47.4	36.5	33.4	24.2	17.0	19.2	19.7	22.9	28.6	36.8	41.0	31.1

Table 1.1-13. Site 4 Climatic Summary for 1994 to 2006 (Continued)

Parameter	Jan	Feb	Mar	Apr	May	Jun	Jul	Aug	Sep	Oct	Nov	Dec	1994–2006
Precipitation (mm)													
Maximum one-hour total	7.37	9.40	5.84	4.32	23.88	9.91	30.99	14.99	16.26	7.37	10.67	6.86	30.99
Maximum daily total	25.40	59.44	30.99	24.64	26.67	16.26	56.90	27.18	28.96	35.81	27.43	31.50	59.44
Average total	26.40	47.70	21.00	11.50	7.50	6.40	18.20	9.30	10.70	12.90	12.30	15.10	199.00
Wind													
Mean Speed (m/s)	4.1	4.6	5.2	5.7	5.1	4.9	4.4	4.2	4.5	4.5	4.2	4.2	4.6
Fastest one-minute													
Speed (m/s)	27.5	32.0	27.8	29.2	29.4	30.4	25.1	32.9	27.3	33.2	26.0	35.8	35.8
Direction (degree)	333.9	315.2	315.2	315.2	011.1	343.0	343.0	340.1	026.3	026.3	339.6	353.2	353.2
Peak three-second gust													
Speed (m/s)	31.7	36.2	31.4	33.3	34.3	35.1	28.3	37.9	32.3	37.2	31.4	39.9	39.9
Solar Radiation (cal/cm ² /min)													
Mean maximum	0.73	0.89	1.17	1.35	1.46	1.51	1.48	1.42	1.29	1.06	0.83	0.71	1.16

Source: BSC 2007e, Table 5-4.

Table 1.1-14. Site 5 Climatic Summary for 1994 to 2006

Parameter	Jan	Feb	Mar	Apr	May	Jun	Jul	Aug	Sep	Oct	Nov	Dec	1994–2006
Temperature (°C)													
Extreme maximum	25.8	26.0	31.9	34.6	42.2	43.7	45.2	43.6	39.9	36.9	31.9	23.2	45.2
Mean maximum	14.2	15.4	20.0	23.2	30.0	35.5	39.2	38.1	33.2	25.9	18.2	13.7	25.5
Mean temperature	7.5	8.8	12.4	15.4	21.7	26.8	30.6	29.5	24.8	17.9	10.9	6.9	17.8
Mean minimum	1.1	2.2	4.7	7.2	12.2	16.6	20.9	20.4	16.3	10.4	4.0	0.3	9.7
Extreme minimum	-9.1	-8.5	-6.7	-4.4	1.4	0.2	12.2	13.1	0.0	-0.2	-8.7	-11.4	-11.4
Average Number of Days													
Precipitation													
0.01 in. or more	3	5	2	3	2	1	2	2	2	3	2	2	30
Temperature													
32°C (90°F) and above	0	0	0	1	12	24	31	30	20	3	0	0	120
0°C (32°F) and below	12	7	4	1	0	0	0	0	0	0	5	14	43
Barometric Pressure (mb)													
Mean barometric pressure	908.5	906.8	905.1	903.8	903.2	903.1	905.3	905.6	904.9	905.9	908.0	909.1	905.8
Mean Relative Humidity (%)													
Hour 0400 PST	55.0	55.3	46.9	43.8	35.4	26.1	27.0	27.7	31.0	34.3	45.3	48.9	39.7
Hour 1000 PST	40.8	40.9	30.3	25.5	19.2	14.4	15.6	16.4	19.0	22.4	30.4	35.2	25.8
Hour 1600 PST	32.7	31.4	21.4	17.1	12.2	7.9	9.4	10.0	12.0	16.6	23.8	28.1	18.6
Hour 2200 PST	51.5	51.5	40.4	35.8	25.7	17.9	19.7	21.0	24.7	30.6	41.6	45.7	33.8

Table 1.1-14. Site 5 Climatic Summary for 1994 to 2006 (Continued)

Parameter	Jan	Feb	Mar	Apr	May	Jun	Jul	Aug	Sep	Oct	Nov	Dec	1994–2006
Precipitation (mm)													
Maximum one-hour total	4.83	7.37	4.83	4.32	10.67	4.06	29.21	11.43	12.70	6.35	6.10	5.84	29.21
Maximum daily total	15.49	50.04	22.86	22.61	18.80	9.65	43.94	18.03	26.67	21.08	24.13	25.65	50.04
Average total	19.30	38.50	14.90	8.90	7.10	3.10	9.40	4.60	11.70	9.10	9.20	11.90	147.70
Wind													
Mean speed (m/s)	4.0	4.4	4.7	4.9	4.6	4.7	4.5	4.7	4.5	4.6	4.1	4.2	4.5
Fastest one-minute													
Speed (m/s)	18.9	20.1	19.7	21.6	20.3	21.2	18.4	21.5	17.1	25.3	18.2	18.4	25.3
Direction (degree)	179.4	159.7	349.1	349.1	349.1	340.8	081.8	322.9	160.2	336.9	336.9	336.9	336.9
Peak three-second gust													
Speed (m/s)	23.7	24.9	24.9	26.4	24.8	28.3	26.5	26.6	20.6	30.4	21.9	22.1	30.4
Solar Radiation (cal/cm ² /min)													
Mean maximum	0.70	0.89	1.15	1.32	1.41	1.45	1.43	1.37	1.23	1.03	0.80	0.69	1.12

Source: BSC 2007e, Table 5-5.

Table 1.1-15. Site 6 Climatic Summary for 1994 to 2006

Parameter	Jan	Feb	Mar	Apr	May	Jun	Jul	Aug	Sep	Oct	Nov	Dec	1994–2006
Temperature (°C)													
Extreme maximum	22.6	23.1	28.4	30.4	38.2	40.3	41.8	41.9	36.3	33.7	25.8	20.5	41.9
Mean maximum	11.2	12.1	16.3	19.3	26.0	31.5	35.3	34.2	29.5	22.5	15.1	10.9	22.0
Mean temperature	5.5	6.3	9.8	12.5	18.8	23.9	27.6	26.4	22.0	15.5	8.8	5.0	15.2
Mean minimum	0.4	0.9	3.2	5.3	10.5	14.8	18.7	17.8	14.3	9.0	2.9	0.2	8.1
Extreme minimum	-11.1	-10.4	-6.9	-4.7	-0.3	2.3	11.3	10.7	4.2	-1.0	-9.3	-11.2	-11.2
Average Number of Days													
Precipitation													
0.01 in. or more	4	6	3	3	2	2	3	2	2	3	3	2	33
Temperature													
32°C (90°F) and above	0	0	0	0	4	16	26	25	8	0	0	0	78
0°C (32°F) and below	14	12	7	3	0	0	0	0	0	0	6	16	57
Barometric Pressure (mb)													
Mean barometric pressure	868.2	867.0	865.8	865.0	864.8	865.8	868.7	869.0	867.3	867.2	867.8	868.6	867.1
Mean Relative Humidity (%)													
Hour 0400 PST	57.0	57.4	50.3	47.9	39.8	29.8	31.5	33.5	35.6	37.9	47.9	50.9	43.3
Hour 1000 PST	42.1	43.6	34.0	29.6	22.1	16.7	17.8	18.6	21.0	24.7	31.8	36.3	28.2
Hour 1600 PST	38.2	36.1	25.9	21.4	15.2	10.6	12.0	12.4	14.6	19.8	28.6	33.8	22.4
Hour 2200 PST	53.8	54.3	43.0	39.3	29.2	20.6	22.4	23.7	27.6	33.5	43.6	47.4	36.5

Table 1.1-15. Site 6 Climatic Summary for 1994 to 2006 (Continued)

Parameter	Jan	Feb	Mar	Apr	May	Jun	Jul	Aug	Sep	Oct	Nov	Dec	1994–2006
Precipitation (mm)													
Maximum one-hour total	11.18	12.95	8.89	6.10	15.24	8.64	16.51	16.51	13.97	5.08	6.35	8.89	16.51
Maximum daily total	31.24	44.70	31.50	29.72	15.75	21.34	20.32	28.19	28.45	35.05	30.23	30.99	44.70
Average total	30.40	56.10	27.10	15.60	9.10	7.20	11.00	10.80	13.50	12.30	15.60	16.60	225.30
Wind													
Mean speed (m/s)	3.6	4.0	4.3	4.6	4.2	4.2	4.1	4.0	3.9	4.1	3.7	3.9	4.0
Fastest one-minute													
Speed (m/s)	20.1	18.5	20.7	21.4	19.7	22.6	17.5	21.9	19.1	19.8	19.9	20.8	22.6
Direction (degree)	358.4	346.0	326.6	326.6	326.6	326.6	326.6	340.3	340.3	345.1	345.1	345.1	326.6
Peak three-second gust													
Speed (m/s)	26.1	27.7	26.5	28.7	28.1	29.9	23.6	27.3	24.0	27.0	26.7	24.9	29.9
Solar Radiation (cal/cm ² /min)													
Mean maximum	0.69	0.87	1.13	1.31	1.39	1.45	1.42	1.38	1.22	1.03	0.79	0.68	1.11

Source: BSC 2007e, Table 5-6.

Table 1.1-16. Site 7 Climatic Summary for 1994 to 2006

Parameter	Jan	Feb	Mar	Apr	May	Jun	Jul	Aug	Sep	Oct	Nov	Dec	1994–2006
Temperature (°C)													
Extreme maximum	24.9	25.3	30.9	33.3	40.7	42.9	44.1	43.0	39.3	36.1	27.8	22.6	44.1
Mean maximum	13.3	14.5	19.0	22.2	29.0	34.4	38.3	37.1	32.2	24.9	17.3	12.9	24.6
Mean temperature	5.7	7.1	10.8	13.8	20.1	25.1	28.8	27.5	22.8	15.9	8.9	5.0	16.0
Mean minimum	-1.8	0.5	1.8	4.2	9.1	13.1	17.1	16.3	12.4	6.2	0.4	-2.8	6.3
Extreme minimum	-11.9	-11.0	-9.1	-6.9	-0.8	0.2	9.3	9.0	2.6	-5.0	-12.5	-16.4	-16.4
Average Number of Days													
Precipitation													
0.01 in. or more	3	6	3	3	1	2	2	2	2	3	3	3	33
Temperature													
32°C (90°F) and above	0	0	0	1	9	22	30	30	17	2	0	0	110
0°C (32°F) and below	22	15	10	4	0	0	0	0	0	1	12	24	88
Barometric Pressure (mb)													
Mean barometric pressure	893.4	892.4	891.0	890.2	889.6	890.1	892.7	892.9	891.7	892.2	893.3	894.4	892.0
Mean Relative Humidity (%)													
Hour 0400 PST	63.1	62.1	54.9	51.6	42.6	32.7	34.7	35.7	39.1	42.0	53.9	57.4	47.5
Hour 1000 PST	42.7	42.0	31.8	26.8	20.3	15.3	16.4	17.4	19.7	23.2	31.0	36.7	26.9
Hour 1600 PST	35.0	33.1	23.7	19.4	13.7	9.4	11.0	11.5	13.5	18.2	25.8	30.3	20.4
Hour 2200 PST	57.1	56.3	45.6	40.3	29.5	21.2	23.8	24.9	28.8	34.4	47.1	52.0	38.4

Table 1.1-16. Site 7 Climatic Summary for 1994 to 2006 (Continued)

Parameter	Jan	Feb	Mar	Apr	May	Jun	Jul	Aug	Sep	Oct	Nov	Dec	1994–2006
Precipitation (mm)													
Maximum one-hour total	10.41	8.38	6.10	4.83	16.76	9.91	31.50	25.65	9.14	7.37	10.16	7.11	31.50
Maximum daily total	23.88	60.20	29.46	24.38	19.30	18.80	64.77	40.89	29.72	30.99	27.18	28.96	64.77
Average total	26.70	48.80	20.90	11.50	7.50	5.80	18.30	11.20	10.20	10.50	13.90	16.30	201.60
Wind													
Mean speed (m/s)	2.6	3.1	3.4	3.9	3.6	3.6	3.4	3.3	3.2	3.1	2.7	2.8	3.2
Fastest one-minute													
Speed (m/s)	17.4	18.4	18.1	21.3	18.9	20.9	15.6	21.8	16.9	23.2	18.0	17.1	23.2
Direction (degree)	000.8	163.7	328.5	328.5	328.5	331.5	164.8	326.1	217.8	331.3	331.3	161.9	331.3
Peak three-second gust													
Speed gust (m/s)	20.7	22.6	22.3	25.5	23.0	26.3	27.2	24.8	26.9	27.7	21.9	21.2	27.7
Solar Radiation (cal/cm ² /min)													
Mean maximum	0.70	0.90	1.14	1.33	1.42	1.46	1.43	1.37	1.23	1.03	0.81	0.71	1.13

Source: BSC 2007e, Table 5-7.

Table 1.1-17. Site 8 Climatic Summary for 1994 to 2006

Parameter	Jan	Feb	Mar	Apr	May	Jun	Jul	Aug	Sep	Oct	Nov	Dec	1994–2006
Temperature (°C)													
Extreme maximum	24.1	24.7	29.8	32.8	40.2	42.0	43.7	42.2	38.2	35.6	27.2	22.2	43.7
Mean maximum	12.7	13.8	18.3	21.4	28.3	33.7	37.5	36.4	31.4	24.2	16.7	12.4	23.9
Mean temperature	6.0	7.1	10.8	13.8	20.1	25.3	29.0	27.7	23.0	16.1	9.3	5.4	16.1
Mean minimum	-0.5	0.5	2.7	5.2	10.2	14.6	18.7	17.9	13.7	7.7	1.9	-1.2	7.6
Extreme minimum	-10.1	-9.6	-8.2	-4.7	0.0	0.2	11.2	11.4	5.3	-3.1	-9.4	-13.1	-13.1
Average Number of Days													
Precipitation													
0.01 in. or more	4	6	3	4	2	1	3	2	2	2	3	3	34
Temperature													
32°C (90°F) and above	0	0	0	0	7	21	30	29	14	1	0	0	102
0°C (32°F) and below	17	12	7	3	0	0	0	0	0	0	8	20	67
Barometric Pressure (mb)													
Mean barometric pressure	888.4	887.3	885.8	885.0	884.2	884.6	887.2	887.4	886.3	887.0	888.0	889.1	886.7
Mean Relative Humidity (%)													
Hour 0400 PST	60.1	60.1	52.4	48.6	40.0	29.9	31.6	32.9	36.4	39.8	51.1	54.2	44.8
Hour 1000 PST	42.2	42.5	31.7	26.7	20.0	14.9	16.1	17.3	19.5	23.0	31.1	36.3	26.8
Hour 1600 PST	35.1	33.5	23.5	18.9	13.2	8.9	10.6	11.2	13.0	18.1	26.1	30.9	20.2
Hour 2200 PST	54.7	54.6	43.2	38.1	28.1	19.6	21.7	23.3	27.1	33.3	44.9	49.0	36.5
Precipitation (mm)													

Table 1.1-17. Site 8 Climatic Summary for 1994 to 2006 (Continued)

Parameter	Jan	Feb	Mar	Apr	May	Jun	Jul	Aug	Sep	Oct	Nov	Dec	1994–2006
Maximum 1-hour total	10.92	8.38	6.86	5.84	9.40	6.86	25.15	27.18	9.14	6.86	10.16	6.60	27.18
Maximum daily total	22.86	54.36	28.96	26.16	17.78	14.73	42.67	30.48	29.46	26.42	25.91	23.11	54.36
Average total	26.00	50.90	21.40	11.30	8.20	5.30	15.50	10.60	9.80	10.80	14.00	14.30	198.10
Wind													
Mean speed (m/s)	2.6	3.0	3.4	3.8	3.5	3.6	3.3	3.2	3.0	2.9	2.5	2.8	3.1
Fastest one-minute													
Speed (m/s)	16.6	18.9	17.7	19.9	17.2	20.8	15.4	20.8	16.7	21.3	16.4	17.1	21.3
Direction (degree)	327.9	327.9	327.9	327.9	327.9	342.8	342.8	333.2	167.4	332.3	004.1	200.7	332.3
Peak three-second gust													
Speed (m/s)	20.5	23.0	25.0	27.6	21.5	27.4	21.5	25.0	21.4	27.3	21.9	20.8	27.6
Solar Radiation (cal/cm ² /min)													
Mean maximum	0.70	0.90	1.15	1.32	1.41	1.46	1.44	1.38	1.23	1.03	0.81	0.71	1.13

Source: BSC 2007e, Table 5-8.

Table 1.1-18. Site 9 Climatic Summary for 1994 to 2006

Parameter	Jan	Feb	Mar	Apr	May	Jun	Jul	Aug	Sep	Oct	Nov	Dec	1994–2006
Temperature (°C)													
Extreme maximum	26.3	26.6	32.6	35.5	42.7	45.1	45.7	44.3	40.7	37.8	28.5	24.0	45.7
Mean maximum	14.8	16.1	20.8	24.0	30.8	36.2	39.9	38.9	33.9	26.5	18.7	14.2	26.2
Mean temperature	7.7	9.2	12.9	16.1	22.4	27.6	31.4	30.3	25.3	18.1	11.1	7.0	18.3
Mean minimum	1.2	2.5	4.9	7.4	12.7	17.1	21.5	20.8	16.4	10.1	4.0	0.3	9.9
Extreme minimum	-10.7	-7.4	-6.0	-3.5	1.2	2.5	12.2	12.8	5.8	0.6	-6.8	-10.8	-10.8
Average Number of Days													
Precipitation													
0.01 in. or more	3	6	2	3	1	1	2	1	2	2	2	2	26
Temperature													
32°C (90°F) and above	0	0	0	2	13	25	31	31	21	4	0	0	127
0°C (32°F) and below	11	7	3	1	0	0	0	0	0	0	5	15	42
Barometric Pressure (mb)													
Mean barometric pressure	920.6	918.8	917.0	915.5	914.4	914.0	916.0	916.3	915.9	917.3	919.7	921.3	917.2
Mean Relative Humidity (%)													
Hour 0400 PST	56.2	55.9	48.5	43.7	35.4	26.0	26.6	27.1	31.6	35.3	46.4	50.3	40.3
Hour 1000 PST	40.8	40.5	30.0	24.4	19.0	14.0	15.0	15.8	18.6	22.0	30.0	35.1	25.4
Hour 1600 PST	31.5	29.9	20.6	16.4	11.8	7.6	8.9	9.6	11.6	15.9	22.6	27.1	17.8
Hour 2200 PST	50.5	49.7	39.4	33.5	24.1	16.6	18.0	19.3	23.5	29.4	40.0	44.8	32.4

Table 1.1-18. Site 9 Climatic Summary for 1994 to 2006 (Continued)

Parameter	Jan	Feb	Mar	Apr	May	Jun	Jul	Aug	Sep	Oct	Nov	Dec	1994–2006
Precipitation (mm)													
Maximum one-hour total	3.30	7.87	5.84	8.38	4.57	4.83	13.72	6.60	6.10	2.54	5.08	5.33	13.72
Maximum daily total	14.22	45.47	18.54	22.35	5.33	11.68	20.07	10.41	28.19	14.48	15.49	19.56	45.47
Average total	15.00	31.20	13.40	8.00	5.00	3.50	3.20	2.50	10.50	5.70	8.10	9.90	116.00
Wind													
Mean speed (m/s)	4.0	4.2	4.6	4.9	4.6	4.7	4.5	4.5	4.4	4.2	4.0	4.0	4.4
Fastest one-minute													
Speed (m/s)	18.3	20.8	19.1	23.0	23.1	19.6	27.5	21.0	18.4	19.1	20.5	21.6	27.5
Direction (degree)	347.8	331.2	331.2	154.1	172.0	154.4	070.1	333.4	242.2	242.2	345.7	336.5	70.1
Peak three-second gust													
Speed (m/s)	22.5	26.9	22.7	27.3	28.4	26.7	33.1	26.2	27.0	23.1	24.3	25.8	33.1
Solar Radiation (cal/cm ² /min)													
Mean maximum	0.77	0.93	1.20	1.40	1.49	1.53	1.51	1.44	1.31	1.07	0.86	0.73	1.19

Source: BSC 2007e, Table 5-9.

Table 1.1-19. Average Annual Total Precipitation

Average Annual Total Precipitation (mm)												
Site	1	2	3	4	5	6	7	8	9	401	405	415
Average	200.9	198.5	223.8	199.0	147.7	225.3	201.6	198.1	116.0	200.9	177.8	181.1

Source: BSC 2007e, Table 5-10.

Table 1.1-20. Annual Total Precipitation at Site 1 from 1994 through 2006

Annual Total Precipitation (mm)													
Year	1994	1995	1996	1997	1998	1999	2000	2001	2002	2003	2004	2005	2006
Total	94.7	232.9	148.6	141.2	366.5	183.4	246.1	179.6	39.6	247.4	285.5	287.5	157.2

Source: BSC 2007e, Table 5-11.

Table 1.1-21. Annual Average Total Precipitation Ranked by Total Amount for 1999 to 2006

Annual Average Total Precipitation (mm) ^a	Site	Elevation (m from mean sea level)
113.4	9	838 ^b
140.4	5	952
177.8	405	1,489
181.1	415	1,442
197.7	8	1,123
198.6	4	1,234
200.9	401	1,563
201.0	7	1,081
201.2	2	1,478
203.3	1	1,144
212.2	6	1,315
223.2	3	1,278

NOTE: ^a Annual average total precipitation from 1999 through 2006 is presented in increasing order.^b Elevation of the original location of Site 9 during most of the measurement period (1993 through May 2, 2006).

Source: BSC 2007e, Table 5-12.

Table 1.1-22. Precipitation Rate and Frequency Results

Site	Average Annual Number of Days ^a	Maximum One-Hour (mm/hr) and Month of Occurrence ^b	Maximum Daily (mm/day) and Month of Occurrence ^c
1	34	21.34 / Aug	54.10 / Feb
2	33	30.23 / Jul	50.04 / Feb
3	34	22.35 / Jul	54.36 / Feb
4	31	30.99 / Jul	59.44 / Feb
5	30	29.21 / Jul	50.04 / Feb
6	33	16.51 / Aug	44.70 / Feb
7	33	31.50 / Jul	64.77 / Jul
8	34	27.18 / Aug	54.36 / Feb
9	26	13.72 / Jul	45.47 / Feb

NOTE: ^aAverage annual number of days with measurable precipitation (total is greater than or equal to 0.01 in.).

^bHighest of the maximum 1 hr precipitation rates, with the corresponding month of occurrence.

^cHighest of the maximum daily precipitation rates, with the corresponding month of occurrence.

Source: BSC 2007e, Table 5-13.

Table 1.1-23. Comparison of 24-Hour Maximum Precipitation from September 21 through 22, 2007, Storm to Values of Previous Maximum Events

Monitoring Site	24-Hour Maximum		Percentage Increase
	September 21 through 22, 2007 (mm)	1994 through 2006 (mm)	
1	81.28	54.10	50.2%
2	85.34	50.04	70.6%
3	83.83	54.36	54.2%
4	87.12	59.44	46.6%
5	76.20	50.04	52.35
6	83.82	44.70	87.5%
7	83.82	64.77	29.4%
8	79.25	54.36	45.8%
9	68.58	45.47	50.8%
401	83.57	NA	NA
405	78.49	NA	NA
415	79.50	NA	NA
Maximum of All Values	87.12	64.77	34.5%

NOTE: NA = not applicable.

Source: Fransioli 2007.

Table 1.1-24. Summary of Mean and Maximum Wind Speeds

Site	Average Annual Mean (m/s)	Peak Three-Second Gust (m/s) and Month of Occurrence	Fastest One-Minute Average Speed (m/s) and Direction (degree) and Month of Occurrence
1	3.5	27.6 / Dec	23.3 / 338.1° / Oct
2	4.4	38.7 / Sep	33.1 / 309.7° / Feb
3	2.7	27.3 / Jun	20.1 / 302.3° / Jun
4	4.6	39.9 / Dec	35.8 / 353.2° / Dec
5	4.5	30.4 / Oct	25.3 / 336.9° / Oct
6	4.0	29.9 / Jun	22.6 / 326.6° / Jun
7	3.2	27.7 / Oct	23.2 / 331.3° / Oct
8	3.1	27.6 / Apr	21.3 / 332.3° / Oct
9	4.4	33.1 / Jul	27.5 / 070.1° / Jul

NOTE: Data cover period 1994 through 2006 for Sites 1, 2, 4 and 9, and 1994 through 1998 for the remaining sites.

Source: BSC 2007e, Table 5-14.

Table 1.1-25. Pasquill Stability Categories Based on Vertical Temperature Differences

Stability Category	Pasquill Stability Category	Ambient Temperature Change With Height (°C/50 m)
Extremely unstable	A	$\Delta T \leq -0.95$
Moderately unstable	B	$-0.95 < \Delta T \leq -0.85$
Slightly unstable	C	$-0.85 < \Delta T \leq -0.75$
Neutral	D	$-0.75 < \Delta T \leq -0.25$
Slightly stable	E	$-0.25 < \Delta T \leq 0.75$
Moderately stable	F	$0.75 < \Delta T \leq 2.0$
Extremely stable	G	$\Delta T > 2.0$

Source: BSC 2007e, Table 4-1.

Table 1.1-26. Joint Frequency Distribution of Wind Speed and Direction for All Hours (1994 to 2006) at Site 1 at 10 m above Ground Level

Wind Direction		Wind Speed Category (m/s)										Total
Degrees Azimuth	Direction	0.5–1.1	1.1–1.6	1.6–2.1	2.1–3.1	3.1–4.1	4.1–5.1	5.1–6.1	6.1–8.1	8.1–10.0	≥ 10.0	
348.75–11.25	North	0.0012	0.0058	0.0094	0.0137	0.0141	0.0118	0.0084	0.0086	0.0024	0.0008	0.0761
11.25–33.75	North-northeast	0.0012	0.0033	0.0035	0.0054	0.0062	0.0058	0.0039	0.0032	0.0007	0.0002	0.0333
33.75–56.25	Northeast	0.0016	0.0048	0.0030	0.0038	0.0034	0.0028	0.0017	0.0009	0.0001	0.0000	0.0221
56.25–78.75	East-northeast	0.0021	0.0047	0.0029	0.0033	0.0017	0.0008	0.0004	0.0002	0.0000	0.0000	0.0160
78.75–101.25	East	0.0019	0.0037	0.0039	0.0030	0.0013	0.0006	0.0002	0.0002	0.0000	0.0000	0.0149
101.25–123.75	East-southeast	0.0015	0.0043	0.0053	0.0050	0.0020	0.0008	0.0003	0.0002	0.0000	0.0000	0.0194
123.75–146.25	Southeast	0.0014	0.0048	0.0087	0.0115	0.0049	0.0014	0.0004	0.0001	0.0000	0.0000	0.0333
146.25–168.75	South-southeast	0.0013	0.0037	0.0099	0.0242	0.0185	0.0094	0.0057	0.0064	0.0029	0.0011	0.0829
168.75–191.25	South	0.0008	0.0028	0.0074	0.0224	0.0335	0.0337	0.0270	0.0327	0.0169	0.0071	0.1842
191.25–213.75	South-southwest	0.0008	0.0027	0.0056	0.0147	0.0148	0.0102	0.0052	0.0027	0.0007	0.0001	0.0574
213.75–236.25	Southwest	0.0008	0.0029	0.0056	0.0105	0.0081	0.0055	0.0020	0.0010	0.0001	0.0000	0.0366
236.25–258.75	West-southwest	0.0009	0.0036	0.0055	0.0085	0.0058	0.0028	0.0008	0.0005	0.0000	0.0000	0.0284
258.75–281.25	West	0.0010	0.0049	0.0070	0.0073	0.0037	0.0015	0.0005	0.0002	0.0001	0.0000	0.0261
281.25–303.75	West-northwest	0.0012	0.0074	0.0127	0.0123	0.0027	0.0013	0.0007	0.0005	0.0001	0.0000	0.0389
303.75–326.25	Northwest	0.0015	0.0114	0.0338	0.0691	0.0393	0.0066	0.0022	0.0021	0.0008	0.0002	0.1671

Table 1.1-26. Joint Frequency Distribution of Wind Speed and Direction for All Hours (1994 to 2006) at Site 1 at 10 m above Ground Level (Continued)

Wind Direction		Wind Speed Category (m/s)										
Degrees Azimuth	Direction	0.5–1.1	1.1–1.6	1.6–2.1	2.1–3.1	3.1–4.1	4.1–5.1	5.1–6.1	6.1–8.1	8.1–10.0	≥ 10.0	Total
326.25–348.75	North-northwest	0.0014	0.0113	0.0358	0.0610	0.0206	0.0075	0.0067	0.0099	0.0055	0.0033	0.1631
—	Total	0.0205	0.0822	0.1600	0.2757	0.1804	0.1025	0.0659	0.0692	0.0304	0.0129	0.9882
									Calms		0.000035	
									Missing/incomplete		0.011768	
									Frequency of calm winds		0.00%	
									Average wind speed		3.54 m/s	

NOTE: Wind speed categories are equal to or greater than the lower limit and are less than the upper limit.

Source: BSC 2007e, Table 5-16.

Table 1.1-27. Joint Frequency Distribution of Wind Speed and Direction (Decimal Fractions) for All Hours (1994 to 2006) at Site 1 at 60 m above Ground Level

Wind Direction		Wind Speed Category (m/s)										Total
Degrees Azimuth	Name	0.5–1.1	1.1–1.6	1.6–2.1	2.1–3.1	3.1–4.1	4.1–5.1	5.1–6.1	6.1–8.1	8.1–10.0	≥ 10.0	
348.75–11.25	North	0.0126	0.0357	0.0245	0.0165	0.0124	0.0127	0.0112	0.0146	0.0076	0.0047	0.1526
11.25–33.75	North-northeast	0.0065	0.0158	0.0160	0.0135	0.0076	0.0082	0.0068	0.0085	0.0033	0.0017	0.0878
33.75–56.25	Northeast	0.0039	0.0073	0.0062	0.0053	0.0035	0.0030	0.0025	0.0022	0.0006	0.0002	0.0347
56.25–78.75	East-northeast	0.0027	0.0048	0.0037	0.0032	0.0018	0.0010	0.0005	0.0004	0.0001	0.0000	0.0183
78.75–101.25	East	0.0023	0.0043	0.0038	0.0031	0.0014	0.0007	0.0004	0.0003	0.0001	0.0001	0.0165
101.25–123.75	East-southeast	0.0020	0.0045	0.0055	0.0045	0.0024	0.0013	0.0005	0.0003	0.0000	0.0000	0.0211
123.75–146.25	Southeast	0.0020	0.0054	0.0082	0.0118	0.0059	0.0023	0.0009	0.0004	0.0000	0.0000	0.0369
146.25–168.75	South-southeast	0.0022	0.0056	0.0111	0.0232	0.0180	0.0111	0.0065	0.0073	0.0049	0.0035	0.0934
168.75–191.25	South	0.0022	0.0056	0.0100	0.0222	0.0278	0.0309	0.0270	0.0421	0.0241	0.0241	0.2160
191.25–213.75	South-southwest	0.0025	0.0052	0.0062	0.0109	0.0100	0.0105	0.0073	0.0059	0.0018	0.0009	0.0613
213.75–236.25	Southwest	0.0032	0.0048	0.0043	0.0067	0.0067	0.0069	0.0042	0.0024	0.0004	0.0002	0.0399
236.25–258.75	West-southwest	0.0031	0.0041	0.0031	0.0037	0.0040	0.0041	0.0023	0.0013	0.0002	0.0000	0.0259
258.75–281.25	West	0.0046	0.0048	0.0025	0.0023	0.0021	0.0020	0.0010	0.0006	0.0001	0.0001	0.0203
281.25–303.75	West-northwest	0.0057	0.0066	0.0029	0.0021	0.0012	0.0015	0.0009	0.0008	0.0003	0.0001	0.0220
303.75–326.25	Northwest	0.0082	0.0134	0.0065	0.0030	0.0016	0.0016	0.0021	0.0027	0.0014	0.0011	0.0415

Table 1.1-27. Joint Frequency Distribution of Wind Speed and Direction (Decimal Fractions) for All Hours (1994 to 2006) at Site 1 at 60 m above Ground Level (Continued)

Wind Direction		Wind Speed Category (m/s)										
Degrees Azimuth	Name	0.5–1.1	1.1–1.6	1.6–2.1	2.1–3.1	3.1–4.1	4.1–5.1	5.1–6.1	6.1–8.1	8.1–10.0	≥ 10.0	Total
326.25–348.75	North-northwest	0.0105	0.0302	0.0220	0.0088	0.0037	0.0041	0.0044	0.0089	0.0079	0.0110	0.1115
—	Total	0.0744	0.1580	0.1366	0.1410	0.1100	0.1018	0.0785	0.0988	0.0530	0.0477	0.9792
										Calms	0.00028	
										Missing/incomplete	0.02049	
										Frequency of calm winds	0.03%	
										Average wind speed	3.94 m/s	

NOTE: Wind speeds are equal to or greater than the lower limit and are less than the upper limit.

Source: BSC 2007e, Table B-2.

Table 1.1-28. Joint Frequency Distribution of Wind Speed and Direction (Decimal Fractions) for All Hours (1994 to 2006) at Site 2 at 10 m above Ground Level

Wind Direction		Wind Speed Category (m/s)										
Degrees Azimuth	Name	0.5–1.1	1.1–1.6	1.6–2.1	2.1–3.1	3.1–4.1	4.1–5.1	5.1–6.1	6.1–8.1	8.1–10.0	≥ 10.0	Total
348.75–11.25	North	0.0003	0.0009	0.0014	0.0027	0.0032	0.0042	0.0043	0.0059	0.0031	0.0014	0.0275
11.25–33.75	North-northeast	0.0004	0.0010	0.0018	0.0042	0.0051	0.0054	0.0051	0.0060	0.0022	0.0012	0.0323
33.75–56.25	Northeast	0.0005	0.0016	0.0028	0.0065	0.0104	0.0111	0.0072	0.0075	0.0020	0.0007	0.0505
56.25–78.75	East-northeast	0.0005	0.0032	0.0068	0.0182	0.0172	0.0082	0.0035	0.0032	0.0009	0.0004	0.0622
78.75–101.25	East	0.0009	0.0048	0.0132	0.0366	0.0333	0.0119	0.0036	0.0018	0.0006	0.0003	0.1071
101.25–123.75	East-southeast	0.0009	0.0044	0.0117	0.0321	0.0291	0.0154	0.0065	0.0023	0.0003	0.0001	0.1029
123.75–146.25	Southeast	0.0009	0.0044	0.0103	0.0248	0.0258	0.0182	0.0104	0.0080	0.0015	0.0002	0.1044
146.25–168.75	South-southeast	0.0008	0.0039	0.0074	0.0159	0.0186	0.0195	0.0166	0.0215	0.0085	0.0020	0.1146
168.75–191.25	South	0.0010	0.0038	0.0066	0.0114	0.0115	0.0134	0.0115	0.0102	0.0023	0.0005	0.0722
191.25–213.75	South-southwest	0.0012	0.0039	0.0066	0.0104	0.0088	0.0097	0.0069	0.0050	0.0013	0.0008	0.0546
213.75–236.25	Southwest	0.0017	0.0056	0.0081	0.0113	0.0130	0.0139	0.0102	0.0069	0.0019	0.0012	0.0738
236.25–258.75	West-southwest	0.0017	0.0053	0.0069	0.0095	0.0077	0.0078	0.0075	0.0107	0.0037	0.0019	0.0626
258.75–281.25	West	0.0016	0.0043	0.0054	0.0076	0.0048	0.0036	0.0033	0.0045	0.0023	0.0011	0.0385
281.25–303.75	West-northwest	0.0008	0.0022	0.0029	0.0036	0.0023	0.0020	0.0023	0.0032	0.0023	0.0029	0.0247
303.75–326.25	Northwest	0.0006	0.0013	0.0018	0.0026	0.0025	0.0025	0.0031	0.0064	0.0057	0.0146	0.0413

Table 1.1-28. Joint Frequency Distribution of Wind Speed and Direction (Decimal Fractions) for All Hours (1994 to 2006) at Site 2 at 10 m above Ground Level (Continued)

Wind Direction		Wind Speed Category (m/s)										
Degrees Azimuth	Name	0.5–1.1	1.1–1.6	1.6–2.1	2.1–3.1	3.1–4.1	4.1–5.1	5.1–6.1	6.1–8.1	8.1–10.0	≥ 10.0	Total
326.25–348.75	North-northwest	0.0004	0.0009	0.0012	0.0022	0.0025	0.0032	0.0033	0.0057	0.0048	0.0065	0.0307
—	Total	0.0144	0.0515	0.0950	0.1994	0.1959	0.1501	0.1056	0.1089	0.0433	0.0358	0.9972
									Calms		0.00003	
									Missing/incomplete		0.00276	
									Frequency of calm Winds		0.00%	
									Average wind speed		4.39 m/s	

NOTE: Wind speeds are equal to or greater than the lower limit and are less than the upper limit.

Source: BSC 2007e, Table B-3.

Table 1.1-29. Joint Frequency Distribution of Wind Speed and Direction (Decimal Fractions) for All Hours (1994 to 1998) at Site 3 at 10 m above Ground Level

Wind Direction		Wind Speed Category (m/s)										
Degrees Azimuth	Name	0.5–1.1	1.1–1.6	1.6–2.1	2.1–3.1	3.1–4.1	4.1–5.1	5.1–6.1	6.1–8.1	8.1–10.0	≥ 10.0	Total
348.75–11.25	North	0.0010	0.0009	0.0005	0.0008	0.0001	0.0001	0.0000	0.0000	0.0000	0.0000	0.0033
11.25–33.75	North-northeast	0.0009	0.0006	0.0002	0.0005	0.0002	0.0001	0.0000	0.0000	0.0000	0.0000	0.0024
33.75–56.25	Northeast	0.0010	0.0008	0.0005	0.0006	0.0003	0.0000	0.0000	0.0000	0.0000	0.0000	0.0033
56.25–78.75	East-northeast	0.0014	0.0015	0.0012	0.0016	0.0006	0.0001	0.0000	0.0000	0.0000	0.0000	0.0064
78.75–101.25	East	0.0029	0.0052	0.0063	0.0114	0.0058	0.0020	0.0007	0.0002	0.0001	0.0000	0.0346
101.25–123.75	East-southeast	0.0047	0.0115	0.0274	0.0409	0.0129	0.0027	0.0005	0.0004	0.0000	0.0000	0.1010
123.75–146.25	Southeast	0.0036	0.0093	0.0183	0.0313	0.0142	0.0032	0.0004	0.0001	0.0000	0.0000	0.0805
146.25–168.75	South-southeast	0.0021	0.0073	0.0137	0.0401	0.0471	0.0309	0.0174	0.0084	0.0015	0.0000	0.1686
168.75–191.25	South	0.0026	0.0074	0.0105	0.0133	0.0050	0.0010	0.0003	0.0001	0.0000	0.0000	0.0403
191.25–213.75	South-southwest	0.0021	0.0067	0.0061	0.0076	0.0013	0.0002	0.0000	0.0000	0.0000	0.0000	0.0241
213.75–236.25	Southwest	0.0032	0.0092	0.0062	0.0097	0.0017	0.0002	0.0001	0.0000	0.0000	0.0000	0.0303
236.25–258.75	West-southwest	0.0028	0.0139	0.0110	0.0097	0.0018	0.0003	0.0000	0.0000	0.0000	0.0000	0.0395
258.75–281.25	West	0.0043	0.0203	0.0278	0.0148	0.0046	0.0009	0.0002	0.0000	0.0000	0.0000	0.0728
281.25–303.75	West-northwest	0.0048	0.0272	0.0749	0.1312	0.0201	0.0111	0.0066	0.0069	0.0029	0.0024	0.2880
303.75–326.25	Northwest	0.0038	0.0135	0.0230	0.0205	0.0128	0.0094	0.0058	0.0055	0.0018	0.0010	0.0971

Table 1.1-29. Joint Frequency Distribution of Wind Speed and Direction (Decimal Fractions) for All Hours (1994 to 1998) at Site 3 at 10 m above Ground Level (Continued)

Wind Direction		Wind Speed Category (m/s)										
Degrees Azimuth	Name	0.5–1.1	1.1–1.6	1.6–2.1	2.1–3.1	3.1–4.1	4.1–5.1	5.1–6.1	6.1–8.1	8.1–10.0	≥ 10.0	Total
326.25–348.75	North-northwest	0.0016	0.0031	0.0010	0.0011	0.0005	0.0002	0.0000	0.0000	0.0000	0.0000	0.0075
—	Total	0.0429	0.1384	0.2286	0.3351	0.1288	0.0624	0.0321	0.0218	0.0064	0.0033	0.9944
									Calms		0.00021	
									Missing/incomplete		0.00536	
									Frequency of calm winds		0.02%	
									Average wind speed		2.68 m/s	

NOTE: Wind speeds are equal to or greater than the lower limit and are less than the upper limit.

Source: BSC 2007e, Table B-4.

Table 1.1-30. Joint Frequency Distribution of Wind Speed and Direction (Decimal Fractions) for All Hours (1994 to 2006) at Site 4 at 10 m above Ground Level

Wind Direction		Wind Speed Category (m/s)										
Degrees Azimuth	Name	0.5-1.1	1.1-1.6	1.6-2.1	2.1-3.1	3.1-4.1	4.1-5.1	5.1-6.1	6.1-8.1	8.1-10.0	≥ 10.0	Total
348.75-11.25	North	0.0005	0.0066	0.0255	0.0309	0.0070	0.0049	0.0048	0.0095	0.0000	0.0000	0.1095
11.25-33.75	North-northeast	0.0006	0.0077	0.0319	0.0454	0.0123	0.0098	0.0107	0.0207	0.0000	0.0000	0.1828
33.75-56.25	Northeast	0.0006	0.0060	0.0165	0.0442	0.0201	0.0118	0.0082	0.0073	0.0000	0.0000	0.1185
56.25-78.75	East-northeast	0.0005	0.0037	0.0074	0.0115	0.0039	0.0015	0.0007	0.0008	0.0000	0.0000	0.0308
78.75-101.25	East	0.0004	0.0031	0.0050	0.0039	0.0016	0.0010	0.0007	0.0009	0.0001	0.0000	0.0172
101.25-123.75	East-southeast	0.0003	0.0024	0.0051	0.0049	0.0019	0.0015	0.0008	0.0006	0.0000	0.0000	0.0178
123.75-146.25	Southeast	0.0002	0.0019	0.0061	0.0096	0.0049	0.0025	0.0010	0.0005	0.0000	0.0000	0.0267
146.25-168.75	South-southeast	0.0003	0.0020	0.0070	0.0208	0.0192	0.0107	0.0050	0.0042	0.0015	0.0000	0.0732
168.75-191.25	South	0.0003	0.0020	0.0082	0.0285	0.0325	0.0309	0.0242	0.0362	0.0000	0.0000	0.2106
191.25-213.75	South-southwest	0.0004	0.0022	0.0055	0.0115	0.0107	0.0111	0.0076	0.0068	0.0000	0.0000	0.0598
213.75-236.25	Southwest	0.0003	0.0021	0.0037	0.0061	0.0047	0.0046	0.0042	0.0036	0.0000	0.0000	0.0306
236.25-258.75	West-southwest	0.0002	0.0018	0.0030	0.0035	0.0022	0.0023	0.0022	0.0020	0.0000	0.0000	0.0181
258.75-281.25	West	0.0003	0.0018	0.0026	0.0027	0.0012	0.0008	0.0009	0.0010	0.0000	0.0000	0.0116
281.25-303.75	West-northwest	0.0004	0.0018	0.0033	0.0024	0.0010	0.0008	0.0006	0.0009	0.0029	0.0024	0.0120
303.75-326.25	Northwest	0.0004	0.0026	0.0049	0.0051	0.0018	0.0013	0.0013	0.0027	0.0018	0.0010	0.0238

Table 1.1-30. Joint Frequency Distribution of Wind Speed and Direction (Decimal Fractions) for All Hours (1994 to 2006) at Site 4 at 10 m above Ground Level (Continued)

Wind Direction		Wind Speed Category (m/s)										
Degrees Azimuth	Name	0.5–1.1	1.1–1.6	1.6–2.1	2.1–3.1	3.1–4.1	4.1–5.1	5.1–6.1	6.1–8.1	8.1–10.0	≥ 10.0	Total
326.25–348.75	North-northwest	0.0005	0.0038	0.0091	0.0175	0.0060	0.0027	0.0023	0.0037	0.0000	0.0000	0.0568
—	Total	0.0061	0.0514	0.1448	0.2484	0.1311	0.0982	0.0752	0.1015	0.0064	0.0033	0.9970
									Calms		0.00009	
									Missing/incomplete		0.00294	
									Frequency of calm winds		0.01%	
									Average wind speed		4.62 m/s	

NOTE: Wind speeds are equal to or greater than the lower limit and are less than the upper limit.

Source: BSC 2007e, Table B-5.

Table 1.1-31. Joint Frequency Distribution of Wind Speed and Direction (Decimal Fractions) for All Hours (1994 to 1998) at Site 5 at 10 m above Ground Level

Wind Direction		Wind Speed Category (m/s)										
Degrees Azimuth	Name	0.5–1.1	1.1–1.6	1.6–2.1	2.1–3.1	3.1–4.1	4.1–5.1	5.1–6.1	6.1–8.1	8.1–10.0	≥ 10.0	Total
348.75–11.25	North	0.0002	0.0025	0.0075	0.0271	0.0512	0.0786	0.0657	0.0400	0.0056	0.0019	0.2802
11.25–33.75	North-northeast	0.0002	0.0019	0.0063	0.0187	0.0390	0.0512	0.0166	0.0029	0.0006	0.0001	0.1373
33.75–56.25	Northeast	0.0002	0.0014	0.0042	0.0105	0.0147	0.0115	0.0024	0.0016	0.0006	0.0002	0.0475
56.25–78.75	East-northeast	0.0001	0.0012	0.0026	0.0049	0.0047	0.0034	0.0030	0.0031	0.0007	0.0005	0.0241
78.75–101.25	East	0.0002	0.0012	0.0020	0.0033	0.0027	0.0021	0.0013	0.0008	0.0003	0.0000	0.0140
101.25–123.75	East-southeast	0.0001	0.0012	0.0020	0.0033	0.0022	0.0007	0.0002	0.0001	0.0000	0.0000	0.0098
123.75–146.25	Southeast	0.0001	0.0010	0.0026	0.0045	0.0021	0.0010	0.0005	0.0005	0.0001	0.0000	0.0126
146.25–168.75	South-southeast	0.0004	0.0020	0.0037	0.0079	0.0077	0.0058	0.0059	0.0099	0.0065	0.0038	0.0535
168.75–191.25	South	0.0002	0.0022	0.0086	0.0195	0.0228	0.0201	0.0193	0.0301	0.0167	0.0133	0.1528
191.25–213.75	South-southwest	0.0005	0.0032	0.0118	0.0300	0.0225	0.0136	0.0064	0.0050	0.0020	0.0011	0.0961
213.75–236.25	Southwest	0.0006	0.0033	0.0079	0.0136	0.0102	0.0059	0.0025	0.0011	0.0004	0.0002	0.0455
236.25–258.75	West-southwest	0.0006	0.0032	0.0043	0.0060	0.0044	0.0034	0.0019	0.0013	0.0003	0.0001	0.0253
258.75–281.25	West	0.0005	0.0029	0.0035	0.0036	0.0022	0.0020	0.0011	0.0008	0.0001	0.0000	0.0167
281.25–303.75	West-northwest	0.0005	0.0026	0.0024	0.0022	0.0011	0.0010	0.0008	0.0009	0.0002	0.0000	0.0117
303.75–326.25	Northwest	0.0003	0.0024	0.0038	0.0039	0.0013	0.0014	0.0017	0.0022	0.0013	0.0007	0.0190

Table 1.1-31. Joint Frequency Distribution of Wind Speed and Direction (Decimal Fractions) for All Hours (1994 to 1998) at Site 5 at 10 m above Ground Level (Continued)

Wind Direction		Wind Speed Category (m/s)										
Degrees Azimuth	Name	0.5–1.1	1.1–1.6	1.6–2.1	2.1–3.1	3.1–4.1	4.1–5.1	5.1–6.1	6.1–8.1	8.1–10.0	≥ 10.0	Total
326.25–348.75	North-northwest	0.0004	0.0025	0.0067	0.0110	0.0068	0.0052	0.0048	0.0071	0.0048	0.0046	0.0539
—	Total	0.0052	0.0345	0.0798	0.1699	0.1954	0.2068	0.1342	0.1074	0.0403	0.0265	0.9930
									Calms		0	
									Missing/incomplete		0.00701	
									Frequency of calm winds		0.00%	
									Average wind speed		4.48 m/s	

NOTE: Wind speeds are equal to or greater than the lower limit and are less than the upper limit.

Source: BSC 2007e, Table B-6.

Table 1.1-32. Joint Frequency Distribution of Wind Speed and Direction (Decimal Fractions) for All Hours (1994 to 1998) at Site 7 at 10 m above Ground Level

Wind Direction		Wind Speed Category (m/s)										
Degrees Azimuth	Name	0.5-1.1	1.1-1.6	1.6-2.1	2.1-3.1	3.1-4.1	4.1-5.1	5.1-6.1	6.1-8.1	8.1-10.0	≥ 10.0	Total
348.75-11.25	North	0.0014	0.0043	0.0087	0.0153	0.0158	0.0156	0.0126	0.0142	0.0042	0.0013	0.0935
11.25-33.75	North-northeast	0.0006	0.0020	0.0037	0.0085	0.0105	0.0119	0.0075	0.0046	0.0011	0.0001	0.0504
33.75-56.25	Northeast	0.0006	0.0013	0.0029	0.0059	0.0035	0.0018	0.0007	0.0001	0.0000	0.0000	0.0169
56.25-78.75	East-northeast	0.0005	0.0013	0.0027	0.0025	0.0010	0.0003	0.0002	0.0001	0.0000	0.0000	0.0086
78.75-101.25	East	0.0005	0.0015	0.0025	0.0021	0.0010	0.0005	0.0002	0.0001	0.0000	0.0000	0.0084
101.25-123.75	East-southeast	0.0008	0.0025	0.0032	0.0039	0.0024	0.0011	0.0006	0.0004	0.0001	0.0000	0.0150
123.75-146.25	Southeast	0.0007	0.0035	0.0088	0.0123	0.0056	0.0017	0.0004	0.0002	0.0001	0.0000	0.0332
146.25-168.75	South-southeast	0.0008	0.0047	0.0125	0.0322	0.0276	0.0155	0.0098	0.0121	0.0070	0.0029	0.1250
168.75-191.25	South	0.0009	0.0032	0.0087	0.0206	0.0250	0.0234	0.0183	0.0203	0.0087	0.0030	0.1320
191.25-213.75	South-southwest	0.0010	0.0028	0.0043	0.0098	0.0110	0.0067	0.0026	0.0015	0.0004	0.0001	0.0402
213.75-236.25	Southwest	0.0015	0.0029	0.0034	0.0048	0.0050	0.0036	0.0011	0.0006	0.0001	0.0001	0.0232
236.25-258.75	West-southwest	0.0032	0.0068	0.0027	0.0031	0.0031	0.0017	0.0006	0.0003	0.0000	0.0000	0.0213
258.75-281.25	West	0.0066	0.0238	0.0068	0.0019	0.0013	0.0012	0.0004	0.0001	0.0000	0.0000	0.0421
281.25-303.75	West-northwest	0.0072	0.0482	0.0386	0.0070	0.0013	0.0009	0.0007	0.0003	0.0001	0.0000	0.1042
303.75-326.25	Northwest	0.0063	0.0383	0.0685	0.0477	0.0059	0.0025	0.0023	0.0032	0.0009	0.0005	0.1763

Table 1.1-32. Joint Frequency Distribution of Wind Speed and Direction (Decimal Fractions) for All Hours (1994 to 1998) at Site 7 at 10 m above Ground Level (Continued)

Wind Direction		Wind Speed Category (m/s)										
Degrees Azimuth	Name	0.5–1.1	1.1–1.6	1.6–2.1	2.1–3.1	3.1–4.1	4.1–5.1	5.1–6.1	6.1–8.1	8.1–10.0	≥ 10.0	Total
326.25–348.75	North-northwest	0.0022	0.0135	0.0279	0.0284	0.0120	0.0061	0.0052	0.0068	0.0046	0.0028	0.1096
—	Total	0.0346	0.1606	0.2057	0.2059	0.1321	0.0946	0.0632	0.0650	0.0274	0.0108	0.9977
									Calms		0.00023	
									Missing/incomplete		0.00210	
									Frequency of calm winds		0.02%	
									Average wind speed		3.24 m/s	

NOTE: Wind speeds are equal to or greater than the lower limit and are less than the upper limit.

Source: BSC 2007e, Table B-7.

Table 1.1-33. Joint Frequency Distribution of Wind Speed and Direction (Decimal Fractions) for All Hours (1994 to 2006) at Site 9 at 10 m above Ground Level

Wind Direction		Wind Speed Category (m/s)										
Degrees Azimuth	Name	0.5–1.1	1.1–1.6	1.6–2.1	2.1–3.1	3.1–4.1	4.1–5.1	5.1–6.1	6.1–8.1	8.1–10.0	≥ 10.0	Total
348.75–11.25	North	0.0002	0.0017	0.0037	0.0113	0.0152	0.0133	0.0072	0.0057	0.0024	0.0008	0.0613
11.25–33.75	North-northeast	0.0003	0.0016	0.0052	0.0247	0.0734	0.0972	0.0318	0.0062	0.0012	0.0003	0.2418
33.75–56.25	Northeast	0.0003	0.0018	0.0060	0.0209	0.0283	0.0264	0.0131	0.0051	0.0015	0.0004	0.1038
56.25–78.75	East-northeast	0.0003	0.0016	0.0047	0.0103	0.0067	0.0042	0.0025	0.0017	0.0004	0.0002	0.0325
78.75–101.25	East	0.0003	0.0017	0.0042	0.0078	0.0034	0.0019	0.0012	0.0006	0.0002	0.0001	0.0215
101.25–123.75	East-southeast	0.0002	0.0017	0.0041	0.0078	0.0044	0.0011	0.0004	0.0003	0.0001	0.0000	0.0201
123.75–146.25	Southeast	0.0004	0.0021	0.0049	0.0106	0.0092	0.0055	0.0029	0.0029	0.0009	0.0003	0.0397
146.25–168.75	South-southeast	0.0003	0.0022	0.0064	0.0169	0.0257	0.0227	0.0204	0.0299	0.0181	0.0115	0.1540
168.75–191.25	South	0.0004	0.0029	0.0097	0.0270	0.0236	0.0183	0.0143	0.0195	0.0121	0.0090	0.1368
191.25–213.75	South-southwest	0.0004	0.0031	0.0085	0.0154	0.0105	0.0046	0.0022	0.0026	0.0013	0.0008	0.0493
213.75–236.25	Southwest	0.0004	0.0022	0.0064	0.0098	0.0056	0.0018	0.0007	0.0006	0.0002	0.0001	0.0278
236.25–258.75	West-southwest	0.0003	0.0018	0.0041	0.0066	0.0039	0.0016	0.0005	0.0003	0.0001	0.0000	0.0192
258.75–281.25	West	0.0003	0.0015	0.0031	0.0050	0.0031	0.0015	0.0006	0.0004	0.0001	0.0000	0.0156
281.25–303.75	West-northwest	0.0002	0.0011	0.0024	0.0041	0.0027	0.0018	0.0011	0.0007	0.0001	0.0001	0.0142
303.75–326.25	Northwest	0.0002	0.0010	0.0022	0.0046	0.0040	0.0038	0.0032	0.0045	0.0022	0.0007	0.0262

Table 1.1-33. Joint Frequency Distribution of Wind Speed and Direction (Decimal Fractions) for All Hours (1994 to 2006) at Site 9 at 10 m above Ground Level (Continued)

Wind Direction		Wind Speed Category (m/s)										
Degrees Azimuth	Name	0.5–1.1	1.1–1.6	1.6–2.1	2.1–3.1	3.1–4.1	4.1–5.1	5.1–6.1	6.1–8.1	8.1–10.0	≥ 10.0	Total
326.25–348.75	North-northwest	0.0002	0.0012	0.0023	0.0061	0.0068	0.0047	0.0038	0.0054	0.0034	0.0022	0.0361
—	Total	0.0046	0.0290	0.0779	0.1889	0.2263	0.2104	0.1060	0.0863	0.0441	0.0264	0.9857
										Calms	0.00002	
										Missing/incomplete	0.01425	
										Frequency of calm winds	0.00%	
										Average wind speed	4.38 m/s	

NOTE: Wind speeds are equal to or greater than the lower limit and are less than the upper limit.

Source: BSC 2007e, Table B-8.

Table 1.1-34. Joint Frequency Distribution of Wind Speed and Direction (Decimal Fractions) for Daytime Hours (1994 to 2006) at Site 1 at 10 m above Ground Level

Wind Direction		Wind Speed Category (m/s)										
Degrees Azimuth	Name	0.5–1.1	1.1–1.6	1.6–2.1	2.1–3.1	3.1–4.1	4.1–5.1	5.1–6.1	6.1–8.1	8.1–10.0	≥ 10.0	Total
348.75–11.25	North	0.0015	0.0053	0.0059	0.0056	0.0061	0.0066	0.0059	0.0070	0.0021	0.0007	0.0467
11.25–33.75	North-northeast	0.0020	0.0047	0.0035	0.0052	0.0072	0.0072	0.0049	0.0044	0.0009	0.0002	0.0402
33.75–56.25	Northeast	0.0030	0.0087	0.0044	0.0059	0.0059	0.0052	0.0031	0.0014	0.0002	0.0000	0.0378
56.25–78.75	East-northeast	0.0039	0.0087	0.0051	0.0059	0.0030	0.0014	0.0006	0.0004	0.0000	0.0000	0.0291
78.75–101.25	East	0.0036	0.0070	0.0073	0.0053	0.0022	0.0010	0.0003	0.0004	0.0000	0.0000	0.0272
101.25–123.75	East-southeast	0.0028	0.0079	0.0097	0.0091	0.0036	0.0014	0.0006	0.0002	0.0000	0.0000	0.0354
123.75–146.25	Southeast	0.0026	0.0089	0.0162	0.0217	0.0091	0.0026	0.0007	0.0001	0.0001	0.0000	0.0620
146.25–168.75	South-southeast	0.0021	0.0061	0.0178	0.0453	0.0345	0.0173	0.0102	0.0116	0.0054	0.0021	0.1524
168.75–191.25	South	0.0013	0.0038	0.0107	0.0369	0.0576	0.0570	0.0453	0.0537	0.0270	0.0121	0.3054
191.25–213.75	South-southwest	0.0010	0.0024	0.0055	0.0159	0.0184	0.0154	0.0079	0.0039	0.0012	0.0002	0.0717
213.75–236.25	Southwest	0.0009	0.0017	0.0037	0.0105	0.0126	0.0101	0.0038	0.0018	0.0003	0.0001	0.0453
236.25–258.75	West-southwest	0.0008	0.0019	0.0026	0.0060	0.0065	0.0043	0.0012	0.0008	0.0000	0.0000	0.0241
258.75–281.25	West	0.0008	0.0018	0.0022	0.0036	0.0032	0.0021	0.0007	0.0003	0.0001	0.0001	0.0149
281.25–303.75	West-northwest	0.0007	0.0029	0.0026	0.0028	0.0022	0.0020	0.0011	0.0005	0.0002	0.0000	0.0150
303.75–326.25	Northwest	0.0010	0.0041	0.0058	0.0066	0.0036	0.0032	0.0027	0.0029	0.0012	0.0002	0.0312

Table 1.1-34. Joint Frequency Distribution of Wind Speed and Direction (Decimal Fractions) for Daytime Hours (1994 to 2006) at Site 1 at 10 m above Ground Level (Continued)

Wind Direction		Wind Speed Category (m/s)										
Degrees Azimuth	Name	0.5–1.1	1.1–1.6	1.6–2.1	2.1–3.1	3.1–4.1	4.1–5.1	5.1–6.1	6.1–8.1	8.1–10.0	≥ 10.0	Total
326.25–348.75	North-northwest	0.0015	0.0055	0.0096	0.0083	0.0050	0.0062	0.0075	0.0102	0.0053	0.0027	0.0616
—	Total	0.0294	0.0813	0.1126	0.1945	0.1805	0.1430	0.0967	0.0998	0.0438	0.0183	0.9843
									Calms		0.00004	
									Missing/incomplete		0.01563	
									Frequency of calm winds		0.00%	
									Average wind speed		4.01 m/s	

NOTE: Daytime hours are from sunrise to sunset.
Wind speeds are equal to or greater than the lower limit and are less than the upper limit.

Source: BSC 2007e, Table C-1.

Table 1.1-35. Joint Frequency Distribution of Wind Speed and Direction (Decimal Fractions) for Night Hours (1994 to 2006) at Site 1 at 10 m above Ground Level

Wind Direction		Wind Speed Category (m/s)										
Degrees Azimuth	Name	0.5–1.1	1.1–1.6	1.6–2.1	2.1–3.1	3.1–4.1	4.1–5.1	5.1–6.1	6.1–8.1	8.1–10.0	≥ 10.0	Total
348.75–11.25	North	0.0009	0.0063	0.0129	0.0219	0.0222	0.0170	0.0109	0.0101	0.0027	0.0008	0.1057
11.25–33.75	North-northeast	0.0003	0.0019	0.0035	0.0056	0.0052	0.0044	0.0028	0.0019	0.0006	0.0001	0.0263
33.75–56.25	Northeast	0.0002	0.0010	0.0016	0.0017	0.0009	0.0003	0.0003	0.0003	0.0000	0.0000	0.0064
56.25–78.75	East-northeast	0.0002	0.0005	0.0007	0.0006	0.0004	0.0001	0.0001	0.0001	0.0000	0.0000	0.0027
78.75–101.25	East	0.0002	0.0004	0.0006	0.0008	0.0003	0.0002	0.0001	0.0001	0.0000	0.0000	0.0026
101.25–123.75	East-southeast	0.0002	0.0007	0.0008	0.0008	0.0004	0.0003	0.0000	0.0001	0.0000	0.0000	0.0033
123.75–146.25	Southeast	0.0003	0.0006	0.0012	0.0013	0.0007	0.0002	0.0001	0.0000	0.0000	0.0000	0.0043
146.25–168.75	South-southeast	0.0004	0.0014	0.0018	0.0030	0.0023	0.0014	0.0012	0.0011	0.0003	0.0000	0.0130
168.75–191.25	South	0.0004	0.0018	0.0040	0.0079	0.0091	0.0102	0.0085	0.0116	0.0067	0.0021	0.0622
191.25–213.75	South-southwest	0.0005	0.0030	0.0057	0.0134	0.0111	0.0050	0.0025	0.0014	0.0002	0.0001	0.0430
213.75–236.25	Southwest	0.0007	0.0042	0.0076	0.0105	0.0036	0.0009	0.0002	0.0002	0.0000	0.0000	0.0279
236.25–258.75	West-southwest	0.0010	0.0054	0.0084	0.0111	0.0050	0.0013	0.0003	0.0002	0.0000	0.0000	0.0327
258.75–281.25	West	0.0013	0.0079	0.0118	0.0110	0.0041	0.0009	0.0003	0.0001	0.0000	0.0000	0.0375
281.25–303.75	West-northwest	0.0016	0.0120	0.0229	0.0219	0.0033	0.0006	0.0003	0.0004	0.0001	0.0000	0.0630
303.75–326.25	Northwest	0.0019	0.0188	0.0621	0.1321	0.0752	0.0101	0.0017	0.0013	0.0005	0.0003	0.3040

Table 1.1-35. Joint Frequency Distribution of Wind Speed and Direction (Decimal Fractions) for Night Hours (1994 to 2006) at Site 1 at 10 m above Ground Level (Continued)

Wind Direction		Wind Speed Category (m/s)										
Degrees Azimuth	Name	0.5–1.1	1.1–1.6	1.6–2.1	2.1–3.1	3.1–4.1	4.1–5.1	5.1–6.1	6.1–8.1	8.1–10.0	≥ 10.0	Total
326.25–348.75	North-northwest	0.0013	0.0172	0.0622	0.1141	0.0364	0.0089	0.0059	0.0097	0.0057	0.0039	0.2653
—	Total	0.0116	0.0831	0.2078	0.3575	0.1804	0.0618	0.0350	0.0385	0.0169	0.0075	0.9921
									Calms		0.00004	
									Missing/incomplete		0.00785	
									Frequency of calm winds		0.00%	
									Average wind speed		3.07 m/s	

NOTE: Wind speeds are equal to or greater than the lower limit and are less than the upper limit.

Source: BSC 2007e, Table C-2.

Table 1.1-36. Joint Frequency Distribution of Wind Speed and Direction (Decimal Fractions) for Daytime Hours (1994 to 2006) at Site 1 at 60 m above Ground Level

Wind Direction		Wind Speed Category (m/s)										
Degrees Azimuth	Name	0.5–1.1	1.1–1.6	1.6–2.1	2.1–3.1	3.1–4.1	4.1–5.1	5.1–6.1	6.1–8.1	8.1–10.0	≥ 10.0	Total
348.75–11.25	North	0.0052	0.0078	0.0045	0.0046	0.0046	0.0049	0.0053	0.0084	0.0045	0.0033	0.0531
11.25–33.75	North-northeast	0.0042	0.0078	0.0062	0.0067	0.0056	0.0069	0.0065	0.0080	0.0032	0.0014	0.0564
33.75–56.25	Northeast	0.0040	0.0059	0.0052	0.0059	0.0048	0.0047	0.0040	0.0035	0.0008	0.0003	0.0391
56.25–78.75	East-northeast	0.0027	0.0056	0.0047	0.0050	0.0030	0.0017	0.0008	0.0006	0.0002	0.0000	0.0242
78.75–101.25	East	0.0026	0.0052	0.0055	0.0046	0.0021	0.0012	0.0007	0.0006	0.0002	0.0001	0.0228
101.25–123.75	East-southeast	0.0025	0.0061	0.0086	0.0074	0.0038	0.0021	0.0007	0.0005	0.0000	0.0000	0.0316
123.75–146.25	Southeast	0.0022	0.0068	0.0132	0.0201	0.0101	0.0039	0.0014	0.0007	0.0001	0.0001	0.0586
146.25–168.75	South-southeast	0.0019	0.0061	0.0164	0.0402	0.0319	0.0194	0.0108	0.0120	0.0085	0.0062	0.1534
168.75–191.25	South	0.0016	0.0046	0.0110	0.0306	0.0435	0.0496	0.0418	0.0635	0.0356	0.0366	0.3184
191.25–213.75	South-southwest	0.0017	0.0032	0.0048	0.0106	0.0125	0.0165	0.0111	0.0086	0.0025	0.0013	0.0729
213.75–236.25	Southwest	0.0016	0.0021	0.0026	0.0061	0.0092	0.0119	0.0072	0.0044	0.0007	0.0003	0.0461
236.25–258.75	West-southwest	0.0014	0.0013	0.0018	0.0032	0.0045	0.0047	0.0032	0.0020	0.0003	0.0001	0.0224
258.75–281.25	West	0.0019	0.0014	0.0009	0.0017	0.0023	0.0027	0.0015	0.0008	0.0001	0.0001	0.0135
281.25–303.75	West-northwest	0.0014	0.0015	0.0008	0.0013	0.0013	0.0020	0.0014	0.0012	0.0003	0.0001	0.0114
303.75–326.25	Northwest	0.0025	0.0027	0.0015	0.0014	0.0015	0.0019	0.0030	0.0038	0.0019	0.0012	0.0214

Table 1.1-36. Joint Frequency Distribution of Wind Speed and Direction (Decimal Fractions) for Daytime Hours (1994 to 2006) at Site 1 at 60 m above Ground Level (Continued)

Wind Direction		Wind Speed Category (m/s)										
Degrees Azimuth	Name	0.5–1.1	1.1–1.6	1.6–2.1	2.1–3.1	3.1–4.1	4.1–5.1	5.1–6.1	6.1–8.1	8.1–10.0	≥ 10.0	Total
326.25–348.75	North-northwest	0.0037	0.0059	0.0040	0.0021	0.0025	0.0039	0.0047	0.0111	0.0082	0.0085	0.0547
—	Total	0.0412	0.0739	0.0917	0.1515	0.1433	0.1379	0.1042	0.1295	0.0669	0.0597	0.9741
									Calms		0.00016	
									Missing/incomplete		0.02575	
									Frequency of calm winds		0.02%	
									Average wind speed		4.66 m/s	

NOTE: Daytime hours are from sunrise to sunset.
Wind speeds are equal to or greater than the lower limit and are less than the upper limit.

Source: BSC 2007e, Table C-3.

Table 1.1-37. Joint Frequency Distribution of Wind Speed and Direction (Decimal Fractions) for Night Hours (1994 to 2006) at Site 1 at 60 m above Ground Level

Wind Direction		Wind Speed Category (m/s)										
Degrees Azimuth	Name	0.5–1.1	1.1–1.6	1.6–2.1	2.1–3.1	3.1–4.1	4.1–5.1	5.1–6.1	6.1–8.1	8.1–10.0	≥ 10.0	Total
348.75–11.25	North	0.0201	0.0638	0.0446	0.0285	0.0203	0.0206	0.0170	0.0207	0.0107	0.0061	0.2525
11.25–33.75	North-northeast	0.0089	0.0238	0.0259	0.0204	0.0095	0.0095	0.0071	0.0090	0.0033	0.0019	0.1193
33.75–56.25	Northeast	0.0039	0.0086	0.0071	0.0046	0.0022	0.0013	0.0010	0.0009	0.0004	0.0001	0.0302
56.25–78.75	East-northeast	0.0027	0.0040	0.0028	0.0014	0.0006	0.0004	0.0002	0.0002	0.0001	0.0000	0.0123
78.75–101.25	East	0.0020	0.0033	0.0021	0.0015	0.0006	0.0003	0.0001	0.0001	0.0001	0.0001	0.0103
101.25–123.75	East-southeast	0.0016	0.0029	0.0024	0.0017	0.0009	0.0005	0.0002	0.0001	0.0001	0.0000	0.0105
123.75–146.25	Southeast	0.0018	0.0040	0.0031	0.0034	0.0017	0.0008	0.0003	0.0001	0.0000	0.0000	0.0152
146.25–168.75	South-southeast	0.0025	0.0051	0.0058	0.0062	0.0041	0.0027	0.0022	0.0026	0.0013	0.0008	0.0332
168.75–191.25	South	0.0027	0.0065	0.0090	0.0138	0.0120	0.0122	0.0122	0.0206	0.0126	0.0116	0.1132
191.25–213.75	South-southwest	0.0033	0.0073	0.0076	0.0112	0.0074	0.0045	0.0035	0.0033	0.0012	0.0004	0.0497
213.75–236.25	Southwest	0.0048	0.0075	0.0061	0.0074	0.0041	0.0019	0.0011	0.0005	0.0001	0.0001	0.0336
236.25–258.75	West-southwest	0.0048	0.0069	0.0044	0.0042	0.0036	0.0034	0.0014	0.0006	0.0001	0.0000	0.0295
258.75–281.25	West	0.0073	0.0083	0.0041	0.0030	0.0019	0.0013	0.0006	0.0004	0.0001	0.0000	0.0271
281.25–303.75	West-northwest	0.0099	0.0118	0.0050	0.0029	0.0011	0.0009	0.0003	0.0004	0.0003	0.0001	0.0327
303.75–326.25	Northwest	0.0140	0.0241	0.0115	0.0047	0.0017	0.0012	0.0013	0.0017	0.0008	0.0009	0.0618

Table 1.1-37. Joint Frequency Distribution of Wind Speed and Direction (Decimal Fractions) for Night Hours (1994 to 2006) at Site 1 at 60 m above Ground Level (Continued)

Wind Direction		Wind Speed Category (m/s)										
Degrees Azimuth	Name	0.5–1.1	1.1–1.6	1.6–2.1	2.1–3.1	3.1–4.1	4.1–5.1	5.1–6.1	6.1–8.1	8.1–10.0	≥ 10.0	Total
326.25–348.75	North-northwest	0.0173	0.0545	0.0401	0.0155	0.0048	0.0042	0.0040	0.0068	0.0077	0.0135	0.1685
—	Total	0.1077	0.2423	0.1817	0.1304	0.0766	0.0656	0.0526	0.0680	0.0390	0.0356	0.9844
									Calms		0.00041	
									Missing/incomplete		0.01516	
									Frequency of calm winds		0.04%	
									Average wind speed		3.20 m/s	

NOTE: Wind speeds are equal to or greater than the lower limit and are less than the upper limit.

Source: BSC 2007e, Table C-4.

Table 1.1-38. Joint Frequency Distribution of Wind Speed and Direction (Decimal Fractions) for Daytime Hours (1994 to 2006) at Site 2 at 10 m above Ground Level

Wind Direction		Wind Speed Category (m/s)										
Degrees Azimuth	Name	0.5–1.1	1.1–1.6	1.6–2.1	2.1–3.1	3.1–4.1	4.1–5.1	5.1–6.1	6.1–8.1	8.1–10.0	≥ 10.0	Total
348.75–11.25	North	0.0001	0.0004	0.0006	0.0017	0.0026	0.0030	0.0026	0.0031	0.0015	0.0005	0.0160
11.25–33.75	North-northeast	0.0000	0.0004	0.0007	0.0027	0.0028	0.0027	0.0022	0.0024	0.0007	0.0006	0.0152
33.75–56.25	Northeast	0.0001	0.0006	0.0015	0.0037	0.0059	0.0052	0.0037	0.0040	0.0009	0.0003	0.0260
56.25–78.75	East-northeast	0.0002	0.0011	0.0032	0.0097	0.0096	0.0060	0.0034	0.0027	0.0008	0.0003	0.0371
78.75–101.25	East	0.0004	0.0023	0.0086	0.0254	0.0224	0.0085	0.0033	0.0022	0.0008	0.0005	0.0742
101.25–123.75	East-southeast	0.0004	0.0028	0.0104	0.0342	0.0297	0.0149	0.0060	0.0028	0.0004	0.0002	0.1016
123.75–146.25	Southeast	0.0005	0.0031	0.0108	0.0280	0.0278	0.0185	0.0100	0.0066	0.0012	0.0002	0.1068
146.25–168.75	South-southeast	0.0003	0.0031	0.0086	0.0193	0.0240	0.0242	0.0194	0.0245	0.0077	0.0021	0.1333
168.75–191.25	South	0.0004	0.0031	0.0081	0.0146	0.0162	0.0204	0.0154	0.0111	0.0026	0.0005	0.0924
191.25–213.75	South-southwest	0.0005	0.0029	0.0076	0.0142	0.0140	0.0174	0.0122	0.0078	0.0019	0.0013	0.0798
213.75–236.25	Southwest	0.0010	0.0038	0.0074	0.0153	0.0224	0.0261	0.0194	0.0128	0.0034	0.0021	0.1136
236.25–258.75	West-southwest	0.0009	0.0028	0.0041	0.0084	0.0099	0.0123	0.0132	0.0195	0.0068	0.0032	0.0810
258.75–281.25	West	0.0009	0.0016	0.0016	0.0039	0.0043	0.0049	0.0053	0.0076	0.0039	0.0017	0.0356
281.25–303.75	West-northwest	0.0002	0.0007	0.0008	0.0017	0.0018	0.0019	0.0025	0.0043	0.0033	0.0035	0.0207
303.75–326.25	Northwest	0.0002	0.0004	0.0007	0.0013	0.0019	0.0027	0.0044	0.0092	0.0074	0.0140	0.0423

Table 1.1-38. Joint Frequency Distribution of Wind Speed and Direction (Decimal Fractions) for Daytime Hours (1994 to 2006) at Site 2 at 10 m above Ground Level (Continued)

Wind Direction		Wind Speed Category (m/s)										
Degrees Azimuth	Name	0.5–1.1	1.1–1.6	1.6–2.1	2.1–3.1	3.1–4.1	4.1–5.1	5.1–6.1	6.1–8.1	8.1–10.0	≥ 10.0	Total
326.25–348.75	North-northwest	0.0001	0.0003	0.0002	0.0012	0.0022	0.0035	0.0041	0.0058	0.0037	0.0031	0.0242
—	Total	0.0063	0.0294	0.0750	0.1855	0.1974	0.1722	0.1270	0.1264	0.0468	0.0341	0.9960
									Calms		0	
									Missing/incomplete		0.00399	
									Frequency of calm winds		0.00%	
									Average wind speed		4.63 m/s	

NOTE: Daytime hours are from sunrise to sunset.
 Wind speeds are equal to or greater than the lower limit and are less than the upper limit.

Source: BSC 2007e, Table C-5.

Table 1.1-39. Joint Frequency Distribution of Wind Speed and Direction (Decimal Fractions) for Night Hours (1994 to 2006) at Site 2 at 10 m above Ground Level

Wind Direction		Wind Speed Category (m/s)										
Degrees Azimuth	Name	0.5–1.1	1.1–1.6	1.6–2.1	2.1–3.1	3.1–4.1	4.1–5.1	5.1–6.1	6.1–8.1	8.1–10.0	≥ 10.0	Total
348.75–11.25	North	0.0006	0.0014	0.0022	0.0036	0.0037	0.0054	0.0061	0.0088	0.0047	0.0024	0.0390
11.25–33.75	North-northeast	0.0008	0.0016	0.0029	0.0057	0.0074	0.0081	0.0081	0.0095	0.0037	0.0018	0.0497
33.75–56.25	Northeast	0.0009	0.0027	0.0042	0.0093	0.0149	0.0171	0.0109	0.0111	0.0031	0.0011	0.0753
56.25–78.75	East-northeast	0.0009	0.0053	0.0104	0.0268	0.0249	0.0104	0.0036	0.0037	0.0010	0.0004	0.0876
78.75–101.25	East	0.0015	0.0074	0.0180	0.0479	0.0444	0.0154	0.0039	0.0013	0.0005	0.0002	0.1404
101.25–123.75	East-southeast	0.0015	0.0061	0.0130	0.0299	0.0285	0.0160	0.0070	0.0019	0.0002	0.0001	0.1042
123.75–146.25	Southeast	0.0013	0.0057	0.0097	0.0215	0.0238	0.0178	0.0109	0.0094	0.0018	0.0001	0.1020
146.25–168.75	South-southeast	0.0014	0.0046	0.0062	0.0123	0.0131	0.0146	0.0138	0.0186	0.0092	0.0019	0.0957
168.75–191.25	South	0.0016	0.0045	0.0051	0.0082	0.0068	0.0063	0.0075	0.0094	0.0019	0.0004	0.0517
191.25–213.75	South-southwest	0.0018	0.0049	0.0056	0.0065	0.0036	0.0019	0.0015	0.0021	0.0008	0.0004	0.0291
213.75–236.25	Southwest	0.0024	0.0074	0.0088	0.0072	0.0036	0.0016	0.0010	0.0009	0.0003	0.0003	0.0336
236.25–258.75	West-southwest	0.0024	0.0078	0.0097	0.0106	0.0054	0.0033	0.0018	0.0018	0.0006	0.0005	0.0440
258.75–281.25	West	0.0024	0.0070	0.0093	0.0113	0.0053	0.0024	0.0013	0.0015	0.0007	0.0004	0.0415
281.25–303.75	West-northwest	0.0014	0.0038	0.0050	0.0055	0.0029	0.0021	0.0022	0.0021	0.0014	0.0023	0.0287
303.75–326.25	Northwest	0.0011	0.0023	0.0029	0.0040	0.0032	0.0023	0.0019	0.0036	0.0039	0.0152	0.0402

Table 1.1-39. Joint Frequency Distribution of Wind Speed and Direction (Decimal Fractions) for Night Hours (1994 to 2006) at Site 2 at 10 m above Ground Level (Continued)

Wind Direction		Wind Speed Category (m/s)										
Degrees Azimuth	Name	0.5–1.1	1.1–1.6	1.6–2.1	2.1–3.1	3.1–4.1	4.1–5.1	5.1–6.1	6.1–8.1	8.1–10.0	≥ 10.0	Total
326.25–348.75	North-northwest	0.0007	0.0014	0.0022	0.0032	0.0029	0.0029	0.0025	0.0057	0.0059	0.0100	0.0373
—	Total	0.0226	0.0739	0.1153	0.2136	0.1944	0.1278	0.0840	0.0913	0.0397	0.0375	0.9984
									Calms		0.00005	
									Missing/incomplete		0.00150	
									Frequency of calm winds		0.01%	
									Average wind speed		4.14 m/s	

NOTE: Wind speeds are equal to or greater than the lower limit and are less than the upper limit.

Source: BSC 2007e, Table C-6.

Table 1.1-40. Joint Frequency Distribution of Wind Speed and Direction (Decimal Fractions) for Daytime Hours (1994 to 1998) at Site 3 at 10 m above Ground Level

Wind Direction		Wind Speed Category (m/s)										
Degrees Azimuth	Name	0.5-1.1	1.1-1.6	1.6-2.1	2.1-3.1	3.1-4.1	4.1-5.1	5.1-6.1	6.1-8.1	8.1-10.0	≥ 10.0	Total
348.75-11.25	North	0.0009	0.0008	0.0004	0.0011	0.0001	0.0001	0.0000	0.0000	0.0000	0.0000	0.0033
11.25-33.75	North-northeast	0.0012	0.0003	0.0000	0.0006	0.0003	0.0000	0.0000	0.0000	0.0000	0.0000	0.0025
33.75-56.25	Northeast	0.0012	0.0010	0.0002	0.0009	0.0005	0.0001	0.0000	0.0000	0.0000	0.0000	0.0040
56.25-78.75	East-northeast	0.0022	0.0018	0.0012	0.0023	0.0007	0.0001	0.0000	0.0000	0.0000	0.0000	0.0083
78.75-101.25	East	0.0047	0.0090	0.0105	0.0202	0.0100	0.0033	0.0012	0.0001	0.0001	0.0000	0.0592
101.25-123.75	East-southeast	0.0075	0.0192	0.0507	0.0768	0.0233	0.0047	0.0009	0.0007	0.0000	0.0000	0.1839
123.75-146.25	Southeast	0.0058	0.0156	0.0315	0.0578	0.0272	0.0063	0.0007	0.0003	0.0000	0.0000	0.1452
146.25-168.75	South-southeast	0.0024	0.0085	0.0163	0.0557	0.0715	0.0482	0.0269	0.0119	0.0023	0.0000	0.2437
168.75-191.25	South	0.0026	0.0052	0.0087	0.0182	0.0082	0.0016	0.0005	0.0003	0.0000	0.0000	0.0453
191.25-213.75	South-southwest	0.0018	0.0039	0.0081	0.0138	0.0022	0.0004	0.0001	0.0000	0.0000	0.0000	0.0303
213.75-236.25	Southwest	0.0026	0.0042	0.0081	0.0167	0.0029	0.0004	0.0002	0.0000	0.0000	0.0000	0.0351
236.25-258.75	West-southwest	0.0015	0.0055	0.0112	0.0160	0.0029	0.0005	0.0000	0.0000	0.0000	0.0000	0.0376
258.75-281.25	West	0.0034	0.0079	0.0096	0.0157	0.0057	0.0010	0.0002	0.0000	0.0000	0.0000	0.0435
281.25-303.75	West-northwest	0.0043	0.0120	0.0142	0.0201	0.0230	0.0140	0.0080	0.0077	0.0025	0.0013	0.1071
303.75-326.25	Northwest	0.0040	0.0060	0.0042	0.0064	0.0076	0.0068	0.0044	0.0045	0.0011	0.0004	0.0455

Table 1.1-40. Joint Frequency Distribution of Wind Speed and Direction (Decimal Fractions) for Daytime Hours (1994 to 1998) at Site 3 at 10 m above Ground Level (Continued)

Wind Direction		Wind Speed Category (m/s)										
Degrees Azimuth	Name	0.5–1.1	1.1–1.6	1.6–2.1	2.1–3.1	3.1–4.1	4.1–5.1	5.1–6.1	6.1–8.1	8.1–10.0	≥ 10.0	Total
326.25–348.75	North-northwest	0.0017	0.0016	0.0003	0.0010	0.0005	0.0004	0.0000	0.0000	0.0000	0.0000	0.0055
—	Total	0.0478	0.1024	0.1754	0.3233	0.1867	0.0878	0.0433	0.0256	0.0061	0.0016	0.9925
									Calms		0.00014	
									Missing/incomplete		0.00738	
									Frequency of calm winds		0.01%	
									Average wind speed		2.91 m/s	

NOTE: Daytime hours are from sunrise to sunset.
 Wind speeds are equal to or greater than the lower limit and are less than the upper limit.

Source: BSC 2007e, Table C-7.

Table 1.1-41. Joint Frequency Distribution of Wind Speed and Direction (Decimal Fractions) for Night Hours (1994 to 1998) at Site 3 at 10 m above Ground Level

Wind Direction		Wind Speed Category (m/s)										
Degrees Azimuth	Name	0.5-1.1	1.1-1.6	1.6-2.1	2.1-3.1	3.1-4.1	4.1-5.1	5.1-6.1	6.1-8.1	8.1-10.0	≥ 10.0	Total
348.75-11.25	North	0.0010	0.0011	0.0007	0.0005	0.0000	0.0000	0.0000	0.0000	0.0000	0.0000	0.0033
11.25-33.75	North-northeast	0.0006	0.0010	0.0003	0.0004	0.0000	0.0001	0.0000	0.0000	0.0000	0.0000	0.0024
33.75-56.25	Northeast	0.0009	0.0006	0.0008	0.0003	0.0001	0.0000	0.0000	0.0000	0.0000	0.0000	0.0027
56.25-78.75	East-northeast	0.0006	0.0012	0.0012	0.0009	0.0005	0.0001	0.0000	0.0000	0.0000	0.0000	0.0046
78.75-101.25	East	0.0011	0.0013	0.0021	0.0026	0.0015	0.0007	0.0002	0.0002	0.0000	0.0000	0.0098
101.25-123.75	East-southeast	0.0020	0.0037	0.0039	0.0046	0.0024	0.0006	0.0001	0.0000	0.0000	0.0000	0.0173
123.75-146.25	Southeast	0.0014	0.0030	0.0050	0.0045	0.0011	0.0002	0.0000	0.0000	0.0000	0.0000	0.0151
146.25-168.75	South-southeast	0.0018	0.0060	0.0110	0.0244	0.0225	0.0135	0.0078	0.0049	0.0007	0.0000	0.0926
168.75-191.25	South	0.0026	0.0097	0.0123	0.0084	0.0017	0.0003	0.0001	0.0000	0.0000	0.0000	0.0352
191.25-213.75	South-southwest	0.0024	0.0096	0.0041	0.0013	0.0004	0.0000	0.0000	0.0000	0.0000	0.0000	0.0179
213.75-236.25	Southwest	0.0038	0.0143	0.0042	0.0026	0.0004	0.0000	0.0000	0.0000	0.0000	0.0000	0.0254
236.25-258.75	West-southwest	0.0042	0.0223	0.0107	0.0033	0.0006	0.0002	0.0000	0.0000	0.0000	0.0000	0.0414
258.75-281.25	West	0.0053	0.0328	0.0461	0.0138	0.0034	0.0008	0.0001	0.0001	0.0000	0.0000	0.1025
281.25-303.75	West-northwest	0.0053	0.0426	0.1362	0.2436	0.0171	0.0081	0.0051	0.0061	0.0034	0.0035	0.4710
303.75-326.25	Northwest	0.0036	0.0211	0.0420	0.0348	0.0179	0.0119	0.0072	0.0066	0.0025	0.0016	0.1492

Table 1.1-41. Joint Frequency Distribution of Wind Speed and Direction (Decimal Fractions) for Night Hours (1994 to 1998) at Site 3 at 10 m above Ground Level (Continued)

Wind Direction		Wind Speed Category (m/s)										
Degrees Azimuth	Name	0.5–1.1	1.1–1.6	1.6–2.1	2.1–3.1	3.1–4.1	4.1–5.1	5.1–6.1	6.1–8.1	8.1–10.0	≥ 10.0	Total
326.25–348.75	North-northwest	0.0015	0.0046	0.0017	0.0011	0.0005	0.0001	0.0000	0.0000	0.0000	0.0000	0.0095
—	Total	0.0380	0.1748	0.2824	0.3470	0.0704	0.0367	0.0208	0.0180	0.0066	0.0050	0.9964
									Calms		0.00028	
									Missing/incomplete		0.00331	
									Frequency of calm winds		0.03%	
									Average wind speed		2.45 m/s	

NOTE: Wind speeds are equal to or greater than the lower limit and are less than the upper limit.

Source: BSC 2007e, Table C-8.

Table 1.1-42. Joint Frequency Distribution of Wind Speed and Direction (Decimal Fractions) for Daytime Hours (1994 to 2006) at Site 4 at 10 m above Ground Level

Wind Direction		Wind Speed Category (m/s)										
Degrees Azimuth	Name	0.5–1.1	1.1–1.6	1.6–2.1	2.1–3.1	3.1–4.1	4.1–5.1	5.1–6.1	6.1–8.1	8.1–10.0	≥ 10.0	Total
348.75–11.25	North	0.0003	0.0021	0.0037	0.0040	0.0023	0.0027	0.0031	0.0064	0.0056	0.0072	0.0374
11.25–33.75	North-northeast	0.0004	0.0030	0.0078	0.0077	0.0047	0.0056	0.0077	0.0157	0.0132	0.0134	0.0790
33.75–56.25	Northeast	0.0003	0.0035	0.0096	0.0257	0.0178	0.0134	0.0095	0.0087	0.0030	0.0017	0.0932
56.25–78.75	East-northeast	0.0003	0.0027	0.0082	0.0189	0.0066	0.0023	0.0011	0.0013	0.0004	0.0004	0.0424
78.75–101.25	East	0.0004	0.0025	0.0048	0.0056	0.0024	0.0014	0.0010	0.0011	0.0005	0.0002	0.0200
101.25–123.75	East-southeast	0.0003	0.0018	0.0041	0.0052	0.0025	0.0020	0.0012	0.0010	0.0002	0.0001	0.0183
123.75–146.25	Southeast	0.0002	0.0018	0.0057	0.0091	0.0050	0.0031	0.0013	0.0008	0.0001	0.0001	0.0273
146.25–168.75	South-southeast	0.0002	0.0020	0.0088	0.0298	0.0284	0.0156	0.0072	0.0059	0.0033	0.0029	0.1042
168.75–191.25	South	0.0002	0.0023	0.0116	0.0467	0.0526	0.0501	0.0399	0.0614	0.0381	0.0434	0.3464
191.25–213.75	South-southwest	0.0004	0.0027	0.0073	0.0161	0.0166	0.0198	0.0139	0.0124	0.0038	0.0029	0.0959
213.75–236.25	Southwest	0.0003	0.0021	0.0038	0.0062	0.0069	0.0086	0.0080	0.0067	0.0017	0.0008	0.0451
236.25–258.75	West-southwest	0.0002	0.0013	0.0019	0.0029	0.0025	0.0037	0.0041	0.0037	0.0011	0.0004	0.0219
258.75–281.25	West	0.0003	0.0013	0.0011	0.0015	0.0010	0.0010	0.0012	0.0016	0.0003	0.0001	0.0094
281.25–303.75	West-northwest	0.0003	0.0009	0.0013	0.0011	0.0008	0.0012	0.0009	0.0016	0.0007	0.0004	0.0093
303.75–326.25	Northwest	0.0002	0.0014	0.0012	0.0015	0.0010	0.0016	0.0019	0.0041	0.0034	0.0027	0.0190

Table 1.1-42. Joint Frequency Distribution of Wind Speed and Direction (Decimal Fractions) for Daytime Hours (1994 to 2006) at Site 4 at 10 m above Ground Level (Continued)

Wind Direction		Wind Speed Category (m/s)										
Degrees Azimuth	Name	0.5–1.1	1.1–1.6	1.6–2.1	2.1–3.1	3.1–4.1	4.1–5.1	5.1–6.1	6.1–8.1	8.1–10.0	≥ 10.0	Total
326.25–348.75	North-northwest	0.0003	0.0016	0.0018	0.0020	0.0013	0.0016	0.0024	0.0047	0.0055	0.0098	0.0312
—	Total	0.0046	0.0330	0.0828	0.1840	0.1526	0.1338	0.1046	0.1370	0.0810	0.0866	0.9960
										Calms	0.00005	
										Missing/incomplete	0.00390	
										Frequency of calm winds	0.01%	
										Average wind speed	5.20 m/s	

NOTE: Daytime hours are from sunrise to sunset.
 Wind speeds are equal to or greater than the lower limit and are less than the upper limit.

Source: BSC 2007e, Table C-9.

Table 1.1-43. Joint Frequency Distribution of Wind Speed and Direction (Decimal Fractions) for Night Hours (1994 to 2006) at Site 4 at 10 m above Ground Level

Wind Direction		Wind Speed Category (m/s)										
Degrees Azimuth	Name	0.5–1.1	1.1–1.6	1.6–2.1	2.1–3.1	3.1–4.1	4.1–5.1	5.1–6.1	6.1–8.1	8.1–10.0	≥ 10.0	Total
348.75–11.25	North	0.0008	0.0112	0.0476	0.0580	0.0117	0.0070	0.0065	0.0126	0.0097	0.0173	0.1825
11.25–33.75	North-northeast	0.0009	0.0124	0.0564	0.0836	0.0200	0.0141	0.0138	0.0258	0.0237	0.0374	0.2880
33.75–56.25	Northeast	0.0008	0.0085	0.0235	0.0629	0.0224	0.0102	0.0070	0.0059	0.0021	0.0009	0.1441
56.25–78.75	East-northeast	0.0006	0.0047	0.0066	0.0040	0.0012	0.0007	0.0003	0.0003	0.0002	0.0003	0.0189
78.75–101.25	East	0.0005	0.0037	0.0053	0.0020	0.0007	0.0007	0.0004	0.0007	0.0003	0.0002	0.0144
101.25–123.75	East-southeast	0.0003	0.0030	0.0062	0.0046	0.0014	0.0009	0.0004	0.0003	0.0001	0.0000	0.0172
123.75–146.25	Southeast	0.0002	0.0020	0.0064	0.0100	0.0048	0.0018	0.0006	0.0002	0.0001	0.0000	0.0262
146.25–168.75	South-southeast	0.0003	0.0020	0.0052	0.0116	0.0100	0.0058	0.0027	0.0025	0.0012	0.0005	0.0419
168.75–191.25	South	0.0004	0.0016	0.0048	0.0100	0.0122	0.0116	0.0082	0.0107	0.0063	0.0073	0.0731
191.25–213.75	South-southwest	0.0004	0.0017	0.0036	0.0069	0.0048	0.0022	0.0012	0.0012	0.0007	0.0005	0.0233
213.75–236.25	Southwest	0.0003	0.0020	0.0036	0.0060	0.0024	0.0006	0.0004	0.0005	0.0001	0.0001	0.0160
236.25–258.75	West-southwest	0.0002	0.0022	0.0041	0.0040	0.0018	0.0010	0.0003	0.0003	0.0001	0.0001	0.0142
258.75–281.25	West	0.0003	0.0023	0.0041	0.0040	0.0014	0.0006	0.0005	0.0003	0.0001	0.0001	0.0138
281.25–303.75	West-northwest	0.0004	0.0028	0.0053	0.0038	0.0012	0.0004	0.0003	0.0002	0.0001	0.0002	0.0147
303.75–326.25	Northwest	0.0005	0.0039	0.0085	0.0089	0.0027	0.0009	0.0008	0.0013	0.0005	0.0008	0.0287

Table 1.1-43. Joint Frequency Distribution of Wind Speed and Direction (Decimal Fractions) for Night Hours (1994 to 2006) at Site 4 at 10 m above Ground Level (Continued)

Wind Direction		Wind Speed Category (m/s)										
Degrees Azimuth	Name	0.5–1.1	1.1–1.6	1.6–2.1	2.1–3.1	3.1–4.1	4.1–5.1	5.1–6.1	6.1–8.1	8.1–10.0	≥ 10.0	Total
326.25–348.75	North-northwest	0.0006	0.0060	0.0164	0.0332	0.0108	0.0038	0.0021	0.0028	0.0019	0.0053	0.0828
—	Total	0.0077	0.0701	0.2077	0.3137	0.1092	0.0621	0.0453	0.0655	0.0472	0.0713	0.9979
									Calms		0.00012	
									Missing/incomplete		0.00195	
									Frequency of calm winds		0.01%	
									Average wind speed		4.03 m/s	

NOTE: Wind speeds are equal to or greater than the lower limit and are less than the upper limit.

Source: BSC 2007e, Table C-10.

Table 1.1-44. Joint Frequency Distribution of Wind Speed and Direction (Decimal Fractions) for Daytime Hours (1994 to 1998) at Site 5 at 10 m above Ground Level

Wind Direction		Wind Speed Category (m/s)										
Degrees Azimuth	Name	0.5-1.1	1.1-1.6	1.6-2.1	2.1-3.1	3.1-4.1	4.1-5.1	5.1-6.1	6.1-8.1	8.1-10.0	≥ 10.0	Total
348.75-11.25	North	0.0002	0.0023	0.0069	0.0195	0.0232	0.0266	0.0188	0.0176	0.0045	0.0016	0.1212
11.25-33.75	North-northeast	0.0003	0.0019	0.0050	0.0111	0.0131	0.0077	0.0040	0.0027	0.0008	0.0001	0.0468
33.75-56.25	Northeast	0.0003	0.0017	0.0045	0.0074	0.0057	0.0031	0.0016	0.0024	0.0011	0.0003	0.0279
56.25-78.75	East-northeast	0.0002	0.0018	0.0033	0.0053	0.0051	0.0043	0.0045	0.0055	0.0012	0.0006	0.0319
78.75-101.25	East	0.0002	0.0014	0.0024	0.0048	0.0040	0.0036	0.0024	0.0012	0.0005	0.0000	0.0204
101.25-123.75	East-southeast	0.0001	0.0018	0.0027	0.0047	0.0032	0.0009	0.0003	0.0001	0.0000	0.0000	0.0138
123.75-146.25	Southeast	0.0002	0.0015	0.0037	0.0063	0.0027	0.0010	0.0007	0.0005	0.0003	0.0000	0.0168
146.25-168.75	South-southeast	0.0006	0.0032	0.0060	0.0126	0.0105	0.0060	0.0064	0.0109	0.0079	0.0053	0.0694
168.75-191.25	South	0.0003	0.0034	0.0147	0.0336	0.0386	0.0333	0.0322	0.0489	0.0271	0.0202	0.2523
191.25-213.75	South-southwest	0.0007	0.0051	0.0209	0.0547	0.0423	0.0254	0.0117	0.0091	0.0037	0.0021	0.1758
213.75-236.25	Southwest	0.0009	0.0043	0.0115	0.0230	0.0191	0.0113	0.0048	0.0019	0.0007	0.0003	0.0777
236.25-258.75	West-southwest	0.0009	0.0034	0.0053	0.0082	0.0077	0.0062	0.0037	0.0024	0.0005	0.0002	0.0385
258.75-281.25	West	0.0005	0.0023	0.0042	0.0048	0.0026	0.0031	0.0019	0.0013	0.0002	0.0000	0.0208
281.25-303.75	West-northwest	0.0004	0.0019	0.0022	0.0027	0.0013	0.0015	0.0014	0.0016	0.0004	0.0000	0.0134
303.75-326.25	Northwest	0.0004	0.0023	0.0034	0.0038	0.0015	0.0023	0.0028	0.0036	0.0022	0.0011	0.0234

Table 1.1-44. Joint Frequency Distribution of Wind Speed and Direction (Decimal Fractions) for Daytime Hours (1994 to 1998) at Site 5 at 10 m above Ground Level (Continued)

Wind Direction		Wind Speed Category (m/s)										
Degrees Azimuth	Name	0.5–1.1	1.1–1.6	1.6–2.1	2.1–3.1	3.1–4.1	4.1–5.1	5.1–6.1	6.1–8.1	8.1–10.0	≥ 10.0	Total
326.25–348.75	North-northwest	0.0004	0.0024	0.0056	0.0089	0.0062	0.0045	0.0043	0.0082	0.0052	0.0042	0.0498
—	Total	0.0066	0.0407	0.1025	0.2112	0.1866	0.1409	0.1015	0.1178	0.0563	0.0360	0.9911
									Calms		0	
									Missing/incomplete		0.00888	
									Frequency of calm winds		0.00%	
									Average wind speed		4.45 m/s	

NOTE: Daytime hours are from sunrise to sunset.
Wind speeds are equal to or greater than the lower limit and are less than the upper limit.

Source: BSC 2007e, Table C-11.

Table 1.1-45. Joint Frequency Distribution of Wind Speed and Direction (Decimal Fractions) for Night Hours (1994 to 1998) at Site 5 at 10 m above Ground Level

Wind Direction		Wind Speed Category (m/s)										
Degrees Azimuth	Name	0.5-1.1	1.1-1.6	1.6-2.1	2.1-3.1	3.1-4.1	4.1-5.1	5.1-6.1	6.1-8.1	8.1-10.0	≥ 10.0	Total
348.75-11.25	North	0.0002	0.0027	0.0081	0.0348	0.0794	0.1312	0.1130	0.0626	0.0067	0.0022	0.4410
11.25-33.75	North-northeast	0.0001	0.0018	0.0076	0.0263	0.0651	0.0951	0.0293	0.0030	0.0005	0.0000	0.2289
33.75-56.25	Northeast	0.0002	0.0011	0.0038	0.0138	0.0238	0.0201	0.0033	0.0009	0.0002	0.0001	0.0672
56.25-78.75	East-northeast	0.0000	0.0006	0.0018	0.0045	0.0043	0.0024	0.0014	0.0006	0.0001	0.0003	0.0161
78.75-101.25	East	0.0002	0.0010	0.0017	0.0018	0.0015	0.0006	0.0002	0.0004	0.0000	0.0001	0.0075
101.25-123.75	East-southeast	0.0001	0.0006	0.0012	0.0019	0.0013	0.0004	0.0001	0.0000	0.0000	0.0000	0.0057
123.75-146.25	Southeast	0.0001	0.0005	0.0014	0.0026	0.0016	0.0011	0.0004	0.0006	0.0000	0.0000	0.0083
146.25-168.75	South-southeast	0.0001	0.0008	0.0013	0.0032	0.0049	0.0055	0.0054	0.0089	0.0050	0.0023	0.0375
168.75-191.25	South	0.0001	0.0010	0.0024	0.0052	0.0067	0.0068	0.0064	0.0111	0.0062	0.0063	0.0522
191.25-213.75	South-southwest	0.0002	0.0013	0.0026	0.0050	0.0024	0.0017	0.0010	0.0009	0.0003	0.0001	0.0155
213.75-236.25	Southwest	0.0002	0.0022	0.0043	0.0041	0.0012	0.0004	0.0001	0.0003	0.0001	0.0000	0.0129
236.25-258.75	West-southwest	0.0002	0.0030	0.0032	0.0037	0.0010	0.0006	0.0001	0.0001	0.0001	0.0000	0.0121
258.75-281.25	West	0.0006	0.0035	0.0029	0.0025	0.0018	0.0008	0.0002	0.0002	0.0000	0.0000	0.0127
281.25-303.75	West-northwest	0.0007	0.0032	0.0026	0.0016	0.0009	0.0005	0.0001	0.0002	0.0000	0.0000	0.0098
303.75-326.25	Northwest	0.0003	0.0024	0.0042	0.0039	0.0012	0.0004	0.0007	0.0008	0.0004	0.0003	0.0146

Table 1.1-45. Joint Frequency Distribution of Wind Speed and Direction (Decimal Fractions) for Night Hours (1994 to 1998) at Site 5 at 10 m above Ground Level (Continued)

Wind Direction		Wind Speed Category (m/s)										
Degrees Azimuth	Name	0.5–1.1	1.1–1.6	1.6–2.1	2.1–3.1	3.1–4.1	4.1–5.1	5.1–6.1	6.1–8.1	8.1–10.0	≥ 10.0	Total
326.25–348.75	North-northwest	0.0005	0.0026	0.0078	0.0131	0.0073	0.0060	0.0054	0.0061	0.0043	0.0050	0.0581
—	Total	0.0037	0.0283	0.0569	0.1281	0.2044	0.2735	0.1673	0.0968	0.0241	0.0168	0.9949
									Calms		0	
									Missing/incomplete		0.00510	
									Frequency of calm winds		0.00%	
									Average wind speed		4.52 m/s	

NOTE: Wind speeds are equal to or greater than the lower limit and are less than the upper limit.

Source: BSC 2007e, Table C-12.

Table 1.1-46. Joint Frequency Distribution of Wind Speed and Direction (Decimal Fractions) for Daytime Hours (1994 to 1998) at Site 7 at 10 m above Ground Level

Wind Direction		Wind Speed Category (m/s)										
Degrees Azimuth	Name	0.5-1.1	1.1-1.6	1.6-2.1	2.1-3.1	3.1-4.1	4.1-5.1	5.1-6.1	6.1-8.1	8.1-10.0	≥ 10.0	Total
348.75-11.25	North	0.0010	0.0023	0.0044	0.0100	0.0099	0.0104	0.0098	0.0096	0.0029	0.0010	0.0612
11.25-33.75	North-northeast	0.0005	0.0018	0.0042	0.0121	0.0146	0.0158	0.0094	0.0050	0.0010	0.0000	0.0644
33.75-56.25	Northeast	0.0006	0.0012	0.0041	0.0102	0.0054	0.0029	0.0009	0.0002	0.0001	0.0000	0.0256
56.25-78.75	East-northeast	0.0004	0.0014	0.0037	0.0045	0.0019	0.0006	0.0002	0.0002	0.0000	0.0000	0.0129
78.75-101.25	East	0.0004	0.0015	0.0034	0.0032	0.0017	0.0007	0.0004	0.0002	0.0000	0.0000	0.0116
101.25-123.75	East-southeast	0.0008	0.0032	0.0041	0.0057	0.0040	0.0019	0.0011	0.0007	0.0002	0.0000	0.0216
123.75-146.25	Southeast	0.0008	0.0048	0.0140	0.0221	0.0099	0.0028	0.0006	0.0005	0.0001	0.0000	0.0555
146.25-168.75	South-southeast	0.0008	0.0063	0.0210	0.0581	0.0513	0.0282	0.0175	0.0228	0.0129	0.0055	0.2244
168.75-191.25	South	0.0010	0.0047	0.0141	0.0335	0.0420	0.0377	0.0303	0.0339	0.0142	0.0056	0.2170
191.25-213.75	South-southwest	0.0011	0.0042	0.0071	0.0163	0.0199	0.0126	0.0049	0.0027	0.0008	0.0002	0.0698
213.75-236.25	Southwest	0.0019	0.0040	0.0055	0.0084	0.0096	0.0070	0.0023	0.0011	0.0003	0.0001	0.0402
236.25-258.75	West-southwest	0.0042	0.0069	0.0035	0.0051	0.0058	0.0032	0.0010	0.0005	0.0000	0.0000	0.0302
258.75-281.25	West	0.0057	0.0146	0.0045	0.0029	0.0024	0.0019	0.0007	0.0001	0.0000	0.0000	0.0328
281.25-303.75	West-northwest	0.0055	0.0148	0.0085	0.0031	0.0021	0.0016	0.0012	0.0006	0.0001	0.0000	0.0377
303.75-326.25	Northwest	0.0041	0.0100	0.0097	0.0057	0.0023	0.0040	0.0037	0.0049	0.0012	0.0007	0.0462

Table 1.1-46. Joint Frequency Distribution of Wind Speed and Direction (Decimal Fractions) for Daytime Hours (1994 to 1998) at Site 7 at 10 m above Ground Level (Continued)

Wind Direction		Wind Speed Category (m/s)										
Degrees Azimuth	Name	0.5–1.1	1.1–1.6	1.6–2.1	2.1–3.1	3.1–4.1	4.1–5.1	5.1–6.1	6.1–8.1	8.1–10.0	≥ 10.0	Total
326.25–348.75	North-northwest	0.0013	0.0048	0.0050	0.0070	0.0044	0.0044	0.0047	0.0084	0.0053	0.0034	0.0487
—	Total	0.0303	0.0863	0.1168	0.2077	0.1872	0.1357	0.0888	0.0914	0.0391	0.0165	0.9959
									Calms		0.00023	
									Missing/incomplete		0.00390	
									Frequency of calm winds		0.02%	
									Average wind speed		3.88 m/s	

NOTE: Daytime hours are from sunrise to sunset.
 Wind speeds are equal to or greater than the lower limit and are less than the upper limit.

Source: BSC 2007e, Table C-13.

Table 1.1-47. Joint Frequency Distribution of Wind Speed and Direction (Decimal Fractions) for Night Hours (1994 to 1998) at Site 7 at 10 m above Ground Level

Wind Direction		Wind Speed Category (m/s)										
Degrees Azimuth	Name	0.5-1.1	1.1-1.6	1.6-2.1	2.1-3.1	3.1-4.1	4.1-5.1	5.1-6.1	6.1-8.1	8.1-10.0	≥ 10.0	Total
348.75-11.25	North	0.0018	0.0063	0.0132	0.0206	0.0219	0.0208	0.0155	0.0189	0.0056	0.0017	0.1262
11.25-33.75	North-northeast	0.0007	0.0022	0.0031	0.0049	0.0064	0.0080	0.0055	0.0040	0.0012	0.0001	0.0362
33.75-56.25	Northeast	0.0006	0.0014	0.0017	0.0016	0.0017	0.0007	0.0005	0.0001	0.0000	0.0000	0.0082
56.25-78.75	East-northeast	0.0006	0.0013	0.0017	0.0005	0.0001	0.0001	0.0001	0.0000	0.0000	0.0000	0.0043
78.75-101.25	East	0.0006	0.0015	0.0017	0.0009	0.0002	0.0003	0.0000	0.0000	0.0000	0.0000	0.0052
101.25-123.75	East-southeast	0.0007	0.0018	0.0022	0.0020	0.0009	0.0002	0.0001	0.0002	0.0000	0.0000	0.0082
123.75-146.25	Southeast	0.0006	0.0022	0.0035	0.0025	0.0012	0.0006	0.0001	0.0000	0.0000	0.0000	0.0107
146.25-168.75	South-southeast	0.0007	0.0031	0.0040	0.0060	0.0037	0.0026	0.0020	0.0012	0.0009	0.0003	0.0244
168.75-191.25	South	0.0007	0.0017	0.0031	0.0075	0.0078	0.0089	0.0062	0.0065	0.0031	0.0003	0.0460
191.25-213.75	South-southwest	0.0008	0.0013	0.0014	0.0032	0.0020	0.0007	0.0004	0.0003	0.0000	0.0000	0.0102
213.75-236.25	Southwest	0.0011	0.0017	0.0013	0.0012	0.0003	0.0002	0.0000	0.0001	0.0000	0.0000	0.0060
236.25-258.75	West-southwest	0.0021	0.0067	0.0017	0.0010	0.0003	0.0001	0.0001	0.0001	0.0000	0.0000	0.0123
258.75-281.25	West	0.0075	0.0332	0.0091	0.0009	0.0002	0.0005	0.0000	0.0000	0.0000	0.0000	0.0515
281.25-303.75	West-northwest	0.0089	0.0820	0.0690	0.0109	0.0004	0.0002	0.0001	0.0000	0.0000	0.0000	0.1715
303.75-326.25	Northwest	0.0086	0.0670	0.1280	0.0902	0.0096	0.0011	0.0009	0.0014	0.0006	0.0003	0.3078

Table 1.1-47. Joint Frequency Distribution of Wind Speed and Direction (Decimal Fractions) for Night Hours (1994 to 1998) at Site 7 at 10 m above Ground Level (Continued)

Wind Direction		Wind Speed Category (m/s)										
Degrees Azimuth	Name	0.5–1.1	1.1–1.6	1.6–2.1	2.1–3.1	3.1–4.1	4.1–5.1	5.1–6.1	6.1–8.1	8.1–10.0	≥ 10.0	Total
326.25–348.75	North-northwest	0.0031	0.0223	0.0511	0.0501	0.0196	0.0079	0.0057	0.0051	0.0040	0.0023	0.1711
—	Total	0.0390	0.2357	0.2956	0.2041	0.0763	0.0530	0.0373	0.0382	0.0156	0.0051	0.9995
									Calms		0.00023	
									Missing/incomplete		0.00028	
									Frequency of calm winds		0.02%	
									Average wind speed		2.60 m/s	

NOTE: Wind speeds are equal to or greater than the lower limit and are less than the upper limit.

Source: BSC 2007e, Table C-14.

Table 1.1-48. Joint Frequency Distribution of Wind Speed and Direction (Decimal Fractions) for Daytime Hours (1994 to 2006) at Site 9 at 10 m above Ground Level

Wind Direction		Wind Speed Category (m/s)										
Degrees Azimuth	Name	0.5–1.1	1.1–1.6	1.6–2.1	2.1–3.1	3.1–4.1	4.1–5.1	5.1–6.1	6.1–8.1	8.1–10.0	≥ 10.0	Total
348.75–11.25	North	0.0002	0.0022	0.0035	0.0074	0.0066	0.0052	0.0045	0.0057	0.0026	0.0010	0.0390
11.25–33.75	North-northeast	0.0003	0.0019	0.0050	0.0174	0.0229	0.0142	0.0052	0.0039	0.0010	0.0002	0.0720
33.75–56.25	Northeast	0.0002	0.0019	0.0061	0.0175	0.0198	0.0144	0.0067	0.0060	0.0021	0.0005	0.0752
56.25–78.75	East-northeast	0.0003	0.0019	0.0049	0.0096	0.0057	0.0042	0.0026	0.0020	0.0005	0.0002	0.0320
78.75–101.25	East	0.0002	0.0019	0.0046	0.0075	0.0039	0.0030	0.0019	0.0009	0.0003	0.0000	0.0243
101.25–123.75	East-southeast	0.0003	0.0021	0.0047	0.0079	0.0030	0.0011	0.0005	0.0003	0.0001	0.0000	0.0200
123.75–146.25	Southeast	0.0005	0.0029	0.0058	0.0106	0.0055	0.0026	0.0013	0.0018	0.0008	0.0003	0.0322
146.25–168.75	South-southeast	0.0003	0.0034	0.0099	0.0229	0.0242	0.0201	0.0204	0.0331	0.0234	0.0165	0.1743
168.75–191.25	South	0.0005	0.0047	0.0170	0.0483	0.0423	0.0329	0.0259	0.0357	0.0215	0.0152	0.2440
191.25–213.75	South-southwest	0.0006	0.0052	0.0153	0.0286	0.0199	0.0086	0.0040	0.0047	0.0023	0.0015	0.0906
213.75–236.25	Southwest	0.0006	0.0038	0.0113	0.0178	0.0106	0.0034	0.0014	0.0010	0.0004	0.0001	0.0504
236.25–258.75	West-southwest	0.0004	0.0031	0.0070	0.0115	0.0072	0.0030	0.0010	0.0005	0.0002	0.0001	0.0339
258.75–281.25	West	0.0003	0.0021	0.0051	0.0081	0.0054	0.0027	0.0011	0.0006	0.0001	0.0000	0.0257
281.25–303.75	West-northwest	0.0002	0.0015	0.0034	0.0056	0.0036	0.0028	0.0017	0.0011	0.0002	0.0001	0.0202
303.75–326.25	Northwest	0.0002	0.0013	0.0027	0.0049	0.0039	0.0040	0.0043	0.0062	0.0035	0.0010	0.0320

Table 1.1-48. Joint Frequency Distribution of Wind Speed and Direction (Decimal Fractions) for Daytime Hours (1994 to 2006) at Site 9 at 10 m above Ground Level (Continued)

Wind Direction		Wind Speed Category (m/s)										
Degrees Azimuth	Name	0.5–1.1	1.1–1.6	1.6–2.1	2.1–3.1	3.1–4.1	4.1–5.1	5.1–6.1	6.1–8.1	8.1–10.0	≥ 10.0	Total
326.25–348.75	North-northwest	0.0003	0.0014	0.0023	0.0053	0.0042	0.0028	0.0034	0.0068	0.0045	0.0032	0.0342
—	Total	0.0055	0.0414	0.1085	0.2311	0.1887	0.1250	0.0860	0.1103	0.0635	0.0400	0.9834
									Calms		0.00002	
									Missing/incomplete		0.01659	
									Frequency of calm winds		0.00%	
									Average wind speed		4.42 m/s	

NOTE: Daytime hours are from sunrise to sunset.
 Wind speeds are equal to or greater than the lower limit and are less than the upper limit.

Source: BSC 2007e, Table C-15.

Table 1.1-49. Joint Frequency Distribution of Wind Speed and Direction (Decimal Fractions) for Night Hours (1994 to 2006) at Site 9 at 10 m above Ground Level

Wind Direction		Wind Speed Category (m/s)										
Degrees Azimuth	Name	0.5–1.1	1.1–1.6	1.6–2.1	2.1–3.1	3.1–4.1	4.1–5.1	5.1–6.1	6.1–8.1	8.1–10.0	≥ 10.0	Total
348.75–11.25	North	0.0003	0.0012	0.0038	0.0151	0.0238	0.0215	0.0099	0.0057	0.0021	0.0005	0.0840
11.25–33.75	North-northeast	0.0002	0.0013	0.0054	0.0321	0.1244	0.1811	0.0588	0.0086	0.0013	0.0003	0.4134
33.75–56.25	Northeast	0.0003	0.0018	0.0058	0.0243	0.0369	0.0386	0.0195	0.0042	0.0010	0.0003	0.1327
56.25–78.75	East-northeast	0.0003	0.0013	0.0044	0.0109	0.0077	0.0042	0.0024	0.0014	0.0002	0.0002	0.0331
78.75–101.25	East	0.0004	0.0014	0.0039	0.0081	0.0029	0.0008	0.0005	0.0003	0.0001	0.0002	0.0186
101.25–123.75	East-southeast	0.0001	0.0013	0.0036	0.0076	0.0058	0.0011	0.0003	0.0003	0.0001	0.0000	0.0203
123.75–146.25	Southeast	0.0002	0.0014	0.0040	0.0106	0.0128	0.0085	0.0044	0.0040	0.0010	0.0003	0.0474
146.25–168.75	South-southeast	0.0003	0.0009	0.0028	0.0108	0.0271	0.0254	0.0203	0.0267	0.0127	0.0065	0.1336
168.75–191.25	South	0.0002	0.0010	0.0025	0.0055	0.0049	0.0034	0.0026	0.0031	0.0026	0.0027	0.0285
191.25–213.75	South-southwest	0.0002	0.0009	0.0016	0.0020	0.0010	0.0005	0.0005	0.0006	0.0002	0.0001	0.0076
213.75–236.25	Southwest	0.0002	0.0007	0.0015	0.0016	0.0005	0.0001	0.0001	0.0001	0.0000	0.0000	0.0049
236.25–258.75	West-southwest	0.0002	0.0006	0.0011	0.0017	0.0005	0.0001	0.0000	0.0001	0.0000	0.0000	0.0043
258.75–281.25	West	0.0003	0.0008	0.0011	0.0018	0.0008	0.0003	0.0001	0.0001	0.0000	0.0000	0.0053
281.25–303.75	West-northwest	0.0002	0.0006	0.0014	0.0026	0.0018	0.0008	0.0004	0.0002	0.0001	0.0000	0.0082
303.75–326.25	Northwest	0.0001	0.0006	0.0017	0.0043	0.0040	0.0036	0.0021	0.0027	0.0008	0.0004	0.0203

Table 1.1-49. Joint Frequency Distribution of Wind Speed and Direction (Decimal Fractions) for Night Hours (1994 to 2006) at Site 9 at 10 m above Ground Level (Continued)

Wind Direction		Wind Speed Category (m/s)										
Degrees Azimuth	Name	0.5–1.1	1.1–1.6	1.6–2.1	2.1–3.1	3.1–4.1	4.1–5.1	5.1–6.1	6.1–8.1	8.1–10.0	≥ 10.0	Total
326.25–348.75	North-northwest	0.0002	0.0009	0.0023	0.0069	0.0094	0.0067	0.0042	0.0039	0.0023	0.0012	0.0380
—	Total	0.0038	0.0165	0.0469	0.1462	0.2644	0.2968	0.1262	0.0621	0.0246	0.0126	0.9881
									Calms		0.00002	
									Missing/incomplete		0.01188	
									Frequency of calm winds		0.00%	
									Average wind speed		4.35 m/s	

NOTE: Wind speeds are equal to or greater than the lower limit and are less than the upper limit.

Source: BSC 2007e, Table C-16.

Table 1.1-50. Joint Frequency Distribution of Wind Speed and Direction (Decimal Fractions) for Stability Category A (Extremely Unstable) (1994 to 2006) at Site 1 at 10 m above Ground Level

Wind Direction		Wind Speed Category (m/s)										Total
Degrees Azimuth	Name	0.5-1.1	1.1-1.6	1.6-2.1	2.1-3.1	3.1-4.1	4.1-5.1	5.1-6.1	6.1-8.1	8.1-10.0	≥ 10.0	
348.75-11.25	North	0.0000	0.0001	0.0001	0.0012	0.0034	0.0047	0.0061	0.0088	0.0025	0.0009	0.0275
11.25-33.75	North-northeast	0.0000	0.0000	0.0001	0.0017	0.0050	0.0070	0.0062	0.0065	0.0010	0.0004	0.0277
33.75-56.25	Northeast	0.0000	0.0000	0.0003	0.0031	0.0056	0.0068	0.0051	0.0023	0.0004	0.0001	0.0234
56.25-78.75	East-northeast	0.0000	0.0002	0.0006	0.0039	0.0030	0.0021	0.0011	0.0006	0.0001	0.0000	0.0114
78.75-101.25	East	0.0000	0.0001	0.0011	0.0035	0.0029	0.0011	0.0004	0.0005	0.0001	0.0000	0.0096
101.25-123.75	East-southeast	0.0000	0.0003	0.0017	0.0067	0.0048	0.0022	0.0007	0.0001	0.0000	0.0000	0.0164
123.75-146.25	Southeast	0.0001	0.0000	0.0027	0.0164	0.0114	0.0041	0.0009	0.0001	0.0001	0.0000	0.0356
146.25-168.75	South-southeast	0.0000	0.0001	0.0026	0.0344	0.0529	0.0334	0.0191	0.0211	0.0113	0.0043	0.1790
168.75-191.25	South	0.0000	0.0002	0.0012	0.0219	0.0809	0.1003	0.0834	0.0961	0.0449	0.0185	0.4472
191.25-213.75	South-southwest	0.0000	0.0001	0.0007	0.0063	0.0206	0.0288	0.0156	0.0065	0.0014	0.0003	0.0800
213.75-236.25	Southwest	0.0000	0.0000	0.0002	0.0040	0.0128	0.0155	0.0068	0.0027	0.0004	0.0001	0.0422
236.25-258.75	West-southwest	0.0000	0.0001	0.0002	0.0022	0.0059	0.0063	0.0018	0.0010	0.0000	0.0000	0.0173
258.75-281.25	West	0.0000	0.0000	0.0002	0.0010	0.0036	0.0040	0.0012	0.0003	0.0001	0.0001	0.0103
281.25-303.75	West-northwest	0.0000	0.0001	0.0001	0.0009	0.0027	0.0032	0.0020	0.0007	0.0002	0.0001	0.0099
303.75-326.25	Northwest	0.0001	0.0001	0.0002	0.0009	0.0025	0.0034	0.0041	0.0042	0.0017	0.0002	0.0172

Table 1.1-50. Joint Frequency Distribution of Wind Speed and Direction (Decimal Fractions) for Stability Category A (Extremely Unstable) (1994 to 2006) at Site 1 at 10 m above Ground Level (Continued)

Wind Direction		Wind Speed Category (m/s)										
Degrees Azimuth	Name	0.5–1.1	1.1–1.6	1.6–2.1	2.1–3.1	3.1–4.1	4.1–5.1	5.1–6.1	6.1–8.1	8.1–10.0	≥ 10.0	Total
326.25–348.75	North-northwest	0.0001	0.0001	0.0001	0.0007	0.0024	0.0068	0.0094	0.0152	0.0083	0.0028	0.0456
—	Total	0.0002	0.0011	0.0118	0.1084	0.2200	0.2295	0.1635	0.1661	0.0721	0.0276	0.9961
									Calms		0	
									Missing/incomplete		0.00389	
									Frequency of calm winds		0.00%	
									Average wind speed		5.22 m/s	

NOTE: Wind speeds are equal to or greater than the lower limit and are less than the upper limit.

Source: BSC 2007e, Table D-1.

Table 1.1-51. Joint Frequency Distribution of Wind Speed and Direction (Decimal Fractions) for Stability Category A (Extremely Unstable) (1994 to 2006) at Site 1 at 60 m above Ground Level

Wind Direction		Wind Speed Category (m/s)										
Degrees Azimuth	Name	0.5–1.1	1.1–1.6	1.6–2.1	2.1–3.1	3.1–4.1	4.1–5.1	5.1–6.1	6.1–8.1	8.1–10.0	≥ 10.0	Total
348.75–11.25	North	0.0000	0.0001	0.0000	0.0008	0.0021	0.0030	0.0039	0.0090	0.0047	0.0034	0.0269
11.25–33.75	North-northeast	0.0000	0.0000	0.0002	0.0013	0.0029	0.0050	0.0056	0.0089	0.0041	0.0018	0.0299
33.75–56.25	Northeast	0.0000	0.0000	0.0001	0.0024	0.0037	0.0052	0.0054	0.0054	0.0011	0.0004	0.0236
56.25–78.75	East-northeast	0.0000	0.0001	0.0006	0.0026	0.0027	0.0019	0.0011	0.0010	0.0000	0.0001	0.0100
78.75–101.25	East	0.0000	0.0001	0.0008	0.0029	0.0022	0.0017	0.0004	0.0007	0.0000	0.0001	0.0089
101.25–123.75	East-southeast	0.0000	0.0003	0.0014	0.0054	0.0050	0.0025	0.0010	0.0004	0.0000	0.0000	0.0160
123.75–146.25	Southeast	0.0000	0.0002	0.0022	0.0111	0.0107	0.0055	0.0017	0.0008	0.0000	0.0001	0.0323
146.25–168.75	South-southeast	0.0000	0.0002	0.0015	0.0231	0.0421	0.0330	0.0191	0.0206	0.0142	0.0121	0.1658
168.75–191.25	South	0.0000	0.0000	0.0011	0.0143	0.0509	0.0865	0.0785	0.1127	0.0591	0.0537	0.4569
191.25–213.75	South-southwest	0.0000	0.0002	0.0005	0.0034	0.0102	0.0248	0.0206	0.0158	0.0037	0.0013	0.0805
213.75–236.25	Southwest	0.0001	0.0001	0.0002	0.0024	0.0070	0.0149	0.0105	0.0076	0.0010	0.0003	0.0439
236.25–258.75	West-southwest	0.0000	0.0000	0.0002	0.0017	0.0039	0.0056	0.0042	0.0026	0.0002	0.0001	0.0185
258.75–281.25	West	0.0000	0.0000	0.0001	0.0007	0.0023	0.0038	0.0026	0.0009	0.0001	0.0001	0.0105
281.25–303.75	West-northwest	0.0000	0.0000	0.0002	0.0006	0.0011	0.0033	0.0023	0.0021	0.0003	0.0001	0.0099
303.75–326.25	Northwest	0.0001	0.0000	0.0001	0.0009	0.0015	0.0023	0.0038	0.0052	0.0025	0.0016	0.0179

Table 1.1-51. Joint Frequency Distribution of Wind Speed and Direction (Decimal Fractions) for Stability Category A (Extremely Unstable) (1994 to 2006) at Site 1 at 60 m above Ground Level (Continued)

Wind Direction		Wind Speed Category (m/s)										
Degrees Azimuth	Name	0.5–1.1	1.1–1.6	1.6–2.1	2.1–3.1	3.1–4.1	4.1–5.1	5.1–6.1	6.1–8.1	8.1–10.0	≥ 10.0	Total
326.25–348.75	North-northwest	0.0001	0.0001	0.0000	0.0005	0.0017	0.0037	0.0057	0.0152	0.0111	0.0104	0.0484
—	Total	0.0002	0.0011	0.0091	0.0742	0.1500	0.2027	0.1665	0.2088	0.1020	0.0854	0.9824
									Calms		0	
									Missing/incomplete		0.01763	
									Frequency of calm winds		0.00%	
									Average wind speed		6.03 m/s	

NOTE: Wind speeds are equal to or greater than the lower limit and are less than the upper limit.

Source: BSC 2007e, Table D-2.

Table 1.1-52. Joint Frequency Distribution of Wind Speed and Direction (Decimal Fractions) for Stability Category B (Moderately Unstable) (1994 to 2006) at Site 1 at 10 m above Ground Level

Wind Direction		Wind Speed Category (m/s)										Total
Degrees Azimuth	Name	0.5–1.1	1.1–1.6	1.6–2.1	2.1–3.1	3.1–4.1	4.1–5.1	5.1–6.1	6.1–8.1	8.1–10.0	≥ 10.0	
348.75–11.25	North	0.0002	0.0004	0.0011	0.0033	0.0054	0.0089	0.0057	0.0074	0.0013	0.0009	0.0345
11.25–33.75	North-northeast	0.0002	0.0000	0.0009	0.0065	0.0081	0.0100	0.0072	0.0046	0.0007	0.0002	0.0384
33.75–56.25	Northeast	0.0000	0.0000	0.0018	0.0076	0.0122	0.0081	0.0044	0.0022	0.0002	0.0000	0.0366
56.25–78.75	East-northeast	0.0000	0.0002	0.0028	0.0124	0.0066	0.0024	0.0006	0.0000	0.0000	0.0000	0.0249
78.75–101.25	East	0.0000	0.0018	0.0074	0.0079	0.0033	0.0015	0.0002	0.0002	0.0000	0.0000	0.0223
101.25–123.75	East-southeast	0.0002	0.0026	0.0137	0.0179	0.0041	0.0018	0.0013	0.0004	0.0000	0.0000	0.0419
123.75–146.25	Southeast	0.0004	0.0022	0.0218	0.0414	0.0164	0.0052	0.0011	0.0000	0.0000	0.0000	0.0884
146.25–168.75	South-southeast	0.0000	0.0007	0.0150	0.0973	0.0637	0.0185	0.0074	0.0105	0.0039	0.0009	0.2178
168.75–191.25	South	0.0000	0.0007	0.0070	0.0611	0.0871	0.0460	0.0297	0.0297	0.0186	0.0085	0.2885
191.25–213.75	South-southwest	0.0000	0.0000	0.0030	0.0181	0.0196	0.0142	0.0055	0.0028	0.0007	0.0002	0.0641
213.75–236.25	Southwest	0.0000	0.0002	0.0022	0.0102	0.0148	0.0118	0.0035	0.0009	0.0002	0.0000	0.0438
236.25–258.75	West-southwest	0.0000	0.0000	0.0015	0.0065	0.0074	0.0046	0.0009	0.0004	0.0000	0.0000	0.0212
258.75–281.25	West	0.0000	0.0000	0.0011	0.0057	0.0037	0.0011	0.0007	0.0004	0.0000	0.0000	0.0127
281.25–303.75	West-northwest	0.0000	0.0000	0.0002	0.0011	0.0024	0.0015	0.0007	0.0002	0.0002	0.0000	0.0063
303.75–326.25	Northwest	0.0000	0.0000	0.0004	0.0015	0.0035	0.0039	0.0022	0.0041	0.0006	0.0002	0.0162

Table 1.1-52. Joint Frequency Distribution of Wind Speed and Direction (Decimal Fractions) for Stability Category B (Moderately Unstable) (1994 to 2006) at Site 1 at 10 m above Ground Level (Continued)

Wind Direction		Wind Speed Category (m/s)										
Degrees Azimuth	Name	0.5–1.1	1.1–1.6	1.6–2.1	2.1–3.1	3.1–4.1	4.1–5.1	5.1–6.1	6.1–8.1	8.1–10.0	≥ 10.0	Total
326.25–348.75	North-northwest	0.0000	0.0000	0.0007	0.0017	0.0044	0.0066	0.0083	0.0126	0.0046	0.0033	0.0423
—	Total	0.0009	0.0089	0.0805	0.3000	0.2627	0.1460	0.0796	0.0762	0.0310	0.0142	0.9983
									Calms		0	
									Missing/incomplete		0.00166	
									Frequency of calm winds		0.00%	
									Average wind speed		4.00 m/s	

NOTE: Wind speeds are equal to or greater than the lower limit and are less than the upper limit.

Source: BSC 2007e, Table D-3.

Table 1.1-53. Joint Frequency Distribution of Wind Speed and Direction (Decimal Fractions) for Stability Category B (Moderately Unstable) (1994 to 2006) at Site 1 at 60 m above Ground Level

Wind Direction		Wind Speed Category (m/s)										
Degrees Azimuth	Name	0.5–1.1	1.1–1.6	1.6–2.1	2.1–3.1	3.1–4.1	4.1–5.1	5.1–6.1	6.1–8.1	8.1–10.0	≥ 10.0	Total
348.75–11.25	North	0.0000	0.0002	0.0006	0.0024	0.0035	0.0047	0.0062	0.0060	0.0045	0.0026	0.0306
11.25–33.75	North-northeast	0.0000	0.0004	0.0013	0.0039	0.0065	0.0091	0.0097	0.0099	0.0026	0.0013	0.0448
33.75–56.25	Northeast	0.0000	0.0004	0.0009	0.0058	0.0095	0.0086	0.0065	0.0030	0.0011	0.0004	0.0362
56.25–78.75	East-northeast	0.0000	0.0006	0.0034	0.0082	0.0058	0.0034	0.0006	0.0004	0.0000	0.0000	0.0222
78.75–101.25	East	0.0000	0.0017	0.0080	0.0076	0.0032	0.0009	0.0013	0.0000	0.0000	0.0000	0.0228
101.25–123.75	East-southeast	0.0004	0.0034	0.0106	0.0134	0.0037	0.0015	0.0013	0.0006	0.0000	0.0000	0.0349
123.75–146.25	Southeast	0.0000	0.0021	0.0138	0.0375	0.0213	0.0050	0.0019	0.0013	0.0000	0.0000	0.0828
146.25–168.75	South-southeast	0.0000	0.0007	0.0119	0.0806	0.0664	0.0299	0.0106	0.0084	0.0069	0.0050	0.2205
168.75–191.25	South	0.0002	0.0007	0.0062	0.0506	0.0735	0.0530	0.0285	0.0368	0.0201	0.0256	0.2951
191.25–213.75	South-southwest	0.0000	0.0002	0.0021	0.0123	0.0157	0.0162	0.0091	0.0060	0.0021	0.0004	0.0640
213.75–236.25	Southwest	0.0000	0.0002	0.0009	0.0063	0.0114	0.0131	0.0076	0.0032	0.0006	0.0004	0.0437
236.25–258.75	West-southwest	0.0000	0.0000	0.0009	0.0049	0.0050	0.0041	0.0035	0.0013	0.0000	0.0000	0.0198
258.75–281.25	West	0.0000	0.0002	0.0009	0.0054	0.0032	0.0034	0.0011	0.0004	0.0002	0.0000	0.0147
281.25–303.75	West-northwest	0.0000	0.0000	0.0002	0.0011	0.0019	0.0021	0.0007	0.0007	0.0004	0.0002	0.0073
303.75–326.25	Northwest	0.0000	0.0000	0.0002	0.0009	0.0021	0.0030	0.0026	0.0032	0.0032	0.0006	0.0157

Table 1.1-53. Joint Frequency Distribution of Wind Speed and Direction (Decimal Fractions) for Stability Category B (Moderately Unstable) (1994 to 2006) at Site 1 at 60 m above Ground Level (Continued)

Wind Direction		Wind Speed Category (m/s)										
Degrees Azimuth	Name	0.5–1.1	1.1–1.6	1.6–2.1	2.1–3.1	3.1–4.1	4.1–5.1	5.1–6.1	6.1–8.1	8.1–10.0	≥ 10.0	Total
326.25–348.75	North-northwest	0.0000	0.0002	0.0009	0.0015	0.0015	0.0050	0.0058	0.0116	0.0101	0.0084	0.0450
—	Total	0.0006	0.0108	0.0629	0.2425	0.2341	0.1629	0.0972	0.0925	0.0517	0.0448	0.9878
									Calms		0	
									Missing/incomplete		0.01216	
									Frequency of calm winds		0.00%	
									Average wind speed		4.57 m/s	

NOTE: Wind speeds are equal to or greater than the lower limit and are less than the upper limit.

Source: BSC 2007e, Table D-4.

Table 1.1-54. Joint Frequency Distribution of Wind Speed and Direction (Decimal Fractions) for Stability Category C (Slightly Unstable) (1994 to 2006) at Site 1 at 10 m above Ground Level

Wind Direction		Wind Speed Category (m/s)										
Degrees Azimuth	Name	0.5–1.1	1.1–1.6	1.6–2.1	2.1–3.1	3.1–4.1	4.1–5.1	5.1–6.1	6.1–8.1	8.1–10.0	≥ 10.0	Total
348.75–11.25	North	0.0002	0.0006	0.0015	0.0047	0.0056	0.0049	0.0054	0.0066	0.0011	0.0006	0.0312
11.25–33.75	North-northeast	0.0002	0.0002	0.0021	0.0064	0.0077	0.0092	0.0058	0.0036	0.0009	0.0000	0.0361
33.75–56.25	Northeast	0.0004	0.0028	0.0047	0.0096	0.0100	0.0045	0.0028	0.0008	0.0000	0.0000	0.0355
56.25–78.75	East-northeast	0.0000	0.0036	0.0109	0.0135	0.0038	0.0009	0.0004	0.0006	0.0000	0.0000	0.0336
78.75–101.25	East	0.0000	0.0062	0.0147	0.0133	0.0024	0.0002	0.0008	0.0002	0.0000	0.0000	0.0378
101.25–123.75	East-southeast	0.0002	0.0085	0.0225	0.0201	0.0047	0.0015	0.0006	0.0004	0.0000	0.0000	0.0584
123.75–146.25	Southeast	0.0000	0.0075	0.0351	0.0500	0.0105	0.0013	0.0009	0.0000	0.0000	0.0000	0.1054
146.25–168.75	South-southeast	0.0000	0.0024	0.0412	0.1069	0.0370	0.0083	0.0066	0.0086	0.0019	0.0008	0.2136
168.75–191.25	South	0.0000	0.0019	0.0154	0.0690	0.0618	0.0346	0.0254	0.0316	0.0152	0.0068	0.2616
191.25–213.75	South-southwest	0.0000	0.0002	0.0071	0.0218	0.0210	0.0085	0.0043	0.0026	0.0009	0.0000	0.0665
213.75–236.25	Southwest	0.0000	0.0002	0.0023	0.0120	0.0152	0.0086	0.0030	0.0011	0.0000	0.0000	0.0425
236.25–258.75	West-southwest	0.0000	0.0000	0.0019	0.0060	0.0083	0.0026	0.0004	0.0006	0.0000	0.0000	0.0197
258.75–281.25	West	0.0000	0.0000	0.0013	0.0043	0.0023	0.0011	0.0002	0.0004	0.0000	0.0002	0.0098
281.25–303.75	West-northwest	0.0004	0.0000	0.0013	0.0011	0.0015	0.0013	0.0002	0.0004	0.0002	0.0000	0.0064
303.75–326.25	Northwest	0.0002	0.0000	0.0011	0.0024	0.0019	0.0023	0.0023	0.0011	0.0013	0.0000	0.0126

Table 1.1-54. Joint Frequency Distribution of Wind Speed and Direction (Decimal Fractions) for Stability Category C (Slightly Unstable) (1994 to 2006) at Site 1 at 10 m above Ground Level (Continued)

Wind Direction		Wind Speed Category (m/s)										
Degrees Azimuth	Name	0.5–1.1	1.1–1.6	1.6–2.1	2.1–3.1	3.1–4.1	4.1–5.1	5.1–6.1	6.1–8.1	8.1–10.0	≥ 10.0	Total
326.25–348.75	North-northwest	0.0002	0.0002	0.0006	0.0024	0.0032	0.0051	0.0062	0.0056	0.0036	0.0023	0.0293
—	Total	0.0017	0.0342	0.1637	0.3437	0.1969	0.0949	0.0652	0.0641	0.0252	0.0105	0.9972
									Calms		0	
									Missing/incomplete		0.00281	
									Frequency of calm winds		0.00%	
									Average wind speed		3.55 m/s	

NOTE: Wind speeds are equal to or greater than the lower limit and are less than the upper limit.

Source: BSC 2007e, Table D-5.

Table 1.1-55. Joint Frequency Distribution of Wind Speed and Direction (Decimal Fractions) for Stability Category C (Slightly Unstable) (1994 to 2006) at Site 1 at 60 m above Ground Level

Wind Direction		Wind Speed Category (m/s)										
Degrees Azimuth	Name	0.5–1.1	1.1–1.6	1.6–2.1	2.1–3.1	3.1–4.1	4.1–5.1	5.1–6.1	6.1–8.1	8.1–10.0	≥ 10.0	Total
348.75–11.25	North	0.0000	0.0002	0.0009	0.0027	0.0049	0.0049	0.0032	0.0076	0.0044	0.0013	0.0302
11.25–33.75	North-northeast	0.0002	0.0013	0.0019	0.0057	0.0051	0.0066	0.0076	0.0068	0.0028	0.0013	0.0395
33.75–56.25	Northeast	0.0008	0.0015	0.0044	0.0074	0.0082	0.0068	0.0038	0.0025	0.0006	0.0000	0.0359
56.25–78.75	East-northeast	0.0004	0.0044	0.0093	0.0129	0.0053	0.0013	0.0004	0.0002	0.0004	0.0000	0.0345
78.75–101.25	East	0.0004	0.0057	0.0125	0.0095	0.0030	0.0002	0.0006	0.0009	0.0002	0.0000	0.0330
101.25–123.75	East-southeast	0.0002	0.0085	0.0180	0.0156	0.0047	0.0025	0.0008	0.0006	0.0000	0.0000	0.0509
123.75–146.25	Southeast	0.0006	0.0068	0.0268	0.0488	0.0139	0.0030	0.0008	0.0006	0.0000	0.0000	0.1012
146.25–168.75	South-southeast	0.0000	0.0034	0.0355	0.1042	0.0418	0.0142	0.0063	0.0089	0.0065	0.0023	0.2230
168.75–191.25	South	0.0000	0.0008	0.0171	0.0533	0.0577	0.0359	0.0207	0.0338	0.0199	0.0224	0.2615
191.25–213.75	South-southwest	0.0000	0.0002	0.0051	0.0140	0.0158	0.0139	0.0076	0.0049	0.0017	0.0013	0.0645
213.75–236.25	Southwest	0.0004	0.0004	0.0030	0.0089	0.0121	0.0120	0.0059	0.0032	0.0006	0.0000	0.0465
236.25–258.75	West-southwest	0.0000	0.0000	0.0021	0.0040	0.0059	0.0046	0.0017	0.0009	0.0000	0.0000	0.0192
258.75–281.25	West	0.0000	0.0000	0.0023	0.0027	0.0030	0.0019	0.0008	0.0006	0.0002	0.0002	0.0116
281.25–303.75	West-northwest	0.0000	0.0002	0.0006	0.0021	0.0015	0.0009	0.0013	0.0000	0.0002	0.0002	0.0070
303.75–326.25	Northwest	0.0004	0.0004	0.0002	0.0015	0.0013	0.0006	0.0019	0.0032	0.0004	0.0013	0.0112

Table 1.1-55. Joint Frequency Distribution of Wind Speed and Direction (Decimal Fractions) for Stability Category C (Slightly Unstable) (1994 to 2006) at Site 1 at 60 m above Ground Level (Continued)

Wind Direction		Wind Speed Category (m/s)										
Degrees Azimuth	Name	0.5–1.1	1.1–1.6	1.6–2.1	2.1–3.1	3.1–4.1	4.1–5.1	5.1–6.1	6.1–8.1	8.1–10.0	≥ 10.0	Total
326.25–348.75	North-northwest	0.0000	0.0002	0.0004	0.0013	0.0017	0.0036	0.0040	0.0084	0.0047	0.0061	0.0304
—	Total	0.0032	0.0340	0.1401	0.2946	0.1860	0.1129	0.0672	0.0831	0.0425	0.0364	0.9873
									Calms		0	
									Missing/incomplete		0.01274	
									Frequency of calm winds		0.00%	
									Average wind speed		4.05 m/s	

NOTE: Wind speeds are equal to or greater than the lower limit and are less than the upper limit.

Source: BSC 2007e, Table D-6.

Table 1.1-56. Joint Frequency Distribution of Wind Speed and Direction (Decimal Fractions) for Stability Category D (Neutral) (1994 to 2006) at Site 1 at 10 m above Ground Level

Wind Direction		Wind Speed Category (m/s)										
Degrees Azimuth	Name	0.5-1.1	1.1-1.6	1.6-2.1	2.1-3.1	3.1-4.1	4.1-5.1	5.1-6.1	6.1-8.1	8.1-10.0	≥ 10.0	Total
348.75-11.25	North	0.0013	0.0039	0.0025	0.0053	0.0057	0.0096	0.0082	0.0121	0.0038	0.0021	0.0544
11.25-33.75	North-northeast	0.0015	0.0044	0.0047	0.0067	0.0087	0.0071	0.0039	0.0039	0.0012	0.0001	0.0423
33.75-56.25	Northeast	0.0020	0.0107	0.0067	0.0076	0.0044	0.0035	0.0018	0.0010	0.0000	0.0000	0.0378
56.25-78.75	East-northeast	0.0031	0.0156	0.0095	0.0053	0.0022	0.0010	0.0003	0.0004	0.0001	0.0000	0.0374
78.75-101.25	East	0.0034	0.0147	0.0141	0.0057	0.0019	0.0013	0.0004	0.0008	0.0002	0.0001	0.0424
101.25-123.75	East-southeast	0.0028	0.0178	0.0179	0.0097	0.0037	0.0016	0.0004	0.0007	0.0001	0.0000	0.0547
123.75-146.25	Southeast	0.0034	0.0214	0.0314	0.0222	0.0072	0.0021	0.0006	0.0003	0.0001	0.0000	0.0885
146.25-168.75	South-southeast	0.0024	0.0151	0.0369	0.0412	0.0177	0.0093	0.0071	0.0084	0.0028	0.0006	0.1416
168.75-191.25	South	0.0013	0.0090	0.0249	0.0506	0.0379	0.0326	0.0301	0.0444	0.0326	0.0137	0.2770
191.25-213.75	South-southwest	0.0013	0.0052	0.0099	0.0191	0.0144	0.0072	0.0035	0.0031	0.0016	0.0003	0.0656
213.75-236.25	Southwest	0.0011	0.0027	0.0042	0.0096	0.0110	0.0061	0.0019	0.0019	0.0003	0.0001	0.0389
236.25-258.75	West-southwest	0.0012	0.0021	0.0026	0.0047	0.0050	0.0032	0.0012	0.0012	0.0000	0.0000	0.0212
258.75-281.25	West	0.0012	0.0015	0.0015	0.0024	0.0021	0.0016	0.0005	0.0004	0.0003	0.0000	0.0114
281.25-303.75	West-northwest	0.0006	0.0016	0.0008	0.0013	0.0015	0.0013	0.0005	0.0010	0.0001	0.0000	0.0086
303.75-326.25	Northwest	0.0008	0.0022	0.0019	0.0021	0.0024	0.0035	0.0029	0.0029	0.0017	0.0009	0.0214

Table 1.1-56. Joint Frequency Distribution of Wind Speed and Direction (Decimal Fractions) for Stability Category D (Neutral) (1994 to 2006) at Site 1 at 10 m above Ground Level (Continued)

Wind Direction		Wind Speed Category (m/s)										
Degrees Azimuth	Name	0.5–1.1	1.1–1.6	1.6–2.1	2.1–3.1	3.1–4.1	4.1–5.1	5.1–6.1	6.1–8.1	8.1–10.0	≥ 10.0	Total
326.25–348.75	North-northwest	0.0019	0.0026	0.0031	0.0029	0.0049	0.0068	0.0076	0.0110	0.0074	0.0086	0.0567
—	Total	0.0291	0.1307	0.1727	0.1965	0.1308	0.0977	0.0710	0.0934	0.0519	0.0264	0.9941
									Calms		0	
									Missing/incomplete		0.00590	
									Frequency of calm winds		0.00%	
									Average wind speed		3.77 m/s	

NOTE: Wind speeds are equal to or greater than the lower limit and are less than the upper limit.

Source: BSC 2007e, Table D-7.

Table 1.1-57. Joint Frequency Distribution of Wind Speed and Direction (Decimal Fractions) for Stability Category D (Neutral) (1994 to 2006) at Site 1 at 60 m above Ground Level

Wind Direction		Wind Speed Category (m/s)										
Degrees Azimuth	Name	0.5-1.1	1.1-1.6	1.6-2.1	2.1-3.1	3.1-4.1	4.1-5.1	5.1-6.1	6.1-8.1	8.1-10.0	≥ 10.0	Total
348.75-11.25	North	0.0021	0.0028	0.0023	0.0038	0.0029	0.0039	0.0057	0.0114	0.0088	0.0080	0.0518
11.25-33.75	North-northeast	0.0016	0.0044	0.0043	0.0057	0.0067	0.0065	0.0060	0.0083	0.0035	0.0020	0.0490
33.75-56.25	Northeast	0.0039	0.0082	0.0078	0.0073	0.0043	0.0030	0.0028	0.0024	0.0008	0.0003	0.0408
56.25-78.75	East-northeast	0.0042	0.0126	0.0085	0.0048	0.0025	0.0012	0.0005	0.0005	0.0003	0.0000	0.0351
78.75-101.25	East	0.0052	0.0115	0.0094	0.0050	0.0019	0.0012	0.0008	0.0008	0.0008	0.0003	0.0369
101.25-123.75	East-southeast	0.0044	0.0131	0.0161	0.0080	0.0041	0.0025	0.0009	0.0008	0.0002	0.0001	0.0501
123.75-146.25	Southeast	0.0041	0.0171	0.0265	0.0243	0.0080	0.0035	0.0018	0.0009	0.0002	0.0001	0.0864
146.25-168.75	South-southeast	0.0028	0.0149	0.0361	0.0444	0.0185	0.0094	0.0075	0.0099	0.0084	0.0053	0.1572
168.75-191.25	South	0.0016	0.0086	0.0222	0.0430	0.0323	0.0243	0.0220	0.0431	0.0340	0.0509	0.2820
191.25-213.75	South-southwest	0.0013	0.0041	0.0073	0.0133	0.0120	0.0090	0.0053	0.0043	0.0023	0.0021	0.0612
213.75-236.25	Southwest	0.0012	0.0018	0.0033	0.0065	0.0079	0.0086	0.0052	0.0026	0.0009	0.0005	0.0384
236.25-258.75	West-southwest	0.0009	0.0009	0.0023	0.0023	0.0038	0.0034	0.0031	0.0019	0.0008	0.0001	0.0195
258.75-281.25	West	0.0009	0.0008	0.0008	0.0013	0.0016	0.0016	0.0009	0.0011	0.0002	0.0003	0.0095
281.25-303.75	West-northwest	0.0008	0.0009	0.0006	0.0013	0.0010	0.0009	0.0010	0.0005	0.0006	0.0000	0.0077
303.75-326.25	Northwest	0.0009	0.0011	0.0012	0.0011	0.0013	0.0018	0.0028	0.0042	0.0020	0.0023	0.0188

Table 1.1-57. Joint Frequency Distribution of Wind Speed and Direction (Decimal Fractions) for Stability Category D (Neutral) (1994 to 2006) at Site 1 at 60 m above Ground Level (Continued)

Wind Direction		Wind Speed Category (m/s)										
Degrees Azimuth	Name	0.5–1.1	1.1–1.6	1.6–2.1	2.1–3.1	3.1–4.1	4.1–5.1	5.1–6.1	6.1–8.1	8.1–10.0	≥ 10.0	Total
326.25–348.75	North-northwest	0.0008	0.0018	0.0014	0.0020	0.0033	0.0036	0.0043	0.0104	0.0099	0.0178	0.0553
—	Total	0.0368	0.1048	0.1503	0.1741	0.1121	0.0841	0.0708	0.1031	0.0735	0.0903	0.9888
									Calms		0.00012	
									Missing/incomplete		0.01112	
									Frequency of calm winds		0.01%	
									Average wind speed		4.58 m/s	

NOTE: Wind speeds are equal to or greater than the lower limit and are less than the upper limit.

Source: BSC 2007e, Table D-8.

Table 1.1-58. Joint Frequency Distribution of Wind Speed and Direction (Decimal Fractions) for Stability Category E (Slightly Stable) (1994 to 2006) at Site 1 at 10 m above Ground Level

Wind Direction		Wind Speed Category (m/s)										
Degrees Azimuth	Name	0.5–1.1	1.1–1.6	1.6–2.1	2.1–3.1	3.1–4.1	4.1–5.1	5.1–6.1	6.1–8.1	8.1–10.0	≥ 10.0	Total
348.75–11.25	North	0.0018	0.0080	0.0157	0.0287	0.0354	0.0326	0.0224	0.0195	0.0053	0.0010	0.1703
11.25–33.75	North-northeast	0.0018	0.0061	0.0072	0.0106	0.0109	0.0090	0.0061	0.0042	0.0011	0.0003	0.0573
33.75–56.25	Northeast	0.0029	0.0080	0.0054	0.0041	0.0022	0.0013	0.0006	0.0006	0.0000	0.0000	0.0252
56.25–78.75	East-northeast	0.0039	0.0075	0.0027	0.0016	0.0011	0.0003	0.0003	0.0001	0.0000	0.0000	0.0176
78.75–101.25	East	0.0040	0.0040	0.0021	0.0016	0.0006	0.0005	0.0001	0.0001	0.0000	0.0000	0.0130
101.25–123.75	East-southeast	0.0028	0.0039	0.0019	0.0019	0.0007	0.0002	0.0000	0.0000	0.0000	0.0000	0.0114
123.75–146.25	Southeast	0.0026	0.0040	0.0036	0.0031	0.0013	0.0001	0.0001	0.0000	0.0000	0.0000	0.0148
146.25–168.75	South-southeast	0.0022	0.0046	0.0049	0.0070	0.0048	0.0022	0.0021	0.0014	0.0002	0.0000	0.0295
168.75–191.25	South	0.0018	0.0047	0.0095	0.0197	0.0243	0.0289	0.0188	0.0210	0.0077	0.0023	0.1387
191.25–213.75	South-southwest	0.0015	0.0065	0.0123	0.0315	0.0260	0.0109	0.0056	0.0032	0.0004	0.0000	0.0978
213.75–236.25	Southwest	0.0012	0.0074	0.0135	0.0223	0.0102	0.0026	0.0005	0.0004	0.0001	0.0000	0.0583
236.25–258.75	West-southwest	0.0021	0.0082	0.0108	0.0151	0.0114	0.0032	0.0009	0.0004	0.0001	0.0000	0.0521
258.75–281.25	West	0.0023	0.0110	0.0106	0.0072	0.0044	0.0016	0.0004	0.0003	0.0000	0.0000	0.0379
281.25–303.75	West-northwest	0.0022	0.0122	0.0153	0.0088	0.0024	0.0008	0.0006	0.0005	0.0002	0.0000	0.0430
303.75–326.25	Northwest	0.0025	0.0150	0.0288	0.0247	0.0061	0.0037	0.0022	0.0024	0.0006	0.0003	0.0864

Table 1.1-58. Joint Frequency Distribution of Wind Speed and Direction (Decimal Fractions) for Stability Category E (Slightly Stable) (1994 to 2006) at Site 1 at 10 m above Ground Level (Continued)

Wind Direction		Wind Speed Category (m/s)										
Degrees Azimuth	Name	0.5–1.1	1.1–1.6	1.6–2.1	2.1–3.1	3.1–4.1	4.1–5.1	5.1–6.1	6.1–8.1	8.1–10.0	≥ 10.0	Total
326.25–348.75	North-northwest	0.0021	0.0133	0.0235	0.0262	0.0173	0.0137	0.0133	0.0205	0.0107	0.0058	0.1465
—	Total	0.0376	0.1243	0.1676	0.2144	0.1593	0.1116	0.0740	0.0746	0.0267	0.0098	0.9924
									Calms		0.00017	
									Missing/incomplete		0.00747	
									Frequency of calm winds		0.02%	
									Average wind speed		3.44 m/s	

NOTE: Wind speeds are equal to or greater than the lower limit and are less than the upper limit.

Source: BSC 2007e, Table D-9.

Table 1.1-59. Joint Frequency Distribution of Wind Speed and Direction (Decimal Fractions) for Stability Category E (Slightly Stable) (1994 to 2006) at Site 1 at 60 m above Ground Level

Wind Direction		Wind Speed Category (m/s)										Total
Degrees Azimuth	Name	0.5–1.1	1.1–1.6	1.6–2.1	2.1–3.1	3.1–4.1	4.1–5.1	5.1–6.1	6.1–8.1	8.1–10.0	≥ 10.0	
348.75–11.25	North	0.0067	0.0101	0.0079	0.0132	0.0176	0.0244	0.0266	0.0411	0.0215	0.0113	0.1804
11.25–33.75	North-northeast	0.0080	0.0135	0.0106	0.0133	0.0109	0.0134	0.0111	0.0161	0.0066	0.0038	0.1073
33.75–56.25	Northeast	0.0070	0.0111	0.0087	0.0058	0.0036	0.0027	0.0017	0.0016	0.0008	0.0003	0.0432
56.25–78.75	East-northeast	0.0048	0.0056	0.0039	0.0026	0.0013	0.0008	0.0006	0.0004	0.0002	0.0000	0.0202
78.75–101.25	East	0.0043	0.0055	0.0032	0.0030	0.0012	0.0008	0.0005	0.0003	0.0000	0.0000	0.0186
101.25–123.75	East-southeast	0.0035	0.0053	0.0036	0.0034	0.0018	0.0011	0.0002	0.0001	0.0000	0.0000	0.0191
123.75–146.25	Southeast	0.0037	0.0065	0.0057	0.0074	0.0038	0.0016	0.0005	0.0002	0.0000	0.0000	0.0293
146.25–168.75	South-southeast	0.0040	0.0085	0.0099	0.0120	0.0086	0.0060	0.0042	0.0055	0.0024	0.0006	0.0618
168.75–191.25	South	0.0033	0.0095	0.0141	0.0250	0.0248	0.0284	0.0276	0.0488	0.0246	0.0156	0.2216
191.25–213.75	South-southwest	0.0038	0.0079	0.0084	0.0142	0.0134	0.0102	0.0066	0.0069	0.0028	0.0006	0.0749
213.75–236.25	Southwest	0.0038	0.0049	0.0041	0.0084	0.0094	0.0063	0.0031	0.0014	0.0003	0.0002	0.0420
236.25–258.75	West-southwest	0.0025	0.0034	0.0025	0.0034	0.0058	0.0073	0.0034	0.0018	0.0002	0.0001	0.0303
258.75–281.25	West	0.0039	0.0033	0.0015	0.0017	0.0019	0.0022	0.0010	0.0006	0.0002	0.0000	0.0161
281.25–303.75	West-northwest	0.0036	0.0028	0.0018	0.0017	0.0014	0.0013	0.0008	0.0007	0.0003	0.0002	0.0147
303.75–326.25	Northwest	0.0037	0.0036	0.0020	0.0025	0.0024	0.0019	0.0025	0.0030	0.0017	0.0014	0.0247

Table 1.1-59. Joint Frequency Distribution of Wind Speed and Direction (Decimal Fractions) for Stability Category E (Slightly Stable) (1994 to 2006) at Site 1 at 60 m above Ground Level (Continued)

Wind Direction		Wind Speed Category (m/s)										
Degrees Azimuth	Name	0.5–1.1	1.1–1.6	1.6–2.1	2.1–3.1	3.1–4.1	4.1–5.1	5.1–6.1	6.1–8.1	8.1–10.0	≥ 10.0	Total
326.25–348.75	North-northwest	0.0048	0.0050	0.0040	0.0046	0.0050	0.0072	0.0081	0.0151	0.0165	0.0253	0.0957
—	Total	0.0714	0.1062	0.0918	0.1222	0.1128	0.1156	0.0986	0.1434	0.0781	0.0596	0.9876
									Calms		0.00021	
									Missing/incomplete		0.01215	
									Frequency of calm winds		0.02%	
									Average wind speed		4.60 m/s	

NOTE: Wind speeds are equal to or greater than the lower limit and are less than the upper limit.

Source: BSC 2007e, Table D-10.

Table 1.1-60. Joint Frequency Distribution of Wind Speed and Direction (Decimal Fractions) for Stability Category F (Moderately Stable) (1994 to 2006) at Site 1 at 10 m above Ground Level

Wind Direction		Wind Speed Category (m/s)										
Degrees Azimuth	Name	0.5-1.1	1.1-1.6	1.6-2.1	2.1-3.1	3.1-4.1	4.1-5.1	5.1-6.1	6.1-8.1	8.1-10.0	≥ 10.0	Total
348.75-11.25	North	0.0017	0.0084	0.0159	0.0241	0.0183	0.0079	0.0021	0.0005	0.0000	0.0000	0.0790
11.25-33.75	North-northeast	0.0019	0.0043	0.0037	0.0046	0.0032	0.0015	0.0006	0.0001	0.0001	0.0000	0.0200
33.75-56.25	Northeast	0.0023	0.0044	0.0013	0.0012	0.0005	0.0002	0.0002	0.0000	0.0000	0.0000	0.0101
56.25-78.75	East-northeast	0.0029	0.0017	0.0004	0.0004	0.0001	0.0000	0.0000	0.0000	0.0000	0.0000	0.0057
78.75-101.25	East	0.0022	0.0009	0.0004	0.0002	0.0001	0.0000	0.0000	0.0000	0.0000	0.0000	0.0037
101.25-123.75	East-southeast	0.0017	0.0009	0.0001	0.0001	0.0000	0.0000	0.0000	0.0000	0.0000	0.0000	0.0028
123.75-146.25	Southeast	0.0012	0.0011	0.0004	0.0001	0.0000	0.0000	0.0000	0.0000	0.0000	0.0000	0.0029
146.25-168.75	South-southeast	0.0014	0.0012	0.0006	0.0004	0.0001	0.0000	0.0000	0.0000	0.0000	0.0000	0.0037
168.75-191.25	South	0.0008	0.0012	0.0016	0.0012	0.0005	0.0000	0.0000	0.0000	0.0000	0.0000	0.0053
191.25-213.75	South-southwest	0.0008	0.0016	0.0036	0.0081	0.0050	0.0007	0.0001	0.0000	0.0000	0.0000	0.0199
213.75-236.25	Southwest	0.0011	0.0036	0.0076	0.0107	0.0016	0.0001	0.0000	0.0000	0.0000	0.0000	0.0246
236.25-258.75	West-southwest	0.0007	0.0060	0.0112	0.0150	0.0027	0.0003	0.0000	0.0001	0.0000	0.0000	0.0360
258.75-281.25	West	0.0009	0.0082	0.0167	0.0177	0.0052	0.0004	0.0000	0.0000	0.0000	0.0000	0.0492
281.25-303.75	West-northwest	0.0016	0.0142	0.0353	0.0382	0.0039	0.0005	0.0002	0.0001	0.0000	0.0000	0.0941
303.75-326.25	Northwest	0.0023	0.0212	0.0794	0.1910	0.0897	0.0077	0.0004	0.0002	0.0000	0.0000	0.3919

Table 1.1-60. Joint Frequency Distribution of Wind Speed and Direction (Decimal Fractions) for Stability Category F (Moderately Stable) (1994 to 2006) at Site 1 at 10 m above Ground Level (Continued)

Wind Direction		Wind Speed Category (m/s)										
Degrees Azimuth	Name	0.5–1.1	1.1–1.6	1.6–2.1	2.1–3.1	3.1–4.1	4.1–5.1	5.1–6.1	6.1–8.1	8.1–10.0	≥ 10.0	Total
326.25–348.75	North-northwest	0.0020	0.0186	0.0658	0.1213	0.0364	0.0058	0.0009	0.0001	0.0000	0.0000	0.2510
—	Total	0.0255	0.0975	0.2440	0.4342	0.1674	0.0251	0.0046	0.0013	0.0003	0.0000	0.9965
									Calms		0	
									Missing/incomplete		0.00355	
									Frequency of calm winds		0.00%	
									Average wind speed		2.48 m/s	

NOTE: Wind speeds are equal to or greater than the lower limit and are less than the upper limit.

Source: BSC 2007e, Table D-11.

Table 1.1-61. Joint Frequency Distribution of Wind Speed and Direction (Decimal Fractions) for Stability Category F (Moderately Stable) (1994 to 2006) at Site 1 at 60 m above Ground Level

Wind Direction		Wind Speed Category (m/s)										
Degrees Azimuth	Name	0.5-1.1	1.1-1.6	1.6-2.1	2.1-3.1	3.1-4.1	4.1-5.1	5.1-6.1	6.1-8.1	8.1-10.0	≥ 10.0	Total
348.75-11.25	North	0.0324	0.0732	0.0466	0.0372	0.0280	0.0245	0.0150	0.0068	0.0004	0.0001	0.2643
11.25-33.75	North-northeast	0.0160	0.0426	0.0430	0.0275	0.0131	0.0107	0.0063	0.0054	0.0008	0.0001	0.1655
33.75-56.25	Northeast	0.0070	0.0152	0.0117	0.0066	0.0022	0.0008	0.0010	0.0011	0.0001	0.0000	0.0456
56.25-78.75	East-northeast	0.0044	0.0064	0.0036	0.0014	0.0004	0.0003	0.0001	0.0000	0.0000	0.0000	0.0166
78.75-101.25	East	0.0026	0.0043	0.0025	0.0010	0.0002	0.0000	0.0000	0.0000	0.0000	0.0000	0.0107
101.25-123.75	East-southeast	0.0022	0.0037	0.0026	0.0007	0.0001	0.0000	0.0000	0.0000	0.0000	0.0000	0.0094
123.75-146.25	Southeast	0.0026	0.0042	0.0028	0.0015	0.0003	0.0001	0.0000	0.0000	0.0000	0.0000	0.0116
146.25-168.75	South-southeast	0.0038	0.0060	0.0044	0.0032	0.0012	0.0004	0.0002	0.0001	0.0000	0.0000	0.0194
168.75-191.25	South	0.0051	0.0095	0.0102	0.0128	0.0077	0.0040	0.0035	0.0019	0.0001	0.0000	0.0547
191.25-213.75	South-southwest	0.0060	0.0112	0.0114	0.0161	0.0080	0.0030	0.0018	0.0008	0.0001	0.0000	0.0584
213.75-236.25	Southwest	0.0084	0.0134	0.0097	0.0096	0.0038	0.0008	0.0001	0.0001	0.0000	0.0000	0.0458
236.25-258.75	West-southwest	0.0087	0.0119	0.0074	0.0054	0.0031	0.0015	0.0003	0.0000	0.0001	0.0000	0.0384
258.75-281.25	West	0.0122	0.0129	0.0065	0.0039	0.0022	0.0012	0.0005	0.0002	0.0000	0.0000	0.0398
281.25-303.75	West-northwest	0.0128	0.0164	0.0073	0.0042	0.0013	0.0007	0.0000	0.0004	0.0001	0.0000	0.0432
303.75-326.25	Northwest	0.0194	0.0232	0.0106	0.0053	0.0017	0.0008	0.0007	0.0003	0.0000	0.0001	0.0621

Table 1.1-61. Joint Frequency Distribution of Wind Speed and Direction (Decimal Fractions) for Stability Category F (Moderately Stable) (1994 to 2006) at Site 1 at 60 m above Ground Level (Continued)

Wind Direction		Wind Speed Category (m/s)										
Degrees Azimuth	Name	0.5–1.1	1.1–1.6	1.6–2.1	2.1–3.1	3.1–4.1	4.1–5.1	5.1–6.1	6.1–8.1	8.1–10.0	≥ 10.0	Total
326.25–348.75	North-northwest	0.0269	0.0440	0.0192	0.0101	0.0050	0.0040	0.0020	0.0019	0.0002	0.0001	0.1135
—	Total	0.1706	0.2982	0.1996	0.1464	0.0782	0.0527	0.0316	0.0191	0.0021	0.0006	0.9884
									Calms		0.00084	
									Missing/incomplete		0.01077	
									Frequency of calm winds		0.09%	
									Average wind speed		2.13 m/s	

NOTE: Wind speeds are equal to or greater than the lower limit and are less than the upper limit.

Source: BSC 2007e, Table D-12.

Table 1.1-62. Joint Frequency Distribution of Wind Speed and Direction (Decimal Fractions) for Stability Category G (Extremely Stable) (1994 to 2006) at Site 1 at 10 m above Ground Level

Wind Direction		Wind Speed Category (m/s)										
Degrees Azimuth	Name	0.5–1.1	1.1–1.6	1.6–2.1	2.1–3.1	3.1–4.1	4.1–5.1	5.1–6.1	6.1–8.1	8.1–10.0	≥ 10.0	Total
348.75–11.25	North	0.0016	0.0122	0.0151	0.0059	0.0014	0.0003	0.0001	0.0000	0.0001	0.0000	0.0366
11.25–33.75	North-northeast	0.0011	0.0030	0.0022	0.0005	0.0000	0.0000	0.0000	0.0000	0.0000	0.0000	0.0069
33.75–56.25	Northeast	0.0011	0.0026	0.0007	0.0002	0.0000	0.0000	0.0000	0.0000	0.0000	0.0000	0.0046
56.25–78.75	East-northeast	0.0012	0.0005	0.0002	0.0000	0.0000	0.0000	0.0000	0.0000	0.0000	0.0000	0.0019
78.75–101.25	East	0.0005	0.0004	0.0000	0.0000	0.0000	0.0000	0.0000	0.0000	0.0000	0.0000	0.0009
101.25–123.75	East-southeast	0.0007	0.0002	0.0000	0.0000	0.0000	0.0000	0.0000	0.0000	0.0000	0.0000	0.0009
123.75–146.25	Southeast	0.0007	0.0001	0.0001	0.0000	0.0000	0.0000	0.0000	0.0000	0.0000	0.0000	0.0008
146.25–168.75	South-southeast	0.0008	0.0003	0.0001	0.0000	0.0000	0.0000	0.0000	0.0000	0.0000	0.0000	0.0011
168.75–191.25	South	0.0005	0.0003	0.0001	0.0001	0.0000	0.0000	0.0000	0.0000	0.0000	0.0000	0.0010
191.25–213.75	South-southwest	0.0007	0.0009	0.0005	0.0002	0.0000	0.0000	0.0000	0.0000	0.0000	0.0000	0.0024
213.75–236.25	Southwest	0.0014	0.0013	0.0013	0.0002	0.0000	0.0000	0.0000	0.0000	0.0000	0.0000	0.0042
236.25–258.75	West-southwest	0.0008	0.0020	0.0020	0.0018	0.0002	0.0000	0.0000	0.0000	0.0000	0.0000	0.0068
258.75–281.25	West	0.0013	0.0040	0.0056	0.0069	0.0023	0.0001	0.0000	0.0000	0.0000	0.0000	0.0202
281.25–303.75	West-northwest	0.0016	0.0105	0.0130	0.0155	0.0034	0.0003	0.0001	0.0001	0.0001	0.0000	0.0445
303.75–326.25	Northwest	0.0023	0.0248	0.0783	0.1721	0.1353	0.0203	0.0014	0.0001	0.0000	0.0000	0.4347

Table 1.1-62. Joint Frequency Distribution of Wind Speed and Direction (Decimal Fractions) for Stability Category G (Extremely Stable) (1994 to 2006) at Site 1 at 10 m above Ground Level (Continued)

Wind Direction		Wind Speed Category (m/s)										
Degrees Azimuth	Name	0.5–1.1	1.1–1.6	1.6–2.1	2.1–3.1	3.1–4.1	4.1–5.1	5.1–6.1	6.1–8.1	8.1–10.0	≥ 10.0	Total
326.25–348.75	North-northwest	0.0019	0.0296	0.1230	0.2165	0.0568	0.0041	0.0002	0.0001	0.0000	0.0000	0.4323
—	Total	0.0184	0.0925	0.2423	0.4199	0.1994	0.0253	0.0018	0.0003	0.0001	0.0000	0.9965
									Calms		0	
									Missing/incomplete		0.00350	
									Frequency of calm winds		0.00%	
									Average wind speed		2.53 m/s	

NOTE: Wind speeds are equal to or greater than the lower limit and are less than the upper limit.

Source: BSC 2007e, Table D-13.

Table 1.1-63. Joint Frequency Distribution of Wind Speed and Direction (Decimal Fractions) for Stability Category G (Extremely Stable) (1994 to 2006) at Site 1 at 60 m above Ground Level

Wind Direction		Wind Speed Category (m/s)										Total
Degrees Azimuth	Name	0.5–1.1	1.1–1.6	1.6–2.1	2.1–3.1	3.1–4.1	4.1–5.1	5.1–6.1	6.1–8.1	8.1–10.0	≥ 10.0	
348.75–11.25	North	0.0302	0.1331	0.0935	0.0352	0.0091	0.0044	0.0008	0.0001	0.0001	0.0000	0.3066
11.25–33.75	North-northeast	0.0087	0.0237	0.0273	0.0233	0.0026	0.0018	0.0005	0.0003	0.0001	0.0001	0.0884
33.75–56.25	Northeast	0.0019	0.0026	0.0031	0.0020	0.0002	0.0001	0.0000	0.0000	0.0000	0.0000	0.0098
56.25–78.75	East-northeast	0.0005	0.0006	0.0004	0.0003	0.0000	0.0000	0.0000	0.0000	0.0000	0.0000	0.0018
78.75–101.25	East	0.0005	0.0001	0.0003	0.0002	0.0000	0.0000	0.0000	0.0000	0.0000	0.0000	0.0012
101.25–123.75	East-southeast	0.0006	0.0003	0.0002	0.0000	0.0000	0.0000	0.0000	0.0000	0.0000	0.0000	0.0012
123.75–146.25	Southeast	0.0003	0.0005	0.0001	0.0000	0.0000	0.0000	0.0000	0.0000	0.0000	0.0000	0.0010
146.25–168.75	South-southeast	0.0009	0.0007	0.0005	0.0002	0.0000	0.0000	0.0000	0.0000	0.0000	0.0000	0.0023
168.75–191.25	South	0.0010	0.0013	0.0011	0.0007	0.0000	0.0000	0.0000	0.0000	0.0000	0.0000	0.0041
191.25–213.75	South-southwest	0.0019	0.0038	0.0037	0.0039	0.0004	0.0001	0.0000	0.0000	0.0000	0.0000	0.0138
213.75–236.25	Southwest	0.0033	0.0044	0.0050	0.0057	0.0008	0.0000	0.0000	0.0000	0.0000	0.0000	0.0192
236.25–258.75	West-southwest	0.0050	0.0055	0.0038	0.0047	0.0013	0.0007	0.0001	0.0000	0.0000	0.0000	0.0210
258.75–281.25	West	0.0083	0.0096	0.0042	0.0031	0.0015	0.0005	0.0002	0.0000	0.0000	0.0000	0.0273
281.25–303.75	West-northwest	0.0158	0.0189	0.0057	0.0026	0.0005	0.0004	0.0000	0.0001	0.0000	0.0001	0.0442
303.75–326.25	Northwest	0.0244	0.0564	0.0275	0.0066	0.0008	0.0001	0.0001	0.0001	0.0000	0.0000	0.1161

Table 1.1-63. Joint Frequency Distribution of Wind Speed and Direction (Decimal Fractions) for Stability Category G (Extremely Stable) (1994 to 2006) at Site 1 at 60 m above Ground Level (Continued)

Wind Direction		Wind Speed Category (m/s)										
Degrees Azimuth	Name	0.5–1.1	1.1–1.6	1.6–2.1	2.1–3.1	3.1–4.1	4.1–5.1	5.1–6.1	6.1–8.1	8.1–10.0	≥ 10.0	Total
326.25–348.75	North-northwest	0.0285	0.1459	0.1254	0.0379	0.0035	0.0004	0.0003	0.0000	0.0001	0.0000	0.3419
—	Total	0.1319	0.4072	0.3019	0.1263	0.0207	0.0086	0.0021	0.0006	0.0002	0.0001	0.9868
									Calms		0.00027	
									Missing/incomplete		0.01293	
									Frequency of calm winds		0.03%	
									Average wind speed		1.64 m/s	

NOTE: Wind speeds are equal to or greater than the lower limit and are less than the upper limit.

Source: BSC 2007e, Table D-14.

Table 1.1-64. Summary of Pasquill Stability Category Occurrences

Hour	A Extremely Unstable	B Moderately Unstable	C Sightly Unstable	D Neutral	E Slightly Stable	F Moderately Stable	G Extremely Stable
1	0.02	0.00	0.07	3.71	27.66	36.10	32.43
2	0.00	0.00	0.04	3.84	26.65	34.95	34.51
3	0.00	0.00	0.11	3.67	26.34	34.67	35.22
4	0.04	0.00	0.04	3.36	25.31	35.99	35.26
5	0.02	0.02	0.02	3.54	23.93	37.15	35.32
6	0.02	0.02	0.02	5.00	26.89	37.39	30.65
7	0.46	0.95	2.46	20.08	31.94	25.48	18.64
8	8.22	8.26	10.85	30.47	20.19	15.39	6.62
9	29.54	12.22	11.13	29.28	12.84	4.78	0.22
10	46.92	11.72	11.55	27.11	2.55	0.07	0.09
11	53.34	14.72	12.70	18.57	0.58	0.00	0.09
12	63.45	11.49	10.39	14.29	0.29	0.00	0.09
13	64.94	11.98	9.65	13.05	0.36	0.00	0.02
14	62.93	11.28	10.27	14.90	0.54	0.04	0.04
15	54.86	13.51	11.00	19.78	0.80	0.04	0.00
16	39.76	9.73	10.68	37.39	2.34	0.09	0.00
17	22.08	9.14	9.65	32.12	23.51	3.47	0.04
18	1.01	5.60	7.92	34.55	35.65	14.36	0.90
19	0.04	0.04	0.00	17.23	55.16	23.69	3.84
20	0.04	0.04	0.02	6.55	49.86	35.37	8.11
21	0.04	0.04	0.02	5.05	40.46	41.16	13.21
22	0.04	0.00	0.04	4.81	36.07	40.81	18.22
23	0.04	0.00	0.04	4.53	30.99	39.78	24.61
24	0.02	0.04	0.07	4.20	28.15	37.59	29.92
Total	18.54	5.01	4.93	14.87	22.12	20.83	13.71
Summary	A to C: 28.48			D: 14.87	E to G: 56.66		

NOTE: Occurrences are the percent of time for each hour that stability was in the seven Pasquill categories shown, from A (extremely unstable) through G (extremely stable). Totals represent percentage of day in a stability category.

Source: BSC 2007e, Table 5-15.

Table 1.1-65. Earthquakes with M_w Greater than 5.0 within 300 km of Yucca Mountain

Date	Origin Time (GMT) (hr:min:s)	North Latitude (degrees)	West Longitude (degrees)	Depth (km)	Magnitude (M_w)	Location
March 26, 1872	10:30:00	36.70	-118.10	—	7.8	Owens Valley, CA
November 17, 1902	19:50:00	37.39	-113.52	—	6	Pine Valley, NV
November 10, 1916	09:11:00	36.20	-116.90	—	6.1	Death Valley, CA
December 21, 1932	06:10:04	38.80	-117.98	—	6.8	Cedar Mountain, NV
January 30, 1934	20:16:35	38.28	-118.37	—	6.1	Excelsior Mountain, NV
April 10, 1947	15:58:06	34.98	-116.55	—	6.5	Manix, CA
December 16, 1954	11:07:11	39.28	-118.12	15	7.1	Fairview Peak, CA
September 22, 1966	18:57:34	37.37	-114.18	7	5.7	Clover Mountain, NV
June 1, 1975	01:38:49	34.52	-116.50	4.5	5.2	Galway Lake, CA
March 15, 1979	21:07:17	34.33	-116.44	2.5	5.5	Homestead Valley, CA
May 25, 1980	16:33:44	37.59	-118.85	10.2	6.2	Mammoth Lakes, CA
May 25, 1980	16:49:27	37.67	-118.92	8.9	5.9	Mammoth Lakes, CA
May 25, 1980	20:35:48	37.63	-118.84	8.2	5.6	Mammoth Lakes, CA
May 27, 1980	14:50:57	37.49	-118.81	16.1	5.9	Mammoth Lakes, CA
September 30, 1981	11:53:26	37.59	-118.87	5.7	5.6	Mammoth Lakes, CA
November 23, 1984	18:08:25	37.46	-118.61	11.5	5.8	Round Valley, CA
July 20, 1986	14:29:45	37.57	-118.44	6.7	5.8	Chalfant Valley, CA
July 21, 1986	14:42:26	37.54	-118.44	10.5	6.3	Chalfant Valley, CA
July 21, 1986	14:51:09	37.49	-118.43	11.8	5.5	Chalfant Valley, CA
July 31, 1986	07:22:40	37.47	-118.37	8.1	5.5	Chalfant Valley, CA
June 28, 1992	11:57:34	34.20	-116.44	1.0	7.3	Landers, CA

Table 1.1-65. Earthquakes with M_w Greater than 5.0 within 300 km of Yucca Mountain (Continued)

Date	Origin Time (GMT) (hr:min:s)	North Latitude (degrees)	West Longitude (degrees)	Depth (km)	Magnitude (M_w)	Location
June 29, 1992	10:14:20	36.72	-116.29	11.8	5.6	Little Skull Mountain, NV
September 2, 1992	10:26:19	37.17	-113.33	9.6	5.9	St. George, UT
May 17, 1993	23:20:50	37.18	-117.83	9.1	6.1	Eureka Valley, CA
August 17, 1995	22:39:58	35.77	-117.65	10.5	5.2	Ridgecrest, CA
September 20, 1995	23:27:36	35.75	-117.64	8.3	5.3	Ridgecrest, CA
August 1, 1999	16:06:22	37.39	-117.08	7.6	5.7	Scotty's Junction, NV
October 16, 1999	09:46:44	34.59	-116.27	5.0	7.1	Hector Mine, CA

NOTE: GMT = Greenwich Mean Time; M_w = moment magnitude.

Table 1.1-66. Summary of Fault Parameters from Probabilistic Seismic Hazard Assessment Seismic Source Characterization

Fault Type	Parameter^a	Probability of Future Activity	Maximum Magnitude	Slip Rate (mm/yr)	Recurrence Interval (ka)
Regional Faults	Amargosa River Fault zone	1.0	6.4 to 7.5	0.005 to 0.2	10 to 128
	Ash Meadows Fault	1.0	6.2 to 8.1	0.001 to 0.1	10 to 180
	Bare Mountain Fault	1.0	6.5 to 7.3	0.01 to 0.28	42 to 143
	Belted Range Fault	1.0	6.1 to 7.7	0.02 to 0.1	9 to 90
	Buried Hills Faults	1.0	6.4 to 7.3	—	—
	Cane Spring Fault	0.6 to 1.0	5.8 to 7.7	0.002 to 0.07	20 to 146
	Carpetbag Fault system	0.8 to 1.0	6.5 to 7.6	0.005 to 0.05	—
	Carrara (Highway 95) Fault	0.1 to 0.85	6.3 to 7.7	0.01 to 0.12	10 to 69
	Death Valley Fault	1.0	6.4 to 7.6	0.08 to 11.5	0.5 to 5
	Death Valley–Furnace Creek Fault	1.0	6.7 to 8.3	3.0 to 8.0	0.5 to 1.0
	East Pintwater Range Fault	1.0	6.8 to 7.8	—	—
	East Specter Range Fault	1.0	6.4 to 6.7	0.004 to 0.021	10 to 128
	Eleana Range Fault	1.0	6.4 to 7.4	0.00006 to 0.2	20 to 146
	Emigrant Valley North Fault	1.0	6.5 to 7.4	—	10 to 69
	Furnace Creek Fault zone	1.0	6.6 to 7.9	2.3 to 10.0	0.5 to 1.0
	Grapevine Fault	1.0	7.0	0.003 to 0.02	0.6 to 0.8
	Grapevine Mountains Fault	1.0	6.7 to 7.4	—	—
	Hunter Mt.–Panamint Valley Faults	1.0	7.0 to 7.6	1.1 to 3.2	—
	Jackass Flats (Gravity) Fault	0.9	6.7 to 7.7	—	—
	Kawich Range Fault zone	1.0	6.5 to 8.0	0.001 to 0.07	—
	Keane Wonder Fault zone	0.6 to 0.8	6.5 to 7.7	0.001 to 0.01	—
	Mine Mountain Fault zone	0.6 to 1.0	6.6 to 7.7	0.002 to 0.06	20 to 146
	Oak Springs Butte Faults	1.0	6.1 to 7.2	0.01 to 0.2	—
	Oasis Valley Fault zone	0.4 to 0.8	5.8 to 7.7	0.001 to 0.01	—
	Pahute Mesa Faults	0.8	6.2 to 7.1	—	—
	Pahrump Fault zone	1.0	6.1 to 8.2	0.005 to 0.2	—
	Panamint Valley Fault	1.0	7.2 to 7.7	1.57 to 3.15	—
	Peace Camp (South Ridge) Fault	1.0	6.3 to 7.3	0.02 to 0.16	—
	Rock Valley Fault zone	1.0	6.1 to 7.8	0.003 to 0.16	33 to 195
	South Silent Canyon Fault	0.8	6.2 to 7.1	—	—
Spotted Range Faults	1.0	6.5 to 7.4	—	—	
Towne Pass Fault	1.0	6.8 to 7.6	0.004 to 0.03	—	

Table 1.1-66. Summary of Fault Parameters from Probabilistic Seismic Hazard Assessment Seismic Source Characterization (Continued)

Fault Type	Parameter^a	Probability of Future Activity	Maximum Magnitude	Slip Rate (mm/yr)	Recurrence Interval (ka)
Regional Faults (Continued)	Wahmonie Fault	0.8 to 1.0	5.6 to 7.3	0.002 to 0.08	20 to 146
	West Pintwater Range Fault	1.0	6.3 to 7.9	0.002 to 0.2	—
	West Specter Range Fault	1.0	6.2 to 7.5	0.001 to 0.021	10 to >128
	West Spring Mountains Fault	1.0	6.2 to 7.8	0.02 to 0.2	20 to 128
	Yucca Fault	1.0	6.0 to 7.7	0.001 to 0.2	20 to 146
	Yucca Butte Fault	1.0	6.7 to 7.4	—	—
	Yucca Lake Fault	0.5 to 1.0	6.3 to 7.6	0.001 to 0.034	20 to 146
Local Faults	Bare Mountain Fault	1.0	5.8 to 7.5	0.005 to 0.25	20 to 200
	Black Cone Fault	0.8	5.0 to 7.0	0.001 to 0.005	—
	Bow Ridge Fault	0.4 to 1.0	5.2 to 7.0	0.002 to 0.007	40 to 350
	Crater Flat Fault system	1.0	5.3 to 7.0	0.001 to 0.003	—
	Crater Flat Fault (central segment)	0.6	5.3 to 7.0	0.001 to 0.005	—
	Crater Flat Fault (southern segment)	1.0	5.4 to 7.0	0.002 to 0.02	40 to 180
	Crater Flat Fault (northern segment)	1.0	5.5 to 7.0	0.001 to 0.005	120 to 160
	Dune Wash Fault	0.1	4.9 to 7.2	0.0001 to 0.001	—
	East Busted Butte Fault	0.4	4.5 to 7.2	0.0005 to 0.003	—
	East Lathrop Cone Fault	1.0	4.6 to 6.9	0.005 to 0.003	—
	Fatigue Wash Fault	1.0	5.5 to 7.3	0.002 to 0.02	50 to 250
	Fatigue Wash–Windy Wash Fault	1.0	5.6 to 7.2	0.005 to 0.024	—
	Ghost Dance Fault zone	0.05 to 0.1	4.5 to 7.0	0.0001 to 0.002	—
	Iron Ridge Fault	0.1 to 1.0	5.1 to 7.0	0.001 to 0.005	—
	Iron Ridge–Solitario Canyon Fault	1.0	5.5 to 7.2	0.005 to 0.024	—
	Midway Valley Fault	0.1	4.9 to 7.1	0.0001 to 0.001	—
	Paintbrush Canyon Fault	1.0	5.9 to 7.4	0.002 to 0.03	20 to 270
	Paintbrush Canyon–Stagecoach Road Fault	1.0	5.6 to 7.3	0.009 to 0.05	15 to 120
	Paintbrush–Stagecoach–Bow Ridge Fault	1.0	5.5 to 7.6	0.005 to 0.02	10 to 75
	Solitario Canyon Fault	1.0	5.6 to 7.4	0.002 to 0.04	35 to 180
Stagecoach Road Fault	1.0	5.3 to 7.1	0.01 to 0.07	5 to 75	
Windy Wash Fault	1.0	6.6 to 7.5	0.01 to 0.027	35 to 100	
Windy Wash Fault (south segment)	1.0	5.7 to 7.1	0.01 to 0.04	20 to 60	

Table 1.1-66. Summary of Fault Parameters from Probabilistic Seismic Hazard Assessment Seismic Source Characterization (Continued)

Fault Type	Parameter^a	Probability of Future Activity	Maximum Magnitude	Slip Rate (mm/yr)	Recurrence Interval (ka)
Local Faults (Continued)	Windy Wash Fault (north segment)	1.0	5.6 to 7.2	0.001 to 0.005	—

NOTE: ^aParameter ranges developed from all teams reporting (i.e., one to six teams); all parameter ranges were provided as probability distributions. Paleoseismic data on the number and timing of surface rupture earthquakes are insufficient to assess slip rate and recurrence interval information for some faults. Yucca Fault and Yucca Butte Fault are both shown as YC on [Figure 1.1-73](#); separate listings for these fault systems in table represent separate parameter evaluations by different PSHA teams.

Table 1.1-67. Mean Fault Displacement Hazard at Nine Demonstration Sites

Site	Location	Mean Displacement (cm) based on Annual Exceedance Probability		
		10^{-4}	5×10^{-5}	10^{-5}
1	Bow Ridge Fault	<0.1	<0.1	7.8
2	Solitario Canyon Fault	<0.1	<0.1	32
3	Drill Hole Wash Fault	<0.1	<0.1	<0.1
4	Ghost Dance Fault	<0.1	<0.1	<0.1
5	Sundance Fault	<0.1	<0.1	0.1
6	Unnamed fault west of Dune Wash	<0.1	<0.1	<0.1
7	100 m east of Solitario Canyon Fault			
7a	2-m small fault	<0.1	<0.1	<0.1
7b	10-cm shear	<0.1	<0.1	<0.1
7c	Fracture	<0.1	<0.1	<0.1
7d	Intact rock	<0.1	<0.1	<0.1
8	Between Solitario Canyon Fault and Ghost Dance Fault			
8a	2-m small fault	<0.1	<0.1	<0.1
8b	10-cm shear	<0.1	<0.1	<0.1
8c	Fracture	<0.1	<0.1	<0.1
8d	Intact rock	<0.1	<0.1	<0.1
9	Midway Valley	<0.1	<0.1	0.1

Table 1.1-68. Summary of Deaggregation Results and Reference Earthquakes

Annual Probability of Exceedance	Spectral response	M* (Modal Magnitude)	R* (Modal Distance)	Reference Earthquake Magnitude and Distance
10 ⁻³	5 to 10 Hz	5.15	8.75	M 6.3, 5 km
	1 to 2 Hz	7.35	51.25	M 6.9, 52 km
	1 to 2 Hz regional sources 1 to 2 Hz local sources	7.35 5.85	51.25 3.75	
5x10 ⁻⁴	5 to 10 Hz	5.15	8.75	M 6.3, 5 km
	1 to 2 Hz 1 to 2 Hz regional sources	7.35 7.35	51.25 51.25	M 7.0, 51 km
10 ⁻⁴	5 to 10 Hz	6.2	3.75	M 6.3, 5 km
	1 to 2 Hz 1 to 2 Hz regional sources	7.7 7.7	51.3 51.3	M 7.7, 52 km
10 ⁻⁵	5 to 10 Hz	6.25	3.75	M 6.4, 4 km
	1 to 2 Hz 1 to 2 Hz regional sources	6.25 7.35	3.75 51.25	M 7.7, 51 km
10 ⁻⁶	5 to 10 Hz	6.15	1.25	M 6.5, 1 km
	1 to 2 Hz 1 to 2 Hz regional sources	6.65 7.65	1.25 51.25	M 7.7, 51 km
10 ⁻⁷	5-10 Hz	6.15	1.25	M 6.5, 1 km
	1 to 2 Hz 1 to 2 Hz regional sources	6.65 7.65	1.25 51.25	M 7.7, 51 km

Source: BSC 2008c, Table 6.4-1.

Table 1.1-69. Preclosure Seismic Ground Motions for Design Analyses

Annual Probability of Exceedance	Site	Design Response Spectra	Time Histories	PGA (g)		10 Hz SA (g)		1 Hz SA (g)		PGV (cm/s)	
				H	V	H	V	H	V	H	V
10 ⁻³	Surface GROA	Horizontal and vertical	5 three-component sets spectrally matched	0.33	0.22	0.82	0.55	0.29	0.15	23.19	—
5 × 10 ⁻⁴	Surface GROA	Horizontal and vertical	5 three-component sets spectrally matched	0.45	0.32	1.17	0.86	0.43	0.23	34.13	—
10 ⁻⁴	Surface GROA	Horizontal and vertical	5 three-component set spectrally matched	0.91	0.72	2.40	2.22	0.96	0.52	74.13	—
10 ⁻³	Repository block emplacement level	Horizontal and vertical	1 three-component set spectrally matched	0.12	0.07	0.27	0.14	0.10	0.082	13.48	6.96
5 × 10 ⁻⁴	Repository block emplacement level	Horizontal and vertical	1 three-component set spectrally matched	0.17	0.12	0.39	0.23	0.15	0.12	19.54	10.10
10 ⁻⁴	Repository block emplacement level	Horizontal and vertical	1 three-component set spectrally matched	0.37	0.32	0.84	0.59	0.30	0.25	41.40	21.51

NOTE: Seismic hazard curves for the surface GROA: horizontal and vertical spectral acceleration at 0.3, 0.5, 1, 5, 10, 20, and 100 Hz (PGA), horizontal PGV. Seismic hazard curves for the repository block emplacement level: horizontal and vertical spectral acceleration at 0.3, 0.5, 1, 5, 10, 20, and 100 Hz (PGA), PGV. H = horizontal; PGA = peak ground acceleration; PGV = peak ground velocity; SA = spectral acceleration; V = vertical.

Source: BSC 2008c, Table E-1.

Table 1.1-70. UE-25 RF#1

Location ^a : N 232375 m (762190 ft); E 174007 m (570890 ft); Elevation 1,124.3 m (3,688.5 ft) Cored Intervals: 10 to 12 ft; 22 to 22.2 ft; 30 to 31 ft; 50.0 to 51.5 ft; 115 to 118 ft; 122 to 127 ft; 140 to 145 ft		
Stratigraphic Unit—Lithology ^b	Depth (ft) ^c	Interval Thickness (ft) ^c
Alluvium Bouldery; clasts of Tiva Canyon welded tuff more than 6 in. across. Carbonate coatings.	0.0 to 120.0	120.0
Tiva Canyon Member^b Ash-flow tuff, moderately welded, light gray. Gray and white vesicular vapor-phase altered pumice. Phenocrysts 5% to 10%, mostly biotite and feldspar. Carbonate and silica minerals along irregular fractures and a small fault dipping 55° at 123.5 ft. Dip of flattened pumice 20° to 25°.	120.0 to 145.0 total depth	25.0

NOTE: ^aNevada State Plane Coordinates.

^bStratigraphic nomenclature used in original description has been retained in this table.

^cMeasurements rounded to nearest 0.5 ft.

Source: Gibson et al. 1992, Appendix A.

Table 1.1-71. UE-25 RF#2

Location ^a : N 231,282 m (758,800 ft); E 173,838 m (570,335 ft); Elevation 1,114.7 m (3,656.8 ft) Cored Intervals: 10 to 11.5 ft; 30.0 to 30.8 ft; 41 to 51 ft		
Stratigraphic Unit—Lithology ^b	Depth (ft) ^c	Interval Thickness (ft) ^c
Alluvium Welded tuff fragments in fine, sandy, silty tan matrix.	0.0 to 35.0	35.0
Tiva Canyon Member^b Ash-flow tuff, densely welded, light gray. 5% phenocrysts, mostly feldspar and biotite. A few fractures having calcite coatings at about 50 ft. Dip of pumice 20°. A few large lithophysal cavities having vapor phase mineral coatings.	35.0 to 51.0 total depth	16.0

NOTE: ^aNevada State Plane Coordinates.

^bStratigraphic nomenclature used in original description has been retained in this table.

^cMeasurements rounded to nearest 0.5 ft.

Source: Gibson et al. 1992, Appendix A.

Table 1.1-72. UE-25 RF#3

Location ^a : N 233,347 m (765,575 ft); E 174,071 m (571,100 ft); Elevation 1,114.9 m (3,657.7 ft) Cored Intervals: continuous core		
Stratigraphic Unit—Lithology ^b	Depth (ft) ^c	Interval Thickness (ft) ^c
Alluvium Light orange-brown, slightly clayey, sandy matrix containing some carbonate; abundant angular clasts of welded tuff, including Tiva Canyon caprock facies.	1.0 to 8.0	7.0
Colluvium Light gray, blocks and fragments of welded tuff and rhyolite lava in tuffaceous, silty, sandy, and gravelly matrix having soft carbonate cement. Clasts are Paintbrush Tuff and rhyolites of Fortymile Canyon.	8.0 to 90.0	82.0
Sandstone and Alluvium Tuffaceous, very light gray or tan to white, clayey, calcareous. Contains a few volcanic clasts 1 to 2 in. in diameter, but mostly pebble- to sand-size fragments that are clay and carbonate-coated. Lower part is mostly tan to very light yellowish-gray.	90.0 to 111.5	21.5
Sandstone Tuffaceous, very light tan, containing abundant clasts of pumiceous light-colored tuff in a matrix of rather uniform, fine-grained tan sand, weakly cemented by carbonate and clay. Pumice clasts are 0.125 to 0.75 in. in diameter. At about 112 ft is a 1-in. thick irregular layer of white chalky opal with a little admixed calcite. Sand is mostly rock grains containing some quartz, biotite, and feldspar. A 0.5-ft concentration of small rock fragments, of pebble to sand size, occurs at base of unit.	111.5 to 115.0	3.5
Sandstone Tuffaceous, light tan, massive to crudely sorted, except for a few thin (1 to 2 in.) zones that are distinctly bedded, especially at base. Contains reworked (?) white to light gray pumice fragments, mostly 0.125 to 0.33 in., but a few as large as 1.5 in. across. Pumice has less than 2% phenocrysts and generally is altered to clay. Matrix contains silt- to sand-size mineral and rock grains similar to those in unit above.	115.0 to 121.5	6.5
Tuff Reworked, grading down into siltstone that is tuffaceous, light tan, massive. 1-in. layer of siltstone at base, dipping 20°	121.5 to 122.0	0.5
Tuff Reworked, very light gray to light tan, massive to crudely sorted; scattered yellowish, pinkish, and white pumice altered to clay. Matrix contains noticeable sand-size rock grains, increasing in size from 0.125 to 0.25 in. in some zones near base of unit. Crystal fragments, which also increase downward to 25%, consist of quartz, feldspar, and biotite. Lower contact abruptly gradational.	122.0 to 131.5	9.5

Table 1.1-72. UE-25 RF#3 (Continued)

Location ^a : N 233,347 m (765,575 ft); E 174,071 m (571,100 ft); Elevation 1,114.9 m (3,657.7 ft) Cored Intervals: continuous core		
Stratigraphic Unit—Lithology ^b	Depth (ft) ^c	Interval Thickness (ft) ^c
Tuff Reworked, or tuff breccia; light tan, coarse-grained with about 5% crystals of quartz, feldspar, and biotite; 20% perlitic colorless glass fragments; and 25% rock grains and fragments as large as 2 in. across, mostly light gray silicic lava containing few phenocrysts; hornblende and sphene noted. Basal contact dips 25° and is sharp and scoured.	131.5 to 134.0	2.5
Sandstone Tuffaceous, tan, well sorted, mostly fine and medium grained; thin zones (0.5 to 1 in.) of reworked white pumice fragments. Dip of stratification 20°. Biotite, quartz, and feldspar grains. Pumice fragments are coarser toward base—as much as 2 in. across; pumice is not vitric, contains sphene and hornblende.	134.0 to 151.0 ^d	17.0
Sandstone Tuffaceous, tan, massive to crudely interbedded with white pumice fragment zones; otherwise similar to overlying unit. Dip of well-developed fine stratification from 10° to 35°. Occasional light brown fine siltstone or clay layers. Contacts, especially lower one, gradational. Pumice is mostly vitric and phenocryst-poor.	151.0 to 180.0	29.0
Tuff Highly pumiceous, very light tan, with interbedded intervals 1 to 3 ft thick of reworked, mostly massive tuffaceous sandstone, as in overlying units. Pumice white to light yellow, similar to overlying units, diameter mostly about 0.75 in. not vitric. Contacts gradational.	180.0 to 187.5	7.5
Sandstone Tuffaceous, tan, fine- to medium-grained, mostly massive with a few zones of gray and purplish-brown lava fragments; a few gray fragments are vitric, average about 0.25 in. across. Scattered white pumice altered to clay. Contacts gradational.	187.5 to 205.0	17.5

Table 1.1-72. UE-25 RF#3 (Continued)

Location ^a : N 233,347 m (765,575 ft); E 174,071 m (571,100 ft); Elevation 1,114.9 m (3,657.7 ft) Cored Intervals: continuous core		
Stratigraphic Unit—Lithology ^b	Depth (ft) ^c	Interval Thickness (ft) ^c
<p>Tuff unit "x" Ash flow, very light gray, highly pumiceous, nonwelded; zeolitic, vesicular pumice. Probably originally a vapor-phase zone. 10% lithic fragments of mostly purplish-gray lava. A 1-in.-thick ash parting at 207 ft, and 0.5 in. siltstone layer at 209.5 ft. Phenocrysts about 5%; include sphene, hornblende, minor biotite, and quartz. Phenocrysts decrease downward. Irregular parting at 209.5 ft. Clay-coated small fault or tension fracture at about 216 ft, dipping 70°; fault is filled with about 2.5 in. of pale pinkish-tan pumiceous tuff containing only a few lithic fragments. Rock is slightly iron-stained in footwall. Irregular blobs of iron staining between 216 and 218 ft. Two small faults at 231.5 ft: one dips 45°, has clay coating and down-dip slickensides; the other dips 80° and truncates the first one. Another tight fault occurs at 232.5 ft, dips 40°; no brecciation. A parting or small fault at 238 ft dips 55°. Two tight faults occur at 239 ft, one dipping 65° and truncating the other, which dips 60°; both have clay coating; first fault has slightly oblique slickensides. Parting or fracture containing fine silt or clay at 245.5 ft. Other faults with clay at 246.5 ft dip 65°, and at 248.5 ft dip about 80°; latter fault widens downward to a zone about 2 in. wide, where it leaves the hole at 250 ft. Faults have no breccia and little opening, seem to be primarily fractures filled by tuffaceous silt and clay. Crudely sorted zone at 251 ft marks basal contact of an ash-flow unit.</p>	205.0 to 251.0	46.0
<p>Tuff White to tan, crudely bedded, some fine sand-size sorted layers 1 to 3 in. thick; abundant small lithic fragments in more massive parts, some clayey coarse pumice in lower part. Subtle unbrecciated fault at 255 ft dips about 70°; unit is broken and clayey below the fault, which is the lower contact of unit.</p>	251.0 to 255.0	4.0
<p>Tuff Ash flow, nonwelded, pumiceous, pale pinkish-tan to light gray, zeolitic. Scattered sparse lithic fragments of tuff and lava, mostly less than 0.25 in across, but a few as large as 1.25 in across. 5% to 10% phenocrysts of feldspar, biotite, green pyroxene, biotite, and sparse quartz; biotite more abundant than in overlying units.</p>	255.0 to 260.0	5.0
<p>Tuff Crudely bedded to massive, light gray, pumiceous zeolitic; a few thin sorted layers of finer pumice dip 25°. Some pumice is pale pink. Phenocrysts same as in overlying unit. Fault marks base, dips 45°, has clay coating and no breccia.</p>	260.0 to 262.0	2.0

Table 1.1-72. UE-25 RF#3 (Continued)

Location ^a : N 233,347 m (765,575 ft); E 174,071 m (571,100 ft); Elevation 1,114.9 m (3,657.7 ft) Cored Intervals: continuous core		
Stratigraphic Unit—Lithology ^b	Depth (ft) ^c	Interval Thickness (ft) ^c
Tuff Crudely bedded, reworked, light yellowish-gray; phenocryst-poor; alternating coarse- and fine-grained layers that dip as much as 50°. Base of unit rests on scoured surface that dips 30° to 50°.	262.0 to 264.5	2.5
Tiva Canyon Member Ash-flow tuff, nonwelded pumiceous, tan grading down to brownish-purple; vapor-phase zone, devitrified, zeolitic and/or clayey; minor biotite and feldspar, but phenocryst content increases downward from less than 5% at top to 10% in lower part. Pumice 0.25 to 1.0 in, yellow and brown. Lower contact gradational.	264.5 to 267.0	2.5
Tiva Canyon Member Ash-flow tuff, slightly welded at top, grading abruptly down into densely welded, light purplish-brown to purplish-brown, devitrified. High-angle fracture containing 0.25 in layer of indurated ash at 270 ft.	267.0 to 271.0	4.0
Tiva Canyon Member Ash-flow tuff, densely welded, purplish to grayish- brown, vitrophyric; partly vitric gray groundmass containing yellowish-brown pumice. Phenocrysts 10%, mostly biotite and feldspar with minor quartz and clinopyroxene. Pumice foliation dips 20° to 25°. Contacts gradational.	271.0 to 275.0	4.0
Tiva Canyon Member Ash-flow tuff, moderately welded at top to slightly welded at base, devitrified, purplish-brown; phenocrysts 5%, mostly bronze biotite; a few high-angle fractures. Contacts gradational.	275.0 to 284.0	9.0
Tiva Canyon Member Ash-flow tuff, slightly to moderately welded in lower part, light purplish-brown (lower caprock zone); 5% to 10% small gray pumice. Phenocrysts 5% to 10%, include biotite, feldspar, minor quartz, and clinopyroxene. Several small faults and fractures have clay filling; unit very rubbly and clayey from 288 to 290 ft and 292 to 301 ft. Irregular fractures and small faults especially common in lower part. Irregular high angle fracture as much as 1.5 in. wide from 300 to 301 ft, filled with clayey pumiceous tuff containing about 5% phenocrysts of sphene and feldspar and some hornblende, quartz, and biotite, as well as a few small lithic fragments; fracture filling probably derived from units above the Tiva Canyon Member.	284.0 to 301.0 total depth	17.0

NOTE: ^aNevada State Plane Coordinates.

^bStratigraphic nomenclature used in original description has been retained in this table.

^cMeasurements rounded to nearest 0.5 ft.

^dAccording to depth markings on blocks in core box, as much as 5 ft of core may be missing from this interval; blocks marked 133.6 ft and 141.0–151.0 ft are only 2 ft apart.

Source: Gibson et al. 1992, Appendix A.

Table 1.1-73. UE-25 RF#3b

Location ^a : N 233,384 m (765,695 ft); E 174,061 m (571,066 ft); Elevation 1,115.9 m (3,661.1 ft) Cored Intervals: 90 to 95 ft; 106 to 111 ft		
Stratigraphic Unit—Lithology ^b	Depth (ft) ^c	Interval Thickness (ft) ^c
Alluvium Probably similar to that found in hole RF#3.	0.0 to 90.0	90.0
Alluvium Light tan, tuffaceous sandy matrix, moderately indurated: lenses of subangular volcanic clasts; calcareous cement and thin calcitic layers.	90.0 to 105.0	15.0
Sandstone Light tan, tuffaceous, containing 0.5- to 1.0-in. white pumice fragments; sphene and hornblende; sparse volcanic clasts; minor carbonate in matrix. Correlates with 111 to 115 ft in hole RF#3.	105.0 to 111.0 total depth	6.0

NOTE: ^aNevada State Plane Coordinates.

^bStratigraphic nomenclature used in original description has been retained in this table.

^cMeasurements rounded to nearest 0.5 ft.

Source: Gibson et al. 1992, Appendix A.

Table 1.1-74. UE-25 RF#4

Location ^a : N 232,285 m (762,091 ft); E 174,365 m (572,063 ft); Elevation 1,108.5 m (3,636.8 ft) Cored Intervals: intermittent		
Stratigraphic Unit—Lithology ^b	Depth (ft) ^c	Interval Thickness (ft) ^c
Alluvium Bouldery, and tuffaceous sandstone. Clasts as much as 8 in. across, nearly all of which are Tiva Canyon Member. Lower part of unit consists almost entirely of welded tuff clasts.	0.0 to 150.0 ^d	150.0
Tuff, Unit "x" Ash flow, nonwelded, very light gray to white, containing sparse fine-grained, pale orange pumice fragments as much as 1.25 in. across, and pale yellow to pink pumice. Lithic fragments 10%, phenocrysts less than 5%. Contacts not cored. Correlates with unit 205 to 251 ft in hole RF#3.	150.0 to 265.0	115.0
Tiva Canyon Member Tuff, ash flow, nonwelded, light reddish- to purplish-brown, gray vesicular pumice in lower part. Pumice as large as 1.5 in. across. Vapor-phase alteration; phenocrysts 2%. Contacts gradational.	265.0 to 291.0	26.0
Tiva Canyon Member Tuff, ash flow, slightly welded, light vapor phase, varicolored pumice; phenocrysts 5%, increasing downward to 15%. Contacts gradational.	291.0 to 300.0	9.0
Tiva Canyon Member Tuff, ash flow, moderately welded, light pinkish- to brownish-gray; vapor-phase crystallization; gray, brown, and white pumice. Phenocrysts 20%, mostly feldspar. Pumice lineation dips 25° at 300 ft.	300.0 to 306.0 total depth	6.0

NOTE: ^aNevada State Plane Coordinates.

^bStratigraphic nomenclature used in original description has been retained in this table.

^cMeasurements rounded to nearest 0.5 ft.

^dContact based on cuttings that do not match well with cored interval.

Source: Gibson et al. 1992, Appendix A.

Table 1.1-75. UE-25 RF#5

Location ^a : N 231,404 m (759,199 ft); E 173,156 m (568,098 ft); Elevation 1,162.4 m (3,813.7 ft) Cored Intervals: 6.0 to 9.0 ft; 21.0 to 23.5 ft; 40.0 to 43.0 ft; 80.0 to 84.0 ft; 102.0 to 107.0 ft; 112.0 to 122.0 ft		
Stratigraphic Unit—Lithology ^b	Depth (ft) ^c	Interval Thickness (ft) ^c
Alluvium Bouldery; clasts as large as 6 in. in diameter in sandy tan calcareous matrix. Lower contact sharp.	0.0 to 102.5	102.5
Tuff, Unit "x" Ash flow, very light gray. A few white to gray vitric pumice and angular clayey pale orange pumice fragments; 5% small lithic fragments as large as 0.5 in. in diameter. A few small black to colorless perlitic glass fragments. Phenocrysts less than 5%: quartz, feldspar, biotite, and sparse sphene.	102.5 to 122.0 total depth	19.5

NOTE: ^aNevada State Plane Coordinates.

^bStratigraphic nomenclature used in original description has been retained in this table.

^cMeasurements rounded to nearest 0.5 ft.

Source: Gibson et al. 1992, Appendix A.

Table 1.1-76. UE-25 RF#7

Location ^a : N 234,331 m (768,804 ft); E 174,093 m (571,171 ft); Elevation 1,144.9 m (3,756.1 ft) Cored Intervals: 30.0 to 33.0 ft; 60.0 to 63.0 ft; 90.0 to 94.0 ft; 120.0 to 125.0 ft; 140.0 to 150.0 ft		
Stratigraphic Unit—Lithology ^b	Depth (ft) ^c	Interval Thickness (ft) ^c
Alluvium Bouldery; clasts to at least 10 in. in diameter, including several of rhyolite lava, in matrix of calcareous, clayey tan sand.	0.0 to 150.0 total depth	150.0

NOTE: ^aNevada State Plane Coordinates.

^bStratigraphic nomenclature used in original description has been retained in this table.

^cMeasurements rounded to nearest 0.5 ft.

Source: Gibson et al. 1992, Appendix A.

Table 1.1-77. UE-25 RF#7A

Location ^a : N 234,320 m (768,768 ft); E 173,818 m (570,269 ft); Elevation 1,144.8 m (3,755.9 ft) Cored Intervals: 30 to 32 ft; 60 to 62 ft; 87 to 90 ft; 120 to 122.5 ft; 150 to 153 ft		
Stratigraphic Unit—Lithology ^b	Depth (ft) ^c	Interval Thickness (ft) ^c
Alluvium Bouldery, carbonate-cemented clayey sand matrix. Clasts as large as 1.5 ft in diameter. Some rhyolite lava clasts.	0.0 to 125.0	125.0
Colluvium Coarse fragments and blocks of densely welded Paintbrush Tuff.	125.0 to 153.0 total depth	28.0

NOTE: ^aNevada State Plane Coordinates.

^bStratigraphic nomenclature used in original description has been retained in this table.

^cMeasurements rounded to nearest 0.5 ft.

Source: Gibson et al. 1992, Appendix A.

Table 1.1-78. UE-25 RF#8

Location ^a : N 234,320 m (768,768 ft); E 173,818 m (570,269 ft); Elevation 1,144.8 m (3,755.9 ft) Cored Intervals: 30 to 32 ft; 60 to 62 ft; 87 to 90 ft; 120 to 122.5 ft; 150 to 153 ft		
Stratigraphic Unit—Lithology ^b	Depth (ft) ^c	Interval Thickness (ft) ^c
Alluvium Tan, tuffaceous, sandy, containing cobble-sized clasts of welded tuff. Calcareous cement. Less indurated and more tuffaceous downward.	0.0 to 45.0 ^d	45.0
Tuff White, massive, but possibly reworked; 15% small lithic fragments. Lower contact gradational.	45.0 to 56.0	11.0
Tuff, unit "x" Ash flow, nonwelded, white, pumiceous; some vitric pumice, pale gray, with a few orange clayey fragments. Phenocrysts 5%, biotite and feldspar with trace of quartz, sphene, and hornblende. 5 to 10% 0.25 to 0.50 in. lithic fragments, some of which are perlitic gray to black glass; fragments of pumice and lithics increase downward. Thin sorted zones of reworked material 1 to 2 in. thick at about 92 and 93.5 ft. Similar to unit from 205 to 251 ft in hole RF#3.	56.0 to 93.5	37.5
Tuff Poorly sorted to crudely bedded; white, coarse, pumiceous. A few lithic fragments.	93.5 to 95.5	2.0
Sandstone Tuffaceous, tan, poorly sorted; scattered white tuff fragments increasing downward; 25% small volcanic rock grains. Lower contact gradational.	95.5 to 97.0	1.5
Tuff Ash flow, white to light gray, pumiceous; pumice mostly white, vitric. A few clasts of black glass. 10% biotite and feldspar, with minor quartz, hornblende, and sphene. Probably the same as interval 205 to 251 ft in hole RF#3. Similar to unit "x," but has more phenocrysts and pumice.	97.0 to 99.5	2.5
Tuff Bedded lapilli, tan, poorly indurated.	99.5 to 100.0	0.5
Tiva Canyon Member Tuff, ash flow, caprock, nonwelded to slightly welded; hole ends in zone of gray vesicular pumice. Dip of pumice 15° to 20°. Low-angle calcite-coated fracture at about 108 ft.	100.0 to 128.0 total depth	28.0

NOTE: ^aNevada State Plane Coordinates.^bStratigraphic nomenclature used in original description has been retained in this table.^cMeasurements rounded to nearest 0.5 ft.^dContact based on cuttings that do not match well with cored interval.

Source: Gibson et al. 1992, Appendix A.

Table 1.1-79. UE-25 RF#9

Location ^a : N 233,460 m (765,945 ft); E 173,932 m (570,643 ft); Elevation 1,119.8 m (3,674.0 ft) Cored Intervals: continuous core		
Stratigraphic Unit—Lithology ^b	Depth (ft) ^c	Interval Thickness (ft) ^c
Colluvium Coarse, bouldery, cemented with calcareous tuffaceous sand. Boulders, as large as 1.5 ft in diameter, are gray to purplish-gray Paintbrush Tuff and rhyolite lava. Latter is gray to pinkish-gray, flow-banded, and contains 5% to 10% biotite, quartz, feldspar, and probably hornblende. Lava boulders and cobbles more abundant in lower part of unit, where they represent about one-third of the clasts.	0.0 to 65.0	65.0
Tiva Canyon Member Tuff, ash flow, mostly devitrified, nonwelded, pale purplish-pink, shardy; lower part has gray vesicular pumice showing vapor-phase crystallization. Phenocrysts 5% to 10%, mostly bronze-colored biotite. Interval, badly broken and crumbly, has several carbonate-coated fractures. Lower contact gradational.	65.0 to 73.0	8.0
Tiva Canyon Member Tuff, ash flow, slightly welded, light grayish-purple with gray vesicular pumice. Pumice and degree of welding increase downward. Phenocrysts about 5%, mostly feldspar and biotite. Botryoidal chalcedony in cavities. Contacts gradational.	73.0 to 85.0	12.0
Tiva Canyon Member Tuff, ash flow, slightly to moderately welded in lower part, purplish-gray; gray vesicular pumice as much as 2.5 in. long, but average about 0.5 in. Phenocrysts 10%, mostly feldspar and subordinate biotite. Some chalcedony in cavities. Contacts gradational. Lithology at 85 ft matches that at 62 ft in hole RF#11.	85.0 to 100.0	15.0
Tiva Canyon Member Tuff, ash flow, moderately welded, light gray pumice as in overlying unit. A few fractures having clay coatings. Dip of flattened pumice 20° to 25°.	100.0 to 106.0 total depth	6.0

NOTE: ^aNevada State Plane Coordinates.^bStratigraphic nomenclature used in original description has been retained in this table.^cMeasurements rounded to nearest 0.5 ft.

Source: Gibson et al. 1992, Appendix A.

Table 1.1-80. UE-25 RF#10

Location ^a : N 233,266 m (765,308 ft); E 173,806 m (570,230 ft); Elevation 1,118.5 m (3,669.7 ft) Cored Interval: 30.0 to 60.0 ft		
Stratigraphic Unit—Lithology ^b	Depth (ft) ^c	Interval Thickness (ft) ^c
Alluvium Cored part light brown calcareous sandstone and siltstone containing scattered welded tuff fragments and numerous thin layers of white to light tan calcium carbonate.	0.0 to 35.0	35.5
Tiva Canyon Member Ash-flow tuff, nonwelded to slightly welded, grayish-purple, light and dark pumice, some as large as 2 in. across, all devitrified with some vapor-phase alteration. Phenocrysts 5%, biotite and feldspar. Near top of unit are fractures that have carbonate filling. Grades downward to light purplish-gray and becomes moderately welded near bottom of hole. Pumice dips about 22°. One fracture at about 43 ft.	35.5 to 60.0 total depth	24.5

NOTE: ^aNevada State Plane Coordinates.

^bStratigraphic nomenclature used in original description has been retained in this table.

^cMeasurements rounded to nearest 0.5 ft.

Source: Gibson et al. 1992, Appendix A.

Table 1.1-81. UE-25 RF#11

Location ^a : N 233,362 m (765,622 ft); E 173,869 m (570,435 ft); Elevation 1,117.2 m (3,665.4 ft) Cored Intervals: 0 to 2.0 ft; 35.0 to 40.0 ft		
Stratigraphic Unit—Lithology ^b	Depth (ft) ^c	Interval Thickness (ft) ^c
Alluvium Coarse, bouldery; clasts of Tiva Canyon welded tuff in calcareous, friable tan sandstone; carbonate seams common.	0.0 to 39.5	39.5
Tiva Canyon Member Tuff, ash flow, nonwelded, light purplish-pink, poorly indurated; broken, crumbly, clay alteration, carbonate along seams and fractures. Less than 5% phenocrysts, mostly biotite and feldspar.	39.5 to 50.5	11.0
Tiva Canyon Member Tuff, ash flow, slightly welded, light purplish-gray; some large 2-in. light and dark pumice with vapor-phase alteration. Phenocrysts 5% to 10%, biotite, feldspar (same as uppermost Tiva Canyon unit in hole RF#10).	50.5 to 61.0	9.5
Tiva Canyon Member Tuff, ash flow, slightly to moderately welded in lower part, light gray with gray and white pumice; vapor-phase alteration. Open fracture at about 64 ft, dipping 75°, chalcedony-coated. Dip of flattened pumice 20° to 25°. Lithology at 62 ft matches lithology at 85 ft in hole RF#9.	61.0 to 76.5 total depth	15.5

NOTE: ^aNevada State Plane Coordinates.

^bStratigraphic nomenclature used in original description has been retained in this table.

^cMeasurements rounded to nearest 0.5 ft.

Source: Gibson et al. 1992, Appendix A.

Table 1.1-82. Rock Mass Parameters for Nonlithophysal Repository Host Horizon Units Calculated using RocLab

Lithostratigraphic unit	Rock Mass Cat.	Hoek-Brown Classification				Hoek-Brown Criterion			Mohr-Coulomb Fit		Rock Mass Parameters				
		σ_{ci} MPa	GSI	mi	D	mb	s	a	C MPa	Φ Degrees	σ_t MPa	σ_c MPa	σ_{cm}' MPa	Em GPa	Average Poisson Ratio
Tptpmn	1	136.36	51	12.39	0	2.153	0.004	0.505	7.36	32.64	-0.27	8.71	26.90	10.59	NA
Tptpmn	2	136.36	59	12.39	0	2.865	0.011	0.503	8.33	35.02	-0.50	13.79	32.02	16.79	NA
Tptpmn	3	136.36	62	12.39	0	3.189	0.015	0.502	8.75	35.91	-0.63	16.34	34.28	19.95	NA
Tptpmn	4	136.36	68	12.39	0	3.951	0.029	0.502	9.73	37.65	-0.99	22.92	39.57	28.18	NA
Tptpmn	5	136.36	72	12.39	0	4.557	0.049	0.501	10.52	38.79	-1.33	28.68	43.90	35.48	NA
Tptpmn (average)	NA	136.36	62	12.39	0	3.189	0.015	0.502	8.75	35.91	-0.63	16.34	34.28	19.95	0.19
Tptpln	1	165.59	57	20.86	0	4.492	0.008	0.504	11.34	38.98	-0.31	14.94	47.53	14.96	NA
Tptpln	2	165.59	61	20.86	0	5.182	0.013	0.503	12.00	40.17	-0.42	18.75	51.66	18.84	NA
Tptpln	3	165.59	64	20.86	0	5.768	0.018	0.502	12.53	41.06	-0.53	22.22	55.07	22.39	NA
Tptpln	4	165.59	69	20.86	0	6.895	0.032	0.501	13.52	42.53	-0.77	29.44	61.49	29.85	NA
Tptpln	5	165.59	72	20.86	0	7.675	0.045	0.501	14.20	43.39	-0.96	34.82	65.92	35.48	NA

Table 1.1-82. Rock Mass Parameters for Nonlithophysal Repository Host Horizon Units Calculated using RocLab (Continued)

Lithostratigraphic unit	Rock Mass Cat.	Hoek-Brown Classification				Hoek-Brown Criterion			Mohr-Coulomb Fit		Rock Mass Parameters				
		σ_{ci} MPa	GSI	m_i	D	mb	s	a	C MPa	Φ Degrees	σ_t MPa	σ_c MPa	σ_{cm}' MPa	Em GPa	Average Poisson Ratio
Tptpln (average)	NA	165.59	65	20.86	0	5.977	0.020	0.502	12.72	41.36	-0.57	23.51	56.27	23.71	0.22

NOTE: Data based on average saturated 50 mm diameter specimens only. The rock mass is characterized within a range of five rock mass categories, with the category 1 representing the lowest ranking. The categories are established by the GSI values corresponding to 5%, 20%, 40%, 70%, and 90% of GSI cumulative frequency of occurrence cutoffs.

a = empirical curve fitting exponent characteristic for a particular rock type; C = cohesion; D = a factor, which depends upon the degree of disturbance to which the rock mass has been subjected by blast damage and stress relaxation; D = 0 for mechanically excavated openings and D = 1.0 for heavily disturbed/damaged ground; Em = rock mass elastic modulus; GSI = Geologic Strength Index; mb = empirical curve fitting parameter, a reduced value of the intact rock material constant m_i ; m_i = intact rock material constant; NA = not applicable; Φ = internal angle of friction; s = material constant for the rock mass; σ_c = unconfined rock mass compression strength; σ_{ci} = unconfined compressive strength of the intact rock material; σ_{cm}' = global rock mass compressive strength; σ_t = rock mass tensile strength.

Source: BSC 2007i, Table 6-76.

Table 1.1-83. Summary of In Situ Stresses at the Repository Host Horizon

Hydraulic Fracturing Measurements				
Parameter	Value		Value^a	
Boreholes	ESF-GDJACK#1 and #5		ESF-AOD-HDFR#1	
Vertical Stress	4.3 to 4.7 MPa		4.7 MPa	
Minimum Horizontal Stress	2.1 MPa	±0.1 MPa	1.7 MPa	±0.1 MPa
Maximum Horizontal Stress	3.5 MPa	±0.4 MPa	2.9 MPa	±0.4 MPa
Bearing of Minimum Horizontal Stress	N65°W	±15°	N75°W	±14°
Bearing of Maximum Horizontal Stress	N25°E	±15°	N15°E	±14°

NOTE: ^aSNL 1997.

Table 1.1-84. Summary of Laboratory Physical Properties Testing of Alluvium from Boreholes UE-25 RF#47 and UE-25 RF#52

Borehole ID UE-25 RF#	Depth (ft)	USCS Group Symbol	Percent >3 in.	Percent Gravel	Percent Sand	Percent Fines	Minus No. 4 Specific Gravity	Absorption Percent
47	4.5 to 8.8	GP-GM	0.0	46.7	41.9	11.4	2.51	5.5
47	8.8 to 13.5	SM	4.0	39.5	43.3	13.2	2.49	6.4
47	13.5 to 15.7	SM	0.0	24.4	56.5	19.1	2.52	6.4
47	15.7 to 18.2	SP-SM	9.7	39.4	40.1	10.8	2.52	5.1
47	18.2 to 20.5	SM	0.0	33.9	48.3	17.8	2.5	5.7
47	20.7 to 21.7	GW-GM	0.0	57.2	34.7	8.1	2.53	5.8
47	21.7 to 26.2	SM	0.0	31.4	51.8	16.8	2.51	6.1
47	26.2 to 28.6	SP-SM	4.0	40.6	44.1	11.3	2.53	6.3
47	28.6 to 31.6	SM	0.0	24.7	53.8	21.5	2.51	6.3
47	31.6 to 34.8	SM	3.6	39.0	43.3	14.1	2.51	6.1
47	34.8 to 36.5	SM	0.0	33.1	47.3	19.6	2.52	6.3
47	36.5 to 40.9	SM	5.6	35.9	44.3	14.2	2.5	5.0
47	40.9 to 43.8	GM	8.3	41.1	38.1	12.5	2.52	5.4
47	43.8 to 51.0	GM	0.0	43.3	42	14.7	2.49	5.1
47	51.9 to 52.7	SP-SM	0.0	35.2	53.9	10.9	2.51	5.6
47	54.1 to 56.8	SM	0.0	36.9	45.4	17.7	2.51	5.3
47	56.8 to 58.2	SM	0.0	21.8	53.1	25.1	2.48	5.3
47	59.0 to 68.6	GM	2.1	43.2	41.0	13.7	2.52	5.8
47	70.0 to 87.5	SM	2.6	37.0	46.6	13.8	2.49	4.9
47	87.5 to 88.9	SM	0.0	31.1	41.3	27.6	2.54	6.7
52	0.0 to 2.9	GM	9.7	38.0	37.0	15.3	2.54	5.9
52	2.9 to 5.4	SP-SM	0.0	40.1	51.5	8.4	2.54	5.6
52	5.4 to 11.0	GW-GM	1.1	48.4	40.3	10.2	2.52	4.8
52	11.0 to 24.2	SM	1.2	36.6	49.4	12.8	2.5	6.1
52	24.2 to 30.7	SM	0.0	15.9	68.0	16.1	2.43	6.9
52	30.7 to 35.2	SP-SM	0.0	43.8	45.4	10.8	2.5	5.1
52	35.2 to 40.3	SM	0.0	37.4	46.8	15.8	2.51	6.0

Table 1.1-84. Summary of Laboratory Physical Properties Testing of Alluvium from Boreholes UE-25 RF#47 and UE-25 RF#52 (Continued)

Borehole ID UE-25 RF#	Depth (ft)	USCS Group Symbol	Percent >3 in.	Percent Gravel	Percent Sand	Percent Fines	Minus No. 4 Specific Gravity	Absorption Percent
52	40.3 to 44.5	GW-GM	3.5	46.7	40.2	9.6	2.52	6.5
52	44.5 to 50.3	SM	0.0	34.7	51.5	13.8	2.51	5.8
52	50.3 to 61.8	GM	1.7	44.2	40.6	13.5	2.51	5.4
52	61.8 to 68.4	SM	2.0	35.8	48.4	13.8	2.51	6.0
52	68.4 to 104.5	SM	1.9	41.8	41.8	14.5	2.53	5.9
52	104.5 to 107.9	GM	14.0	36.0	34.1	15.9	2.52	3.7
52	109.5 to 148.2	GM	8.6	42.9	35.7	12.8	2.52	15.8
52	149.8 to 152.5	SM	0.0	38.3	44.5	17.2	2.53	6.7
52	152.5 to 155.8	GM	16.9	35.7	35.1	12.3	2.54	5.0
52	157.8 to 160.7	GM	5.9	44.5	36.6	13.0	2.53	4.7

NOTE: USCS = Unified Soil Classification System

Source: SNL 2008a, Table 6.2-3.

Table 1.1-85. Summary of In-Place Soil Density Tests and Relative Density

Test Pit No. TP-WHB-	Sample Depth (ft)	Sample Management Facility Sample No. 01041	USCS Group Symbol	Volume of Test Hole (ft ³)	Total Mass of Test Material (lbs)	Moisture Content (%)	In Place Wet Density (lbm/ft ³)	In Place Dry Density (lbm/ft ³)	Relative Density (%)
5	4	600	GP-GM	16.07	1,963.55	6.9	122.20	114.3	102
5	12	602	GW	20.0	2,293.30	4.8	114.70	109.4	102
5	19	603	GP	14.36	1,640.05	4.6	114.21	109.2	72
6	4	601	SP-SM	21.24	2,486.80	4.7	117.10	111.8	81
6	12	700	SP-SM	20.96	2,319.65	5.3	110.67	105.1	61
6	19	604	SP-SM	15.72	1,735.40	3.7	110.39	106.5	60
7	4	605	GW-GM	15.14	1,712.00	4.5	113.08	108.2	74
7	12	606	SP	12.77	1,537.30	4.9	120.38	114.8	100
7	19	607	SP-SM	14.34	1,691.35	3.8	117.95	113.6	68

NOTE: USCS = Unified Soil Classification System

Source: SNL 2008a, Table 6.2-4.

Table 1.1-86. Median, 16th Percentile, and 84th Percentile of Seismic Wave Velocities in Each Stratigraphic Unit from Free-Free Resonant Column Tests

Stratigraphic Unit	Number of Specimens	Depth of Unit (ft)		V _s (ft/s)			V _c (ft/s)			V _p (ft/s)		
		Top	Bottom	Median	16th Percentile	84th Percentile	Median	16th Percentile	84th Percentile	Median	16th Percentile	84th Percentile
Tmr	2	0	60	2,497	1,177	5,297	4,283	2,193	8,363	5,108	2,916	8,946
Tpki	2	60	100	3,668	3,597	3,740	5,828	5,556	6,113	6,656	6,618	6,694
Tpcrn	3	100	120	4,409	3,399	5,718	6,855	5,446	8,629	7,685	6,340	9,316
Tpcrl	2	120	140	3,579	2,072	6,183	6,042	3,481	10,487	7,803	4,818	12,638
Tpcpul	3	140	160	7,165	6,926	7,412	11,486	10,915	12,086	12,185	11,549	12,856
Tpcpmn	2	160	180	8,855	8,691	9,022	13,188	12,307	14,132	13,419	12,245	14,707
Tpcpll	2	180	200	4,612	4,108	5,178	7,683	6,852	8,616	10,525	9,552	11,598
Tpcpln	2	200	220	8,901	8,242	9,612	13,639	12,910	14,409	14,184	13,812	14,566
Tpcpv	1 ^a	220	260	5,273	5,273	5,273	8,039	8,039	8,039	8,902	8,272	9,580
Tpy	3	260	280	4,035	3,377	4,822	6,260	5,052	7,757	6,599	5,415	8,041
Tpbt3	4	280	300	3,306	2,803	3,900	5,141	4,203	6,288	5,978	5,065	7,055
Tpp	3	300	360	3,615	3,078	4,246	5,540	4,795	6,400	5,935	4,986	7,064
Tpbt2	2	360	420	2,297	1,970	2,677	3,610	3,138	4,153	4,091	3,834	4,365
Tptrn	6 ^b	420	540	6,491	6,033	6,983	10,022	9,237	10,873	10,589	9,951	11,267
Tptrl	2	540	560	3,824	3,628	4,031	7,164	7,118	7,210	8,084	6,984	9,358
Tptpul	12	560	700	5,771	4,760	6,997	9,158	7,529	11,141	11,169	9,996	12,481
Ttptmn	9	700	840	8,817	8,657	8,980	13,307	12,942	13,681	13,610	13,157	14,077
Ttptll	7 ^c	840	1,100	6,203	5,248	7,330	9,610	7,900	11,691	11,107	9,844	12,531

Table 1.1-86. Median, 16th Percentile, and 84th Percentile of Seismic Wave Velocities in Each Stratigraphic Unit from Free-Free Resonant Column Tests (Continued)

Stratigraphic Unit	Number of Specimens	Depth of Unit (ft)		V _s (ft/s)			V _c (ft/s)			V _p (ft/s)		
		Top	Bottom	Median	16th Percentile	84th Percentile	Median	16th Percentile	84th Percentile	Median	16th Percentile	84th Percentile
Tptpln	8	1,100	1,240	8,633	8,007	9,308	13,421	12,780	14,093	13,952	13,400	14,527
Tptpv	5	1,240	1,360	4,886	3,415	6,990	7,428	5,144	10,726	8,871	6,072	12,960
Tac	10	1,360	1,660	4,397	3,316	5,830	6,851	5,330	8,807	7,451	5,939	9,347
Tcp	21	1,660	2,020	5,438	4,434	6,670	8,491	6,986	10,319	8,989	7,454	10,840
Tcpbt	1	2,020	2,060	5,475	5,475	5,475	8,004	8,004	8,004	8,052	8,052	8,052
Tcb	12	2,060	2,440	5,814	4,159	8,126	8,849	6,284	12,459	10,275	8,202	12,871
Tcbbt	2	2,440	2,480	6,924	6,756	7,096	10,750	10,551	10,953	11,159	10,979	11,342
Tct	5	2,480	3,300	5,096	4,684	5,545	8,023	7,482	8,603	8,734	8,370	9,115

NOTE: ^aOne specimen broken after V_p test and V_c and V_s test
^bData of one outlier specimen discarded
^cData of two outlier specimens discarded.

Source: SNL 2008a, Table 6.5-7.

Table 1.1-87. Median, 16th Percentile and 84th Percentile of Material Damping Ratios in Each Stratigraphic Unit

Strat. Unit	No. of Specimens	Depth of Unit (ft)		D _{Smin} (%)			D _{Cmin} (%)		
		Top	Bottom	Median	16th Percentile	84th Percentile	Median	16th Percentile	84th Percentile
Tmr	1 ^a	0	60	0.42	0.42	0.42	0.14	0.14	0.14
Tpki	2	60	100	1.23	0.97	1.55	0.80	0.73	0.87
Tpcrn	3	100	120	0.95	0.49	1.82	0.57	0.36	0.89
Tpcrl	2	120	140	1.61	0.76	3.45	1.29	0.94	1.78
Tpcpul	3	140	160	0.34	0.29	0.40	0.29	0.21	0.41
Tpcpmn	2	160	180	0.26	0.18	0.37	0.27	0.17	0.42
Tpcpll	2	180	200	1.06	0.44	2.55	0.42	0.20	0.89
Tpcpln	2	200	220	0.18	0.15	0.22	0.14	0.12	0.16
Tpcpv	1 ^b	220	260	0.73	0.73	0.73	0.43	0.43	0.43
Tpy	3	260	280	1.02	0.53	1.98	0.63	0.37	1.09
Tpbt3	4	280	300	1.21	0.76	1.93	1.01	0.64	1.59
Tpp	3	300	360	0.69	0.53	0.89	0.52	0.39	0.68
Tpbt2	1 ^a	360	420	0.75	0.75	0.75	0.69	0.69	0.69
Tptrn	6 ^a	420	540	0.33	0.27	0.40	0.30	0.22	0.42
Tptrl	2	540	560	0.84	0.51	1.40	0.55	0.30	0.98
Tptpul	11 ^a	560	700	0.80	0.51	1.26	0.55	0.34	0.88
Tptpmn	9	700	840	0.22	0.15	0.30	0.20	0.13	0.29
Tptpll	7 ^c	840	1100	0.58	0.36	0.93	0.49	0.34	0.72

Table 1.1-87. Median, 16th Percentile and 84th Percentile of Material Damping Ratios in Each Stratigraphic Unit (Continued)

Strat. Unit	No. of Specimens	Depth of Unit (ft)		D _{Smin} (%)			D _{Cmin} (%)		
		Top	Bottom	Median	16th Percentile	84th Percentile	Median	16th Percentile	84th Percentile
Tptpln	8	1100	1240	0.24	0.12	0.49	0.26	0.18	0.37
Tptpv	5	1240	1360	1.13	0.53	2.40	1.38	0.67	2.82
Tac	9 ^a	1360	1660	0.57	0.30	1.10	0.53	0.26	1.09
Tcp	21	1660	2020	0.56	0.41	0.77	0.45	0.33	0.60
Tcpbt	1	2020	2060	0.86	0.86	0.86	0.75	0.75	0.75
Tcb	12	2060	2440	0.83	0.31	2.25	0.55	0.23	1.31
Tcbbt	2	2440	2480	0.59	0.48	0.72	0.56	0.53	0.59
Tct	5	2480	3300	1.11	0.59	2.09	0.64	0.31	1.30

NOTE: ^aData of one outlier specimen discarded

^bOne specimen broken after V_P test and V_C and V_S test

^cData of two outlier specimens discarded.

Source: SNL 2008a, Table 6.5-8.

Table 1.1-88. Measured Radionuclide Concentrations at Gate 510 Air Sampling Station

Radionuclide	Average Concentration (pCi/m ³)	
	2004	2005
³ H	0.73	0.28
²⁴¹ Am	4.69×10^{-6}	4.01×10^{-6}
²³⁸ Pu	1.76×10^{-6}	1.08×10^{-6}
²³⁹⁺²⁴⁰ Pu	3.07×10^{-6}	2.99×10^{-6}

Source: Grossman 2005, Table 4.0; Grossman 2006, Table 4.0.

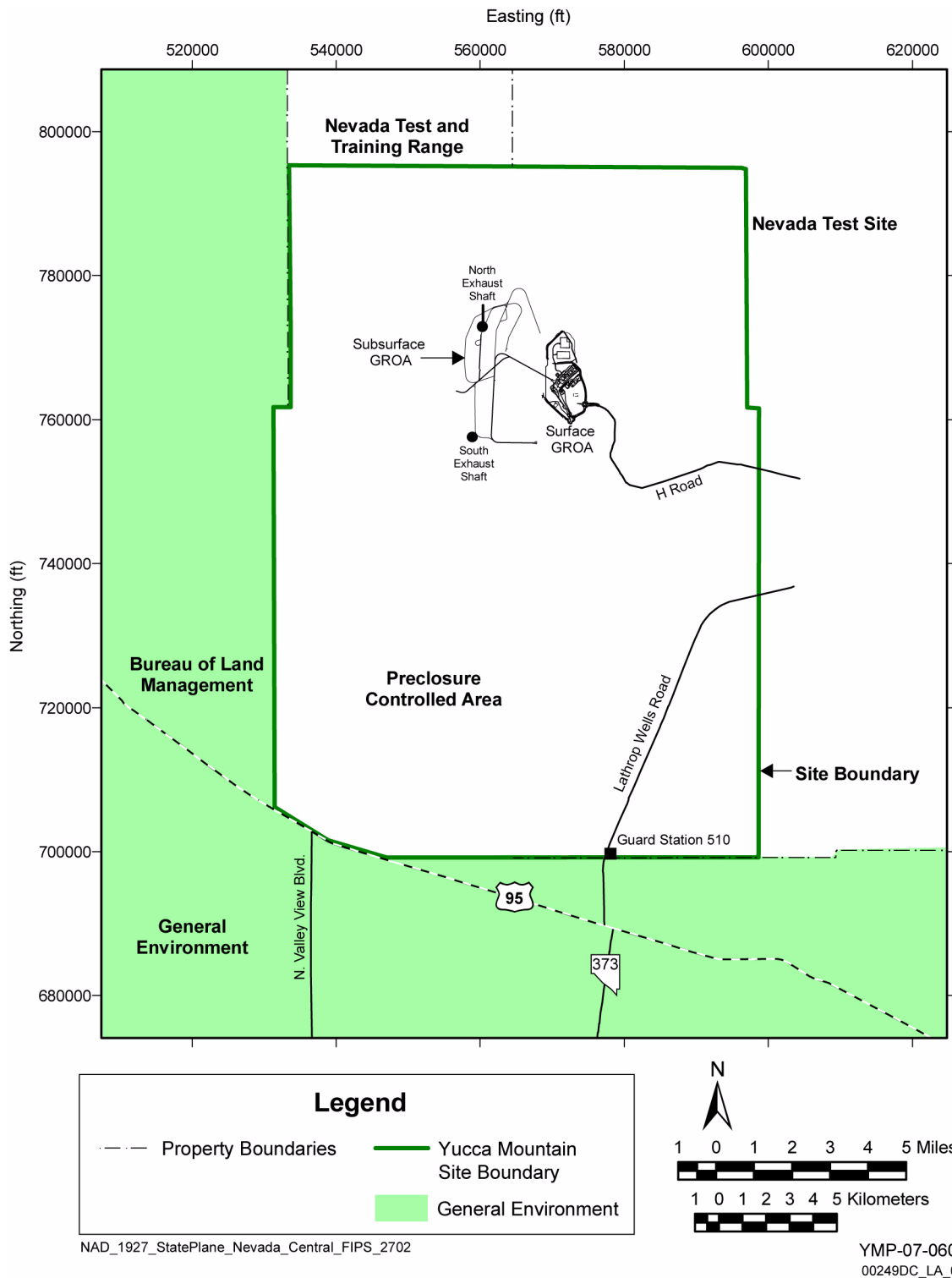


Figure 1.1-1. Site Boundary

NOTE: The preclosure controlled area is also called the site and the land withdrawal area.

INTENTIONALLY LEFT BLANK

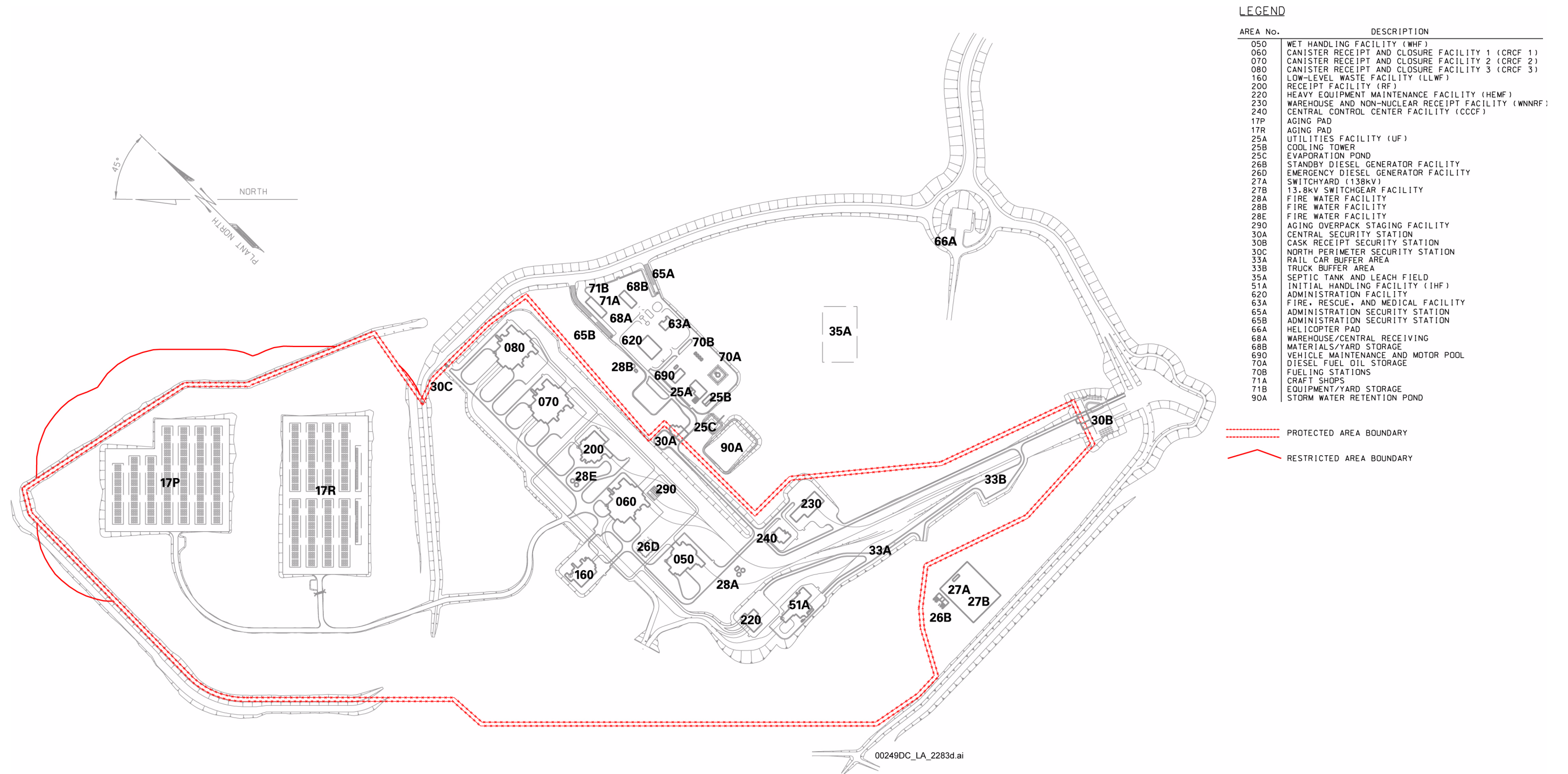
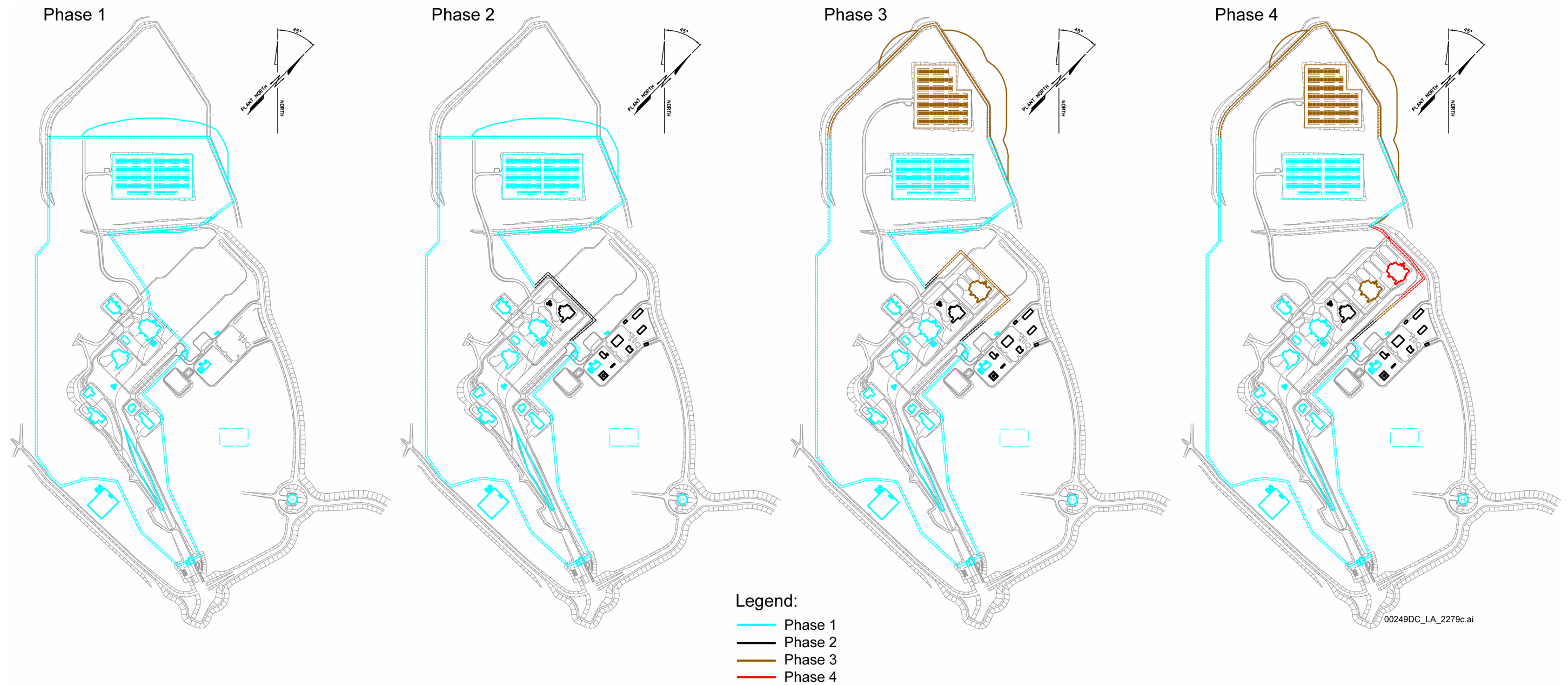


Figure 1.1-2. Boundaries of Surface Geologic Repository Operations Area at Maximum Extent of the Restricted Area

INTENTIONALLY LEFT BLANK



NOTE: Exhaust shafts will also be part of the surface GROA. The legend for boundaries and facility names is shown in Figure 1.1-2

Figure 1.1-3. Surface Geologic Repository Operations Area Showing Changes of Restricted Area and Protected Area during Phased Repository Development

INTENTIONALLY LEFT BLANK

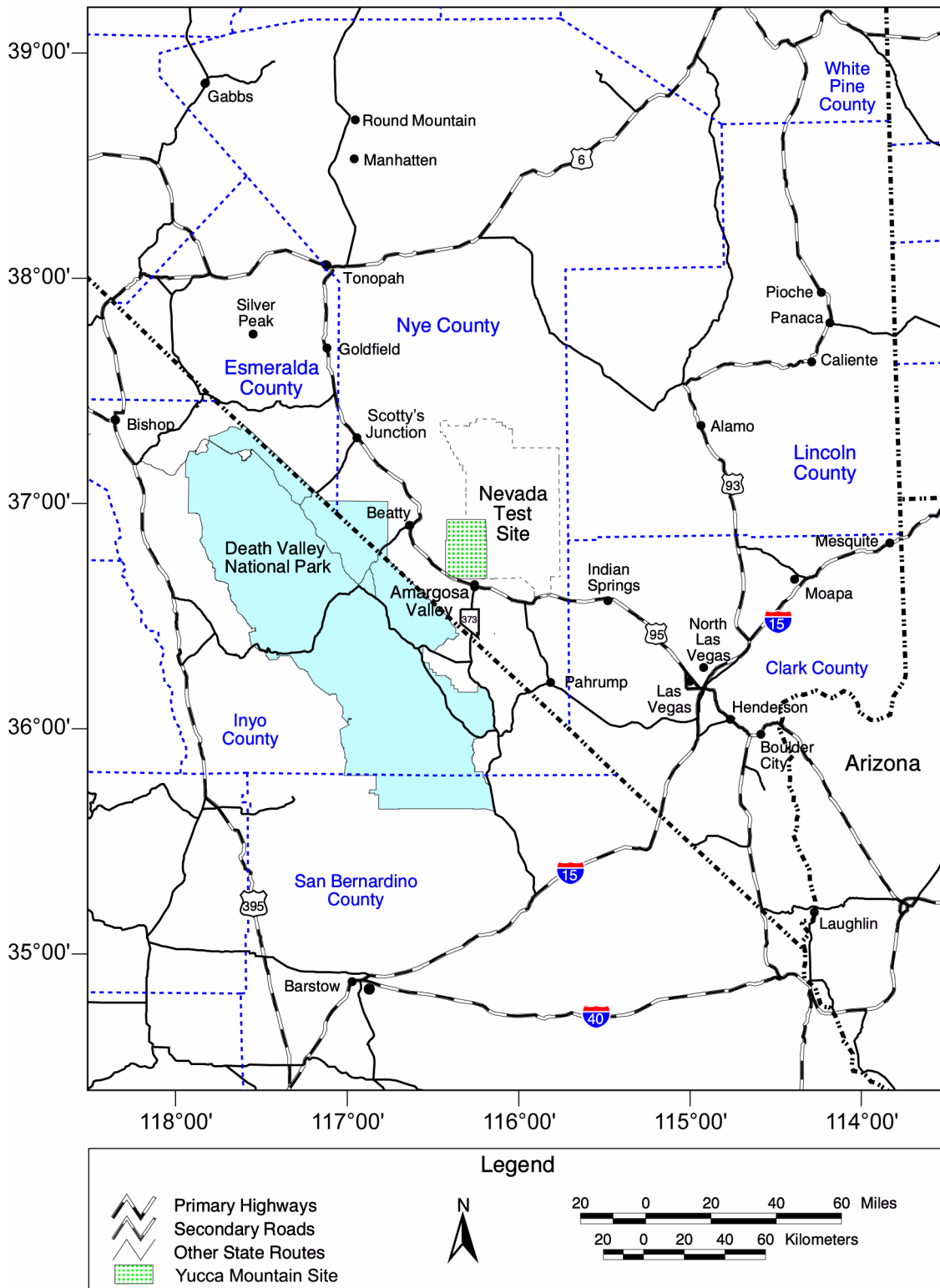


Figure 1.1-4. Map Showing the Location of Yucca Mountain Site

00249DC_LA_1137b.ai

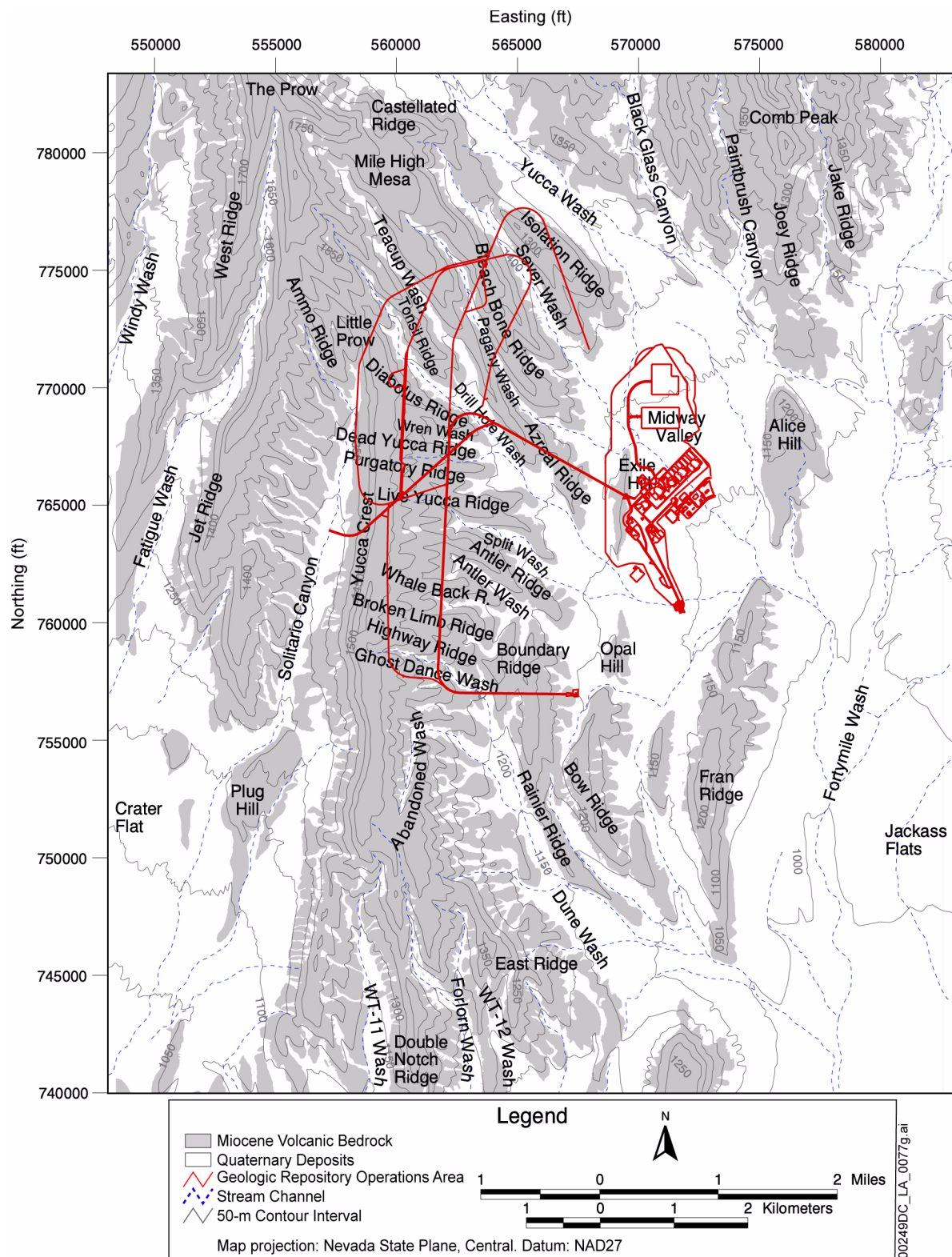


Figure 1.1-5. Topography and Drainage System in the Vicinity of the Repository

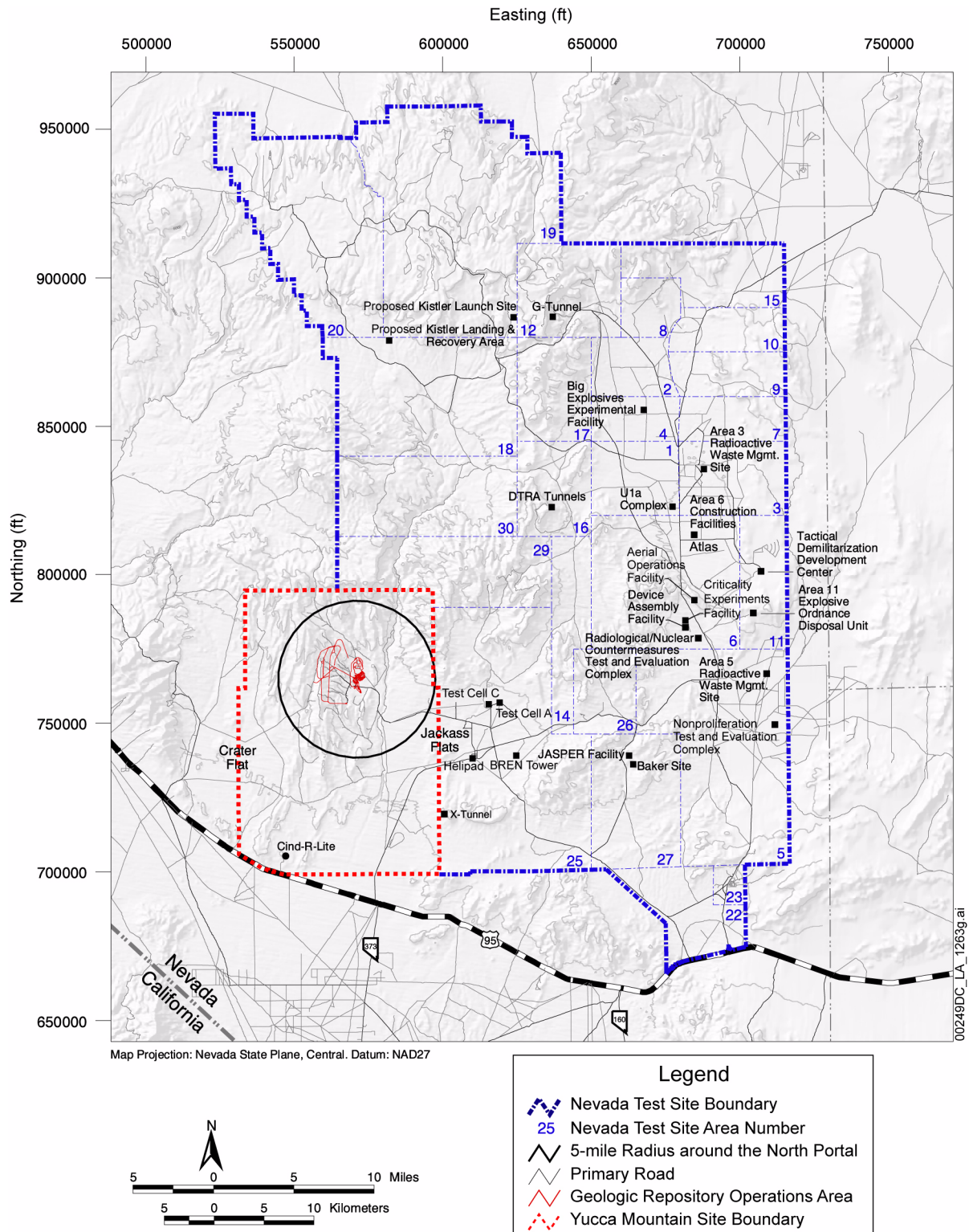
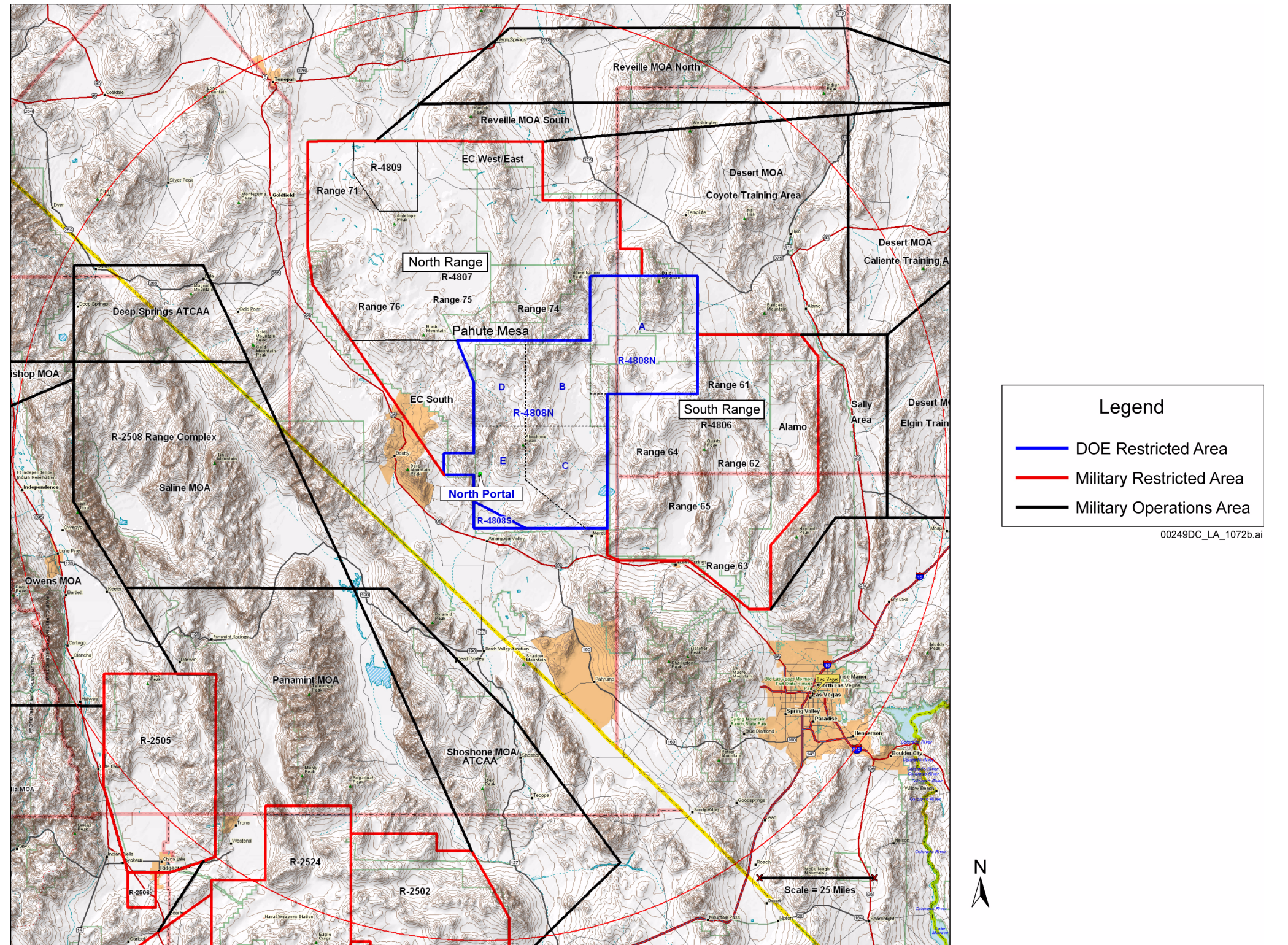


Figure 1.1-6. Nevada Test Site Regional Location Map

NOTE: Nevada State Plane coordinates pertain only to Nevada portion of map. BREN = Bare Reactor Experiment-Nevada; DTRA = Defense Threat Reduction Agency; JASPER = Joint Actinide Shock Physics Experimental Research.

INTENTIONALLY LEFT BLANK



NOTE: ATCAA = air traffic control assigned airspace; EC = electronic combat; MOA = military operations area.

Figure 1.1-7. 100-mi Regional Airspace Setting Surrounding Yucca Mountain

INTENTIONALLY LEFT BLANK

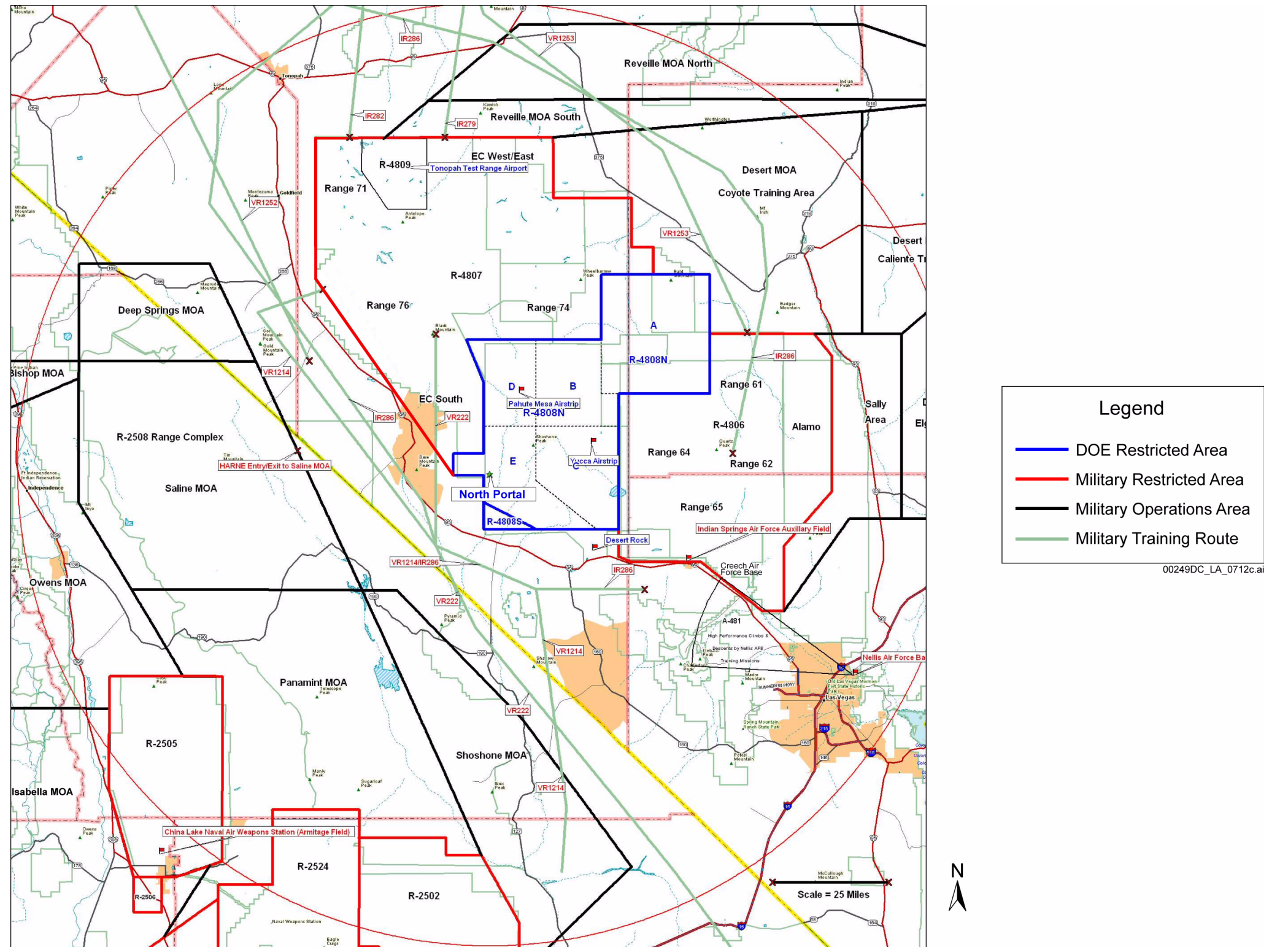


Figure 1.1-8. Military Airports, Military Training Routes, and Navigation Aids in the Regional Setting

NOTE: EC = electronic combat; MOA = military operations area.

INTENTIONALLY LEFT BLANK

INTENTIONALLY LEFT BLANK